NANYANG TECHNOLOGICAL UNIVERSITY

SYNTHESIS AND REACTIVITIES OF NOVEL DIVALENT GROUP 14 ELEMENTS SPECIES

WANG LILIANG

SCHOOL OF PHYSICAL AND MATHEMATICAL SCIENCES

2017

SYNTHESIS AND REACTIVITIES OF NOVEL DIVALENT GROUP 14 ELEMENTS SPECIES WANG LILIANG 2017

SYNTHESIS AND REACTIVITIES OF NOVEL DIVALENT GROUP 14 ELEMENTS SPECIES

WANG LILIANG

WANG LILIANG

School of Physical and Mathematical Sciences

A thesis submitted to the Nanyang Technological University

in fulfilment of the requirements for the degree of

Doctor of Philosophy

2017

Acknowledgements

I would first like to express my sincere appreciation to my supervisor, Nanyang Assistant Professor Dr. Rei Kinjo, for recruiting me into the research group and giving the chance to immerse myself in the research life. I should also thank my supervisor Dr. Kinjo for his guidance, patience and support throughout the years of my Ph.D study. Without his advice and help, I cannot finish my Ph.D thesis, even would never be a Doctor of Chemistry in my life.

I would always like to extend my gratitude to my colleagues in the years through the Ph.D study. I have learnt a lot of knowledge from them. Without their help, it would be tough for me. In particular, I want to thank the former members Dr. Kong Lingbing, Dr. Chong Che Chang, Dr. Cui Jingjing, Dr. Chandrakanta Dash, Dr. Kiran Kumarvarma Chakrahari, and Mr. Hu Haitao; and current members Dr. Wang Baolin, Dr. Lu Wei, Dr. Rao Bin, Dr. Su Yuanting, Mr. Wu Di, Mr. Su Bochao, and Ms. Gillian Goh Kor Hwee.

I would like to express my sincere thanks to Dr. Li Yongxin and Dr. Rakesh Ganguly for their expertise in X-ray crystallography analysis. I am also thankful to Ms. Goh Ee Ling and Mr. Keith Leung for their kind assistance in NMR analysis. I am grateful to appreciate the supports and help from all staffs in CBC.

I would also like to appreciate the Nanyang Technological University, Singapore (NTU) for giving me the opportunity to pursue my degree and awarding me a research scholarship.

I should finally thank my father Mr. Wang Yuhe, my mother Mrs. Du Yumei, and my young sister Ms. Wang Xinyue for their supports and encouragement throughout the four years.

Table of Contents

List of Abbreviations

NMR	Nuclear magnetic resonance
δ	chemical shift
eq.	equivalent
g	gram
h	hour
IR	infra-red
J	coupling constant
s	singlet
d	doublet
q	quartet
m	multiplet
t	triplet
br	broad
Hz	Hertz
MHz	megahertz
calcd	calculated
HOMO	Highest Occupied Molecular Orbital
LUMO	Lowest Unoccupied Molecular Orbital
P_4	white phosphorus
HRMS	High Resolution Mass Spectrometry
M	concentration in mol/L
M^+	parent ion peak in mass spectrum
mL	milliliter
mmol	millimole
mol%	mole percent
M.p.	melting point
m/z	mass to charge ratio (mass spectrum)

dec	decomposition
ppm	parts per million
r.t.	room temperature
THT	tetrahydrothiophene
THF	tetrahydrofuran
DCM	dichloromethane
L	ligands
Ad	adamantyl
Ar	aryl (substituted aromatic ring)
^{n}Bu	*n*-butyl
^{t}Bu	*tert*-butyl
CAAC	cyclic (alkyl)(amino) carbene
aNHC	abnormal *N*-heterocyclic carbene
NHC	*N*-heterocyclic carbene
AAC	(alkyl)(amino) carbene
DAC	diamidocarbene
NHSis	*N*-heterocyclic silylenes
NHGes	*N*-heterocyclic germylenes
Dipp	2,6-diisopropylphenyl
DFT	Density Functional Theory
FLPs	frustrated Lewis Pairs
H	hydrogen
Me	methyl
Et	Ethyl
^{i}Pr	*iso*-propyl
Ph	phenyl
Mes	2,4,6-trimethylphenyl
OTf	triflate (trifluoromethanesulfonate)

List of Schemes

List of Figures

List of Tables

Abstract

In this thesis, we have first synthesized a cyclic (alkyl)(amino) germylene (**CAAGe**) which possesses the high-lying HOMO−1 and low-lying LUMO, which was supported by DFT calculations. The reactivities have been investigated subsequently. The reaction of CAAGe with S_8 was first carried out, where led to the formation of the sulfido-bridged dimers as a mixture of two diastereomers involving Ge_2S_2 four-membered ring framework. But, when **CAAGe** was reacted with N_2O, and only trans product was obtained. The treatment of **CAAGe** with TEMPO was also performed and led to the formation of a 1:2 adduct. **CAAGe** was also reacted with hydrosilanes in the presence of 20 mol% $B(C_6F_5)_3$, where **CAAGe** was transformed into germylenes **10** and **11** via silyl group exchange. Lastly, the reactions of **CAAGe** with various gold(I), palladium(0) and palladium(II) complexes have been performed. The Au−Cl bond insertion products [ClGe−Au−NHC] were further reacted with various silver reagents to afford the corresponding [Ge−Au−NHC]•X complex.

A new gold(I) complex featuring a pyrid-2-ylidene ligand was synthesized and fully characterized. It has been employed in hydroamination of alkynes with ammonia, which provided an efficient synthetic method for the construction of pyridine derivatives. It has also been utilized in the hydroimination of alkynes with imines, which indicated an apparent anti-Markovnikov regioselectivity to form 2-aza-1,3-dienes.

Chapter 1 General Introduction

1.1 A brief history of stable divalent species of Group 14 elements

1.1.1 A brief history of carbenes

Carbenes are neutral divalent species in which the carbon atom possesses six electrons in its valence shell. These species were first recognized by Geuther and Hermann in 1855. These authors proposed the formation of dichlorocarbene as an intermediate in the reaction of chloroform with potassium hydroxide.[1]

Carbenes were considered diradical species (Figure 1.1, triplet state) until 1951 when Lennard-Jones and Pople hypothesized that carbene could exist in both singlet and triplet states.[2-3] Seventeen years later, Hoffmann *et al.* described the difference between the triplet and singlet states of carbenes (Figure 1.1).

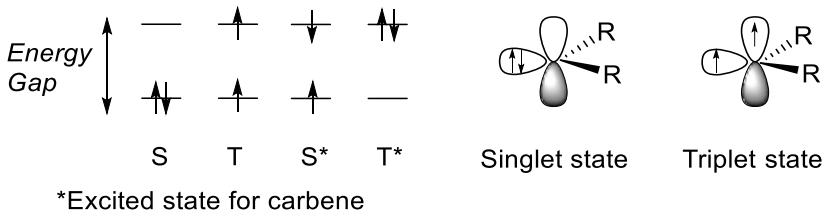

Figure 1.1 Electronic states of a carbene.

Hoffmann *et al.* suggested that the enhanced stability of singlet carbenes might be attributed to the π-overlapping between the empty *p* orbital of the carbene carbon and the π electrons of the adjacent electron withdrawing substituents, as well as their σ-electronegativity effect such as N, O, halogen etc. (Figure 1.2). [4-7]

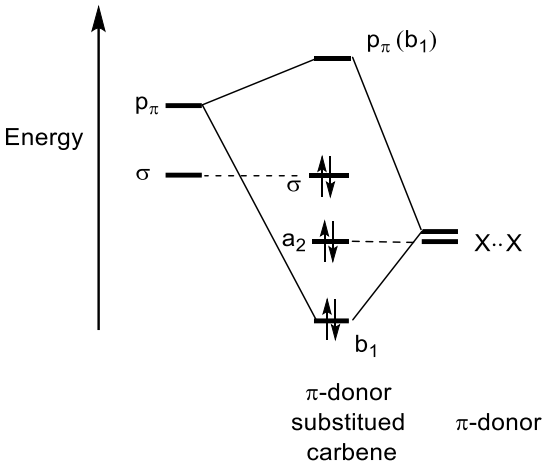

Figure 1.2 The electronic configuration of singlet carbenes with π donor substituents.

For example, dichlorocarbene (Cl_2C**:**) is a reactive intermediate in organic synthesis in its singlet state,[8-9] and has been detected by IR spectroscopy at low temperatures (Figure 1.3).[10]

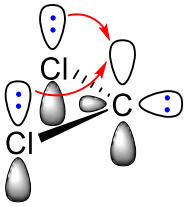

Figure 1.3 Electronic structure of dichlorocarbene.

Carbenes were originally regarded as transient species until the free [bis(diisopropylamino)phosphino]trimethylsilylcarbene **1** was successfully synthesized and isolated by Bertrand *et al.* in 1988.[11-12] In 1991, *N*-heterocyclic carbenes (NHCs) **2** were reported by Arduengo *et al.* (Figure 1.4) and have since become the most widely investigated type of singlet carbenes.[4]

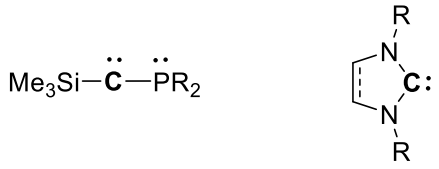

1 **2**

1988, Bertrand **1991, Arduengo**

Figure 1.4 The first isolable carbenes **1** and *N*-heterocyclic carbenes **2**.

Subsequently, the chemistry of heteroatom-stabilized singlet carbene has seen dramatic developments and the effect of the adjacent substituents on the properties of these carbenes has been studied in detail.[5, 13-18] Carbenes can be classified into two categories based on the number of adjacent substituents and their electronic properties.[19-21] The first category is comprised of carbenes that possess only one π electron donor substituent (Figure 1.5).[16, 22] This includes (alkyl)(amino)carbenes (**AACs**) which are known to react with CO to yield amino ketenes.[23] Other examples of this category include cyclic (alkyl)(amino) carbenes (CAACs) **3**.[22] **CAACs** exhibit strong electrophilic and nucleophilic properties and can react with small molecules such as CO,[23] H_2,[24] and NH_3.[24-25] Abnormal *N*-heterocyclic carbenes (**aNHCs**) are strong electron donor ligands that can activate CO_2 similar to **CAACs 3** to afford betaines.[16, 26]

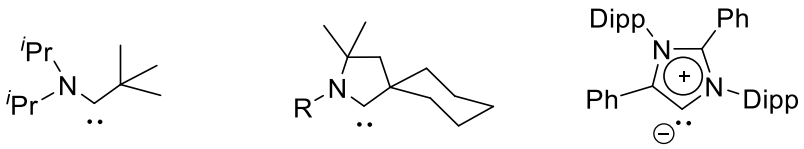

AAC **CAACs 3** **aNHC**

Figure 1.5 Stable carbenes with one π electron donor substituent.

The second category is composed of carbenes that contain two π electron donor substituents. A representative example of this category is NHCs, which are also the most prevalent singlet carbenes (Figure 1.6).[5, 27-30] NHCs show poor electrophilicity, but are strong σ donors (even stronger than the electron rich trialkylphosphines).[31-32] These carbenes are amphoteric because

of the presence of an empty *p* orbital and an occupied *s* orbital. NHCs are used as ligands in transition metal complexes and are relevant to catalytic reactions.[31, 33] Such carbenes can also stabilize the low valent main group species.[34-45]

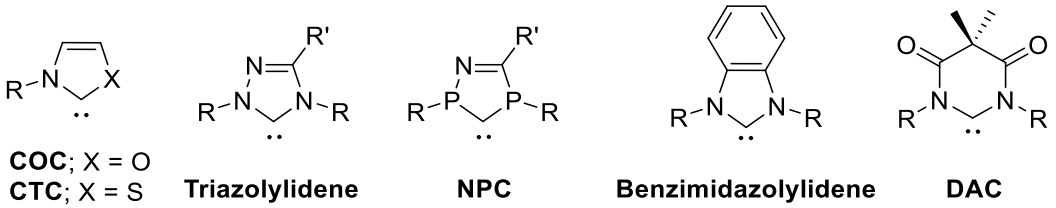

Figure 1.6 Stable carbenes with two π electron donor substituents.

1.1.2 Group 14 metallylenes

Group 14 metallylenes such as silylene (R_2Si:), germylene (R_2Ge:), stannylene (R_2Sn:), and plumbylene (R_2Pb:) are heavier carbene analogues that are also neutral and divalent with six electrons in the valence shells of Si, Ge, Sn, and Pb atoms.

Silylenes have many striking similarities with germylenes in terms of their synthetic route, reactivity, and geometry. Thus, the chemistry of silylene is also a means to understand that of germylene.[46] Meanwhile, stannylene (R_2Sn:) and plumbylene (R_2Pb:) have not been discussed in this chapter because they are thermodynamically stable under ambient conditions and lack representative reactivity.

In contrast to carbenes, metallylenes exist preferably in the singlet state[46-47] owing to a gradually increasing singlet-triplet energy difference (ΔEst). ΔEst of H_2E: (E = C, Si, Ge, Sn, and Pb) increases on descending down the group, from −9.0 kcal mol^{-1} for H_2C:, 21.0 kcal mol^{-1} for H_2Si:, 23 kcal mol^{-1} for H_2Ge:, 24 kcal mol^{-1} for H_2Sn:, and 37 kcal mol^{-1} for H_2Pb:. There are mainly two reasons why carbenes may prefer to exist in the triplet state, i.e., either the magnitude of ΔE_{st} is small and/or the extent of repulsion between the two paired electrons in the *s* orbital of metallylenes decreases upon descending the Group 14 due to the progressively

increasing radius of the *s* orbital.[48-54]

The first transient silylene **4** was observed by Skell and Goldstein in 1964 in the Si–H insertion reaction of dimethylsilylene **4** with trimethylsilane (Scheme 1.1a).[55] The transient dimethylgermylene **6** could be generated either via thermolysis or via photolysis of 7-germanorbornadienes (Scheme 1.1b).[56-60]

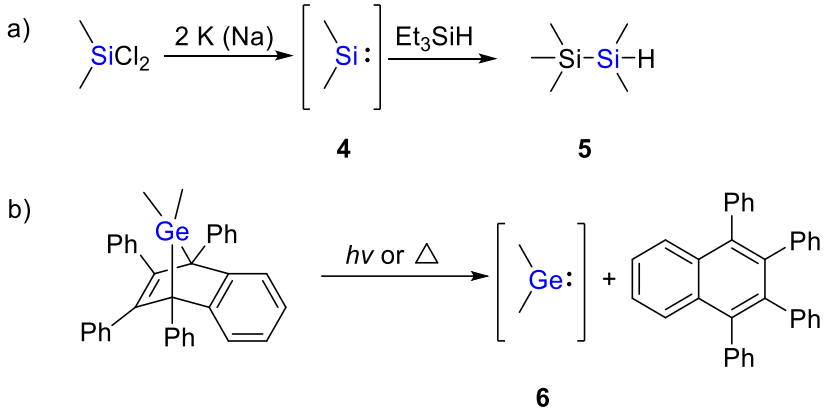

Scheme 1.1 a) Generation of silylene **4** and its insertion reaction; b) Generation of transient dimethylgermylene **6**.

In 1985, Apeloig *et al.* performed theoretical calculations to study the influence of different substituents on the properties of silylenes. It was found that electronegative substituents increase the energy gap between the HOMO and LUMO while σ donors (such as Me, $SiMe_3$, and SiH_3) decrease this energy gap.[61-63] These results have helped experimental chemists to access the stable and isolable metallylenes.

The first isolable dicoordinated germylene **7** stabilized by electronegative substituents was obtained by Harris *et al.* in 1974.[64] They employed the reaction of $GeCl_2$•dioxane with the appropriate lithium amide ($Li(NR^1R^2)$) to generate acyclic diamino germylene **7** (Scheme 1.2). Germylene **7** was further utilized for the synthesis of the first acyclic disilylgermylene **8**.[65] In the solid state, **8** formed a dimeric structure to give the digermene **9**, which can be considered as a heavy homonuclear analogue of alkenes.

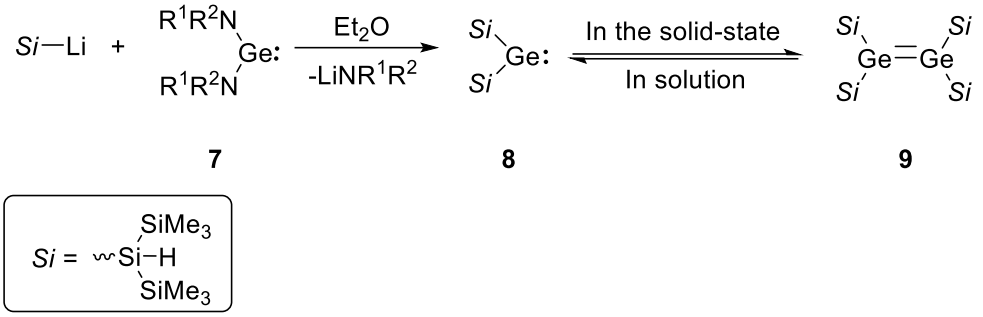

Scheme 1.2 Synthesis of disilylgermylene **8** in solution and its dimer **9** in the solid state.

In 2012, Power *et al.*[66] and Aldridge *et al.*[67] independently reported two different types of acyclic dicoordinated silylenes **10** and **11** that were found to be stable at ambient temperature (Scheme 1.3). To date, no stable acyclic diaminosilylene has been reported.[68]

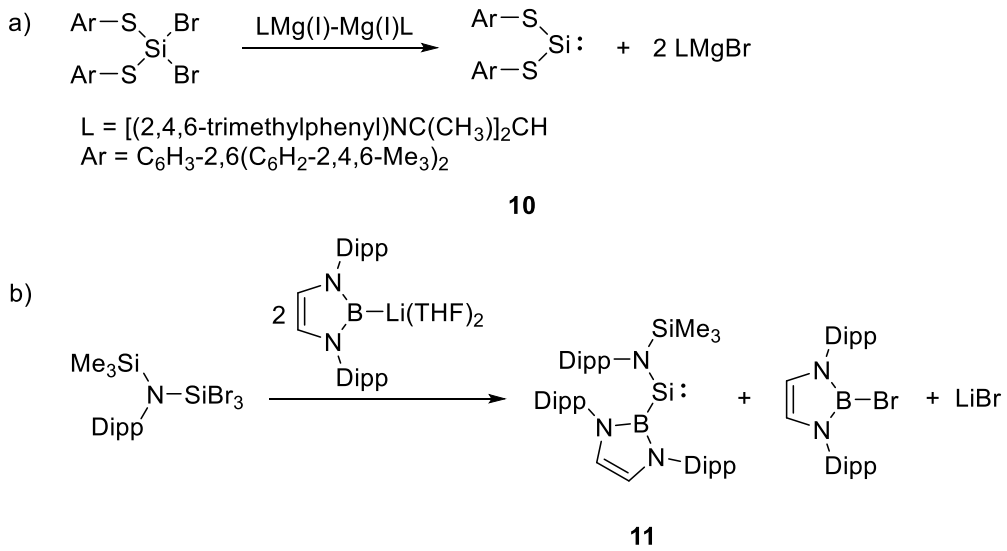

Scheme 1.3 Synthesis of acyclic dicoordinated silylenes.

Several stable heavy Group 14 analogues of alkenes $R_2E{=}ER_2$ and alkynes RE≡ER (E = Si, Ge, and Sn) (Figure 1.7) have been obtained, which are typically formed from the homocoupling of corresponding divalent species because of the lack of thermodynamic and/or kinetic stability.

34, 38, 48, 65, 69-79

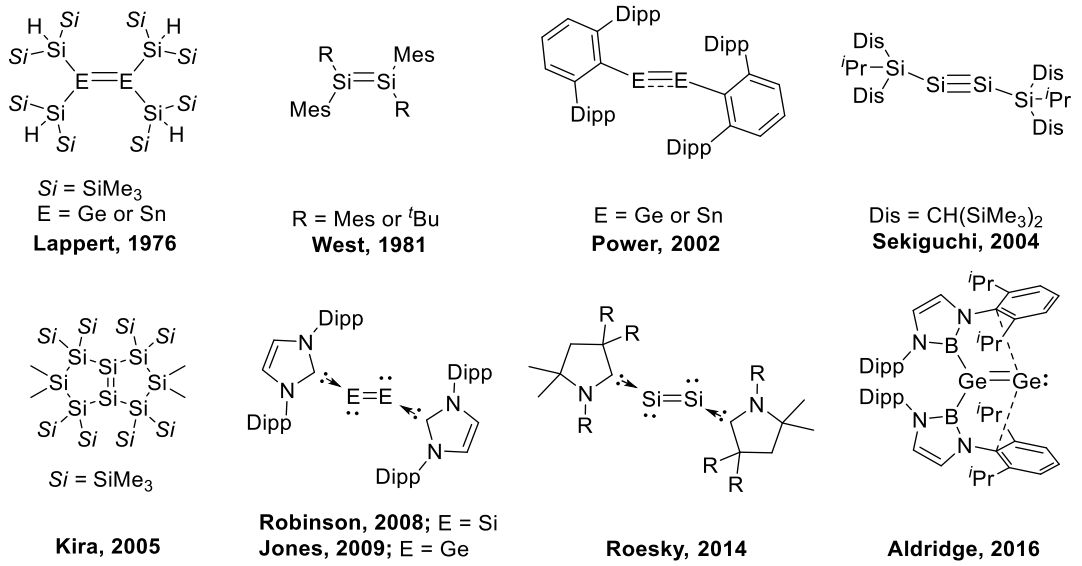

Figure 1.7 Stable heavy Group 14 analogues of alkenes and alkynes.

The reactivities of metallylenes have attracted a lot of attention to synthesize stable metallylenes. The first stable *N*-heterocyclic silylene **12** (NHSi) and *N*-heterocyclic germylene **13** (NHGe) were synthesized by West *et al.* in 1994 and Herrmann *et al.* in 1992, respectively. Diamino groups were employed as substituents to protect the metallylene center from dimerization (Scheme 1.4).[80-81]

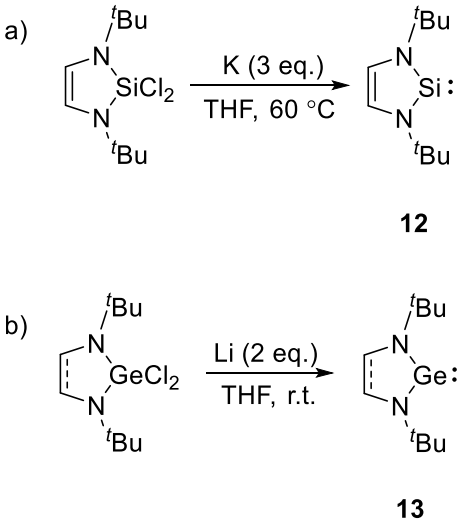

Scheme 1.4 a) Synthesis of the stable silylene **12**; b) synthesis of the stable germylene **13**.

Since their discovery, the field of stable metallylenes has attracted significant attention. Various ligands with subtle differences in their steric and electronic characteristics have been utilized to stabilize the metallylene center (Figure 1.8).[80-92]

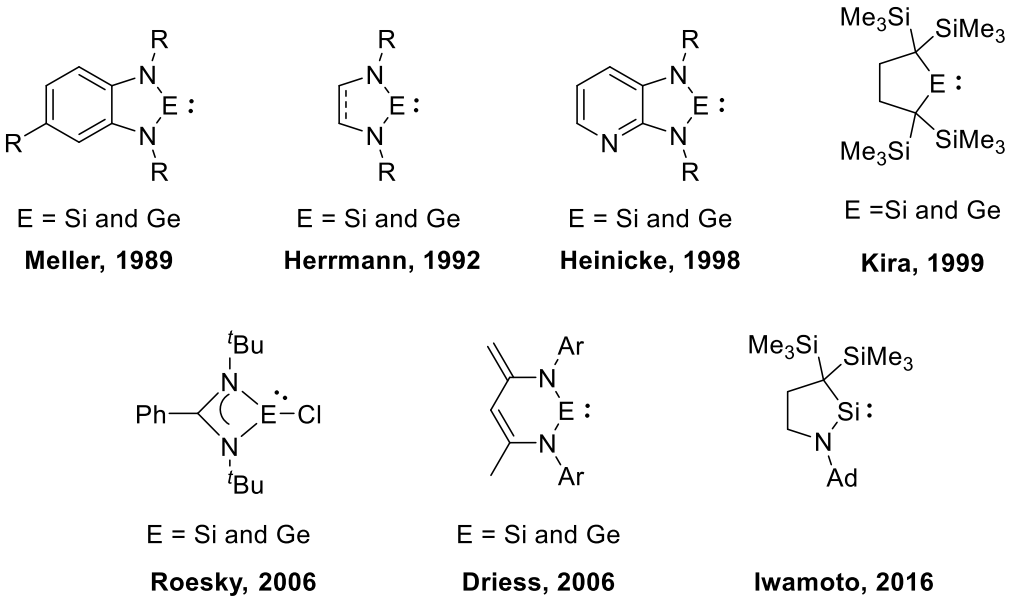

Figure 1.8 Common cyclic metallylenes stabilized by various ligands.

1.2 The reactions of divalent species of Group 14 elements (C-Ge)

As discussed above, the ground state of metallylenes is singlet and they are amphoteric in nature due to the filled *s* orbital and the vacant *p* orbital in their structure. They commonly undergo four categories of reactions: a) insertion into σ bonds, b) addition toward π bonds, c) oxidation, and d) complexation reactions.

1.2.1 Insertion of divalent species of Group 14 elements into σ bonds

The insertion of metallylenes into σ bonds (X–Y) such as hydrogen (H–H), ammonia (H_2N–H), and chlorosilanes (R_3Si–Cl) may proceed via two possible mechanisms, either the σ_{X-Y} bond or the lone pair electrons of X attack the empty *p* orbital of the metallylene (Figure 1.9).

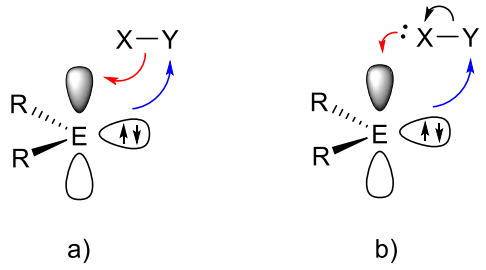

Figure 1.9 Orbital interactions involved in the insertion of metallylenes into X–Y bonds.

Although NHCs have been known for more than three decades, most of them are inert toward the σ_{H-N} bond of ammonia due to the insufficient π acceptor ability of the carbene carbon that arises because of two adjacent nitrogen donors.[8, 25] However, cyclic (alkyl)(amino) carbenes **3** can be used for the activation of ammonia (Scheme 1.5a).[24] Meanwhile, metallylenes also show reactivity toward the activation of ammonia.[46] Roesky *et al.* have utilized metallylenes featuring β-diketiminato ligands **13** in order to perform the activation of ammonia, which resulted in different products, **14** and **15** (Scheme 1.5b).[93-94]

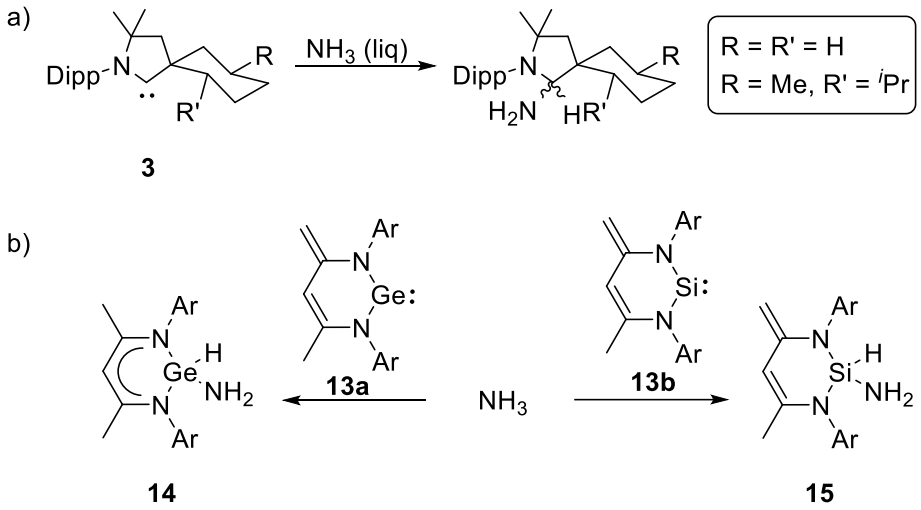

Scheme 1.5 Activation of ammonia by metallylenes **13**.

The reaction of metallylenes **16** with tetrachlorosilane and germanium tetrachloride was carried out by Kira and co-workers to obtain **17**. The reduction reactions of **17** with potassium graphite were carried out to obtain the heavier analogues of allenes **18**, which could be considered as silicon(0) and germanium(0) stabilized by two homometallylenes **16** (Scheme 1.6).[95-97]

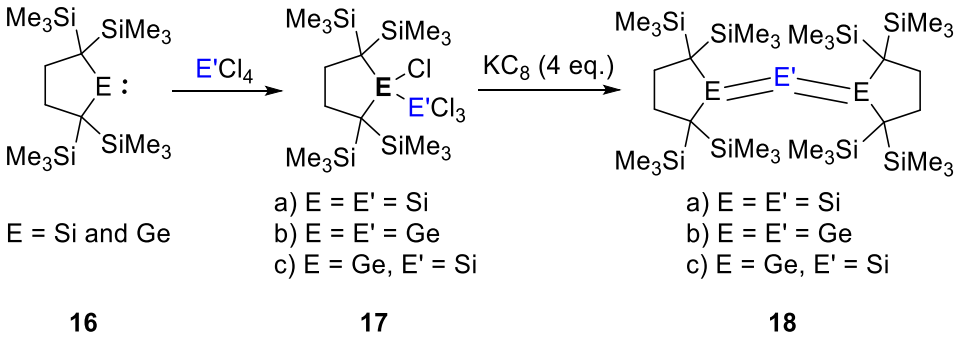

Scheme 1.6 Synthesis of **17** and the heavier elements allenes **18**.

The reactions of metallylenes with H–Si, Cl–C, and H–C bonds are quite common and have not been discussed in detail here (for more information, please see the cited references).[46, 68, 91-92, 98]

1.2.2 Addition of Group 14 divalent species to π bonds

The trapping reactions of transient metallylenes with unsaturated substrates such as alkenes, alkynes, and nitriles have also been reported. Similar reactions with the isolable metallylenes have been frequently employed for the synthesis of novel compounds containing heavier Group 14 elements and for the investigation of the reactivity of metallylenes. The mechanism of the addition reaction involves an interaction between the π-bond of the substrates with the empty *p* orbital of the divalent species in the initial step.

In carbene chemistry, only one stable carbene **19** is known to react with alkynes to form the bicyclic product **21** via a [2+1] cycloaddition. This reaction has been applied for the synthesis of cyclobutene species from both terminal and internal alkyl and aryl alkynes.[99] When NHC **2** was utilized in the reaction with acetylene, the C–H insertion product **20** was obtained (Scheme 1.7).[100]

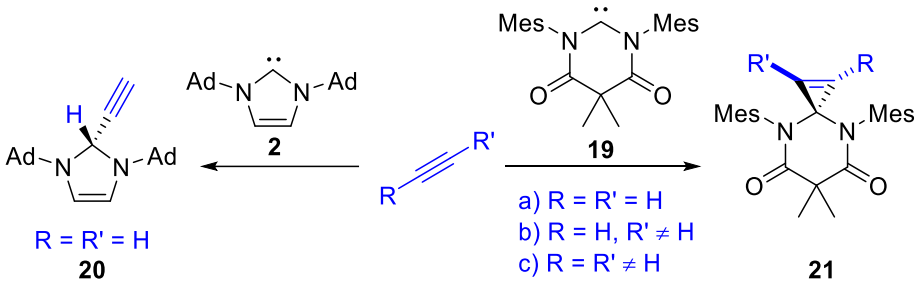

Scheme 1.7 Reactions of stable carbenes **2** and **19** with alkynes.

Interesting reactions of metallylenes **13** with alkynes have been reported by Driess and co-workers. With germylene **13a**, the [4+2] cycloaddition product **23b** was formed in addition to the C–H insertion product **23a** (Scheme 1.8a). When silylene **13b** was used as the substrate, two products were formed, the insertion product **22a** and the [1+2] cycloaddition product **22b**.[101-102] While the reaction of silylene **24** with diphenylacetylene was carried out, the corresponding [1+2] cycloaddition product **25** was obtained in 63% yield (Scheme 1.8b).[92]

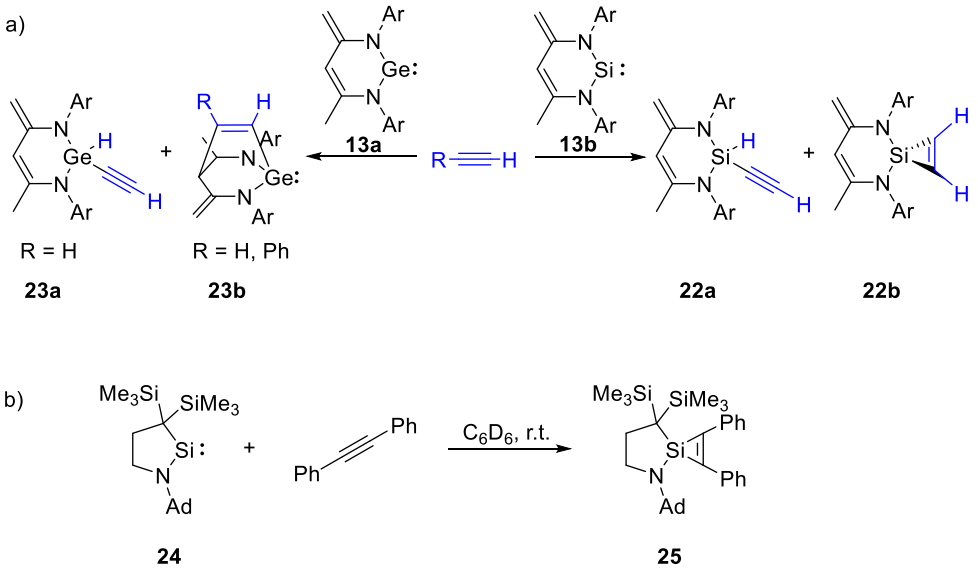

Scheme 1.8 Reactions of metallylenes **13** and silylene **24** with alkynes.

Carbon monoxide (CO) is the simplest oxocarbon and consists of one carbon atom and one oxygen atom that is connected by a triple bond. It can be activated by transient triplet carbenes to give the corresponding ketenes. Although it is spin-allowed, very few stable carbenes have access to the activation of the CO triple bond.[103-104] In 2006, Bertrand and co-workers reported the fixation of CO by CAAC **3** and **AAC** (Scheme 1.9a), which afforded the corresponding ketenes **26**.[23] The stable carbenes **AAC**[23], **DAC**,[105] and **ferrocenophane-NHC**[8] (Scheme 1.9b) have also been employed in the formation of ketenes via activation of CO.

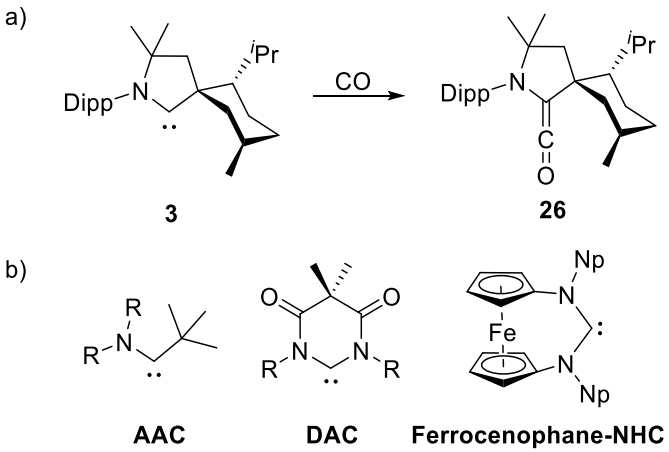

Scheme 1.9 a) Reactions of CAAC **3** with CO; b) Stable carbenes applied for the activation of CO.

Power *et al.* have reported that acyclic germylene **27** react with CO (Scheme 1.10).[106] The reaction of **27** with two equivalents of CO involved C–H insertion to afford germylenes **28** and **29**.

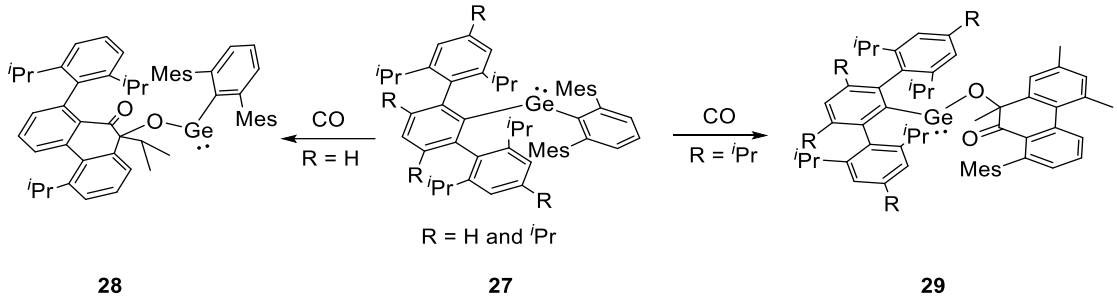

Scheme 1.10 Reactions of germylene **27** with CO.

Imines (R_2C=NR) are important functional groups that are routinely utilized in organic synthesis. Among the reported NHC-catalyzed reactions with imines,[107-109] only one addition reaction of NHCs **30** with imine has been described, in which intramolecular cyclization occurred to afford the cyclic product **31** (Scheme 1.11).[110]

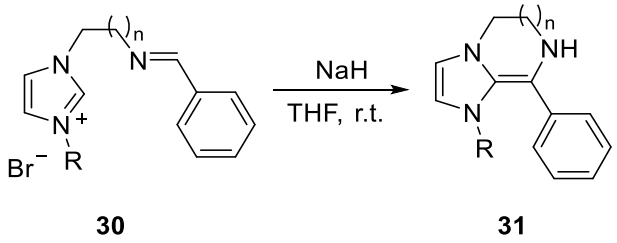

Scheme 1.11 Intramolecular cyclization of NHCs **30** involving an imine moiety.

Cycloaddition of metallylenes with imines has also been reported. Silylene **11** reacted with diimine to afford the corresponding [1+4] cycloaddition product **32** which was isolated by sublimation and fully characterized (Scheme 1.12a).[111] Cycloaddition of dialkylsilylene **33** with various aldimines was performed by Li *et al.* to obtain the two products **34** and **35** in high yields. With aldimines bearing strong withdrawing groups, silaazetidines **35** were obtained via a 1,2-trimethylsilyl migration (Scheme 1.12b).[112]

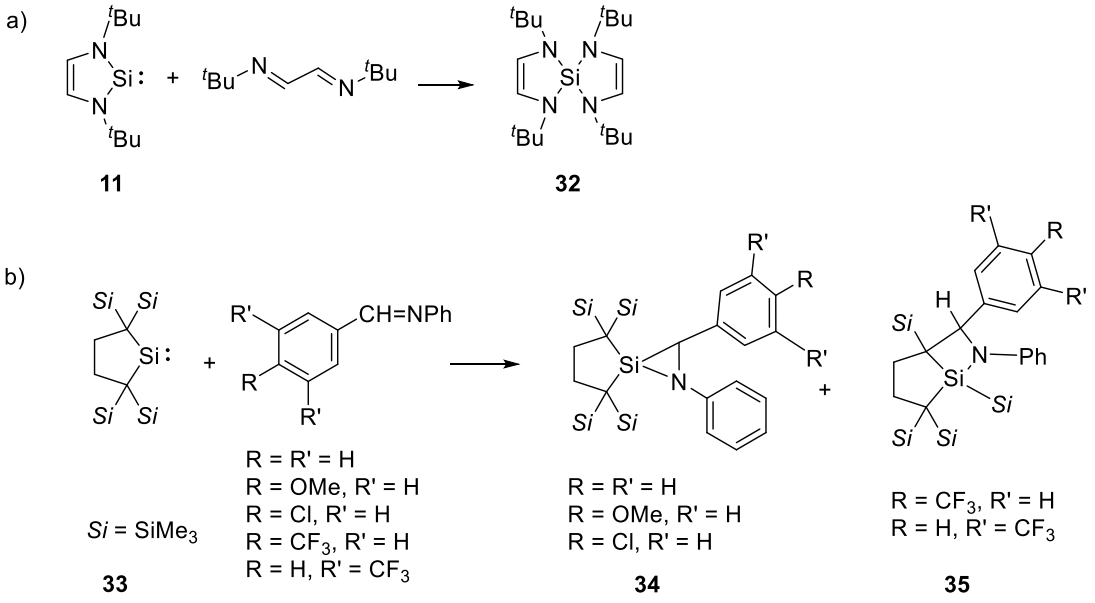

Scheme 1.12 Reactions of silylenes **11** and **33** with imines.

Li and co-workers further investigated the activation of aromatic nitriles by dialkylsilylene **33** which underwent [1+2+2] cycloadditions giving two products **36** and **37** (Scheme 1.13). It was found that when the nitrile substituted electron withdrawing groups were employed, symmetric 1,3-diaza-2-siloles **37** were formed.[113]

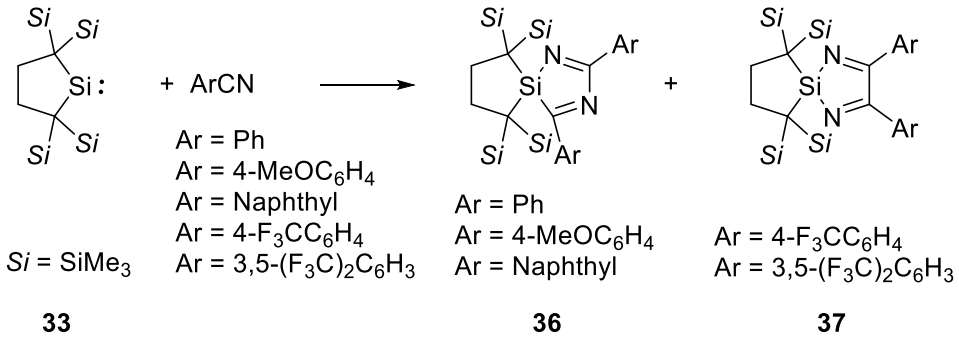

Scheme 1.13 Reactions of silylene **33** with various aromatic nitriles.

The activation of nitriles by stable germylenes has not been reported so far.[114] However, its carbon analogues **1** and **40** were applicable to the [1+2] cycloaddition of stable carbenes toward nitriles, which generated 2*H*-azirines **39** and **41**, respectively (Scheme 1.14).[99, 115]

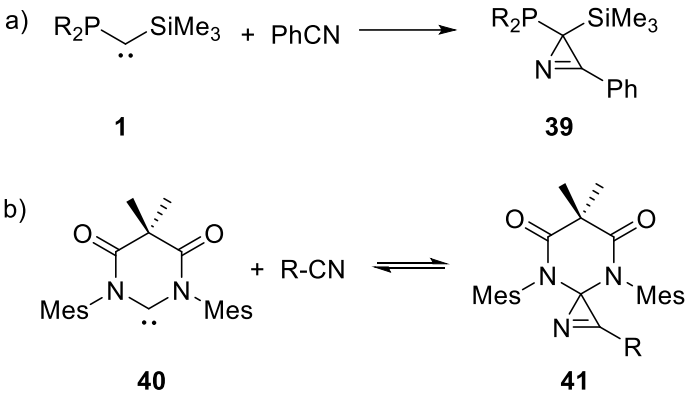

Scheme 1.14 The synthesis of 2*H*-azirines **39** and **41** via cycloaddition.

1.2.3 Oxidation reactions of divalent species of Group 14 elements

Carbenes are readily oxidized by chalcogens and this reaction is frequently employed to confirm the generation of transient carbenes.[29, 116-117] In 1995, Enders and co-workers reported the reaction of triazolylidene **42** with O_2, S_8, and selenium to generate corresponding urea derivatives **43** (Scheme 1.15). [29]

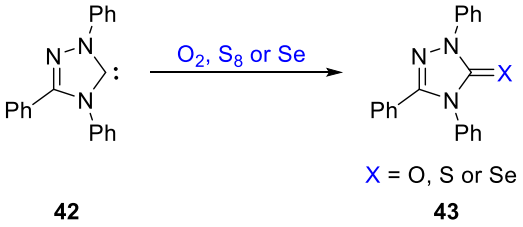

Scheme 1.15 Reactions of carbene **42** with chalcogens.

The oxidation reaction of stable metallylenes with chalcogens has been well documented. As almost all of the stable silylenes react with chalcogens, only a representative example is given in this introduction. The reaction of silylene **11** with chalcogens afforded the corresponding centrosymmetric spirocyclic dimers **44** (Scheme 1.16) via a proposed [Si=X] double bond intermediate.[111]

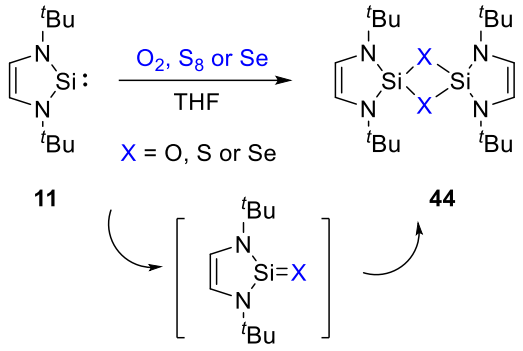

Scheme 1.16 Reactions of silylene **11** with chalcogens.

The activation of white phosphorus (P_4) by various carbenes[118-120] and silylenes[121-124] has also been extensively investigated. Bertrand *et al.* have reported the reaction of various carbenes with P_4 and it has been found that with cyclic carbenes **2** and **3**, the corresponding products **46** were generated.[119-120] In contrast, when an acyclic carbene **45** was utilized in this reaction, product **47** was obtained (Scheme 1.17).[118]

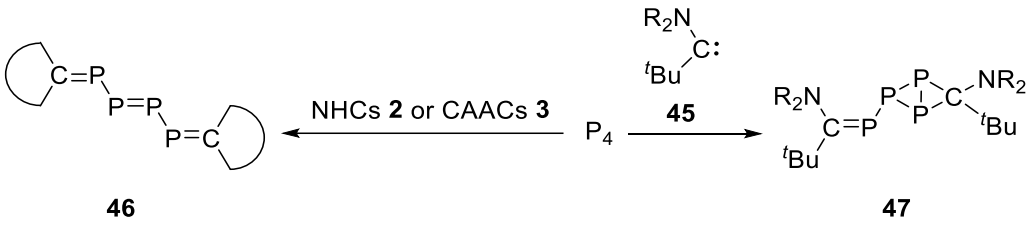

Scheme 1.17 Reactions of various carbenes with P_4.

Various P containing compounds were thus formed by the oxidation reaction of silylenes with P_4 (Figure 1.10). Product **48** was obtained by the reaction of silylene **13** with P_4, which further reacted with another equivalent of silylene **13** to afford **49**.[123] A few other examples have been reported by Roesky *et al.*[121, 124] Different products were obtained in the reaction of silylenes **50** with P_4 depending on the molar ratio. With **50a**:P_4 molar ratio = 6:1, the yellow product **51** was generated in 60% yield while in the reaction of silylene **52b** with P_4 (molar ratio **50b**:P_4 = 2:1), the purple-colored product **52** was obtained in 50% yield after work-up.

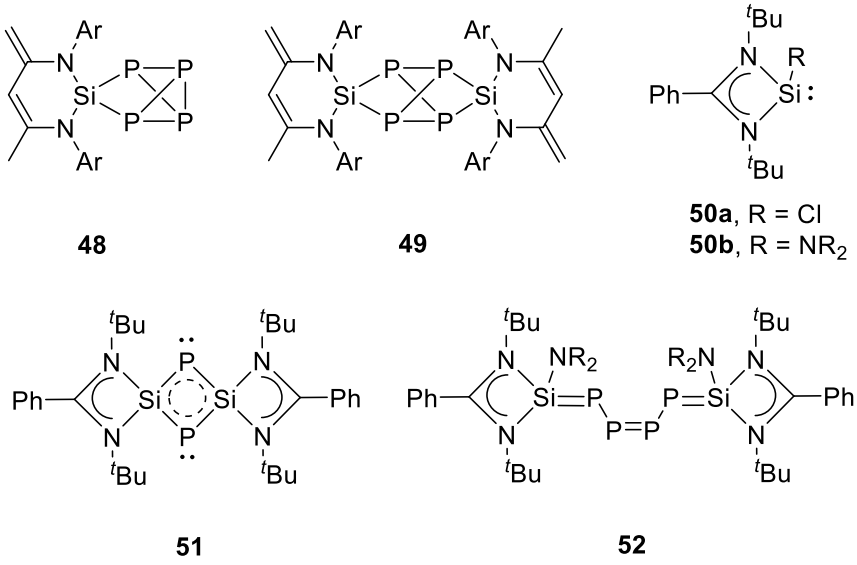

Figure 1.10 Products generated by oxidation of silylenes with P_4.

1.2.4 Coordination of metallylenes to transition metals

Metallylene transition metal complexes are organometallic compounds featuring metallylene ligands that are coordinated to the metal center. There are two types of bonding involved in their formation, namely, σ-donation of the lone pair of electrons from the ligand to the transition metal and the π-backdonation of the *d* electrons of the transition metal to the empty *p* orbital of the metallylene ligand (Figure 1.11).[125-126]

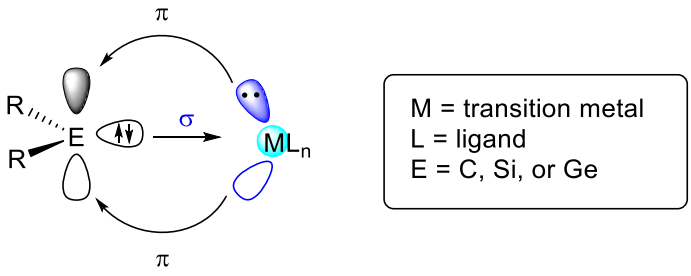

Figure 1.11 The bonding of a metallylene to a transition metal center.

The NHC-metal complexes **53** and **54** (Figure 1.12) were reported as early as 1968 by Wanzlick[127] and Öfele[128] respectively. Various transition metal NHC complexes have been

synthesized in the subsequent decades. NHCs are excellent ligands owing to their σ-donor and π-acceptor abilities in organometallic chemistry.[129-132]

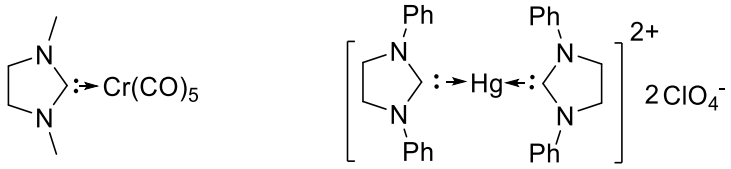

53 **54**

Figure 1.12 The first NHC metal complexes.

Among the different NHC transition metal complexes, zero-valent mononuclear metal complexes such as **53** have been reported independently by Bertrand *et al.* and Roesky *et al.*[133-138] This type of complexes are unique because the metal center stabilized by the two CAAC units is in its zero-oxidation state (Figure 1.12). Although the transition metal complexes **55** have similar C–M–C angles that are close to 180 °C, density functional theory (DFT) calculations suggest that they possess different electronic configurations. For Au, Cu, Ni, Mn, and Zn complexes, the electronic density is mainly delocalized within the CAAC units. In the case of iron and cobalt, most of the electronic density is localized o·n the metal center rather than the CAAC units.

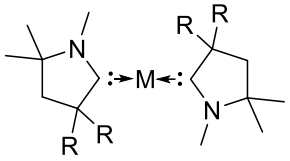

M = Au, Cu, Co, Fe, Ni, Mn, Zn

55

Figure 1.13 Isolated dicoordinated metal(0) complexes **55**.

Although NHCs and stable metallylenes have not been documented in the formation of metal (0) complexes, they are usually utilized to the insertion of M–X bonds. Recently, Cabeza *et al.* have reported that germylene **56** undergoes a ligand exchange reaction with chloro(tetrahydrothiophene) gold(I) (THTAuCl) to afford the germylene gold complex **57**. However, when germylene is reacted with either $AgBF_4$ or $CuBF_4$, the dicoordinated germylene M(I) complex **58** is obtained (Scheme 1.13).[139] Similar ligand exchange reactions have also been reported by Marschner *et al.*[140]

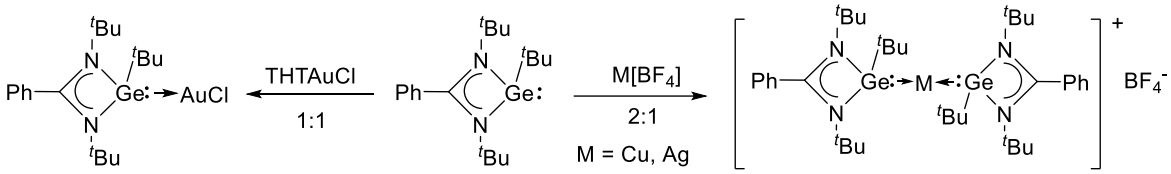

57 **56** **58**

Scheme 1.18 Synthesis of germylene metal complexes **57** and **58**.

1.3 Project Objectives

Based on the knowledge of the chemistry of Group 14 divalent species, it can be envisaged that the heavier analogues of cyclic (alkyl)(amino) carbenes (CAACs) may exhibit peculiar electronic characters, chemical and physical properties, and reactivities. This realization prompted us to develop hitherto unknown cyclic (alkyl)(amino) metallylenes.

This project focuses on the synthesis of cyclic (alkyl)(amino) metallylenes and an investigation of their reactivities. The behavior of these compounds as ligands in transition metal complexes has also been investigated. Furthermore, the performance of transition metal-metallylene complexes in catalytic hydroamination of alkynes with ammonia has been studied.

1.4 References

1. Hermann, M., *Justus Liebigs Annalen der Chemie* **1855,** *95*, 211-225.
2. Lennard-Jones, J.; Pople, J. A., *Discuss. Faraday Soc.* **1951,** *10*, 9-18.
3. Walsh, A. D., *J. Chem. Soc.,* **1953**, 2260-2266.
4. Arduengo, A. J.; Harlow, R. L.; Kline, M., *J. Am. Chem. Soc.* **1991,** *113*, 361-363.
5. Bourissou, D.; Guerret, O.; Gabbaï, F. P.; Bertrand, G., *Chem. Rev.* **2000,** *100*, 39-92.
6. Pauling, L., *J. Chem. Soc., Chem. Commun.* **1980**, 688-689.
7. Irikura, K. K.; Goddard, W. A.; Beauchamp, J. L., *J. Am. Chem. Soc.* **1992,** *114*, 48-51.
8. Siemeling, U.; Farber, C.; Bruhn, C.; Leibold, M.; Selent, D.; Baumann, W.; von Hopffgarten, M.; Goedecke, C.; Frenking, G., *Chem. Sci.* **2010,** *1*, 697-704.
9. Smith, M. B.; March, J., Carbocations, Carbanions, Free Radicals, Carbenes, and Nitrenes. In *March's Advanced Organic Chemistry*, John Wiley & Sons, Inc.: 2006; pp 234-295.
10. Andrews, L., *J. Chem. Phys.* **1968,** *48*, 979-982.
11. Igau, A.; Grutzmacher, H.; Baceiredo, A.; Bertrand, G., *J. Am. Chem. Soc.* **1988,** *110*, 6463-6466.
12. Baceiredo, A.; Bertrand, G.; Sicard, G., *J. Am. Chem. Soc.* **1985,** *107*, 4781-4783.
13. Lavallo, V.; Canac, Y.; Donnadieu, B.; Schoeller, W. W.; Bertrand, G., *Science* **2006,** *312*, 722-724.
14. Dixon, D. A.; Dobbs, K. D.; Arduengo, A. J.; Bertrand, G., *J. Am. Chem. Soc.* **1991,** *113*, 8782-8785.
15. Buron, C.; Gornitzka, H.; Romanenko, V.; Bertrand, G., *Science* **2000,** *288*, 834-836.
16. Aldeco-Perez, E.; Rosenthal, A. J.; Donnadieu, B.; Parameswaran, P.; Frenking, G.; Bertrand, G., *Science* **2009,** *326*, 556-559.
17. Vignolle, J.; Cattoën, X.; Bourissou, D., *Chem. Rev.* **2009,** *109*, 3333-3384.
18. Lavallo, V.; Mafhouz, J.; Canac, Y.; Donnadieu, B.; Schoeller, W. W.; Bertrand, G., *J. Am. Chem. Soc.* **2004,** *126*, 8670-8671.

19. Mieusset, J.-L.; Brinker, U. H., *J. Org. Chem.* **2008,** *73*, 1553-1558.

20. Pérez, P., *J. Phys. Chem. A* **2003,** *107*, 522-525.

21. Sander, W.; Kötting, C.; Hübert, R., *J. Phys. Org. Chem.* **2000,** *13*, 561-568.

22. Lavallo, V.; Canac, Y.; Präsang, C.; Donnadieu, B.; Bertrand, G., *Angew. Chem. Int. Ed.* **2005,** *44*, 5705-5709.

23. Lavallo, V.; Canac, Y.; Donnadieu, B.; Schoeller, W. W.; Bertrand, G., *Angew. Chem. Int. Ed.* **2006,** *45*, 3488-3491.

24. Frey, G. D.; Lavallo, V.; Donnadieu, B.; Schoeller, W. W.; Bertrand, G., *Science* **2007,** *316*, 439-441.

25. Hudnall, T. W.; Moerdyk, J. P.; Bielawski, C. W., *Chem. Commun.* **2010,** *46*, 4288-4290.

26. Kuchenbeiser, G.; Soleilhavoup, M.; Donnadieu, B.; Bertrand, G., *Chem. Asian J.* **2009,** *4*, 1745-1750.

27. Melaimi, M.; Soleilhavoup, M.; Bertrand, G., *Angew. Chem. Int. Ed.* **2010,** *49*, 8810-8849.

28. Schuster, O.; Yang, L.; Raubenheimer, H. G.; Albrecht, M., *Chem. Rev.* **2009,** *109*, 3445-3478.

29. Enders, D.; Breuer, K.; Raabe, G.; Runsink, J.; Teles, J. H.; Melder, J.-P.; Ebel, K.; Brode, S., *Angew. Chem. Int. Ed. Engl.* **1995,** *34*, 1021-1023.

30. Martin, D.; Baceiredo, A.; Gornitzka, H.; Schoeller, W. W.; Bertrand, G., *Angew. Chem. Int. Ed.* **2005,** *44*, 1700-1703.

31. Glorius, F., *N-Heterocyclic Carbenes in Transition Metal Catalysis. [electronic resource]*. Berlin, Heidelberg : Springer Berlin Heidelberg : Imprint: Springer, 2007.: 2007.

32. Nolan, S. P., *N-Heterocyclic carbenes in synthesis*. Weinheim : Wiley-VCH ; Chichester : John Wiley [distributor], c2006.: 2006.

33. Cazin, C. S. J., *N-Heterocyclic Carbenes in Transition Metal Catalysis and Organocatalysis. [electronic resource]*. Dordrecht : Springer Science+Business Media B.V., 2011.: 2011.

34. Wang, Y.; Xie, Y.; Wei, P.; King, R. B.; Schaefer, H. F.; von R. Schleyer, P.; Robinson, G. H., *Science* **2008,** *321*, 1069-1071.

35. Wang, Y.; Xie, Y.; Wei, P.; King, R. B.; Schaefer, I. I. I. H. F.; Schleyer, P. v. R.; Robinson, G. H., *J. Am. Chem. Soc.* **2008,** *130*, 14970-14971.

36. Wang, Y.; Quillian, B.; Wei, P.; Xie, Y.; Wannere, C. S.; King, R. B.; Schaefer, H. F.; Schleyer, P. v. R.; Robinson, G. H., *J. Am. Chem. Soc.* **2008,** *130*, 3298-3299.

37. Wang, Y.; Quillian, B.; Wei, P.; Wannere, C. S.; Xie, Y.; King, R. B.; Schaefer, H. F.; Schleyer, P. v. R.; Robinson, G. H., *J. Am. Chem. Soc.* **2007,** *129*, 12412-12413.

38. Sidiropoulos, A.; Jones, C.; Stasch, A.; Klein, S.; Frenking, G., *Angew. Chem. Int. Ed.* **2009,** *48*, 9701-9704.

39. Braunschweig, H.; Dewhurst, R. D.; Hammond, K.; Mies, J.; Radacki, K.; Vargas, A., *Science* **2012,** *336*, 1420-1422.

40. Filippou, A. C.; Chernov, O.; Schnakenburg, G., *Angew. Chem. Int. Ed.* **2009,** *48*, 5687-5690.

41. Ghadwal, R. S.; Roesky, H. W.; Merkel, S.; Henn, J.; Stalke, D., *Angew. Chem. Int. Ed.* **2009,** *48*, 5683-5686.

42. Bissinger, P.; Braunschweig, H.; Kraft, K.; Kupfer, T., *Angew. Chem. Int. Ed.* **2011,** *50*, 4704-4707.

43. Filippou, A. C.; Lebedev, Y. N.; Chernov, O.; Straßmann, M.; Schnakenburg, G., *Angew. Chem. Int. Ed.* **2013,** *52*, 6974-6978.

44. Kong, L.; Li, Y.; Ganguly, R.; Vidovic, D.; Kinjo, R., *Angew. Chem. Int. Ed.* **2014,** *53*, 9280-9283.

45. Xiong, Y.; Yao, S.; Inoue, S.; Epping, J. D.; Driess, M., *Angew. Chem. Int. Ed.* **2013,** *52*, 7147-7150.

46. Mizuhata, Y.; Sasamori, T.; Tokitoh, N., *Chem. Rev.* **2009,** *109*, 3479-3511.

47. Karatsu, T.; Miller, R. D.; Sooriyakumaran, R.; Michl, J., *J. Am. Chem. Soc.* **1989,** *111*, 1140-1141.

48. Lee, V. Y.; Sekiguchi, A., Heavy Analogs of Carbenes: Silylenes, Germylenes, Stannylenes and Plumbylenes. In *Organometallic Compounds of Low-Coordinate Si, Ge, Sn and Pb*, John Wiley & Sons, Ltd: 2010; pp 139-197.

49. Berkowitz, J.; Greene, J. P.; Cho, H.; Ruščić, B., *J. Chem. Phys.* **1987,** *86*, 1235-1248.

50. Balasubramanian, K.; McLean, A. D., *J. Chem. Phys.* **1986,** *85*, 5117-5119.

51. Balasubramanian, K., *J. Chem. Phys.* **1988,** *89*, 5731-5738.

52. Trinquier, G., *J. Am. Chem. Soc.* **1990,** *112*, 2130-2137.

53. Apeloig, Y.; Pauncz, R.; Karni, M.; West, R.; Steiner, W.; Chapman, D.,

Organometallics **2003,** *22*, 3250-3256.

54. Driess, M.; Grützmacher, H., *Angew. Chem. Int. Ed. Engl.* **1996,** *35*, 828-856.

55. Skell, P. S.; Goldstein, E. J., *J. Am. Chem. Soc.* **1964,** *86*, 1442-1443.

56. Koecher, J.; Lehnig, M.; Neumann, W. P., *Organometallics* **1988,** *7*, 1201-1207.

57. Kolesnikov, S. P.; Egorov, M. P.; Galminas, A. M.; Ezhova, M. B.; Nefedov, O. M.; Leshina, T. V.; Taraban, M. B.; Kruppa, A. I.; Maryasova, V. I., *J. Organomet. Chem.* **1990,** *391*, c1-c6.

58. Shusterman, A. J.; Landrum, B. E.; Miller, R. L., *Organometallics* **1989,** *8*, 1851-1855.

59. Wataru, A.; Takeshi, T.; Akira, S., *Chem. Lett.* **1987,** *16*, 317-318.

60. Ando, W.; Itoh, H.; Tsumuraya, T., *Organometallics* **1989,** *8*, 2759-2766.

61. Apeloig, Y.; Karni, M., *J. Chem. Soc., Chem. Commun.* **1985**, 1048-1049.

62. Gillette, G. R.; Noren, G. H.; West, R., *Organometallics* **1987,** *6*, 2617-2618.

63. Apeloig, Y.; Karni, M.; West, R.; Welsh, K., *J. Am. Chem. Soc.* **1994,** *116*, 9719-9729.

64. Harris, D. H.; Lappert, M. F., *J. Chem. Soc., Chem. Commun.* **1974**, 895-896.

65. Davidson, P. J.; Harris, D. H.; Lappert, M. F., *J. Chem. Soc., Dalton Trans.* **1976**, 2268-2274.

66. Rekken, B. D.; Brown, T. M.; Fettinger, J. C.; Tuononen, H. M.; Power, P. P., *J. Am. Chem. Soc.* **2012,** *134*, 6504-6507.

67. Protchenko, A. V.; Birjkumar, K. H.; Dange, D.; Schwarz, A. D.; Vidovic, D.; Jones, C.; Kaltsoyannis, N.; Mountford, P.; Aldridge, S., *J. Am. Chem. Soc.* **2012,** *134*, 6500-6503.

68. Driess, M., *Nat. Chem.* **2012,** *4*, 525-526.

69. Pu, L.; Phillips, A. D.; Richards, A. F.; Stender, M.; Simons, R. S.; Olmstead, M. M.; Power, P. P., *J. Am. Chem. Soc.* **2003,** *125*, 11626-11636.

70. Stender, M.; Phillips, A. D.; Wright, R. J.; Power, P. P., *Angew. Chem. Int. Ed.* **2002,** *41*, 1785-1787.

71. Phillips, A. D.; Wright, R. J.; Olmstead, M. M.; Power, P. P., *J. Am. Chem. Soc.* **2002,** *124*, 5930-5931.

72. Fink, M. J.; Michalczyk, M. J.; Haller, K. J.; Michl, J.; West, R., *Organometallics* **1984,** *3*, 793-800.

73. Michalczyk, M. J.; West, R.; Michl, J., *J. Am. Chem. Soc.* **1984,** *106*, 821-822.

74. Sekiguchi, A.; Kinjo, R.; Ichinohe, M., *Science* **2004,** *305*, 1755-1757.

75. Rit, A.; Campos, J.; Niu, H.; Aldridge, S., *Nat. Chem.* **2016,** *8*, 1022-1026.

76. WEST, R.; FINK, M. J.; MICHL, J., *Science* **1981,** *214*, 1343-1344.

77. Kobayashi, H.; Iwamoto, T.; Kira, M., *J. Am. Chem. Soc.* **2005,** *127*, 15376-15377.

78. Mondal, K. C.; Samuel, P. P.; Roesky, H. W.; Aysin, R. R.; Leites, L. A.; Neudeck, S.; Lübben, J.; Dittrich, B.; Holzmann, N.; Hermann, M.; Frenking, G., *J. Am. Chem. Soc.* **2014,** *136*, 8919-8922.

79. Hall, M. B., *J. Am. Chem. Soc.* **1978,** *100*, 6333-6338.

80. Denk, M.; Lennon, R.; Hayashi, R.; West, R.; Belyakov, A. V.; Verne, H. P.; Haaland, A.; Wagner, M.; Metzler, N., *J. Am. Chem. Soc.* **1994,** *116*, 2691-2692.

81. Herrmann, W. A.; Denk, M.; Behm, J.; Scherer, W.; Klingan, F.-R.; Bock, H.; Solouki, B.; Wagner, M., *Angew. Chem. Int. Ed. Engl.* **1992,** *31*, 1485-1488.

82. Meller, A.; Pfeiffer, J.; Noltemeyer, M., *Z. Anorg. Allg. Chem.* **1989,** *572*, 145-150.

83. Gehrhus, B.; Lappert, M. F.; Heinicke, J.; Boese, R.; Blaser, D., *J. Chem. Soc., Chem. Commun.* **1995**, 1931-1932.

84. Heinicke, J.; Oprea, A.; Kindermann, M. K.; Karpati, T.; Nyulászi, L.; Veszprémi, T., *Chem. Eur. J.* **1998,** *4*, 541-545.

85. Kira, M.; Ishida, S.; Iwamoto, T.; Kabuto, C., *J. Am. Chem. Soc.* **1999,** *121*, 9722-9723.

86. Mitsuo, K.; Shintaro, I.; Takeaki, I.; Masaaki, I.; Chizuko, K.; Lubov, I.; Hideki, S., *Chem. Lett.* **1999,** *28*, 263-264.

87. So, C.-W.; Roesky, H. W.; Magull, J.; Oswald, R. B., *Angew. Chem. Int. Ed.* **2006,** *45*, 3948-3950.

88. Jones, C.; Rose, R. P.; Stasch, A., *Dalton Trans.* **2008**, 2871-2878.

89. Driess, M.; Yao, S.; Brym, M.; van Wüllen, C.; Lentz, D., *J. Am. Chem. Soc.* **2006,** *128*, 9628-9629.

90. Driess, M.; Yao, S.; Brym, M.; van Wüllen, C., *Angew. Chem. Int. Ed.* **2006,** *45*, 4349-4352.

91. Asay, M.; Jones, C.; Driess, M., *Chem. Rev.* **2011,** *111*, 354-396.

92. Kosai, T.; Ishida, S.; Iwamoto, T., *Angew. Chem. Int. Ed.* **2016,** *55*, 15554-15558.

93. Jana, A.; Schulzke, C.; Roesky, H. W., *J. Am. Chem. Soc.* **2009,** *131*, 4600-4601.

94. Jana, A.; Objartel, I.; Roesky, H. W.; Stalke, D., *Inorg. Chem.* **2009,** *48*, 798-800.

95. Ishida, S.; Iwamoto, T.; Kabuto, C.; Kira, M., *Nature* **2003,** *421*, 725-727.

96. Iwamoto, T.; Abe, T.; Kabuto, C.; Kira, M., *Chem. Commun.* **2005**, 5190-5192.

97. Iwamoto, T.; Masuda, H.; Kabuto, C.; Kira, M., *Organometallics* **2005,** *24*, 197-199.

98. Kira, M.; Ishida, S.; Iwamoto, T., *The Chemical Record* **2004,** *4*, 243-253.

99. Moerdyk, J. P.; Bielawski, C. W., *J. Am. Chem. Soc.* **2012,** *134*, 6116-6119.

100. Arduengo Iii, A. J.; Calabrese, J. C.; Davidson, F.; Rasika Dias, H. V.; Goerlich, J. R.; Krafczyk, R.; Marshall, W. J.; Tamm, M.; Schmutzler, R., *Helv. Chim. Acta* **1999,** *82*, 2348-2364.

101. Yao, S.; van Wüllen, C.; Sun, X.-Y.; Driess, M., *Angew. Chem. Int. Ed.* **2008,** *47*, 3250-3253.

102. Yao, S.; van Wullen, C.; Driess, M., *Chem. Commun.* **2008**, 5393-5395.

103. Sander, W.; Hübert, R.; Kraka, E.; Gräfenstein, J.; Cremer, D., *Chem. Eur. J.* **2000,** *6*, 4567-4579.

104. Visser, P.; Zuhse, R.; Wong, M. W.; Wentrup, C., *J. Am. Chem. Soc.* **1996,** *118*, 12598-12602.

105. Hudnall, T. W.; Bielawski, C. W., *J. Am. Chem. Soc.* **2009,** *131*, 16039-16041.

106. Wang, X.; Zhu, Z.; Peng, Y.; Lei, H.; Fettinger, J. C.; Power, P. P., *J. Am. Chem. Soc.* **2009,** *131*, 6912-6913.

107. He, L.; Jian, T.-Y.; Ye, S., *J. Org. Chem.* **2007,** *72*, 7466-7468.

108. He, M.; Bode, J. W., *J. Am. Chem. Soc.* **2008,** *130*, 418-419.

109. Li, G.-Q.; Dai, L.-X.; You, S.-L., *Chem. Commun.* **2007**, 852-854.

110. Simonovic, S.; Frison, J.-C.; Koyuncu, H.; Whitwood, A. C.; Douthwaite, R. E., *Org. Lett.* **2009,** *11*, 245-247.

111. Haaf, M.; Schmiedl, A.; Schmedake, T. A.; Powell, D. R.; Millevolte, A. J.; Denk,

M.; West, R., *J. Am. Chem. Soc.* **1998,** *120*, 12714-12719.

112. Chen, W.; Wang, L.; Li, Z.; Lin, A.; Lai, G.; Xiao, X.; Deng, Y.; Kira, M., *Dalton Trans.* **2013,** *42*, 1872-1878.

113. Wang, L.; Chen, W.; Li, Z.; Xiao, X.-Q.; Lai, G.; Liu, X.; Xu, Z.; Kira, M., *Chem. Commun.* **2013,** *49*, 9776-9778.

114. Miller, K. A.; Watson, T. W.; Bender; Banaszak Holl, M. M.; Kampf, J. W., *J. Am. Chem. Soc.* **2001,** *123*, 982-983.

115. Alcaraz, G.; Wecker, U.; Baceiredo, A.; Dahan, F.; Bertrand, G., *Angew. Chem. Int. Ed. Engl.* **1995,** *34*, 1246-1248.

116. Wanzlick, H. W., *Angew. Chem.* **1962,** *74*, 129-134.

117. Enders, D.; Breuer, K.; Runsink, J.; Henrique Teles, J., *Liebigs Ann.* **1996,** *1996*, 2019-2028.

118. Back, O.; Kuchenbeiser, G.; Donnadieu, B.; Bertrand, G., *Angew. Chem. Int. Ed.* **2009,** *48*, 5530-5533.

119. Masuda, J. D.; Schoeller, W. W.; Donnadieu, B.; Bertrand, G., *Angew. Chem. Int. Ed.* **2007,** *46*, 7052-7055.

120. Masuda, J. D.; Schoeller, W. W.; Donnadieu, B.; Bertrand, G., *J. Am. Chem. Soc.* **2007,** *129*, 14180-14181.

121. Khan, S.; Michel, R.; Sen, S. S.; Roesky, H. W.; Stalke, D., *Angew. Chem. Int. Ed.* **2011,** *50*, 11786-11789.

122. Driess, M.; Fanta, A. D.; Powell, D. R.; West, R., *Angew. Chem. Int. Ed. Engl.* **1989,** *28*, 1038-1040.

123. Xiong, Y.; Yao, S.; Brym, M.; Driess, M., *Angew. Chem. Int. Ed.* **2007,** *46*, 4511-4513.

124. Sen, S. S.; Khan, S.; Roesky, H. W.; Kratzert, D.; Meindl, K.; Henn, J.; Stalke, D.; Demers, J.-P.; Lange, A., *Angew. Chem. Int. Ed.* **2011,** *50*, 2322-2325.

125. Hahn, F. E.; Jahnke, M. C., *Angew. Chem. Int. Ed.* **2008,** *47*, 3122-3172.

126. Fillman, K. L.; Przyojski, J. A.; Al-Afyouni, M. H.; Tonzetich, Z. J.; Neidig, M. L., *Chem. Sci.* **2015,** *6*, 1178-1188.

127. Wanzlick, H. W.; Schönherr, H. J., *Angew. Chem. Int. Ed. Engl.* **1968,** *7*, 141-142.

128. Öfele, K., *J. Organomet. Chem.* **1968,** *12*, P42-P43.

129. Rovis, T.; Nolan, S. P., *Synlett* **2013,** *24*, 1188-1189.

130. Arduengo, A. J.; Bertrand, G., *Chem. Rev.* **2009,** *109*, 3209-3210.

131. Bugaut, X.; Glorius, F., *Chem. Soc. Rev.* **2012,** *41*, 3511-3522.

132. Soleilhavoup, M.; Bertrand, G., *Acc. Chem. Res.* **2015,** *48*, 256-266.

133. Weinberger, D. S.; Melaimi, M.; Moore, C. E.; Rheingold, A. L.; Frenking, G.; Jerabek, P.; Bertrand, G., *Angew. Chem. Int. Ed.* **2013,** *52*, 8964-8967.

134. Weinberger, D. S.; Amin Sk, N.; Mondal, K. C.; Melaimi, M.; Bertrand, G.; Stückl, A. C.; Roesky, H. W.; Dittrich, B.; Demeshko, S.; Schwederski, B.; Kaim, W.; Jerabek, P.; Frenking, G., *J. Am. Chem. Soc.* **2014,** *136*, 6235-6238.

135. Ung, G.; Rittle, J.; Soleilhavoup, M.; Bertrand, G.; Peters, J. C., *Angew. Chem. Int. Ed.* **2014,** *53*, 8427-8431.

136. Mondal, K. C.; Samuel, P. P.; Li, Y.; Roesky, H. W.; Roy, S.; Ackermann, L.; Sidhu, N. S.; Sheldrick, G. M.; Carl, E.; Demeshko, S.; De, S.; Parameswaran, P.; Ungur, L.; Chibotaru, L. F.; Andrada, D. M., *Eur. J. Inorg. Chem.* **2014,** *2014*, 818-823.

137. Samuel, P. P.; Mondal, K. C.; Roesky, H. W.; Hermann, M.; Frenking, G.; Demeshko, S.; Meyer, F.; Stückl, A. C.; Christian, J. H.; Dalal, N. S.; Ungur, L.; Chibotaru, L. F.; Pröpper, K.; Meents, A.; Dittrich, B., *Angew. Chem. Int. Ed.* **2013,** *52*, 11817-11821.

138. Singh, A. P.; Samuel, P. P.; Roesky, H. W.; Schwarzer, M. C.; Frenking, G.; Sidhu, N. S.; Dittrich, B., *J. Am. Chem. Soc.* **2013,** *135*, 7324-7329.

139. Álvarez-Rodríguez, L.; Cabeza, J. A.; García-Álvarez, P.; Polo, D., *Organometallics* **2015,** *34*, 5479-5484.

140. Hlina, J.; Arp, H.; Walewska, M.; Flörke, U.; Zangger, K.; Marschner, C.; Baumgartner, J., *Organometallics* **2014,** *33*, 7069-7077.

Chapter 2 Synthesis & Characterization of a Cyclic (Alkyl)(amino) germylene

2.1 Introduction

Germylene is the germanium analogue of carbene (R_2Ge:), and is favored in the singlet ground state rather than triplet ground state (Figure 2.1).[1-2] In contrast to carbene, germylene prefers the $4s^24p^2$ valence electron configuration in the germanium centre, which possesses a vacant *p*-orbital and a lone pair of valence orbital.[3-5] Based on the theoretical calculation, the singlet-triplet separation (ΔE_{ST}) of germylene (23 kcal mol^{-1}) is higher than that of carbene (–9 kcal mol^{-1}),[6] which indicates that the singlet state germylene is more stable than its triplet state.

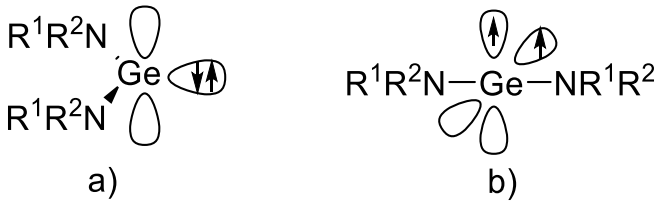

Figure 2.1 Proposed structure for germylene **I**: a) singlet ground state, b) triplet ground state.

To date, a lot of isolable germylenes have been synthesized by stabilization effects of bulky substituents and/or coordinating ligands.[4] Germylenes usually exhibit the electrophilic character in contrast to the nucleophilicity of carbenes.[4, 7] The seminal work was reported in 1974 by Harris and Lappert, presenting that the reaction of $GeCl_2$•dioxane with lithium amide ($Li(NR^1R^2)$) in ether afforded germylene **I** (Figure 2.2).[8]

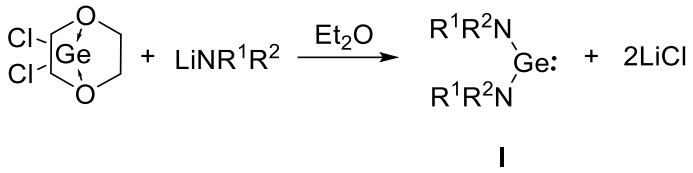

Figure 2.2 Synthesis of germylene **I**.

Since then, a plethora of studies on the synthesis and reactivity of isolable germylenes were reported.[4, 9] Germylenes can be summed up in two types: a) ionic germylenes **II**–**IV**[10-14] (Figure 2.3); b) neutral germylenes **V-XII** [15-35] (Figure 2.4).

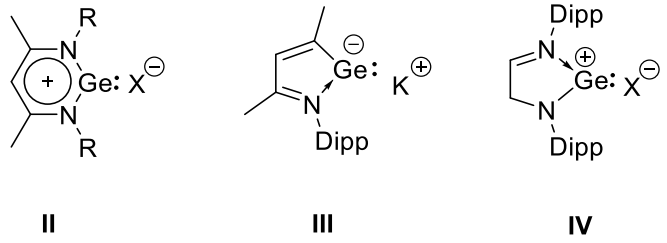

Figure 2.3 Selected ionic germylenes **II**, **III**, and **IV**.

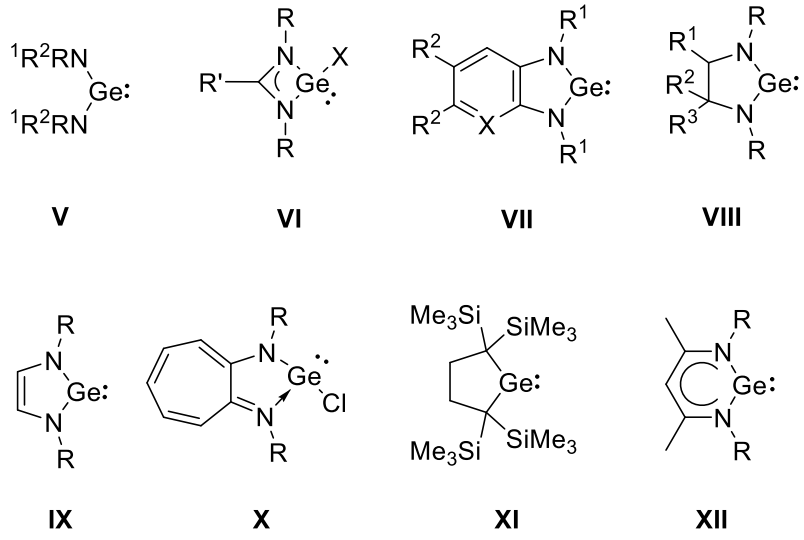

Figure 2.4 Selected neutral germylenes **V**-**XII**.

These germylenes **I-XII** can be isolated and stored under an inert atmosphere, and their

thermal stability depends on the steric and electronic effects from the adjacent substituents of germanium centre. Germylene **II** was first reported by Roesky *et al.* in 2001, and it was prepared from β-diketiminatolithium salt **II'** with germanium dichloride in ether.[29-30] Subsequently, Driess and co-workers reported the reduction of **II** with two equivalents of potassium to afford germylene **III** in 33% yield.[14] (Figure 2.5)

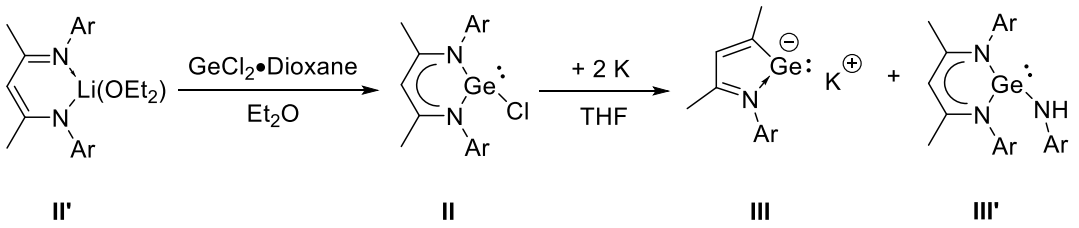

Figure 2.5 Syntheses of ionic germylene **II** and **III**.

Unlike other neutral five-membered germylenes, cationic germylenes **IVa-b** were synthesized in an astounding route reported by Müller and co-workers in 2009. They employed the protonation of germylene **IX** with $HB(C_6F_5)_4$ in diethyl ether or $Et_3SiB(C_6F_5)_4$ in benzene to generate corresponding cationic germylenes **IVa-b** (Figure 2.6).[11]

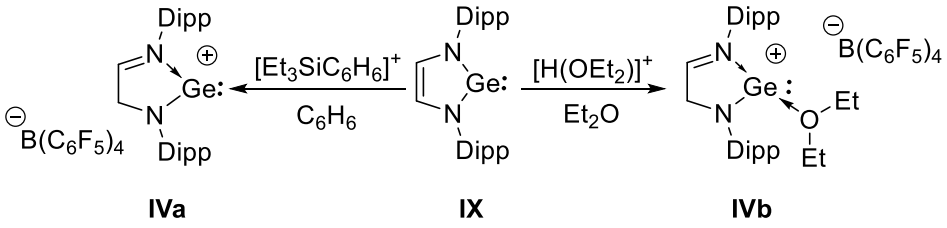

Figure 2.6 Protonation of germylene **IX** with $[H(OEt_2)_2]•[B(C_6F_5)_4]$ in ether or $[Et_3Si(C_6H_6)]•[B(C_6F_5)_4]$ in benzene.

Acyclic germylene **Va** reacted with diisopropylcarbodiimide via an addition reaction to afford a base-coordinated germylene **VIa** (Figure 2.7).[16] This is the only example of a synthetic route to access a tricoordinate germylene **VIa** from another acyclic germylene **Va**.

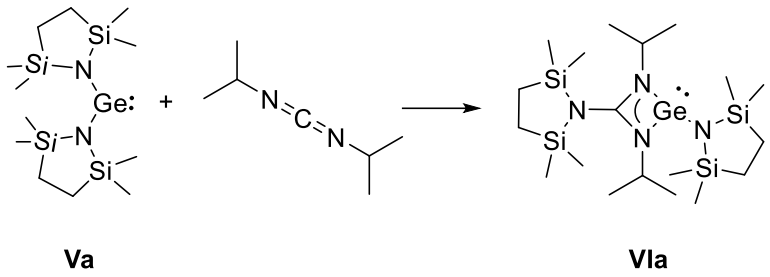

Va **VIa**

Figure 2.7 Formation of germylene **VIa** by the reaction of germylene **Va** with diisopropylcarbodiimide.

The five-membered *N*-heterocyclic germylene **VII** was first reported by Meller in 1989. Benzene-1,2-diamine was reacted with ^{n}BuLi to afford amidinate lithium salt, after which $GeCl_2$•dioxane was added to the mixture to afford **VII** (Figure 2.8).[20-21] It should be noted that both acyclic germylene **V** and cyclic six-membered germylene **XII** were obtained by the reaction of amidinate lithium salt with $GeCl_2$.[12-13, 29-37]

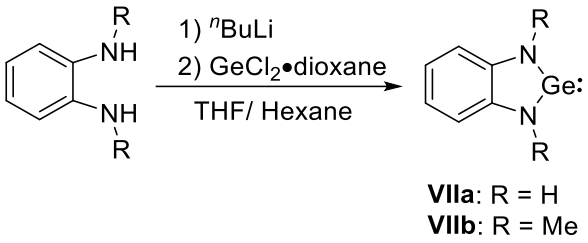

VIIa: R = H
VIIb: R = Me

Figure 2.8 Syntheses of germylene **VII**.

Compound **XI"** can be obtained by the reaction of 1,1,4,4-tetrakis(trimethylsilyl)-butane-1,4-diyl lithium salt **XI'** with $GeCl_4$. The reduction of dichlorogermane **XI"** with KC_8 afforded the first stable dialkylgermylene **XI** (Figure 2.9a).[28] In comparison with **XI**, both saturated *N*-heterocyclic germylene **VIII** and unsaturated *N*-heterocyclic germylene **IX** were synthesized by the reduction of dichlorogermane precursors (Figure 2.9b).[24, 26]

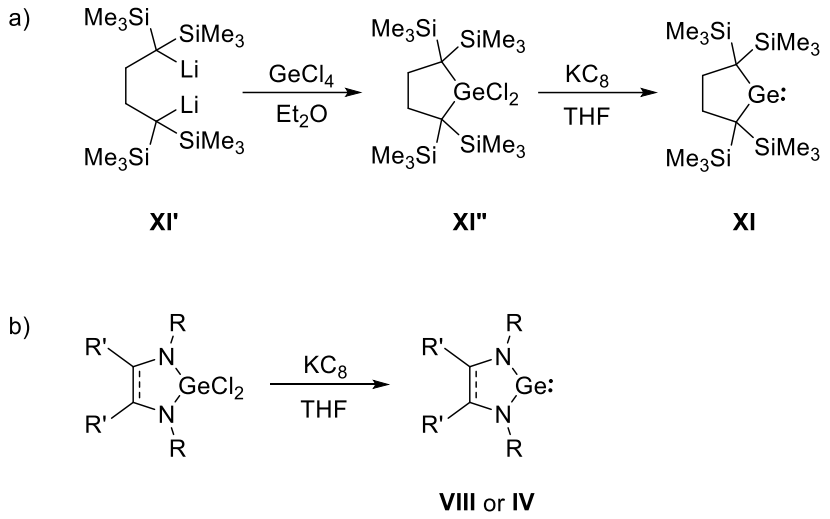

Figure 2.9 a) Syntheses of dialkylgermylene **XI**; b) the reductions of dichlorogermane precursors with KC_8.

In contrast to **XI**, *N*-heterocyclic germylenes are sterically protected by bulky groups and electronically stabilized by both π-donation and σ-withdrawing from the adjacent nitrogen atom.[38] Nevertheless, Germylene **XI** is sterically protected by bulky Me_3Si-groups without the electronic protections from them. In other words, germylene **XI** is the least electronically perturbed among all known isolable germylenes.

Most studies of germylenes have been focused on *N*-heterocyclic germylenes (NHGes). Indeed, the investigation of NHGes predated those of its counterpart: *N*-heterocyclic carbenes (NHCs) and *N*-heterocyclic silylenes (NHSis). However, few germylenes have been reported to expand the diversity of cyclic germylene skeletons,[19, 23, 26, 39-46] including the dialkylgermylene developed by Kira and co-workers.[28, 47-51] In carbene chemistry, Bertrand and co-workers have successfully developed cyclic (alkyl)(amino) carbenes (CAACs) **XIII**, in which one of the adjacent amino group was replaced with a quaternary carbon compared with NHCs **XIV** (Figure 2.10a).

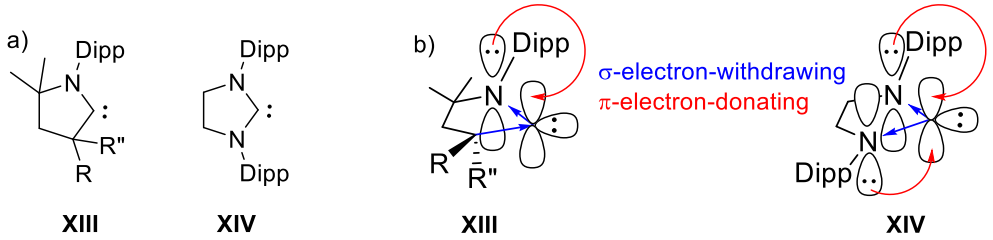

XIII **XIV** **XIII** **XIV**

Figure 2.10 a) Selected CAAC **XIII** and NHC **XIV**; b) orbital diagrams of **XIII** and **XIV**.

The theoretical research unclosed that the HOMO of **XIII** (−4.9eV) is slightly higher than that of **XIV** (−5.2eV) in energy and that CAACs **XIII** exhibit σ-donating and π-accepting abilities stronger than those of NHCs **XIV** (Figure 2.10b).[7, 52-56] Bertrand *et al.* utilized the peculiar steric and electronic properties of **XIII** for the synthesis of novel low-valence main group elements species such as boron[57-59], phosphorus[60-63], antimony[64], silicon[65], and even carbon[66]. Additionally, **XIII** are also great ligands for the stabilization of zero oxidation state transition metals complexes including copper[67], gold[68], iron[69], nickel[70], cobalt[69], manganese[71], and zinc[72].

Herein, we design a new germylene **1** (Figure 2.11), one of the amino group was replaced with a quaternary carbon complied with **IX**. The different reactivity and electronic property from other known germylenes have been expected. We propose that cyclic (alkyl)(amino) germylene (CAAGe) **1** features both stronger σ-donor and π-accepter ability, which can perform some different reactions from other germylenes toward small molecules, main group elements and transition metals complexes.

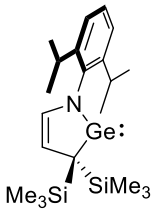

1

Figure 2.11 Cyclic (alkyl)(amino) germylene **1**.

2.2 Results and Discussions

*2.2.1 Comparison of molecular orbitals of germylenes (**VIII', IX', XI', and 1'**)*

Prior to preparation of germylene **1**, we carried out a brief inspection to compare the molecular orbitals (MOs) of cyclic germylenes (**VIII'**, **IX'**, and **XI'**) with our target germylene **1'**, based on the theoretical calculation at the B3LYP/6-31G(d,p) level (Figure 2.12).

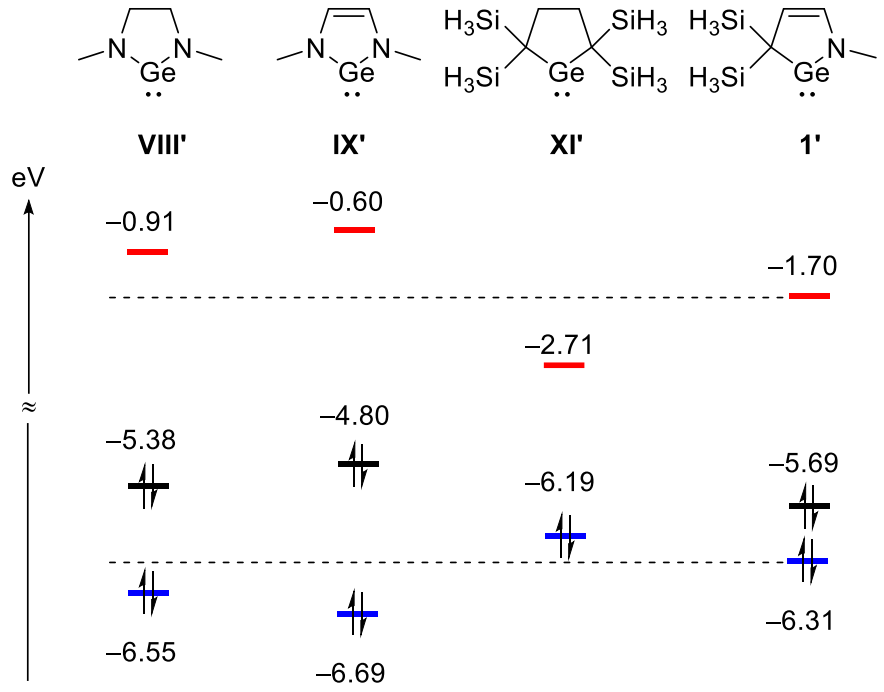

Figure 2.12 Energy (eV) of frontier orbitals of *N*-heterocyclic germylenes **VIII'**, **IX'**, cyclic dialkylgrmylene **XI'** and cyclic (alkyl)(amino) germylene **1'**, calculated at the B3LYP/6-31G(d,p) level of theory.

The calculated result indicated that the germanium lone pair of **VIII'**, **IX'** and **1'** are located at the HOMO−1, and the HOMO−1 of **1'** (−6.31 eV) is slightly higher than NHGes **VIII'** and **IX'** in energy (Figure 2.12). Energies of the LUMOs are predominantly unoccupied p-orbital on the germanium center for all germylenes **VIII'**, **IX'**, **XI'** and **1'**, which decrease in the order **IX'** > **VIII'** > **1'** > **XI'** from −0.60 eV to −2.71 eV. By calculation, it can be concluded that the electrophilicity of germylene **1'** would be enhanced for the replacement of a π-electron donating

as well as a σ-withdrawing amino group with a σ-donating alkyl group, and the nucleophilicity of the germanium center would be concomitantly raised.

*2.2.2 Preparation of cyclic (alkyl)(amino) dichlorogermane **4***

Our strategy for the synthesis of cyclic (alkyl)(amino) germylene is based on oxidative 1,4-addition of germylene with 1,3-diene and subsequent reduction.[73-74] We envisaged that dichlorogermylene would undergo cyclization with α,β-unsaturated imine to afford a dichlorogermane precursor featuring the GeC_3N five-membered ring skeleton, which could be reduced to access germylene. To validate our hypothesis, we carried out the reaction of 3,3-bis(trimethylsilyl)acrylaldehyde[75] and 2,6-diisopropylaniline in Et_2O, from which α, β-unsaturated imine **3** was obtained in 72% isolated yield (Scheme 2.1). The solid state molecular structure of α, β-unsaturated imine **3** was determined by single crystal X-ray diffraction analysis (Figure 2.13).

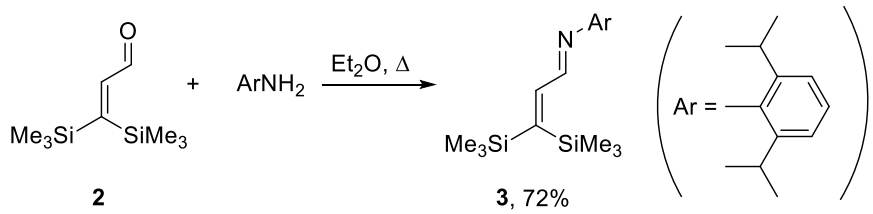

Scheme 2.1 Synthesis of α,β-unsaturated imine **3**.

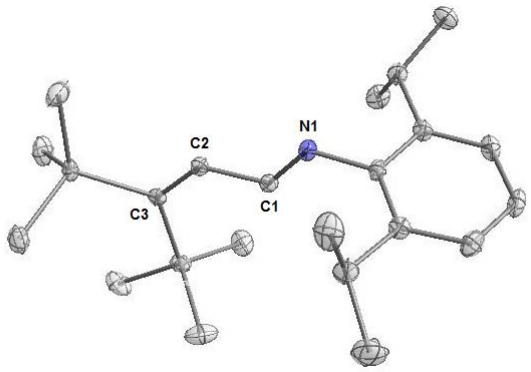

Figure 2.13 Solid state structure of **3**. Hydrogen atoms are omitted for clarity. Thermal ellipsoids are shown at the 50% probability level. Selected bond lengths [Å] and angles [º]: N1-C1 1.2789(19), C1-C2 1.464(2), C2-C3 1.352(2); N1-C1-C2 120.05(13), C1-C2-C3 126.66(14).

Treatment of a stoichiometric amount of dichlorogermylene dioxane complex with **3** in benzene successfully underwent a 1,4-addition via a redox reaction between them, which gave a cyclic dichlorogermane derivative **4** in 96% yield. The result presents the first example of 1,4-addition of Cl_2Ge: to α,β-unsaturated imine. (Scheme 2.2) A single crystal of **4** was grown in hexane at room temperature under an inert atmosphere, and the solid state molecular structure of **4** was confirmed by single crystal X-ray diffraction analysis (Figure 2.14).

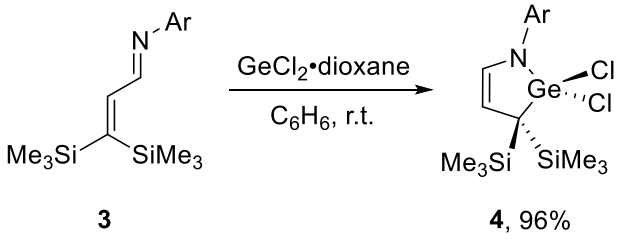

Scheme 2.2 Synthesis of cyclic (alkyl)(amino) dichlorogermanium **4**.

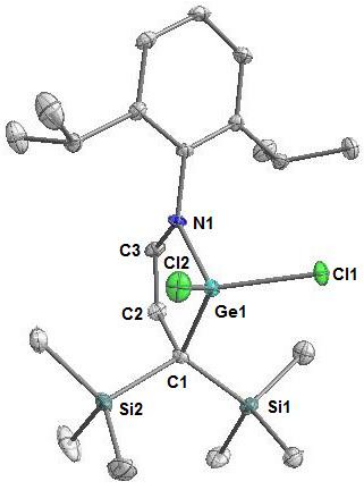

Figure 2.14 Solid state structure of **4**. Hydrogen atoms are omitted for clarity. Thermal ellipsoids are shown at the 50% probability level. Selected bond lengths [Å] and angles [°]: Ge1-N1 1.822(2), Ge1-C1 1.959(3), C1-C2 1.531(4), C2-C3 1.340(4), C3-N1 1.408(4), C1-Si11.909(3), C1-Si2 1.911(3); N1-Ge1-C1 94.90(11), Ge1-C1-C2 98.41(18), C1-C2-C3 119.91(3), C2-C3-N1 119.0(3), C3-N1-Ge1 107.13(18).

To compare the ^{1}H NMR spectrum of **3** with that of **4**, a singlet peak for Me_3Si group of **4** appears at 0.25 ppm, while two singlet peaks for those of **3** were observed at 0.24 ppm and 0.26 ppm.; A doublet peak for CH_3 of isopropyl group of **3** appears at 1.18 ppm, while it is separated to a doublet of doublets appearing at 1.17 ppm and 1.35 ppm for **4**. It means that **4** has a planar symmetric structure. There is a significant difference on the C(sp^2)*H* protons: two doublet peaks appear at 7.39 ppm and 8.15 ppm for **3**, but at 4.63 ppm and 6.34 ppm for **4**. (Figure 2.15)

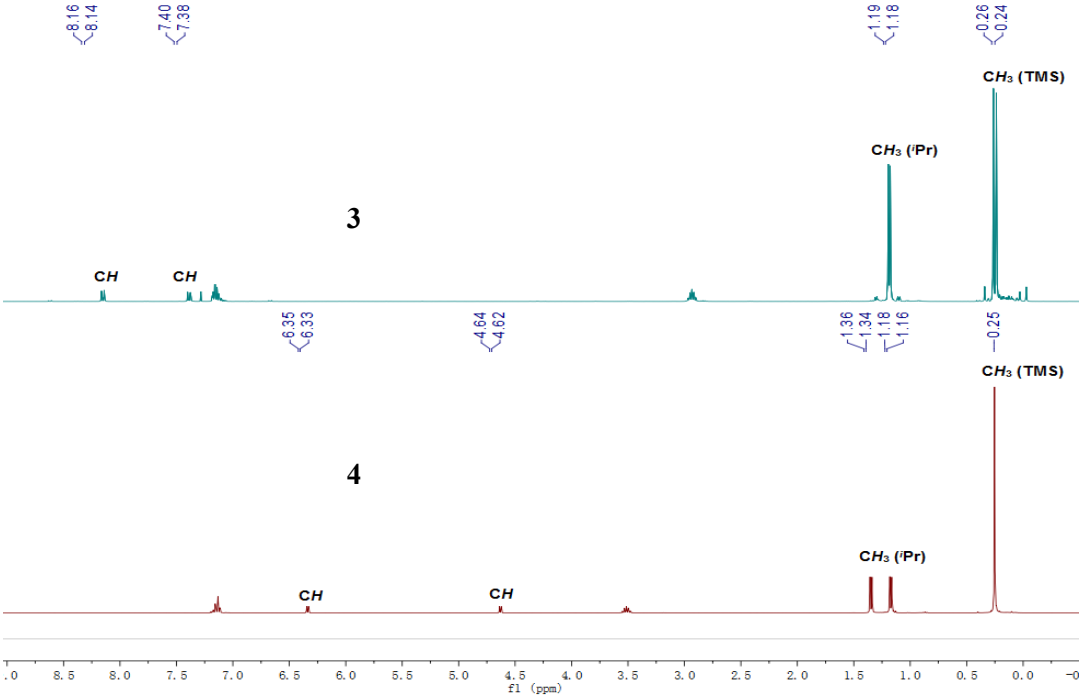

Figure 2.15 ^{1}HNMR spectra of **3** (top) and **4** (bottom).

*2.2.3 Synthesis of cyclic (alkyl)(amino) germylene **1***

A mixture of **4** and three equivalents of potassium graphite (KC_8) was heated at 60 °C in benzene. After work-up, germylene **1** was isolated as a dark red solid in 90% yield. (Scheme 2.3) In the ^{1}H NMR spectrum of **1**, a singlet for Me_3Si group appears at 0.21 ppm, which is identical to that (0.22 ppm) of **4** (Figure 2.16). The ^{13}C NMR spectrum of **1** displays two peaks at 118.9 ppm and 146.7 ppm for the $C(sp^2)$-H carbon atoms in the $GeNC_3$ five-membered ring, which are significantly shifted downfield in comparison to those (99.0 ppm and 139.1 ppm) of **4**. (Figure 2.17)

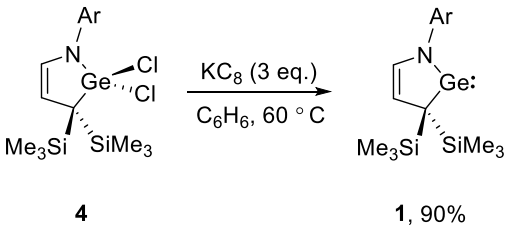

4 **1**, 90%

Scheme 2.3 Synthesis of cyclic (alkyl)(amino) germylene **1**.

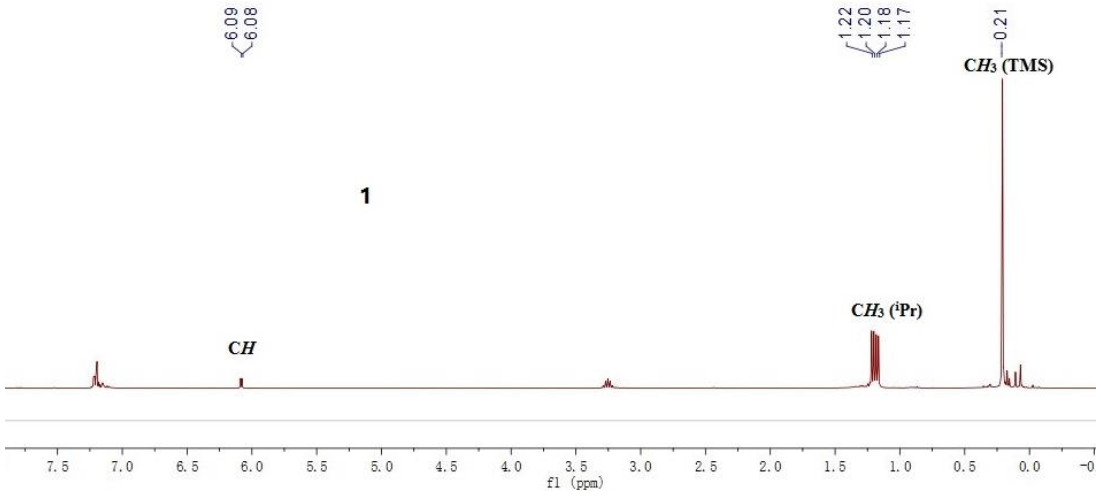

Figure 2.16 ^{1}H NMR spectrum of **4**.

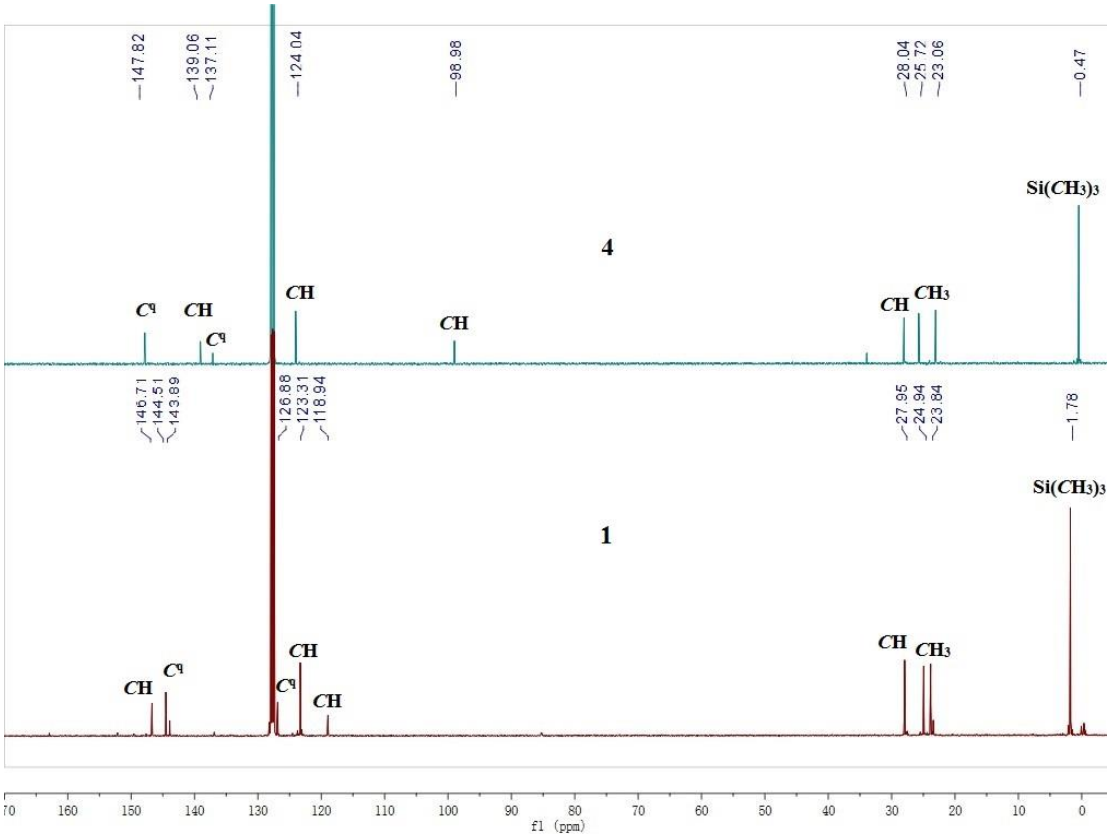

Figure 2.17 ^{13}C NMR spectra of **4** (top) and **1** (bottom).

The solid state molecular structure of germylene **1** was determined by single crystal X-ray diffraction analysis (Figure 2.18). Five atoms in the $GeNC_3$ five-membered ring of **1** and **4** are coplanar (the sum of internal pentagon angles = 539.91 and 539.34 º), and 2,6-diisopropylphenyl ring at the N1 atom and the

$GeNC_3$ skeleton are nearly perpendicular to each other. The Ge1−N1 bond (1.859(11) Å) and the Ge1−C15 bond (1.998(14) Å) distances are slightly longer than those (Ge1−N1 1.822(2) Å, Ge1−C1 1.959(3) Å) of **4** (Figure 2.14). The N1−Ge1−C15 bond angle of 86.5(5) º in **1** is acuter than the N1−Ge1−C1 bond angle (94.90(11) º) in **4**, the corresponding N−Ge−N bond angle (84.8(1) º) in **VIII**[24] as well as the corresponding C−Ge−C bond angle [90.97(9) º] in **X** [28].

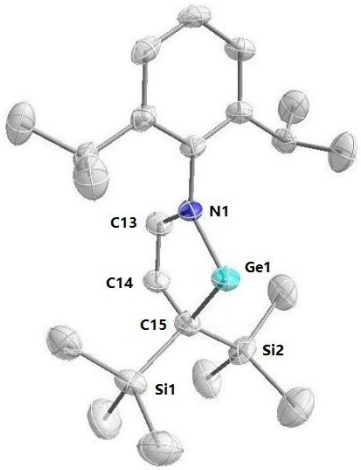

Figure 2.18 Solid state structure of **1**. Hydrogen atoms are omitted for clarity. Thermal ellipsoids are shown at the 50% probability level. Selected bond lengths [Å] and angles [º]: Ge1-N1 1.859(11), Ge1-C15 1.998(14), C14-C15 1.466(19), C13-C14 1.390(13), C13-N1 1.410(16), C15-Si1 1.907(11), C15-Si2 1.876(6); N1-Ge1-C15 86.5(5), Ge1-C15-C14 106.6(6), C13-C14-C15 117.8(11), C13-C14-N1 113.8(11), C13-N1-Ge1 115.3(6).

To gain insight into the electronic features, we carried out quantum chemical calculations on **1** at the B3LYP/6-31G(d,p) level. A lone-pair orbital at the Ge atom was found in the HOMO−1, whereas the HOMO displays a Ge−N π-bonding involving the two C−Si σ-bonds which exhibit anti-bonding conjugation with the π-orbital of the C=C moiety (Figure 2.19). The LUMO is mainly the empty p orbital of the Ge center. Natural bond orbital (NBO) analysis gave Wiberg bond index (WBI) values of the Ge−N bond (0.78) and the Ge−C bond (0.73), indicating single bond nature of these bonds. Natural population analysis (NPA) manifested the second order perturbation energy of 33.97 kcal·mol^{-1} for the interaction between a lone-pair on the N atom and formally unoccupied *p*-orbital of the Ge atom.

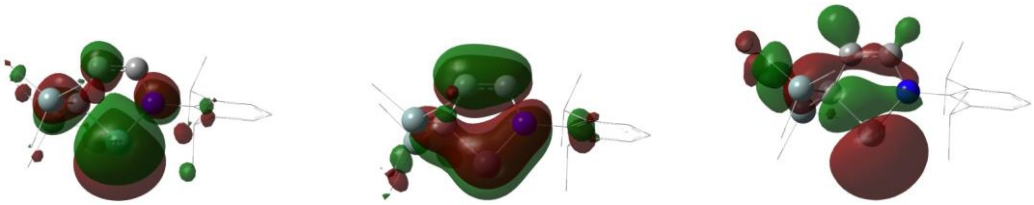

LUMO (-1.44 eV) HOMO (-5.39 eV) HOMO–1 (-5.86 eV)

Figure 2.19 Plots of the LUMO (left), HOMO (middle) and HOMO–1 (right) of **1** calculated at the B3LYP/6-31G(d,p) level of theory (hydrogen atoms are omitted for clarifying).

A UV-vis spectrum of **1** in hexane exhibits a broad peak with λ_{max} at 368 nm, which is due to HOMO-LUMO transition, responsible for the dark red colour of **1** (Figure 2.20).

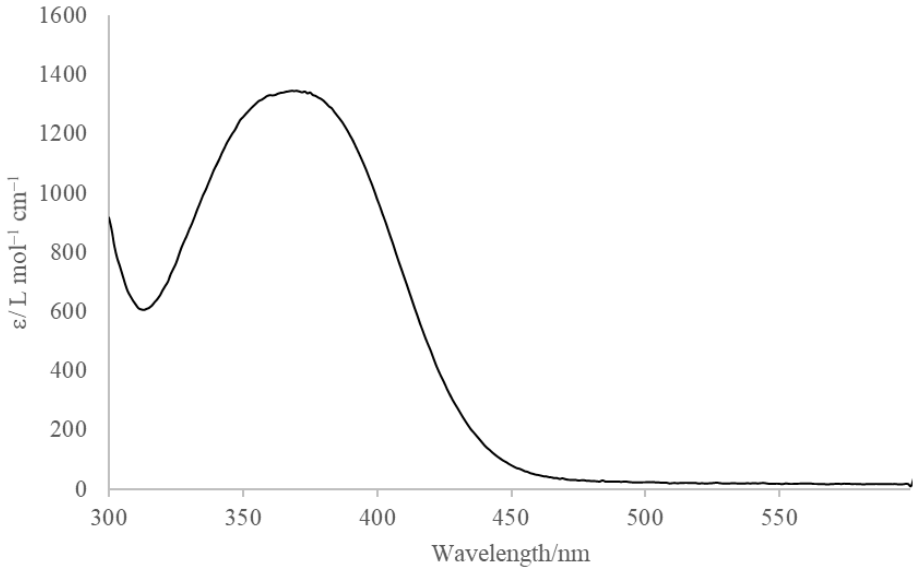

Figure 2.20 UV-visible spectrum of germylene **1** in hexane at room temperature.

2.3 Conclusion

In conclusion, we have developed a direct approach for the synthesis of a dichlorogermane derivative **4** featuring the five-membered $GeNC_3$ ring skeleton through a simple 1,4-addition of dichlorogermylene•dioxane complex with α,β-unsaturated imine **3**. Subsequently, the reduction of **4** with KC_8 gave cyclic (alkyl)(amino) germylene (CAAGe) **1** possessing the high-lying HOMO−1 and low-lying LUMO, which was supported by DFT calculations.

2.4 Experimental Section

2.4.1 General Information

All reactions were performed under an atmosphere of argon by using standard Schlenk or dry box techniques; solvents were dried over Na metal, K metal or CaH_2. All the substrates were obtained from the commercial sources or synthesized following literature procedures. Analytical thin layer chromatography was performed on triethylamine deactivated 0.25 mm silica gel 60-F254. Visualization was carried out with UV light. ^{1}H, and ^{13}C spectrum were obtained with AVIII 400MHz BBFO1 spectrometer at 298 K. NMR multiplicities are abbreviated as follows: s = singlet, d = doublet, t = triplet, m = multiplet, br = broad signal. Coupling constants J are given in Hz. Electrospray ionization (ESI) mass spectrum was obtained at the Mass Spectrometry Laboratory at the Division of Chemistry and Biological Chemistry, Nanyang Technological University. Melting points were measured with an OpticMelt Stanford Research System.

*2.4.2 Synthesis of imine **3***

2,6-diisopropylaniline (55 mmol, 9.75 g) and 3,3-bis(trimethylsilyl)acrylaldehyde (50 mmol, 10.00 g) were mixed in ether (100 mL). The mixture was refluxed overnight. After cooling to room temperature, the product was purified by silica gel column chromatography

(petroleum ether/ ethyl acetate = 10:1) to afford **3** as a yellow solid (12.9 g, 72%). Mp: 109 ℃; ^{1}H NMR (400 MHz, $CDCl_3$) δ 8.13 (d, *J* = 10.1 Hz, 1H, C*H*), 7.36 (d, *J* = 10.1 Hz, 1H, C*H*), 7.18 – 7.07 (m, 3H, Ar-*H*), 2.91 (dt, *J* = 13.7, 6.9 Hz, 2H, C*H*), 1.17 (s, 6H, CH_3), 1.15 (s, 6H, CH_3), 0.24 (s, 9H, Si(CH_3)$_3$), 0.21 (s, 9H, Si(CH_3)$_3$); ^{13}C NMR (100 MHz, $CDCl_3$) δ 163.40 (*C*H), 162.04 (*C*^{q}), 151.12 (*C*H), 148.79 (*C*^{q}), 137.23 (*C*^{q}), 124.26 (*C*^{q}), 122.96 (*C*H), 27.73 (*C*H), 23.61 (*C*H_3), 2.39 (Si(*C*H_3)$_3$), 0.05 (Si(*C*H_3)$_3$); HRMS (ESI): m/z calcd for $C_{21}H_{38}NSi_2$: 359.2465 [(M+H)]$^{+}$; found: 359.2468.

*2.4.3 Synthesis of cyclic (alkyl)(amino) dichlorogermane **4***

(E)-N-(2,6-diisopropylphenyl)-3,3-bis(trimethylsilyl)prop-2-en-1-imine **1** (4 mmol, 1.42 g) and dichlorogermadiyl dioxane (4 mmol, 0.93 g) were mixed in benzene (20 mL). The mixture was stirred at room temperature overnight and then vacuumed to remove the solvent. The product **4** was obtained as a yellow solid (1.93 g, 96%). Mp: 154 ℃; ^{1}H NMR (400 MHz, C_6D_6) δ 7.15 – 6.88 (m, 3H, Ar-*H*), 6.30 (d, *J* = 6.3 Hz, 1H, C*H*), 4.60 (d, *J* = 6.3 Hz, 1H, C*H*), 3.48 (dt, *J* = 13.7, 6.9 Hz, 2H, C*H*), 1.31 (d, *J* = 6.9 Hz, 6H, CH_3), 1.14 (d, *J* = 6.9 Hz, 6H, CH_3), 0.22 (s, 18H, Si(CH_3)$_3$); ^{13}C NMR (100 MHz, C_6D_6) δ 147.82 (*C*^{q}), 139.06 (*C*H), 137.11 (*C*^{q}), 127.91 (*C*H), 124.04 (*C*H), 98.98 (*C*H), 33.96, (*C*^{q}), 28.04 (*C*H), 25.72 (*C*H_3), 23.06 (*C*H_3), 0.47 (Si(*C*H_3)$_3$); HRMS (ESI): m/z calcd for $C_{21}H_{38}NSi_2Cl_2Ge$: 504.1132 [(M+H)]$^{+}$; found: 504.1156.

*2.4.4 Synthesis of cyclic (alkyl)(amino) germylene **1***

7 (2 mmol, 1.02 g) and KC_8(6 mmol, 0.81 g) were mixed in benzene (30 mL). The mixture was stirred at 60 ℃ for 6 h. After stirring for another 30 min at room temperature, the mixture was filtered and concentrated under vacuum. The product **1** was obtained as a dark red solid (0.78 g, 90%). Mp: 95 ℃; ^{1}H NMR (400 MHz, C_6D_6) δ 7.22 (d, *J* = 4.1 Hz, 1H, C*H*), 7.22 – 7.21 (m, 3H, Ar-*H*), 6.08 (d, *J* = 4.1 Hz, 1H, C*H*), 3.25 (dt, *J* = 13.8, 6.9 Hz, 2H, C*H*), 1.21 (d, *J* = 6.9 Hz, 6H, CH_3), 1.17 (d, *J* = 6.9 Hz, 6H, CH_3), 0.21 (s, 18H, Si(CH_3)$_3$); ^{13}C NMR (100 MHz, C_6D_6) δ 147.10 (*C*H), 144.88 (*C*^{q}), 127.82 (*C*^{q}), 127.28 (*C*H), 123.69 (*C*H), 119.35 (*C*H),

28.34 (*C*H), 25.35 (*C*H_3), 24.23 (*C*H_3), 2.18 (Si(*C*H_3)$_3$); UV-vis (Hexane, 298 K) with λ_{max}/nm at 368 nm; HRMS (ESI): m/z calcd for $C_{21}H_{38}NSi_2Ge$: 434.1755 $[(M+H)]^+$; found: 434.1761.

2.4.5 ^{1}H and ^{13}C NMR Spectra

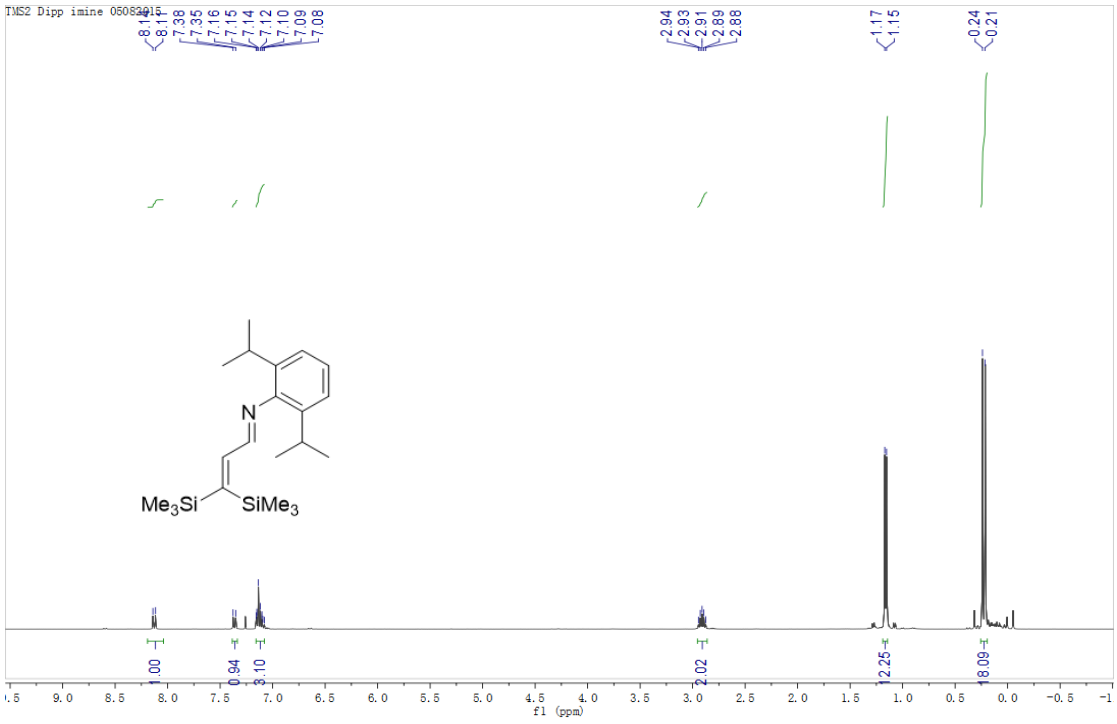

Figure 2.21 ^{1}H NMR spectrum of **3**

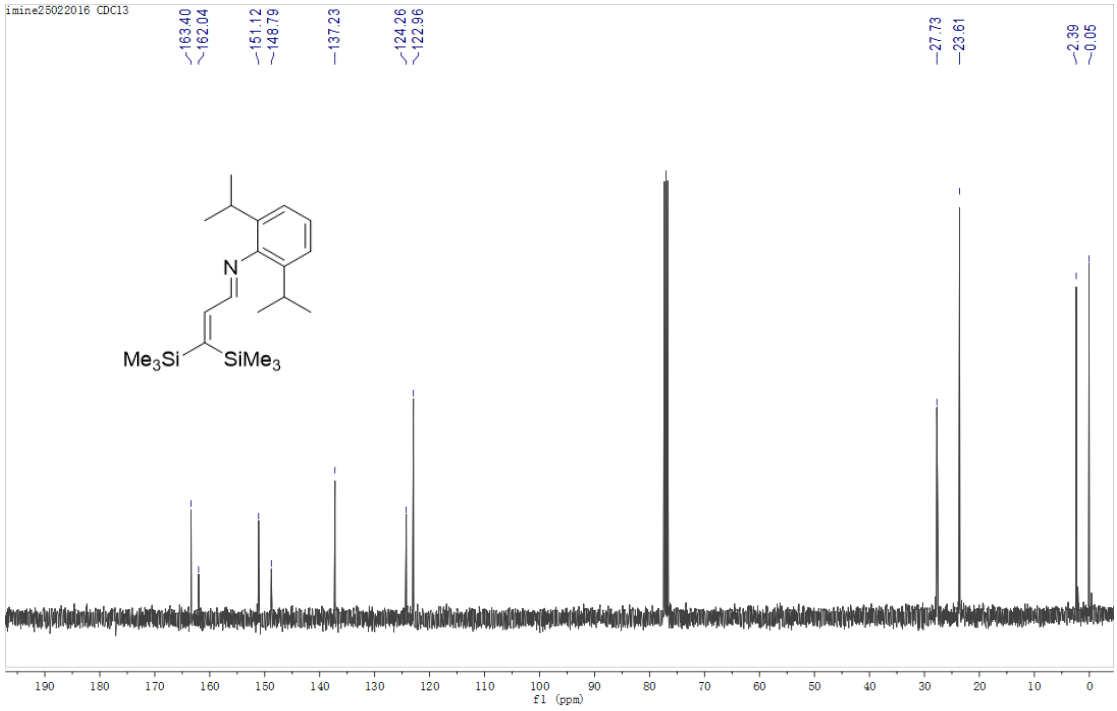

Figure 2.22 ^{13}C NMR spectrum of **3**

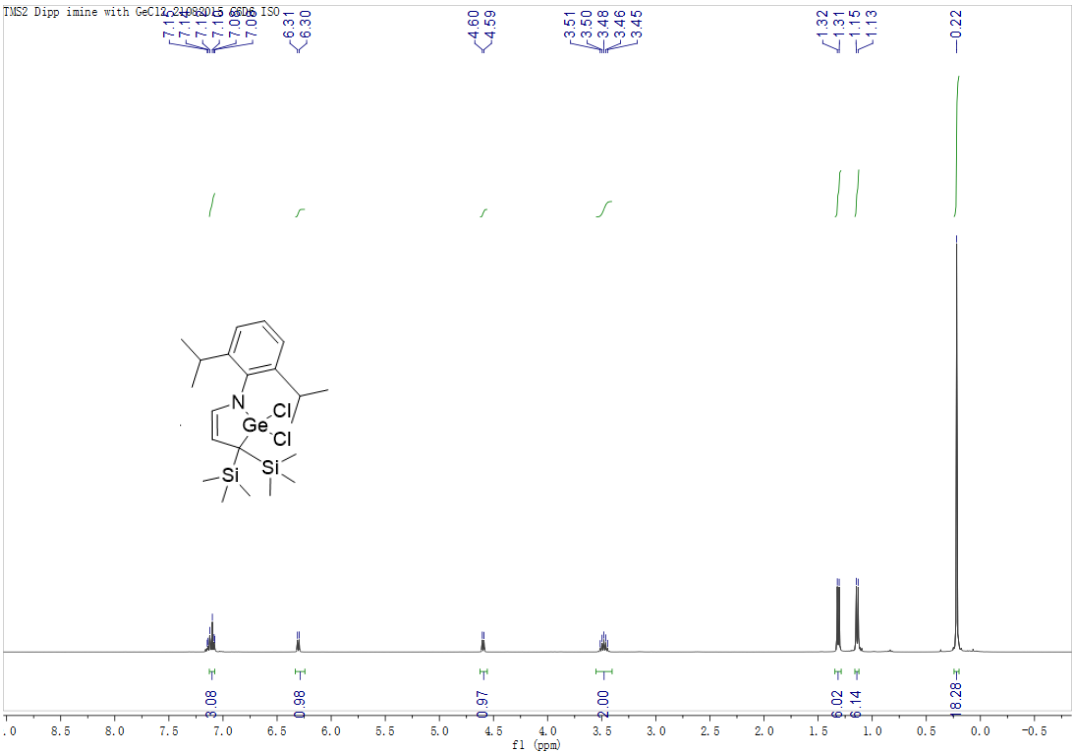

Figure 2.23 ^{1}H NMR spectrum of **4**

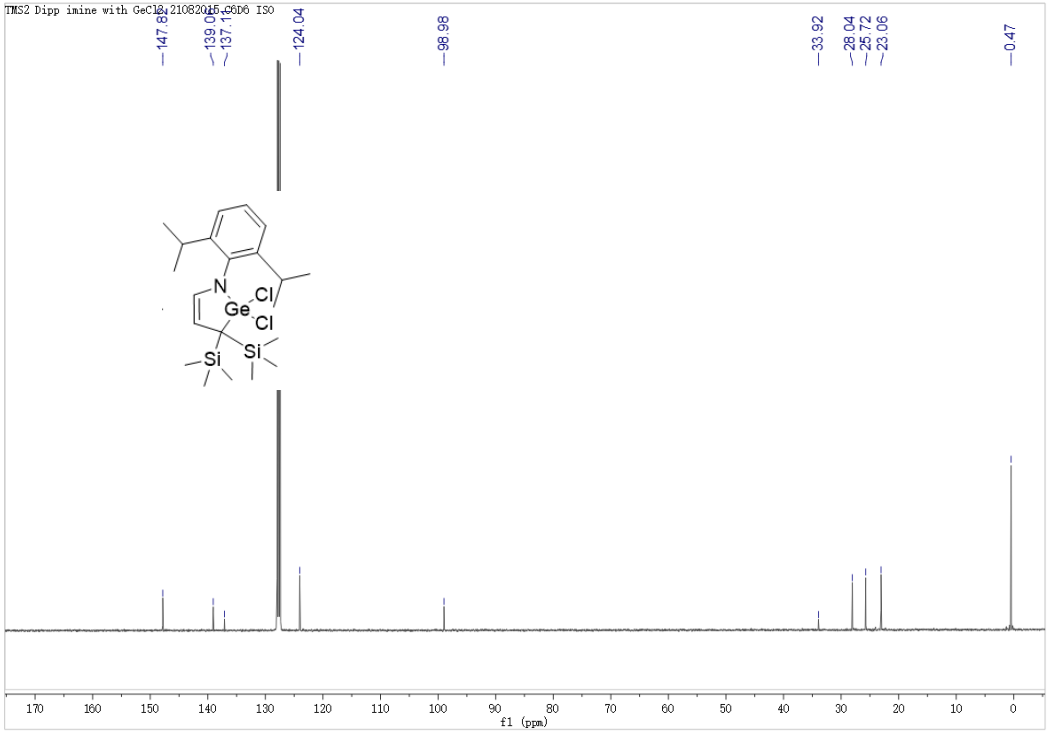

Figure 2.24 ^{13}C NMR spectrum of **4**

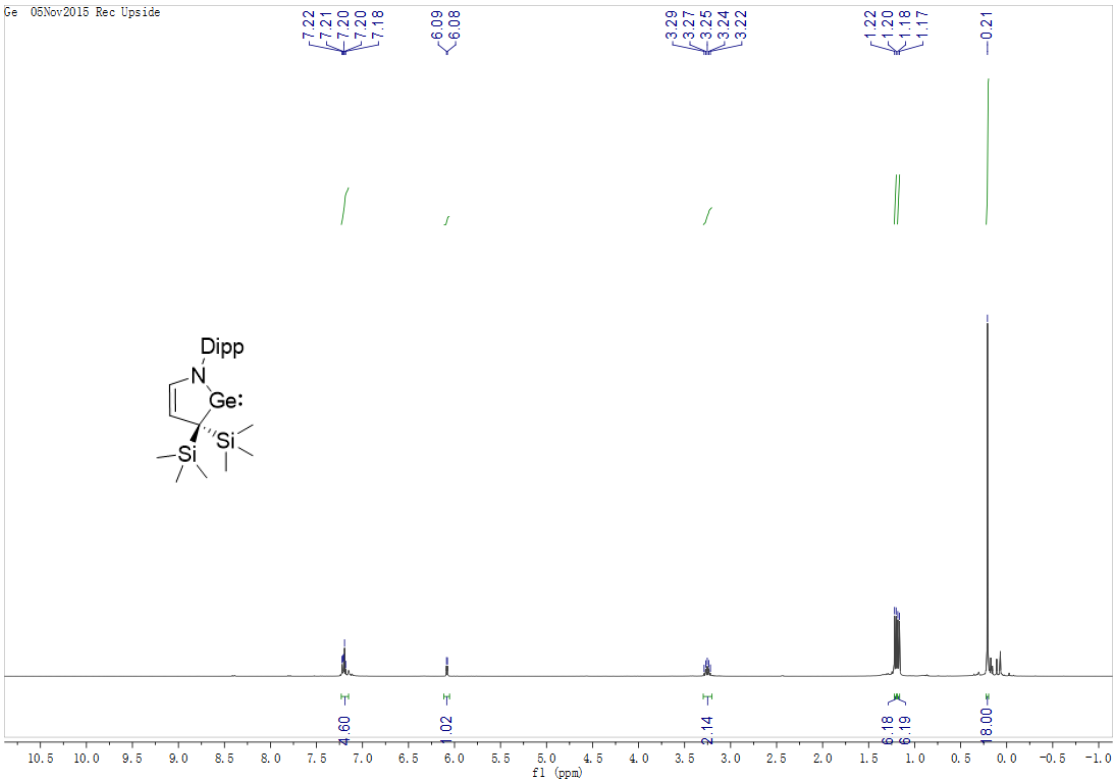

Figure 2.25 ^{1}H NMR spectrum of **1**

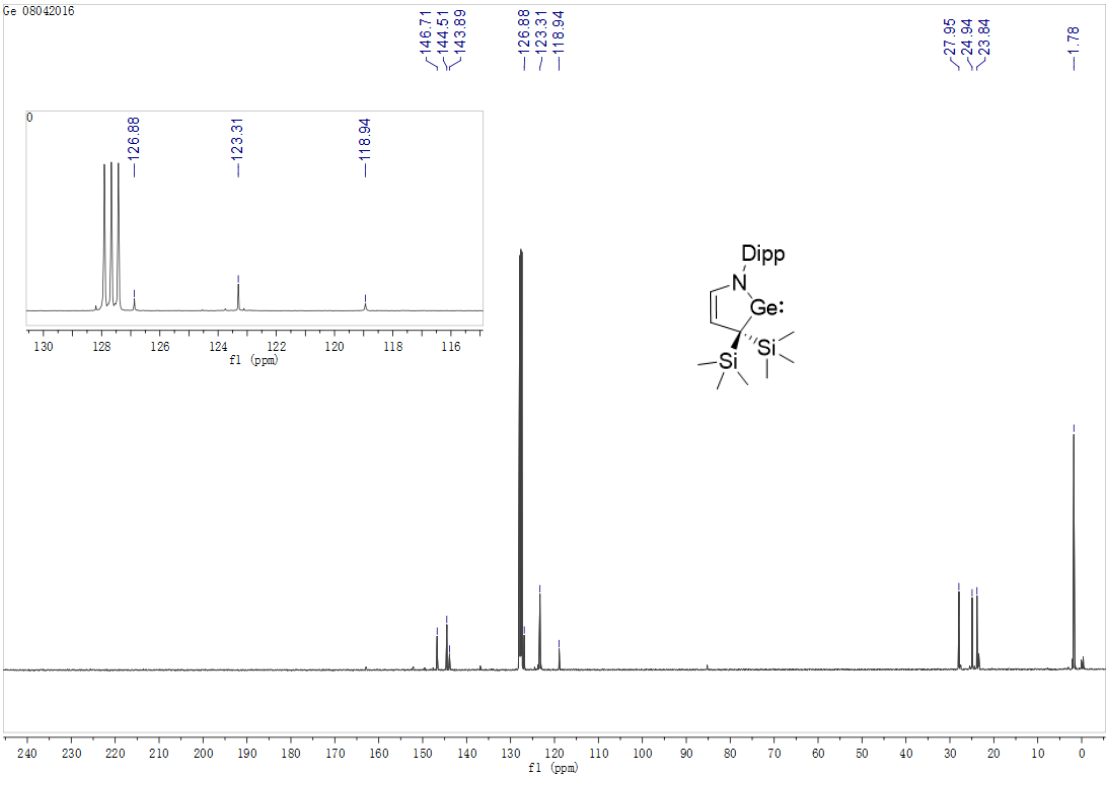

Figure 2.26 ^{13}C NMR spectrum of **1**

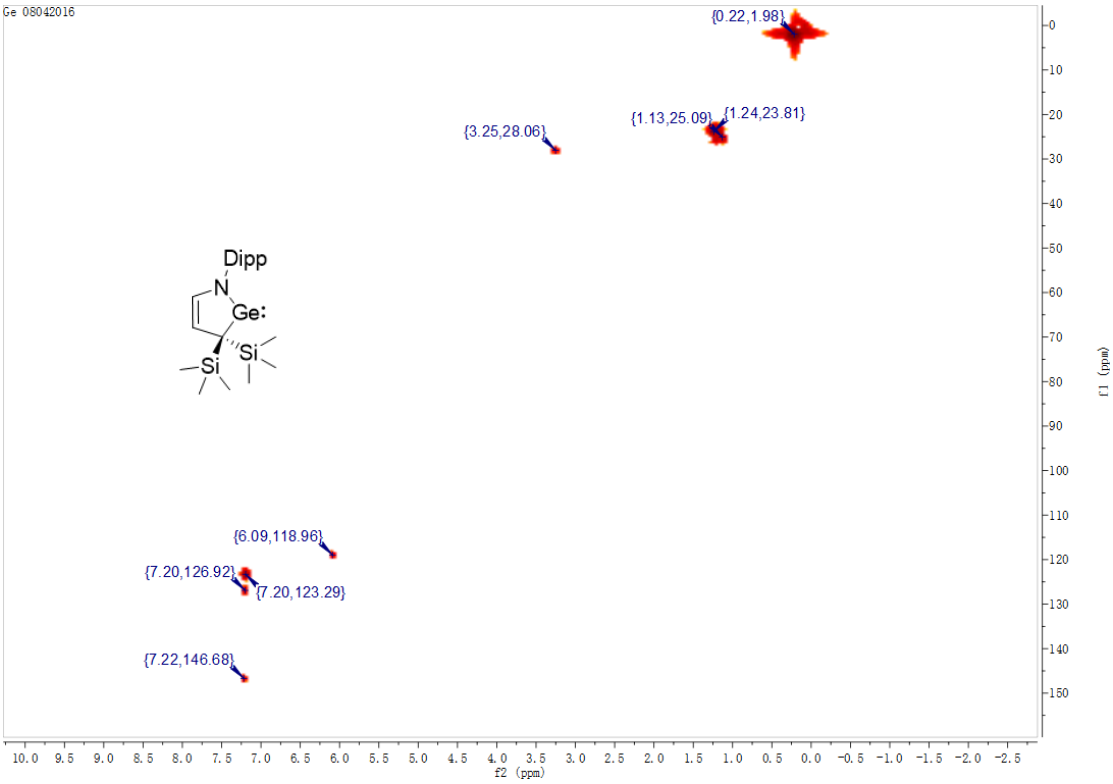

Figure 2.27 ^{1}H-^{13}C HSQC spectrum of **1**.

2.5 References

1. Gynane, M. J. S.; Harris, D. H.; Lappert, M. F.; Power, P. P.; Riviere, P.; Riviere-Baudet, M., *J. Chem. Soc., Dalton Trans.* **1977**, 2004-2009.

2. Davidson, P. J.; Harris, D. H.; Lappert, M. F., *J. Chem. Soc., Dalton Trans.* **1976**, 2268-2274.

3. Bourissou, D.; Guerret, O.; Gabbaï, F. P.; Bertrand, G., *Chem. Rev.* **2000,** *100*, 39-92.

4. Mizuhata, Y.; Sasamori, T.; Tokitoh, N., *Chem. Rev.* **2009,** *109*, 3479-3511.

5. Sasamori, T.; Tokitoh, N., Group 14 Multiple Bonding. In *Encyclopedia of Inorganic Chemistry*, John Wiley & Sons, Ltd: 2006.

6. Trinquier, G., *J. Am. Chem. Soc.* **1990,** *112*, 2130-2137.

7. Soleilhavoup, M.; Bertrand, G., *Acc. Chem. Res.* **2015,** *48*, 256-266.

8. Harris, D. H.; Lappert, M. F., *J. Chem. Soc., Chem. Commun.* **1974**, 895-896.

9. Asay, M.; Jones, C.; Driess, M., *Chem. Rev.* **2011,** *111*, 354-396.

10. West, R.; Moser, D. F.; Guzei, I. A.; Lee, G.-H.; Naka, A.; Li, W.; Zabula, A.; Bukalov, S.; Leites, L., *Organometallics* **2006,** *25*, 2709-2711.

11. Schäfer, A.; Saak, W.; Haase, D.; Müller, T., *Chem. Eur. J.* **2009,** *15*, 3945-3950.

12. Stender, M.; Phillips, A. D.; Power, P. P., *Inorg. Chem.* **2001,** *40*, 5314-5315.

13. Akkari, A.; Byrne, J. J.; Saur, I.; Rima, G.; Gornitzka, H.; Barrau, J., *J. Organomet. Chem.* **2001,** *622*, 190-198.

14. Wang, W.; Yao, S.; van Wüllen, C.; Driess, M., *J. Am. Chem. Soc.* **2008,** *130*, 9640-9641.

15. Jones, C.; Rose, R. P.; Stasch, A., *Dalton Trans.* **2008**, 2871-2878.

16. Chen, T.; Hunks, W.; Chen, P. S.; Stauf, G. T.; Cameron, T. M.; Xu, C.; DiPasquale, A. G.; Rheingold, A. L., *Eur. J. Inorg. Chem.* **2009,** *2009*, 2047-2049.

17. Foley, S. R.; Bensimon, C.; Richeson, D. S., *J. Am. Chem. Soc.* **1997,** *119*, 10359-10363.

18. Foley, S. R.; Zhou, Y.; Yap, G. P. A.; Richeson, D. S., *Inorg. Chem.* **2000,** *39*, 924-929.

19. Heinicke, J.; Oprea, A.; Kindermann, M. K.; Karpati, T.; Nyulászi, L.; Veszprémi, T., *Chem. Eur. J.* **1998,** *4*, 541-545.

20. Meller, A.; Pfeiffer, J.; Noltemeyer, M., *Z. Anorg. Allg. Chem.* **1989,** *572*, 145-150.

21. Pfeiffer, J.; Maringgele, W.; Noltemeyer, M.; Meller, A., *Chem. Ber.* **1989,** *122*, 245-252.

22. Heinicke, J.; Oprea, A., *Heteroat. Chem* **1998,** *9*, 439-444.

23. Baker, R. J.; Jones, C.; Mills, D. P.; Pierce, G. A.; Waugh, M., *Inorg. Chim. Acta* **2008,** *361*, 427-435.

24. Herrmann, W. A.; Denk, M.; Behm, J.; Scherer, W.; Klingan, F.-R.; Bock, H.; Solouki, B.; Wagner, M., *Angew. Chem. Int. Ed. Engl.* **1992,** *31*, 1485-1488.

25. Kühl, O.; Lönnecke, P.; Heinicke, J., *Polyhedron* **2001,** *20*, 2215-2222.

26. Tomasik, A. C.; Hill, N. J.; West, R., *J. Organomet. Chem.* **2009,** *694*, 2122-2125.

27. Dias, H. V. R.; Wang, Z., *J. Am. Chem. Soc.* **1997,** *119*, 4650-4655.

28. Mitsuo, K.; Shintaro, I.; Takeaki, I.; Masaaki, I.; Chizuko, K.; Lubov, I.; Hideki, S., *Chem. Lett.* **1999,** *28*, 263-264.

29. Ding, Y.; Roesky, H. W.; Noltemeyer, M.; Schmidt, H.-G.; Power, P. P., *Organometallics* **2001,** *20*, 1190-1194.

30. Ding, Y.; Hao, H.; Roesky, H. W.; Noltemeyer, M.; Schmidt, H.-G., *Organometallics* **2001,** *20*, 4806-4811.

31. Ayers, A. E.; Klapötke, T. M.; Dias, H. V. R., *Inorg. Chem.* **2001,** *40*, 1000-1005.

32. Chorley, R. W.; Hitchcock, P. B.; Lappert, M. F.; Leung, W.-P.; Power, P. P.; Olmstead, M. M., *Inorg. Chim. Acta* **1992,** *198–200*, 203-209.

33. Schnepf, A., *Z. Anorg. Allg. Chem.* **2006,** *632*, 935-938.

34. Veith, M.; Rammo, A., *Z. Anorg. Allg. Chem.* **2001,** *627*, 662-668.

35. Hitchcock, P. B.; Lappert, M. F.; Thorne, A. J., *J. Chem. Soc., Chem. Commun.* **1990**, 1587-1589.

36. Arii, H.; Nakadate, F.; Mochida, K., *Organometallics* **2009,** *28*, 4909-4911.

37. Yang, Z.; Ma, X.; Roesky, H. W.; Yang, Y.; Zhu, H.; Magull, J.; Ringe, A., *Z. Anorg. Allg. Chem.* **2008,** *634*, 1490-1492.

38. Lee, V. Y.; Sekiguchi, A., Heavy Analogs of Carbenes: Silylenes, Germylenes,

Stannylenes and Plumbylenes. In *Organometallic Compounds of Low-Coordinate Si, Ge, Sn and Pb*, John Wiley & Sons, Ltd: 2010; pp 139-197.

39. Li, Y.; Mondal, K. C.; Stollberg, P.; Zhu, H.; Roesky, H. W.; Herbst-Irmer, R.; Stalke, D.; Fliegl, H., *Chem. Commun.* **2014,** *50*, 3356-3358.

40. Fedushkin, I. L.; Skatova, A. A.; Chudakova, V. A.; Khvoinova, N. M.; Baurin, A. Y.; Dechert, S.; Hummert, M.; Schumann, H., *Organometallics* **2004,** *23*, 3714-3718.

41. Ullah, F.; Oprea, A. I.; Kindermann, M. K.; Bajor, G.; Veszprémi, T.; Heinicke, J., *J. Organomet. Chem.* **2009,** *694*, 397-403.

42. Huang, M.; Kireenko, M. M.; Zaitsev, K. V.; Oprunenko, Y. F.; Churakov, A. V.; Howard, J. A. K.; Lermontova, E. K.; Sorokin, D.; Linder, T.; Sundermeyer, J.; Karlov, S. S.; Zaitseva, G. S., *Eur. J. Inorg. Chem.* **2012,** *2012*, 3712-3724.

43. Karwasara, S.; Yadav, D.; Jha, C. K.; Rajaraman, G.; Nagendran, S., *Chem. Commun.* **2015,** *51*, 4310-4313.

44. Okazaki, R.; Tokitoh, N., *Acc. Chem. Res.* **2000,** *33*, 625-630.

45. Leung, W.-P.; Chiu, W.-K.; Chong, K.-H.; Mak, T. C. W., *Chem. Commun.* **2009**, 6822-6824.

46. Ding, Y.; Ma, Q.; Usón, I.; Roesky, H. W.; Noltemeyer, M.; Schmidt, H.-G., *J. Am. Chem. Soc.* **2002,** *124*, 8542-8543.

47. Ishida, S.; Hirakawa, F.; Furukawa, K.; Yoza, K.; Iwamoto, T., *Angew. Chem. Int. Ed.* **2014,** *53*, 11172-11176.

48. Iwamoto, T.; Hirakawa, F.; Ishida, S., *Angew. Chem. Int. Ed.* **2012,** *51*, 12111-12114.

49. Ishida, S.; Hirakawa, F.; Iwamoto, T., *J. Am. Chem. Soc.* **2011,** *133*, 12968-12971.

50. Kira, M.; Yauchibara, R.; Hirano, R.; Kabuto, C.; Sakurai, H., *J. Am. Chem. Soc.* **1991,** *113*, 7785-7787.

51. Kira, M.; Ishida, S.; Iwamoto, T.; Kabuto, C., *J. Am. Chem. Soc.* **1999,** *121*, 9722-9723.

52. Martin, D.; Soleilhavoup, M.; Bertrand, G., *Chem. Sci.* **2011,** *2*, 389-399.

53. Martin, C. D.; Soleilhavoup, M.; Bertrand, G., *Chem. Sci.* **2013,** *4*, 3020-3030.

54. Mondal, K. C.; Roy, S.; Maity, B.; Koley, D.; Roesky, H. W., *Inorg. Chem.* **2016,** *55*, 163-169.

55. Arduengo, A. J.; Bock, H.; Chen, H.; Denk, M.; Dixon, D. A.; Green, J. C.;

Herrmann, W. A.; Jones, N. L.; Wagner, M.; West, R., *J. Am. Chem. Soc.* **1994,** *116*, 6641-6649.

56. Back, O.; Henry-Ellinger, M.; Martin, C. D.; Martin, D.; Bertrand, G., *Angew. Chem. Int. Ed.* **2013,** *52*, 2939-2943.

57. Kinjo, R.; Donnadieu, B.; Celik, M. A.; Frenking, G.; Bertrand, G., *Science* **2011,** *333*, 610-613.

58. Ruiz, D. A.; Melaimi, M.; Bertrand, G., *Chem. Commun.* **2014,** *50*, 7837-7839.

59. Ruiz, D. A.; Ung, G.; Melaimi, M.; Bertrand, G., *Angew. Chem. Int. Ed.* **2013,** *52*, 7590-7592.

60. Back, O.; Kuchenbeiser, G.; Donnadieu, B.; Bertrand, G., *Angew. Chem. Int. Ed.* **2009,** *48*, 5530-5533.

61. Back, O.; Donnadieu, B.; Parameswaran, P.; Frenking, G.; Bertrand, G., *Nat. Chem.* **2010,** *2*, 369-373.

62. Kinjo, R.; Donnadieu, B.; Bertrand, G., *Angew. Chem. Int. Ed.* **2010,** *49*, 5930-5933.

63. Back, O.; Celik, M. A.; Frenking, G.; Melaimi, M.; Donnadieu, B.; Bertrand, G., *J. Am. Chem. Soc.* **2010,** *132*, 10262-10263.

64. Kretschmer, R.; Ruiz, D. A.; Moore, C. E.; Rheingold, A. L.; Bertrand, G., *Angew. Chem. Int. Ed.* **2014,** *53*, 8176-8179.

65. Mondal, K. C.; Roesky, H. W.; Schwarzer, M. C.; Frenking, G.; Tkach, I.; Wolf, H.; Kratzert, D.; Herbst-Irmer, R.; Niepötter, B.; Stalke, D., *Angew. Chem. Int. Ed.* **2013,** *52*, 1801-1805.

66. Li, Y.; Mondal, K. C.; Samuel, P. P.; Zhu, H.; Orben, C. M.; Panneerselvam, S.; Dittrich, B.; Schwederski, B.; Kaim, W.; Mondal, T.; Koley, D.; Roesky, H. W., *Angew. Chem. Int. Ed.* **2014,** *53*, 4168-4172.

67. Weinberger, D. S.; Amin Sk, N.; Mondal, K. C.; Melaimi, M.; Bertrand, G.; Stückl, A. C.; Roesky, H. W.; Dittrich, B.; Demeshko, S.; Schwederski, B.; Kaim, W.; Jerabek, P.; Frenking, G., *J. Am. Chem. Soc.* **2014,** *136*, 6235-6238.

68. Weinberger, D. S.; Melaimi, M.; Moore, C. E.; Rheingold, A. L.; Frenking, G.; Jerabek, P.; Bertrand, G., *Angew. Chem. Int. Ed.* **2013,** *52*, 8964-8967.

69. Ung, G.; Rittle, J.; Soleilhavoup, M.; Bertrand, G.; Peters, J. C., *Angew. Chem. Int. Ed.* **2014,** *53*, 8427-8431.

70. Mondal, K. C.; Samuel, P. P.; Li, Y.; Roesky, H. W.; Roy, S.; Ackermann, L.; Sidhu, N. S.; Sheldrick, G. M.; Carl, E.; Demeshko, S.; De, S.; Parameswaran, P.; Ungur, L.; Chibotaru, L. F.; Andrada, D. M., *Eur. J. Inorg. Chem.* **2014,** *2014*, 818-823.

71. Samuel, P. P.; Mondal, K. C.; Roesky, H. W.; Hermann, M.; Frenking, G.; Demeshko, S.; Meyer, F.; Stückl, A. C.; Christian, J. H.; Dalal, N. S.; Ungur, L.; Chibotaru, L. F.; Pröpper, K.; Meents, A.; Dittrich, B., *Angew. Chem. Int. Ed.* **2013,** *52*, 11817-11821.

72. Singh, A. P.; Samuel, P. P.; Roesky, H. W.; Schwarzer, M. C.; Frenking, G.; Sidhu, N. S.; Dittrich, B., *J. Am. Chem. Soc.* **2013,** *135*, 7324-7329.

73. Al-Rafia, S. M. I.; Momeni, M. R.; McDonald, R.; Ferguson, M. J.; Brown, A.; Rivard, E., *Angew. Chem. Int. Ed.* **2013,** *52*, 6390-6395.

74. Tokitoh, N.; Manmaru, K.; Okazaki, R., *Organometallics* **1994,** *13*, 167-171.

75. Yan, L.; Sun, X.; Li, H.; Song, Z.; Liu, Z., *Org. Lett.* **2013,** *15*, 1104-1107.

Chapter 3 Oxidation and related reactivity of cyclic (alkyl)(amino) germylene with N_2O, S_8 and TEMPO

3.1 Introduction

Ketone is a very important compound with the structure of $R_2C=O$, and has high application value in both industry and biology.[1-3] It usually exists in monomeric forms rather than dimeric, oligomeric or polymeric forms. As a germanium analog of ketone, germanone has a more polarized Ge=O bond than that of ketone, so germanone generally exists as oligomeric or polymeric forms.[4]

The first monomeric germanone **I** was isolated by Tamao and co-workers in 2012,[5] which was stabilized by the introduction of bulk groups (Figure 3.1). It is well known that the Ge=O double bond of germanone is weak, and its bond dissociation energy (108 kcal mol^{-1}) is obviously lower than that (172 kcal mol^{-1}) of the C=O double bond of ketone.[4] Germanone favored to dimerize or oligomerize, because the germannium atom lack of the effective *sp*-hybridization due to its radial extensions.[6-9]

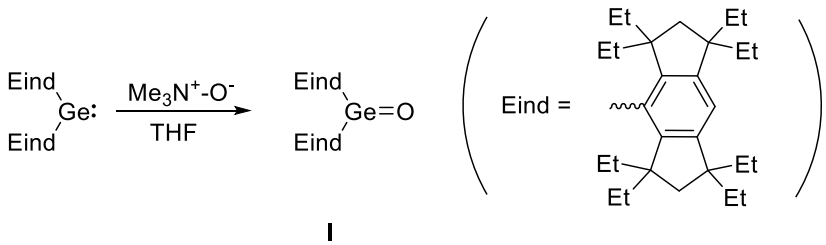

I

Figure 3.1 Synthesis of germanone **I**.

3.1.1 Intramolecular base stabilization of germanthione

The first stable heavy germanthione ($R_2Ge=S$) **II** with a terminal sulfur atom was reported by Veith and co-workers in 1989, which is stabilized by the coordination of intramolecular amine

(Figure 3.2).[10-12] Meanwhile, the reaction of germylene **III** with oxygen gave the dimer **IV** instead of germanone **V** (Figure 3.2).[4, 10, 13] Meanwhile, the reaction of germylene **III** with oxygen gave the dimer **IV** instead of germanone **V** (Figure 3.2), which is probably due to the higher bond polarity of Ge=O (1.44) than that of Ge=S (0.86). The bond polarity is a concept to describe the sharing of electrons between atoms within a covalent bond, in which the electron pairs shared between two atoms are not shared equally.

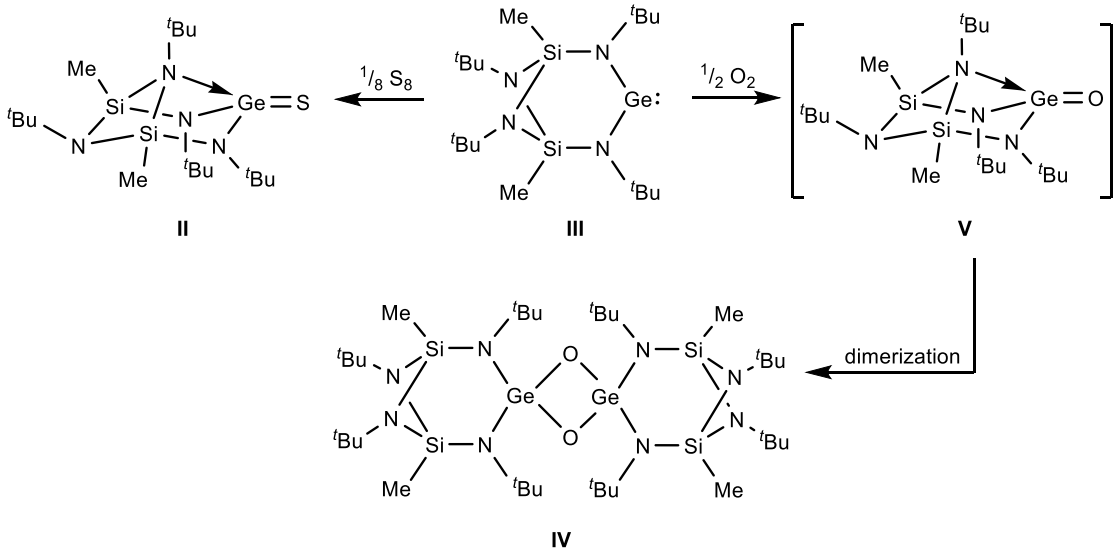

Figure 3.2 Reaction of germylene **III** with S_8 and O_2.

The second isolable germanthione **VII** stabilized by the intramolecular coordination of nitrogen atoms was reported by Parkin and co-workers in 1994 (Figure 3.3), where the stability of **VII** was also contributed from the coordination between nitrogen lone pair of electrons and *d*-orbital of germanium atom. To date, there are still not such germanones stabilized by the intramolecular coordination.[14]

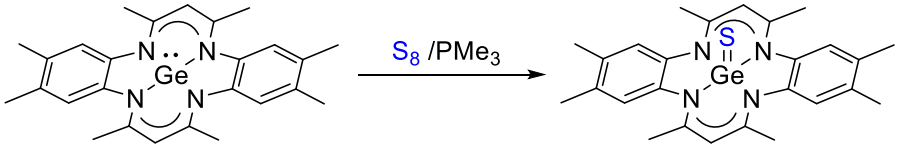

VI **VII**

Figure 3.3 Reaction of germylene **VI** with S_8 /PMe_3.

Germanthiones **II** and **VII** were stabilized by the intramolecular donors that can donate the lone pair of electrons into the vacant *d*-orbital of germanium atom increasing its electron density and decreasing the net atomic charges of germannium. The intramolecular donors incidentally decreas the polarity of Ge=X double bonds as well to enhace the stabilty of germanthiones **II** and **VII**.[15-17]

3.1.2 Intermolecular base stabilization of germanone

The germanones and germanthiones stabilized intermolecularly by base also have been reported. Driess and co-workers reported the reactions of silylene/germylene DMAP/NHC adducts with N_2O to afford silanone and germanone adducts, respectively (Figure 3.4).[18-19] This synthetic strategy has been first applied for the preparation of silanone adducts. (Figure 3.4)[20-23] As the result, the nucleophilicity of germylene has been increased by the donors. In contrast to the free germylene **VIII**, **VIII** cannot react with nitrous oxide at all.[18]

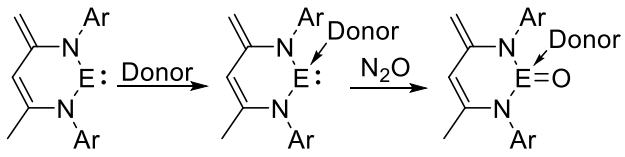

VIII **IX** **V**

(E = Si, Ge; Donor = DMAP, NHC)

Figure 3.4 Reaction of germylene or silylene **VIII** with N_2O.

3.1.3 Steric-stabilization of germanone and germanthione

As mentioned in the introduction of Chapter 3.1, the first transient germanones was reported in 1971 by Satgé and co-workers,[24] whereas the isolable monomeric germanone was reported in 2012.[5] Two decades ago, its sulfur congeners, germanthione without inter- or intramolecular coordination of donors were isolated and characterized by Okazaki and co-workers (Figure 3.5).[25]

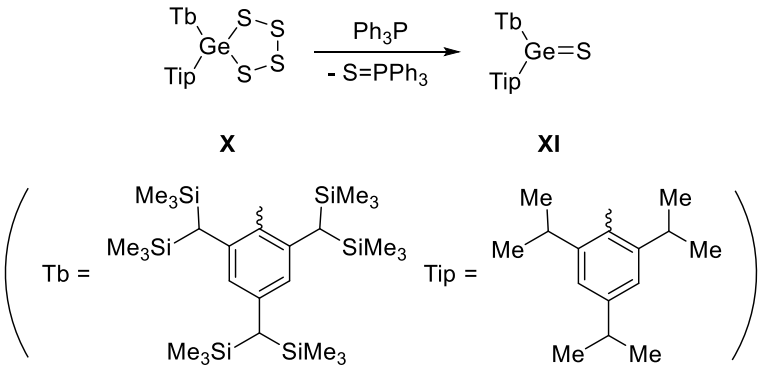

Figure 3.5 Reaction of tetrathiagermolane **X** with triphenylphosphine.

It should be noted that when mesityl (Mes) group was employed instead of Tip group, a dimer of germanthione **XI** was formed indicating that Mes is not bulky enough to stabilize the reactive germanthione **XI**.[26-27]

Nagendran and co-workers reported a new germanone intramolecularly stabilized by both donor and acceptor sites.[28] Interestingly, when they employed the μ-oxo dimer **XIII** instead of germylene **XII**, the addition of Lewis acids to **XIII** afforded the Lewis acids-germanone adducts **XIV** in a high yield. They also investigate the reactivity of germylene $ZnCl_2$ adduct **XV** with N_2O, from which the same product **XIV** was obtained in 96% yield (Figure 3.6).

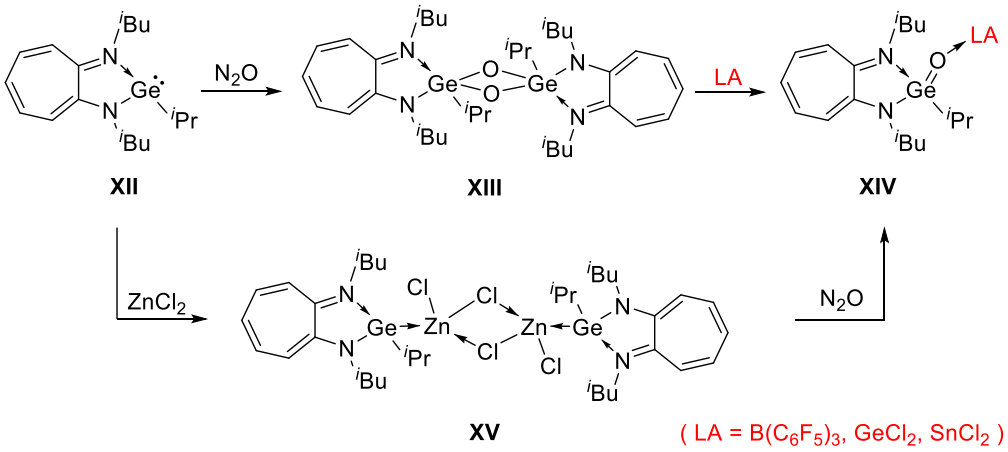

Figure 3.6 Generation of germanone **XIV**.

Although a few isolable germanones and germanthiones have been reported, more dimers or oligomers of germanones and germanthiones have been synthesized due to the deficiency of steric hindrance and/ or the high polarity of Ge=X (X = O or S) double bonds.[6-7, 28]

3.2 Results and Discussions

As has been mentioned in *chapter 2*, we have synthesized cyclic (alkyl)(amino) germylene **1** which possesses a high-lying HOMO and low-lying LUMO, as well as bulky substituents to protect germanium center. Herein, we present oxidation reactions toward S_8, N_2O and TEMPO.

*3.2.1 Reaction of germylene **1** with S_8*

At first, we tested the reaction of germylene **1** with excess S_8. The corresponding dimers **2a** and **2b** were obtained as a mixture of two diastereomers instead of the monomer. We carried out the optimization of the condition. Finally, the reaction gave the highest yield of 59% under the 8:1 ratio of **1** and S_8 at ambient temperature. (Scheme 3.1).

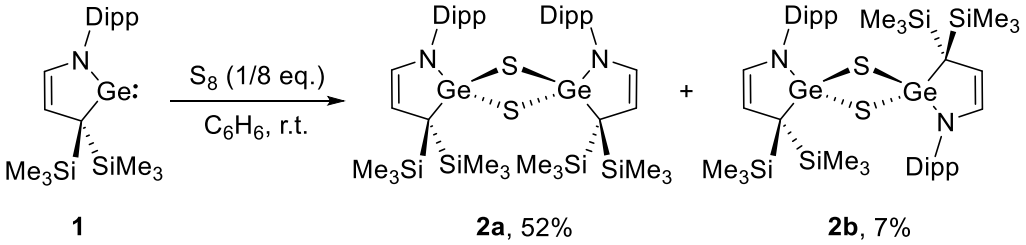

1 **2a**, 52% **2b**, 7%

Scheme 3.1 Reaction of germylene **1** with S_8.

Remarkably, the products **2a** and **2b** have great thermodynamics stability, and they even can be purified by column chromatography under air atmosphere. Subsequently, X-ray crystallographic analysis (Figure 3.7) confirmed that the structure of the major product **2a** possesses two 2,6-diisopropylphenyl groups located on the same side of the Ge_2S_2 plane. Both **2a** and **2b** involve a planar Ge_2S_2 four-membered ring. The S−Ge−S and Ge−S−Ge bond angles are 93.47(5) º and 86.56(5) º for **2a**, and 94.01(12) º and 85.99(12) º for **2b**, respectively. The Ge−S bond distances [**2a**: 2.2462(13) Å and 2.2406(13) Å, **2b**: 2.231(3) Å and 2.237(3) Å] are in the range reported of Ge−S single bonds (2.17-2.25 Å),[29] and longer than the Ge=S double bond length of 2.049(3) Å in [Tb(Trip)Ge=S] (Tb = 2,4,6-$((Me_3Si)_2CH)_3C_6H_2$, Trip = 2,4,6-$^{i}Pr_3C_6H_2$).[25]

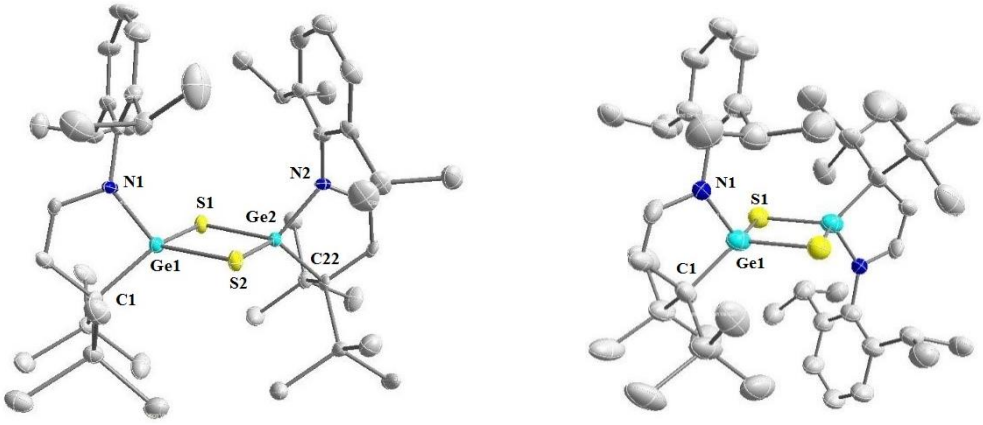

Figure 3.7 Solid-state structures of **2a** (left) and **2b** (right). Hydrogen atoms are omitted for clarity. Thermal ellipsoids are shown at the 50% probability level. Selected bond lengths [Å] and angles [º]: **2a**) Ge1-S1 2.2462(13), Ge1-S2 2.2406(13), Ge2-S1 2.2356(13), Ge2-S2 2.2483(13); S2-Ge1-S1 93.47(5), S1-Ge2-S2 93.55(5). **2b**) Ge1-S1 2.248(3), Ge1-S1 2.247(4); S1-Ge1-S1 94.27(12).

As mentioned in Chapter 3.1, when germanthiones can be isolated, that should be stable enough through the protections of thermodynamic and kinetic factors. To get the isolable germanthione, we introduced both intermolecular donors [pyridine, Me_3N, Ph_3P, and Et_3N] and acceptors [$AlCl_3$, $GaCl_3$, BPh_3 and $B(C_6F_5)_3$] to the mixture of **1** and S_8 (0.25 eq.). However, only the dimers **2** were obtained.[28, 30-31]

According to the ^1H NMR spectra, $AlCl_3$ and $B(C_6F_5)_3$ strongly interact with **1** over $GaCl_3$ (Figure 3.8). In the ^1H NMR spectra, a doublet for C*H* of **1** appears at 6.09 ppm, while the doublet was observed at 5.69 ppm with $B(C_6F_5)_3$, 5.82 ppm with $AlCl_3$, 6.06 ppm with $GaCl_3$, respectively (Figure 3.8).

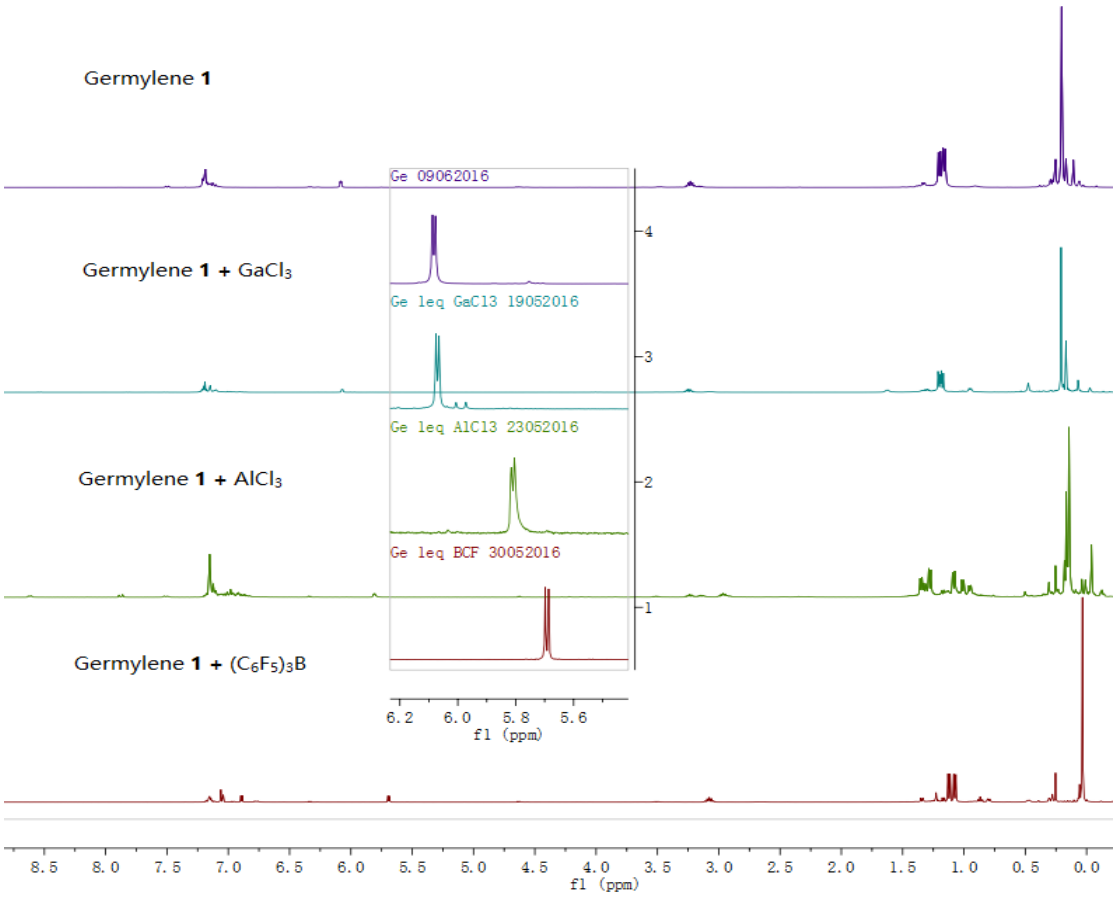

Figure 3.8 Comparison of the ^{1}H NMR spectra of germylene **1** and its Lewis acid adducts.

An unexpected product **3** was obtained from the reaction of **1** with $GaCl_3$ (Scheme 3.2). **3'** is a new germylene adduct which was stabilized by the imine N atom intramolecularly. The reaction of germylene **1** with HCl was hypothesized to generate intermediate **3'**, where HCl was generated from the hydrolysis of $GaCl_3$ possibly. The single crystal of **3** was obtained by recrystallization and its solid-state structure was confirmed by X-ray crystallographic analysis (Figure 3.9).

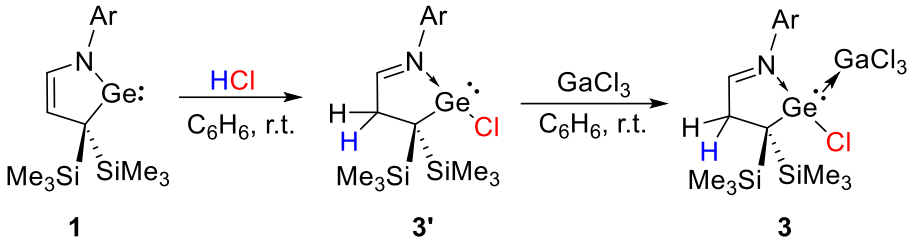

Scheme 3.2 Generation of germylene **3**.

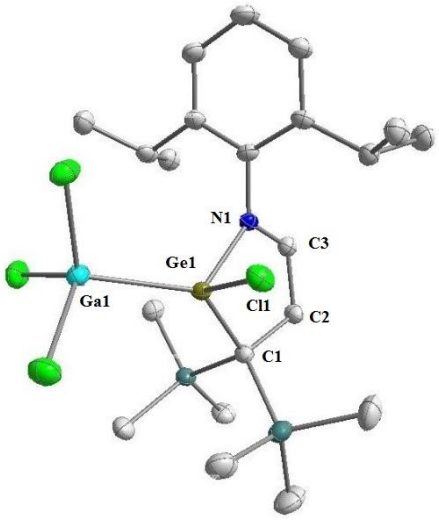

Figure 3.9 Solid-state structure of **3**. Hydrogen atoms are omitted for clarity. Thermal ellipsoids are shown at the 50% probability level. Selected bond lengths [Å] and angles [º]: Ga1-Ge1 2.4857(5), Ge1-C1 1.969(3), Ge1-N1 1.988(3), Ge1-Cl1 2.1997(8), C3-N1 1.280(4), C1-C2 1.565(4), C2-C3 1.488(4); C1-Ge1-Ga1 133.64(9), C1-Ge1-N1 89.53(12), C3-N1-Ge1 110.7(2), C3-C2-C1 113.4(3), C2-C1-Ge1 104.2(2), N1-C3-C2 120.6(3).

The $GeNC_3$ five-membered ring of **3** are coplanar (the sum of internal pentagon angles = 538.43 º for **3**). The Ge1−N1 bond [1.988(3) Å] distance is slightly longer than that [Ge1−N1 1.859(11) Å] of **1** (Figure 2.18), indicating a property of dative bond rather than a covalent bond. The N1−C3 bond [1.280(4) Å] distances are slightly shorter than that C13−N1 [1.410(16) Å] of **1**. The N1−Ge1−C1 bond angle [89.53(12) º] in **4** is more obtuse than the N1−Ge1−C15 bond angle of 86.5(5) º in **1**.

*3.2.2 Reaction of germylene **1** with N_2O*

Next we investigated the reaction of **1** with nitrous oxide that is well known as a powerful oxidizer for transition metals complexes and low-valent main group compounds.[18-19, 28, 32-36] As mentioned in the introduction of chapter 3.1, Driess and co-workers reported the reactivity of germylene **VIII** toward N_2O; however, there was no reaction in the absence of the donors.[18-19]

We carried out the reaction of germylene **1** with N_2O. After 1 hour at 40 °C, 1,3-digemadioxetane **4**, the dimeric form of germanone **4'**, was obtained in 90% yield (Scheme 3.3). **4** was purified by recrystallization as a white solid, and the solid-state structure was confirmed by X-ray crystallographic analysis (Figure 3.10).

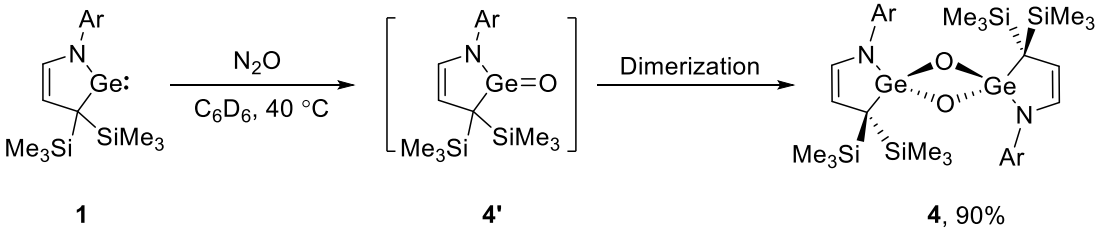

Scheme 3.3 Reaction of germylene **1** with N_2O.

Product **4** displays a spiro-structure involving a nearly planar Ge_2O_2 four-membered ring in which two 2,6-diisopropylphenyl groups are located on the opposite side with respect to the Ge_2O_2 plane. The O−Ge−O and Ge−O−Ge bond angles are 86.35(8) ° and 93.65(8) °, respectively. The Ge−O bond distances [1.8084(16) Å and 1.8090(17) Å] are almost identical to those [1.821(2) Å and 1.822(2) Å] in digermadioxetane reported by Kira *et al*.[37-38]

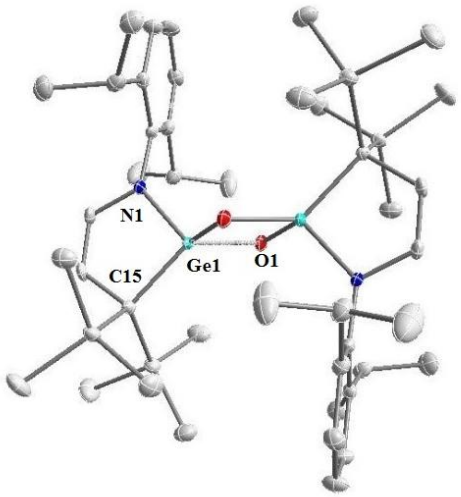

Figure 3.10 Solid-state structures of **4**. Hydrogen atoms are omitted for clarity. Thermal ellipsoids are shown at the 50% probability level. Selected bond lengths [Å] and angles [º]: Ge1-O1 1.8084(16), Ge1-N1 1.836(2), C15-Ge1 1.957(2); O1-Ge1-O1 86.35(8), N1-Ge1-C15 93.59(9), Ge1-O1-Ge1 93.65(8).

Next, we also introduced the intermolecular Lewis bases [pyridine, Me_3N, Ph_3P, and Et_3N] and Lewis acids [$AlCl_3$, $GaCl_3$, Ph_3B and $B(C_6F_5)_3$] to lower the polar of Ge=O double bond in the trapping reaction of the germanone **4'**,[28, 30-31] which afforded **4** as the final product. To compare the bond lengths of Ge–O in **4** with that of Ge–S bond in **3**, we can find that Ge−O bond distances [1.8084(16) Å and 1.8090(17) Å] are strikingly shorter than Ge−S bond distances [2.2462(13) Å and 2.2406]. Based on that, I think the stereoselectivity of the product **4** is depend on the steric effect, where the (Z) isomer is less stability than (E)-isomer.

*3.2.3 Reaction of germylene **1** with TEMPO*

2,2,6,6-tetramethylpiperidin-1-oxyl (TEMPO) is a well-known stable radical reagent used in oxidation reactions.[39] Kira and co-workers reported the reactions of TEMPO and metallylenes **XVI** (Scheme 3.4a),[38] which prompted us to explore the reaction of TEMPO with germylene **1**. We implemented the reaction of germylene **1** with two equivalents of TEMPO at ambient temperature, which afforded **5** in 71% yield (Scheme 3.4b). We also investigated 1:1 reaction

between **1** and TEMPO, which gave **5** again, and un-reacted **1** was recovered after the reaction. The thermolysis of **5** in benzene led to a complex mixture.

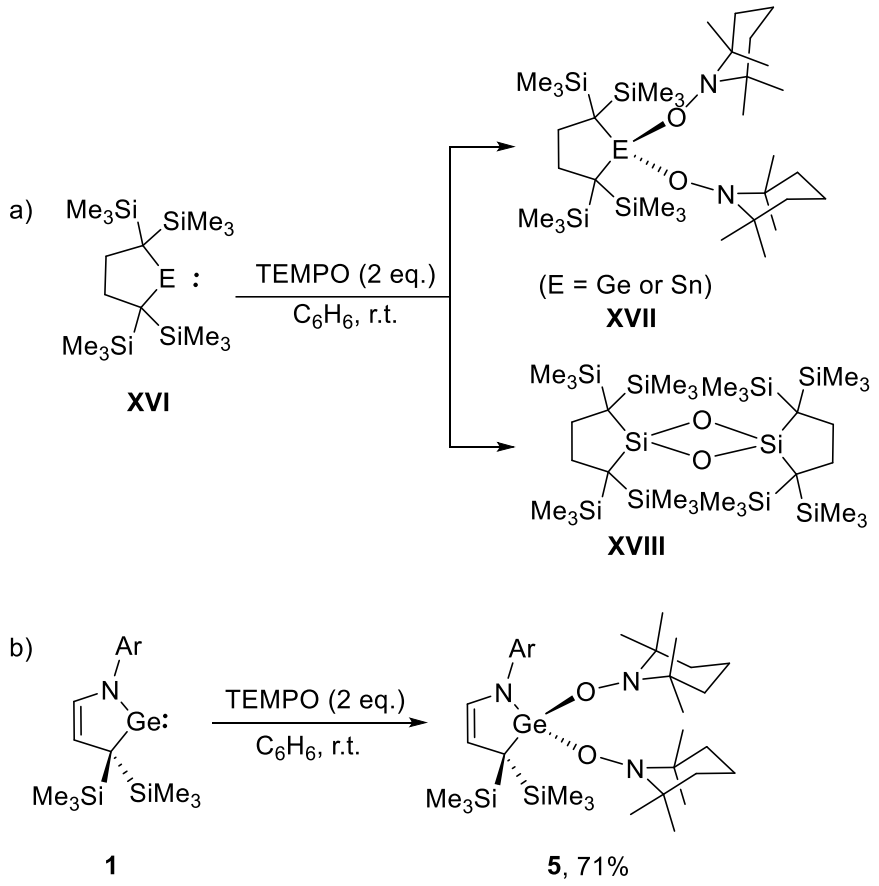

Scheme 3.4 The reaction of metallylenes with TEMPO.

The molecular structure of **5** was determined by X-ray crystallography in Figure 3.11. The Ge−O bond distances [1.814(3) Å and 1.796(3) Å] in **5** are lengthened with respect to the Ge=O double bond distance of 1.6468(5) Å in $(Eind)_2Ge{=}O$ (Eind = 1,1,3,3,5,5,7,7-octaethyl-s-hydrindacen-4-yl group),[5] and comparable to those [1.824(2) Å and 1.826(2) Å] in its homolog **XVII**.[37-38]

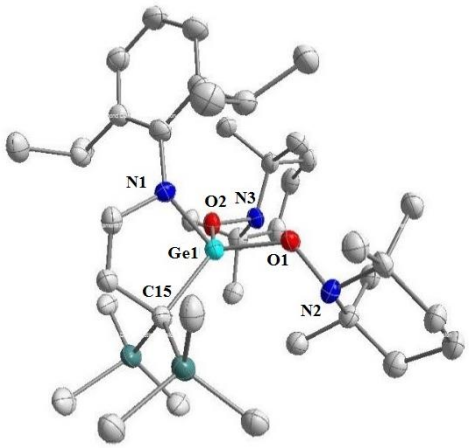

Figure 3.11 Solid-state structure of **5**. Hydrogen atoms are omitted for clarity. Thermal ellipsoids are shown at the 50% probability level. Selected bond lengths [Å] and angles [º]: Ge1-O2 1.814(3), Ge1-O1 1.796(3), N2-O1 1.479(4), N3-O2 1.479(4), Ge1-N1 1.871(3), C15-Ge1 2.020(4); O1-Ge1-O2 104.32(13), N1-Ge1-C15 92.67(16).

3.3 Conclusion

In this chapter, we have investigated the reactivity of germylene **1** with S_8 and N_2O with and without Lewis acids. The oxidation reaction of **1** by S_8 led to the formation of the sulfido-bridged dimers **3** as a mixture of two diastereomers involving Ge_2S_2 four-membered ring framework. In contrast, when **1** was oxidized by N_2O, and only trans product containing the Ge_2O_2 four-membered ring skeleton was obtained. The reaction of **1** with TEMPO led to the formation of a 1:2 adduct **5**.

3.4 Experimental Section

3.4.1 General Information

All reactions were performed under an atmosphere of argon by using standard Schlenk or dry box techniques; solvents were dried over sodium metal, potassium metal or CaH_2. All the substrates were obtained from the commercial sources or synthesized following literature procedures. Analytical thin layer chromatography was performed on triethylamine deactivated 0.25 mm silica gel 60-F254. Visualization was carried out with UV light. ^{1}H, and ^{13}C spectra were obtained with AVIII 400MHz BBFO1 spectrometer at 298 K. NMR multiplicities are abbreviated as follows: s = singlet, d = doublet, t = triplet, m = multiplet, br = broad signal. Coupling constants *J* are given in Hz. Electrospray ionization (ESI) mass spectra were obtained at the Mass Spectrometry Laboratory at the Division of Chemistry and Biological Chemistry, Nanyang Technological University. Melting points were measured with an OpticMelt Stanford Research System.

*3.4.2 Reaction of germylene **1** with S_8*

Cyclooctasulfur (S_8) (0.03 mmol, 7.4 mg) and **1** (0.23 mmol, 100 mg) were mixed in benzene (2 mL) and stirred for 1 hour at room temperature. After the solvent was removed under vacuum, the product was purified by silicone gel column chromatography (petroleum ether/ ethyl acetate = 10:1) to afford colorless crystals of **2a** (56 mg, 52%) and **2b** (7.5 m g, 7%).

2a: Mp: 230 °C (dec); ^{1}H NMR (400 MHz, $CDCl_3$) δ 7.10 (t, *J* = 7.7 Hz, 2H, Ar-*H*), 6.89 (d, *J* = 7.7 Hz, 4H, Ar-*H*), 6.19 (d, *J* = 6.1 Hz, 2H, C*H*), 4.75 (d, *J* = 6.1 Hz, 2H, C*H*), 3.00 (dt, *J* = 13.6, 6.8 Hz, 4H, C*H*), 0.96 (d, *J* = 6.9 Hz, 12H, CH_3), 0.93 (d, *J* = 6.7 Hz, 12H, CH_3), 0.27 (s, 36H, Si(CH_3)$_3$); ^{13}C NMR (100 MHz, $CDCl_3$) δ 146.96 (C^q), 140.92 (*C*H), 139.61 (C^q), 126.38 (*C*H), 123.58 (*C*H), 98.98 (*C*H), 28.18 (*C*H), 26.00 (*C*H_3), 22.91 (*C*H_3), 1.05 (Si(*C*H_3)$_3$); HRMS (ESI): m/z calcd for $C_{42}H_{75}N_2S_2Si_4Ge_2$: 931.2872. $[(M+H)]^+$; found: 931.2892.

2b: Mp: 237 °C (dec); ^{1}H NMR (400 MHz, $CDCl_3$) δ 7.18 (m, 6H, Ar-*H*), 6.32 (d, *J* = 6.0 Hz, 2H, C*H*), 4.68 (d, *J* = 6.0 Hz, 2H, C*H*), 3.24 (dt, *J* = 13.5, 6.8 Hz, 4H, C*H*), 1.32 (d, *J* = 6.8 Hz, 12H, CH_3), 1.04 (d, *J* = 6.8 Hz, 12H, CH_3), −0.01 (s, 36H, Si(CH_3)$_3$); ^{13}C NMR (100 MHz, $CDCl_3$) δ 147.88 (*C*^{q}), 140.31 (*C*H), 139.73 (*C*^{q}), 126.90 (*C*H), 123.67 (*C*H), 98.65 (*C*H), 28.55 (*C*H), 26.56 (*C*H_3), 22.27 (*C*H_3), 0.61 (Si(*C*H_3)$_3$); HRMS (ESI): m/z calcd for $C_{42}H_{75}N_2S_2Si_4Ge_2$: 931.2872. [(M+H)]$^{+}$; found: 931.2898.

*3.4.3 Reaction of germylene **1** with gallium trichloride*

Gallium trichloride (0.23 mmol, 41 mg) and **1** (0.23 mmol, 100 mg) were mixed in benzene (2 mL) and stirred for 5 min at room temperature. After the solvent was removed under vacuum, the mixture was washed with hexane and then recrystallized with benzene to afford colorless crystal of **3** (47 mg, 31%). ^{1}H NMR spectrum is very broad (Figure 3.16), which cannot be determined.

*3.4.4 Reaction of germylene **1** with nitrous oxide*

Nitrous oxide (0.23 mmol, 10 mg) was carefully condensed at liquid nitrogen in benzene solution of **1** (0.23 mmol, 100 mg). The reaction mixture was heated and stirred at 40 °C for 1 hour. After the solvent was removed under vacuum, the product was purified by recrystallization to afford colorless crystal of **4** (93 mg, 90%). Mp: 278 °C (dec). ^{1}H NMR (400 MHz, C_6D_6) δ 7.19 (m, 2H, Ar-*H*), 7.15 – 7.11 (m, 4H, Ar-*H*), 6.34 (d, J = 6.3 Hz, 2H, C*H*), 4.65 (d, J = 6.3 Hz, 2H, C*H*), 3.50 (dt, J = 13.6, 6.8 Hz, 4H, C*H*), 1.42 (d, J = 6.8 Hz, 12H, CH_3), 1.21 (d, J = 6.8 Hz, 12H, CH_3), 0.05 (s, 36H, Si(CH_3)$_3$); ^{13}C NMR (100 MHz, C_6D_6) δ 147.81 (*C*^{q}), 141.12 (*C*H), 140.44 (*C*^{q}), 123.91 (*C*H), 120.00 (*C*H), 97.48 (*C*H), 28.23 (*C*H), 26.01 (*C*H_3), 22.70 (*C*H_3), 0.25 (Si(CH_3)$_3$); HRMS (ESI): m/z calcd for $C_{42}H_{75}N_2O_2Si_4Ge_2$: 899.3329. [(M+H)]$^{+}$; found: 899.3361.

*3.4.5 Reaction of germylene **1** with TEMPO*

TEMPO (0.50 mmol, 78 mg) and **1** (0.23 mmol, 100 mg) were mixed in benzene (2 mL) and stirred for 5 min at room temperature. After the solvent was removed under vacuum, the product was recrystallized from hexane to afford colorless crystal of **5** (120 mg, 71%). Mp: 195 °C. ^{1}H NMR (400 MHz, C_6D_6) δ 7.18 (s, 3H, Ar-*H*), 6.43 (d, *J* = 6.6 Hz, 1H, C*H*), 4.66 (d, *J* = 6.6 Hz, 1H, C*H*), 3.87 (s, 2H, C*H*), 2.15 – 0.87 (m, 48H), 0.47 (s, 18H, Si(CH_3)$_3$); ^{13}C NMR (100 MHz, C_6D_6) δ 147.32 (*C*^{q}), 144.21 (*C*^{q}), 140.67 (*C*H), 126.43 (*C*H), 123.63 (*C*H), 97.13 (*C*H), 61.35 (*C*^{q}), 61.15 (*C*^{q}), 41.85 (*C*H$_3$), 41.35 (*C*H$_3$), 34.30 (*C*H$_2$), 28.10 (*C*H$_2$),26.47 (*C*H), 21.83 (*C*H$_2$), 16.96 (*C*H$_3$), 4.16 (Si(*C*H$_3$)$_3$); HRMS (ESI): m/z calcd for $C_{39}H_{74}N_3O_2Si_2Ge$: 746.4531. $[(M+H)]^+$; found: 746.4509.

3.4.6 ^{1}H and ^{13}C NMR Spectra

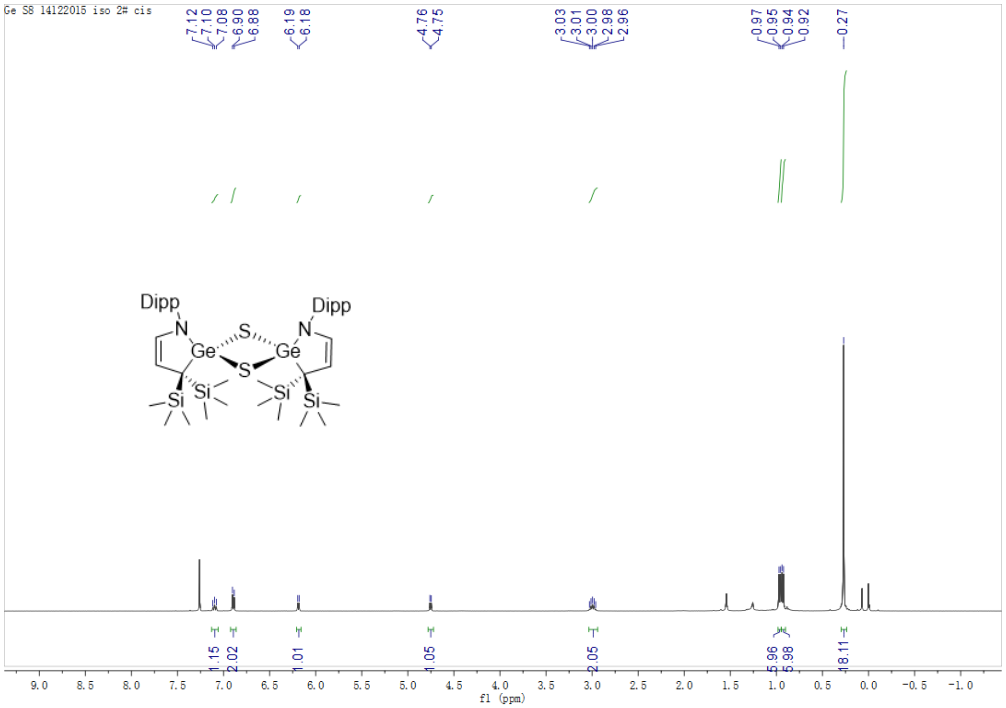

Figure 3.12 ^{1}H NMR spectrum of **2a**.

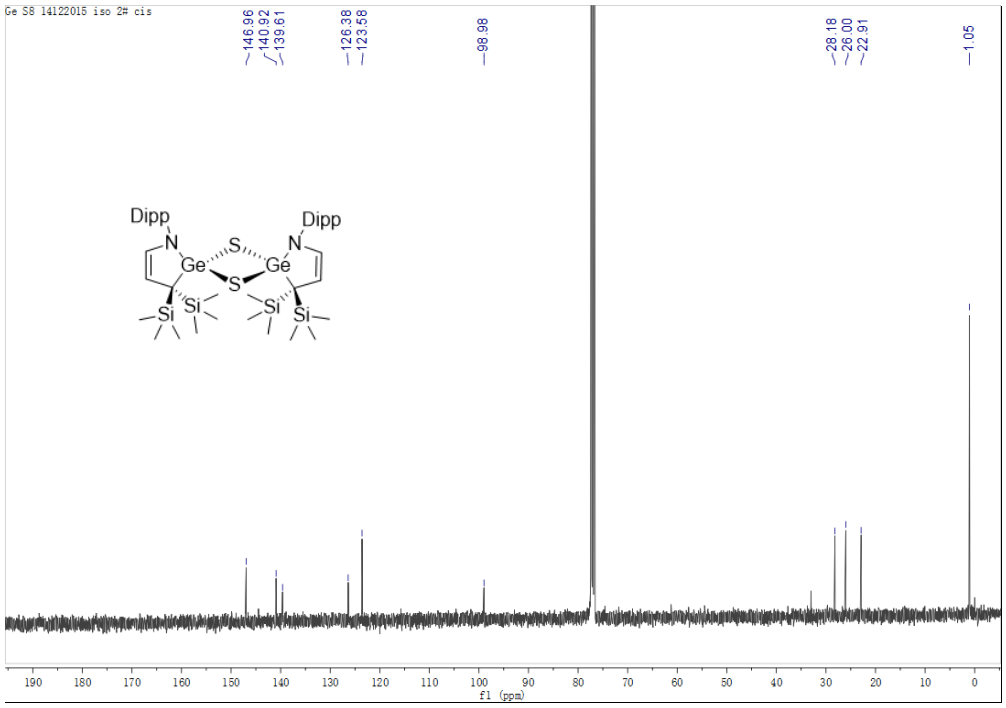

Figure 3.13 ^{13}C NMR spectrum of **2a**.

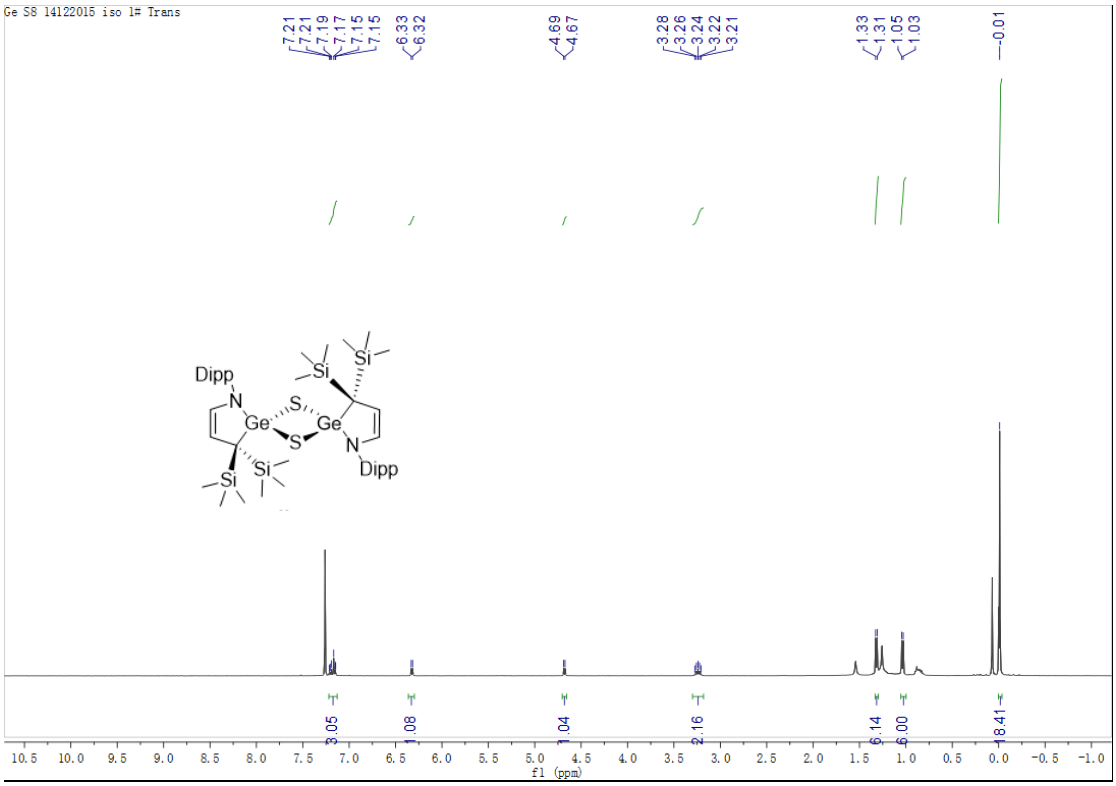

Figure 3.14 ^{1}H NMR spectrum of **2b**.

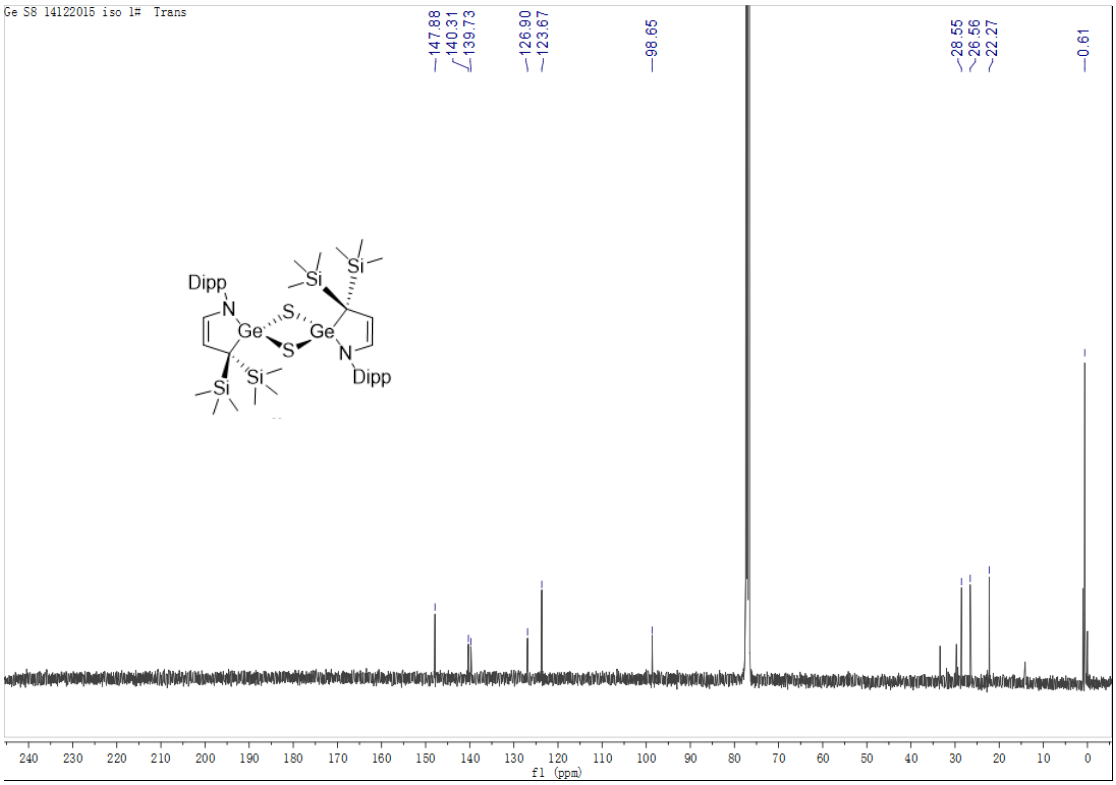

Figure 3.15 ^{13}C NMR spectrum of **2b**.

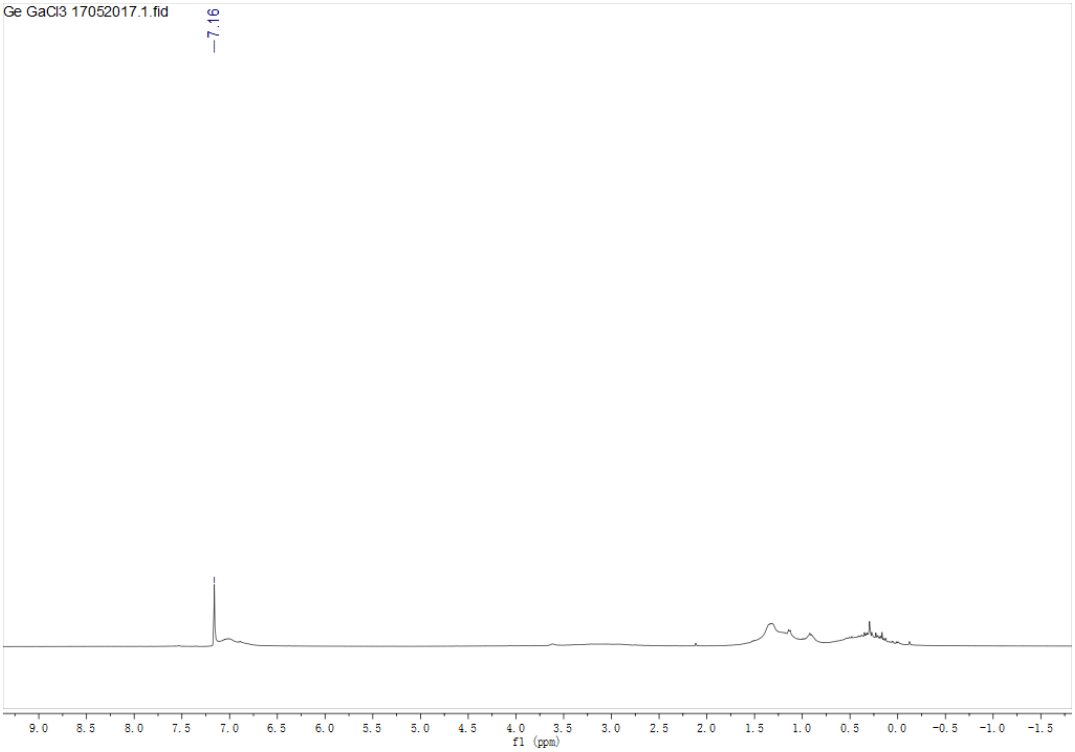

Figure 3.16 ^{1}H NMR spectrum of **3**.

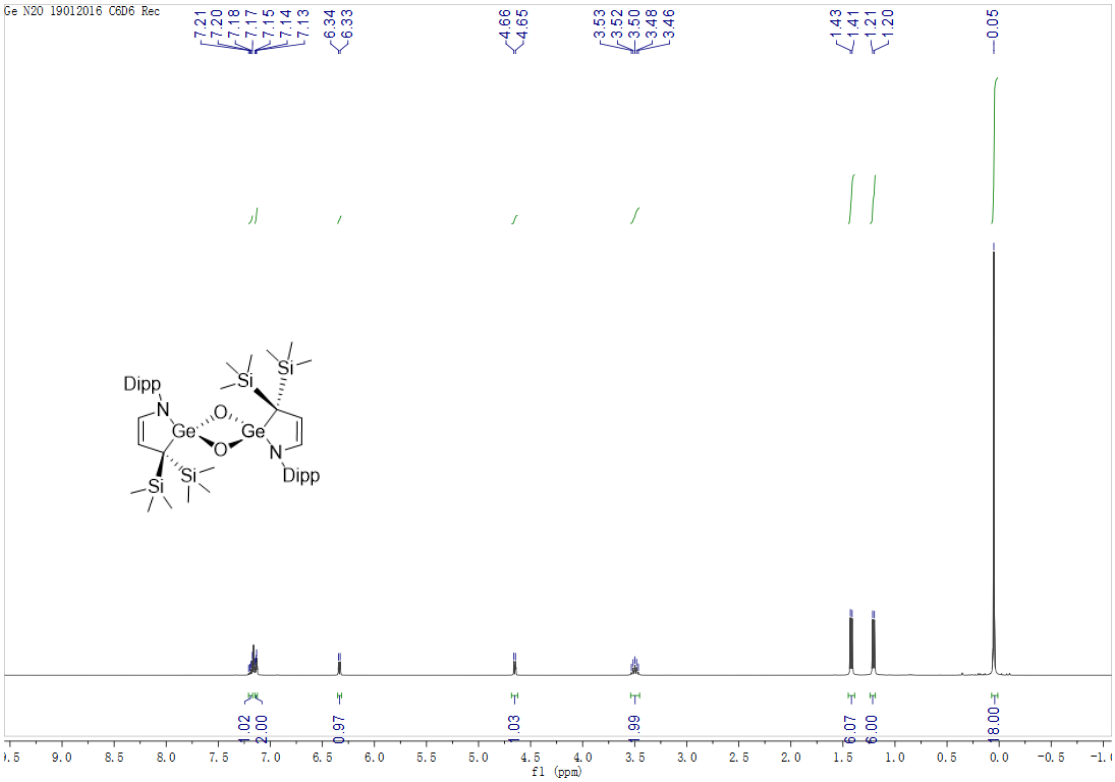

Figure 3.17 ^{1}H NMR spectrum of **4**.

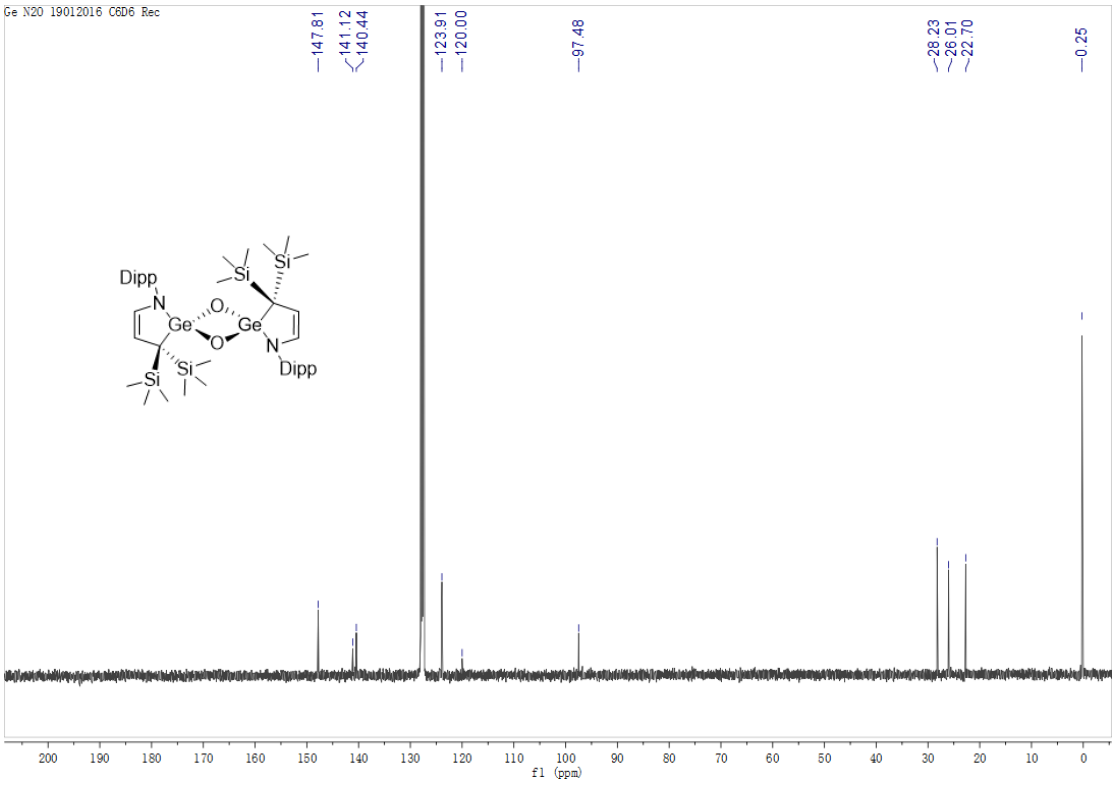

Figure 3.18 ^{13}C NMR spectrum of **4**.

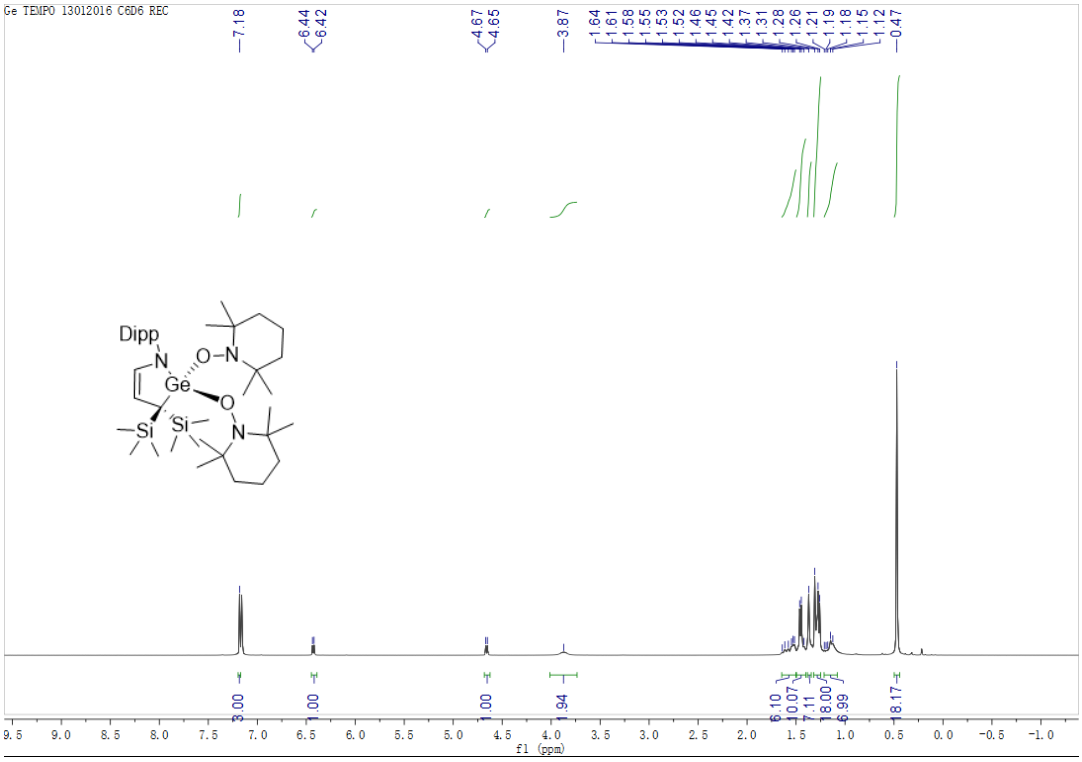

Figure 3.19 ^{1}H NMR spectrum of **5**.

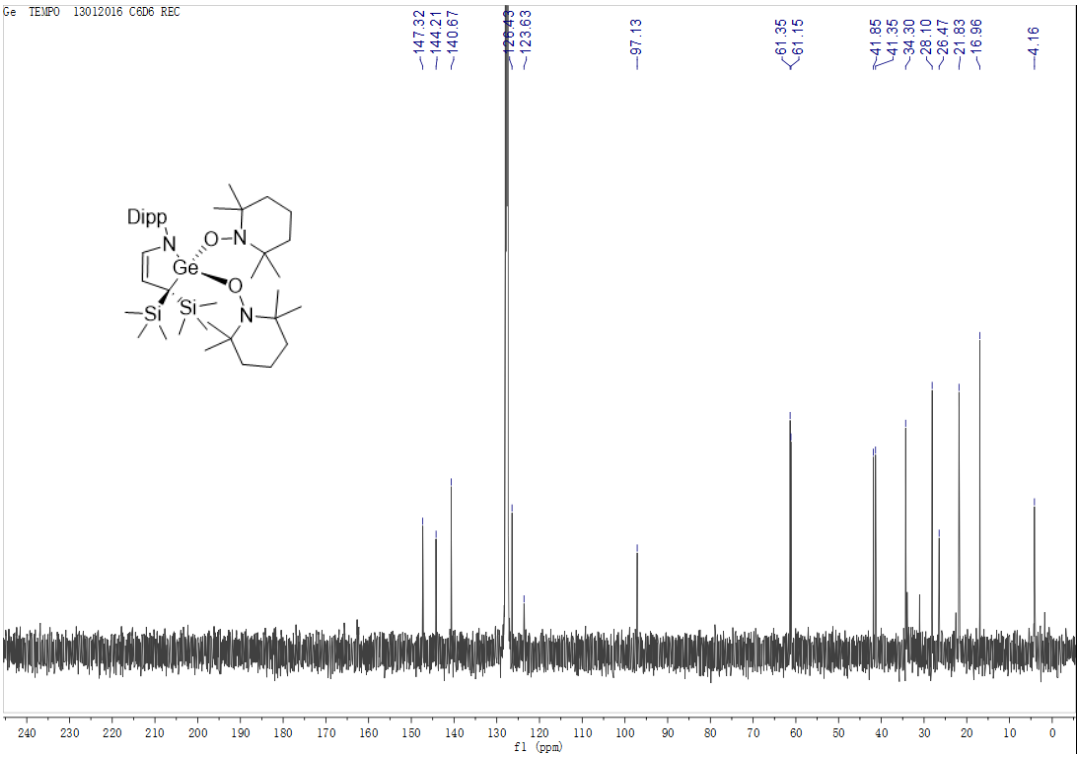

Figure 3.20 ^{13}C NMR spectrum of **5**.

3.5 Reference

1. Bräutigam, S.; Dennewald, D.; Schürmann, M.; Lutje-Spelberg, J.; Pitner, W.-R.; Weuster-Botz, D., *Enzyme Microb. Technol.* **2009,** *45*, 310-316.

2. Du, P.-X.; Wei, P.; Lou, W.-Y.; Zong, M.-H., *Microb Cell Fact.* **2014,** *13*, 84.

3. Bechara, W. S.; Pelletier, G.; Charette, A. B., *Nat. Chem.* **2012,** *4*, 228-234.

4. Trinquier, G.; Pelissier, M.; Saint-Roch, B.; Lavayssiere, H., *J. Organomet. Chem.* **1981,** *214*, 169-181.

5. Li, L.; Fukawa, T.; Matsuo, T.; Hashizume, D.; Fueno, H.; Tanaka, K.; Tamao, K., *Nat. Chem.* **2012,** *4*, 361-365.

6. Kapp, J.; Remko, M.; Schleyer, P. v. R., *J. Am. Chem. Soc.* **1996,** *118*, 5745-5751.

7. Kapp, J.; Remko, M.; Schleyer, P. v. R., *Inorg. Chem.* **1997,** *36*, 4241-4246.

8. Kutzelnigg, W., *Angew. Chem. Int. Ed. Engl.* **1984,** *23*, 272-295.

9. Benson, S. W., *Chem. Rev.* **1978,** *78*, 23-35.

10. Veith, M.; Becker, S.; Huch, V., *Angew. Chem. Int. Ed. Engl.* **1989,** *28*, 1237-1238.

11. Veith, M.; Detemple, A.; Huch, V., *Chem. Ber.* **1991,** *124*, 1135-1141.

12. Veith, M.; Detemple, A., *Phosphorus, Sulfur Silicon Relat. Elem.* **1992,** *65*, 17-24.

13. Trinquier, G.; Barthelat, J. C.; Satge, J., *J. Am. Chem. Soc.* **1982,** *104*, 5931-5936.

14. Kuchta, M. C.; Parkin, G., *J. Chem. Soc., Chem. Commun.* **1994**, 1351-1352.

15. Okazaki, R.; Tokitoh, N., *Acc. Chem. Res.* **2000,** *33*, 625-630.

16. Ossig, G.; Meller, A.; Brönneke, C.; Müller, O.; Schäfer, M.; Herbst-Irmer, R., *Organometallics* **1997,** *16*, 2116-2120.

17. Bender; Banaszak Holl, M. M.; Kampf, J. W., *Organometallics* **1997,** *16*, 2743-2745.

18. Yao, S.; Xiong, Y.; Driess, M., *Chem. Commun.* **2009**, 6466-6468.

19. Yao, S.; Xiong, Y.; Wang, W.; Driess, M., *Chem. Eur. J.* **2011,** *17*, 4890-4895.

20. Yao, S.; Xiong, Y.; Brym, M., *J. Am. Chem. Soc.* **2007,** *129*, 7268-7269.

21. Xiong, Y.; Yao, S.; Driess, M., *J. Am. Chem. Soc.* **2009,** *131*, 7562-7563.

22. Yao, S.; Xiong, Y.; Driess, M., *Chem. Eur. J.* **2010,** *16*, 1281-1288.

23. Xiong, Y.; Yao, S.; Müller, R.; Kaupp, M.; Driess, M., *J. Am. Chem. Soc.* **2010,** *132*, 6912-6913.

24. Barrau, J.; Massol, M.; Mesnard, D.; Satgé, J., *J. Organomet. Chem.* **1971,** *30*, C67-C69.

25. Tokitoh, N.; Matsumoto, T.; Manmaru, K.; Okazaki, R., *J. Am. Chem. Soc.* **1993,** *115*, 8855-8856.

26. Tokitoh, N.; Suzuki, H.; Matsumoto, T.; Matsuhashi, Y.; Okazaki, R.; Goto, M., *J. Am. Chem. Soc.* **1991,** *113*, 7047-7049.

27. Kühl, O.; Lönnecke, P.; Heinicke, J., *Polyhedron* **2001,** *20*, 2215-2222.

28. Sinhababu, S.; Yadav, D.; Karwasara, S.; Sharma, M. K.; Mukherjee, G.; Rajaraman, G.; Nagendran, S., *Angew. Chem. Int. Ed.* **2016,** *55*, 7742-7746.

29. Matsumoto, T.; Tokitoh, N.; Okazaki, R., *J. Am. Chem. Soc.* **1999,** *121*, 8811-8824.

30. Xiong, Y.; Yao, S.; Karni, M.; Kostenko, A.; Burchert, A.; Apeloig, Y.; Driess, M., *Chem. Sci.* **2016,** *7*, 5462-5469.

31. Xiong, Y.; Yao, S.; Driess, M., *Angew. Chem. Int. Ed.* **2013,** *52*, 4302-4311.

32. Lee, D.-H.; Mondal, B.; Karlin, K. D., Nitrogen Monoxide and Nitrous Oxide Binding and Reduction. In *Activation of Small Molecules*, Wiley-VCH Verlag GmbH & Co. KGaA: 2006; pp 43-79.

33. Tolman, W. B., *Angew. Chem. Int. Ed.* **2010,** *49*, 1018-1024.

34. Horn, B.; Limberg, C.; Herwig, C.; Feist, M.; Mebs, S., *Chem. Commun.* **2012,** *48*, 8243-8245.

35. Jana, A.; Roesky, H. W.; Schulzke, C., *Dalton Trans.* **2010,** *39*, 132-138.

36. Azhakar, R.; Pröpper, K.; Dittrich, B.; Roesky, H. W., *Organometallics* **2012,** *31*, 7586-7590.

37. Iwamoto, T.; Masuda, H.; Ishida, S.; Kabuto, C.; Kira, M., *J. Organomet. Chem.* **2004,** *689*, 1337-1341.

38. Iwamoto, T.; Masuda, H.; Ishida, S.; Kabuto, C.; Kira, M., *J. Am. Chem. Soc.* **2003,** *125*, 9300-9301.

39. Barriga, S., *Synlett* **2001,** *2001*, 0563.

Chapter 4 Equilibrium of silylium exchange: germylene activation of hydrosilanes under $B(C_6F_5)_3$ catalysis

4.1 Introduction

Hydrosilanes, which are organosilanes containing both organic substituents and at least one silicon−hydrogen bond, were utilized as the hydrogen source to reduce organic compounds, such as alcohol,[1-4] ether,[3-5] and ketone.[6-11] Although the H atom in hydrosilanes exhibits certain hydridic nature due to the difference in electronegativity between Si (χ = 1.9) and H (χ = 2.1), they are not intrinsic nucleophiles. In general, hydrosilanes do not react spontaneously with organic substrates unless the substrates are strong electrophiles. Alternatively, hydrosilanes can be activated with electrophiles or Lewis acids, such as carbocation $(R_3C)^+$, and tris(pentafluorophenyl)borane $B(C_6F_5)_3$.[3, 12-13]

The activation of hydrosilanes with Group 14 divalent species has attracted much attention due to the oxidation processes that occur at the metallylene center under mild conditions. These are also considered the challenge in the chemistry of Group 14 metallylenes.[14-15]

4.1.1 Activating the Si−H bond in hydrosilanes by carbenes

For many years, it was hypothesized that only transition-metal centers were able to activate hydrosilanes due to the high bond dissociation energy of the Si−H bond (90 kcal/mol), which is comparable to that of the C−H bond (92 kcal/mol).[16-18] In 2010, the first example of hydrosilane activation by cyclic (alkyl)(amino) carbenes (CAACs) **I** and *N*-heterocyclic carbene (NHC) **II** was reported by Bertrand *et al.*; the corresponding products **III** and **IV** were generated via the insertion of the Si−H bond at the carbene center (Scheme 4.1).[15]

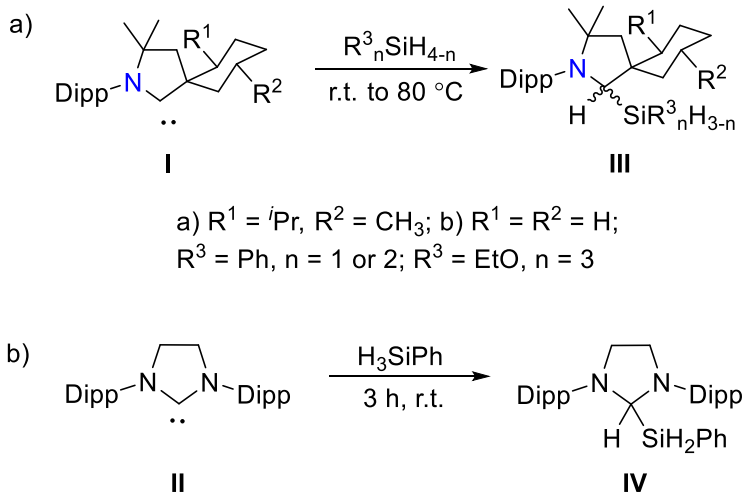

Scheme 4.1 Hydrosilane activation by CAACs **I** and NHC **II**.

In 2012, Radius and co-workers observed the ring expansion of the NHCs when hydrosilane was treated at a higher reaction temperature. This ring expansion involved the cleavage of a C−N bond in the NHCs **II** (Scheme 4.2).[19] A proposed reaction pathway for the formation of **V** is shown in Scheme 4.3. First, carbenes **II** are inserted into the hydrosilane Si−H bond to afford product **VI**. The subsequent C−N bond cleavage of NHCs is concomitant with the formation of a Si−N bond that generates the zwitterionic intermediate **VII**. The final step may involve the migration of a hydrogen atom from the Si center to the adjacent C atom to provide **Vb**.

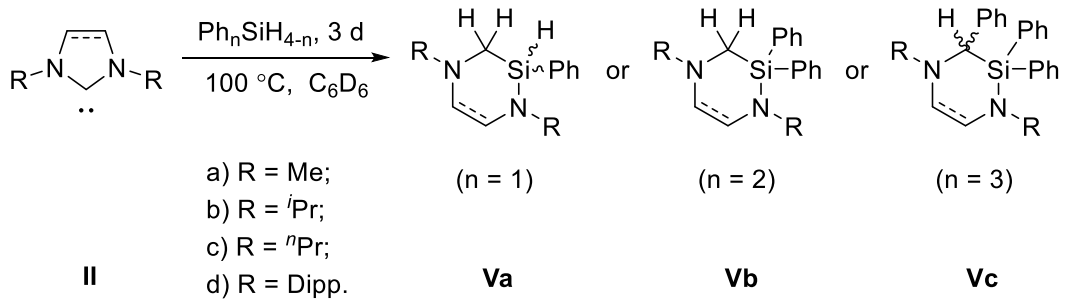

Scheme 4.2 Reaction of various NHCs **II** with hydrosilanes.

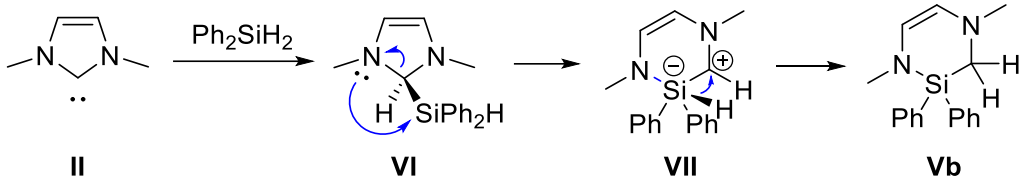

Scheme 4.3 Proposed reaction path for the formation of **Vb**.

In 2015, Bielawski *et al.* reported another Si−H bond activation by DAC **VIII** to form **IX** (Scheme 4.4).[20] This reaction is similar to the hydrosilanes activation by CAACs **I**[15] and NHCs **II**[19]. Collectively, the initial step is the formation of carbene→hydrosilane (supervalent) complexes, which has been considered the key step in the aforementioned Si–H bond activations.[21]

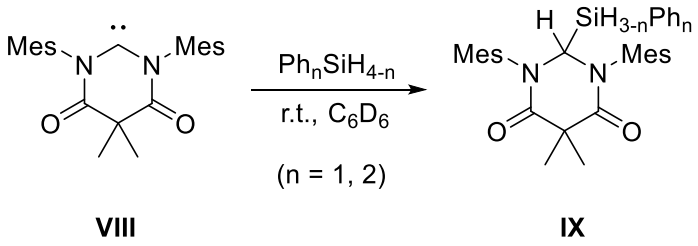

Scheme 4.4 Reactions of DAC **VIII** with hydrosilanes.

4.1.2 Activating the Si−H bond in hydrosilanes by silylenes

Hydrosilanes activation by silylenes, the silicon analogues of carbenes, has also been reported. In 2003, Kira and co-workers showed that the reactions of silylene **XI** with various chlorosilanes afforded either the Si−H insertion **X** or Si−Cl bond insertion **XII** products (Scheme 4.5).[22] The corresponding Si−H bond insertion products **X** were obtained exclusively, when the reactions of silylene **XI** with dimethylchlorosilane and trimethylsilane were performed. These reactions indicated that the Si−Cl insertion was more sensitive to steric hindrance than Si−H insertion.

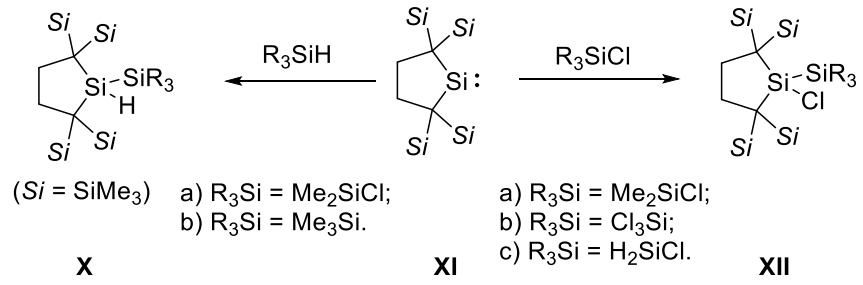

Scheme 4.5 Reactions of silylene **XI** with various silanes.

Most recently, a reversible activation of hydrosilane by silylene **XIII** was reported by Kato *et al*.[14] Silylene **XIII** readily reacted with phenylsilane at ambient temperature to afford the corresponding Si−H bond insertion product **XIV** in 49% isolated yield (Scheme 4.6). It is noteworthy that the **XIII**: **XIV** ratio was temperature dependent. The proportional decrease with increasing temperature indicated that the reaction involved an equilibrium process.

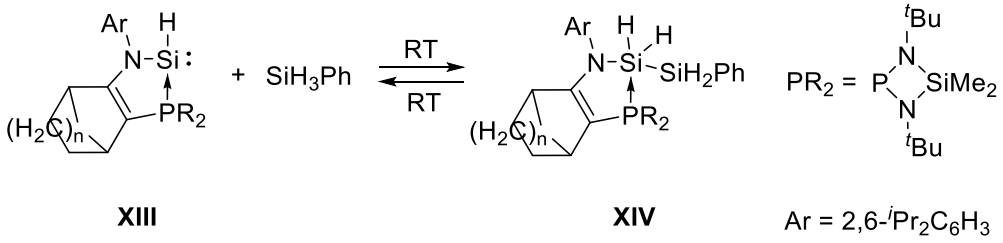

Scheme 4.6 Reversible insertion reaction of silylene **XIII** with hydrosilane.

4.1.3 Activating the Si−H bond in hydrosilane by germylene

In 2015, Tobita and co-workers reported the activation of hydrosilane by cationic germylene **XV** that contained tungsten and NHC units.[23] The reaction of germylene **XV** with hydrosilane at room temperature underwent the Si−H bond insertion to afford the product **XVI** (Scheme 4.7). Notably, **XV** regenerated to achieve equilibrium when a fluorobenzene solution of **XVI** was heated to 60 ℃. Although this Si−H bond activation process is reversible, the decomposition of both **XV** and **XVI** was observed when the mixture was heated above 80 ℃.

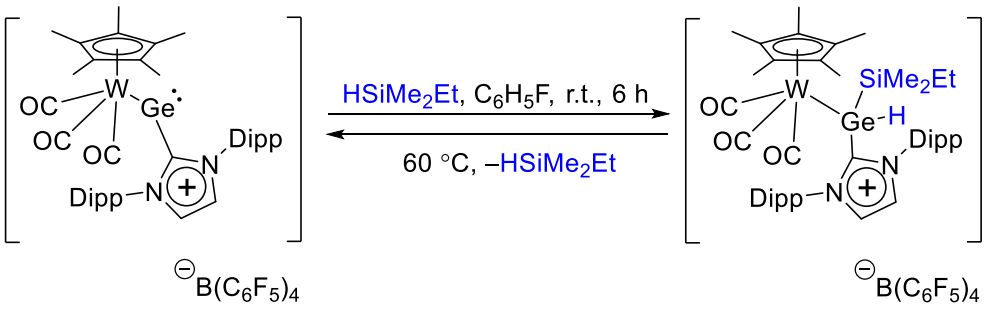

XV **XVI**

Scheme 4.7 Reaction of cationic germylene **XV** with hydrosilane.

Kato *et al.* subsequently reported the activation of hydrosilane by germylene **XVII**/$B(C_6F_5)_3$ adduct **XVIII**, where germylene **XVII** was regarded as a donor component of frustrated Lewis pairs (FLPs).[24] The adduct **XVIII** reacted with hydrosilane to provide cationic germylene **XIX** via the Si−H bond cleavage (Scheme 4.8). In contrast, the reaction of **XVIII** with phenylsilane afforded **XX**, which was likely formed by an initial Si−H bond activation from the P/B Lewis pair. This was followed by the insertion of germylene into the Si−H bond of another phenylsilane.

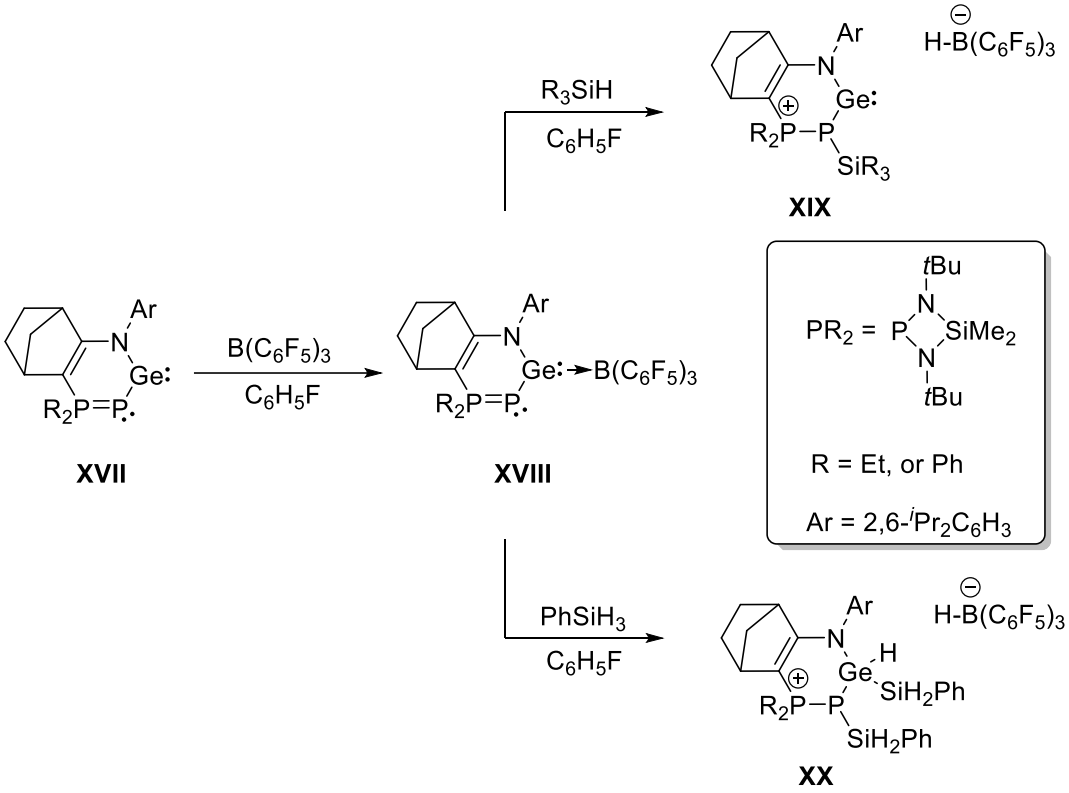

Scheme 4.8 Reactions of germylene/$B(C_6F_5)_3$ adduct **XVIII** with hydrosilanes.

It is well known that $B(C_6F_5)_3$ can be utilized for hydrosilanes activation, and ion-like silylium of the type $R_3Si^{\delta+}Y^{\delta-}$ **XXI** are key species for reducing various organic substrates.[25-29] Hydrosilanes activation by $B(C_6F_5)_3$ is reversible. Although **XXI** are not free silylium ions, they can act like silylium ions (Scheme 4.9).[3, 24-25, 30-33]

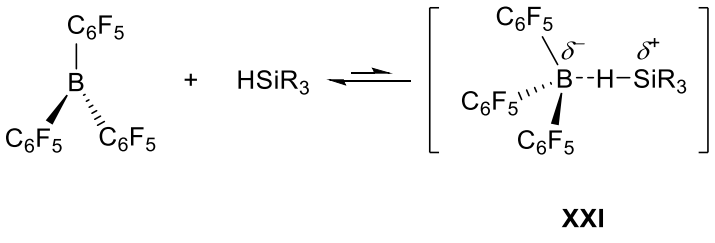

XXI

Scheme 4.9 Reversible activation of hydrosilanes by $B(C_6F_5)_3$.

Hydrosilane activation by germylene has been reported both by Tobita *et al.*[23] and Kato *et al.*[24] To the best of our knowledge, although the direct activation of hydrosilane by neutral

isolable germylene is unknown, the activation of Et_3SiH was utilized by Baines and co-workers trapping the transient germylene and affording the insertion product of Si-H bond.[34] Because we synthesized a cyclic (alkyl)(amino) germylene **1** possessing the high-lying HOMO and low-lying LUMO, as described in *Chapter 2*, here we present the reaction of germylene **1** with hydrosilanes under mild conditions.

4.2 Results and Discussions

*4.2.1 Reaction of germylene **1** with hydrosilanes*

First, the reaction of diphenylsilane **2a** with germylene **1** was examined at room temperature. No reaction was observed until the mixture was heated to 100 °C for three days (Scheme 4.10). Despite such harsh conditions and prolonged reaction time, only 30% conversion from germylene **1** to an indeterminate symmetric product **3** was observed as determined by ^{1}H NMR spectroscopy. The activation of triethylsilane (Et_3SiH) by germylene **1** was also investigated under the same conditions, but no reaction was observed.

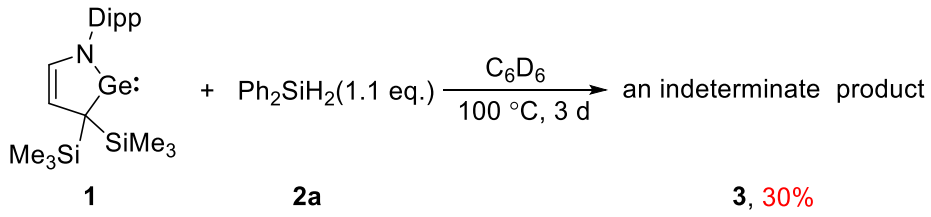

Scheme 4.10 Activation of silane **2** with germylene **1**.

As introduced in *Chapter 4.1.3*, $B(C_6F_5)_3$ can be utilized for hydrosilane activation. Herein, it is expected that $B(C_6F_5)_3$ can promote hydrosilane activation by **1**. Hence, 20 mol% $B(C_6F_5)_3$ was employed for the reaction of germylene **1** with 10 equivalents of diphenylsilane **2a**. After 3 h at 90 °C, three products formed, including the indeterminate symmetric product **3** (Scheme 4.11). The other two products were assigned to germylenes **4a** and **5**, respectively, based on ^{1}H NMR spectroscopy. Three new doublet peaks appeared for one of the respective *C(sp^2)H* proton in the five-membered ring at 6.67 ppm (**5**), 6.45 ppm (**4a**) and 6.37 ppm (**3**). There was a peak with a chemical shift of 4.19 ppm, which overlapped with the *C(sp^2)H* proton in **3** and belonged to the Me_3Si-*H* proton in **6** (Figure 4.1).

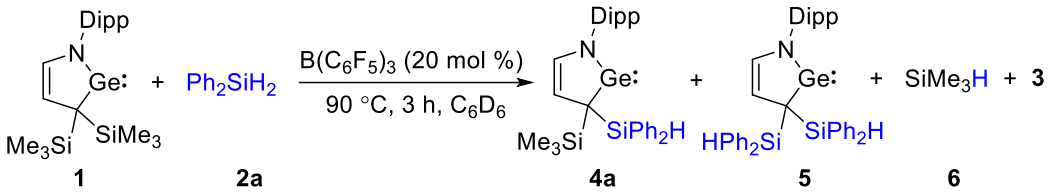

Scheme 4.11 Activating diphenylsilane **2a** by germylene **1** in the presence of catalytic $B(C_6F_5)_3$.

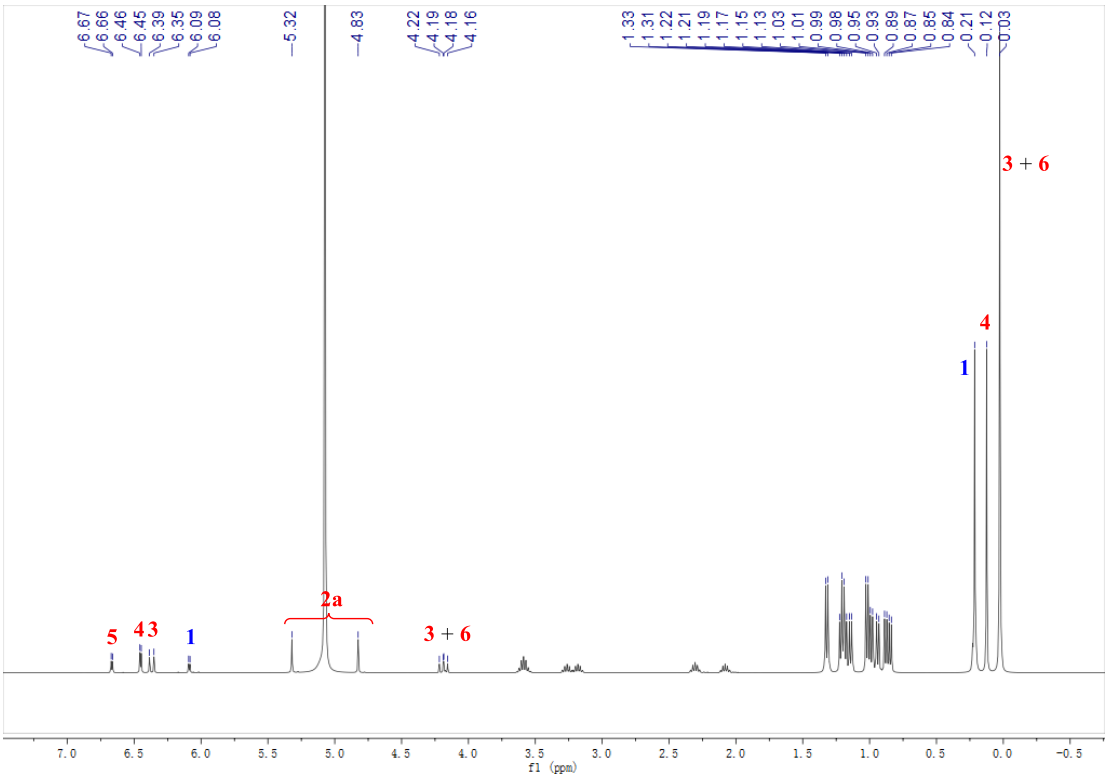

Figure 4.1 ^{1}H NMR spectrum (fitted) of the **2a** and **1** mixture after 3 h at 90 °C.

The reaction of Et_3SiH **2b** with germylene **1** in the presence of catalytic $B(C_6F_5)_3$ for 3 d at 100 °C produced similar results, and included indeterminate symmetric product **3** and germylene **4b** via the unimolecular substitution reaction (Scheme 4.12).

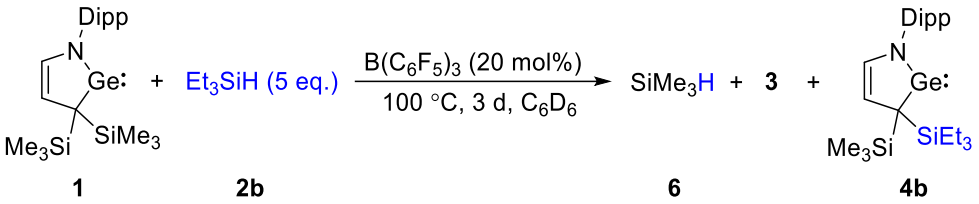

Scheme 4.12 Activation of triethylsilane **2b** with germylene **1** in the presence of catalytic $B(C_6F_5)_3$.

The proposed mechanism for the formation of germylene **4** is shown in Scheme 4.13. Two key equilibrium steps are involved in the reaction: a) the reaction of hydrosilane **2** with $B(C_6F_5)_3$ is the initial step to afford silylium-like **2'**, which further reacts with germylene **1** to generate the intermediate **1a**; b) silylium **6'** reacts with $[HB(C_6F_5)_3]^-$ to provide free $B(C_6F_5)_3$ and trimethylsilane **6**. Germylene **4** is formed from **1a'** via a silyl [1,2] migration (Scheme 4.13).

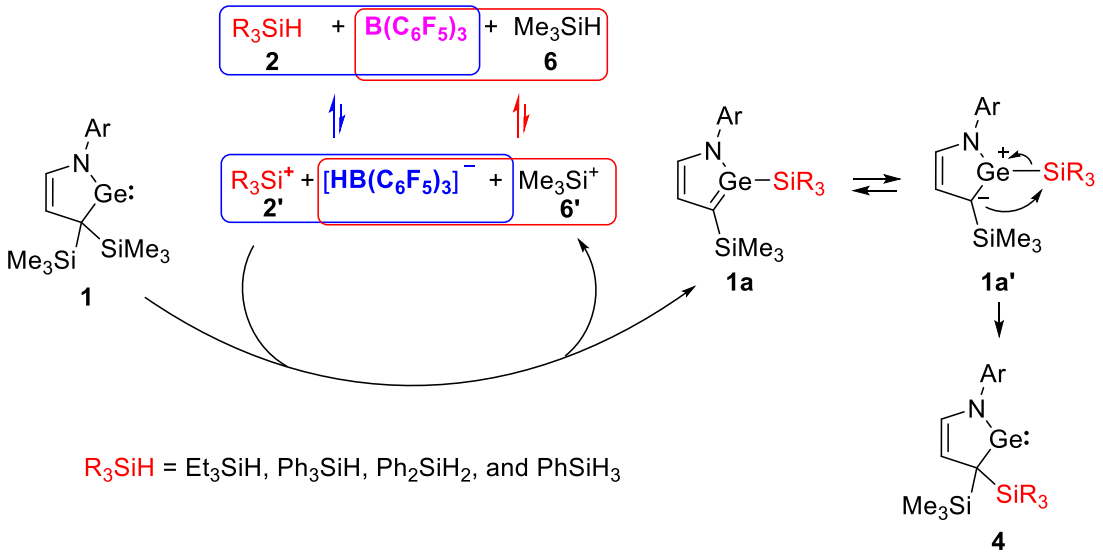

Scheme 4.13 Proposed mechanism for the formation of products **4**.

Based on the proposed mechanism, it is hypothesized that an increase in the nucleophilicity of germylene **1** will promote the reactivity of germylene **1** by forming [germylene-SiR_3]$^+$ adduct due to enhanced bond (Ge−Si) dissociation energy. Therefore, we modified the germylene **1** by replacing the 2,6-diisopropylphenyl group with a stronger electron-donating inductive effect (+I) 1-admantyl group to increase the electron density at the germanium center.[35]

First, we briefly analyzed the molecular orbitals (MOs) of germylenes **1** and **7** using a DFT calculation at the theoretical B3LYP/6-31G(d,p) level (Figure 4.2). The HOMO−1 of **7** corresponds to the lone pair of germylenes, which is higher in energy than that of **1**. The HOMO−LUMO gap (3.98 eV) of germylene **7** is slightly larger than that (3.94 eV) of **1**. This short analysis indicated that the modified germylene **7** would exhibit a stronger nucleophilicity than germylene **1**, which fit our expectations.

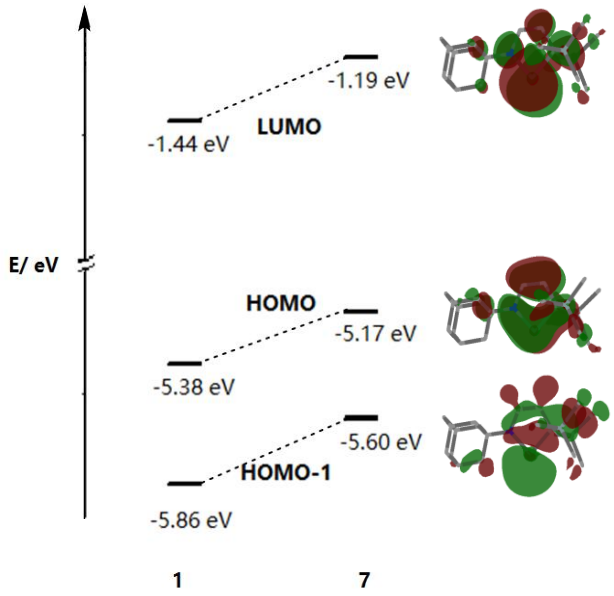

Figure 4.2 a) MOs comparison between **1** and **7**; b) Plots of LUMO (top), HOMO (middle), and HOMO–1 (bottom) of **7** at the B3LYP/6-31G(d,p) level (the hydrogen atoms are omitted for clarity).

*4.2.2 Synthesis of modified germylene **7***

As indicated in *Chapter 2*, the synthesis of modified cyclic (alkyl)(amino) germylene **7** is based on the synthetic route to germylene **1**. First, the reaction of 3,3-bis(trimethylsilyl)acrylaldehyde with amantadine was conducted in toluene, from which α,β-unsaturated imine **8** was obtained in 65% isolated yield (Scheme 4.14). The solid-state molecular structure of α,β-unsaturated imine **8** was determined by single-crystal X-ray diffraction analysis

(Figure 4.3b). Then α,β-unsaturated imine **8** was reacted with 1.2 equivalents of germanium dichloride–dioxane complex to afford a dichlorogermane **9**.

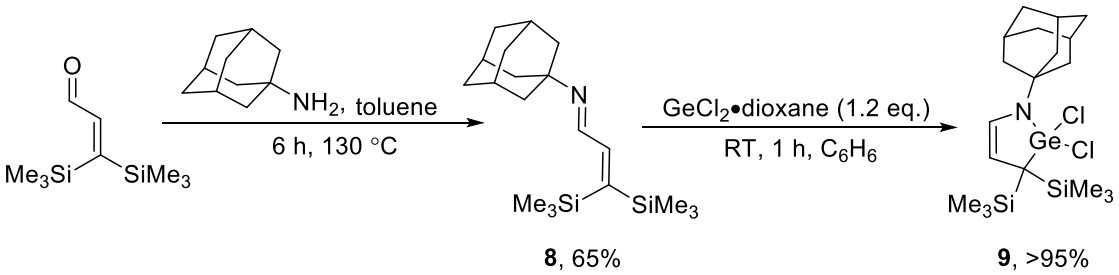

8, 65% **9**, >95%

Scheme 4.14 Synthesis of α,β-unsaturated imine **8** and dichlorogermane **9**.

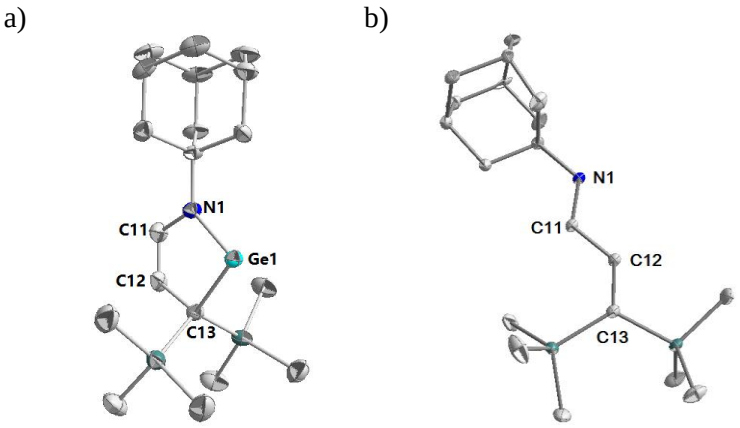

7 **8**

Figure 4.3 Solid state structures of **7** (left) and **8** (right). Hydrogen atoms are omitted for clarity. Thermal ellipsoids are shown at the 50% probability level. Selected bond lengths [Å] and angles [°]: a) N1-C11 1.365(5), C11-C12 1332(6), C12-C13 1.517(5), Ge1-C13 2.002(4), Ge1-N1 1.859(3); N1-C11-C12 121.8, N1-Ge1-C13 87.07(15), C11-N1-Ge1 113.5(3), Ge1-C13-C12 104.7(3), Si1-C13-Si2 119.9(2); b) N1-C11 1.276(2), C11-C12 1.465(2), C12-C13 1.356(2); N1-C11-C12 119.51(14), C11-C12-C13 126.74(14).

The reaction of **9** with 2.5 equivalents of potassium graphite (KC_8) was performed at −30 °C in THF for 20 h. Germylene **7** was isolated as a yellow solid in 93% yield after purification (Scheme 4.15). The solid-state structure of germylene **7** was determined by single-crystal X-ray diffraction analysis, it showed similar metric parameters to those of germylene **1** (Figure 4.3a).[36]

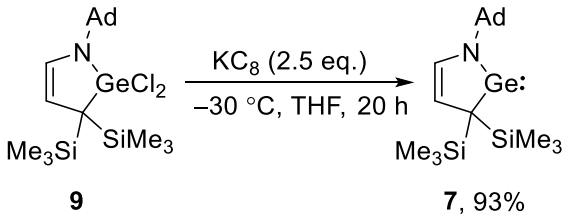

9 **7**, 93%

Scheme 4.15 Synthesis of germylene **7**.

In the ^{1}H NMR spectrum of **7**, a singlet for Me_3Si group appears at 0.18 ppm, which is nearly identical to that (0.21 ppm) of germylene **1**. Two doublets appear at 7.65 ppm and 6.22 ppm corresponding to the C*(sp^2)-H* protons in germylene **7**, which are significantly shifted downfield compared with the corresponding peaks of germylene 1, 7.22 ppm and 6.09 ppm (Figure 4.4).

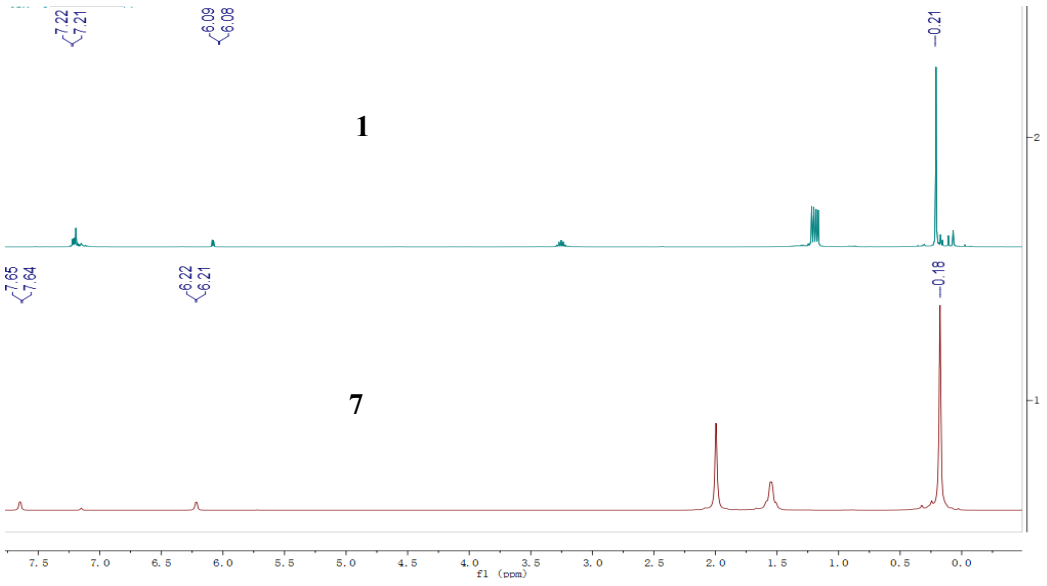

Figure 4.4 ^{1}H NMR spectra of germylene **1** (top) and germylene **7** (bottom).

4.2.3 Reaction of germylene 7 with hydrosilanes in the presence of $B(C_6F_5)_3$

The reaction of **7** with hydrosilanes **2** in the presence of 20 mol% $B(C_6F_5)_3$ was examined. Different products were obtained depending on the hydrosilane substrates. When four equivalents of diphenylsilane **2a** were used in the reaction, the corresponding germylene product **10** was obtained in 91% isolated yield (Scheme 4.16). Germylene **10** was characterized using ^{1}H NMR spectroscopy (Figure 4.5) and single-crystal X-ray diffraction analysis (Figure 4.6). In comparison with **7**, the Si1-C3-Si2 bond angle of 113.20(16) º in **10** is more acute than the Si1-C13-Si2 bond angle [119.3(2) º] in **7**. It is noteworthy that only **10** was observed in this reaction, germylene **11** with one $SiMe_3$ group and one $SiPh_2H$ group was not observed.

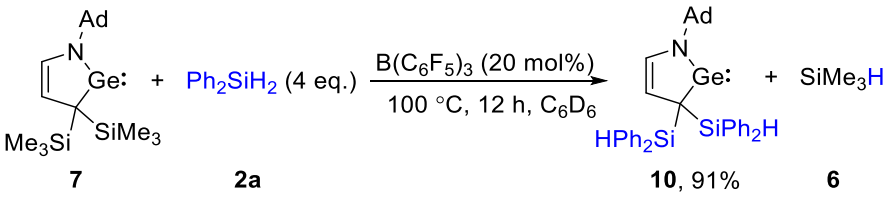

Scheme 4.16 Reaction of germylene **7** with diphenylsilane **2a**.

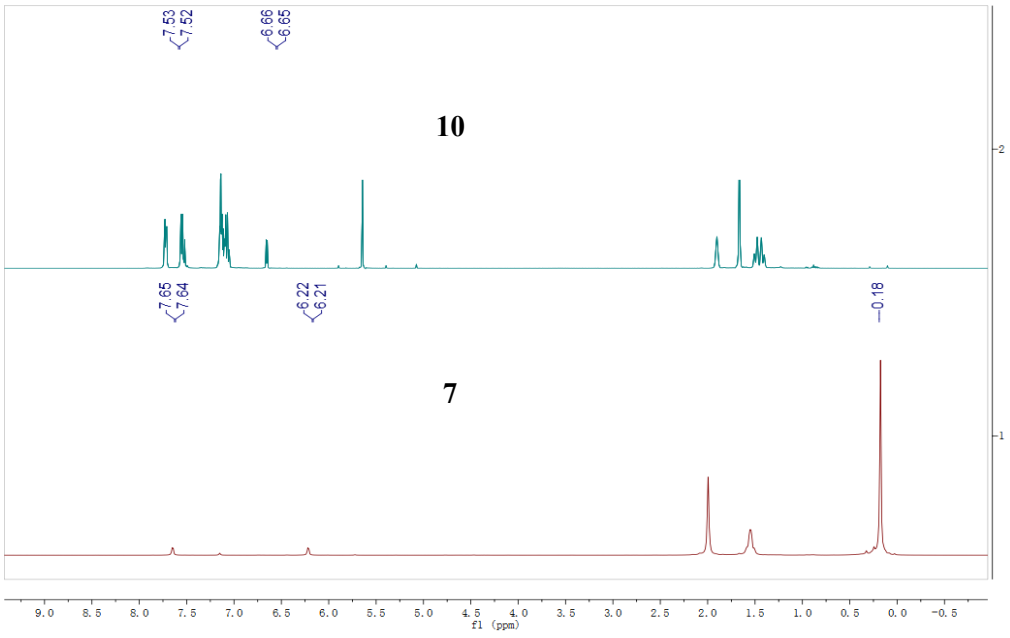

Figure 4.5 ^{1}H NMR spectra of germylene **10** (top) and germylene **7** (bottom).

According to the ^{1}H NMR spectrum of **10** (Figure 4.5), compound **10** does not possess the Me_3Si group because there are no peaks around 0.2 ppm. The ^{1}H NMR spectra also showed same chemical shifts of two C*(sp^2)-H* protons: First, one doublet peak appeared at 7.65 ppm for germylene **7**, which was slightly shifted to high-field at 7.53 ppm for germylene **10**. Second, another doublet peak appeared at 6.22 ppm for **7**, but the corresponding peak was significantly shifted down-field at 6.66 ppm for **10** (Figure 4.5).

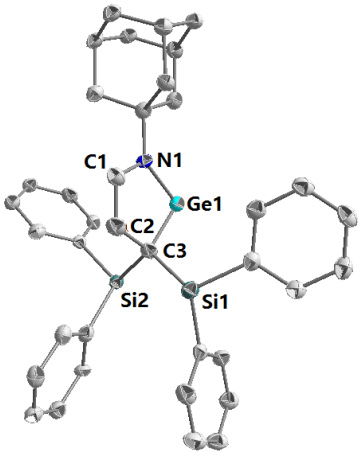

Figure 4.6 Solid state structures of **10**. Hydrogen atoms are omitted for clarity. Thermal ellipsoids are shown at the 50% probability level. Selected bond lengths [Å] and angles [°]: N1-Ge1 1.862(3), N1-C1 1.385(4), C1-C2 1.371(5), C2-C3 1.462(5), C3-Ge1 2.036, C3-Si1 1.880(4), C3-Si2 1.880(4); N1-Ge1-C3 85.52(12), N1-C1-C2 116.4(3), C1-C2-C3 116.9(3), C2-C3-Ge1 106.2(2), Ge1-N1-C1 115.0(2), Si1-C3-Si2 113.20(16).

The reactions of germylene **7** with Et_3SiH **2b**, $PhSiH_3$ **2c** and Ph_3SiH **2d** were also conducted in the presence of $B(C_6F_5)_3$ to afford germylenes **11** (Scheme 4.17). The reaction of germylene **7** with 4 equivalents of Et_3SiH **2b** was performed in the presence of 20 mol% $B(C_6F_5)_3$ catalyst, the mixture was heated at 50 °C for 7 h to reach equilibrium (Figure 4.7 (middle)). Based on the proposed mechanism in *Scheme 4.12*, when the reaction of germylene **7** with **2b** attained equilibrium, the removal of Me_3SiH **6** was performed to promote the equilibrium and the generation of product **11b** (Figure 4.7 (bottom)).

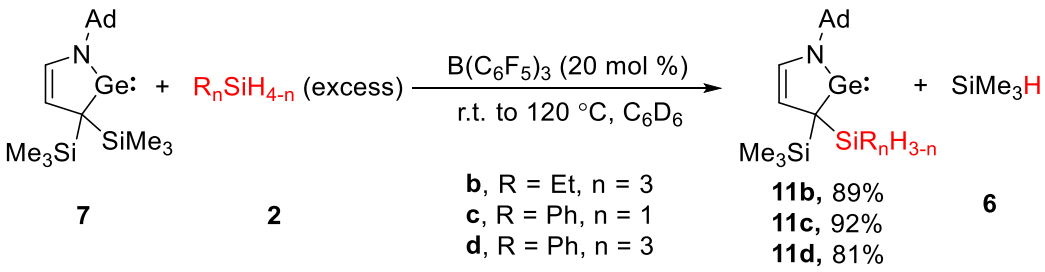

Scheme 4.17 Reactions of germylene **7** with various hydrosilanes **2**.

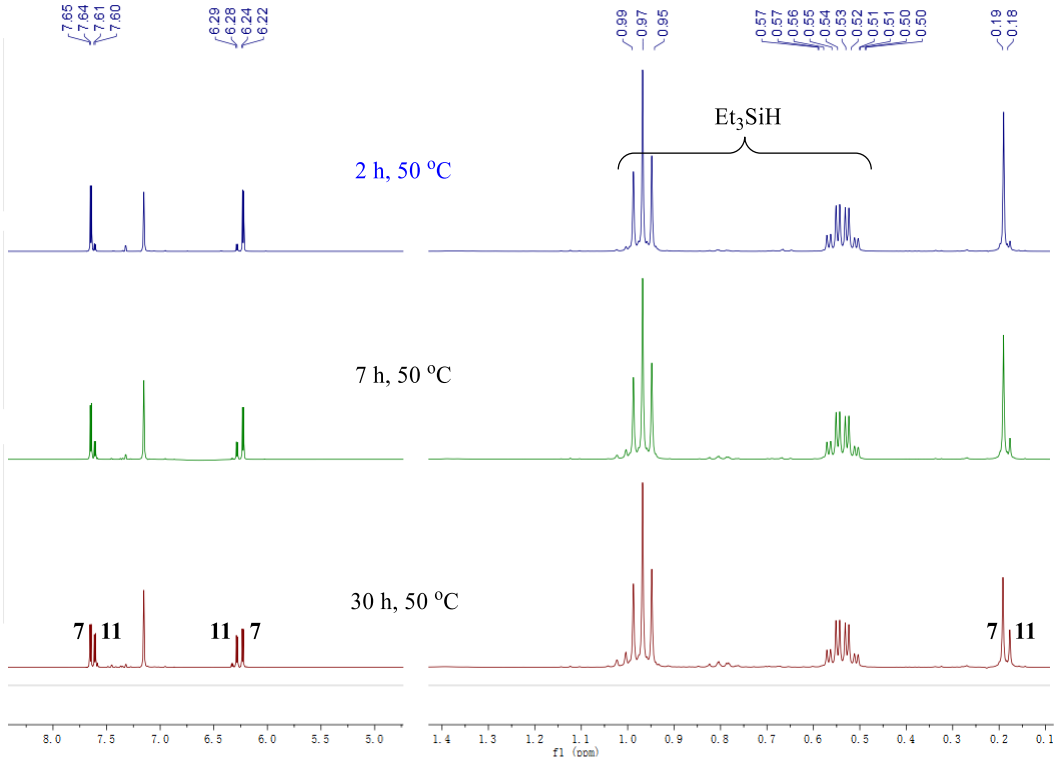

Figure 4.7 ^{1}H NMR spectra (fitted) for the reaction of germylene **7** with Et_3SiH for various times (2 h (top), 7 h (middle) and 30 h (bottom)).

When phenylsilane **2c** was reacted with germylene **7** as well as 20 mol% $B(C_6F_5)_3$ at ambient temperature, the corresponding germylene **11c** was also afforded in high yield. The products **11b** and **11c** were determined by ^{1}H NMR spectroscopy. Attempts to obtain single crystals of **11b** and **11c** failed.

In the ^{1}H NMR spectrum of germylene **11c**, the integral of the singlet for the $SiMe_3$ group at 0.22 ppm is half that of germylene **7**, which implies that one $SiMe_3$ group has been replaced with the $SiPhH_2$ group. Two doublets appear at 5.12 ppm and 4.80 ppm belonging to the $SiPhH_2$ group (Figure 4.8). This evidence supports the formation of germylene **11c** from the reaction.

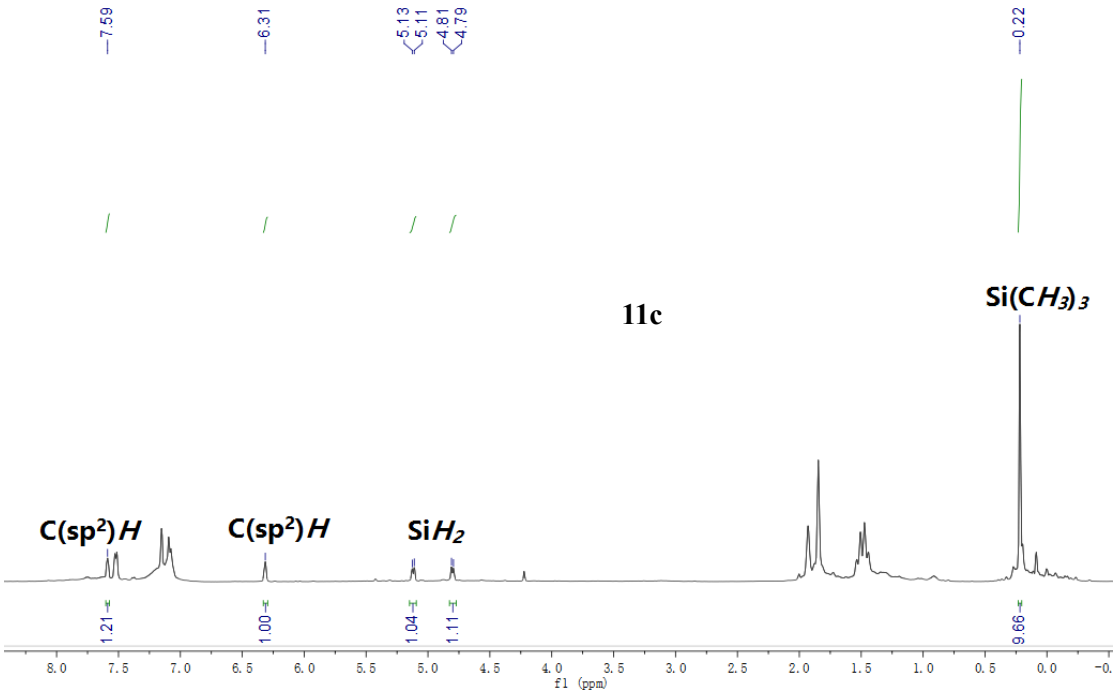

Figure 4.8 ^{1}H NMR spectrum of germylene **11c**.

The reaction of germylene **7** with triphenylsilane **2d** was performed at 120 ℃. After 12 h, solvent and by-product Me_3SiH **6** were removed under vacuum. By repeating the same processes three times, 81% of germylene **7** was converted to germylene **11d**. The reaction was monitored by ^{1}H NMR spectroscopy, which showed that a doublet at 6.25 ppm and a singlet at 0.20 ppm for germylene **7** decreased gradually while the corresponding peaks at 6.55 ppm and 0.02 ppm for **11d** increased concomitantly (Figure 4.9). Unfortunately, attempts to obtain a single crystal of **11d** failed.

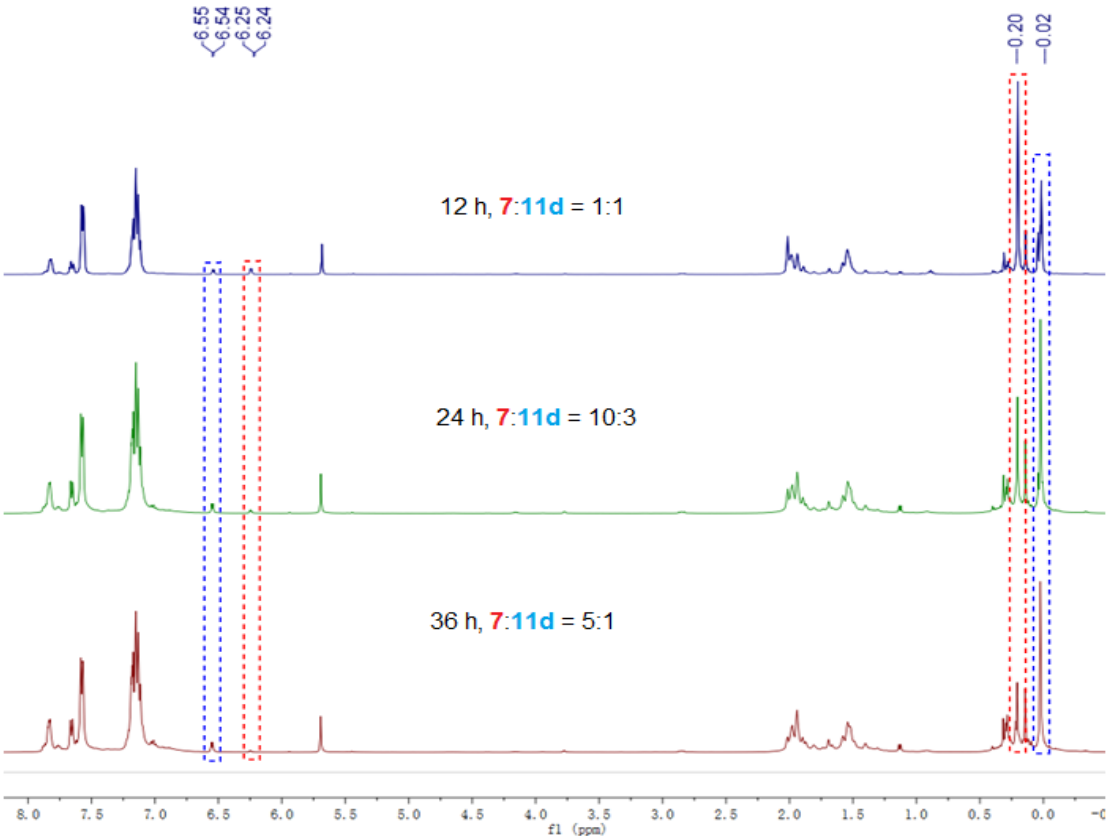

Figure 4.9 ^{1}H NMR spectra for the reaction of germylene **7** with triphenylsilane **2d** in the presence of $B(C_6F_5)_3$ for 12 h (top), 24 h (middle), and 36 h (bottom).

Although all attempts to obtain single crystals of **11** failed, the corresponding products **12** were afforded as yellow solids when the stoichiometry trapping reactions of germylene **11** with one equivalent of diphenyl diselenide were carried out at room temperature in benzene (scheme 4.18).[37-38] These products **12** were characterized using NMR spectroscopy and single-crystal X-ray diffraction analysis (Figure 4.10).

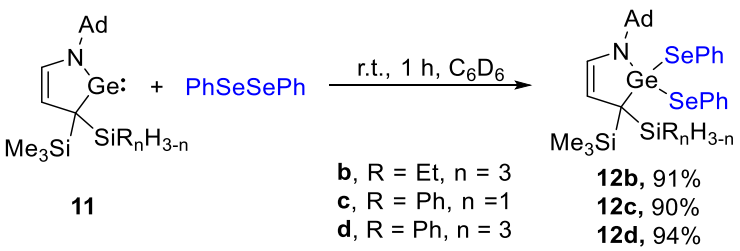

Scheme 4.18 Reactions of germylene **11** with diphenyl diselenide.

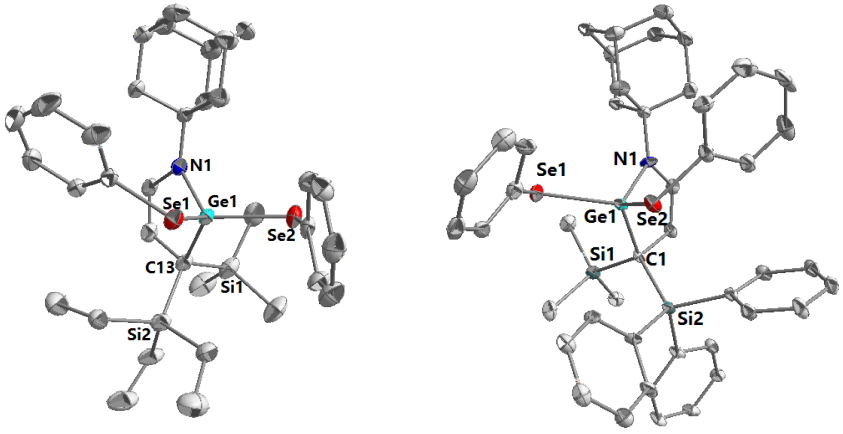

12b **12d**

Figure 4.10 Solid state structures of **12b** and **12d**. Hydrogen atoms are omitted for clarity. Thermal ellipsoids are shown at the 50% probability level. Selected bond lengths [Å] and angles [°]: **12b**) C13-Ge1 1.981(5), Ge1-N1 1.858(4), Ge1-Se2 2.3663(7), Ge1-Se1 2.3897(7), C13-Si2 1.900(5), C13-Si1 1.919(5); Se2-Ge1-Se1 103.28(2), N1-Ge1-C13 92.31(19), Si2-C13-Si1 114.2(2); **12d**) Ge1-N1 1.827(6), Ge1-Se1 2.3871(11), Ge1-Se2 2.3930(10), C1-Ge1 1.990(7), C1-Si2 1.896(8), C1-Si1 1.913(7); Si2-C1-Si1 114.2(4), N1-Ge1-C1 93.3(3), Se1-Ge1-Se2 107.54(4).

In comparison to the bond parameters of compounds **12b** and **12d**, the Ge1-Se1 bond length of 2.3663(7) Å in **12b** is notably shorter than that of 2.3871(11) Å in **12d**. Moreover, the C13-Si1 bond length of 1.919(5) Å in **12b** is slightly longer than that of C1-Si1 1.913(7) in **12d**. The Se1-Ge1-Se2 bond angle of 103.28(2) ° in **12b** is more acute than the Se1-Ge1-Se2 bond angle [107.54(4) °] in **12d**. The difference might have resulted from the steric effect, where the Ph_3Si group is bulkier than the Et_3Si group.

4.2.4 Mechanism elucidation and kinetic studies

To verify the hypothesized mechanism (Scheme 4.13), the reaction of germylene **7** with 1 equivalent of $B(C_6F_5)_3$ was performed in C_6D_6 at room temperature, which afforded the corresponding adduct **12** (Scheme 4.19a). In the ^1H NMR spectrum, the doublets at 7.51 ppm

and 6.09 ppm for adduct **12** shifted compared with the corresponding peaks of germylene **7**, 7.65 ppm and 6.23 ppm (Figure 4.11).

In the proposed mechanism, the formation of germylene **11** involved the intermediate **1a**. The reaction of germylene **7** with $Et_3SiB(C_6F_5)_4$ was conducted in benzene at ambient temperature subsequently certifying the hypothesis (Scheme 4.19b). The reaction was monitored by ^1H NMR spectroscopy, in which the formation of germylene **11b** was observed. The proportion of **11b** increased gradually and was 33% for 37 h (Figure 4.11).

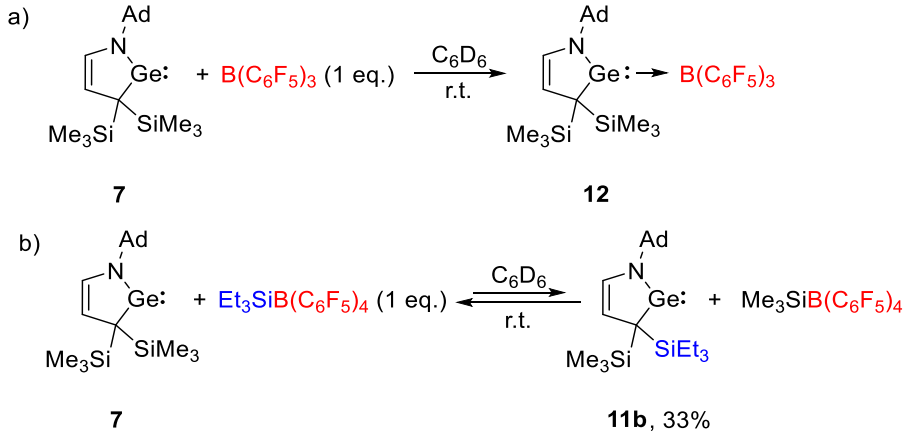

Scheme 4.19 Reaction of germylene **7** with $B(C_6F_5)_3$ or $Et_3SiB(C_6F_5)_4$.

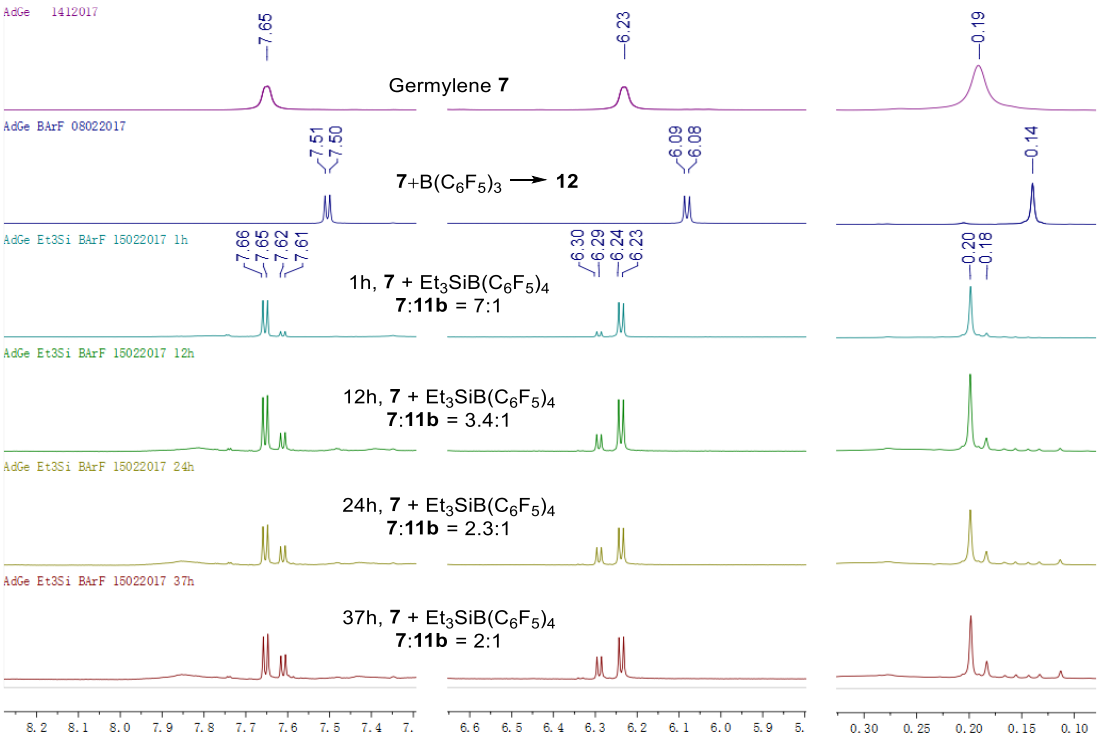

Figure 4.11 ^{1}HNMR spectra of the mixture of germylene **7** with $B(C_6F_5)_3$ or $Et_3SiB(C_6F_5)_4$.

When the reaction of germylene **7** with 1 equivalent of $Et_3SiB(C_6F_5)_4$ and 1 equivalent of $NaHB(C_6F_5)_3$ as the H^- source was conducted, germylene **11b** formed with a 41% after 36 h. The reaction was promoted by the addition of $NaHB(C_6F_5)_3$ (Scheme 4.20).

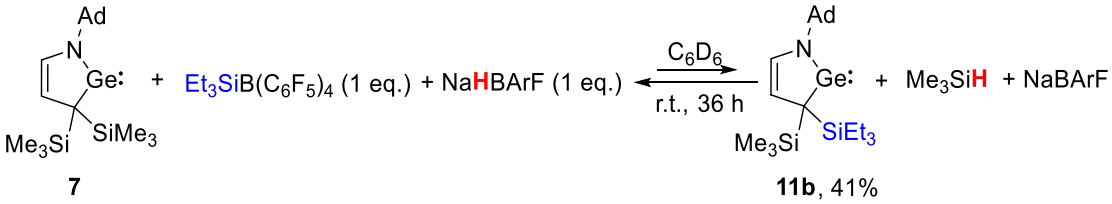

Scheme 4.20 Reaction of germylene **7** with $Et_3SiB(C_6F_5)_4$ and $NaHB(C_6F_5)_3$.

To further elucidate the mechanism for the reaction of germylene **7** with hydrosilanes **2** in the presence of $B(C_6F_5)_3$, kinetic experiments were also conducted. First, the reactions of germylene **7** with excess Et_3SiH were plotted as a pseudo first-order reaction versus time (Figure 4.12) or a pseudo second-order reaction versus time at 333 K using the initial rate data (Figure

4.13). The slope remains stationary when Et_3SiH are conducted more than 5 equivalents, but there is a low R-squared value for the first-order reaction equation, which indicates the pseudo reaction is second-order under these conditions.

Other kinetic studies were performed at various temperatures (323 K – 343 K), in which the reaction of germylene **7** with 1.7 equivalents of Et_3SiH in the presence of 20 mol% of $B(C_6F_5)_3$ were conducted (Table 4.1). The highest concentration of germylene **11b** was determined at 323 K.

T (K)	323	333	343
Concentration (M) of **11b**	0.0319	0.0317	0.0292

Table 4.1 Concentration of **11b** at various temperatures, when the reaction reached equilibrium. (Determined by ^1H NMR spectroscopy)

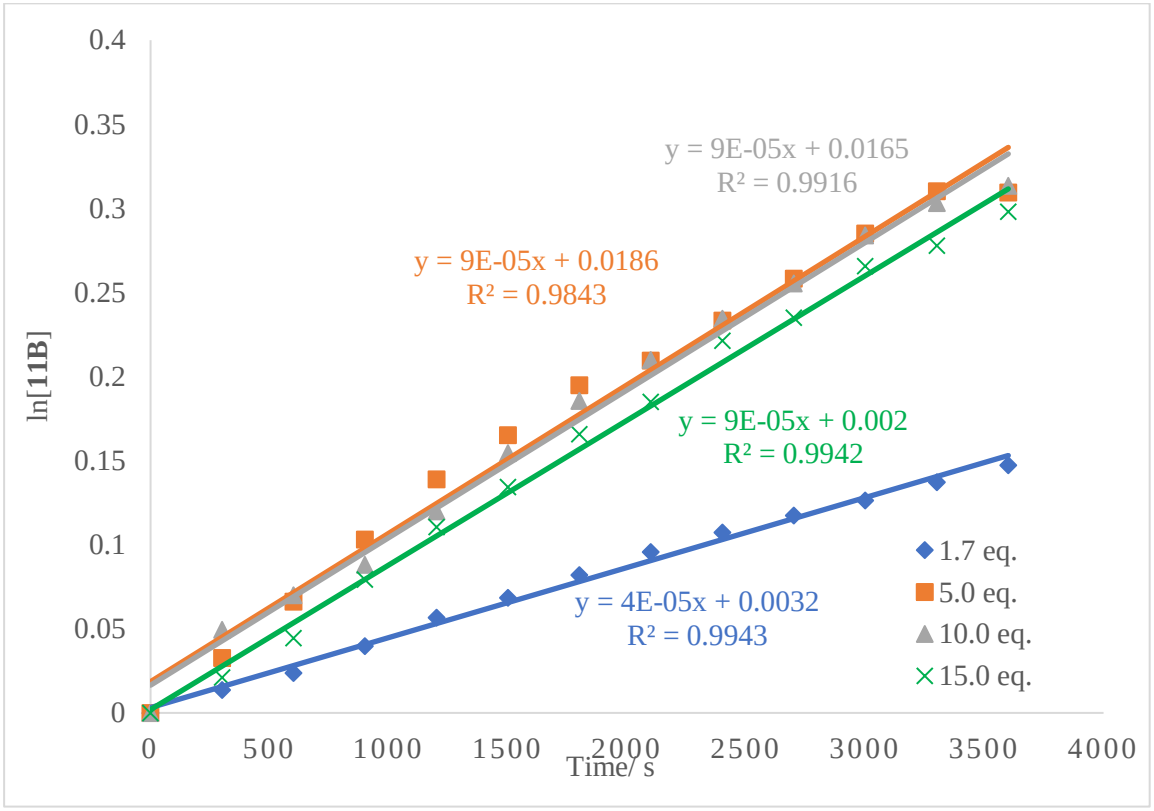

Figure 4.12 Pseudo-first order plots for the reaction of germylene **7** with various equivalents of Et_3SiH at 333 K.

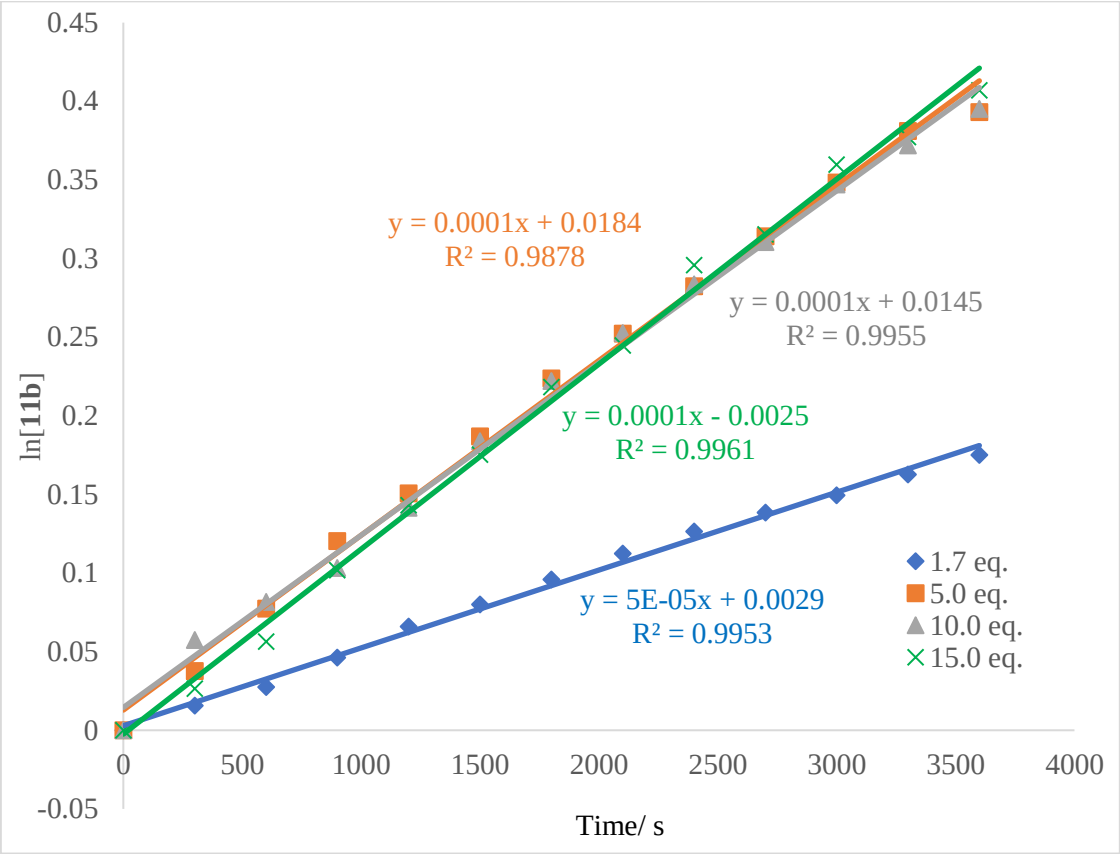

Figure 4.13 Pseudo-second order plots for the reaction of germylene **7** with various equivalents of Et_3SiH at 333 K.

4.3 Conclusion

In conclusion, a modified germylene **7** with an adamantyl group on the N atom was developed. In the reaction of **7** with hydrosilanes in the presence of 20 mol% $B(C_6F_5)_3$, germylene **7** was transformed into germylenes **10** and **11** via silyl group exchange. Our mechanistic study suggests that the initial step is hydrosilane activation by $B(C_6F_5)_3$ to generate silylium ion which subsequently forms an adduct with germylene **7**. Elimination of one silyl group on the sp^3-carbon in the $GeNC_3$ five-membered ring would yield the cyclic germene intermediate **1b**, from which germylenes **10** and **11** may be formed via a migration of the silyl group from the Ge atom to the adjacent C atom.

4.4 Experimental Section

4.4.1 General Information

All reactions were performed under an atmosphere of argon by using standard Schlenk or dry box techniques; solvents were dried over Na metal, K metal or CaH_2. All the substrates were obtained from the commercial sources or synthesized following literature procedures. ^{1}H, ^{13}C and ^{29}Si spectra were obtained with AVIII 400 MHz BBFO1 and BBFO2 spectrometers at 298 K. NMR multiplicities are abbreviated as follows: s = singlet, d = doublet, t = triplet, m = multiplet, br = broad signal. Coupling constants J are given in Hz. Electrospray ionization (ESI) mass spectrum was obtained at the Mass Spectrometry Laboratory at the Division of Chemistry and Biological Chemistry, Nanyang Technological University. Melting points were measured with an OpticMelt Stanford Research System.

*4.4.2 Synthesis of imine **8***

Amantadine (45 mmol, 6.81 g) and 3,3-bis(trimethylsilyl)acrylaldehyde (50 mmol, 10.00 g) were mixed in toluene (100 mL). The mixture was refluxed overnight. After cooling to room temperature, the product was purified by recrystallization in pentane to afford **8** as a white solid (12.9 g, 72%). Mp: 92 °C; ^{1}H NMR (400 MHz, $CDCl_3$) δ 8.27 (d, *J* = 9.1 Hz, 1H, C*H*), 7.16 (d, *J* = 9.1 Hz, 1H, C*H*), 2.16 (s, 3H, C*H*), 1.79 – 1.66 (m, 12H, CH_2), 0.26 (s, 9H, Si(CH_3)$_3$), 0.17 (s, 9H, Si(CH_3)$_3$); ^{13}C NMR (101 MHz, $CDCl_3$) δ 157.01 (*C*H), 152.42 (*C*H), 57.84 (*C*^{q}), 43.17 (*C*H_2), 36.50 (*C*H_2), 29.53 (*C*H), 2.37 (Si(*C*H_3)$_3$), 0.10 (Si(*C*H_3)$_3$); HRMS (ESI): m/z calcd for $C_{19}H_{35}NSi_2$: 333.2308. $[(M+H)]^{+}$; found: 334.2392.

*4.4.3 Synthesis of cyclic (alkyl)(amino) dichlorogermane **9***

(E)-N-(adamantan-1-yl)-3,3-bis(trimethylsilyl)prop-2-en-1-imine **8** (4 mmol, 1.42 g) and dichlorogermadiyl dioxane (4 mmol, 0.93 g) were mixed in benzene (20 mL). The mixture was

stirred at room temperature overnight and then vacuumed to remove the solvent. The product **9** was obtained as a white solid (1.93 g, 96%). Mp: 134 ℃; ^{1}H NMR (400 MHz, C_6D_6) δ 6.61 (d, *J* = 6.6 Hz, 1H, C*H*), 4.72 (s, 1H, C*H*), 1.94 (s, 6H, CH_2), 1.88 (s, 6H, CH_2), 1.45 (s, 6H, C*H*), 0.27 (s, 18H, Si(CH_3)$_3$); ^{13}C NMR (101 MHz, C_6D_6) δ 132.08 (*C*H), 98.46 (*C*H), 55.81 (*C*^{q}), 43.75 (*C*H_2), 35.97 (*C*H_2), 29.82 (*C*H), 0.46 (Si(*C*H_3)$_3$); HRMS (ESI): m/z calcd for $C_{19}H_{35}Cl_2GeNSi_2$: 477.0897. [(M+H)]$^{+}$; found: 478.0979.

*4.4.4 Synthesis of modified cyclic (alkyl)(amino) germylene **7***

9 (2 mmol, 1.02 g) and KC_8 (6 mmol, 0.81 g) were mixed in benzene (30 mL). The mixture was stirred at 60 ℃ for 24 h. After stirring for another 30 min at room temperature, the mixture was filtered and concentrated under vacuum to afford product **7** as a light-yellow solid (0.78 g, 90%). Mp: 73 ℃; ^{1}H NMR (400 MHz, C_6D_6) δ 7.65 (d, *J* = 3.6 Hz, 1H, C*H*), 6.22 (d, *J* = 3.5 Hz, 1H, C*H*), 2.00 (s, 9H, s), 1.55 (d, *J* = 4.1 Hz, 6H, CH_2), 0.18 (s, 18H, Si(CH_3)$_3$); ^{13}C NMR (101 MHz, C_6D_6) δ 140.08 (*C*H), 119.08 (*C*H), 78.53 (*C*^{q}), 57.41 (*C*^{q}), 47.13 (*C*H_2), 36.24 (*C*H_2), 30.11 (*C*H), 1.42 (Si(*C*H_3)$_3$); ^{29}Si NMR (79 MHz, C_6D_6) δ −8.32 (*Si*(CH$_3$)$_3$); HRMS (ESI): m/z calcd for $C_{19}H_{35}GeNSi_2$: 407.1520. [(M+H)]$^{+}$; found: 408.1598.

*4.4.5 Reactions of hydrosilanes **2** with germylene **7** in the presence of $B(C_6F_5)_3$*

Germylene **7** (0.05 mmol, 20 mg) and hydrosilanes **2a** (0.20 mmol, 37 mg) were mixed in C_6D_6 (0.5 mL) in the presence of $B(C_6F_5)_3$ (0.01 mmol, 5 mg), and the mixture was heated at 100 ℃ for 12 hours. After all volatiles were removed under vacuum, recrystallization in pentane afforded **10** as a light-yellow solid in 91% (29 mg). Mp: 129 ℃; ^{1}H NMR (400 MHz, C_6D_6) δ 7.76 – 7.68 (m, 4H, Ar-*H*), 7.55 (dd, *J* = 7.8, 1.5 Hz, 4H, Ar-*H*), 7.53 (d, *J* = 4.3 Hz, 1H, C*H*), 7.13 (dt, *J* = 5.9, 3.4 Hz, 8H, Ar-*H*), 7.08 (dt, *J* = 13.8, 4.1 Hz, 4H, Ar-*H*), 6.65 (d, *J* = 4.3 Hz, 1H, C*H*), 5.64 (t, 2H, Ph_2Si-*H*), 1.90 (s, 3H, CH_2), 1.67 (d, *J* = 2.2 Hz, 6H, CH_2), 1.46 (dd, *J* = 29.3, 12.0 Hz, 6H, C*H*); ^{13}C NMR (101 MHz, C_6D_6) δ 142.69 (*C*H), 135.21 (*C*^{q}), 135.14 (*C*H), 134.99 (*C*H), 129.50 (*C*H), 129.24 (*C*H), 127.68 (*C*H), 127.35 (*C*H), 116.84 (*C*H), 67.69 (*C*^{q}),

57.10 (C^q), 46.49 (CH_2), 36.08 (CH_2), 29.95 (CH); ^{29}Si NMR (79 MHz, C_6D_6) δ −24.33 (d, J = 201.8 Hz, SiPh$_2$H); HRMS (ESI): m/z calcd for $C_{37}H_{39}GeNSi_2$: 627.1833. $[(M+H)]^+$; found: 628.1895.

Germylene **7** (0.05 mmol, 20 mg) and hydrosilanes **2b** (0.20 mmol, 24 mg) were mixed in C_6D_6 (0.5 mL) in the presence of $B(C_6F_5)_3$ (0.01 mmol, 5 mg), and the mixture was heated at 60 ℃ for 5 hours. After the mixture was cooled to room temperature, all volatiles were removed under vacuum. Because the germylene **11b** was failed to isolate, PhSeSePh (0.05 mmol, 16 mg) was added to a benzene (1 mL) solution of **11b**. After stirring at ambient temperature for 30 minutes, the solvent was removed under vacuum to afford **12b**. The product **12b** as a light-yellow solid in 91% (31 mg). Mp: 102 ℃ (dec); ^{1}H NMR (400 MHz, C_6D_6) δ 7.89 – 7.72 (m, 2H, Ar-*H*), 7.50 – 7.35 (m, 2H, Ar-*H*), 7.07 – 6.99 (m, 3H, Ar-*H*), 6.92 (t, J = 6.8 Hz, 3H, Ar-*H*), 6.61 (d, J = 6.2 Hz, 1H, C*H*), 4.92 (d, J = 6.2 Hz, 1H, C*H*), 1.87 (s, 3H, C*H*), 1.81 – 1.69 (m, 7H, CH_2), 1.49 – 1.35 (m, 6H, CH_2), 1.20 – 1.11 (m, 14H, C*H*), 0.46 (s, 9H, Si(CH_3)$_3$); ^{13}C NMR (101 MHz, C_6D_6) δ 137.86 (*C*H), 137.12 (*C*H), 135.79 (*C*H), 133.75 (*C*H), 130.08 (C^q), 128.98 (C^q), 128.68 (*C*H), 128.61 (*C*H), 128.13 (*C*H), 126.55 (*C*H), 99.93 (*C*H), 55.58 (C^q), 43.81 (CH_2), 36.18 (C^q), 32.24 (*C*H), 30.02 (*C*H), 8.73 (CH_3), 6.47 (CH_2), 1.92 (Si(CH_3)$_3$); ^{29}Si NMR (79 MHz, C_6D_6) δ 5.28 (SiEt$_3$), −0.87 (Si(CH$_3$)$_3$); HRMS (ESI): m/z calcd for $C_{34}H_{51}GeNSe_2Si_2$: 763.1102. $[(M+H)]^+$; found: 764.1177.

Germylene **7** (0.05 mmol, 20 mg) and hydrosilanes **2c** (0.20 mmol, 21 mg) were mixed in C_6D_6 (0.5 mL) in the presence of $B(C_6F_5)_3$ (0.01 mmol, 5 mg), and the mixture was stirred at room temperature for 12 hours. Then the mixture was removed under vacuum. Because the germylene **11c** was failed toisolate, PhSeSePh (0.05 mmol, 16 mg) was added to benzene (1 mL) solution of **11c**. After stirring at room temprtaure for 30 minutes, the solvent was removed under vaccum to afford **13c** as a light-yellow oil. HRMS (ESI): m/z calcd for $C_{34}H_{43}GeNSe_2Si_2$: 755.0476. $[(M+H)]^+$; found: 756.0436.

Germylene **7** (20 mg, 0.05 mmol) and hydrosilanes **2d** (52 mg, 0.20 mmol) were mixed in C_6D_6 (0.5 mL) in the presence of $B(C_6F_5)_3$ (5 mg, 0.01 mmol) and the mixture was heated at 120 ℃ for 12 hours. After the mixture was cooled to room temperature, the sovent was removed under vacuum. Because germylene **11d** was failed to isolate, PhSeSePh (0.05 mmol, 16 mg) was added to benzene (1 mL) solution. After stirring at ambient temperature for 30 minutes, the solvent was removed under vacuum to afford **13d** as a light-yellow solid in 94% (38 mg). Mp: 154 ℃ (dec); ^{1}H NMR (400 MHz, C_6D_6) δ 8.09 (s, 5H, C*H*), 7.91 – 7.82 (m, 2H, C*H*), 7.22 (m, 9H, C*H*), 7.12 – 6.97 (m, 3H, C*H*), 6.86 – 6.64 (m, 4H, C*H*), 6.58 – 6.44 (m, 2H, C*H*), 5.38 (d, *J* = 6.2 Hz, 1H, C*H*), 1.86 – 1.82 (m, 3H, CH_2), 1.79 – 1.71 (m, 3H, CH_2), 1.60 – 1.53 (m, 3H, CH_2), 1.48 – 1.33 (m, 6H, C*H*), 0.23 (s, 9H, Si(CH_3)$_3$); ^{13}C NMR (101 MHz, C_6D_6) δ 138.49, 138.00 (*C*H), 136.97 (*C*H), 134.73 (*C*H), 129.23 (*C*H), 128.93 (*C*^{q}), 128.75 (*C*^{q}), 128.58 (*C*H), 128.15 (*C*H), 127.29 (*C*H), 126.74 (*C*H), 99.91 (*C*H), 55.12 (*C*^{q}), 43.67 (*C*H_2), 36.10 (*C*H_2), 30.00 (*C*H), 29.68 (*C*^{q}), 1.71 (Si(*C*H_3)$_3$); ^{29}Si NMR (79 MHz, C_6D_6) δ −0.27 (*Si*(CH$_3$)$_3$), −14.43 (*Si*Ph$_3$); HRMS (ESI): m/z calcd for $C_{46}H_{51}GeNSe_2Si_2$: 907.1102. $[(M+H)]^+$; found: 908.1219.

4.4.6 Kinetic studies

General method for pseudo-first order reactions: Germylene **7** (20 mg, 0.05 mmol), Et_3SiH **2b** (100 mg, 0.86 mmol; or 150 mg, 1.29 mmol), the internal standard *p*-xylene (2.65 mg, 0.025 mmol) and C_6D_6 (0.5 mL) were loaded into a dried J. Young NMR tube and sealed. The reaction was heated at 333.15 K and monitored automatically by NMR spectroscopy with 5 minutes interval. Based on the integration of germylene **11b**, which was plotted versus time following a pseudo-first order kinetic equation.

*General procedures for the activation of Et_3SiH **2b** by germylene **7** at various temperatures*: Germylene **7** (20 mg, 0.05 mmol), Et_3SiH **2b** (10 mg, 0.086 mmol), the internal standard *p*-xylene (2.65 mg, 0.025 mmol) and C_6D_6 (0.5 mL) were loaded into a dried J. Young NMR tube in glovebox. The mixture was heated at a temperature range from 323.15 K to 343.15 K, which

was automatically monitored by NMR spectroscopy with 5 minutes interval. Based on the integration of germylene **11b**, the logarithmic plot of the concentration of germylene **11b** was plotted against time.

4.4.7 ^{1}H, ^{13}C, and ^{29}Si NMR spectra

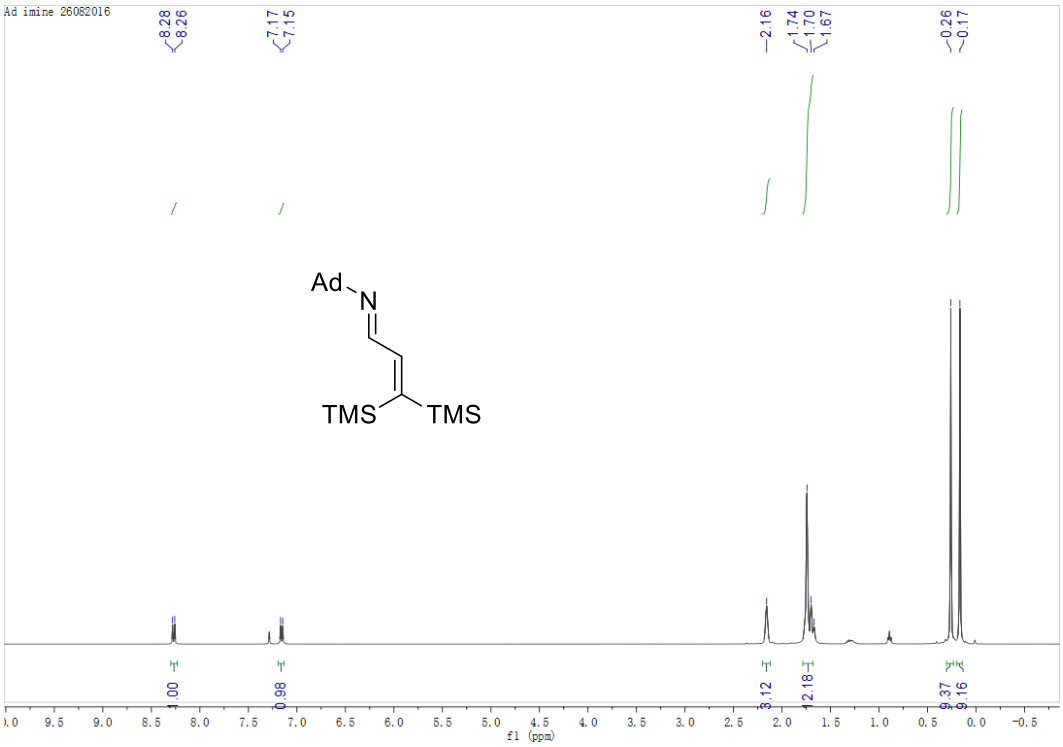

Figure 4.14 ^{1}H NMR spectrum of **8**

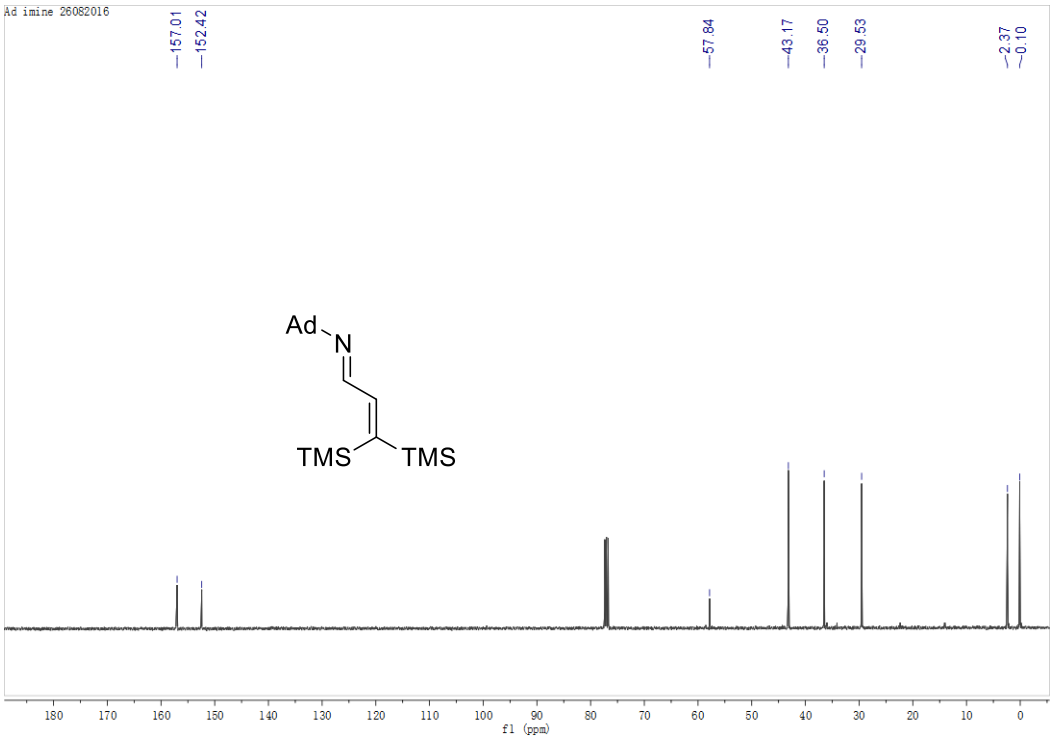

Figure 4.15 ^{13}C NMR spectrum of **8**

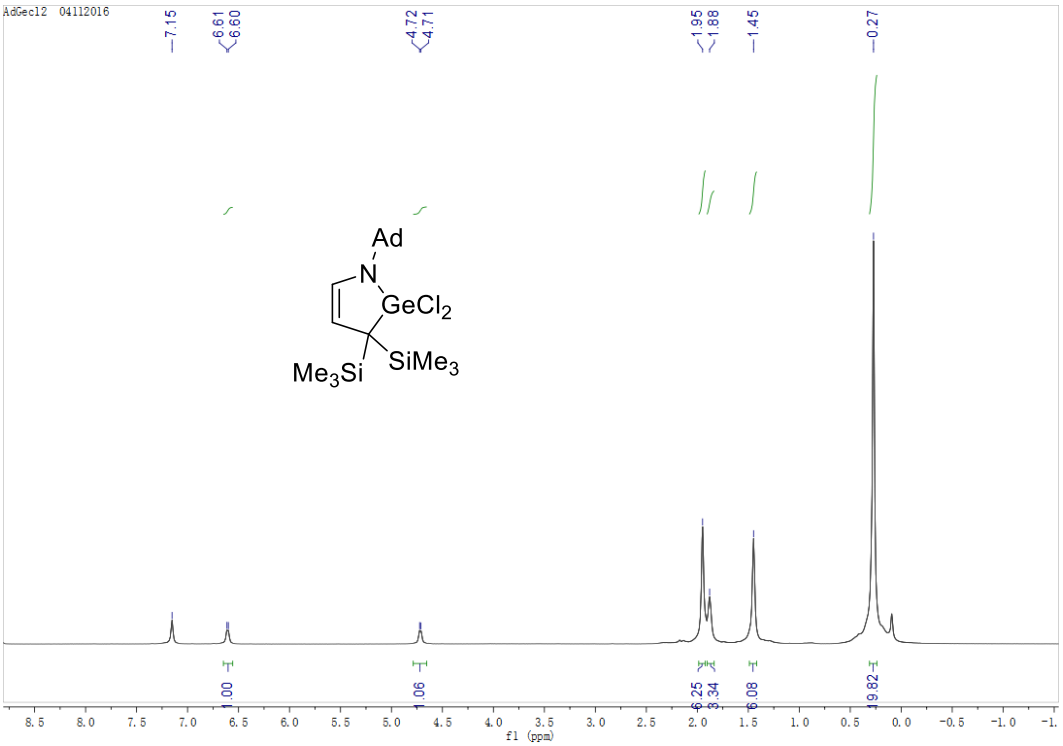

Figure 4.16 ^{1}H NMR spectrum of **9**

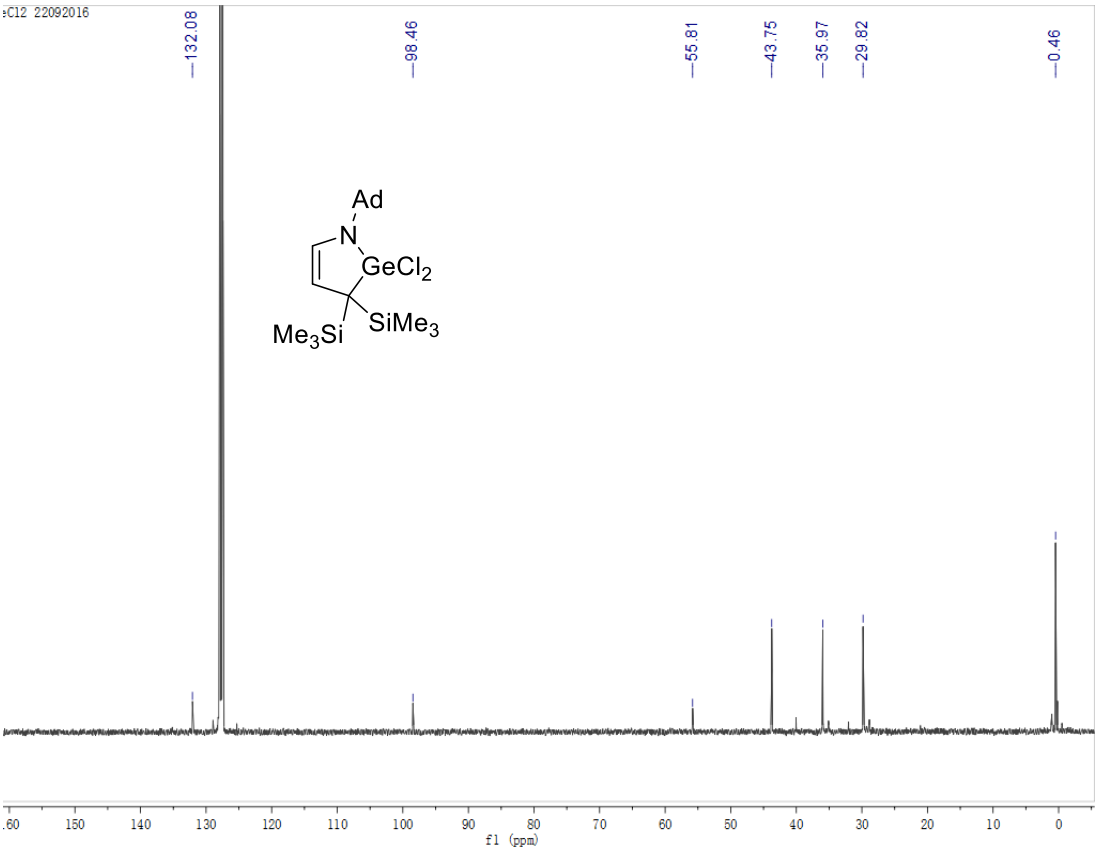

Figure 4.17 ^{13}C NMR spectrum of **9**

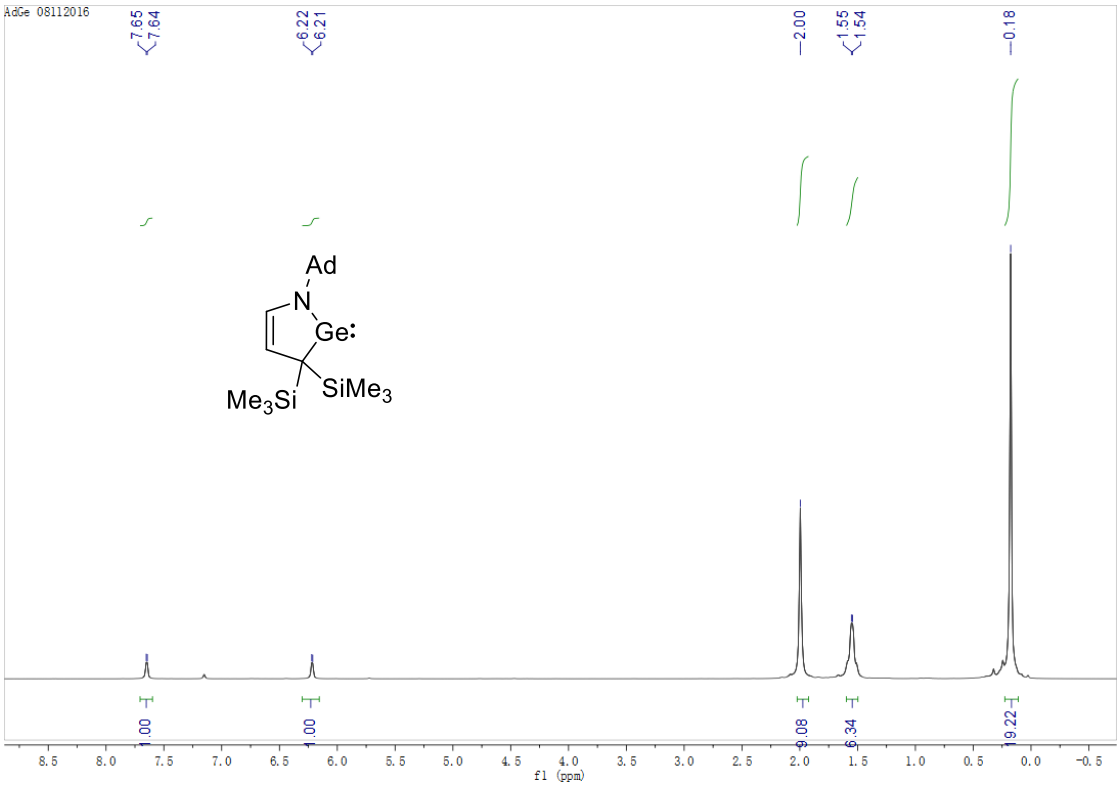

Figure 4.18 ^{1}H NMR spectrum of **7**

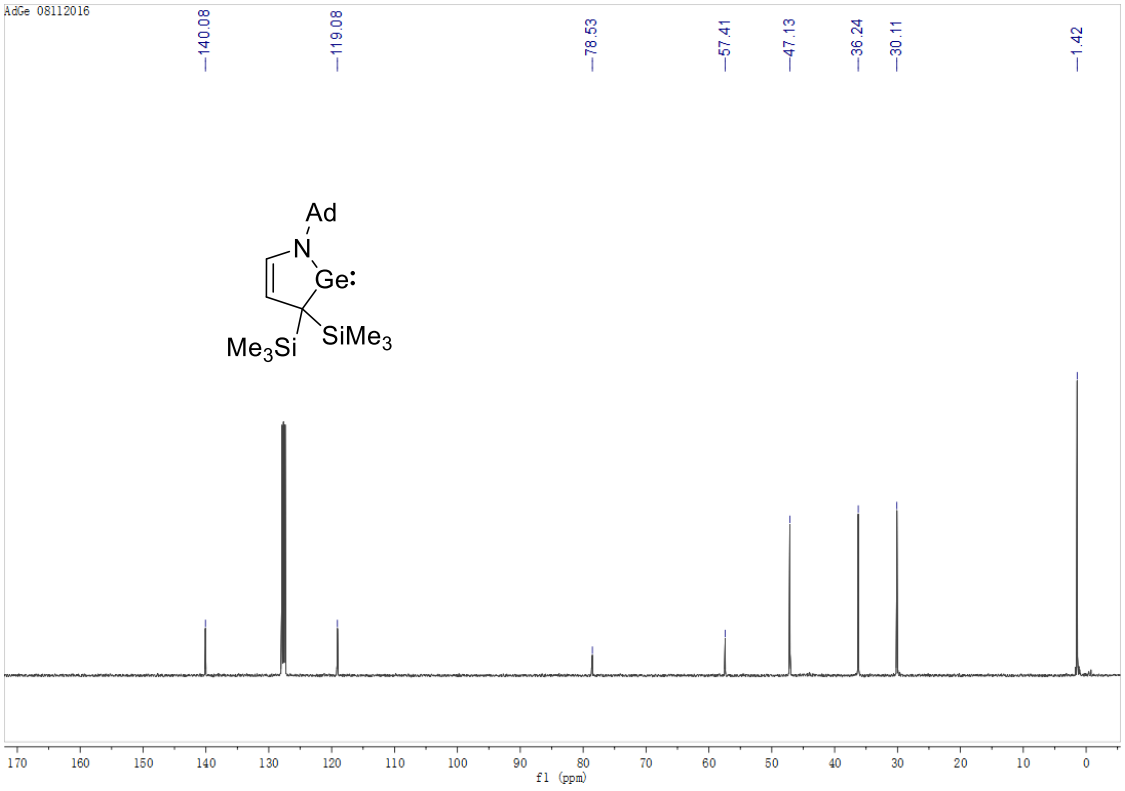

Figure 4.19 ^{13}C NMR spectrum of **7**

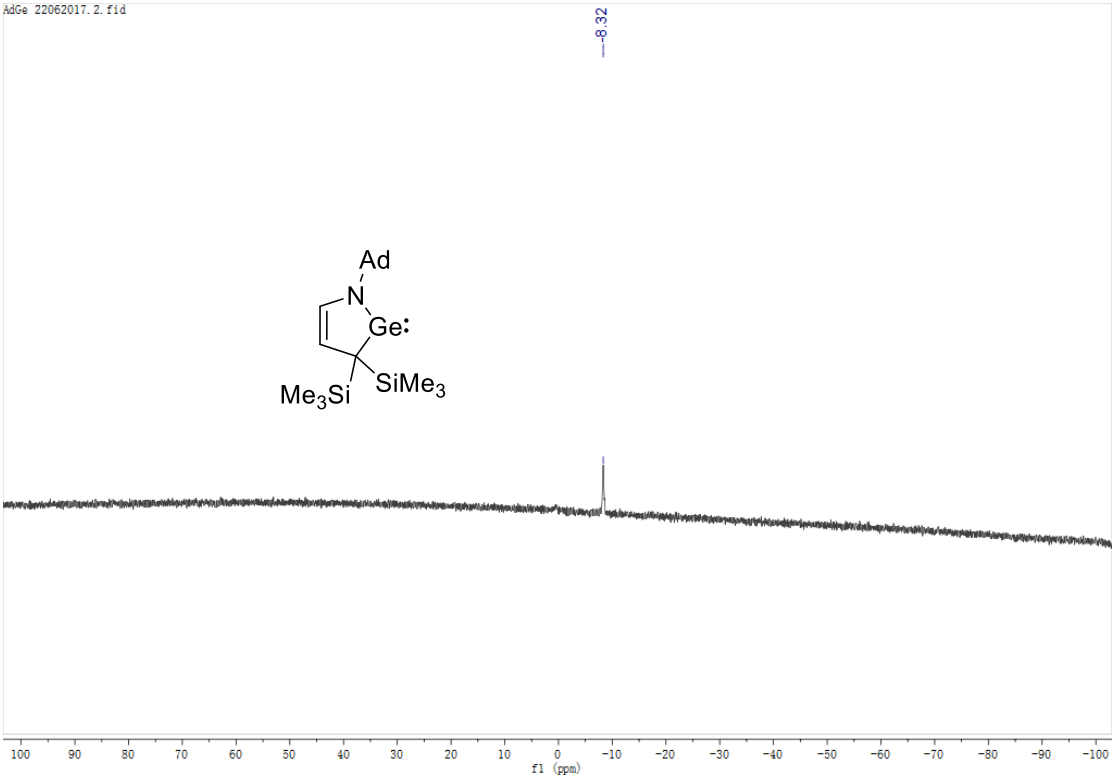

Figure 4.20 ^{29}Si NMR spectrum of **7**

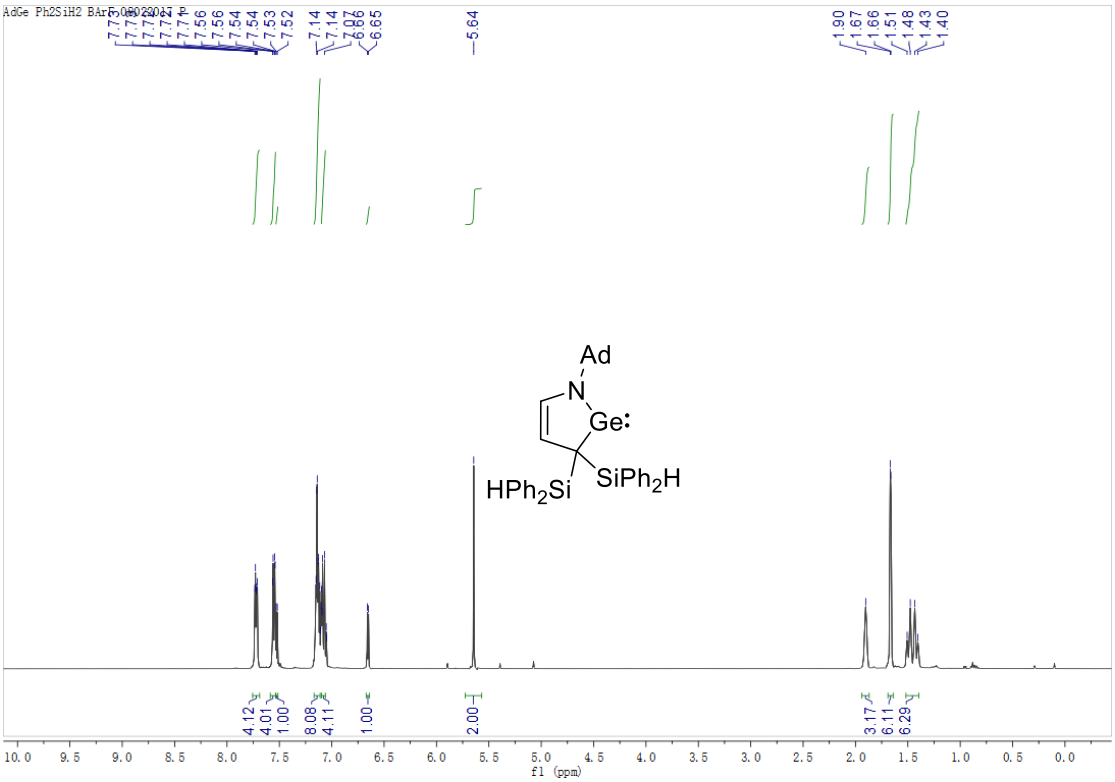

Figure 4.21 ^{1}H NMR spectrum of **10**

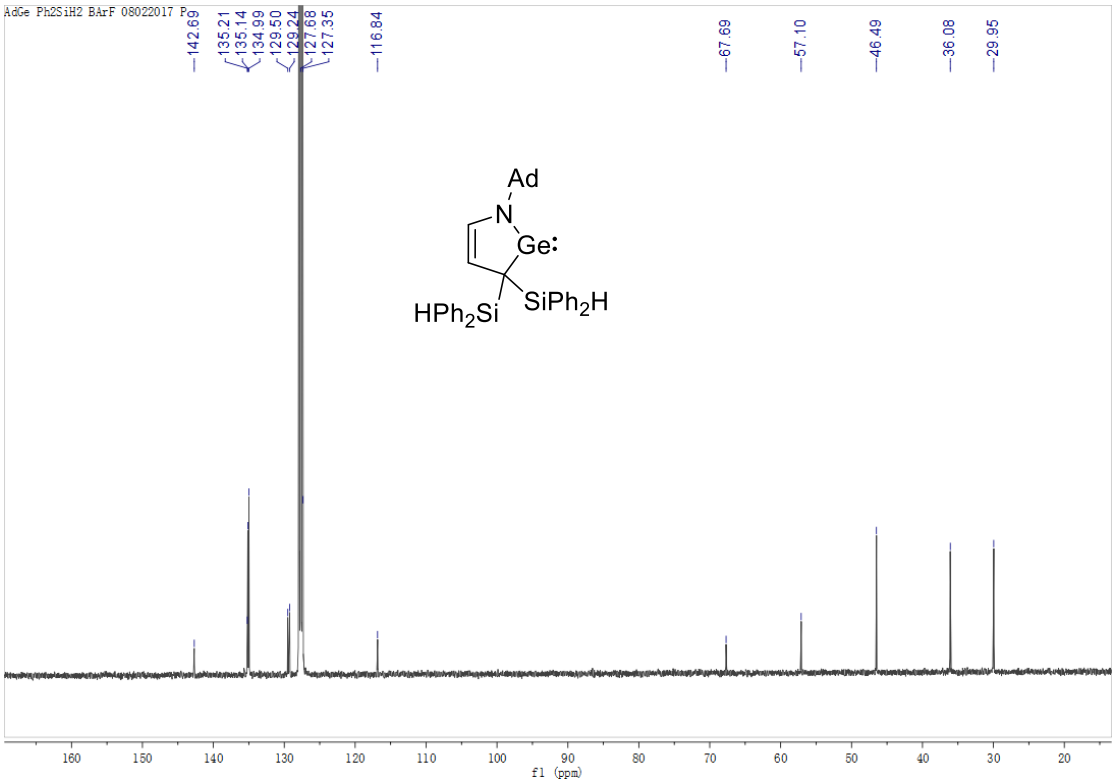

Figure 4.22 ^{13}C NMR spectrum of **10**

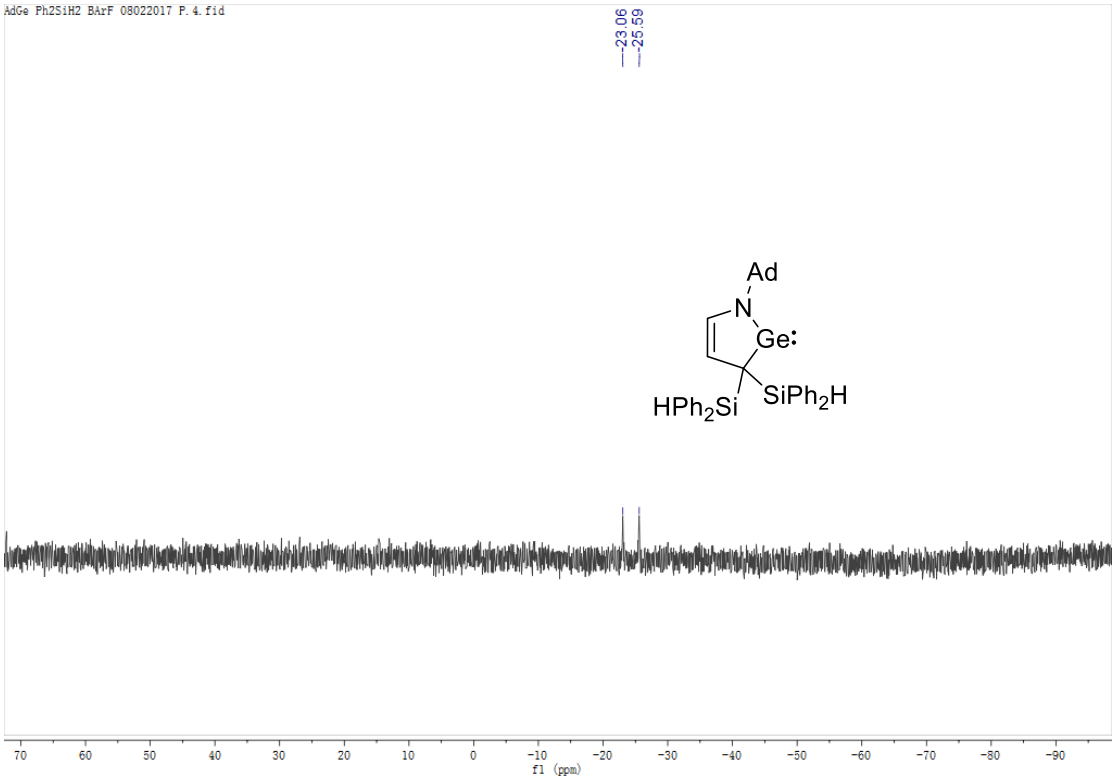

Figure 4.23 ^{29}Si NMR spectrum of **10**

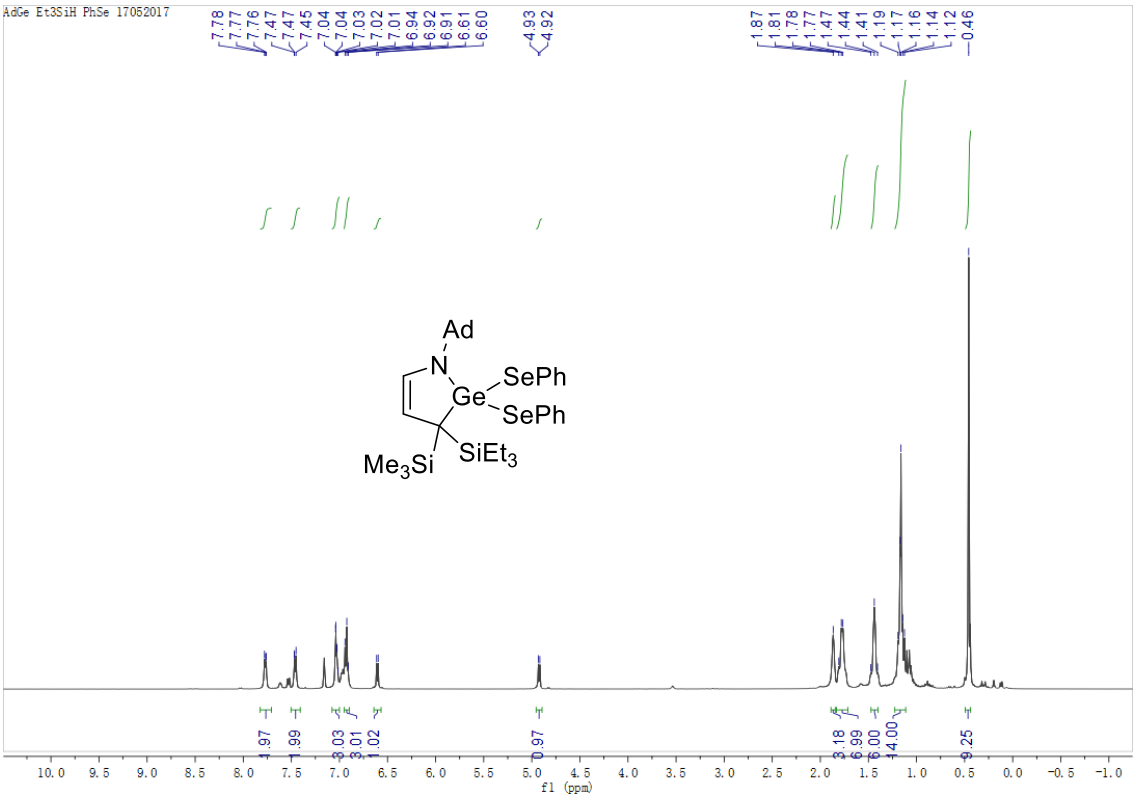

Figure 4.24 ^{1}H NMR spectrum of **12b**

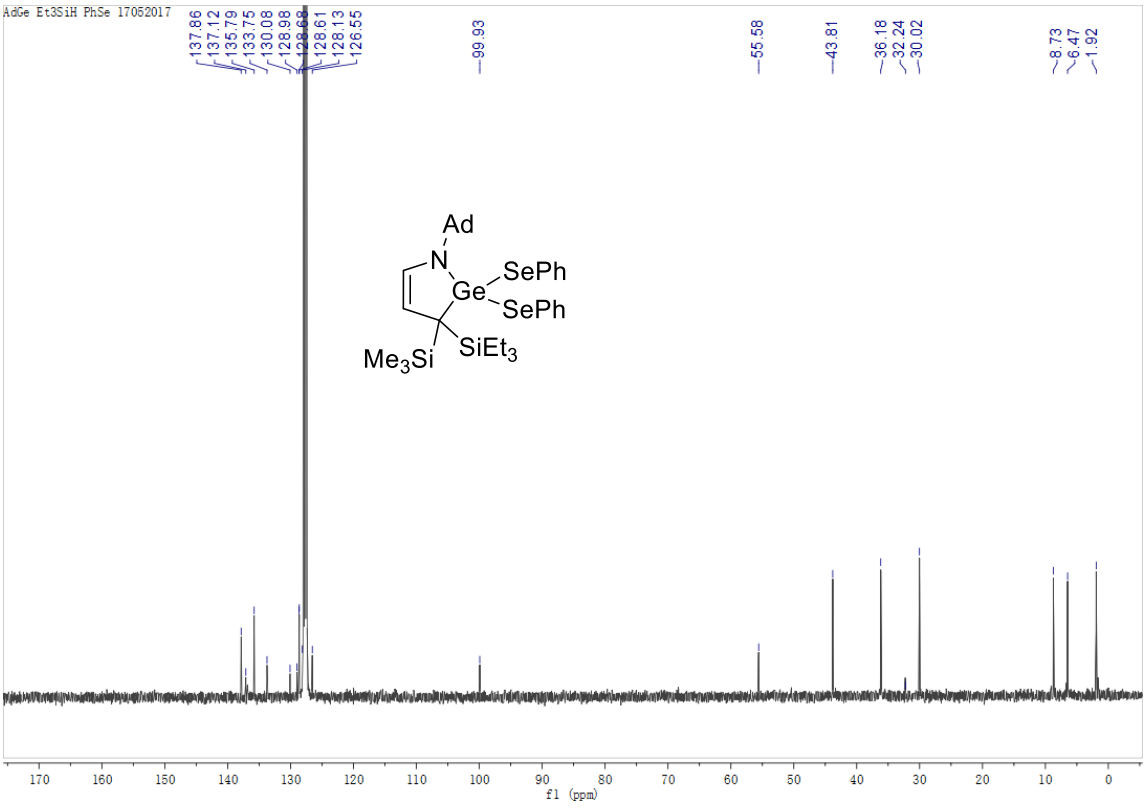

Figure 4.25 ^{13}C NMR spectrum of **12b**

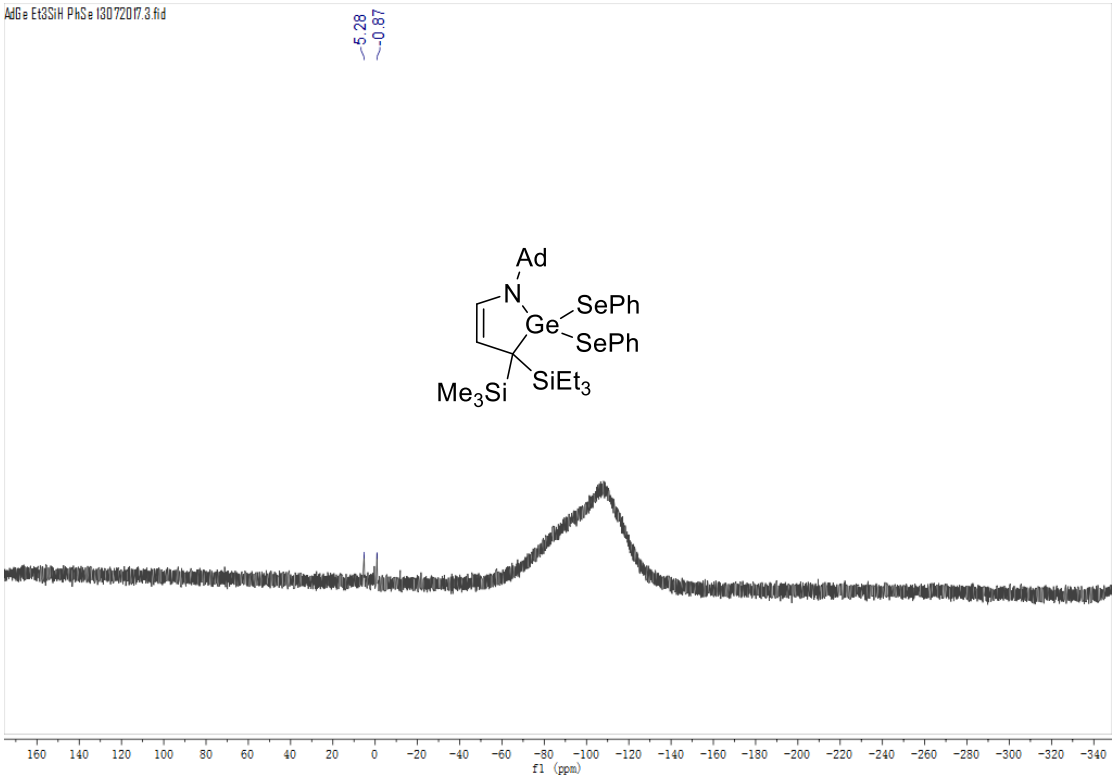

Figure 4.26 ^{29}Si NMR spectrum of **12b**

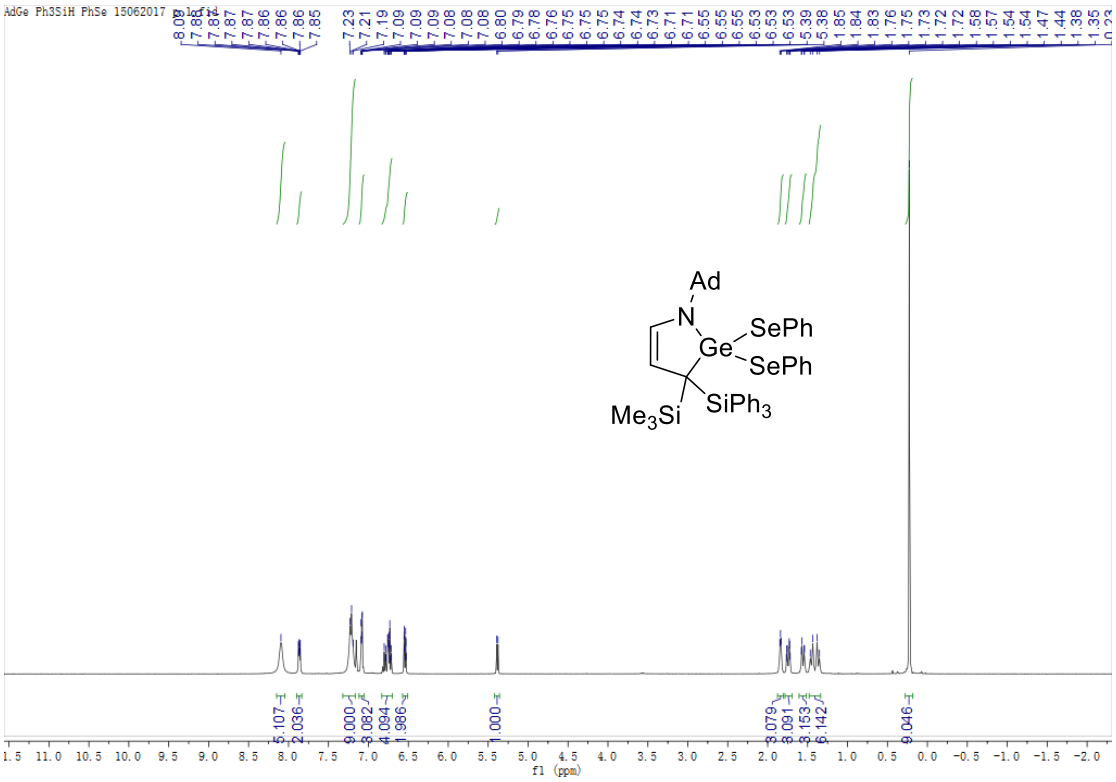

Figure 4.27 ^{1}H NMR spectrum of **12d**

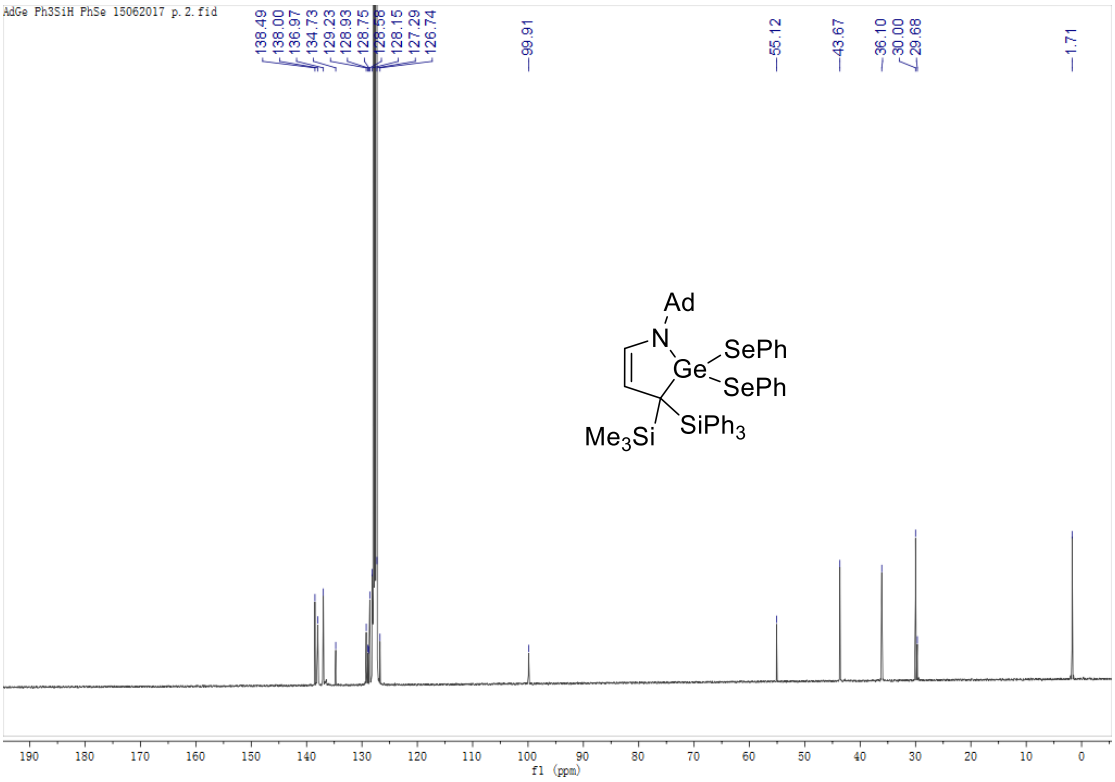

Figure 4.28 ^{13}C NMR spectrum of **12d**

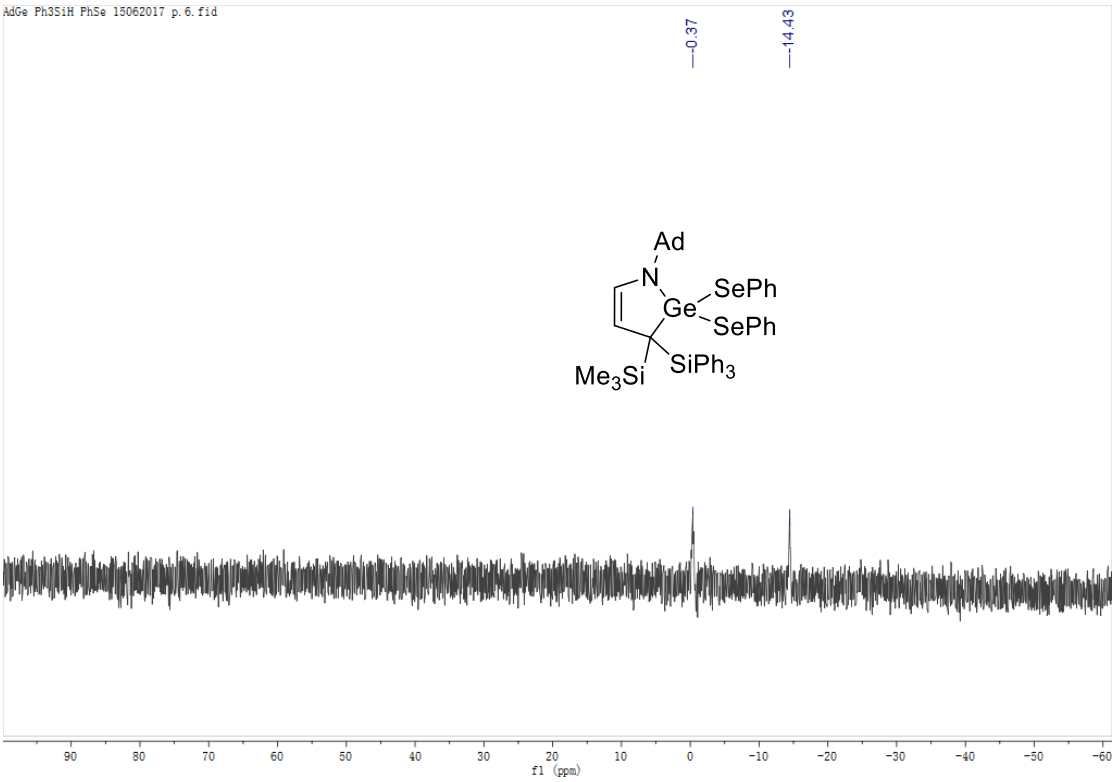

Figure 4.29 ^{29}Si NMR spectrum of **12d**

4.5 Reference

1. Carey, F. A.; Tremper, H. S., *J. Org. Chem.* **1971,** *36*, 758-761.

2. Smonou, I.; Orfanopoulos, M., *Tetrahedron Lett.* **1988,** *29*, 5793-5796.

3. Gevorgyan, V.; Rubin, M.; Benson, S.; Liu, J.-X.; Yamamoto, Y., *J. Org. Chem.* **2000,** *65*, 6179-6186.

4. Gevorgyan, V.; Liu, J.-X.; Rubin, M.; Benson, S.; Yamamoto, Y., *Tetrahedron Lett.* **1999,** *40*, 8919-8922.

5. Chandrasekhar, S.; Raji Reddy, C.; Jagadeeshwar Rao, R., *Tetrahedron* **2001,** *57*, 3435-3438.

6. Zheng, G. Z.; Chan, T. H., *Organometallics* **1995,** *14*, 70-79.

7. Shunichi, F.; Morifumi, F., *Chem. Lett.* **1991,** *20*, 2059-2062.

8. Corriu, R. J. P.; Moreau, J. J. E., *J. Chem. Soc., Chem. Commun.* **1973**, 38-39.

9. Klei, S. R.; Tilley, T. D.; Bergman, R. G., *Organometallics* **2002,** *21*, 4648-4661.

10. Lipke, M. C.; Tilley, T. D., *J. Am. Chem. Soc.* **2014,** *136*, 16387-16398.

11. Bleith, T.; Gade, L. H., *J. Am. Chem. Soc.* **2016,** *138*, 4972-4983.

12. L. Larson, G.; L. Fry, J., Ionic and Organometallic-Catalyzed Organosilane Reductions. In *Organic Reactions*, John Wiley & Sons, Inc.: 2004.

13. Carey, F. A.; Tremper, H. S., *J. Am. Chem. Soc.* **1968,** *90*, 2578-2583.

14. Rodriguez, R.; Contie, Y.; Nougué, R.; Baceiredo, A.; Saffon-Merceron, N.; Sotiropoulos, J.-M.; Kato, T., *Angew. Chem. Int. Ed.* **2016,** *55*, 14355-14358.

15. Frey, G. D.; Masuda, J. D.; Donnadieu, B.; Bertrand, G., *Angew. Chem. Int. Ed.* **2010,** *49*, 9444-9447.

16. Walsh, R., *Acc. Chem. Res.* **1981,** *14*, 246-252.

17. Kanabus-Kaminska, J. M.; Hawari, J. A.; Griller, D.; Chatgilialoglu, C., *J. Am. Chem. Soc.* **1987,** *109*, 5267-5268.

18. Gronert, S.; Glaser, R.; Streitwieser, A., *J. Am. Chem. Soc.* **1989,** *111*, 3111-3117.

19. Schmidt, D.; Berthel, J. H. J.; Pietsch, S.; Radius, U., *Angew. Chem. Int. Ed.* **2012,** *51*, 8881-8885.

20. Lastovickova, D. N.; Moerdyk, J. P.; Kelley, A. R.; Bielawski, C. W., *J. Phys. Org. Chem.* **2015,** *28*, 75-78.

21. Momeni, M. R.; Rivard, E.; Brown, A., *Organometallics* **2013,** *32*, 6201-6208.

22. Ishida, S.; Iwamoto, T.; Kabuto, C.; Kira, M., *Silicon Chem.* **2003,** *2*, 137-140.

23. Inomata, K.; Watanabe, T.; Miyazaki, Y.; Tobita, H., *J. Am. Chem. Soc.* **2015,** *137*, 11935-11937.

24. Del Rio, N.; Lopez-Reyes, M.; Baceiredo, A.; Saffon-Merceron, N.; Lutters, D.; Müller, T.; Kato, T., *Angew. Chem. Int. Ed.* **2017,** *56*, 1365-1370.

25. Rendler, S.; Oestreich, M., *Angew. Chem. Int. Ed.* **2008,** *47*, 5997-6000.

26. Chase, P. A.; Jurca, T.; Stephan, D. W., *Chem. Commun.* **2008**, 1701-1703.

27. Chatterjee, I.; Porwal, D.; Oestreich, M., *Angew. Chem. Int. Ed.* **2017,** *56*, 3389-3391.

28. Liu, Z.-Y.; Wen, Z.-H.; Wang, X.-C., *Angew. Chem.* **2017,** *129*, 5911-5914.

29. Fasano, V.; Radcliffe, J. E.; Ingleson, M. J., *ACS Catalysis* **2016,** *6*, 1793-1798.

30. Parks, D. J.; Piers, W. E., *J. Am. Chem. Soc.* **1996,** *118*, 9440-9441.

31. Corre, Y.; Rysak, V.; Capet, F.; Djukic, J.-P.; Agbossou-Niedercorn, F.; Michon, C., *Chem. Eur. J.* **2016,** *22*, 14036-14041.

32. Parks, D. J.; Blackwell, J. M.; Piers, W. E., *J. Org. Chem.* **2000,** *65*, 3090-3098.

33. Berkefeld, A.; Piers, W. E.; Parvez, M., *J. Am. Chem. Soc.* **2010,** *132*, 10660-10661.

34. Baines, K. M.; Cooke, J. A.; Vittal, J. J., *J. Chem. Soc., Chem. Commun.* **1992**, 1484-1485.

35. Tolman, C. A., *J. Am. Chem. Soc.* **1970,** *92*, 2953-2956.

36. Wang, L.; Lim, Y.; Li, Y.; Ganguly, R.; Kinjo, R., *Molecules* **2016,** *21*, 990.

37. Tomoda, S.; Shimoda, M.; Takeuchi, Y.; Kajii, Y.; Obi, K.; Tanaka, L.; Honda, K., *J. Chem. Soc., Chem. Commun.* **1988**, 910-912.

38. Brown, D. H.; Cross, R. J.; Millington, D., *J. Chem. Soc., Dalton Trans.* **1977**, 159-161.

Chapter 5 Reactions of germylenes with metal complexes

5.1 Introduction

The existence of stable carbenes was first described by Fischer *et al*. in 1964 in the complex $W(CO)_5(COCH_3)(CH_3)$).[1] Since this report, carbenes have become ubiquitous neutral ligands in coordination chemistry of transition metals.[2-7]

In this chapter, the various synthetic routes of dicarbene gold(I) complexes and their electronic properties have been summarized. The first dicarbene gold(I) complex **I** was synthesized by Burini and co-workers in 1989, by reacting *C*-imidazolyl lithium salts with chloro(triphenylphosphine)gold(I) (Scheme 5.1). The same method has been applied for the synthesis of the corresponding dicarbene silver(I) complexes.[8]

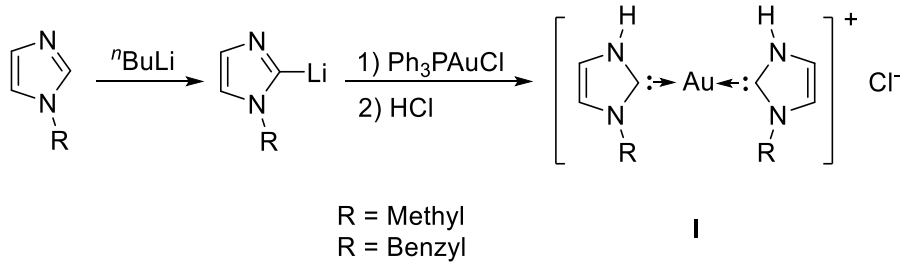

Scheme 5.1 Synthesis of dicarbene gold(I) complexes **I**.

The dicarbene gold(I) complexes have also been synthesized via carbene transfer from corresponding W or Cr carbene complexes.[9-11] In 1998, Liu and co-workers reported that the transfer reaction between the *N*-heterocyclic carbene (NHC) tungsten carbonyl complex **II** and $(Me_2S)AuCl$, led to the formation of di-NHC gold(I) complex **III**, which was obtained as a yellow liquid in 64% yield (Scheme 5.2).[9]

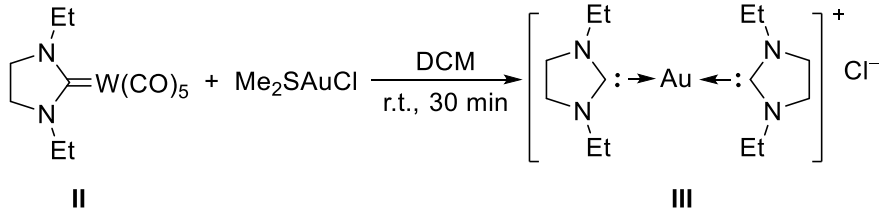

II III

Scheme 5.2 Transfer reaction between NHC tungsten complex **II** and (Me_2S)AuCl.

Following these reports in the literature, the chemistry of dicarbene gold(I) has been intensively studied both experimentally and theoretically. Conventionally, dicarbene gold(I) complexes are synthesized through the direct reaction of tetrahydrothiophene gold(I) chloride ((THT)AuCl) with two equivalents of NHCs or imidazolium salt.[12-15] In 2006, Baker *et al.* reported the synthesis of di-NHC gold(I) complexes **IV** by the reaction of two equivalents of NHCs with (Me_2S)AuCl, wherein the NHCs were prepared *in situ* by the deprotonation of the imidazolium salt with lithium bis(trimethylsilyl)azanide (LiHMDS) at room temperature (Scheme 5.3).[16]

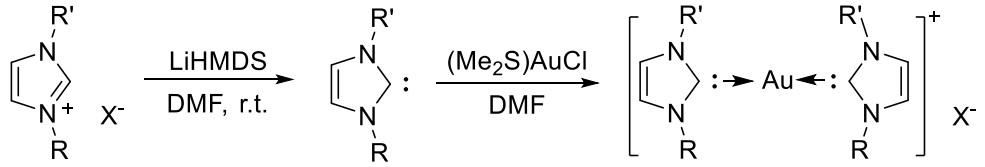

R = R' = Me, ^{i}Pr, ^{n}Bu, ^{t}Bu, and Cy; X = Cl
R = R' = Me; X = Br
R = Me; R' = Et; X = PF_6

IV

Scheme 5.3 Synthesis of di-NHC gold(I) complexes **II**.

The dicarbene gold(I) complexes can also be synthesized in a stepwise manner. In 2008, Bertrand and co-workers reported the formation of the dicyclic (alkyl)(amino) carbenes (CAACs) gold(I) complex **IV**.[17] These **CAACs,** which feature bulky and rigid substituents at the carbon adjacent to the carbene center, reacted with one equivalent of (Me_2S)AuCl to afford the corresponding CAAC gold(I) chloride **V**. Alternatively, di-CAAC gold(I) complexes **VI** were

obtained when the CAACs containing the smaller and more flexible cyclohexyl or cyclohexylene groups were used as reactants (Scheme 5.4a). Complex **VI** could further react with lithium at room temperature in THF to afford electron rich the di-CAAC stabilized gold(0) complex (Scheme 5.4b).[18]

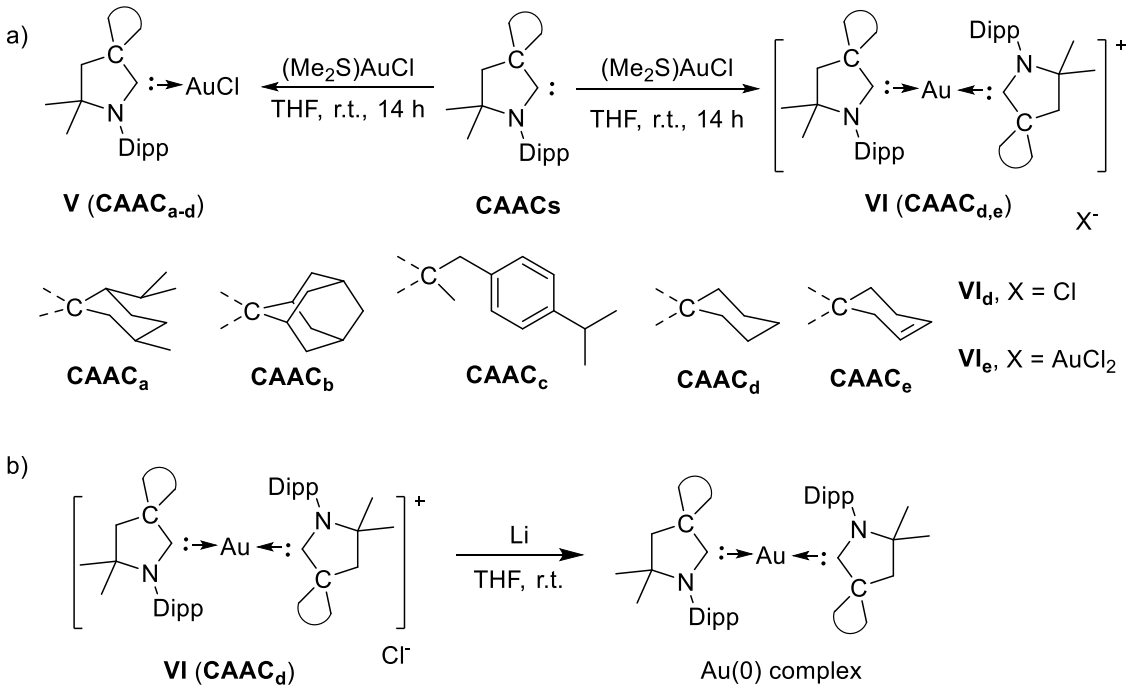

Scheme 5.4 a) Reactions of **CAACs** with $(Me_2S)AuCl$; b) reactions of complexes $\mathbf{VI_d}$ with lithium to afford the gold(0) complex.

In addition to the above mentioned synthetic route, di-NHC gold(I) complex **VII** was synthesized by the reaction of 0.5 equivalents of $(SMe_2)AuCl$ with the corresponding *in situ* generated NHC Ag(I) complex (Scheme 5.5). This reaction was reported by Hong *et al.* in 2013 and performed at ambient temperature in dichloromethane (DCM).[19]

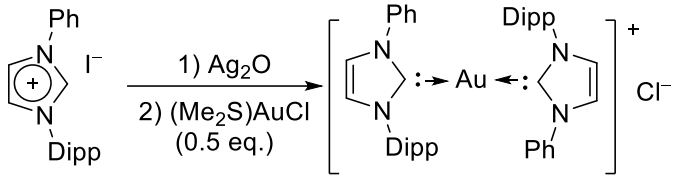

VII

Scheme 5.5 Synthesis of dicarbene gold(I) complex **VII**.

Hetero-di-NHC gold(I) complexes containing two different NHCs have generally been synthesized by the reaction of mono NHC gold(I) complexes with one equivalent of a different free NHC or its precursor imidazolium salt.[20-22] The first hetero-di-NHC gold(I) complex **IX** was reported by Raubenheimer and co-workers in 1995,[21] where one equivalent of CF_3SO_3H was reacted with **VIII** to afford complex **IX** (Scheme 5.6).

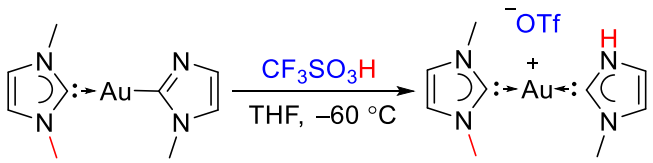

VIII **IX**

Scheme 5.6 Synthesis of the first hetero-di-NHC gold(I) complex **IX**.

In 2013, Huynh and co-workers reported the synthesis of hetero-di-NHC gold(I) complexes **XI**,[22] which involved the reaction of the NHC gold(I) acetate **X** with imidazolium salts (Scheme 5.7). Homo-di-NHC gold(I) complexes were formed when the reaction time was prolonged.

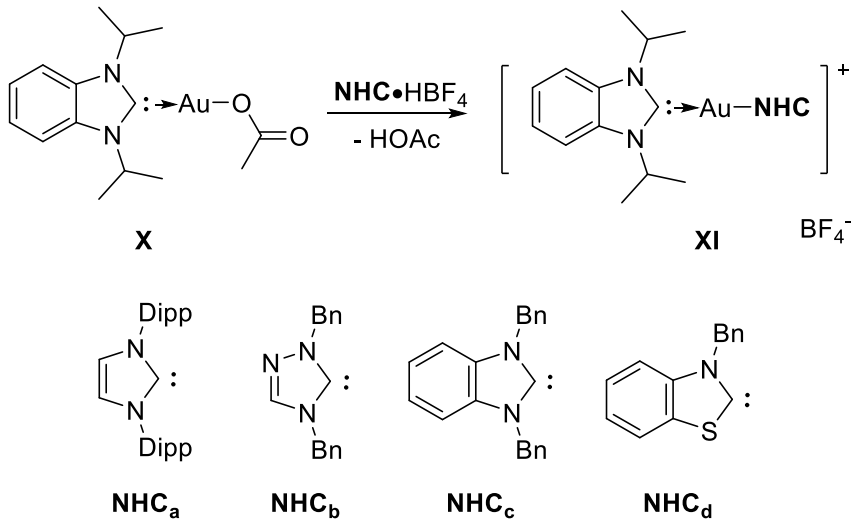

Scheme 5.7 Reactions of complex **X** with different imidazolium salts.

Moreover, the bonding and electronic properties of di-NHC gold(I) complexes have also been studied theoretically. Formally, the bonding in a di-NHC gold(I) complex involves both NHC:→Au(I)←:NHC σ-donation and NHC:←Au(I)→:NHC π-back-donation. However, NHCs are often considered as pure σ donors because the empty *p* orbital of carbene is filled by the π electrons from the nitrogen atom.[23-28]

In 2004, Frenking and co-workers reported a computational study on the π-interactions between Group 11 metals in the +1 oxidation state and NHC ligands.[12] The energy decomposition analysis (EDA) clarified the contributions of σ and π orbital interactions (Figure 5.1).[29-31] The out-of-plane $\pi_{\perp}$ back-donation was found to contribute about 20% to the total orbital interaction energies, and the in-of-plane of $\pi_{\parallel}$ back-donation accounted for 10% of the entire interaction energy.

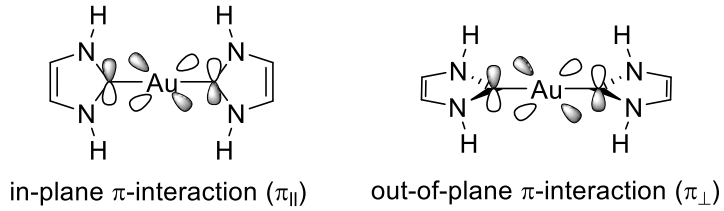

Figure 5.1 The interactions between in-of-plane($\pi_{\parallel}$) and out-of-plane($\pi_{\perp}$).

In 2014, Zuccaccia *et al.* also reported their studies on the interactions between gold(I) and NHC ligands. Their calculations suggested that π back-donation is a sensitive and tunable component of the $C_{carbene}$−Au bond. Moreover, the π/σ contribution ratio can be modulated from more than half of σ-donation to pure σ-donation depending on the auxiliary ligand(L) of the [NHC−Au(I)−L] complex (Figure 5.2).[32] The nature of bonding between the CAAC ligand and gold(I) metal in **IV** was also calculated by Frenking *et al.* These authors suggested that the CAAC ligands are stronger π-acceptors than σ-donors in **IV**,[33] they prefer to accept the *d* electrons of the gold(I) atom.

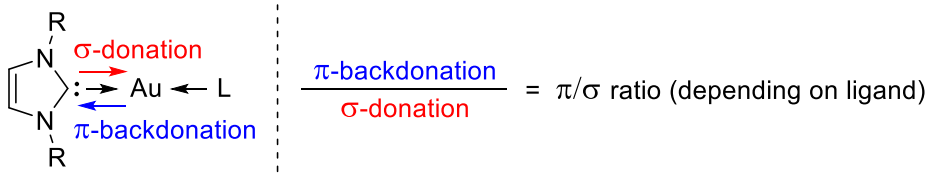

Figure 5.2 The two components of the Au−NHC bond in [NHC−Au−L] systems.

While di-NHC gold(I) complexes have been extensively studied, neither disilylenes nor digermylenes gold(I) complexes have been reported so far. As a relevant study, it has been reported that the reactions of Lewis base-stabilized germylenes with gold(I) halides furnishes germylene-gold(I) species. In 2012, Castel *et al.* reported that the reaction of phosphaalkenyl germylene **XII** with gold(I) halide complexes afforded the germylene gold(I) chloride complex **XIII** (Scheme 5.8a).[34] Leung and co-workers reported the synthesis of the pyridine-coordinated germanium(II) gold(I) complex **XV** by the direct complexation reaction between germanium(II)

XIV and gold(I) iodide (Scheme 5.8b).[35]

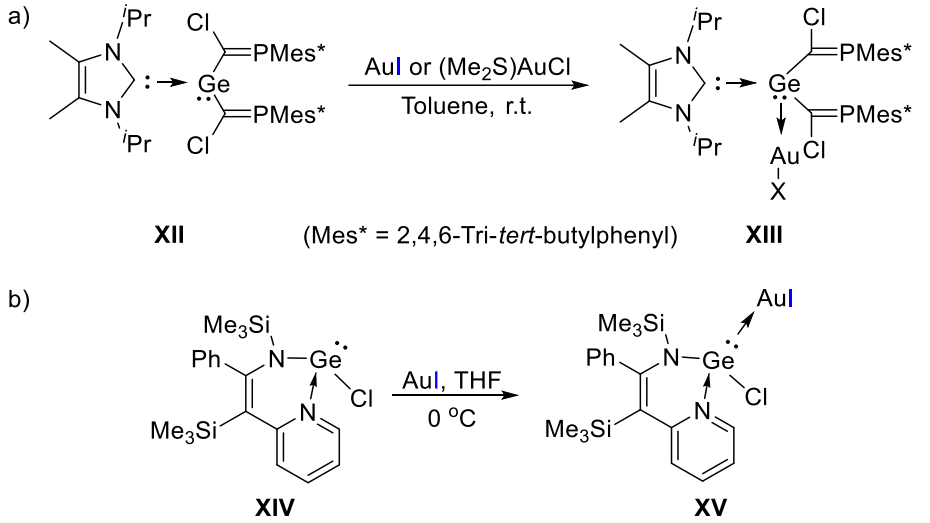

Scheme 5.8 Complexation reactions of germylenes with gold(I) halides.

Compounds containing Au−Ge σ bonds can be synthesized either vis the insertion reaction of germylenes into gold(I)−halide bonds,[36-38] or by the displacement reaction of the R_3Ge^- anion with gold(I) halide species.[39-40] The insertion reaction of $GeCl_2$•dioxane into the Au−Cl bond was first reported by Schmidbaur *et al.* in 1995 in the synthesis of the germanium-gold(I) complex **XVI** (Scheme 5.9a).[38] Analogously, Sharp and co-workers reported that germylene **XVII** inserted into the Au−Cl bond of R_3PAuCl complexes to form germanium-gold(I) complexes **XVIII**(Cl) (Scheme 5.9b).[41] Moreover, when the Cl^- of L→Au−Cl was replaced with the tetrafluoroborate (BF_4^-) analogue in the preceding reaction, fluoride abstraction took place from the BF_4^- anion and the complex **XVIII**(F) was formed.

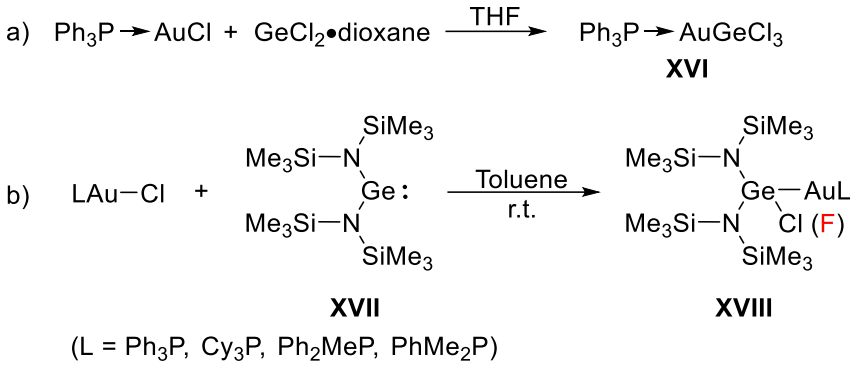

Scheme 5.9 Insertion reactions of germylenes into the Au−Cl bond.

The displacement reaction of the R_3Ge^- anion with gold(I) chloride complexes was first reported by Gade and co-workers in 1996. In this study, the triamidometalate **XIX** was reacted with $[R_4P]^+[AuX_2]^-$ to afford the corresponding digermaaurates **XX** (Scheme 5.7).[40]

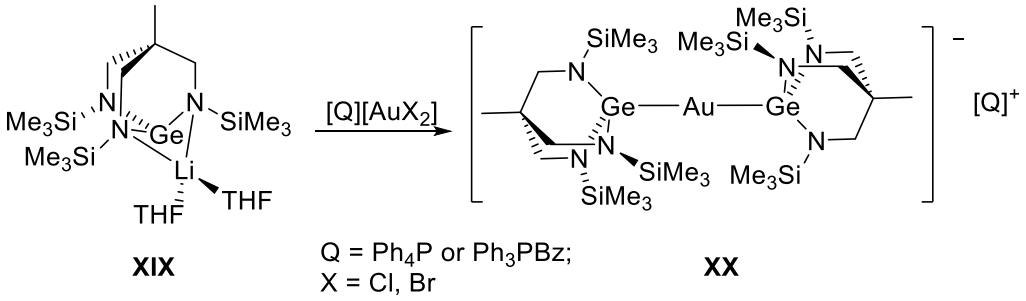

Scheme 5.10 Reactions of the triamidogermalithium **XIV** with gold(I) complexes.

Recently, Majumdar *et al.* have reported the preparation of the dicationic bis(germanium(II)) gold(I) complex **XXI**, in which the sequestered germanium(II) center was coordinated by an acyclic tetradentate bis(α-iminopyridine) ligand (Scheme 5.11).[42] The pentacationic gold(I) complex **XXII** shows a linear geometry with the Ge–Au–Ge bond angle of 166.538(16) º. All Ge–N bonds distances are shorter than that of dicationic germanium(II) **XXI**, which indicates an enhanced donation from the N atoms of both imines and pyridines to the cationic germanium(II) center.

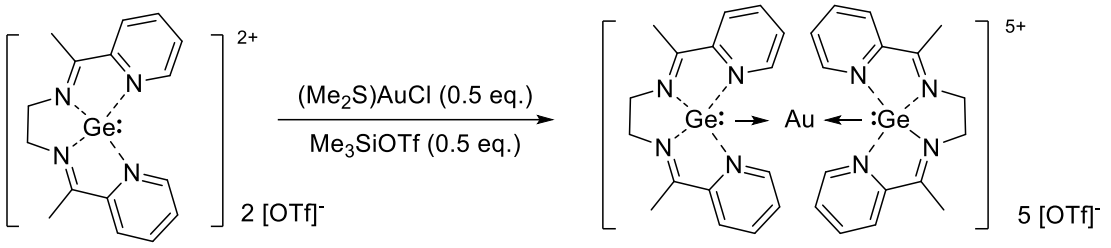

XXI **XXII**

Scheme 5.11 Synthsis of bis(α-iminopyridine) germanium(II) gold(I) complex **XXII**.

Although some germylene and germanium gold(I) complexes have been reported, neither bis(germylenes) gold(I) complexes nor hetero ligands coordinated-gold(I) complexes containing germylene are known. Based on this literature survey, we made an attept to extend the reactions of cyclic (alkyl)(amino) germylenes (CAAGe) **1** with transition metals such as gold(I), palladium(0), and palladium(II). In the cases where the reactions of CAAGe **1** with other transition metals were successful, the corresponding products were further investigated to gain an insight into their geometries and electronic structures, as well as the possibility of their application as catalysts in organic chemistry.

5.2 Results and Discussions

*5.2.1 Reaction of CAAGe **1** with triphenylphosphine gold(I) chloride*

The reaction of CAAGe **1** with one equivalent of tetrahydrothiophene gold(I) chloride ((THT)AuCl) in C_6D_6 at room temperature led to the formation of the corresponding germanium dichloride **2**, and unreacted CAAGe **1**. When 2.2 equivalents of (THT)AuCl were utilized under the same reaction conditions, germanium dichloride **2** was obtained quantitively (Scheme 5.12), the gold nanoparticles were also observed after the reaction on the surface of NMR tube.

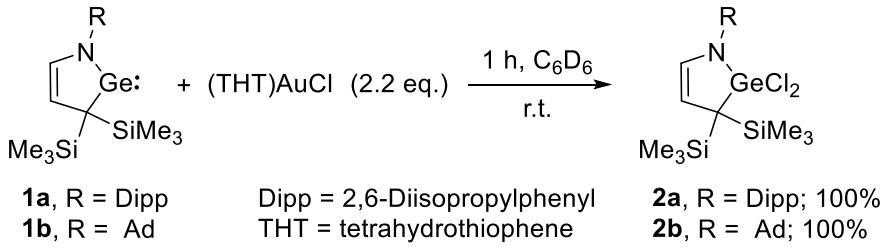

Scheme 5.12 Reactions of CAAGe **1** with (THT)AuCl.

In contrast, when CAAGe **1a** and **1b** were treated with triphenylphosphine gold(I) chloride, insertion into the Au−Cl bond led to the formation of 3a and 3b in 92% and 94% yield respectively (Scheme 5.13). Single crystals of **3a** and **3b** were grown by the volatilization method at room temperature in benzene, and their solid-state structure of **3a** and **3b** were determined by single crystal X-ray diffraction analysis (Figure 5.3). The Ge1–Au1 distances of 2.4037(4) Å in **3a** and 2.4000(5) Å in **3b** are similar to the known Au−Ge(IV) bond lengths,[37, 40-41] but significantly longer than Ge(II)−Au distances in **VIII** and **X** (2.3449(3) Å and 2.346(2) Å, respectively). previously reported Ge(II)–Au distances.[34-35] The Ge–Au–P bond angle in **3a** is 173.08(3) º, which indicates a nearly linear geometry. The Au atoms are not coplanar with the five-membered ring. The dihedral angle of the five-membered ring plane and Au1−Ge1 bond in **3a** is 51.272 º, which is close to that in **3b** (52.183 º).

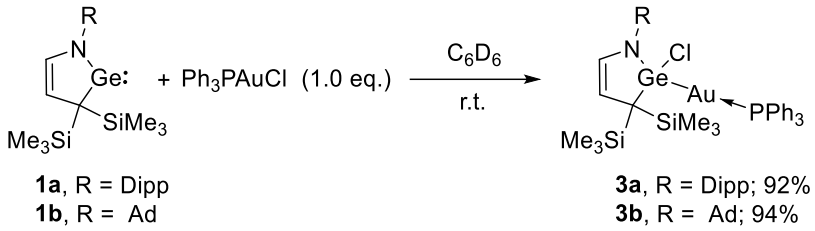

1a, R = Dipp
1b, R = Ad

3a, R = Dipp; 92%
3b, R = Ad; 94%

Scheme 5.13 Reactions of CAAGe **1a** and **1b** with triphenylphosphine gold(I) chloride.

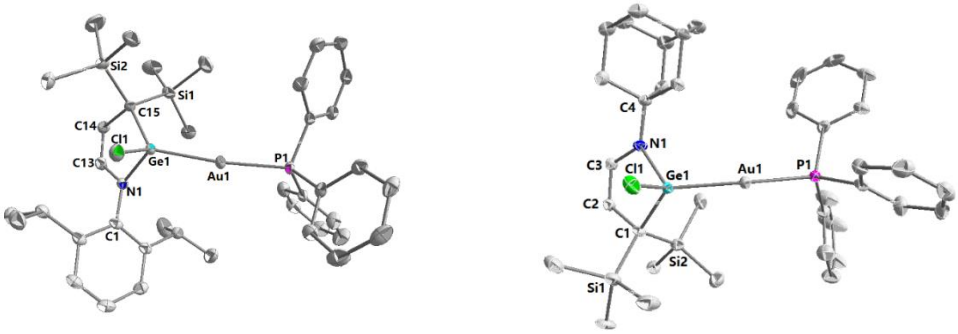

3a **3b**

Figure 5.3 Solid state structures of **3a** and **3b**. Hydrogen atoms are omitted for clarity. Thermal ellipsoids are shown at the 50% probability level. Selected bond lengths [Å] and angles [°]: **3a**) Au1-P1 2.3174(8), Au1-Ge1 2.4037(4), Cl1-Ge1 2.2669(9), Ge1-N1 1.875(3), C15-Ge1 2.000(4), C13-N1 1.386(5), C13-C14 1.339(5), C14-C15 1.524(5), C1-N1 1.434(5); P1-Au1-Ge1 173.08(3), Cl1-Ge1-Au1 105.01(3), N1-Ge1-C15 90.25(14); **3b**) Au1-P1 2.3066(12), Au1-Ge1 2.4000(5), Ge1-N1 1.866(4), Ge1-C1 1.991(4), Ge1-Cl1 2.2704(13), C1-C2 1.510(6), C1-Si1 1.897(5), C1-Si2 1.897(5), C2-C3 1.355(6), C3-N1 1.389(6), C4-N1 1.468(8); P1-Au1-Ge1 167.62(3), N1-Ge1-C1 90.97(18), C1-Ge1-Au1 123.59(14).

*5.2.2 Reaction of germylene **1** with NHC gold(I) chloride*

The reaction of CAAGe **1** with a stoichiometric amount of *N*-heterocyclic carbene gold(I) chloride was conducted at ambient temperature in benzene. Similar to the aforementioned reaction with Ph_3PAuCl, the insertion of **1** into the Au−Cl bond took place and the corresponding gold(I) complexes **4** were obtained in high yields (Scheme 5.14).

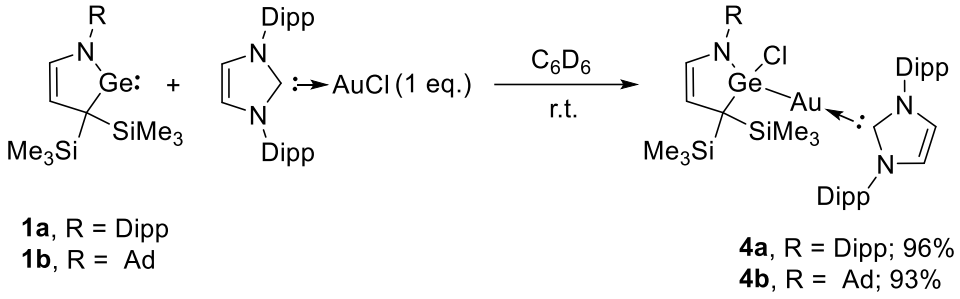

Scheme 5.14 Reaction of CAAGe **1** with NHC gold(I) chloride.

Colorless single crystals of **4a** and **4b** were obtained by volatilization with chloroform at room temperature. Their solid-state structures were determined by single crystal X-ray diffraction analysis and are shown in *Figure 5.4*. The Ge1–Au1–C1 bond angle of **4a** is 173.08(3) º which is more acute than that of **4b** (177.37(11) º). The differences in structural parameters of these complexes may likely be a result of the steric effect of the bulky adamantyl group. The Ge1−Au1 bond length of **4a** (2.3892(5) Å) is slightly longer than that in **4b** (2.3877(4) Å). However, the Ge1−Au1 bond length in **4a** and **4b** are shorter than that of **3** and the previously reported Ge(IV)–Au bond length.[34-35, 40]

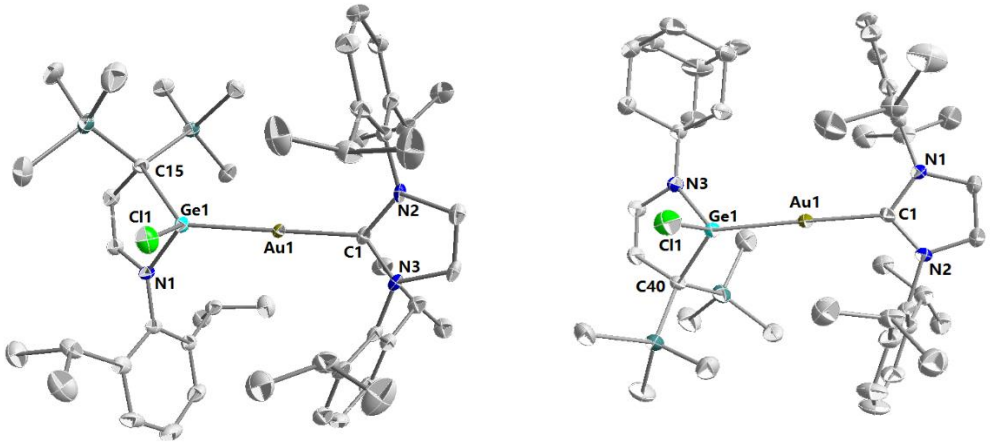

4a **4b**

Figure 5.4 Solid state structures of **4a** and **4b**. Hydrogen atoms are omited for clarity. Thermal ellipsoids are shown at the 50% probability level. Selected bond lengths [Å] and angles [º]: **4a** Au1-C1 2.058(4), Au1-Ge1 2.3892(5), C1-N3 1.348(6), C1-N2, 1.354(6), C15-Ge1 2.012(4), Cl1-Ge1 2.2696(12), Ge1-N1 1.882(4); C1-Au1-Ge1 171.52(12), N3-C1-N2 105.4(3), Cl1-Ge1-Au1 101.16(3), N1-Ge1-C15 89.91(17); **4b** Au1-C1 2.059(4), Au1-Ge1 2.3877(4), C1-N1 1.347(5), C1-N2 1.357(5), C40-Ge1 1.980(4), Cl1-Ge1 2.3078(11), Ge1-N3 1.865(3); C1-Au1-Ge1 177.37(11), N1-C1-N2 104.8(3), N3-Ge1-C40 89.88(16), Cl1-Ge1-Au1 104.77(3).

In the ^{1}H NMR spectrum of **4a**, two multiplet peaks for the C*H* of isopropyl groups of the NHC ligand appear at 2.71 ppm and 2.56 ppm, while one singlet was observed at 2.65 ppm for these protons in **4b**; one singlet for the skeleton *CH* of NHC ligand appears at 7.22 ppm in **4b**, while the corresponding protons are separated into two doublets peaks appearing at 7.08 ppm and 6.76 ppm in **4a** (Figure 5.5).

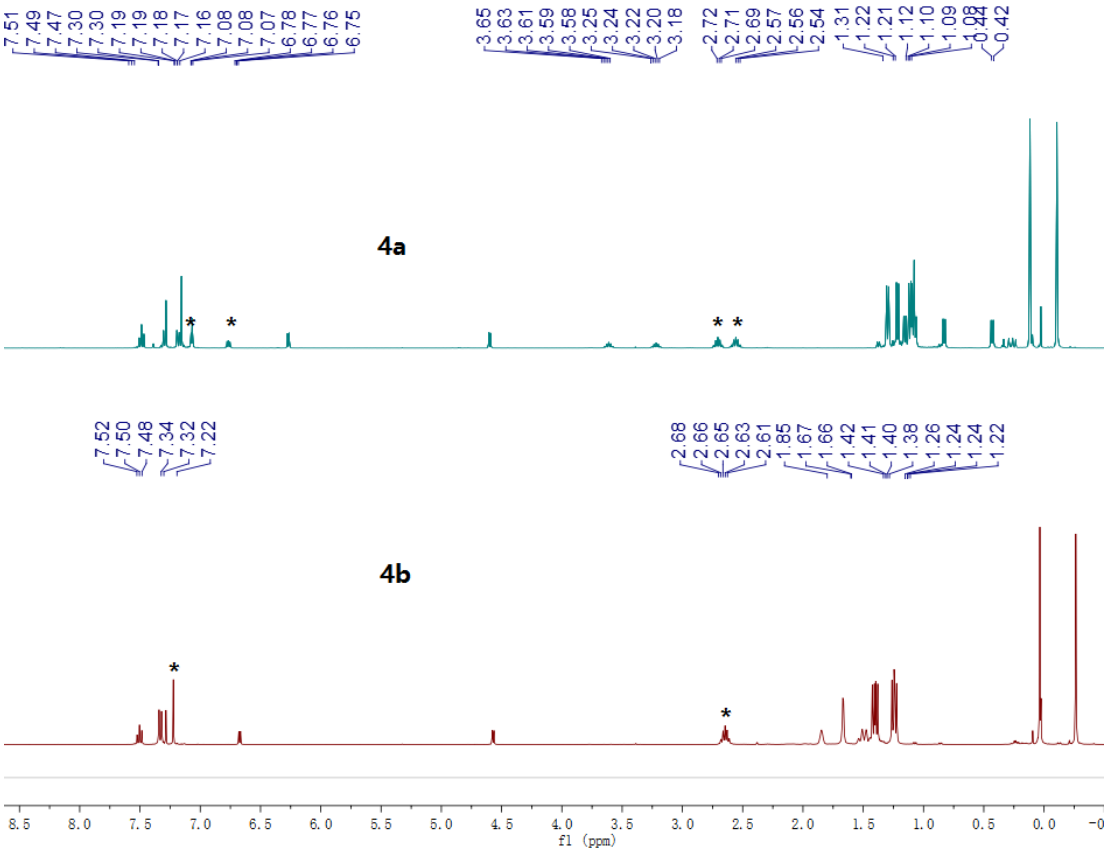

Figure 5.5 ^{1}H NMR spectra of **4a** and **4b**.

5.2.3 Reaction of germanium gold(I) complexes with silver reagents

With the successful synthesis of germanium gold(I) complexes **3** and **4**, these complexes were then utilized for the synthesis of a cationic gold(I) complex supported by germylene and NHC. First, the reactions of **3a** with AgX (X = BF_4, SbF_6, PF_6 and $Al(OC(CF_3)_3)_4$) were performed at ambient temperature in $CDCl_3$. After work-up, unidentifiable products were obtained. Meanwhile, the reactions of **4a** with AgX (X = BF_4, SbF_6, PF_6 and $Al(OC(CF_3)_3)_4$) at room temperature in $CDCl_3$ afforded the corresponding gold(I) complexes **5** (Scheme 5.15). The complex **5d** was characterized by NMR spectroscopy and single crystal X-ray diffraction analysis (Figure 5.6). Complex **4b** was also reacted with AgX (X = BF_4, SbF_6, PF_6 and $Al(OC(CF_3)_3)_4$) under the same conditions, which unfortunately led to its decomposition.

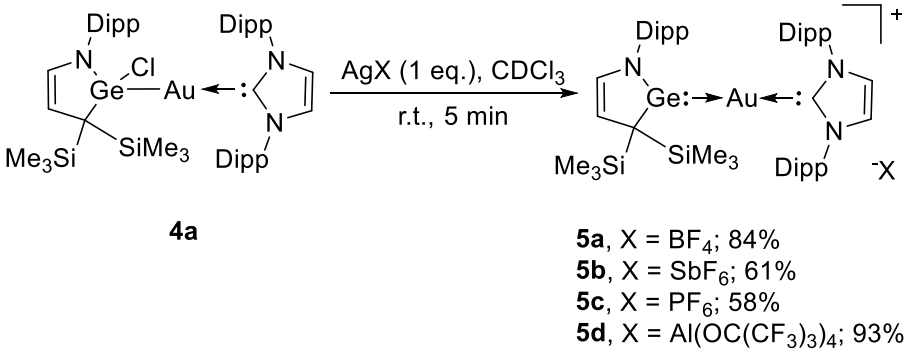

4a

5a, X = BF_4; 84%
5b, X = SbF_6; 61%
5c, X = PF_6; 58%
5d, X = $Al(OC(CF_3)_3)_4$; 93%

Scheme 5.15 Reactions of germanium gold(I) complexes **4a** with silver reagents.

5d possesses a nearly linear Ge1−Au1−C1 skeleton (176.62(15) º). The dihedral angle between the CAAGe five-membered ring and the NHC plane is 31.335 º, which may be a result of the steric effect that resists the π conjugation of both planes. The Ge1−Au1 bond distances (2.3634(6) Å) were found to be slightly shorter than the Au−Ge bonds in **XX** (2.423(2) Å) and those in **XXII** (2.3857(6) Å) but longer than that in **XX** (2.346(2) Å).[40, 42] Complex **5d** has remarkably shorter Ge1–N1 bond distances (1.807(5) Å) in comparison with that in **1a** (1.859(11) Å), indicating an enhanced donation of the N lone pair electrons to the Ge atom.

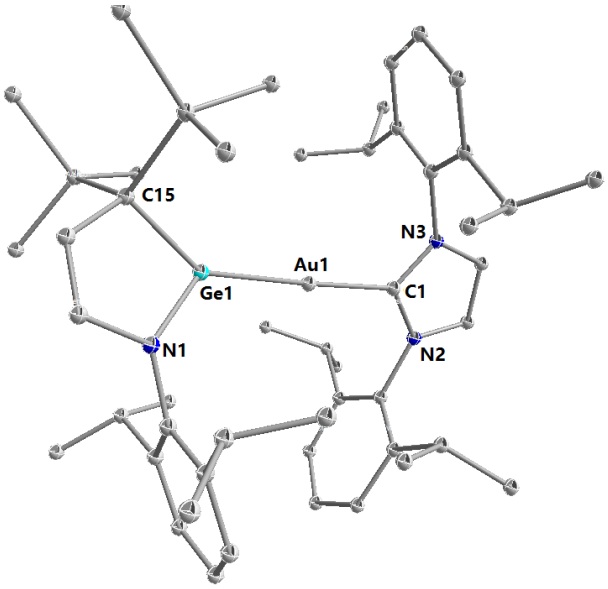

Figure 5.6 Solid-state structure of **5d**. Hydrogen atoms and counter ion are omitted for clarity. Thermal ellipsoids are shown at the 50% probability level. Selected bond lengths [Å] and angles [º]: Au1-C22 2.047(6), Au1-Ge1 2.3634(6), C15-Ge1 1.925(6), Ge1-N1 1.807(5), C22-N2 1.337(7), C22-N3 1.346(7); C22-Au1-Ge1 176.62(15), N2-C22-N3 105.7(5), N1-Ge1-C15 91.2(2).

In order to investigate the electronic nature of **5d**, density functional theory (DFT) calculations (at the B3LYP/6-31G(d,p) level for Ge, Si, C, N, H and M05-2X/LANL2DZ level for Au) on the cationic part of compound **5d** were performed. According to NBO analysis, the Wiberg bond indices for the Ge–Au and C–Au bonds were 0.68 and 0.44, respectively. This suggested that the interaction between germylene and Au centre is stronger than that between Au and carbene. The HOMO─7 corresponds to the σ-donation of electron pairs from the Ge and C to gold(I), in which the latter is energetically stabilized by both carbene and germylene ligands (Figure 5.7a). The π-interaction between the Ge p_z orbitals and empty *p*-orbitals of carbene moiety can be observed clearly (LUMO, Figure 5.7b).

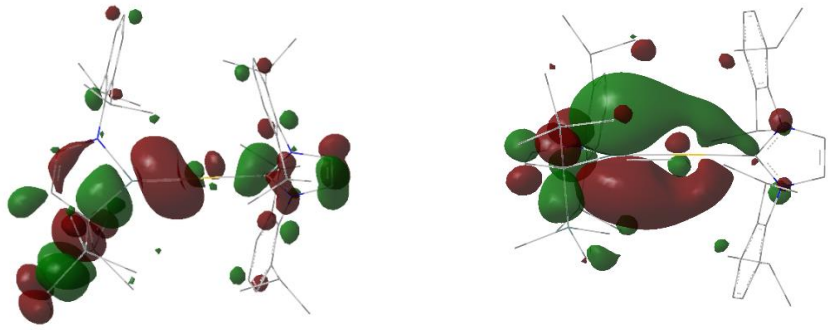

a) HOMO−7 b) LUMO

Figure 5.7 Relevant contour plots of the cationic part of **5d** at an isovalue of 0.03 au.

5.2.4 A brief introduction to the chemistry of germylene palladium complexes

The formation of germylene palladium(0) complex **XXIVa** was first synthesized by Hitchcock and co-workers in 1985 through the reaction of acyclic diamino germylene **XXIII** with [Pd(cod)Cl_2] under the mild condition in toluene, where the platinum analogues of **XXIVb** was also obtained by the reaction of [Pt(cod)Cl_2] and excess of **XXIII** (Scheme 5.16).[43]

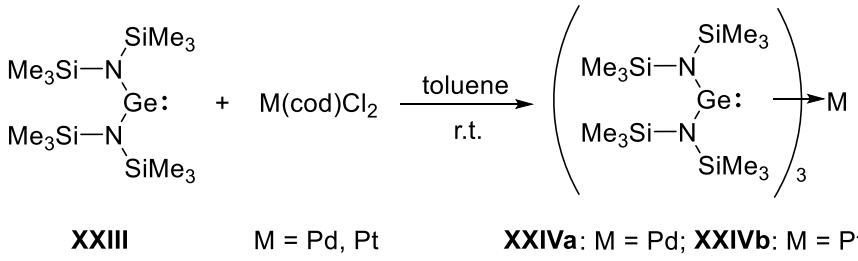

XXIII M = Pd, Pt **XXIVa**: M = Pd; **XXIVb**: M = Pt

Scheme 5.16 Formation of germylene metal complexes **XXIV**.

The reactions of acyclic diamino germylene **XXIII** with palladium(0) complexes have been reported by Holl and co-workers in 2002. The **XVIII** was reacted with 1 equivalent of tetrakis(phosphine) palladium(0) led to the formation of germylene palladium complex **XXV** (Scheme 5.17).[44]

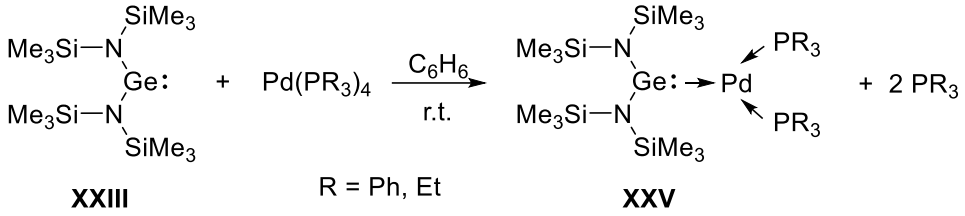

Scheme 5.17 Reactions of germylene **XXIII** with palladium(0) complexes.

The chemical behavior of dimeric germylene **XXVI** in relation to Pd(0) and Pd(II) complexes was studied by Zaitsev et al., where they carried out the reaction of **XXVI** with $Pd(PPh_3)_4$ resulting in tetrakis(germylene) palladium(0) complex **XXVII** and bis(phosphine)-mono(germylene) palladium(0) complex **XXVIII** (Scheme 5.18a). When **XXVI** was treated with $Pd(PPh_3)_2Cl_2$ at ambient temperatures in toluene, **XXVII** and Ge(IV) **XXIX** were obtained, as a result of the oxidation/reduction process (Scheme 5.18b).[45]

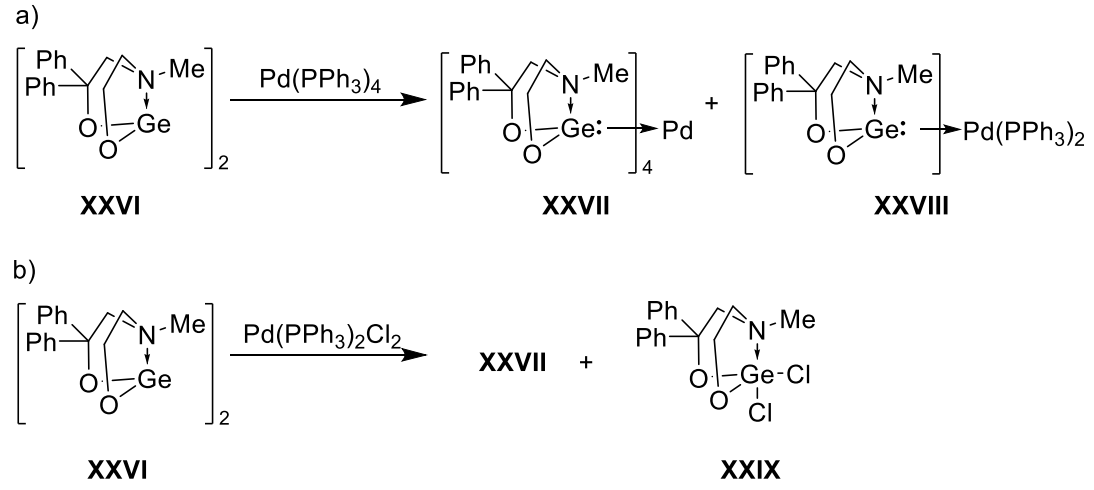

Scheme 5.18 Reaction of dimeric germylene **XXVI** with Pd(0) and Pd(II) complexes.

*5.2.5 Reaction of germylene **1a** with palladium complexes*

As CAAGe **1a** has a high-lying HOMO−1 and low-lying LUMO, we conceived of a bis(germylene **1a**) palladium(0) complex, which is different with the examples mentioned. The reaction of **1a** with tetrakis(triphenylphosphine) palladium(0) was first carried out in benzene

(Scheme 5.19a) to obtain germylene bis(triphenylphosphine) palladium(0) **6**. The structure of **6** was determined by NMR spectroscopy and single crystal X-ray diffraction analysis (Figure 5.8). When two equivalents of **1a** were reacted with one equivalent of bis(triphenylphosphine) palladium(II)dichloride at ambient temperature in C_6D_6 for 1 h, palladium(0) complex **6** was obtained, albeit in a lower yield (31%) (Scheme 5.19b).

The Ge1−Pd1 bond distance of **6** (2.3539(7) Å) is strikingly longer than that in **XXIV** (2.330(5) Å) and slightly shorter than the Au1−Ge1 bond length in **5d** (2.3634(6) Å). The Ge1−Pd1−P1 bond angle for **6** is 124.34(4) º, which is similar to that observed in the case of **XXIV** (125.66(2) º). The P1−Pd1−P2 bond angle is 119.80(5) º, which is also close to that in **XXIV** (119.45(4) º). The Ge1–N1 bond distance of **6** (1.870(4) Å) is slightly longer than that in **1a** (1.859(11) Å) and significantly longer than that in **5d** (1.807(5) Å), which indicated that the donation of electron density from the N atom to the empty *p*-orbital of Ge atom was subdued in complex **6** and enhanced in complex **5d**.

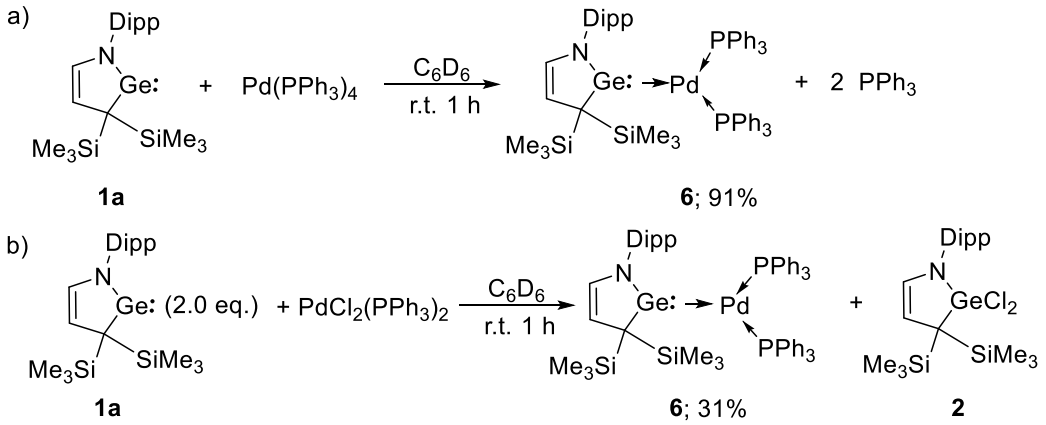

Scheme 5.19 Reactions of CAAGe **1a** with phosphine palladium complexes.

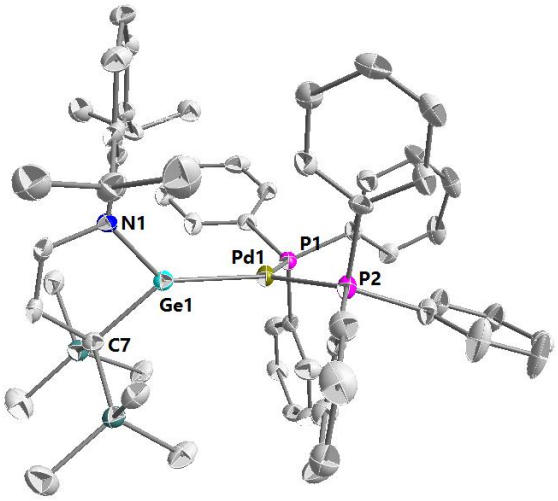

Figure 5.8 Solid state structure of **6**. Hydrogen atoms are omitted for clarity. Thermal ellipsoids are shown at the 50% probability level. Selected bond lengths [Å] and angles [º]: Ge1-Pd1 2.3539(7), P1-Pd1 2.3112(13), P2-Pd1 2.3332(13), Ge1-N1 1.870(4), C7-Ge1 1.995(5); N1-Ge1-C7 88.41(18), P1-Pd1-P2 119.80(5), P1-Pd1-Ge1 124.34(4), P2-Pd1-Ge1 115.82(4).

5.3 Conclusion

The reactions of CAAGe **1** with various gold(I), palladium(0) and palladium(II) complexes have been examined. The Au−Cl bond insertion products [ClGe−Au−PPh_3] **3** and [ClGe−Au−NHC] **4** were formed in the reactions of germylenes **1** with triphenylphosphine gold(I) chloride and NHC gold(I) chloride respectively. The reactions of **4a** with various silver reagents afforded the corresponding [Ge−Au−NHC]•X complex **5**. Furthermore, the reaction of **1a** with $Pd(PPh_3)_4$ resulted in the formation of germylene bis(triphenylphosphine) palladium(0) **6**, which was also formed by the reaction of **1a** with $Pd(PPh_3)_2Cl_2$.

5.4 Experimental Section

5.4.1 General Information

All reactions were performed under an atmosphere of argon by using standard Schlenk or dry box techniques; solvents were dried over sodium metal, potassium metal or CaH_2. All the substrates were obtained from the commercial sources or synthesized following literature procedures. ^{1}H, ^{13}C, ^{19}F and ^{31}P spectra were obtained with AVIII 400MHz BBFO1 spectrometer at 298 K. NMR multiplicities are abbreviated as follows: s = singlet, d = doublet, t = triplet, m = multiplet, br = broad signal. Coupling constants *J* are given in Hz. Electrospray ionization (ESI) mass spectra were obtained at the Mass Spectrometry Laboratory at the Division of Chemistry and Biological Chemistry, Nanyang Technological University. Melting points were measured with an OpticMelt Stanford Research System.

*5.4.2 Reaction of germylene **1** with (THT)AuCl*

(THT)AuCl (0.02 mmol, 6.5 mg) and **1** (0.01 mmol) were mixed in a sealed Young-NMR tube and the reaction mixture was shaken in C_6D_6 (0.5 mL) for 5 min at room temperature. Compounds **2** was then determined by NMR spectroscopy.

*5.4.3 Reaction of germylene **1** with Ph_3PAuCl*

Ph_3PAuCl (0.10 mmol, 50 mg) and **1** (0.10 mmol) were mixed in benzene (2 mL) and the reaction mixture was stirred for 1 h at room temperature. After that, the solvent was removed under vacuum, the mixture was washed with hexane to remove soluble part. The volatile was removed under vacuum, compound **3** was obtained as colorless solid: **3a** (86 mg, 92%), **3b** (85 mg, 94%).

3a: Mp: 157 °C (dec); ^{1}H NMR (400 MHz, C_6D_6) δ 7.24 (tt, *J* = 14.8, 7.4 Hz, 9H, Ar-*H*), 7.04 – 6.94 (m, 3H, Ar-*H*), 6.90 (m, 6H, Ar-*H*), 6.74 (d, *J* = 5.2 Hz, 1H, C*H*), 5.00 (d, *J* = 5.2

Hz, 1H, C*H*), 4.25 (dt, *J* = 13.3, 6.5 Hz, 1H, C*H*), 4.08 (dt, *J* = 13.1, 6.5 Hz, 1H, C*H*), 1.58 (d, *J* = 6.6 Hz, 3H, CH_3), 1.42 (d, *J* = 6.6 Hz, 3H, CH_3), 1.26 (d, *J* = 6.5 Hz, 3H, CH_3), 1.07 (d, *J* = 6.9 Hz, 3H, CH_3), 0.64 (s, 9H, Si(CH_3)$_3$), 0.49 (s, 9H, Si(CH_3)$_3$); ^{13}C NMR (101 MHz, C_6D_6) δ 149.02 (*C*^{q}), 146.32 (*C*^{q}), 142.48 (*C*^{q}), 141.79 (*C*H), 134.06 (*C*H), 133.92 (*C*H), 131.11 (*C*H), 129.05 (*C*H), 128.94 (*C*H), 127.97 (*C*H), 125.83 (*C*H), 124.92 (*C*H), 122.58 (*C*H), 98.88 (*C*H), 37.22 (*C*^{q}), 29.05 (*C*H_3), 28.02 (*C*H_3), 26.16 (*C*H_3), 24.97 (*C*H_3), 22.96 (*C*H_3), 2.51 (Si(*C*H_3)$_3$), 1.35 (Si(*C*H_3)$_3$); ^{31}P NMR (162 MHz, C_6D_6) δ 46.29 (*P*Ph$_3$); HRMS (ESI): m/z calcd for $C_{39}H_{52}AuClGeNPSi_2$: 927.1942. [(M+H)]$^+$; found: 928.1945.

3b: Mp: 149 °C (dec); ^{1}H NMR (400 MHz, C_6D_6) δ ^{1}H NMR (400 MHz, C_6D_6) δ 7.36 (m, 6H, Ar-*H*), 7.08 (d, *J* = 5.5 Hz, 1H, C*H*), 6.99 – 6.82 (m, 9H, Ar-*H*), 5.11 (d, *J* = 5.4 Hz, 1H, C*H*), 2.35 (q, *J* = 11.1 Hz, 6H, CH_2), 2.02 (s, 3H, C*H*), 1.69 – 1.50 (m, 6H, CH_2), 0.66 (s, 9H, Si(CH_3)$_3$), 0.47 (s, 9H, Si(CH_3)$_3$); ^{13}C NMR (101 MHz, C_6D_6) δ 134.67 (*C*H), 134.09 (*C*H), 133.95 (*C*H), 131.18 (*C*H), 131.16 (*C*H), 130.31 (*C*^{q}), 129.83 (*C*^{q}), 129.09 (*C*H), 128.98 (*C*H), 98.85 (*C*H), 54.05 (*C*^{q}), 46.19 (*C*H_2), 36.68 (*C*H_2), 30.39 (*C*H), 2.62 (Si(*C*H_3)$_3$), 1.30 (Si(*C*H_3)$_3$); ^{31}P NMR (162 MHz, C_6D_6) δ 46.16 (*P*Ph$_3$); HRMS (ESI): m/z calcd for $C_{37}H_{50}AuClGeNPSi_2$: 901.1785. [(M+H)]$^+$; found: 902.1864.

*5.4.4 Reaction of germylene **1** with NHCAuCl*

The mixture of NHCAuCl (0.10 mmol, 62 mg) with **1** (0.10 mmol) was stirred in benzene (2 mL) at room temperature for 1 h. After the solvent was removed under vacuum, the mixture was washed with hexane to remove unreacted germylene **1**. The volatile was then removed under vacuum, compound **4** was obtained as colorless solid: **4a** (101 mg, 96%), **4b** (95 mg, 93%).

4a: Mp: 187 °C (dec); ^{1}H NMR (400 MHz, $CDCl_3$) δ 7.49 (t, *J* = 7.8 Hz, 2H, Ar-*H*), 7.30 (d, *J* = 1.3 Hz, 1H, Ar-*H*), 7.22 – 7.14 (m, 4H, Ar-*H*), 7.09 – 7.04 (m, 2H, Ar-*H*), 6.80 – 6.72 (m, 1H, C*H*), 6.27 (d, *J* = 5.2 Hz, 1H, C*H*), 4.60 (d, *J* = 5.2 Hz, 1H, C*H*), 3.61 (dt, *J* = 13.6, 6.8 Hz, 1H, C*H*), 3.22 (dt, *J* = 13.8, 6.9 Hz, 1H, C*H*), 2.71 (dt, *J* = 13.7, 6.9 Hz, 2H, C*H*), 2.56 (dt, *J* =

13.7, 6.8 Hz, 2H, C*H*), 1.30 (d, *J* = 6.9 Hz, 6H, CH_3), 1.22 (d, *J* = 6.9 Hz, 6H, CH_3), 1.16 (d, *J* = 6.7 Hz, 3H, CH_3), 1.13 – 1.05 (m, 15H, CH_3), 0.83 (d, *J* = 6.8 Hz, 3H, CH_3), 0.43 (d, *J* = 7.0 Hz, 3H, CH_3), 0.12 (s, 9H, Si(CH_3)$_3$), -0.11 (s, 9H, Si(CH_3)$_3$); ^{13}C NMR (101 MHz, $CDCl_3$) δ 197.21 ($C_{carbene}$), 148.78 (C^q), 146.74 (C^q), 145.35 (C^q), 145.31 (C^q), 142.46 (C^q), 140.64 (C^q), 134.17 (C^q), 130.42 (*C*H), 124.64 (*C*H), 124.50 (*C*H), 124.23 (*C*H), 123.54 (*C*H), 123.27 (*C*H), 122.27 (*C*H), 98.54 (*C*H), 35.38 (C^q), 28.81 (*C*H_3), 28.71 (*C*H_3), 27.91 (*C*H), 27.51 (*C*H), 26.27 (*C*H_3), 25.89 (*C*H), 24.50 (*C*H_3), 24.47 (*C*H_3), 24.30 (*C*H_3), 24.16 (*C*H), 23.74 (*C*H_3), 22.93 (*C*H), 2.53 (Si(*C*H_3)$_3$), 1.00 (Si(*C*H_3)$_3$); HRMS (ESI): m/z calcd for $C_{48}H_{73}AuClGeN_3Si_2$: 1053.3903. $[(M+H)]^+$; found: 1054.3987.

4b: Mp: 182 °C (dec); ^{1}H NMR (400 MHz, $CDCl_3$) δ 7.50 (t, *J* = 7.8 Hz, 2H, Ar-*H*), 7.33 (d, *J* = 8.1 Hz, 4H, Ar-*H*), 7.22 (s, 2H, C*H*), 6.67 (d, *J* = 5.4 Hz, 1H, C*H*), 4.57 (d, *J* = 5.4 Hz, 1H, C*H*), 2.65 (dt, *J* = 13.8, 6.9 Hz, 4H, C*H*), 1.85 (s, 3H, C*H*), 1.67 (d, *J* = 2.2 Hz, 6H, CH_2), 1.49 (d, *J* = 12.9 Hz, 6H, CH_2), 1.40 (dd, *J* = 11.1, 6.9 Hz, 12H, CH_3), 1.24 (dd, *J* = 8.5, 7.0 Hz, 12H, CH_3), 0.04 (s, 9H, Si(CH_3)$_3$), −0.26 (s, 9H, Si(CH_3)$_3$); ^{13}C NMR (101 MHz, $CDCl_3$) δ 197.39 ($C_{carbene}$), 145.53 (C^q), 145.36 (C^q), 134.17 (*C*H), 134.03 (C^q), 130.59 (*C*H), 129.04 (*C*H), 128.20 (C^q), 124.31 (*C*H), 124.12 (*C*H), 123.44 (*C*H), 119.97 (*C*H), 98.85 (*C*H), 53.52 (C^q), 45.22 (*C*H_2), 36.60 (*C*H_2), 33.31 (C^q), 29.94 (*C*H), 28.91 (*C*H), 28.87 (*C*H), 24.61 (*C*H_3), 24.53 (*C*H_3), 24.22 (*C*H_3), 24.05 (*C*H_3), 2.39 (Si(*C*H_3)$_3$), 0.89 (Si(*C*H_3)$_3$); HRMS (ESI): m/z calcd for $C_{46}H_{71}AuClGeN_3Si_2$: 1027.3747. $[(M+H)]^+$; found: 1028.3844.

*5.4.5 Reaction of **4a** with AgX*

The mixture of gold(I) complex **4a** (0.05 mmol, 50 mg) with AgX (0.05 mmol) ($AgBF_4$, 10 mg; $AgSbF_6$, 17 mg; $AgPF_6$, 13 mg) was carried out in $CDCl_3$ (0.5 mL) at room temperature for 5 min. After the mixture was monitored by NMR spectroscopy to determine the yield (**5a** 84%; **5b** 61%; **5c** 58%).

The mixture of gold(I) complex **4a** (0.10 mmol, 105 mg) with $AgAl(OC(CF_3)_3)_4$, 107 mg)

was carried out in $CHCl_3$ (2 mL) at room temperature for 5 min. After AgCl was filtered off. All volatiles were removed under vacuum to afford **5d** as a yellow solid (183 mg, 93%). Mp: 244 °C (dec). ^{1}H NMR (400 MHz, $CDCl_3$) δ 7.55 (t, *J* = 7.8 Hz, 2H, Ar-*H*), 7.34 (d, *J* = 7.8 Hz, 1H, Ar-*H*), 7.28 (d, *J* = 2.8 Hz, 5H, Ar-*H*), 7.19 (d, *J* = 4.8 Hz, 1H, C*H*), 7.13 (d, *J* = 7.8 Hz, 2H, C*H*), 6.25 (d, *J* = 4.8 Hz, 1H, C*H*), 2.54 (dt, *J* = 13.8, 6.9 Hz, 2H, C*H*), 2.45 – 2.28 (m, 4H, C*H*), 1.22 (d, *J* = 6.9 Hz, 12H, CH_3), 1.08 (d, *J* = 6.8 Hz, 6H, CH_3), 1.07 (d, *J* = 6.9 Hz, 12H, CH_3), 0.72 (d, *J* = 6.9 Hz, 6H, CH_3), 0.05 (s, 18H, Si(CH_3)$_3$); ^{13}C NMR (101 MHz, $CDCl_3$) δ 188.12 ($C_{carbene}$), 145.46 (C^q), 144.00 (C^q), 143.81 (*C*H), 138.72 (C^q), 132.70 (C^q), 131.49 (*C*H), 128.43 (*C*H), 124.55 (*C*H), 124.42 (*C*H), 123.59 (C^q), 122.72 (*C*H), 119.80 (*C*H), 119.11 (C^q), 75.74 (C^q), 28.79 (*C*H), 27.97 (*C*H), 25.24 (C^q), 25.00 (*C*H_3), 23.59 (*C*H_3), 23.44 (*C*H_3), 1.87 (Si(*C*H_3)$_3$); ^{19}F NMR (376 MHz, $CDCl_3$) δ -75.46 (C*F*$_3$); HRMS (ESI): m/z calcd for $[C_{48}H_{73}AuGeN_3Si_2]^+$: 1018.4220. $[M]^+$; found: 1018.4235.

*5.4.6 Reaction of germylene **1a** with $Pd(PPh_3)_2Cl$ and $Pd(PPh_3)_4$*

$Pd(PPh_3)_2Cl_2$ (0.1 mmol, 71 mg) and **1a** (0.2 mmol, 87 mg) were mixed in benzene (1 mL), and the mixture was stirred for 1 hour at room temperature. After the solvent was removed under vacuum, the mixture was washed with hexane. Recrystallization with benzene afford **6** as red crystal (66 mg, 31%).

$Pd(PPh_3)_4$ (0.1 mmol, 116 mg) and **1a** (0.1 mmol, 44 mg) were mixed in benzene (1 mL), and the mixture was stirred for 1 hour at ambient temperature, then recrystallized with benzene to afford **6** as red crystal (85 mg, 81%).

Mp: 167 °C (dec). ^{1}H NMR (400 MHz, C_6D_6) δ 7.39 (dd, *J* = 9.0, 7.1 Hz, 10H, Ar-*H*), 7.26 (dd, *J* = 8.5, 6.5 Hz, 1H, Ar-*H*), 7.19 (d, *J* = 7.0 Hz, 2H, Ar-*H*), 7.07 (d, *J* = 4.6 Hz, 1H, C*H*), 6.98 – 6.84 (m, 20H, Ar-*H*), 5.80 (d, *J* = 4.6 Hz, 1H, C*H*), 3.57 (dt, *J* = 13.6, 6.8 Hz, 2H, C*H*), 1.21 (d, *J* = 6.8 Hz, 6H, CH_3), 0.78 (d, *J* = 6.8 Hz, 6H, CH_3), 0.28 (s, 18H, Si(CH_3)$_3$); ^{13}C NMR (101 MHz, C_6D_6) δ 145.36 (*C*H), 145.23 (C^q), 144.61 (C^q), 138.72 (*C*H), 138.59 (*C*H), 138.47

(*C*H), 133.96 (*C*H), 133.87 (*C*H), 133.79 (*C*H), 128.31 (*C*H), 126.04 (*C*H), 123.52 (*C*H), 111.82 (*C*H), 71.69 (C^q), 28.15 (*C*H), 24.77 (CH_3), 23.84 (CH_3), 1.53 ($Si(CH_3)_3$); HRMS (ESI): m/z calcd for $C_{57}H_{67}PdGeNP_2Si_2$: 1063.2534. $[(M+H)]^+$; found: 1064.2646.

5.4.6 ^{1}H, ^{13}C, ^{19}F and ^{31}P NMR Spectra

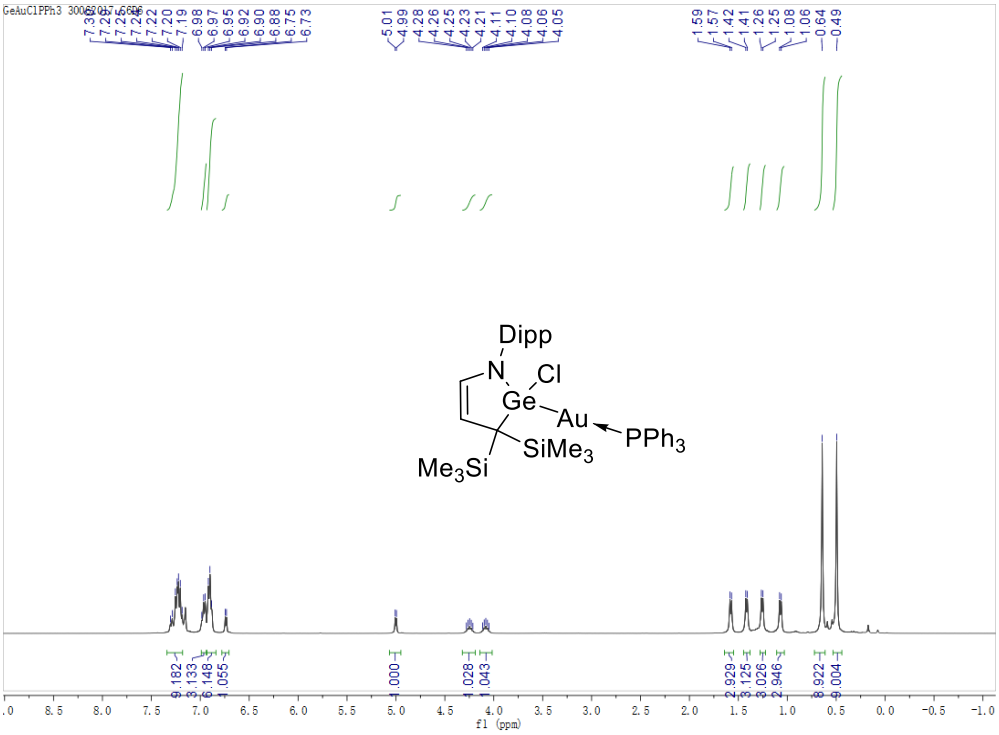

Figure 5.9 ^{1}H NMR spectrum of **3a**

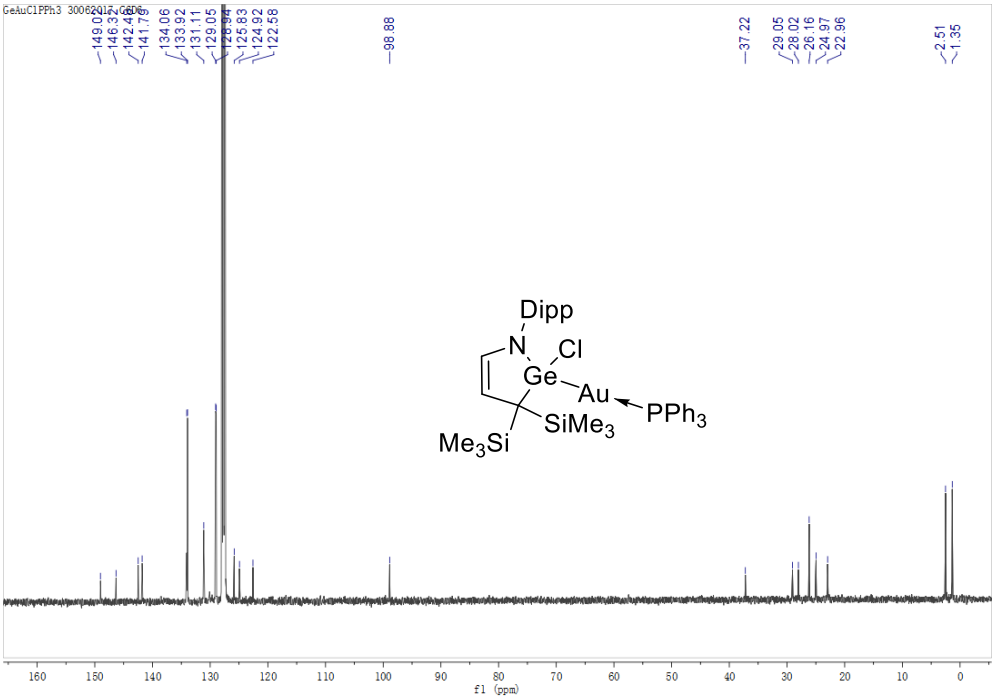

Figure 5.10 ^{13}C NMR spectrum of **3a**

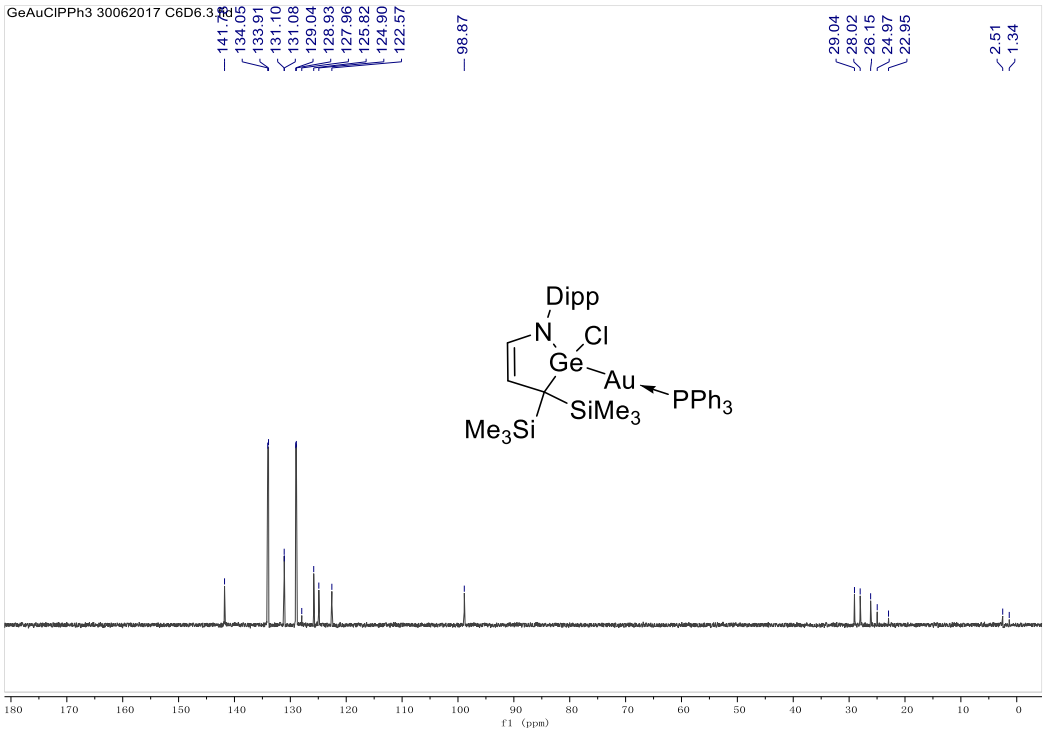

Figure 5.11 DEPT-135 spectrum of **3a**

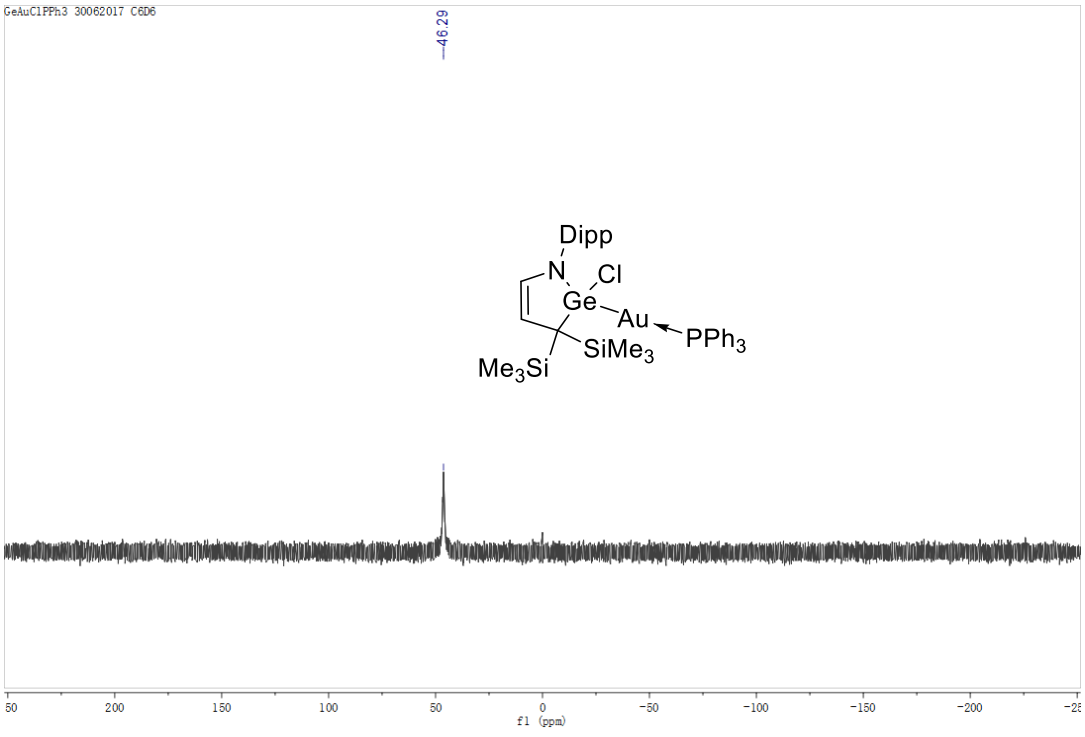

Figure 5.12 ^{31}P NMR spectrum of **3a**

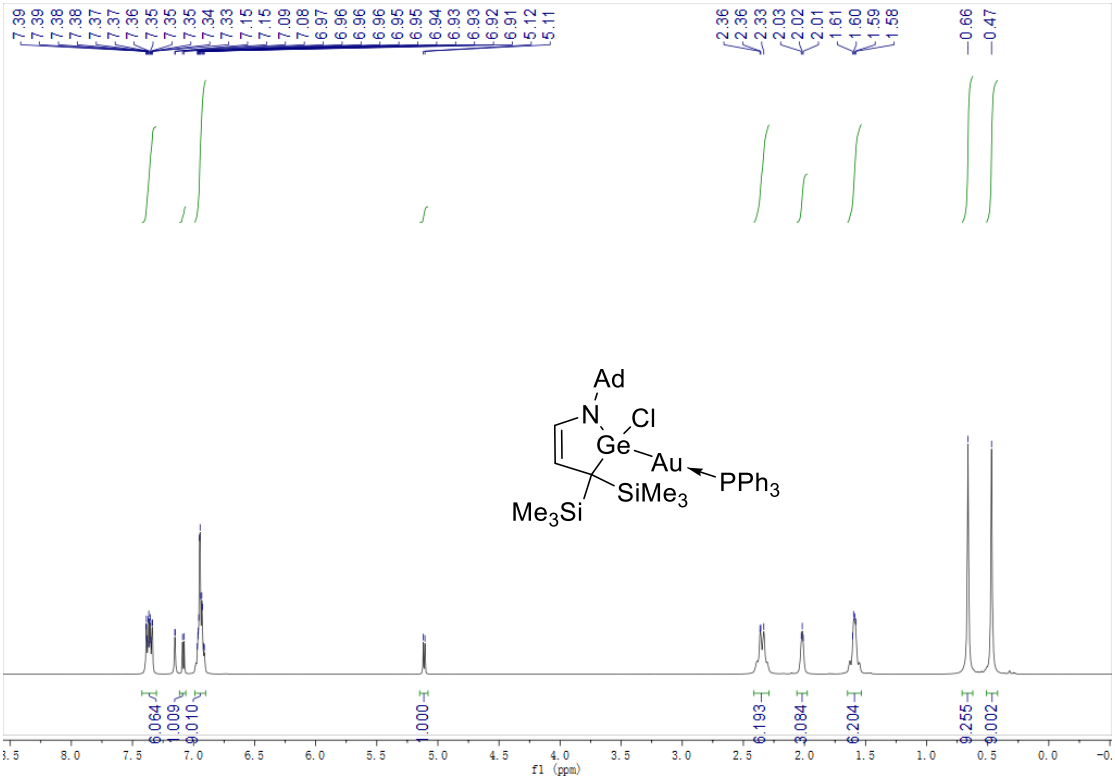

Figure 5.13 ^{1}H NMR spectrum of **3b**

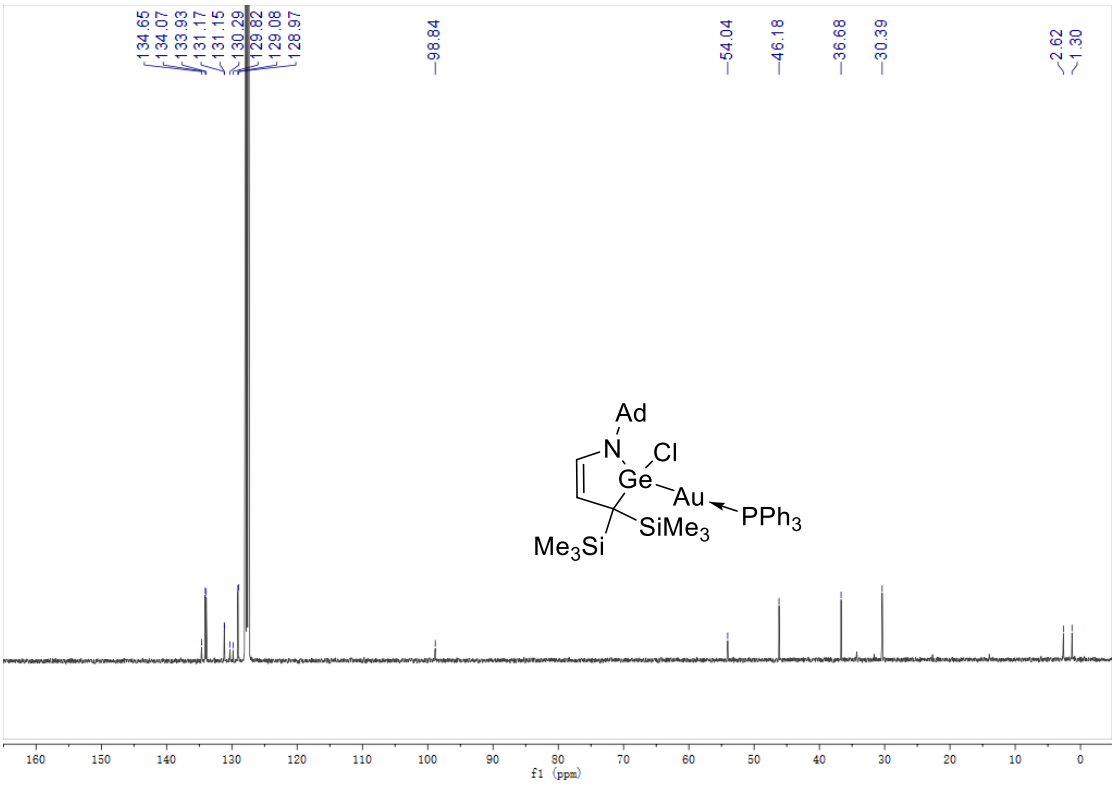

Figure 5.14 ^{13}C NMR spectrum of **3b**

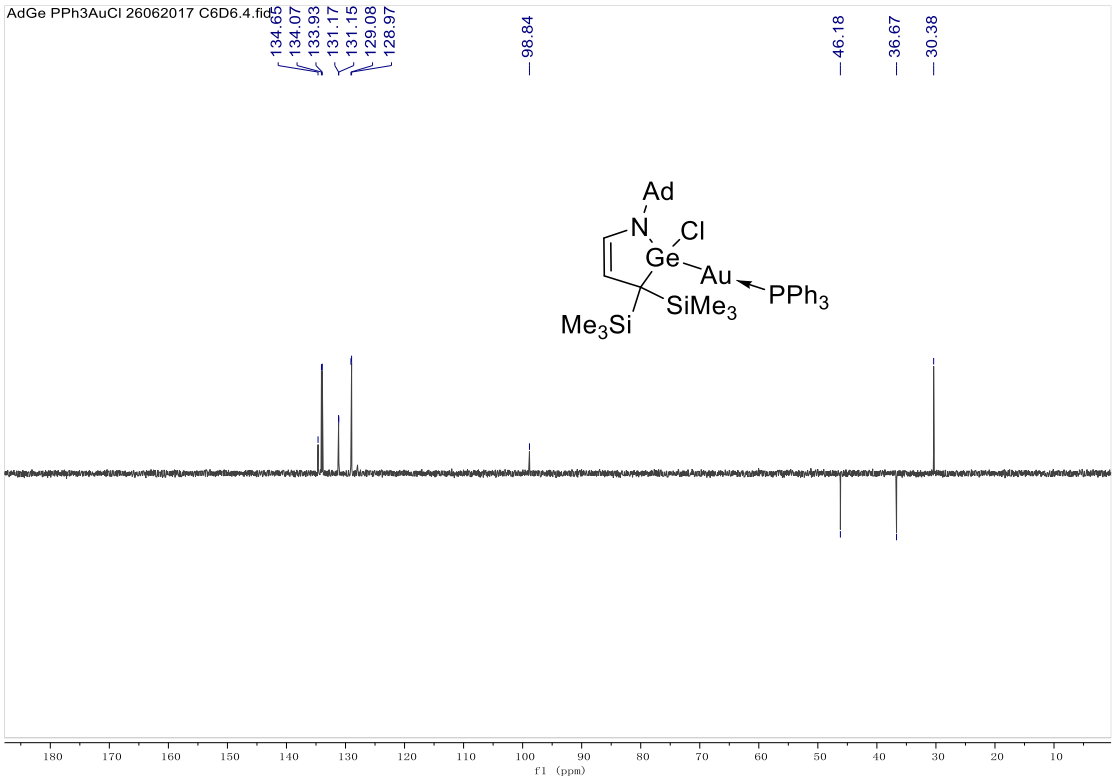

Figure 5.15 DEPT-135 spectrum of **3b**

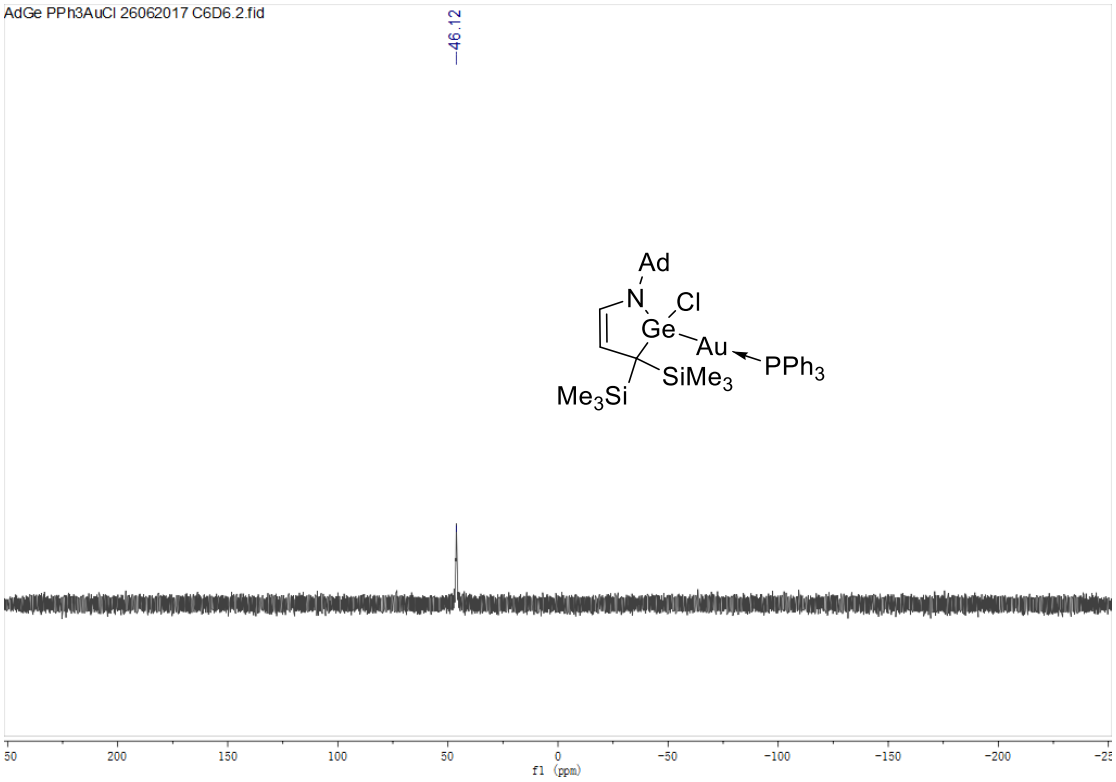

Figure 5.16 ^{31}P NMR spectrum of **3b**

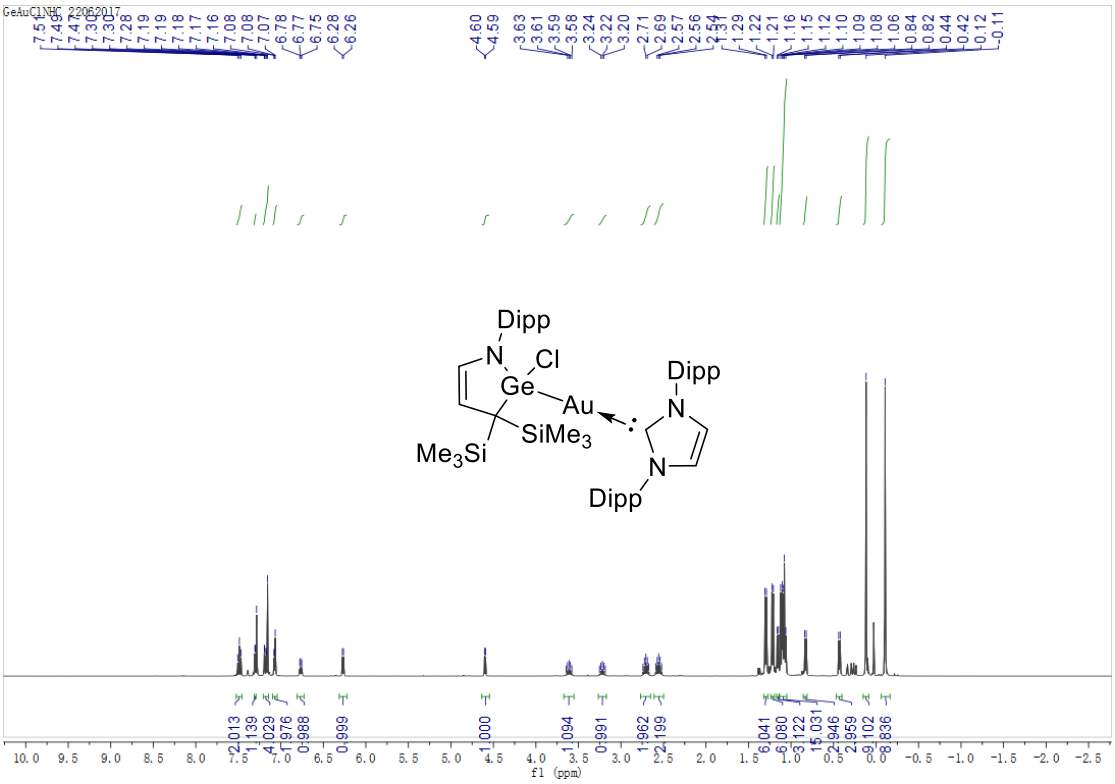

Figure 5.17 ^{1}H NMR spectrum of **4a**

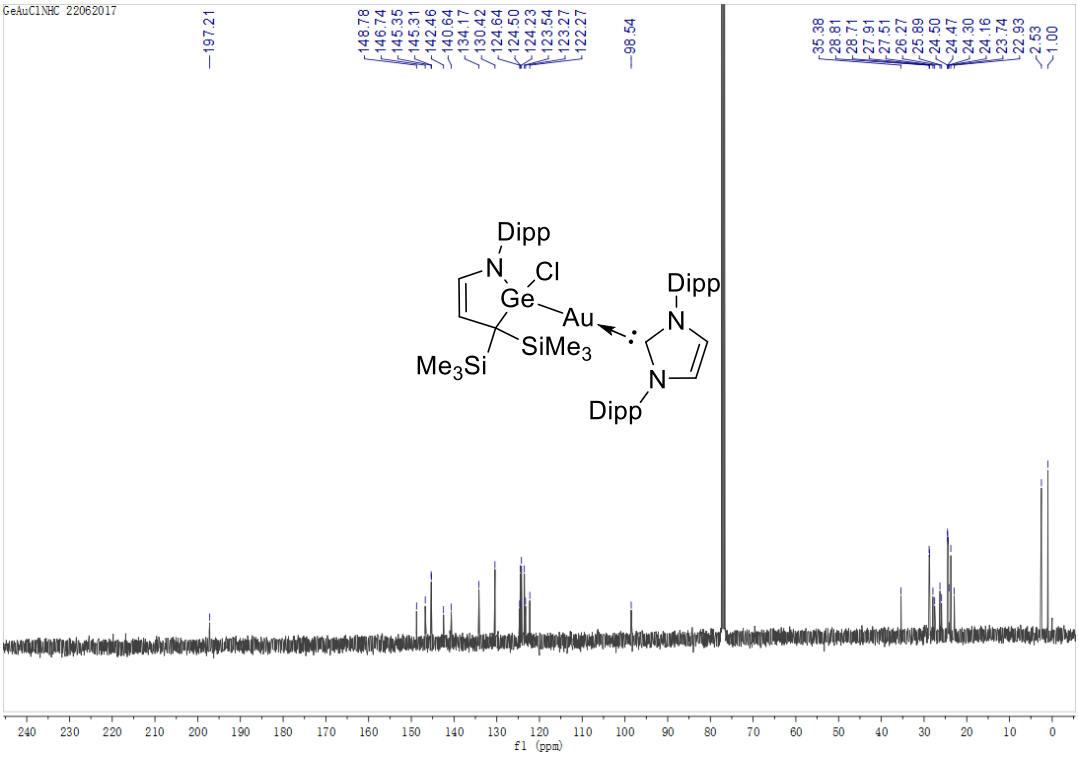

Figure 5.18 ^{13}C NMR spectrum of **4a**

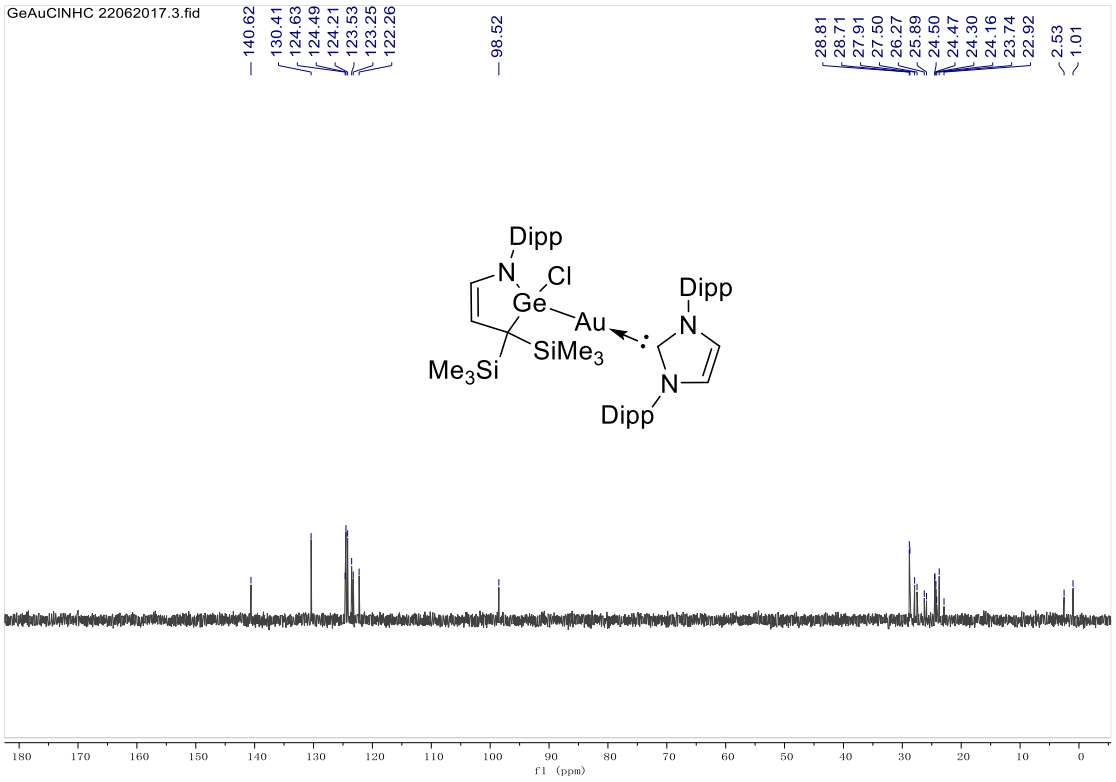

Figure 5.19 DEPT-135 spectrum of **4a**

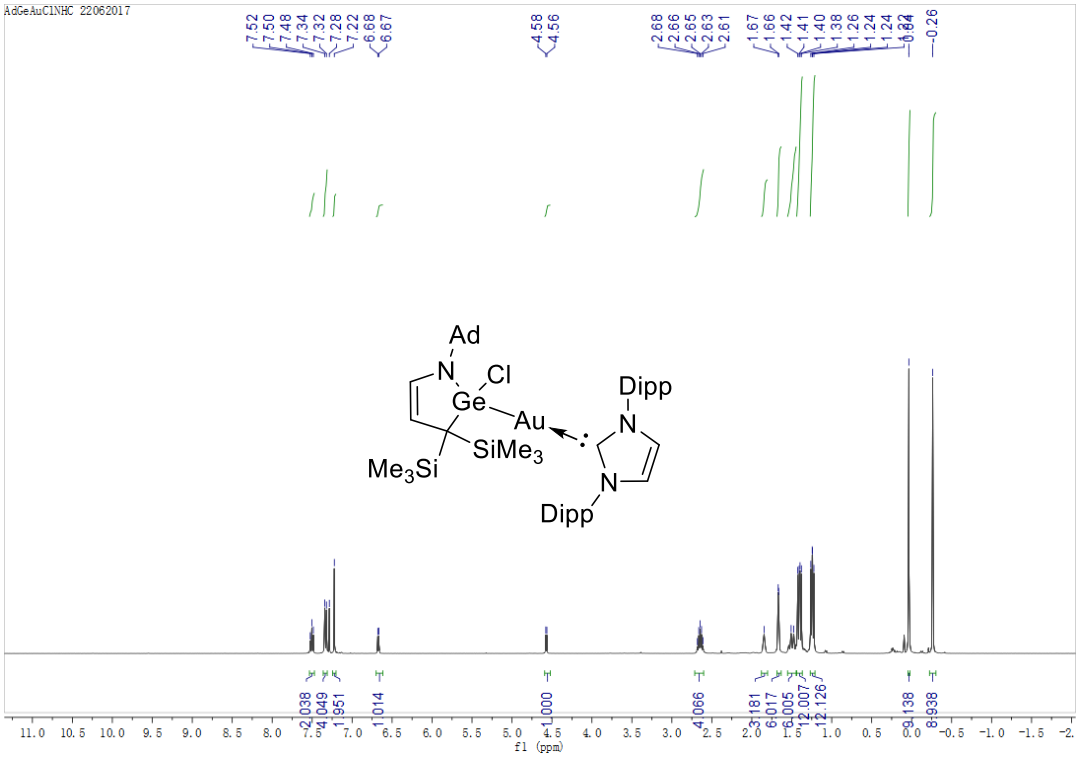

Figure 5.20 ^{1}H NMR spectrum of **4b**

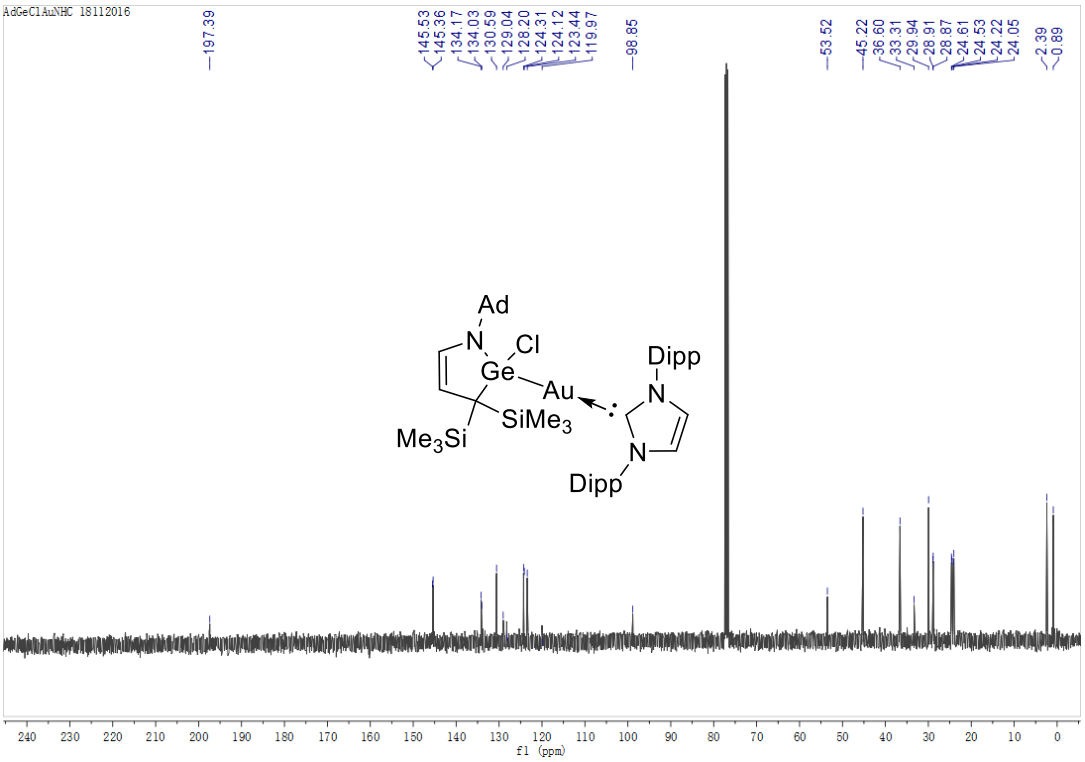

Figure 5.21 ^{13}C NMR spectrum of **4b**

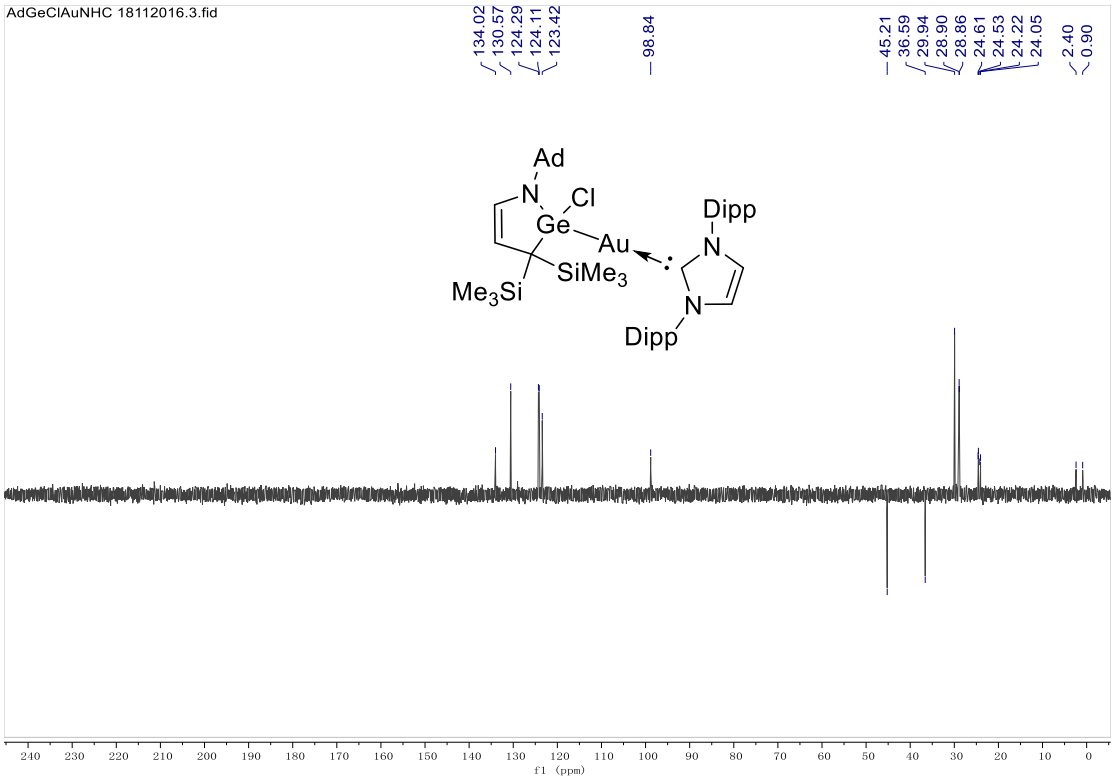

Figure 5.22 DEPT-135 spectrum of **4b**

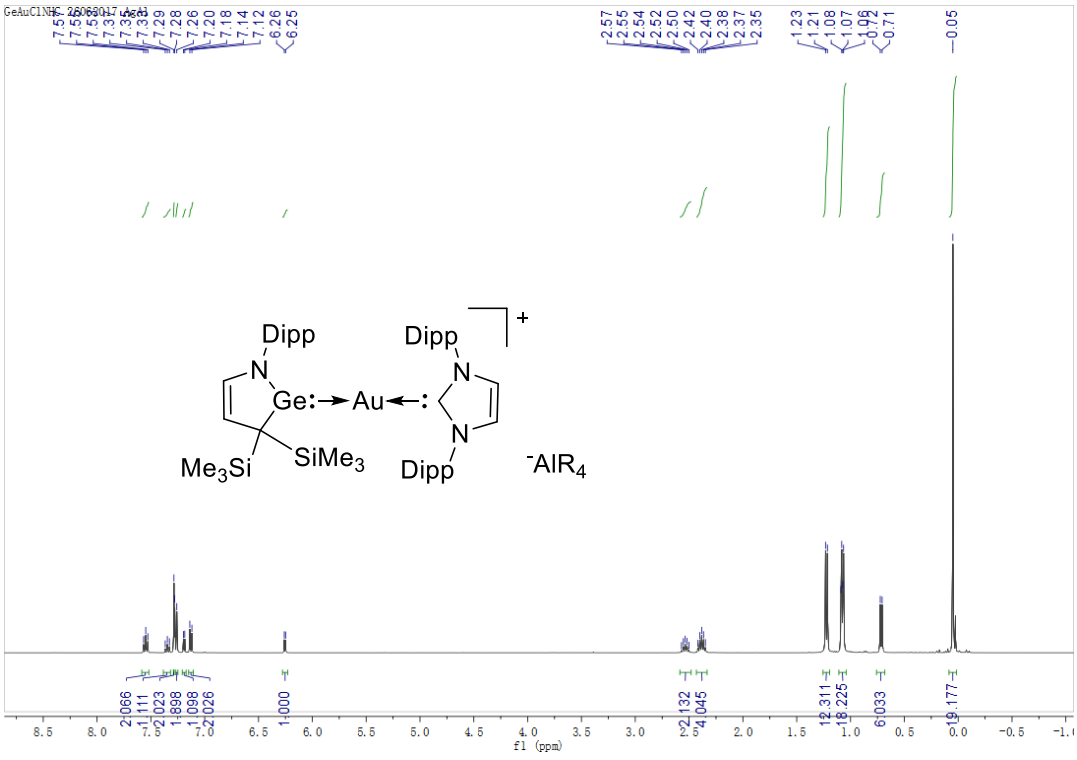

Figure 5.23 ^{1}H NMR spectrum of **5**

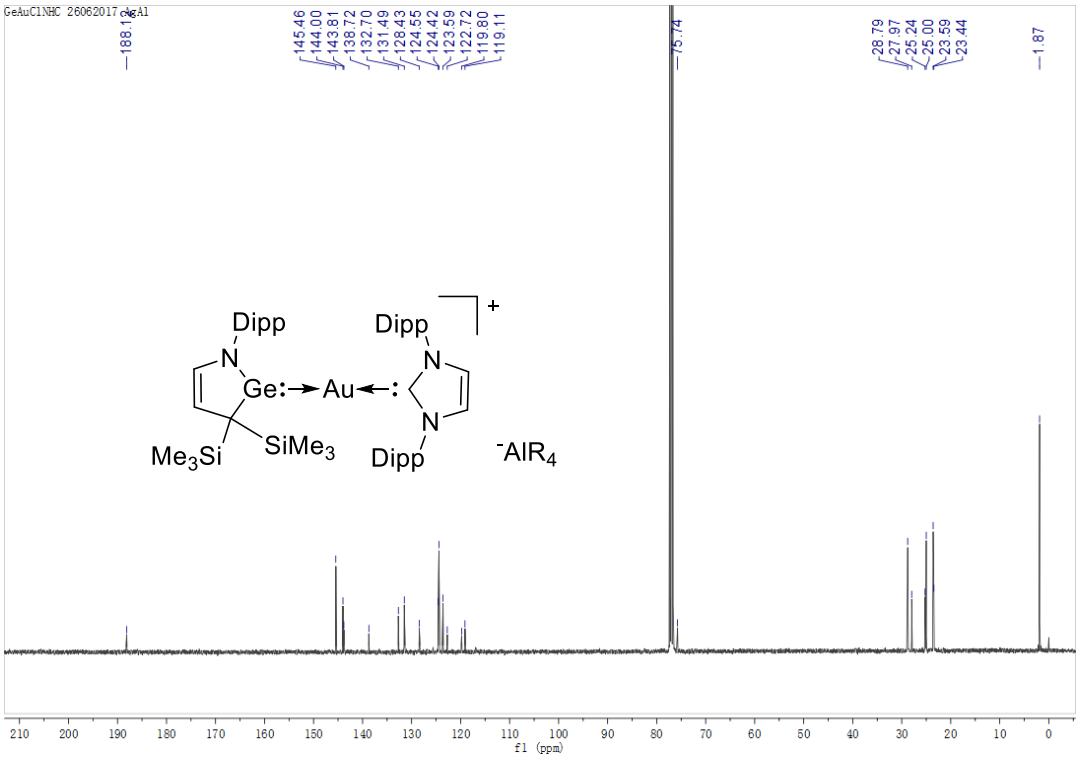

Figure 5.24 ^{13}C NMR spectrum of **5**

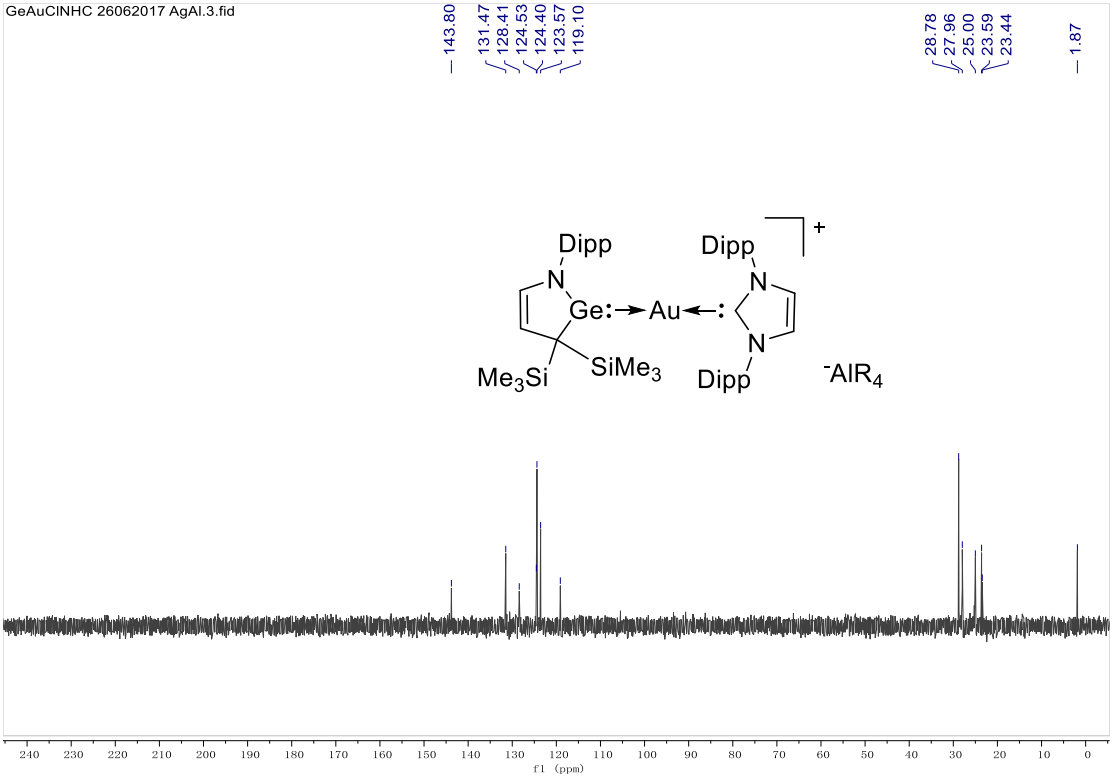

Figure 5.25 DEPT-135 NMR spectrum of **5**

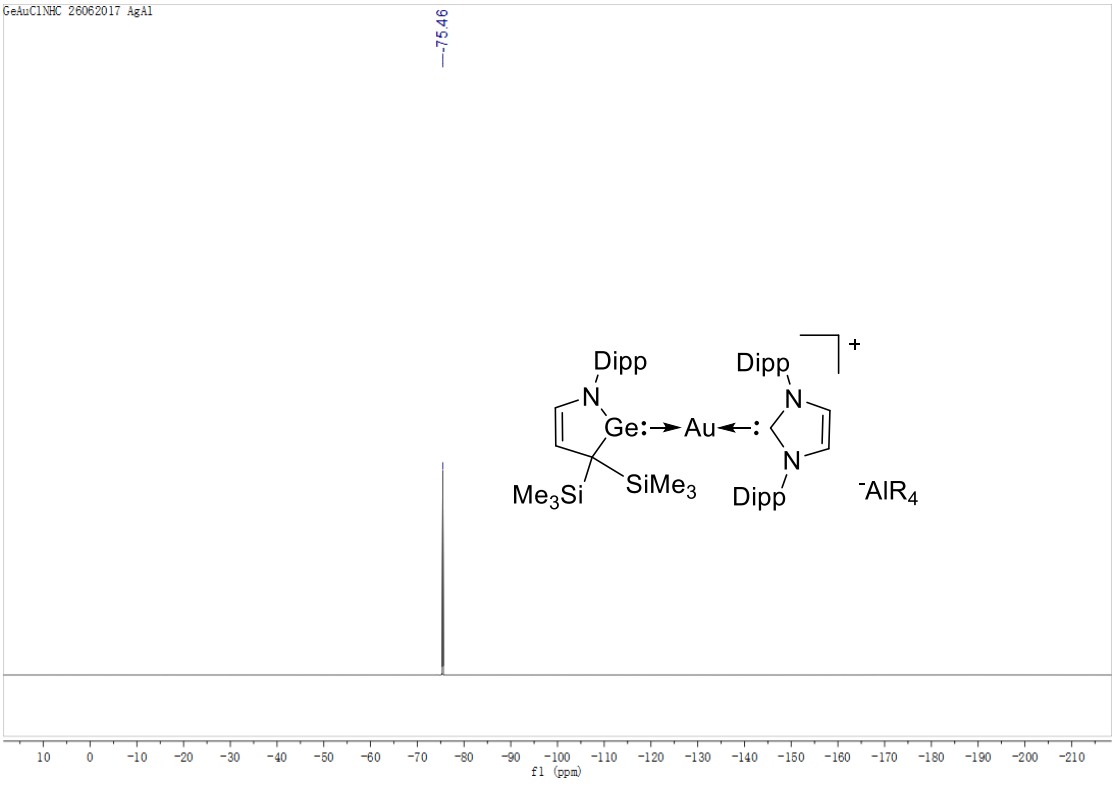

Figure 5.26 ^{19}F NMR spectrum of **5**

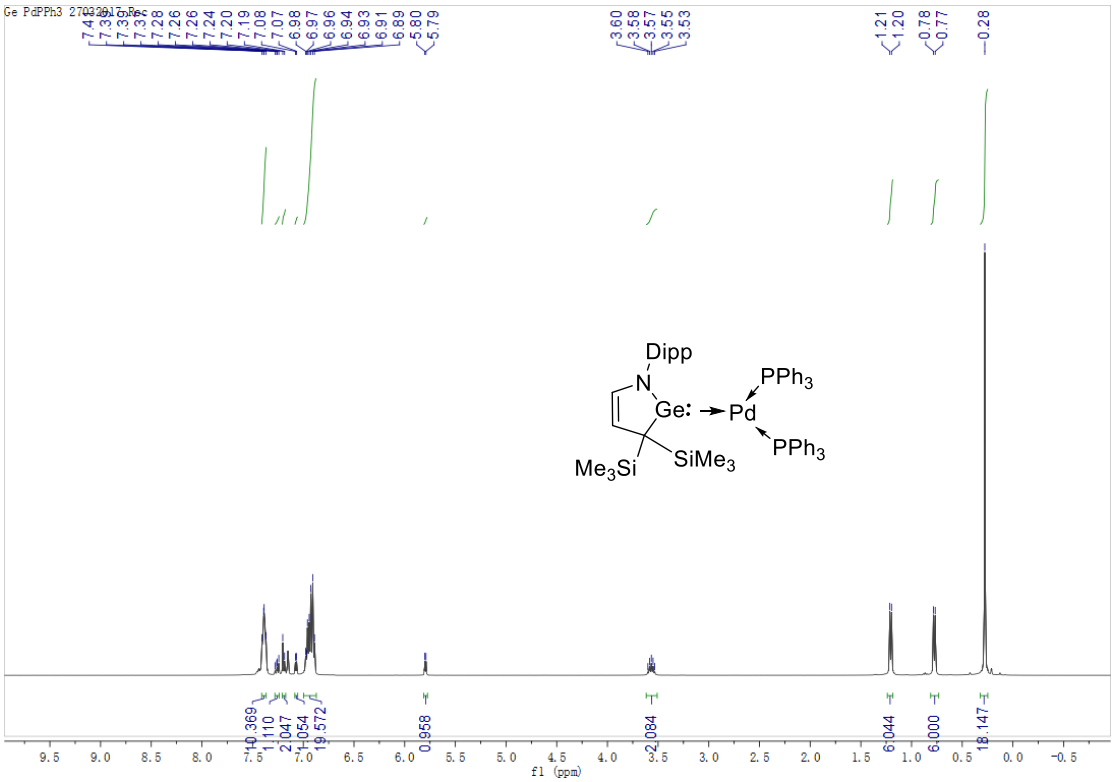

Figure 5.27 ^{1}H NMR spectrum of **6**

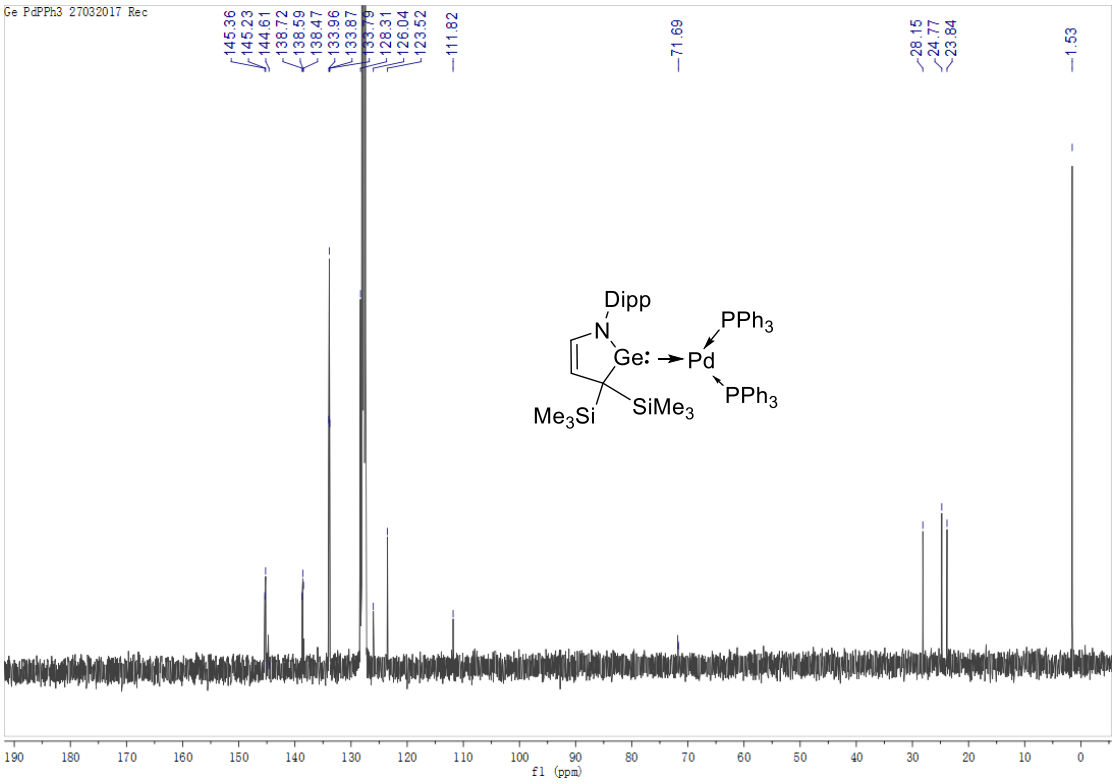

Figure 5.28 ^{13}C NMR spectrum of **6**

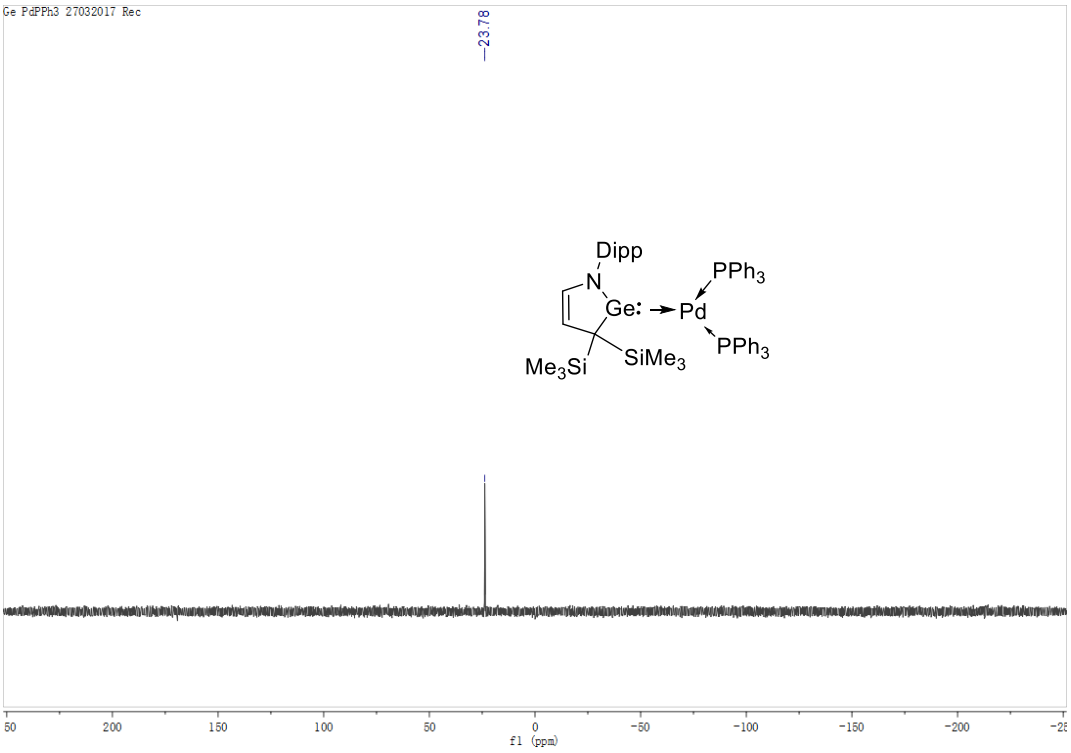

Figure 5.29 ^{31}P NMR spectrum of **6**

5.5 Reference

1. Fischer, E. O.; Maasböl, A., *Angew. Chem. Int. Ed. Engl.* **1964,** *3*, 580-581.

2. Vignolle, J.; Cattoën, X.; Bourissou, D., *Chem. Rev.* **2009,** *109*, 3333-3384.

3. Martin, C. D.; Soleilhavoup, M.; Bertrand, G., *Chem. Sci.* **2013,** *4*, 3020-3030.

4. Arduengo, A. J.; Bertrand, G., *Chem. Rev.* **2009,** *109*, 3209-3210.

5. Bourissou, D.; Guerret, O.; Gabbaï, F. P.; Bertrand, G., *Chem. Rev.* **2000,** *100*, 39-92.

6. Martin, D.; Soleilhavoup, M.; Bertrand, G., *Chem. Sci.* **2011,** *2*, 389-399.

7. Cazin, C. S. J., *N-Heterocyclic Carbenes in Transition Metal Catalysis and Organocatalysis. [electronic resource]*. Dordrecht : Springer Science+Business Media B.V., 2011.: 2011.

8. Bonati, F.; Burini, A.; Pietroni, B. R.; Bovio, B., *J. Organomet. Chem.* **1989,** *375*, 147-160.

9. Liu, S.-T.; Hsieh, T.-Y.; Lee, G.-H.; Peng, S.-M., *Organometallics* **1998,** *17*, 993-995.

10. Fañanás-Mastral, M.; Aznar, F., *Organometallics* **2009,** *28*, 666-668.

11. Ku, R.-Z.; Huang, J.-C.; Cho, J.-Y.; Kiang, F.-M.; Reddy, K. R.; Chen, Y.-C.; Lee, K.-J.; Lee, J.-H.; Lee, G.-H.; Peng, S.-M.; Liu, S.-T., *Organometallics* **1999,** *18*, 2145-2154.

12. Nemcsok, D.; Wichmann, K.; Frenking, G., *Organometallics* **2004,** *23*, 3640-3646.

13. Hu, X.; Castro-Rodriguez, I.; Olsen, K.; Meyer, K., *Organometallics* **2004,** *23*, 755-764.

14. Baker, M. V.; Barnard, P. J.; Brayshaw, S. K.; Hickey, J. L.; Skelton, B. W.; White, A. H., *Dalton Trans.* **2005**, 37-43.

15. Jothibasu, R.; Huynh, H. V.; Koh, L. L., *J. Organomet. Chem.* **2008,** *693*, 374-380.

16. Baker, M. V.; Barnard, P. J.; Berners-Price, S. J.; Brayshaw, S. K.; Hickey, J. L.; Skelton, B. W.; White, A. H., *Dalton Trans.* **2006**, 3708-3715.

17. Frey, G. D.; Dewhurst, R. D.; Kousar, S.; Donnadieu, B.; Bertrand, G., *J. Organomet. Chem.* **2008,** *693*, 1674-1682.

18. Weinberger, D. S.; Melaimi, M.; Moore, C. E.; Rheingold, A. L.; Frenking, G.;

Jerabek, P.; Bertrand, G., *Angew. Chem. Int. Ed.* **2013,** *52*, 8964-8967.

19. Xu, X.; Kim, S. H.; Zhang, X.; Das, A. K.; Hirao, H.; Hong, S. H., *Organometallics* **2013,** *32*, 164-171.

20. Gaillard, S.; Nun, P.; Slawin, A. M. Z.; Nolan, S. P., *Organometallics* **2010,** *29*, 5402-5408.

21. Raubenheimer, H. G.; Lindeque, L.; Cronje, S., *J. Organomet. Chem.* **1996,** *511*, 177-184.

22. Guo, S.; Sivaram, H.; Yuan, D.; Huynh, H. V., *Organometallics* **2013,** *32*, 3685-3696.

23. Herrmann, W. A.; Köcher, C., *Angew. Chem. Int. Ed. Engl.* **1997,** *36*, 2162-2187.

24. Heinemann, C.; Müller, T.; Apeloig, Y.; Schwarz, H., *J. Am. Chem. Soc.* **1996,** *118*, 2023-2038.

25. Boehme, C.; Frenking, G., *J. Am. Chem. Soc.* **1996,** *118*, 2039-2046.

26. Arduengo, A. J.; Gamper, S. F.; Calabrese, J. C.; Davidson, F., *J. Am. Chem. Soc.* **1994,** *116*, 4391-4394.

27. Frison, G.; Sevin, A., *J. Organomet. Chem.* **2002,** *643*, 105-111.

28. Frison, G.; Sevin, A., *J. Phys. Chem. A* **1999,** *103*, 10998-11003.

29. Morokuma, K., *J. Chem. Phys.* **1971,** *55*, 1236-1244.

30. Ziegler, T.; Rauk, A., *Theoretica. chimica. acta.* **1977,** *46*, 1-10.

31. Kitaura, K.; Morokuma, K., *Int. J. Quantum Chem.* **1976,** *10*, 325-340.

32. Marchione, D.; Belpassi, L.; Bistoni, G.; Macchioni, A.; Tarantelli, F.; Zuccaccia, D., *Organometallics* **2014,** *33*, 4200-4208.

33. Jerabek, P.; Roesky, H. W.; Bertrand, G.; Frenking, G., *J. Am. Chem. Soc.* **2014,** *136*, 17123-17135.

34. Matioszek, D.; Kocsor, T.-G.; Castel, A.; Nemes, G.; Escudie, J.; Saffon, N., *Chem. Commun.* **2012,** *48*, 3629-3631.

35. Leung, W.-P.; So, C.-W.; Chong, K.-H.; Kan, K.-W.; Chan, H.-S.; Mak, T. C. W., *Organometallics* **2006,** *25*, 2851-2858.

36. Bauer, A.; Schmidbaur, H., *J. Chem. Soc., Dalton Trans.* **1997**, 1115-1116.

37. Bauer, A.; Schmidbaur, H., *J. Am. Chem. Soc.* **1996,** *118*, 5324-5325.

38. Bauer, A.; Schier, A.; Schmidbaur, H., *J. Chem. Soc., Dalton Trans.* **1995**, 2919-2920.

39. Glockling, F.; Wilbey, M. D., *J. Chem. Soc. A* **1968**, 2168-2171.

40. Contel, M.; Hellmann, K. W.; Gade, L. H.; Scowen, I. J.; McPartlin, M.; Laguna, M., *Inorg. Chem.* **1996,** *35*, 3713-3715.

41. Anandhi, U.; Sharp, P. R., *Inorg. Chim. Acta* **2006,** *359*, 3521-3526.

42. Raut, R. K.; Majumdar, M., *Chem. Commun.* **2017,** *53*, 1467-1469.

43. Hitchcock, P. B.; Lappert, M. F.; Misra, M. C., *J. Chem. Soc., Chem. Commun.* **1985**, 863-864.

44. Cygan, Z. T.; Bender; Litz, K. E.; Kampf, J. W.; Banaszak Holl, M. M., *Organometallics* **2002,** *21*, 5373-5381.

45. Kireenko, M. M.; Zaitsev, K. V.; Oprunenko, Y. F.; Churakov, A. V.; Tafeenko, V. A.; Karlov, S. S.; Zaitseva, G. S., *Dalton Trans.* **2013,** *42*, 7901-7912.

Chapter 6 Hydroamination of terminal alkynes with ammonia catalysed by *2*-pyridyene gold(I) catalyst to construct pyridine derivatives

6.1 Introduction

Carbenes are neutral divalent species and have both nucleophilic and electrophilic abilities. Carbenes have been utilized in the synthetic chemistry as supporting ligands and compared with the electron-rich phosphine ligands from the viewpoint of the donating ability.[1-4] DFT calculations on *N*-heterocyclic carbene (NHC)-metal complexes showed that σ donation of NHCs contributes approximately 70% to the overall orbital interaction energy whereas π-interactions including both π donation and π back-donation contribute the remaining 15-30%.[5-7]

As the first metal-carbene complex, methoxyphenylmethylene tungsten (0) pentacarbonyl **I** was reported by Fisher *et al.* in 1964 and its structure was identified by X-ray diffractometry and NMR spectroscopy (Figure 6.1).[8] They employed the same method to access the chromium (0), iron (0), and manganese (0) carbene complexes where the adjacent methoxy and phenyl groups were replaced by different alkoxy and alkyl groups.[9]

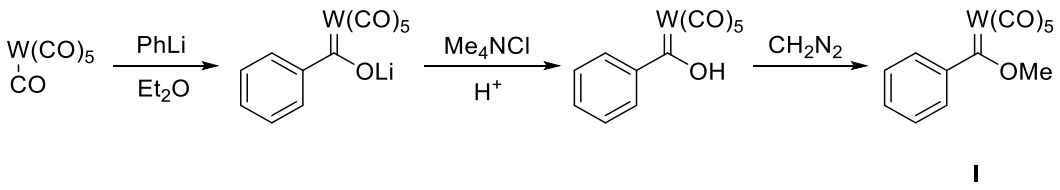

I

Figure 6.1 Synthesis of the first metal-carbene complex **I**.

Since then various carbene complexes have been reported, while it was difficult to isolate free carbenes due to their intrinsic instability. The first stable carbene **III** was reported by Bertrand and co-workers in 1988. By the flash thermolysis of (trimethylsilyl)

[bis(diisopropylamino)phosphino]-diazomethane **II** at 250 °C under vacuum, carbene **III** was synthesized and it was stabilized by the adjacent phosphorous and silicon substituents (Figure 6.2).[10-13]

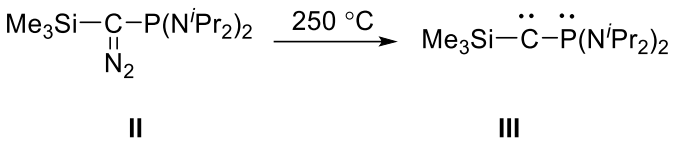

II **III**

Figure 6.2 Synthesis of the first carbene **III**.

Three years later, Arduengo and co-workers reported the synthesis of carbene **IVa** by the deprotonation of the corresponding imidazolium salt with sodium hydride at ambient temperature in THF with a catalytic amount of dimethyl sulfoxide (DMSO). The solid-state structure of **IVa** was unambiguously characterized by X-ray crystallographic analysis (Figure 6.3).[14-15]

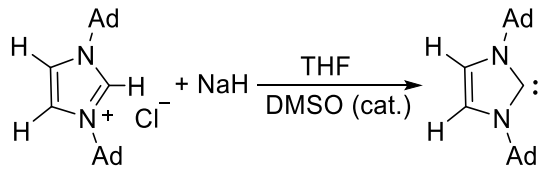

IVa

Figure 6.3 Synthesis of carbene **IVa**.

This seminal discovery led to the great development of experimental and theoretical investigations on the synthesis and analysis of NHCs. Following the pioneering work by Arduengo, various stable NHCs have been developed (Figure 6.4)[14, 16-18], which was usually stabilized by employing the bulky substituents.[11] Moreover, Bertrand *et al.* have successfully developed cyclic (alkyl)(amino) carbenes (CAACs) **IX** where one of the adjacent amino groups was replaced with a quaternary carbon compared with NHCs **V** (Figure 6.4). They also investigated the reactivities and electronic properties by experimental and theoretical studies,

and uncovered that CAACs **IX** exhibit both stronger σ-donating and π-accepting ability than NHCs.[19-21]

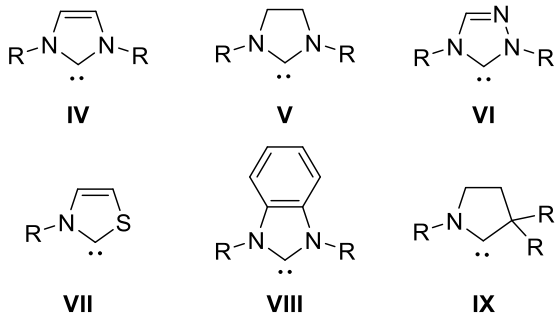

Figure 6.4 Selected examples of NHCs.

Homogenous transition-metal catalysts have been successfully applied to a range of hydroaminations.[22-26] Thus far, metal complexes such as ruthenium,[27-30] iridium,[31-33] nickel,[34] rhodium,[31, 33, 35-37] palladium,[38-41] and platinum,[42-43] copper,[44] silver,[45] gold,[46-49] and zinc[50-51] have been widely utilized. Gold(I) complexes are also known to excel in the hydroamination of alkynes.[52-54]

The hydroamination of unsaturated substrates with ammonia has attracted much attention as the 100% atom-economic synthetic approach for the construction of nitrogen carbon bonds, in which the total molecular mass of the reactants is the same as the molecular mass of products without any byproducts. The hydroamination of olefins with ammonia in an anti-Markovnikov addition was regarded as one of the top ten challenges for catalysis.[55] Direct functionalization of ammonia is still a great challenge in synthetic chemistry because of the following reasons:

First, Werner complex afforded by the coordination of either ammonia or amine substrates to transition metal is usually inert. Second, the activation of the enthalpically strong N−H bond (107 kcal/mol) of ammonia requires harsh conditions such as high temperature and high pressure. Third, ammonia disfavor proton exchanges either to or from it, due to the moderate basicity of ammonia.[56]

In 2008, the gold-catalyzed hydroamination of alkynes with ammonia[48] was reported by Bertrand and co-workers, where CAACs **IX** have been employed as the supporting ligands in the gold complexes (Figure 6.5). Similar catalysis with hydrazine has also been reported.[49]

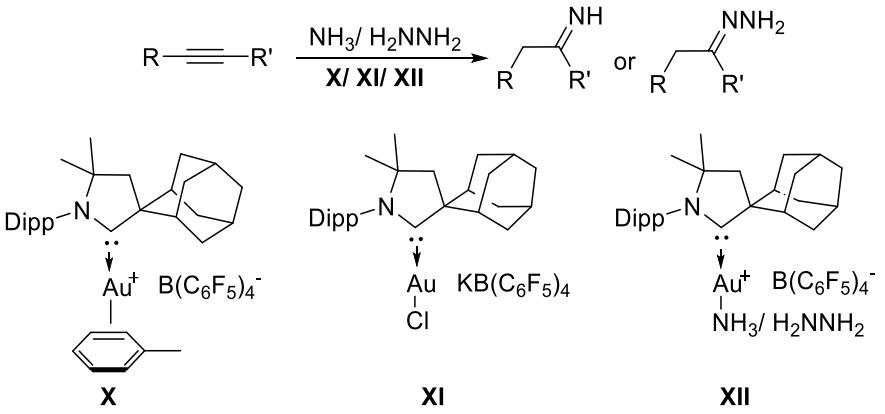

Figure 6.5 Hydroamination of alkynes with ammonia or hydrazine catalyzed by CAACAu(I) complexes.

The reported transition-metal catalytic reactions with ammonia can be classified into three cases. The first one involves tandem processes in which ammonia reacts with aldehyde without the ruthenium catalyst (Figure 6.6).[57]

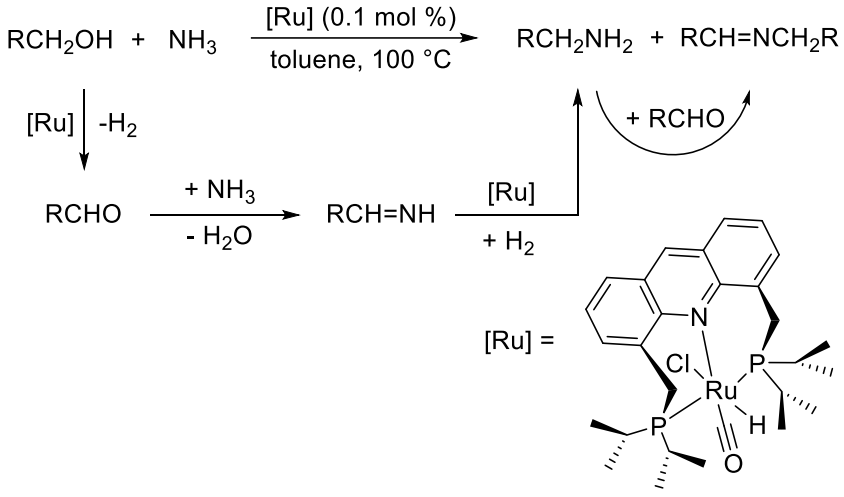

Figure 6.6 The formation of amines and imines catalyzed by ruthenium catalyst.

The second one involves the catalytic processes during which ammonia reacts with the copper center to form a metal ammonia complex. Oxidative-addition and reductive-elimination of copper complexes with substrates occur subsequently to afford the finial products.[58] The substrates were limited to electron-poor heteroaromatic halides, and electron-poor arenes in these reactions (Figure 6.7). The selectivity of primary amines was not under control, the secondary amines were generated accompanying.[59-62]

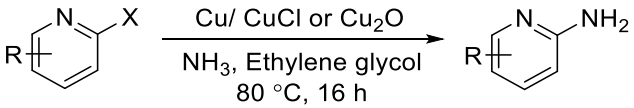

Figure 6.7 The formation of primary amines catalyzed by copper complexes.

The third is the catalytic hydroamination of unsaturated substrates, which has been mentioned in this chapter earlier. In this reaction, CAACs play an important role. Werner-type complexes generated by the reaction of pre-catalysts with ammonia was inert and prevented the use of ammonia as a substrate in the catalytic reaction. However, the CAACs possessed of both strong σ donor and π acceptor properties that enable the gold complex to liberate ammonia molecule and to activate alkynes effectively.

In 2011, G. Kovács and co-workers reported the theoretical studies on hydroamination of alkynes with ammonia catalyzed by CAAC-Au(I).[63] They revealed that the mechanism involves three steps: 1) coordination of the unsaturated substrates to the cationic gold center; 2) nucleophilic attack of ammonia on the C≡C bond; 3) the proton transfer from ammonia to the unsaturated carbon (C=C) atom, which is the key step in this reaction (Figure 6.8).

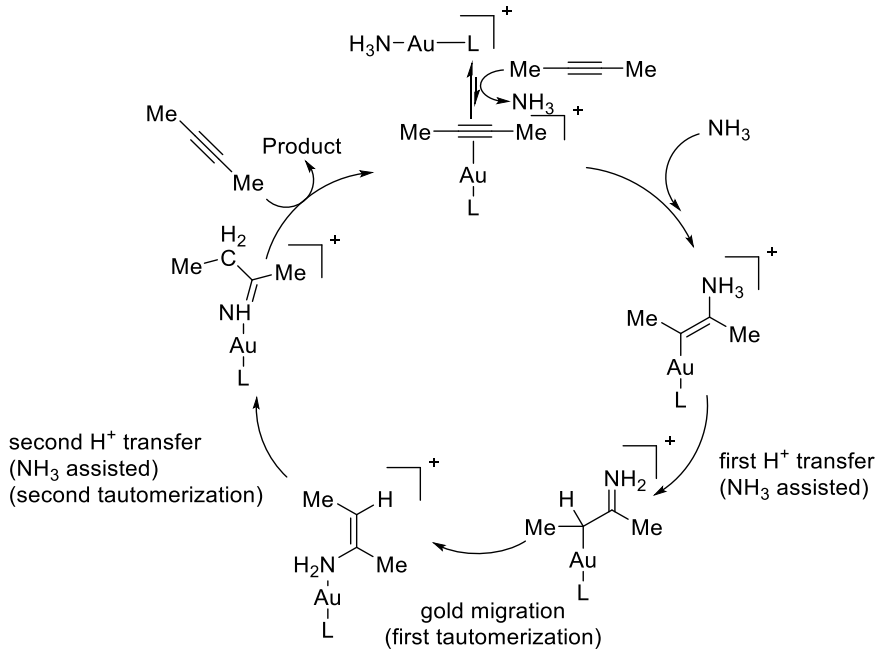

Figure 6.8 The proposed mechanism of hydroamination catalyzed by CAAC-Au(I).

From the above theoretical studies on hydroamination, we can hypothesize that if a stronger σ donating and π accepting ligand is employed to replace with the CAACs ligand of **XI**, the catalytic activity of L→Au(I) complex will be promoted. In 2009, M. S. Nechaev *et al* reported the theoretical study on thermodynamic stability and ligand properties of NHCs using the DFT calculation.[64] The representative samples include imidazolin-*2*-ylidene(**IV**), imidazolidin-*2*-ylidene(**V**), CAAC (**IX**), pyrazolin-*3*-ylidene (**VI**), pyridin-*2*-ylidene (**XIII**), and pyridin-*4*-ylidene (**XIV**) (Figure 6.9).

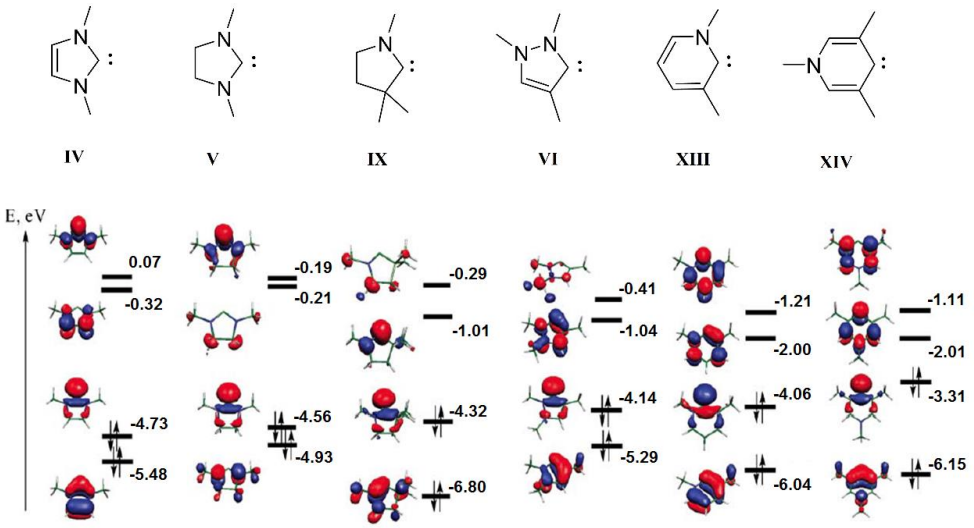

Figure 6.9 Energy level of the frontier orbitals of selected carbenes.

According to their calculation results, the HOMOs increase in the order **IV**<**V**<**IX**<**VI**<**XIII**<**XIV** from −4.73eV to −3.31eV, which are higher than the strong σ-donor phosphine P^{t}Bu$_3$ (−4.92 eV).[65] Experimentally, the C–O stretching frequencies of L→nickel carbonyl and L→iridium carbonyl complex has been analyzed, which indicated that NHCs complexes have lower frequencies than their phosphine counterparts.[65-68] This result indicates that carbenes are stronger σ-donors than phosphines. It is interesting that pyridine-based carbenes **XIII** and **XIV** have by far low LUMO, indicating that they could readily accept the *d*-electrons of metals and serve as good π-acceptor ligands. Pyridylidene **XIII** also possesses a higher HOMO energy compared with NHCs, and even CAACs. Hence, **XIII** could be considered as a better σ-donating and π-accepting ligand instead of CAACs, and will balance the polarity of M−NH$_3$ bond to promote substrate exchange, which is necessary for a turnover in catalysis and the stability of the complex.[64, 69-70]

Free and isolable pyridylidenes are not available so far. In 2012, Itami *et al.* synthesized a *2*-pyridylidene→Au(I) complex **XV** by the deprotonation of the corresponding pyridinium salts followed by the addition of Me$_2$SAuCl (Figure 6.10).[71] It should be noted that no *2*-pyridylidene species were observed in this reaction. There are two possibilities why *2*-pyridylidene cannot be

isolated. First, the adjacent substituents were not bulky enough to stabilize the free pyridylidenes. The second possibility is considered from the electronic effect, the 2,6-dimethylphenyl can be thought as donor for the σ-π conjugation between the σ-bond of methyl group and π-aromatic moieties, which will cause the thermodynamic stability going down.[72-73]

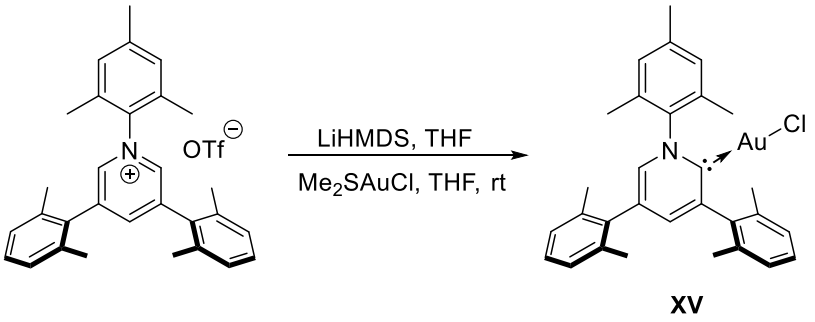

Figure 6.10 Synthesis of *2*-pyridylidene gold complex **XV**.

Hence, we designed a novel *2*-pyridylidene featuring two 3,5-di-tert-butylphenyl groups which are bulkier than 2,6-dimethylphenyl groups on the pyridylidene ring hindering the dimerization or polymerization. It will possess strong σ-donating and π-accepting abilities that can be utilized as a ligand to prepare *2*-pyrdilidene-gold complex **1** (Figure 6.11).[64] *2*-pyrdilidene-gold complex **1** is expected to be able to catalyze the hydroamination of unsaturated substrates with ammonia and conduct the regioselectivity of reaction for the bulky substituents.[22, 74]

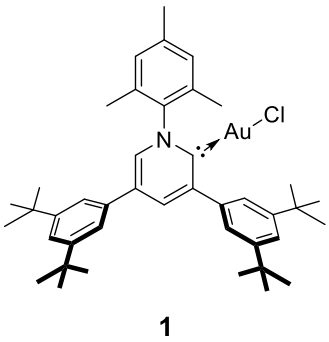

Figure 6.11 The new *2*-pyrdilidene-gold complex **1**.

6.2 Results and Discussions

The synthetic route to *2*-pyridyilene gold complex **1** is shown in Scheme 6.1. Pyridinium salt **4** bearing bulky substituents on 1,3,5-positions was chosen as the precursor of **1**. The reaction of 3,5-dibromopyridine with 2 equivalents of boronic acid in the presence of $Pd(PPh_3)_4$ and $Ba(OH)_2$ afforded the product **2** in 90% yield. The next reaction of **2** with 1-chloro-2,4-dinitrobenzene was carried out in ethanol at 90 ℃ for 4 days providing a Zincke salt **3** in 70% isolated yield. The chloride anion exchange reaction of **3** took place in the presence of silver reagent (AgOTf), and then the 2,4-dinitrophenyl group was replaced by a mesityl (1,3,5-trimethylphenyl) group at 150 ℃ in situ. Finally, the product **4** was obtained as a brown solid in 90% isolated yield.

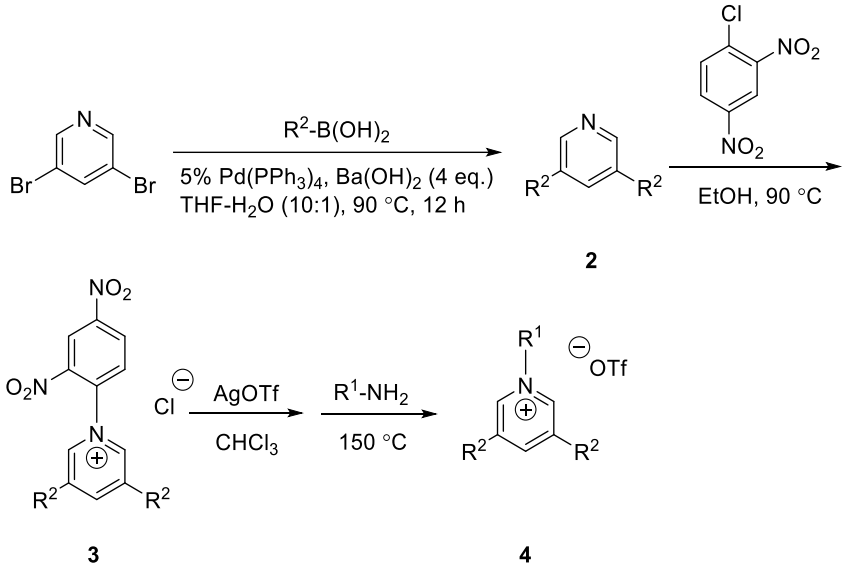

Scheme 6.1 Synthesis of pyridinium salt **4**. (R^1 = Mes, R^2 = 3,5-^{t}Bu$_2$-C_6H_3)

With the precursor pyridinium **4** in hand, the deprotonation of **4** was carried out with lithium hexamethyldisilazide (LiHMDS) in THF at room temperature (Scheme 6.2). While no free 2-pyridylidene was observed in this deprotonation reactions at all. When THTAuCl was added to the mixture of reaction, the corresponding 2-pyridylidene–gold(I) complex **1** was obtained in 27% isolated yield. The structure of **1** has been confirmed by X-ray diffractometry (Figure 6.12)

and its characteristic signal for the carbon of carbene was observed at 187.8 ppm in the ^{13}C NMR spectroscopy. The pyridylidene six-membered ring of **1** is coplanar (the sum of internal pentagon angles = 720 º). It should be noted that the Au–C bond length of **1** (1.989(4) Å) is shorter than that of **XV** (2.0113(195) Å) which indicates the stronger interaction between the 2-pyridylidene ligand and gold in **1**.

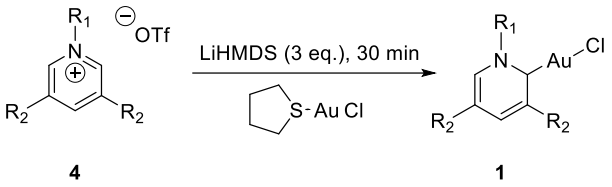

4 1

Scheme 6.2 Synthesis of *2*-pyridyilene gold complex **1**. (R_1 = Mes, R_2 = 3,5-^{t}Bu$_2$-C$_6$H$_3$)

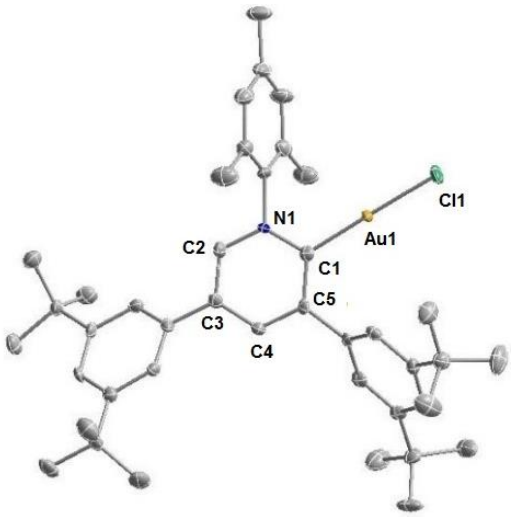

Figure 6.12 Solid state structure of **1**. Hydrogen atoms are omitted for clarity. Thermal ellipsoids are shown at the 50% probability level. Selected bond lengths [Å] and angles [º]: Au1-C1 1.989(4), Au1-Cl1 2.2842(11), C1-N1 1.373(5), C3-C4 1.394(5), C1-C5 1.424(5), C2-N1 1.355(5), C2-C3 1.378(5), C4-C5 1.383(6); C1-Au1-Cl1 177.84(12), N1-C1-Au1 119.9(3), C5-C1-Au1 125.3(3), C4-C5-C1 120.0(4), C2-C3-C4 116.3(4), C2-N1-C1 125.1(3), C5-C4-C3 122.9(4), N1-C2-C3 120.9(4), N1-C1-C5 114.8(4).

As mentioned in chapter 6.1, due to the strong σ-donor property of CAACs promoted the

leaving of ammonia and π-acceptor property of CAACs incrseaed the activity of alkynes of gold(I) π-complexes, CAACs gold complex could catalyze the hydroamination of ammonia or hydrazine with unsaturated substrates such as C=C double bonds and C≡C triple bonds. It has been well discussed in *chapter 6.1* that *2*-pyridylidenes possess stronger σ-donor and π-acceptor properties than CAACs.[64] Therefore, it is expected that *2*-pyridylidene-gold complex **1** has a better catalytic activity than CAACs gold complex **XI** in hydroamination. With *2*-pyridylidene–gold(I) complex **1** in hand, we have initially carried out the catalytic hydroamination of ethynylbenzene **5a** with ammonia in the presence of **1** (5 mol%) in order to compare its catalytic activity with **XI** (Scheme 6.3).[48]

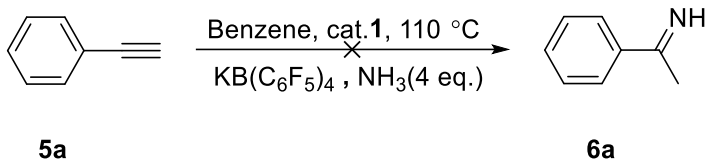

Scheme 6.3 Hydroamination of ethynylbenzene with ammonia catalyzed by complex **1**.

The reaction was carried out for 12 h, instead of the expected product 1-phenylethan-1-imine **6a,** an unexpected product was observed from the NMR spectra. In the ^{13}C NMR spectrum, a characteristic peak was detected at 45.0 ppm, which was assigned to CH_2 carbon. Initially, the compound from the anti-Markovnikov addition of ammonia to ethynylbenzene **5a** was proposed according to the NMR spectra. Interestingly, the product 2-benzyl-4,6-diphenylpyridine **7a** was confirmed by NMR spectroscopy (Scheme 6.4). Pyridine derivatives are important class heterocyclic compounds in natural products, pharmaceuticals, and efficient materials. Historically, the synthesis of pyridine relies on the condensation of the amine with carbonyl compounds.

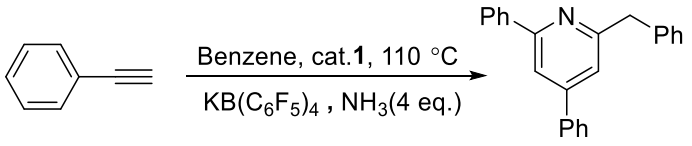

5a **7a**

Scheme 6.4 Synthesis of **7a** from hydroamination of ethynylbenzene with ammonia.

Pyridine derivatives are the important class of heterocyclic compounds in natural products, pharmaceuticals, and efficient materials. Historically, the synthesis of pyridine relies on the condensation of amines with carbonyl compounds, which is similar to many condensation methods. Ammonia was commonly utilized in the synthesis of pyridine derivatives. Autoxidation was also a necessary step for the aromatization. (Scheme 6.5).[75]

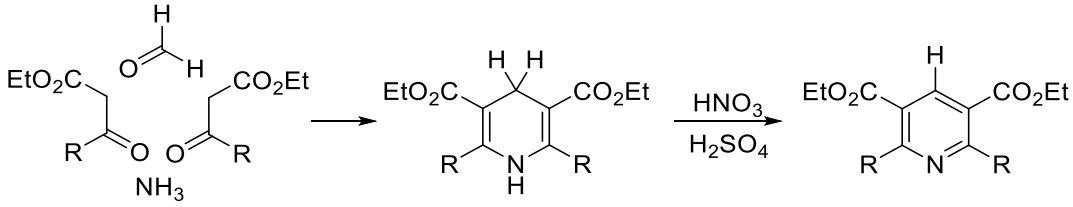

Scheme 6.5 Synthesis of pyridine derivatives.

In 2005, Craig and Henry reported the synthesis of alkyl-, aryl- and ester substituted pyridines. They utilized the ozonolysis of 1,6-dienes to afford ketones which further reacted with ammonia to afford the finial products (Scheme 6.6). It was established in azaheterocycle for the construction of pyridine ring.[76-77]

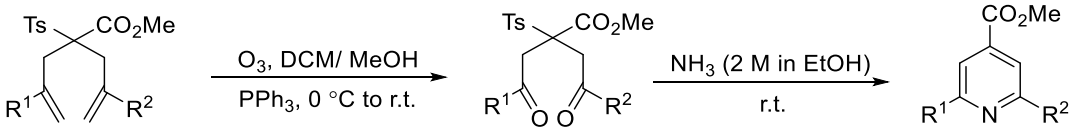

Scheme 6.6 Synthesis of polysubstituted pyridines.

Transition metal catalyzed cyclization and coupling reactions offer a series of new routes

to functionalize pyridine derivatives.[76] In 2002, Larock and *et al.* reported that Pd(II) complex has been utilized to synthesize pyridine derivatives (Scheme 6.7). This reaction included two steps: a) the coupling reaction of haloalkenes with terminal alkynes catalyzed by palladium; b) cyclization catalyzed by CuI.[78]

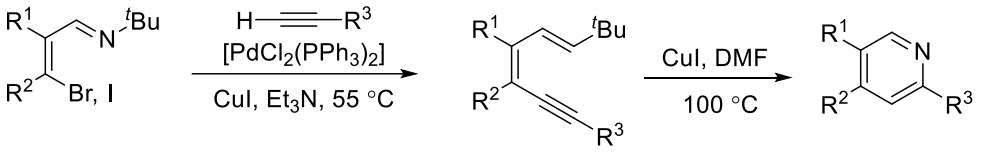

Scheme 6.7 Synthesis of pyridines catalyzed by transition metals.

In 2005, Suzuki *et al.* reported the synthesis of pyridine derivatives. The reaction involved a titanium intermediate which reacted with substituted alkynes, and quenched by E^+ to provide 2,3,4,6-tetrasubstituted pyridines (Scheme 6.8).[79]

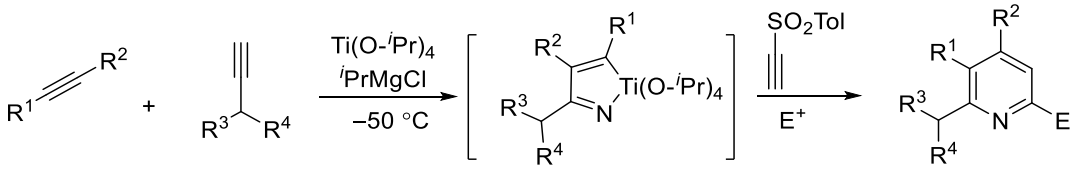

R^1, R^2 = ^{n}Bu, R^3 = OMe, R^4 = H, E^+ = H, 76%
R^1 = ^{n}Hx, R^2 = TMS, R^3 = OMe, R^4 = H, E^+ = H, 58%
R^1 = ^{n}Hx, R^2 = TMS, R^3 = OMe, R^4 = H, E^+ = I, 50%
R^1 = ^{n}Hx, R^2 = TMS, R^3 = OMe, R^4 = *R*-OTBS, E^+ = H, 49%, 99% *ee*

Scheme 6.8 Synthesis of 2,3,4,6-tetrasubstituted pyridines.

In our case, the possible mechanism for the formation of **7a** is shown in scheme 6.9. The initial step is the formation of 1-phenylethane-1-imine **6** via Markovnikov addition of NH_3 to alkyne. Then, imine **6** attacks another alkyne activated by the gold complex, which undergoes Anti-Markovnikov addition affording the 1-phenyl-N-styrylethan-1-imine intermediate **12**. **13** is considered as the tautomer of **12**, which reacts with the third alkyne to generate **15** without the activity of cationic Au species[80-81] and then undergoes an aromatization to generate the final product **7a**.

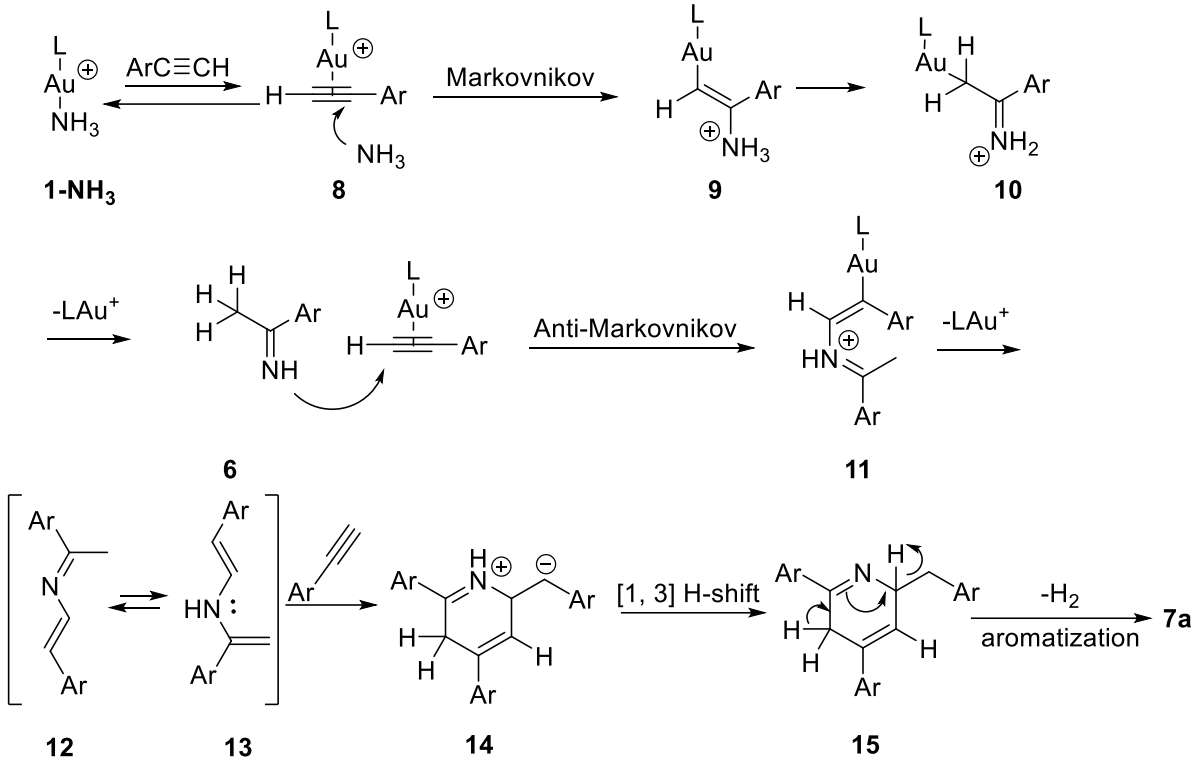

Scheme 6.9 The mechanism of hydroamination proposed.

To verify the hypothesized mechanism, the reaction of phenylacetylene **5a** with 1-phenylethan-1-imine **6a** has been carried out (Scheme 6.10). As expected, when a large excess of phenylacetylene **5a** was treated with ammonia, 2-benzyl-4,6-diphenylpyridine **7a** was obtained as the major product in 51% yield after 5 h, indicating that the 1-phenylethan-1-imine **6a** was involved in the reaction process. Although attempts have been made to monitor the other reaction intermediates **12** by varying the reaction temperature, time, and substrates ratio, 2-benzyl-4,6-diphenylpyridine **7a** was the only detectable product in this reaction.

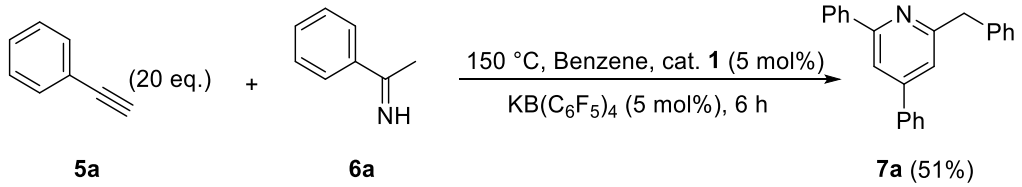

Scheme 6.10 Reaction of phenylacetylene **5a** with 1-phenylethan-1-imine **6a**.

The reaction of ^{13}C-labeling alkyne **5a*** with ammonia has been carried out under the same condition in the presence of gold catalyst **1** affording the corresponding **7a*** (Scheme 6.11), which supported the proposed reaction mechanism (Scheme 6.9) upon the corresponding $^{13}CNMR$ spectrum.

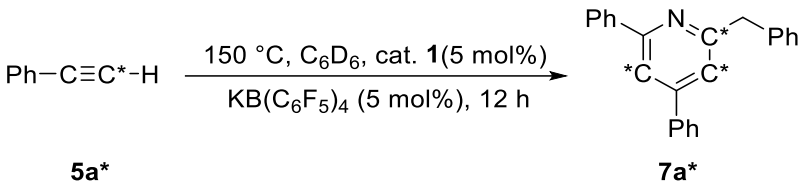

Scheme 6.11 Reaction of ^{13}C-labeling phenylacetylene **5a*** with ammonia.

When the reaction conditions were optimized. At the beginning, the amount of ammonia was determined at 0.4 equivalent (Table 6.1, Entries 3, and 5-8). there was no reaction when the temperature was below 100 ℃, and until it was heated at 150 ℃ giving the highest yield (Table 6.1, Entries 1-3). The impact of catalyst loading has been tested, and almost showed no effect on the reaction (Table 6.1, Entries 3 and 4). The optimized conditions were determined at 150 ℃, 1 mol% of catalyst loading, and 0.4 equivalent of ammonia (Table 6.1, Entry 3). The reaction of **5a** with a large excess of ammonia exclusively afforded 1-phenylethan-1-imine **6a** (Table 6.1, Entry 8), indicating that the initial step was a Markovnikov hydroamination of an alkyne with ammonia.

Table 6.1 Optimization of reaction conditions for the construction of pyridine **7a**.[a]

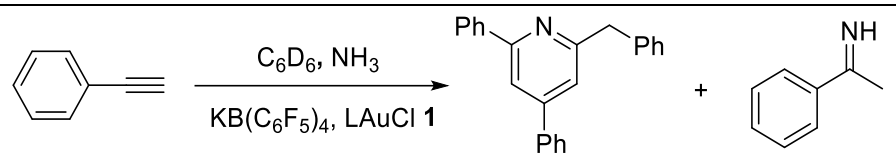

5a **7a** **6a**

Entry	Catalyst [mol%]	*t* [h]	T [°C]	NH_3[eq.]	Yield (**7a**) [%][b]	Yield (**6a**) [%][b]
1	1	12	r.t.	0.4	NR	NR
2	1	12	100	0.4	NR	NR
3	**1**	**12**	**150**	**0.4**	**43**	**0**
4	5	6	150	0.4	41	0
5	1	12	150	0.8	26	25
6	1	12	150	2	10	45
7	1	12	150	10	8	50
8	1	12	150	100	0	75

Notes: a. Reaction condition **5a** (1 mmol), C_6D_6 (0.7 mL). b. Yield was determined by ^{1}H NMR spectroscopy using 1,4-di-t-butylbenzene as an internal standard.

With the optimized reaction condition in hand, the scope of the catalytic reaction was briefly examined with a variety of terminal alkynes **5** involving electron-donating (Table 6.2, entries 3, 9 and 10) as well as electron-withdrawing aromatic groups (Table 6.2, entries 2, and 4-8). The corresponding products (**5a-l**) were obtained in 20%~48% yields. The relatively low yield of **5h** was probably due to the extremely strong electron-withdrawing CF_3-group (Table 6.2, entry 8), inducing the weak basicity of imine **6h** and impeding its addition to second alkynes (Scheme 6.5). 2-Ethynylthiophene and 3-ethynylthiophene also exhibited tolerance to the reaction conditions (Table 6.2, entries 11 and 12). We have also obtained two single crystals of **7b** and **7g** supporting our speculation for the structure of **7** (Figure 6.13).

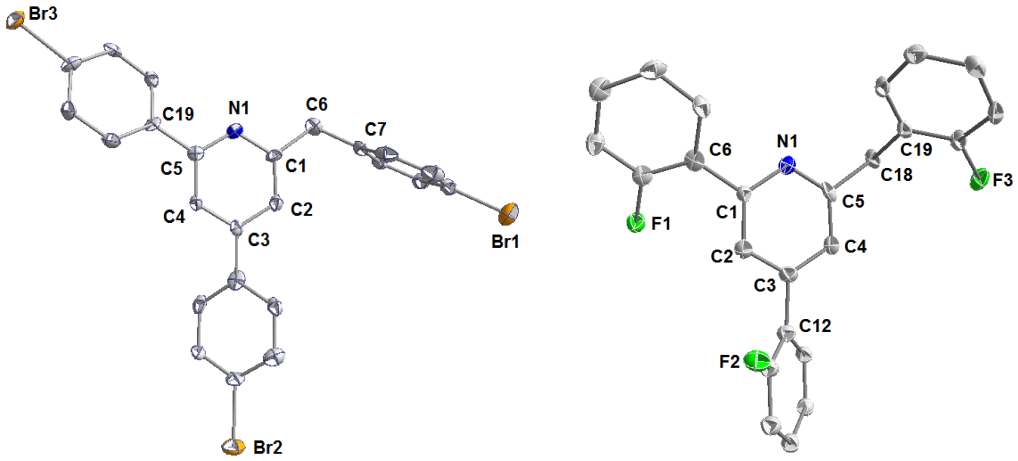

7b **7g**

Figure 6.13 Solid state structure of **7b** (left) and **7g** (right). Hydrogen atoms are omitted for clarity. Thermal ellipsoids are shown at the 50% probability level. Selected bond lengths [Å] and angles [º]: **7b)** N1-C1 1.3492(95), C1-C2 1.3867(116), C2-C3 1.3828(124), C3-C4 1.3771(98), C4-C5 1.4184(116), C5-N1 1.3344(113), C1-C6 1.5297(144), C6-C7 1.5083(117); C1-C6-C17 115.435(801); **7g)** C1-N1 1.365(13), C1-C2 1.391(14), C2-C3 1.387(14), C3-C4 1.415(15), C4-C5 1.379(14), C5-N1 1.349(13), C5-C18 1.521(15), C18-C19 1.511(16); C19-C18-C5 111.4(9).

Table 6.2 The construction of pyridine derivatives catalyzed by **1** from alkynes and ammonia.[a]

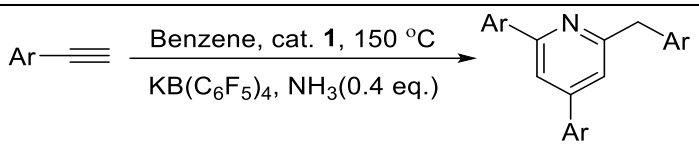

5 **7**

Entry		Substrate	**7** Yield [b,c]	Entry		Substrate	**7** Yield [b,c]
1	**5a**	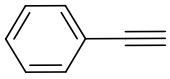	**7a** 43% (40%)	7	**5g**	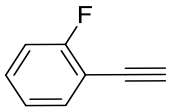	**7g** 41% (38%)
2	**5b**	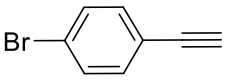	**7b** 38% (34%)	8	**5h**	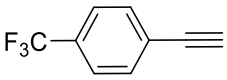	**7h** 23% (19%)
3	**5c**	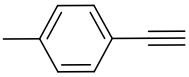	**7c** 33% (30%)	9	**5i**	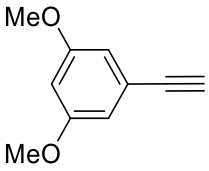	**7i** 30% (28%)
4	**5d**	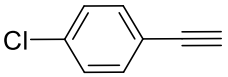	**7d** 31% (27%)	10	**5j**	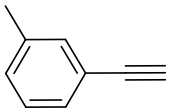	**7j** 41% (37%)
5	**5e**	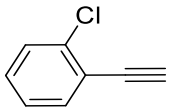	**7e** 31% (28%)	11	**5k**	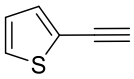	**7k** 20% (17%)
6	**5f**	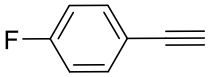	**7f** 45% (43%)	12	**5l**	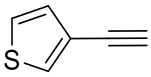	**7l** 48% (45%)

Notes: a. Reaction condition **5** (1 mmol), ammonia (0.25 mmol), LAuCl and $KB(C_6F_5)_4$ (1 mol%), and C_6D_6 (0.7 mL). b. Yields were determined by ^1H NMR spectroscopy using 1,4-di-t-butylbenzene as an internal standard. c. Isolated yields were given in parentheses.

Based on the results in *table 6.2*, we attempted to extend this strategy by employing two different terminal alkynes for the construction of rather complex pyridine derivatives **16** (Table 6.3). It was noteworthy to mention that the electron withdrawing alkynes were attacked in the anti-Markovnikov addition step and in absence of the initiative Markovnikov addition with ammonia and final aromatization steps. Why did the electron withdrawing alkynes only

attend the anti-Markovnikov addition step? The basicity of imine **6** was the key point for the formation of the 1-phenyl-N-styrylethan-1-imine intermediate **12**. The nucleophilic attack of imine **6** to another alkyne was blocked, if imine **6** was featuring an electron-withdrawing substituent (Scheme 6.12). When imine **6** fearing electron donating group reacts with the second alkyne substituted by electron withdrawing group, the reaction will be promoted to give complex pyridine derivatives **16**. **16d** was characterized by X-ray crystallographic analysis, which aided us to speculate the structure of **16** (Figure 6.14). **16** has similar bonds lengths and angles of a skeleton to that of **7**.

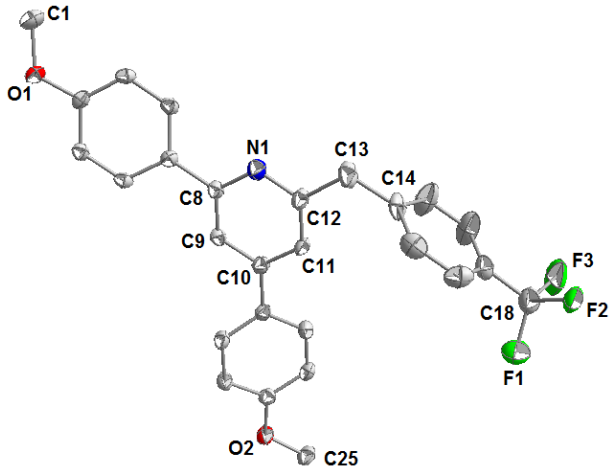

Figure 6.14 Solid state structure of **16d**. Hydrogen atoms are omitted for clarity. Thermal ellipsoids are shown at the 50% probability level. Selected bond lengths [Å] and angles [º]: N1-C12 1.3662(34), C11-C12 1.3646(35), C10-C11 1.3728(27), C9-C10 1.3862(33), C8-C9 1.3919(32), C8-N1 1.3616(27), C12-C13 1.512(34), C13-C14 1.5080(39); C12-C13-C14 114.654(206).

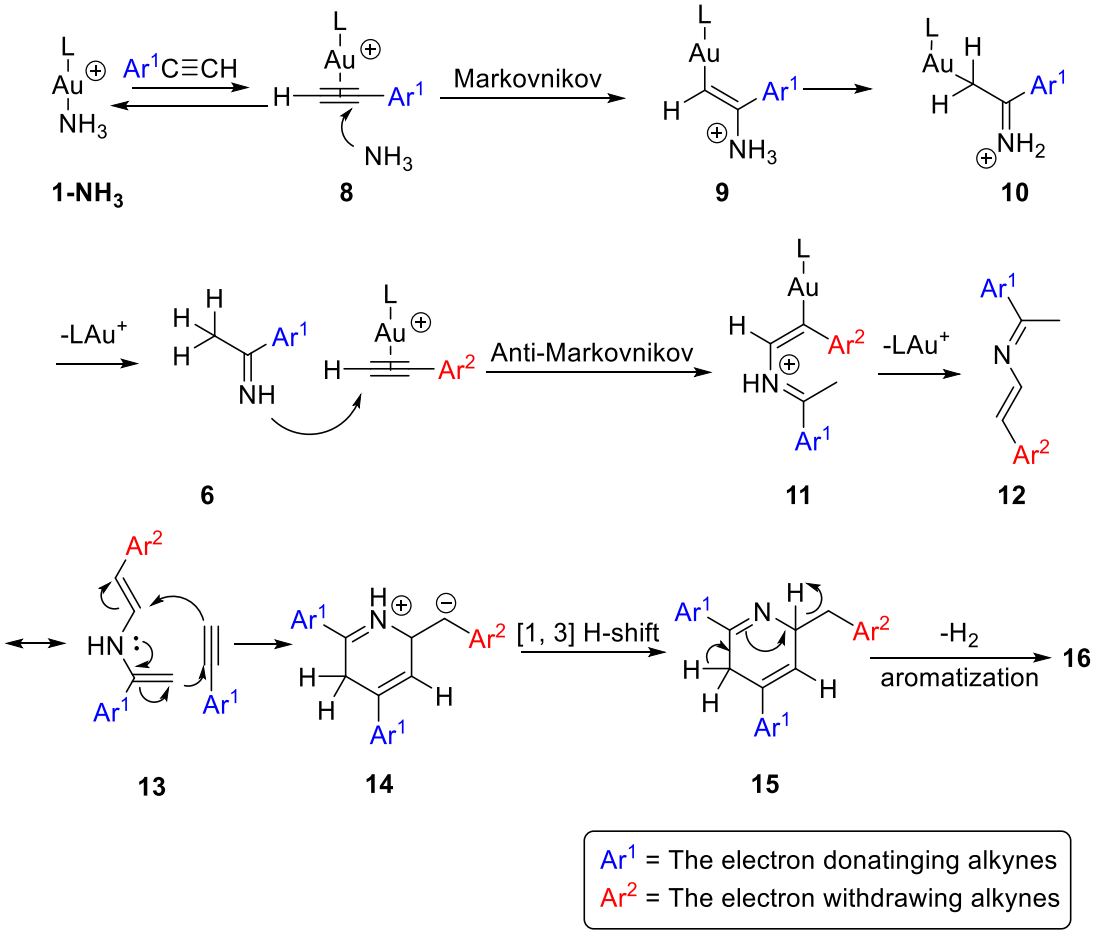

Scheme 6.12 The mechanism of formation on **16** proposed.

Table 6.3 Au-catalyzed three-component coupling reaction[a]

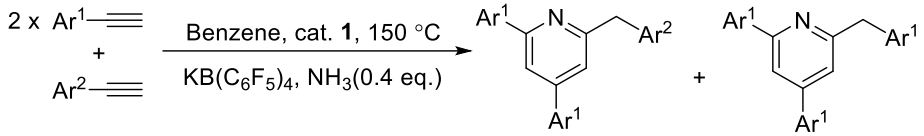

5 **16** **7**

Entry	Substrate Ar^1	Substrate Ar^2	**16** Yield [b]	**7** Yield [b]
1	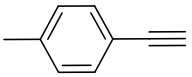	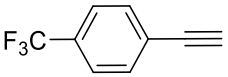	**16a** 15 %	**7c** 18%
2	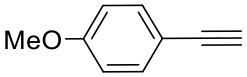	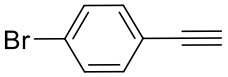	**16b** 10%	**7m** 12%
3	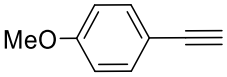	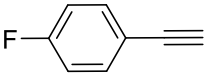	**16c** 11%	**7m** 12%
4	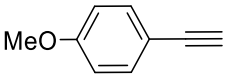	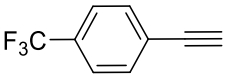	**16d** 8 %	**7m** 12%
5	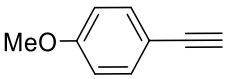	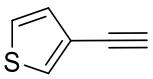	**16e** 14%	**7m** 11%

Notes: a. Reaction condition **5** (1 mmol), ammonia (0.25 mmol), LAuCl **1** and $KB(C_6F_5)_4$ (1 mol%), and C_6D_6 (0.7 mL). b. Isolated yields were given.

The reaction of alkyne **5a** with 1-phenylethan-1-imine **6a** in the presence of LAuCl **1** and $KB(C_6F_5)_4$ afforded 2-benzyl-4,6-diphenylpyridine **7a** as the major product in 51% yield rather than the anti-Markovnikov addition product. It encouraged us to extend the substrates by replacing the methyl group with bulk groups to increase the stability of **12**.

In 2011 Toste and co-workers reported that the reaction of phenylacetylene **5a** with *N*,1-diphenylmethanimine PhN=CHPh in the presence of gold catalyst afforded propargylamine where alkynes were nucleophiles (Scheme 6.13a).[82] Four years later, Zhao *et al.* reported nickel-catalyzed intermolecular coupling between internal alkynes and aromatic N–H ketimines

(Scheme 6.13b).[83]

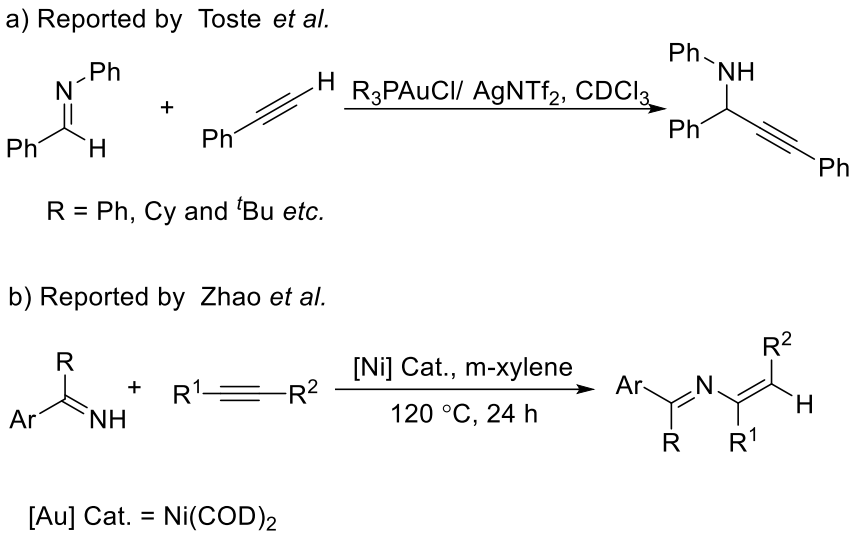

Scheme 6.13 Reported reactions of imines with alkynes.

To our best knowledge, the anti-Markovnikov addition of benzophenone imines **17** to terminal alkynes **5** has never been reported so far. We first examined the reaction of terminal alkynes **5a** with benzophenone imine **17a** catalyzed by **1** and $KB(C_6F_5)_4$ under the similar reaction conditions to that of ammonia (Scheme 5.14a). A mixture of (Z)-1,1-diphenyl-N-styrylmethanimine **18a** and 1,1-diphenyl-N-(1-phenylvinyl) methanimine **19a** were generated after 1 hour, and the yield of the anti-Markovnikov adduct **18a** was nearly identical to that of Markovnikov adduct **19a**. When the reaction time was extended to 6 h, **19a** gradually decomposed to an unidentified mixture under the reaction conditions. Finally, the highest yield of **18a** was obtained at 51% for 6 h. To further probe the formation of the anti-Markovnikov product, a ^{13}C-labeling experiment with a ^{13}C-labeled phenylacetylene **5a*** was performed, which decisively afforded **18a***(Scheme 6.14b).

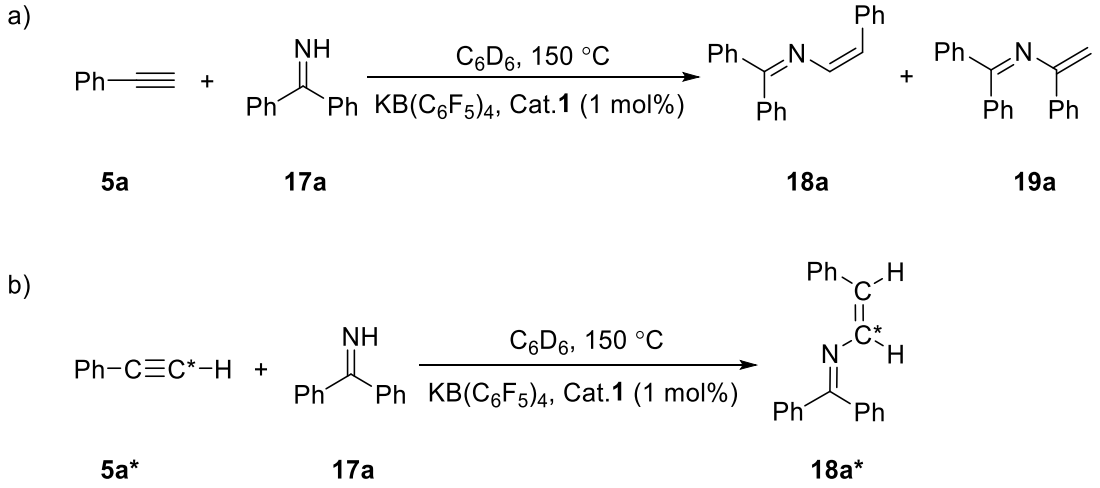

Scheme 6.14 Reaction of imine **17a** with alkyne catalyzed by gold catalyst **1**.

When the reaction was carried out (Table 6.4, entry 1), the anti-Markovnikov product **18a** was observed prior to Markovnikov product **19a** in the early stage of the reaction, and the highest yield (51%) of **18a** was obtained, and Markovnikov product **19a** completely decomposed after 6 h. When 1-bromo-4-ethynylbenezene **5b** and 4-ethynyltoluene **5c** were introduced, the similar results were presented (Table 6.4, entries 2 and 3). The scope of the hydroimination with respect to imines has been investigated, which involving various imine substrates such as *p*-methylphenyl groups **17b**, *p*-fluorophenyl groups **17c**, as well as methyl benzimidate **17d**. The corresponding 2-aza-1,3-dienes **18a-l** were afforded from the hydroimination of these imines **17a-d** with alkynes **5a**–**c** in moderate yields (Table 6.4, entries 1-12). It should be noted that the formation of **18** and **19** from terminal alkynes and imines has never been reported so far. The reaction of 2,2,4,4-tetramethylpentan-3-imine (^{t}Bu$_2$C=NH) with **5a** has also been performed, which gave a complex mixture. The two single crystals of **18h** and **18i** have also been obtained to support our speculation for the structure of **18** (Figure 6.15) and the anti-Markovnikov addition step.

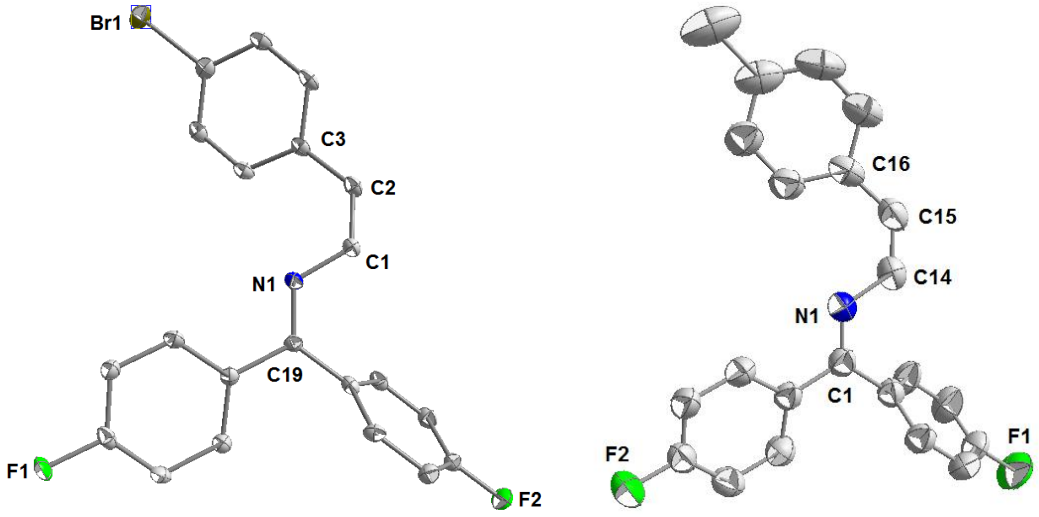

18h **18i**

Figure 6.15 Solid state structure of **18b** (left) and **18g** (right). Hydrogen atoms are omitted for clarity. Thermal ellipsoids are shown at the 50% probability level. Selected bond lengths [Å] and angles [º]: **18h** C2-C3 1.4657(51), C1-C2 1.3470(67), C1-N1 1.4003(45), N1-C9 1.1294(51); C9-N1-C1 120.412(294), N1-C1-C2 122.561(323), C1-C2-C3 127.792(421); **18i** C15-C16 1.4457(32), C14-C15 1.3366(35), C1-N1 1.2933(29), N1-C14 1.3877(30); C14-N1-C1 121.115(205), N1-C14-C15 123.547(231), C14-C15-C16 123.972(255).

Table 6.4 Au-catalyzed hydroimination of terminal arylalkynes[a]

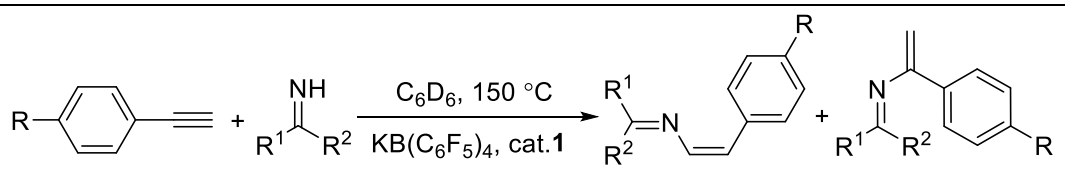

5 **17** **18** **19**

Entry	**5**	**17**	Time (h)	Yield (%)[b,c]	Ratio (18:19)
1	**5a** (R = H)	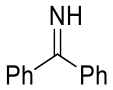	6	**18a** 51(47)	6.2 : 1
2	**5b** (R = Br)		6	**18b** 54(50)	100 : 0
3	**5c** (R = Me)	**17a**	6	**18c** 43(39)	100 : 0
4	**5a** (R = H)	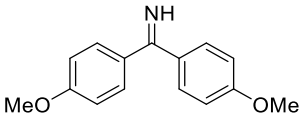	6	**18d** 40(37)	100 : 0
5	**5b** (R = Br)		6	**18e** 48(44)	100 : 0
6	**5c** (R = Me)	**17b**	6	**18f** 42(37)	100 : 0
7	**5a** (R = H)	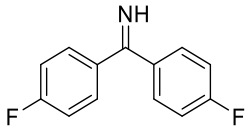	6	**18g** 50(47)	100 : 0
8	**5b** (R = Br)		6	**18h** 48(42)	100 : 0
9	**5c** (R = Me)	**17c**	5	**18i** 36(32)	100 : 0
10	**5a** (R = H)	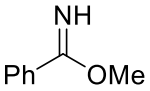	4	**18j** 51(47)	4.3 : 1
11	**5b** (R = Br)		3	**18k** 55(51)	6.1 : 1
12	**5c** (R = Me)	**17d**	3	**18l** 43(39)	6.1 : 1

Notes: a. Reaction condition **5** (1 mmol), ammonia (0.25 mmol), LAuCl and $KB(C_6F_5)_4$ (1 mol%), and C_6D_6 (0.7 mL). b. Yields were determined by ^1H NMR spectroscopy using 1,4-di-t-butylbenzene as an internal standard. c. Isolated yields are given in parentheses.

The anti-Markovnikov products **18** were stable enough to be isolated by chromatography, which encouraged us to extend the substrates. We further tested the reaction of **17a** with diphenylacetylene, which afforded N-(1,2-diphenylvinyl)-1,1-diphenylmethanimine in 78% yield (Scheme 6.15).[83]

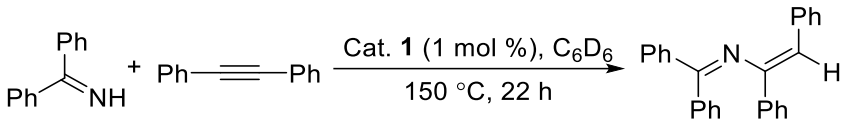

17a

Scheme 6.15 Reaction of imine **17a** with diphenylacetylene catalyzed by gold catalyst **1**.

6.3 Conclusion

A new gold complex **1** featuring a pyrid-*2*-ylidene ligand was synthesized and fully characterized. **1** has been employed in hydroamination of alkynes with ammonia, which provided an efficient synthetic method for the construction of pyridine derivatives **7**. **1** has also been utilized in the hydroimination of alkynes with imines, which indicated an apparent anti-Markovnikov regioselectivity to form 2-aza-1,3-dienes **18**. A plausible mechanism involving both Markovnikov and Anti-Markovnikov addition was proposed and certified by the experimental studies.

6.4 Experimental Section

All manipulations were performed under an atmosphere of dry argon or nitrogen using standard Schlenk techniques unless otherwise stated. Solvents were dried by standard methods and distilled under nitrogen. ^{1}H, ^{13}C and ^{19}F NMR spectra were recorded on Bruker BBFO1 400 or BBFO2 400 spectrometers at 298 K. Mass spectra were performed at the NTU Mass Spectrometry Laboratory. X-ray analyses were performed using Bruker X8-APEX X-ray diffraction instrument with Mo-radiation.

*6.4.1 Synthesis of compound 3,5-bis(3,5-di-tert-butylphenyl)pyridine **2***

3,5-dibromopyridine (10 mmol, 2.35 g), (3,5-di-tert-butylphenyl)boronic acid (25 mmol, 5.85 g), $Pd(PPh_3)_4$ (0.5 mmol, 0.58 g), $Ba(OH)_2$ (40 mmol, 6.88 g) were dissolved in THF and H_2O (10:1, 180 mL, degassed). The mixture was refluxed overnight. After cooling to room temperature, ethyl acetate was added and the organic layer was dried over $MgSO_4$. The product was purified by silica gel column chromatography (petroleum ether: ethyl acetate = 10:1) to afford **2** as a yellow solid (4.1 g, 90%). M.P. 146 ℃; ^{1}H NMR δ (400 MHz, $CDCl_3$): 1.43 (s, 36H, CH_3); 7.45-7.46 (d, *J* = 4 Hz, 4H, Ar-*H*); 7.53 (s, 2H); 8.02-8.03 (t, *J* = 4 Hz, 1H, Py-*H*); 8.80-8.81 (d, *J* = 4 Hz, 2H, Py-*H*). ^{13}C NMR (101 MHz, $CDCl_3$): δ 31.3 (*C*H_3), 35.2 (CH_3)$_3$-*C*), 122.0 (*C*H), 122.5 (*C*H), 133.8 (*C*H), 137.6 (*C*^{q}), 137.9 (*C*^{q}), 147.2 (*C*H), 151.8 (*C*^{q}). HRMS $[M+H]^+$ *m/z* Calcd for $C_{33}H_{46}N$: 456.3630. Found: 456.3638.

*6.4.2 Synthesis of compound **3***

Compound **2** (10 mmol, 4.55 g) and *1*-chloro-*2,4*-dinitrobenzene (15 mmol, 3.0 g) were dissolved in ethanol (50 mL) and the mixture was heated at 90 ℃ for 4 days. After removal of the solvent, the product was purified by silica gel column (petroleum ether: ethyl acetate = 10:1, 500 mL; ethanol, 300 mL) to afford Zincke salt as a red solid (4.6 g, 70%). M.P. 184 ℃; ^{1}H NMR (400 MHz, $CDCl_3$): *δ* 1.41 (s, 36H, CH_3); 7.17 (s, 2H, Ar-*H*); 7.48 (d, *J* = 4Hz, 4H, Ar-*H*);

7.66 (t, *J* = 12 Hz, 2H, Ar-*H*); 8.75 (d, *J* = 8 Hz, 2H, Py-*H*); ^{13}C NMR (101 MHz, $CDCl_3$): δ 17.6 (*C*H_3), 21.2 (*C*H_3), 31.5 (*C*$(CH_3)_3$), 35.3 (*C*$(CH_3)_3$), 122.7 (*C*H), 125.5 (*C*H), 130.5 (*C*H), 132.3 (C^q), 139.3 (C^q), 141.2 (*C*H), 142.2 (C^q), 143.1 (*C*H), 144.2 (C^q), 153.0 (C^q). HRMS $[M+H]^+$ *m/z* Calcd for $C_{39}H_{49}O_4ClN_3$: 658.3412. Found: 658.3416.

*6.4.3 Synthesis of compound **4***

Zincke salt **3** (10 mmol, 6.57 g) was dissolved in $CHCl_3$ (80 mL) and 2.56 g (10 mmol) of AgOTf was added. The mixture was stirred at room temperature for 30 min. After filtration, the solvent was removed under vacuum and 2,4,6-trimethylaniline (15 mL) was added. The mixture was heated at 150 ℃ for 3 h. After distillation to remove excess 2,4,6-trimethylaniline, the residue was purified by chromatography (PE:EA = 3:1, 300 mL; ethanol, 200 mL) to give 5.1 g (90%) of **4** as a brown solid; M.P. 198 ℃; ^{1}H NMR (400 MHz, $CDCl_3$): δ 1.41 (s, 36H, C*H*$_3$); 2.22 (s, 6H, C*H*$_3$); 2.43 (s, 3H, C*H*$_3$); 7.18 (s, 2H, Ar-*H*); 7.28 (s, 2H, Ar-*H*); 7.52 (d, *J* = 8 Hz, 4H, Ar-*H*); 7.67 (t, *J* = 4 Hz, 2H, Ar-*H*); 8.76 (d, *J* = 8 Hz, 2H, Ar-*H*); 8.78 (d, *J* = 12 Hz, 2H, Py-*H*). ^{13}C NMR (101 MHz, $CDCl_3$): δ 17.7(*C*H_3), 21.2(*C*H_3), 31.3 (*C*$(CH_3)_3$), 35.2 (*C*$(CH_3)_3$), 122.2(*C*H), 125.3(*C*H), 130.5(*C*H), 132.4 (C^q), 139.5 (C^q), 141.3(*C*H), 142.2 (C^q), 142.9(*C*H), 144.2 (C^q), 153.1 (C^q). HRMS $[M+H]^+$ *m/z* Calcd for $C_{43}H_{57}F_3NO_3S$: 724.4011. Found: 724.4009.

*6.4.4 Synthesis of compound **1***

A THF solution of LiHMDS (115 mmol, 1.0 M, 115 mL) was added to a THF solution (20.0 mL) of pyridinium triflate **4** (38.0 mmol, 25.0 g). The mixture was stirred at room temperature for 20 min. Chloro(tetrahydrothiophene) gold(I) (38.0 mmol, 11.5 g) was added to the mixture. The solution was filtered and concentrated under vacuum. The crude product was purified by silica gel column chromatography (MeOH: $CHCl_3$ = 1:20) and **1** was obtained as a pale-yellow crystal by recrystallization with $CHCl_3$/toluene at room temperature (6.8 g, 27%), M.P. 231 ℃. ^{1}H NMR (400 MHz, $CDCl_3$): δ 1.41-1.45 (d, *J* = 16 Hz, 36H, C*H*$_3$); 2.15 (s, 6H, C*H*$_3$); 2.41 (s,

3H, C*H*$_3$); 7.10 (s, 2H, Mes-*H*); 7.38-7.39 (d, *J* = 4 Hz, 2H, Ar-*H*); 7.28(s, 2H, Ar-*H*); 7.61 (s, 2H, Ar-*H*); 7.62(d, *J* = 4 Hz, 2H, Ar-*H*); 7.79(d, *J* = 12 Hz, 2H, Ar-*H*); 8.32(d, *J* =8 Hz, 1H, *p*-C*H*); 8.39 (d, *J* = 4 Hz, 1H, *o*-C*H*). ^{13}C NMR (100 MHz, $CDCl_3$): δ 18.04 (*C*H$_3$), 21.29 (*C*H$_3$), 31.47 (*C*H$_3$), 31.57 (*C*H$_3$), 35.14 (*C*(CH$_3$)$_3$), 35.19 (*C*(CH$_3$)$_3$), 121.21 (*C*H),122.93 (*C*H), 123.88 (*C*H), 123.95 (*C*H), 129.86 (*C*H), 132.22 (*C*^{q}), 134.01 (*C*^{q}), 136.94 (*C*^{q}), 136.97 (*C*H), 138.33 (*C*H), 139.77 (*C*^{q}), 139.93 (*C*^{q}), 145.84 (*C*^{q}), 151.10 (*C*^{q}), 152.29 (*C*^{q}), 152.63 (*C*^{q}), 187.52 (*C*^{carbene}). HRMS $[M+H]^+$ *m/z* Calcd for $C_{42}H_{57}AuClN$: 807.3845. Found: 807.3852.

6.4.5 Au-catalyzed construction of pyridine derivatives 7

General procedure: Complex LAuCl **1** (8 mg, 5 mol%) and $KB(C_6F_5)_4$ (7 mg, 5 mol%) were introduced in a Wilmad CQPV thick-walled (1.4 mm) NMR tube. The C_6D_6 (0.7 mL), 1,4-di-t-butylbenzene (0.2 mmol, 38 mg), the desired alkyne **5** (1 mmol) were added in this reaction. NH_3 (0.4 mmol, 6.8 mg) was carefully condensed at −60 °C. The reaction mixture was heated at 150 °C and monitored periodically by ^{1}H NMR. Upon completion, the products were purified on triethylamine deactivated silica gel with the appropriate mixture of *n*-hexane and ethyl acetate.

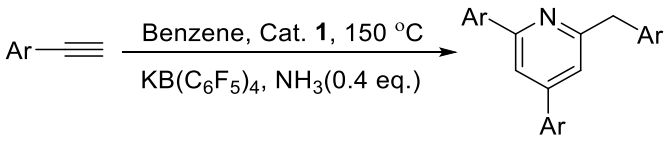

5 **7**

7a: Yellow oil; 40% yield (isolated); ^{1}H NMR (400 MHz, $CDCl_3$): δ = 8.11 (d, *J* = 7.1 Hz, 2H, Ar-*H*), 7.79 (d, *J* = 1.3 Hz, 1H, Ar-*H*), 7.64 (dd, *J* = 8.1, 1.3 Hz, 2H, Ar-*H*), 7.55 – 7.40 (m, 9H, Ar-*H*), 7.36 (t, *J* = 7.5 Hz, 2H, Ar-*H*), 7.28 (d, *J* = 1.3 Hz, 1H, Ar-*H*), 4.34 (s, 2H, C*H*$_2$); ^{13}C NMR (100 MHz, $CDCl_3$): δ = 161.4 (*C*^{q}), 157.5 (*C*^{q}), 149.8 (*C*^{q}), 139.7 (*C*^{q}), 139.7 (*C*^{q}), 138.9 (*C*^{q}), 129.3 (*C*H), 129.0 (*C*H), 128.9 (*C*H), 128.8 (*C*H), 128.7 (*C*H), 128.6 (*C*H), 127.2 (*C*H), 127.1 (*C*H), 126.4 (*C*H), 119.6 (*C*H), 116.5 (*C*H), 45.0 (*C*H$_2$); HRMS (ESI): m/z calcd for $C_{24}H_{20}N$: 322.1596 $[(M+H)]^+$; Found: 322.1595.

7a*: Yellow oil; 38% yield (isolated); ^{1}H NMR (400 MHz, $CDCl_3$): δ = 8.10-8.05 (m, 2H, Ar-*H*), 7.60 (d, *J* = 7.0 Hz, 2H, Ar-*H*), 7.49-7.39 (m, 9H, Ar-*H*), 7.32 (t, *J* = 7.6 Hz, 3H, Ar-*H*), 7.24 (d, *J* = 7.0 Hz, 1H, Ar-*H*), 4.30 (dd, *J* = 7.0, 3.6 Hz, 2H, CH_2); ^{13}C NMR (100 MHz, $CDCl_3$): δ = 161.4 (dd, *J* = 58.5, 10.2 Hz, *C**), 119.5 (d, *J* = 58.4 Hz, *C**), 116.5 (d, *J* = 9.0 Hz, *C**); HRMS (ESI): m/z calcd for $C_{21}{}^{13}C_3H_{20}N$: 325.1696 $[(M+H)]^+$; Found: 325.1702.

7b: Yellow solid; MP: 134 °C; 34% yield (isolated); ^{1}H NMR (400 MHz, $CDCl_3$): δ = 7.86 (d, *J* = 8.5 Hz, 2H, Ar-*H*), 7.60 (s, 1H, Ar-*H*), 7.53 (dd, *J* = 8.6, 2.5 Hz, 4H, Ar-*H*), 7.38 (dd, *J* = 10.4, 8.5 Hz, 4H, Ar-*H*), 7.18 (d, *J* = 3.3 Hz, 1H, Ar-*H*), 7.15 (s, 1H, Ar-*H*), 7.11 (s, 1H, Ar-*H*), 4.13 (s, 2H, CH_2); ^{13}C NMR (100 MHz, $CDCl_3$): δ = 161.1 (C^q), 156.6 (C^q), 149.0 (C^q), 138.4 (C^q), 138.2 (C^q), 137.4 (C^q), 132.3 (*C*H), 131.9 (*C*H), 131.7 (*C*H), 130.9 (*C*H), 128.7 (*C*H), 123.6 (C^q), 123.6 (C^q), 120.4 (C^q), 119.5 (*C*H), 116.0 (*C*H), 44.3 (CH_2); HRMS (ESI): m/z calcd for $C_{24}H_{17}Br_3N$: 555.8911 $[(M+H)]^+$; Found: 555.8897.

7c: Yellow oil; 30% yield (isolated); ^{1}H NMR (400 MHz, $CDCl_3$): δ = 7.96 (d, *J* = 8.2 Hz, 2H, Ar-*H*), 7.70 (d, *J* = 1.4 Hz, 1H, Ar-*H*), 7.50 (d, *J* = 8.1 Hz, 2H, Ar-*H*), 7.30-7.24 (m, 6H, Ar-*H*), 7.18 (d, *J* = 1.4 Hz, 1H, Ar-*H*), 7.12 (d, *J* = 7.8 Hz, 2H, Ar-*H*), 4.23 (s, 2H,CH_2), 2.41 (s, 3H, CH_3), 2.40 (s, 3H, CH_3), 2.32 (s, 3H, CH_3); ^{13}C NMR (100 MHz, $CDCl_3$): δ = 161.5 (C^q), 157.4 (C^q), 149.5 (C^q), 138.8 (C^q), 138.7 (C^q), 137.1 (C^q), 136.8 (C^q), 136.1 (C^q), 135.7 (C^q), 129.7 (*C*H), 129.4 (*C*H), 129.2 (*C*H), 129.1 (*C*H), 127.0 (*C*H), 126.9 (*C*H), 119.0 (*C*H), 115.9 (*C*H), 44.6 (CH_2), 21.3 (CH_3), 21.2 (CH_3), 21.1 (CH_3); HRMS (ESI): m/z calcd for $C_{27}H_{26}N$: 364.2065 $[(M+H)]^+$; Found: 364.2071.

7d: Colorless solid; MP: 118 °C; 27% yield (isolated); ^{1}H NMR (400 MHz, $CDCl_3$): δ = 8.00 (d, *J* = 8.6 Hz, 2H, Ar-*H*), 7.68 (d, *J* = 1.3 Hz, 1H, Ar-*H*), 7.54 (d, *J* = 8.5 Hz, 2H, Ar-*H*), 7.48-7.42 (m, 4H, Ar-*H*), 7.29 (s, 4H, Ar-*H*), 7.19 (d, *J* = 1.3 Hz, 1H, Ar-*H*), 4.23 (s, 2H, CH_2); ^{13}C NMR (100 MHz, $CDCl_3$): δ = 161.1 (C^q), 156.5 (C^q), 148.9 (C^q), 137.8 (C^q), 137.7 (C^q), 136.9 (C^q), 135.3 (*C*H), 135.2 (*C*H), 132.3 (*C*H), 130.5 (*C*H), 129.3 (*C*H), 128.9 (C^q), 128.7 (C^q),

128.3 (*C*^{q}), 119.4 (*C*H), 116.0 (*C*H), 44.1 (*C*H_2); HRMS (ESI): m/z calcd for $C_{24}H_{17}Cl_3N$: 427.0427 $[(M+H)]^+$; Found: 427.0427.

7e: Yellow oil; 28% yield (isolated); ^{1}H NMR (400 MHz, $CDCl_3$): δ = 7.66 (dd, *J* = 7.5, 1.9 Hz, 1H, Ar-*H*), 7.60 (d, *J* = 1.4 Hz, 1H, Ar-*H*), 7.49-7.46 (m, 2H, Ar-*H*), 7.42-7.31 (m, 7H, Ar-*H*), 7.22 (td, *J* = 7.3, 1.8 Hz, 2H, Ar-*H*), 7.15 (d, *J* = 1.4 Hz, 1H, Ar-*H*), 4.44 (s, 2H, CH_2); ^{13}C NMR (100 MHz, $CDCl_3$): δ = 159.2 (*C*^{q}), 156.3 (*C*^{q}), 147.3 (*C*^{q}), 139.2 (*C*^{q}), 137.9 (*C*^{q}), 137.0 (*C*^{q}), 134.3 (*C*H), 132.3 (*C*H), 131.8 (*C*H), 131.5 (*C*H), 131.0 (*C*H), 130.2 (*C*H), 130.1 (*C*H), 129.6 (*C*H), 129.5 (*C*H), 128.0 (*C*H), 127.1 (*C*^{q}), 127.0 (*C*^{q}), 126.9 (*C*^{q}), 123.2 (*C*H), 122.2 (*C*H), 42.0 (*C*H_2); HRMS (ESI): m/z calcd for $C_{24}H_{17}Cl_3N$: 427.0427 $[(M+H)]^+$; Found: 427.0427.

7f: Yellow oil; 43% yield (isolated); ^{1}H NMR (400 MHz, $CDCl_3$): δ = 8.05 (dd, *J* = 8.9, 5.4 Hz, 2H, Ar-*H*), 7.66 (d, *J* = 1.4 Hz, 1H, Ar-*H*), 7.59 (dd, *J* = 8.8, 5.3 Hz, 2H, Ar-*H*), 7.33 (dd, *J* = 8.6, 5.5 Hz, 2H, Ar-*H*), 7.17 (m, 5H, Ar-*H*), 7.02 (t, *J* = 8.7 Hz, 1H, Ar-*H*), 4.24 (s, 2H, CH_2); ^{13}C NMR (100 MHz, $CDCl_3$): δ = 163.8 (d, J_{CF} = 195.5 Hz, *C*^{q}), 163.5 (d, J_{CF} = 229.6 Hz, *C*^{q}), 161.3 (d, J_{CF} = 172.2 Hz, *C*^{q}), 161.3 (*C*^{q}), 156.6 (*C*^{q}), 149.0 (*C*^{q}), 135.6 (d, J_{CF} = 3.1 Hz, *C*^{q}), 135.2 (d, J_{CF} = 3.1 Hz, *C*^{q}), 134.7 (d, J_{CF} = 3.3 Hz, *C*^{q}), 130.6 (d, J_{CF} = 7.9 Hz, *C*H), 128.9 (d, J_{CF} = 5.5 Hz, *C*H), 128.8 (d, J_{CF} = 5.4 Hz, *C*H), 119.2 (*C*H), 116.0 (d, *J* = 21.5 Hz, *C*H), 115.6 (d, *J* = 21.6 Hz, *C*H), 115.3 (d, *J* = 21.2 Hz, *C*H), 44.0 (*C*H_2); ^{19}F NMR (376 MHz, $CDCl_3$): δ = –112.6 (m, 1F), –112.9 (m, 1F), –116.80 (m, 1F); HRMS (ESI): m/z calcd for $C_{24}H_{17}F_3N$: 376.1313 $[(M+H)]^+$; Found: 376.1308.

7g: Yellow solid; MP: 90 °C; 38% yield (isolated); ^{1}H NMR (400 MHz, $CDCl_3$): δ = 8.03 (td, *J* = 7.8, 1.7 Hz, 1H, Ar-*H*), 7.82 (s, 1H, Ar-*H*), 7.45 (td, *J* = 7.7, 1.5 Hz, 1H, Ar-*H*), 7.36 (dd, *J* = 13.4, 6.4 Hz, 3H, Ar-*H*), 7.28 (s, 1H, Ar-*H*), 7.25-7.22 (m, 1H, Ar-*H*), 7.21 (s, 1H, Ar-*H*), 7.15 (d, *J* = 1.4 Hz, 1H, Ar-*H*), 7.09 (s, 1H, Ar-*H*), 4.33 (s, 2H, CH_2); ^{13}C NMR (100 MHz, $CDCl_3$): δ = 161.0 (d, *J* = 245.6 Hz, *C*^{q}), 160.6 (d, *J* = 249.7 Hz, *C*^{q}), 159.8 (d, *J* = 250.1 Hz, *C*^{q}), 159.9 (*C*^{q}), 153.1 (*C*^{q}), 144.5 (*C*^{q}), 131.5 (d, *J* = 4.4 Hz, *C*H), 131.3 (d, *J* = 2.9 Hz, *C*H), 130.4

(m),130.3 (*C*H), 128.3 (d, *J* = 8.0 Hz, *C*H), 127.5 (d, *J* = 11.6 Hz, C^q), 126.6 (d, *J* = 12.9 Hz, C^q), 126.4 (d, *J* = 16.0 Hz, C^q), 124.6 (d, *J* = 3.7 Hz, *C*H), 124.5 (d, *J* = 3.5 Hz, *C*H), 124.2 (d, *J* = 3.5 Hz, *C*H), 122.3 (d, *J* = 3.2 Hz, *C*H), 122.2 (d, *J* = 3.2 Hz, *C*H), 121.5 (d, *J* = 2.5 Hz, *C*H), 116.4 (d, *J* = 20.6 Hz, *C*H), 116.1 (d, *J* = 21.2 Hz, *C*H), 115.3 (d, *J* = 22.0 Hz, *C*H), 37.6 (d, *J* = 2.8 Hz, *C*H_2); ^{19}F NMR (376 MHz, $CDCl_3$): δ = –116.9 (m, 2F), –117.5 (m, 1F); HRMS (ESI): m/z calcd for $C_{24}H_{17}F_3N$: 376.1313 $[(M+H)]^+$; Found: 376.1307.

7h: Yellow oil;19% yield (isolated); ^{1}H NMR (400 MHz, $CDCl_3$): δ = 8.18 (d, *J* = 8.1 Hz, 2H, Ar-*H*), 7.76 (d, *J* = 7.8 Hz, 3H, Ar-*H*), 7.70 (d, *J* = 8.1 Hz, 2H, Ar-*H*), 7.65 (d, *J* = 8.0 Hz, 1H, Ar-*H*), 7.47 (d, *J* = 8.1 Hz, 2H, Ar-*H*), 7.36 (d, *J* = 8.0 Hz, 2H, Ar-*H*), 7.20 (d, *J* = 8.1 Hz, 2H, Ar-*H*), 4.24 (s, 2H, C*H*$_2$); ^{13}C NMR (100 MHz, $CDCl_3$): δ = 156.7 (C^q), 154.8 (C^q), 143.4 (q, C^q), 142.8 (q, C^q), 142.0 (q, C^q), 138.70 (*C*H), 130.4 (q, *J* = 38.2 Hz, C^q), 129.55 (*C*H), 129.17 (*C*H), 127.18 (*C*H), 125.76 (q, *J* = 3.7 Hz, *C*H), 125.51 (q, *J* = 3.7 Hz, *C*H), 125.18 (q, *J* = 3.7 Hz, *C*H), 122.6 (q, C^q), 118.5 (*C*H), 41.6 (*C*H_2); ^{19}F NMR (376 MHz, $CDCl_3$): δ = –63.3 (s, 1F), –63.5 (s, 1F), –63.5 (s, 1F); HRMS (ESI): m/z calcd for $C_{27}H_{17}F_9N$: 526.1217 $[(M+H)]^+$; Found: 526.1212.

7i: Yellow oil; 28% yield (isolated); ^{1}H NMR (400 MHz, $CDCl_3$): δ = 7.68 (d, *J* = 1.3 Hz, 1H, Ar-*H*), 7.25-7.22 (m, 3H, Ar-*H*), 6.72 (d, *J* = 2.2 Hz, 2H, Ar-*H*), 6.56 – 6.52 (m, 4H, Ar-*H*), 6.34 (t, *J* = 2.3 Hz, 1H, Ar-*H*), 4.21 (s, 2H, C*H*$_2$), 3.87 (s, 6H, OC*H*$_3$), 3.83 (s, 6H, OC*H*$_3$), 3.76 (s, 6H, OC*H*$_3$); ^{13}C NMR (100 MHz, $CDCl_3$): δ = 161.2 (C^q), 161.1 (C^q), 160.9 (C^q), 160.8 (C^q), 157.1 (C^q), 149.9 (C^q), 141.8 (C^q), 141.8 (C^q), 141.0 (C^q), 119.9 (*C*H), 116.7 (*C*H), 107.4 (*C*H), 105.5 (*C*H), 105.3 (*C*H), 100.1 (*C*H), 100.5 (*C*H), 98. 2 (*C*H), 55.5 (*C*H_3), 55.5 (*C*H_3), 55.2 (*C*H_3), 45.0 (*C*H_2); HRMS (ESI): m/z calcd for $C_{30}H_{32}NO_6$: 502.2230 $[(M+H)]^+$; Found: 502.2229.

7j: Yellow oil; 37% yield (isolated); ^{1}H NMR (400 MHz, $CDCl_3$): δ = 7.89 (s, 1H, Ar-*H*), 7.85 (d, *J* = 7.8 Hz, 1H, Ar-*H*), 7.72 (s, 1H, Ar-*H*), 7.45 – 7.32 (m, 5H, Ar-*H*), 7.22 (t, *J* = 8.3

Hz, 5H, Ar-*H*), 7.04 (d, *J* = 7.1 Hz, 1H, Ar-*H*), 4.26 (s, 2H, CH_2), 2.46 (s, 3H, CH_3), 2.42 (s, 3H, CH_3), 2.34 (s, 3H, CH_3); ^{13}C NMR (100 MHz, $CDCl_3$): δ = 161.3 (C^q), 157.6 (C^q), 149.8 (C^q), 139.8 (C^q), 139.6 (C^q), 138.9 (C^q), 138.6 (C^q), 138.3 (C^q), 138.0 (C^q), 130.0 (*C*H), 129.5 (*C*H), 129.5 (*C*H), 128.8 (*C*H), 128.60 (*C*H), 128.4 (*C*H), 127.9 (*C*H), 127.8 (*C*H), 127.0 (*C*H), 126.2 (*C*H), 124.3 (*C*H), 124.2 (*C*H), 119.5 (*C*H), 116.6 (*C*H), 44.9 (*C*H_2), 21.61 (*C*H_3), 21.50 (*C*H_3), 21.44 (*C*H_3); HRMS (ESI): m/z calcd for $C_{27}H_{26}N$: 364.2065 $[(M+H)]^+$; Found: 364.2062.

7k: Yellow oil; 17% yield (isolated); ^{1}H NMR (400 MHz, $CDCl_3$): δ = 7.68 (d, *J* = 3.2 Hz, 2H, Ar-*H*), 7.49-7.42 (m, 1H, Ar-*H*), 7.40 (t, *J* = 4.1 Hz, 2H, Ar-*H*), 7.23 (d, *J* = 1.2 Hz, 1H, Ar-*H*), 7.20 (dd, *J* = 4.9, 1.4 Hz, 1H, Ar-*H*), 7.1-7.11 (m, 2H, Ar-*H*), 6.97-6.95 (m, 2H, Ar-*H*), 4.38 (s, 2H, CH_2); ^{13}C NMR (100 MHz, $CDCl_3$): δ = 160.5 (C^q), 152.9 (C^q), 145.0 (C^q), 142.9 (C^q), 141.5 (C^q), 141.5 (C^q), 128.4 (*C*H), 128.1 (*C*H), 127.8 (*C*H), 127.1 (*C*H), 126.9 (*C*H), 125.9 (*C*H), 125.5 (*C*H), 124.9 (*C*H), 124.6 (CH), 117.3 (*C*H), 113.2 (*C*H), 38.7 (*C*H_2); HRMS (ESI): m/z calcd for $C_{18}H_{14}NS_3$: 340.0288 $[(M+H)]^+$; Found: 340.0290.

7l: Yellow oil; 45% yield (isolated); ^{1}H NMR (400 MHz, $CDCl_3$): δ = 7.95 (dd, *J* = 3.0, 1.2 Hz, 1H, Ar-*H*), 7.70 (dd, *J* = 5.0, 1.2 Hz, 1H, Ar-*H*), 7.62 (d, *J* = 1.4 Hz, 1H, Ar-*H*), 7.61 (dd, *J* = 2.5, 1.8 Hz, 1H, Ar-*H*), 7.43-7.35 (m, 3H, Ar-*H*), 7.27 (dd, *J* = 4.9, 3.0 Hz, 1H, Ar-*H*), 7.18 (d, *J* = 1.4 Hz, 1H, Ar-*H*), 7.10 (dd, *J* = 2.0, 1.0 Hz, 1H, Ar-*H*), 7.08 (dd, *J* = 4.9, 1.2 Hz, 1H, Ar-*H*), 4.23 (s, 2H, CH_2); ^{13}C NMR (100 MHz, $CDCl_3$): δ = 160.9 (C^q), 153.7 (C^q), 144.0 (C^q), 142.47 (C^q), 140.0 (C^q), 139.6 (C^q), 128.7 (*C*H), 126.9 (*C*H), 126.4 (*C*H), 126.2 (*C*H), 125.9 (*C*H), 125.6 (*C*H), 123.7 (*C*H), 122.9 (*C*H), 121.8 (*C*H), 118.3 (*C*H), 115.3 (*C*H), 39.4 (*C*H_2); HRMS (ESI): m/z calcd for $C_{18}H_{14}NS_3$: 340.0288 $[(M+H)]^+$; Found: 340.0290.

7m: Yellow oil; 14% yield (isolated); ^{1}H NMR (400 MHz, $CDCl_3$): δ = 8.02 (d, *J* = 8.5 Hz, 2H, Ar-*H*), 7.64 (d, *J* = 1.1 Hz, 1H, Ar-*H*), 7.56 (d, *J* = 8.8 Hz, 2H, Ar-*H*), 7.30 (d, *J* = 8.5 Hz, 2H, Ar-*H*), 7.13 (d, *J* = 1.0 Hz, 1H, Ar-*H*), 6.99 (dd, *J* = 12.1, 8.8 Hz, 4H, Ar-*H*), 6.86 (d, *J* = 8.6 Hz, 2H, Ar-*H*), 4.20 (s, 2H, CH_2), 3.87 (s, 3H, OCH_3), 3.85 (s, 3H, OCH_3), 3.79 (s, 3H, OCH_3);

^{13}C NMR (100 MHz, $CDCl_3$): δ = 161.5 (*C*^{q}), 160.3 (*C*^{q}), 160.3 (*C*^{q}), 158.1 (*C*^{q}), 157.0 (*C*^{q}), 149.1 (*C*^{q}), 132.5 (*C*^{q}), 131.9 (*C*^{q}), 131.3 (*C*^{q}), 130.2 (*C*H), 128.3 (*C*H), 128.2 (*C*H), 118.2 (*C*H), 115.1 (*C*H), 114.3 (*C*H), 114.0 (*C*H), 113.9 (*C*H), 55.4 (O*C*H$_3$), 55.2 (O*C*H$_3$), 44.1 (*C*H$_2$); HRMS (ESI): m/z calcd for $C_{27}H_{26}NO_3$: 412.1913 $[(M+H)]^+$; Found: 412.1915.

16a: Colorless solid; Mp: 110 °C; 12% yield (isolated); ^{1}H NMR (400 MHz, $CDCl_3$): δ = 7.95 (d, *J* = 8.1 Hz, 2H, Ar-*H*), 7.74 (s, 1H, Ar-*H*), 7.57 (d, *J* = 8.3 Hz, 2H, Ar-*H*), 7.51 (m, 4H, Ar-*H*), 7.28 (m, 4H, Ar-*H*), 7.20 (s, 1H, Ar-*H*), 4.31 (s, 2H, C*H*$_2$), 2.42 (s, 3H, C*H*$_3$), 2.41 (s, 3H, C*H*$_3$); ^{13}C NMR (100 MHz, $CDCl_3$): δ = 160.2 (*C*^{q}), 157.9 (*C*^{q}), 150.0 (*C*^{q}), 144.08 (*C*^{q}), 139.2 (*C*^{q}), 139.1 (*C*^{q}), 136.9 (*C*^{q}), 135.9 (*C*^{q}), 129.9 (*C*H), 129.6 (*C*H), 129.6 (*C*H), 128.6 (q, *J* = 31.8 Hz, *C*^{q}), 127.1 (*C*H), 127.0 (*C*H), 125.8 (q, *C*^{q}) 125.5 (q, *J* = 3.7 Hz, *C*H), 119.2 (*C*H), 116.3 (*C*H), 44.8 (*C*H$_2$), 21.4 (*C*H$_3$), 21.3 (*C*H$_3$); ^{19}F NMR (376 MHz, $CDCl_3$): δ = –62.3 (s, 1F); HRMS (ESI): m/z calcd for $C_{27}H_{23}NF_3$: 418.1783 $[(M+H)]^+$; Found: 418.1779.

16b: Yellow oil; 10% yield (isolated); ^{1}H NMR (400 MHz, $CDCl_3$): δ = 8.01 (d, *J* = 8.8 Hz, 2H, Ar-*H*), 7.66 (s, 1H, Ar-*H*), 7.57 (d, *J* = 8.7 Hz, 2H, Ar-*H*), 7.43 (d, *J* = 8.4 Hz, 2H, Ar-*H*), 7.25 (d, *J* = 5.3 Hz, 2H, Ar-*H*), 7.13 (s, 1H, Ar-*H*), 7.00 (dd, *J* = 8.8, 6.8 Hz, 4H, Ar-*H*), 4.19 (s, 2H, C*H*$_2$), 3.88 (s, 3H, OC*H*$_3$), 3.86 (s, 3H, OC*H*$_3$); ^{13}C NMR (100 MHz, $CDCl_3$): δ = 160.6 (*C*^{q}) 160.5 (*C*^{q}), 160.5 (*C*^{q}), 157.4 (*C*^{q}), 149.4 (*C*^{q}), 139.0 (*C*^{q}), 132.5 (*C*^{q}), 131.7 (*C*H), 131.2 (*C*^{q}), 131.1 (*C*H), 128.5 (*C*H), 128.3 (*C*H), 120.3 (*C*^{q}), 118.4 (*C*H), 115.4 (*C*H), 114.6 (*C*H), 114.2 (*C*H), 55.5 (O*C*H$_3$), 55.5 (O*C*H$_3$), 44.4 (*C*H$_2$); HRMS (ESI): m/z calcd for $C_{26}H_{23}NO_2Br$: 460.0912 $[(M+H)]^+$; Found: 460.0911.

16c: Colorless oil; 10% yield (isolated); ^{1}H NMR (400 MHz, $CDCl_3$): δ = 8.01 (d, *J* = 8.9 Hz, 2H, Ar-*H*), 7.66 (d, *J* = 1.4 Hz, 1H, Ar-*H*), 7.57 (d, *J* = 8.8 Hz, 2H, Ar-*H*), 7.34 (dd, *J* = 8.7, 5.5 Hz, 2H, Ar-*H*), 7.13 (d, *J* = 1.4 Hz, 1H, Ar-*H*), 7.00 (dd, *J* = 9.3, 7.9 Hz, 6H, Ar-*H*), 4.22 (s, 2H, C*H*$_2$), 3.88 (s, 3H, OC*H*$_3$), 3.86 (s, 3H, OC*H*$_3$); ^{13}C NMR (100 MHz, $CDCl_3$): δ = 162.9 (d, *J* = 192.1 Hz, *C*^{q}), 161.0 (*C*^{q}), 160.5 (d, *J* = 3.1 Hz, *C*^{q}), 157.3 (*C*^{q}), 149.4 (*C*^{q}), 135.7 (*C*^{q}), 135.6

(C^q), 132.5 (C^q), 131.3 (C^q), 130.8 (d, J = 7.8 Hz, *C*H), 128.5 (d, J = 13.2 Hz, *C*H), 118.4 (*C*H), 115.5 (*C*H), 115.3 (*C*H), 115.3 (*C*H), 114.5 (*C*H), 114.2 (*C*H), 55.5 (O*C*H$_3$), 55.5 (O*C*H$_3$), 44.2 (*C*H$_2$); ^{19}F NMR (376 MHz, $CDCl_3$): δ = –117.1 (m, 1F); HRMS (ESI): m/z calcd for $C_{26}H_{23}NFO_2$: 400.1713 $[(M+H)]^+$; Found: 400.1709.

16d: Colorless solid; Mp: 113 °C; 6% yield (isolated); ^{1}H NMR (400 MHz, $CDCl_3$): δ = 8.03 (d, J = 8.8 Hz, 2H, Ar-*H*), 7.69 (s, 1H, Ar-*H*), 7.58 (d, J = 8.8 Hz, 4H, Ar-*H*), 7.51 (d, J = 8.1 Hz, 2H, Ar-*H*), 7.17 (s, 1H, Ar-*H*), 7.01 (t, J = 8.2 Hz, 4H, Ar-*H*), 4.30 (s, 2H, C*H*$_2$), 3.88 (s, 3H, OC*H*$_3$), 3.86 (s, 3H, OC*H*$_3$); ^{13}C NMR (100 MHz, $CDCl_3$): δ = 160.6 (C^q), 160.5 (C^q), 160.0 (C^q), 157.4 (C^q), 149.5 (C^q), 144.1 (C^q), 144.1 (C^q), 132.4 (C^q), 131.1 (C^q), 129.6 (*C*H), 128.5 (q, J = 32.1 Hz, C^q), 128.4 (*C*H), 128.3 (*C*H), 127.8 (q, J = 261.9 Hz, C^q), 125.5 (q, J = 3.7 Hz, *C*H), 118.5 (*C*H), 115.5 (*C*H), 114.6 (*C*H), 114.2 (*C*H), 55.5 (O*C*H$_3$), 55.5 (O*C*H$_3$), 44.8 (*C*H$_2$); ^{19}F NMR (377 MHz, $CDCl_3$): δ = –62.3 (s, 1F); HRMS (ESI): m/z calcd for $C_{27}H_{23}NO_2F_3$: 450.1681 $[(M+H)]^+$; Found: 450.1681.

16e: Colorless solid; Mp: 103 °C; 14% yield (isolated); ^{1}H NMR (400 MHz, $CDCl_3$): δ = 8.02 (d, J = 8.8 Hz, 2H, Ar-*H*), 7.67 (s, 1H, Ar-*H*), 7.58 (d, J = 8.7 Hz, 2H, Ar-*H*), 7.28 (dd, J = 4.8, 3.1 Hz, 1H, Ar-*H*), 7.18 (s, 1H, Ar-*H*), 7.17 – 7.03 (m, 2H, Ar-*H*), 7.00 (t, J = 8.2 Hz, 4H, Ar-*H*), 4.27 (s, 2H, C*H*$_2$), 3.88 (s, 3H, OC*H*$_3$), 3.86 (s, 3H, OC*H*$_3$); ^{13}C NMR (100 MHz, $CDCl_3$): δ = 160.7 (C^q), 160.5 (C^q), 160.5 (C^q), 157.3 (C^q), 149.3 (C^q), 140.0 (C^q), 132.6 (C^q), 131.3 (C^q), 128.9 (*C*H), 128.5 (*C*H), 128.4 (*C*H), 125.6 (*C*H), 121.8 (*C*H), 118.3 (*C*H), 115.4 (*C*H), 114.5 (*C*H), 114.2 (*C*H), 55.5 (O*C*H$_3$), 55.5 (O*C*H$_3$), 39.7 (*C*H$_2$); HRMS (ESI): m/z calcd for $C_{24}H_{22}NSO_2$: 388.1371 $[(M+H)]^+$; Found: 388.1372.

*6.4.7 Au-catalyzed hydroimination of terminal aryl alkynes **5***

General procedure: Complex LAuCl **1** (8mg, 5 mol%) and $KB(C_6F_5)_4$ (7 mg, 5 mol%) were introduced in a J-Young NMR tube. The C_6D_6 (0.5 mL), 1,3,5-trimethoxybenzene (0.1 mmol, 16.8 mg), the desired alkyne **5** (0.4 mmol) and imine **17** (0.2 mmol) were added in this reaction.

The reaction mixture was heated at 150 °C and monitored periodically by ^{1}H NMR. Upon completion, the products were purified on triethylamine deactivated silica gel with the appropriate mixture of *n*-hexane and ethyl acetate.

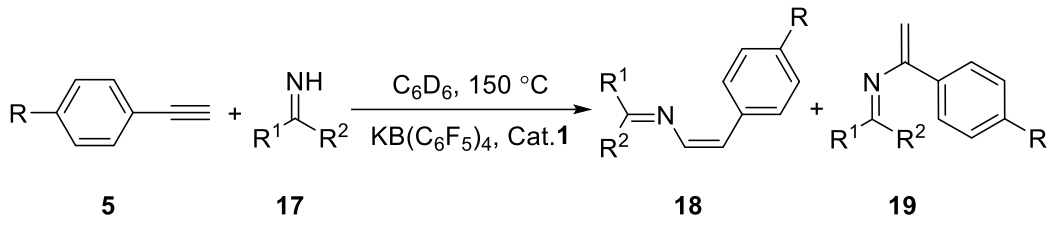

18a: Yellow oil; 47% yield (isolated); ^{1}H NMR (400 MHz, $CDCl_3$): δ = 8.01-7.96 (m, 2H, Ar-*H*), 7.82 (m, 2H, Ar-*H*), 7.51 (m, 3H, Ar-*H*), 7.41 (m, 5H, Ar-*H*), 7.31-7.28 (m, 3H, Ar-*H*), 6.86 (d, *J* = 8.6 Hz, 1H, C*H*), 6.10 (d, *J* = 8.6 Hz, 1H, C*H*); ^{13}C NMR (100 MHz, $CDCl_3$): δ = 167.4 (N=*C*), 139.6 (*C*^{q}), 136.8 (*C*^{q}), 136.4 (*C*H), 136.2 (*C*^{q}), 130.8 (*C*H), 130.6 (*C*H), 129.5 (*C*H), 129.0 (*C*H), 129.0 (*C*H), 128.5 (*C*H), 128.3 (*C*H), 128.3 (*C*H), 127.3 (*C*H), 125.5 (*C*H); HRMS (ESI): m/z calcd for $C_{21}H_{18}N$: 284.1439 $[(M+H)]^+$; found: 284.1437.

18a*: Yellow oil; 46% yield (isolated); ^{1}H NMR (400 MHz, $CDCl_3$): δ = 7.95 (d, *J* = 7.5 Hz, 2H, Ar-*H*), 7.84-7.75 (m, 2H, Ar-*H*), 7.52-7.34 (m, 8H, Ar-*H*), 7.28-7.25 (m, 3H, Ar-*H*), 6.83 (dd, *J* = 164.5, 8.6 Hz, 1H, C*H*), 6.07 (dd, *J* = 8.5, 1.5 Hz, 1H, C*H*); ^{13}C NMR (100 MHz, $CDCl_3$): δ = 136.2 (*C**); HRMS (ESI): m/z calcd for $C_{20}{}^{13}CH_{18}N$: 285.1473 $[(M+H)]^+$; Found: 285.1478.

18b: Yellow oil; 50% yield (isolated); ^{1}H NMR (400 MHz, $CDCl_3$): δ = 7.83 (d, *J* = 8.5 Hz, 2H, Ar-*H*), 7.79-7.74 (m, 2H, Ar-*H*), 7.51-7.46 (m, 5H, Ar-*H*), 7.46-7.37 (m, 3H, Ar-*H*), 7.26 (m, 2H, Ar-*H*), 6.84 (d, *J* = 8.5 Hz, 1H, C*H*), 6.00 (d, *J* = 8.6 Hz, 1H, C*H*); ^{13}C NMR (100 MHz, $CDCl_3$): δ = 168.0 (N=*C*), 139.4 (*C*^{q}), 137.0 (*C*H), 136.1 (*C*^{q}), 135.8, (*C*^{q}) 132.3 (*C*H), 131.4 (*C*H), 130.8 (*C*H), 129.5 (*C*H), 129.2 (*C*H), 129.0 (*C*H), 128.6 (*C*H), 128.4 (*C*H), 124.2 (*C*H), 121.3 (*C*^{q}); HRMS (ESI): m/z calcd for $C_{21}H_{17}BrN$: 362.0544 $[(M+H)]^+$; found: 362.0548.

18c: Yellow oil; 39% yield (isolated); ^{1}H NMR (400 MHz, $CDCl_3$): δ = 7.89 (d, J = 8.1 Hz, 2H, Ar-*H*), 7.82 (m, 2H, Ar-*H*), 7.54-7.47 (m, 3H, Ar-*H*), 7.47-7.38 (m, 3H, Ar-*H*), 7.29 (m, 2H, Ar-*H*), 7.22 (d, J = 8.0 Hz, 2H, Ar-*H*), 6.82 (d, J = 8.5 Hz, 1H, C*H*), 6.08 (d, J = 8.5 Hz, 1H, C*H*), 2.40 (s, 3H, CH_3); ^{13}C NMR (100 MHz, $CDCl_3$): δ = 166.8 (C^q), 139.7 (C^q), 137.2 (C^q), 136.3 (C^q), 135.6 (*C*H), 134.1 (C^q), 130.8 (*C*H), 130.4 (*C*H), 129.4 (*C*H), 129.0 (*C*H), 129.0 (*C*H), 128.9 (*C*H), 128.5 (*C*H), 128.3 (*C*H), 125.7 (*C*H), 21.4 (*C*H_3); HRMS (ESI): m/z calcd for $C_{22}H_{20}N$: 298.1596 $[(M+H)]^+$; found: 298.1595.

18d: Yellow oil; 37% yield (isolated); ^{1}H NMR (400 MHz, $CDCl_3$): δ = 7.94 (d, J = 7.4 Hz, 2H, Ar-*H*), 7.75 (d, J = 8.9 Hz, 2H, Ar-*H*), 7.35 (t, J = 7.7 Hz, 2H, Ar-*H*), 7.25-7.18 (m, 3H, Ar-*H*), 6.99 (d, J = 8.7 Hz, 2H, Ar-*H*), 6.91 (d, J = 8.9 Hz, 2H, Ar-*H*), 6.84 (d, J = 8.6 Hz, 1H, C*H*), 6.01 (d, ^{3}J = 8.6 Hz, 1H, C*H*), 3.88 (s, 3H, OCH_3), 3.86 (s, 3H, OCH_3); ^{13}C NMR (100 MHz, $CDCl_3$): δ = 166.9 (N=*C*), 161.7 (C^q), 160.1 (C^q), 137.2 (C^q), 136.9 (*C*H), 131.3 (*C*H), 130.8 (*C*H), 130.6 (*C*H), 128.5 (C^q), 128.2 (*C*H), 126.9 (*C*H), 123.9 (*C*H), 113.8 (*C*H), 113.7 (*C*H), 55.5 (O*C*H_3), 55.4 (O*C*H_3); HRMS (ESI): m/z calcd for $C_{23}H_{22}NO_2$: 344.1651 $[(M+H)]^+$; found: 344.1649.

18e: Yellow oil; 44% yield (isolated); ^{1}H NMR (400 MHz, $CDCl_3$): δ = 7.82 (d, J = 8.5 Hz, 2H, Ar-*H*), 7.73 (d, J = 8.9 Hz, 2H, Ar-*H*), 7.47 (d, J = 8.5 Hz, 2H, Ar-*H*), 7.20 (d, J = 8.6 Hz, 2H, Ar-*H*), 6.99 (d, J = 8.6 Hz, 2H, Ar-*H*), 6.91 (d, J = 8.9 Hz, 2H, Ar-*H*), 6.86 (d, J = 8.6 Hz, 1H, C*H*), 5.93 (d, J = 8.6 Hz, 1H, C*H*), 3.88 (s, 3H, OCH_3), 3.86 (s, 3H, OCH_3); ^{13}C NMR (100 MHz, $CDCl_3$): δ = 167.4 (N=*C*), 161.9 (C^q), 160.2 (C^q), 137.6 (*C*H), 136.1 (C^q), 132.7 (C^q), 132.1 (*C*H), 131.3 (*C*H), 131.3 (*C*H), 130.8 (*C*H), 128.3 (Cq), 122.6 (*C*H), 120.8 (C^q), 113.8 (*C*H), 113.7 (*C*H), 55.5 (O*C*H_3), 55.5 (O*C*H_3); HRMS (ESI): m/z calcd for $C_{23}H_{21}NO_2Br$: 422.0756 $[(M+H)]^+$; found: 422.0752.

18f: Yellow oil; 37% yield (isolated); ^{1}H NMR (400 MHz, $CDCl_3$): δ = 7.85 (d, J = 8.1 Hz, 2H, Ar-*H*), 7.75 (d, J = 8.9 Hz, 2H, Ar-*H*), 7.19 (m, 4H, Ar-*H*), 6.99 (d, J = 8.7 Hz, 2H, Ar-*H*),

6.91 (d, *J* = 8.9 Hz, 2H, Ar-*H*), 6.81 (d, *J* = 8.6 Hz, 1H, C*H*), 5.99 (d, *J* = 8.6 Hz, 1H, C*H*), 3.88 (s, 3H, OCH_3), 3.86 (s, 3H, OCH_3), 2.37 (s, 3H, CH_3); ^{13}C NMR (100 MHz, $CDCl_3$): δ = 166.3 (N=*C*), 161.6 (*C*^{q}), 160.0 (*C*^{q}), 136.8 (*C*^{q}), 136.1 (*C*H), 134.4 (*C*^{q}), 132.9 (*C*^{q}), 131.2 (*C*H), 130.8 (*C*H), 130.6 (*C*H), 129.0 (*C*H), 128.6 (*C*^{q}), 124.1 (*C*H), 113.8 (*C*H), 113.6 (*C*H), 55.5 (O*C*H_3), 55.4 (O*C*H_3), 21.4 (*C*H_3); HRMS (ESI): m/z calcd for $C_{24}H_{24}rNO_2$: 358.1807 [(M+H)]$^+$; found: 358.1809.

18g: Yellow oil; 47% yield (isolated); ^{1}H NMR (400 MHz, $CDCl_3$): δ = 7.91 (d, *J* = 7.5 Hz, 2H, Ar-*H*), 7.76 (dd, *J* = 8.8, 5.6 Hz, 2H, Ar-*H*), 7.37 (t, *J* = 7.7 Hz, 2H, Ar-*H*), 7.25 (dd, *J* = 7.4, 4.3 Hz, 3H, Ar-*H*), 7.19 (t, *J* = 8.6 Hz, 2H, Ar-*H*), 7.08 (t, *J* = 8.6 Hz, 2H, Ar-*H*), 6.77 (d, *J* = 8.6 Hz, 1H, C*H*), 6.09 (d, *J* = 8.6 Hz, 1H, C*H*); ^{13}C NMR (100 MHz, $CDCl_3$): δ = 165.8 (d, J_{C-F} = 145.9 Hz, *C*^{q}), 165.1 (N=*C*), 163.3 (d, J_{C-F} = 143.1 Hz, *C*^{q}), 136.7 (*C*^{q}), 135.9 (*C*H), 135.8 (d, J_{C-F} = 2.8 Hz, *C*^{q}), 131.8 (d, J_{C-F} = 3.5 Hz, *C*^{q}), 131.4 (d, J_{C-F} = 8.4 Hz, *C*H), 131.1 (d, J_{C-F} = 8.4 Hz, *C*H), 130.8 (*C*H), 128.3 (*C*H), 127.4 (*C*H), 125.9 (*C*H), 116.0 (d, J_{C-F} = 21.4 Hz, *C*H), 115.6 (d, J_{C-F} = 21.6 Hz, *C*H); ^{19}F NMR (376 MHz, $CDCl_3$): δ = –109.7 (m, 1F), –111.2 (m, 1F); HRMS (ESI): m/z calcd for $C_{21}H_{16}NF_2$: 320.1251 [(M+H)]$^+$; found: 320.1252.

18h: Yellow solid; 42% yield (isolated); Mp: 113 °C; ^{1}H NMR (400 MHz, $CDCl_3$): δ = 7.78 (d, *J* = 8.5 Hz, 2H, Ar-*H*), 7.73 (dd, *J* = 8.8, 5.6 Hz, 2H, Ar-*H*), 7.49 (d, *J* = 8.5 Hz, 2H, Ar-*H*), 7.28-7.17 (m, 4H, Ar-*H*), 7.08 (t, *J* = 8.6 Hz, 2H, Ar-*H*), 6.79 (d, *J* = 8.5 Hz, 1H, C*H*), 6.02 (d, *J* = 8.6 Hz, 1H, C*H*); ^{13}C NMR (100 MHz, $CDCl_3$): δ = 165.9 (d, J_{C-F} = 148.6 Hz, *C*^{q}), 165.6 (N=*C*), 163.43 (d, J_{C-F} = 146.5 Hz, *C*^{q}), 136.5 (*C*H), 135.7 (d, J_{C-F} = 2.9 Hz, *C*^{q}), 135.6 (*C*^{q}), 132.2 (*C*H), 131.6 (d, J_{C-F} = 3.6 Hz, *C*^{q}), 131.5 (d, J_{C-F} = 9.3 Hz, *C*H), 131.4 (*C*H), 131.1 (d, J_{C-F} = 8.1 Hz, *C*H), 124.6 (CH), 121.4 (*C*^{q}), 116.0 (d, J_{C-F} = 21.2 Hz, *C*H), 115.6 (d, J_{C-F} = 21.7 Hz, *C*H); ^{19}F NMR (376 MHz, $CDCl_3$): δ = –109.2 (m, 1F), –110.9 (m, 1F); HRMS (ESI): m/z calcd for $C_{21}H_{15}NF_2Br$: 398.0356 [(M+H)]$^+$; found: 398.0353.

18i: Yellow solid; 32% yield (isolated); Mp: 97 °C; ^{1}H NMR (400 MHz, $CDCl_3$): δ = 7.84 (d, J = 8.1 Hz, 2H, Ar-*H*), 7.81-7.73 (m, 2H, Ar-*H*), 7.28 (m, 2H, Ar-*H*), 7.24-7.17 (m, 4H, Ar-*H*), 7.10 (t, *J* = 8.7 Hz, 2H, Ar-*H*), 6.76 (d, *J* = 8.5 Hz, 1H, C*H*), 6.10 (d, *J* = 8.5 Hz, 1H, C*H*), 2.40 (s, 3H, CH_3); ^{13}C NMR (100 MHz, $CDCl_3$): δ = 165.7 (d, $J_{C\text{-}F}$ = 143.1 Hz, C^q), 164.5 (N=*C*), 163.2 (d, $J_{C\text{-}F}$ = 140.4 Hz, C^q), 137.4 (C^q), 135.9 (d, $J_{C\text{-}F}$ = 3.0 Hz, C^q), 135.2 (*C*H), 133.9 (C^q), 131.8 (d, $J_{C\text{-}F}$ = 3.6 Hz, C^q), 131.4 (d, $J_{C\text{-}F}$ =8.4 Hz, *C*H), 131.1 (d, $J_{C\text{-}F}$ =8.2 Hz, *C*H), 130.7 (*C*H), 129.1 (*C*H), 126.1 (*C*H), 115.9 (d, $J_{C\text{-}F}$ = 21.4 Hz, *C*H), 115.5 (d, $J_{C\text{-}F}$ = 21.5 Hz, *C*H), 21.4 (*C*H_3); ^{19}F NMR (376 MHz, $CDCl_3$): δ = –109.9 (m), –111.3 (m); HRMS (ESI): m/z calcd for $C_{22}H_{18}NF_2$: 334.1407 $[(M+H)]^+$; found: 334.1411.

18j: Yellow oil; 47% yield (isolated); ^{1}H NMR (400 MHz, $CDCl_3$): δ = 7.91 (d, *J* = 7.5 Hz, 2H, Ar-*H*), 7.56 (m, 2H, Ar-*H*), 7.45 (m, 3H, Ar-*H*), 7.34 (t, *J* = 7.7 Hz, 2H, Ar-*H*), 7.21 (t, *J* = 7.4 Hz, 1H, Ar-*H*), 6.76 (d, *J* = 8.7 Hz, 1H, C*H*), 5.81 (d, J = 8.7 Hz, 1H, C*H*), 4.03 (s, 3H, OCH_3); ^{13}C NMR (100 MHz, $CDCl_3$): δ = 162.9 (N=*C*), 137.2 (C^q), 133.3 (*C*H), 131.3 (C^q), 130.6 (*C*H), 129.6 (*C*H), 129.2 (*C*H), 128.4 (*C*H), 128.2 (*C*H), 126.5 (*C*H), 119.8 (*C*H), 54.3 (O*C*H_3); HRMS (ESI): m/z calcd for $C_{16}H_{186}NO$: 238.1230 $[(M+H)]^+$; found: 238.1230.

18k: Yellow oil; 51% yield (isolated); ^{1}H NMR (400 MHz, $CDCl_3$): δ = 7.79 (d, *J* = 8.5 Hz, 2H, Ar-*H*), 7.57-7.51 (m, 2H, Ar-*H*), 7.46 (m, 5H, Ar-*H*), 6.79 (d, *J* = 8.6 Hz, 1H, C*H*), 5.74 (d, *J* = 8.6 Hz, 1H, C*H*), 4.02 (s, 3H, OCH_3); ^{13}C NMR (100 MHz, $CDCl_3$): δ = 163.5 (N=*C*), 136.2 (C^q), 134.0 (*C*H), 131.2 (*C*H), 131.1 (C^q), 131.1 (*C*H), 130.7 (*C*H), 129.2 (*C*H), 128.5 (*C*H), 120.2 (C^q), 118.5 (*C*H), 54.4 (O*C*H_3); HRMS (ESI): m/z calcd for $C_{16}H_{15}NOBr$: 316.0337 $[(M+H)]^+$; found: 316.0337.

18l: Yellow oil; 39% yield (isolated); ^{1}H NMR (400 MHz, $CDCl_3$): δ = 7.82 (d, *J* = 8.1 Hz, 2H, Ar-*H*), 7.57 (m, 2H, Ar-*H*), 7.45 (m, 3H, Ar-*H*), 7.17 (d, *J* = 8.0 Hz, 2H, Ar-*H*), 6.73 (d, *J* = 8.6 Hz, 1H, C*H*), 5.80 (d, *J* = 8.6 Hz, 1H, C*H*), 4.04 (s, 3H, OCH_3), 2.37 (s, 3H, CH_3); ^{13}C NMR (100 MHz, $CDCl_3$): δ = 162.6 (N=*C*), 136.2 (C^q), 134.4 (C^q), 132.4 (*C*H), 131.3 (C^q),

130.5 (*C*H), 129.5 (*C*H), 129.2 (*C*H), 128.9 (*C*H), 128.4 (*C*H), 119.8 (*C*H), 54.3 (O*C*H_3), 21.4 (*C*H_3); HRMS (ESI): m/z calcd for $C_{17}H_{18}NO$: 252.1388 $[(M+H)]^+$; found: 252.1385.

6.4.7 *^{1}H, ^{13}C and ^{19}F NMR Spectra*

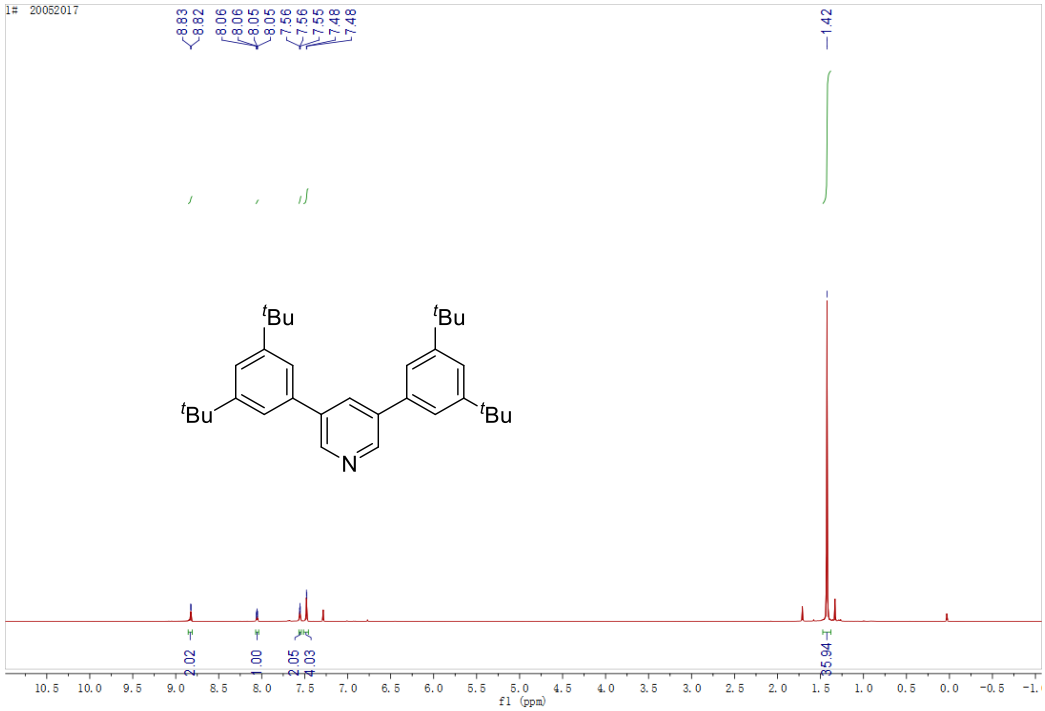

Figure 6.16 ^{1}H NMR spectrum of **2**

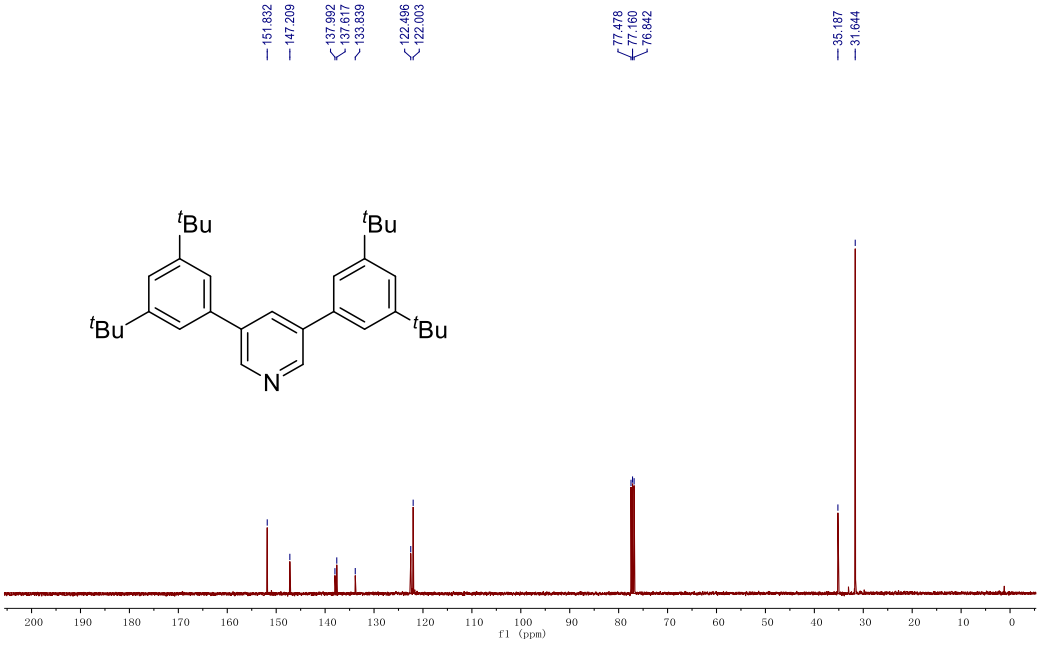

Figure 6.17 ^{13}C NMR spectrum of **2**

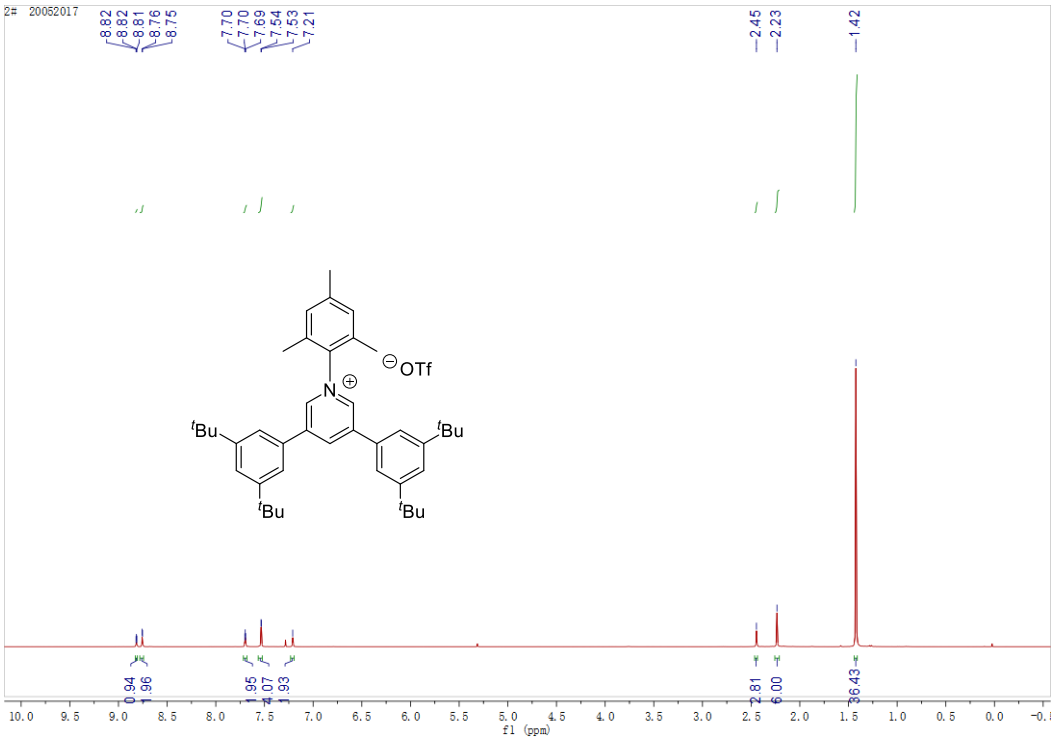

Figure 6.18 ^{1}H NMR spectrum of **4**

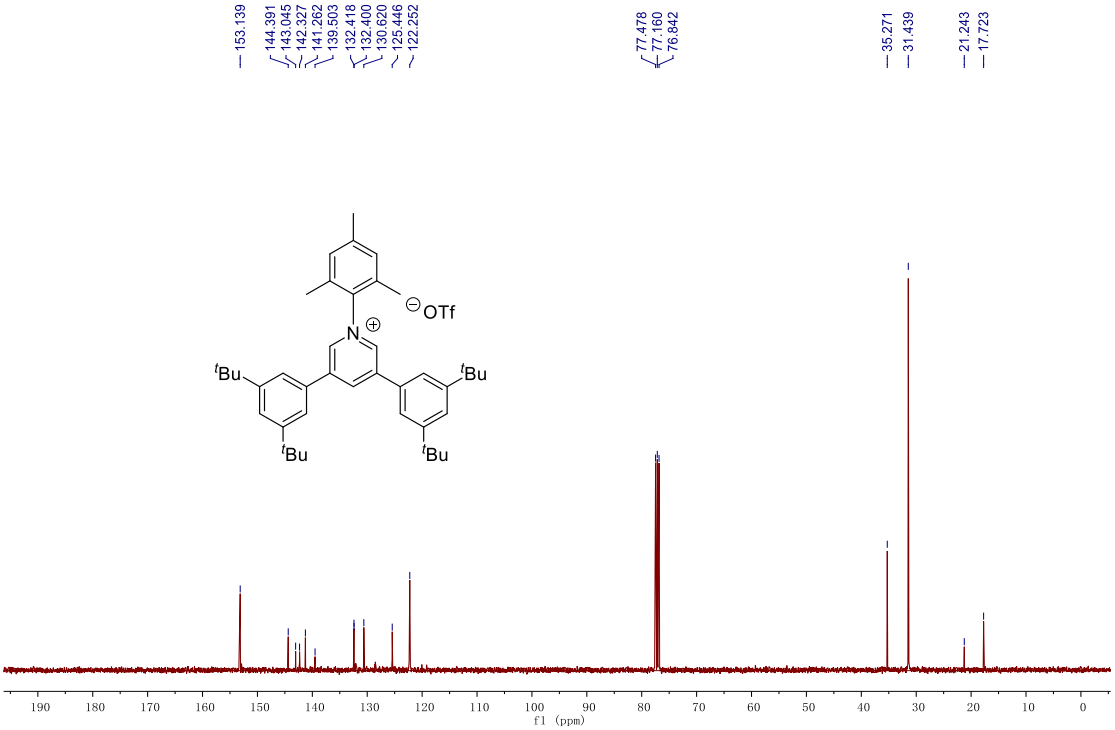

Figure 6.19 ^{13}C NMR spectrum of **4**

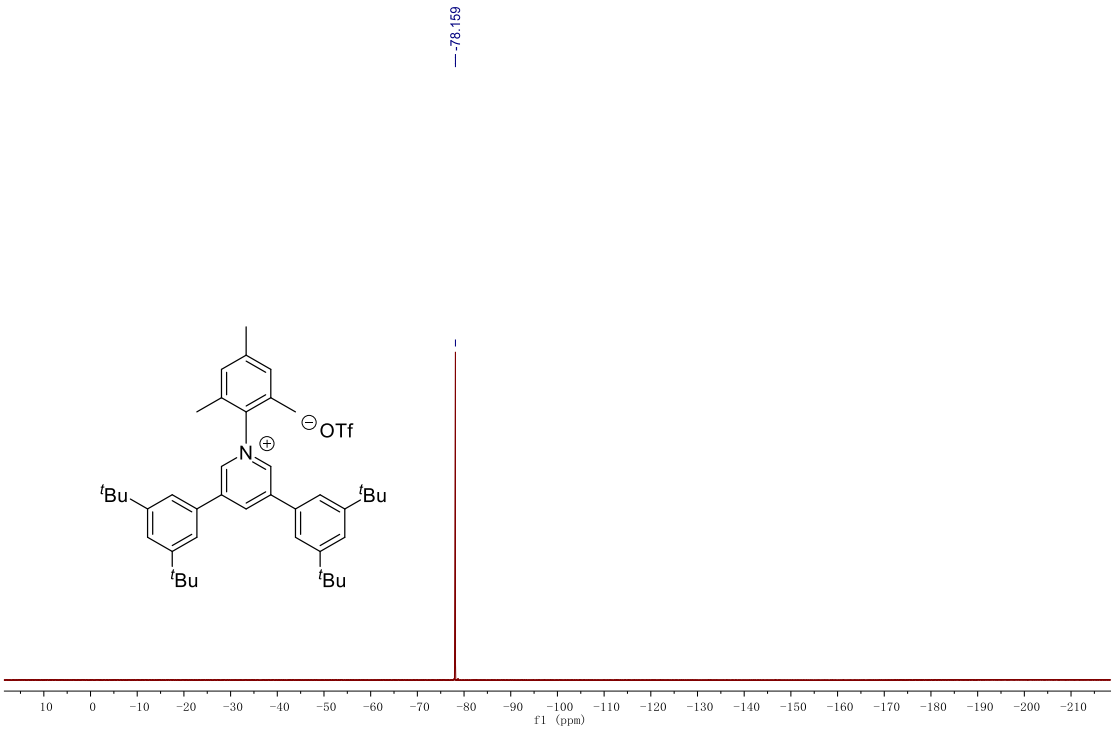

Figure 6.20 ^{19}F NMR spectrum of **4**

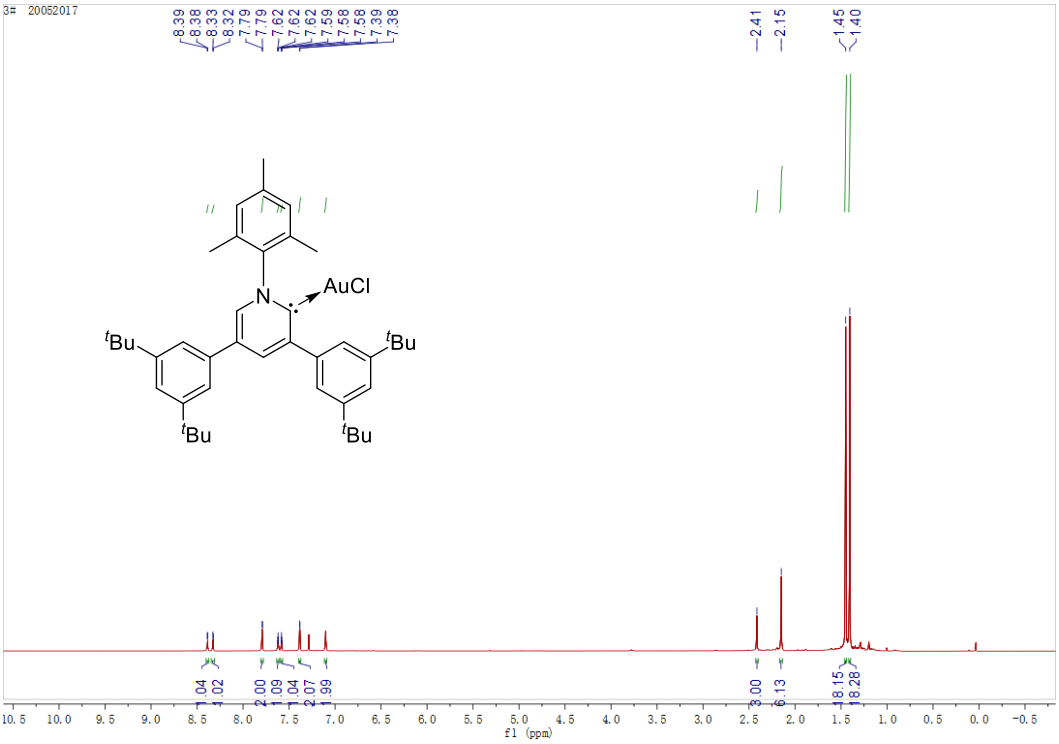

Figure 6.21 ^{1}H NMR spectrum of **1**

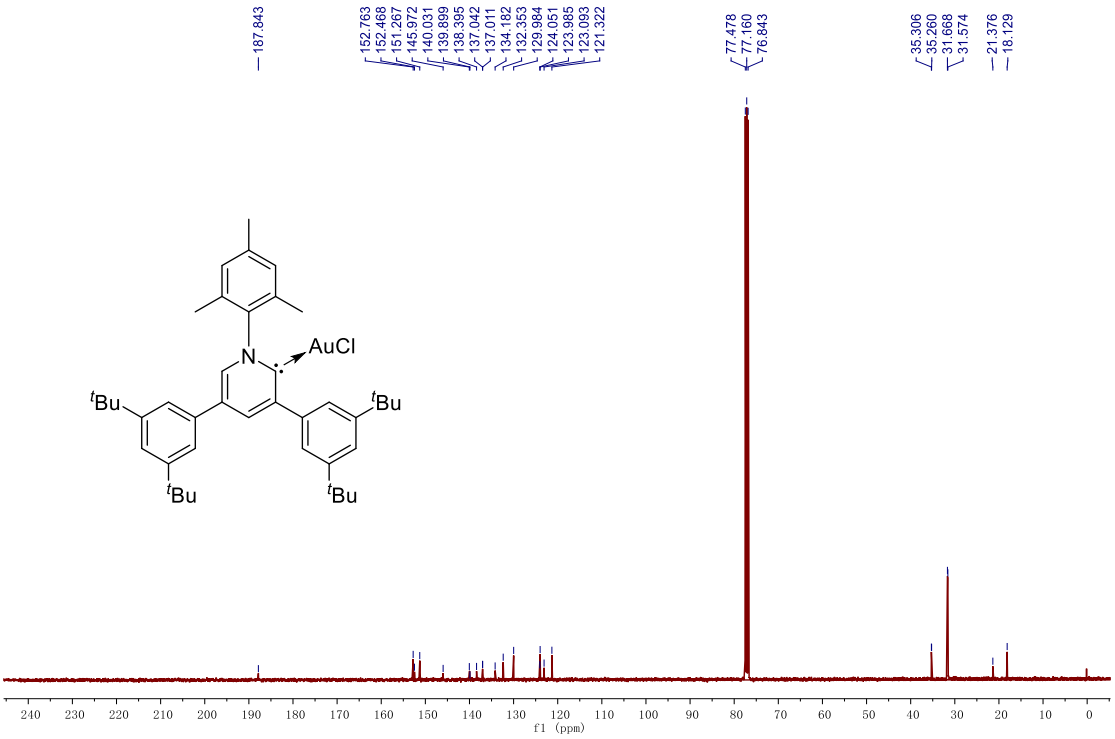

Figure 6.22 ^{13}C NMR spectrum of **1**

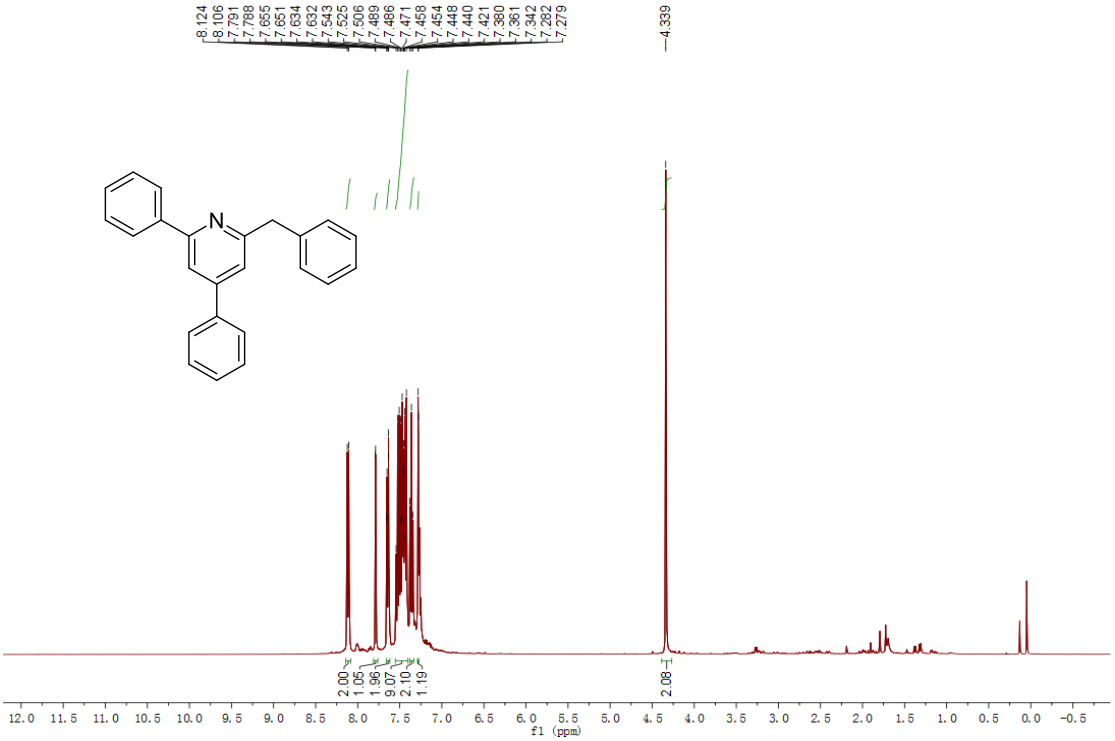

Figure 6.23 ^{1}H NMR spectrum of **7a**

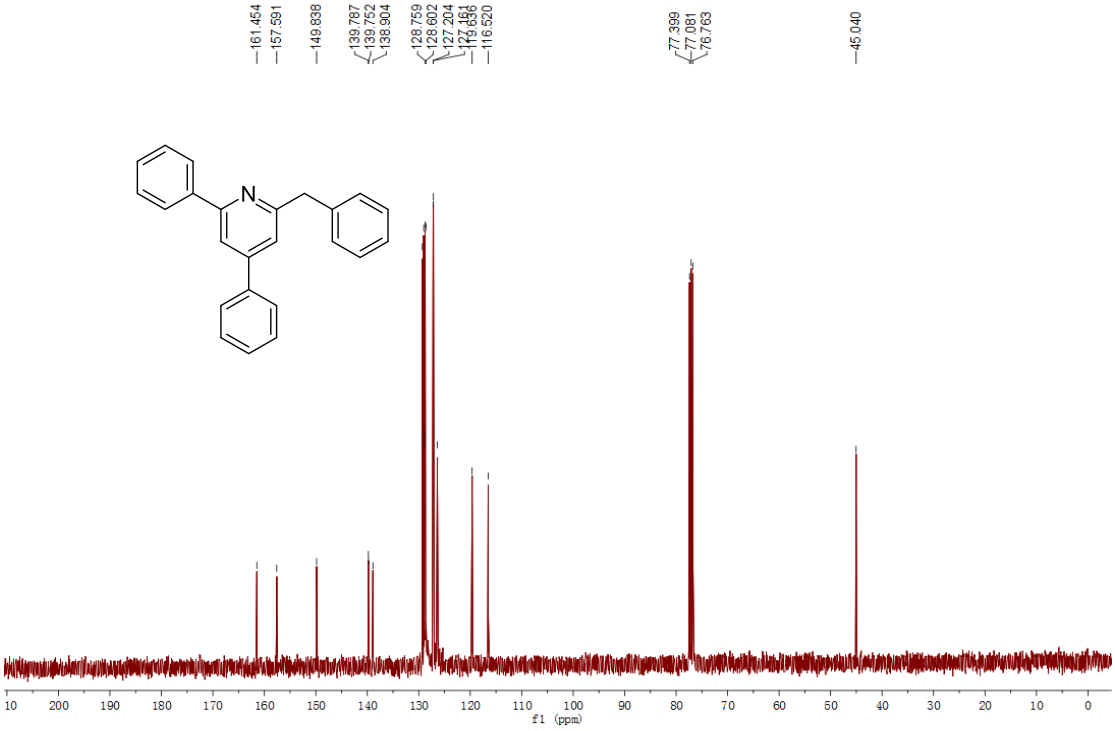

Figure 6.24 ^{13}C NMR spectrum of **7a**

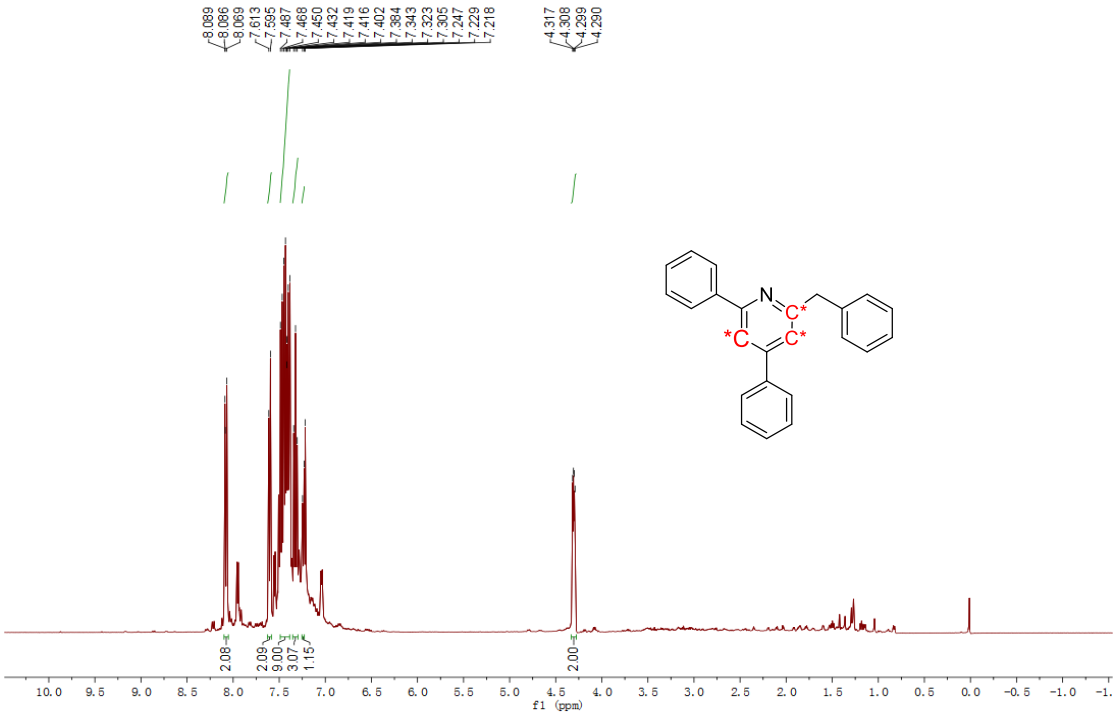

Figure 6.25 ^{1}H NMR spectrum of **7a***

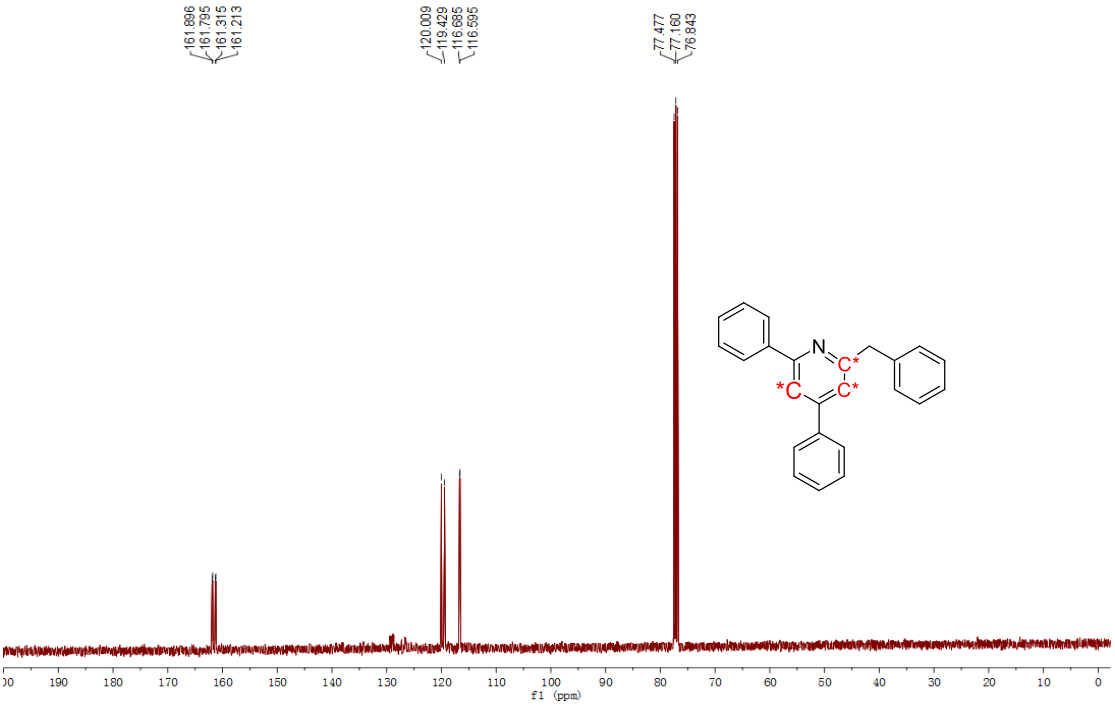

Figure 6.26 ^{13}C NMR spectrum of **7a***

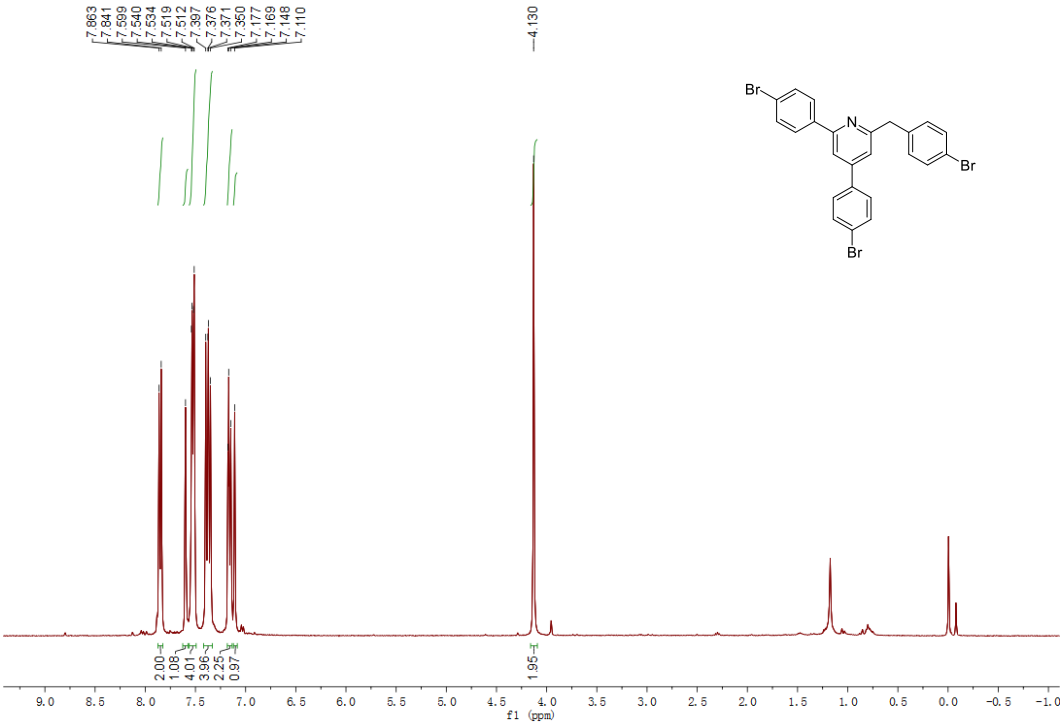

Figure 6.27 ^{1}H NMR spectrum of **5b**

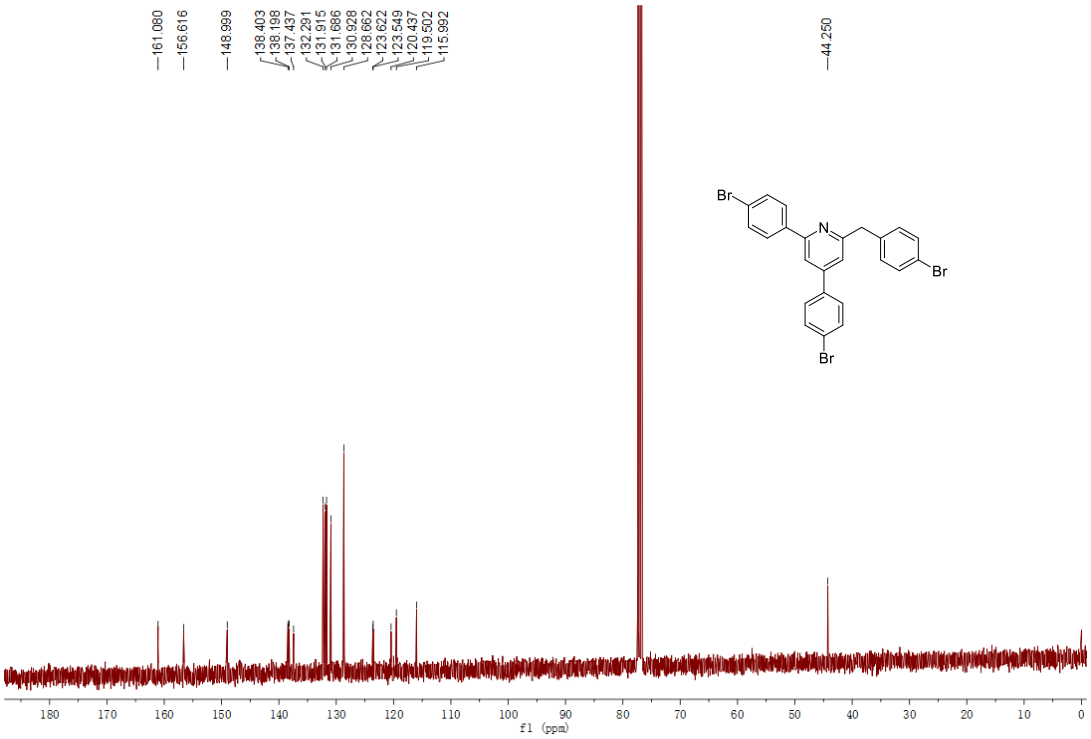

Figure 6.28 ^{13}C NMR spectrum of **5b**

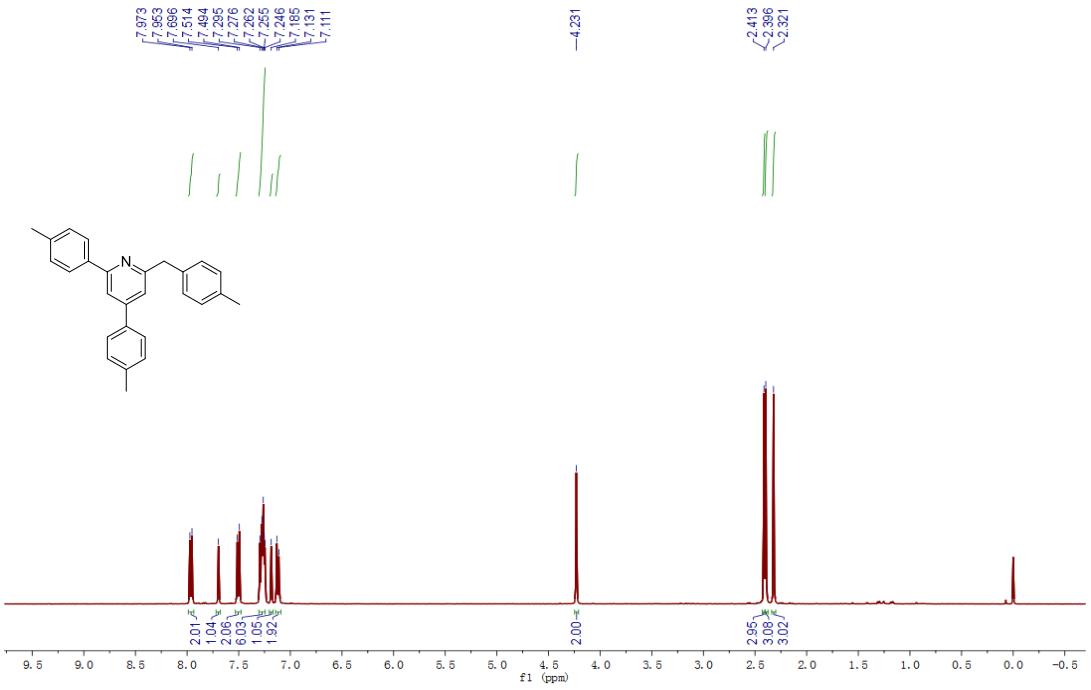

Figure 6.29 ^{1}H NMR spectrum of **5c**

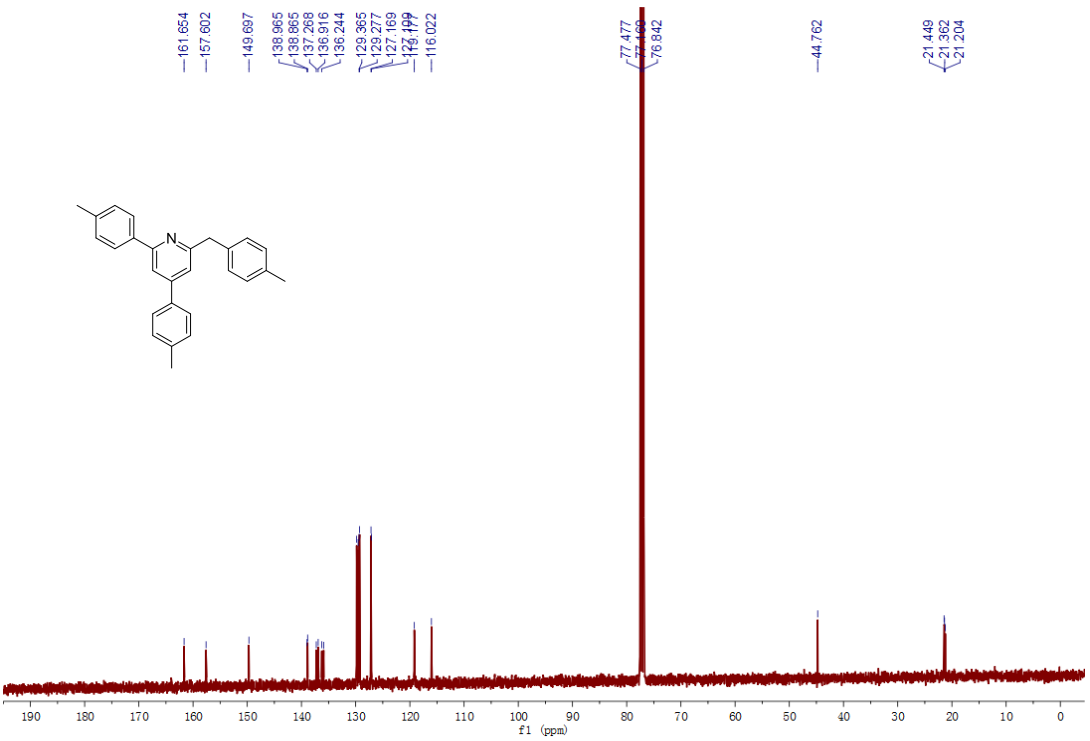

Figure 6.30 ^{13}C NMR spectrum of **5c**

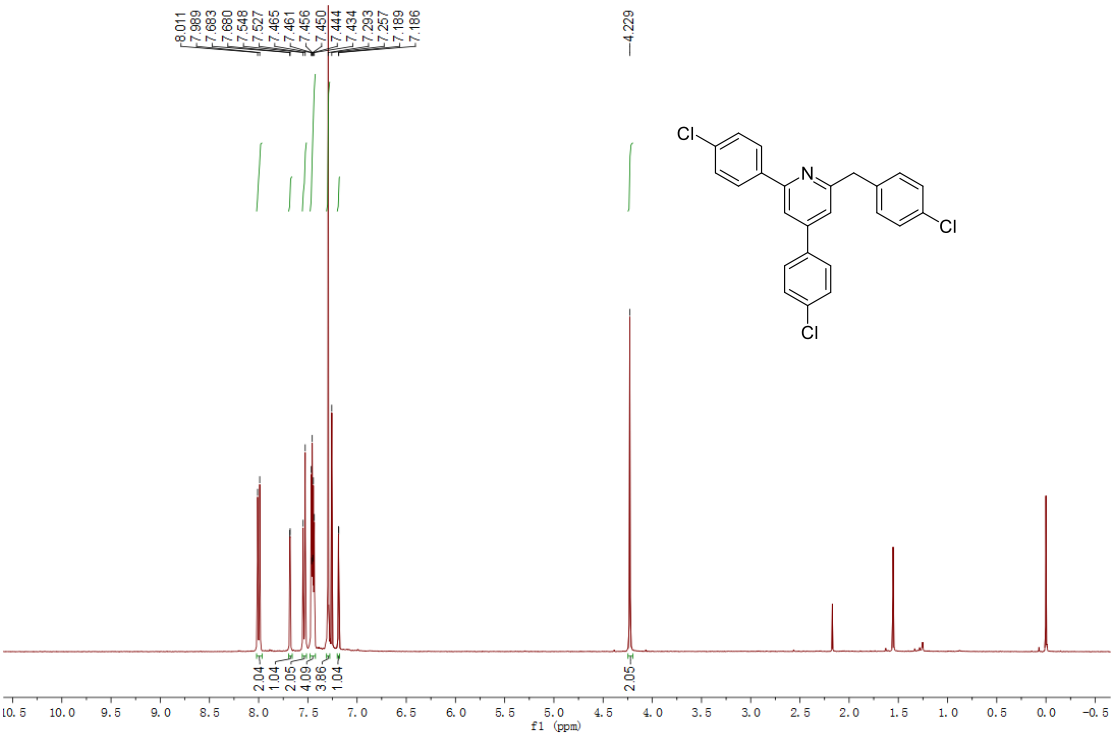

Figure 6.31 ^{1}H NMR spectrum of **5d**

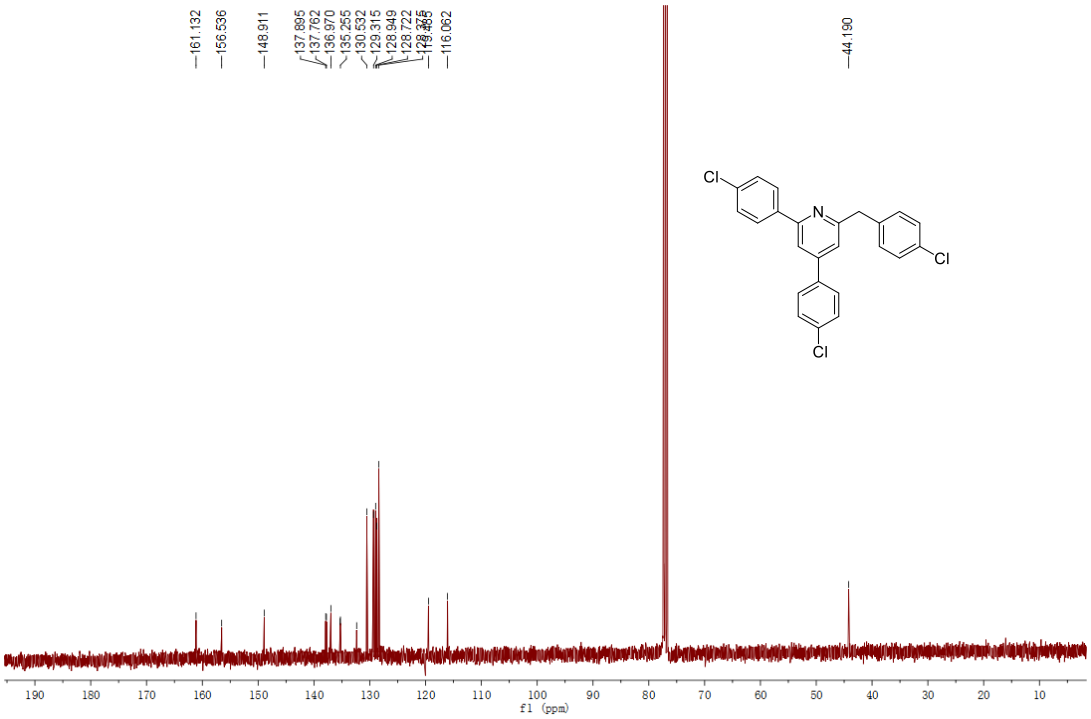

Figure 6.32 ^{13}C NMR spectrum of **5d**

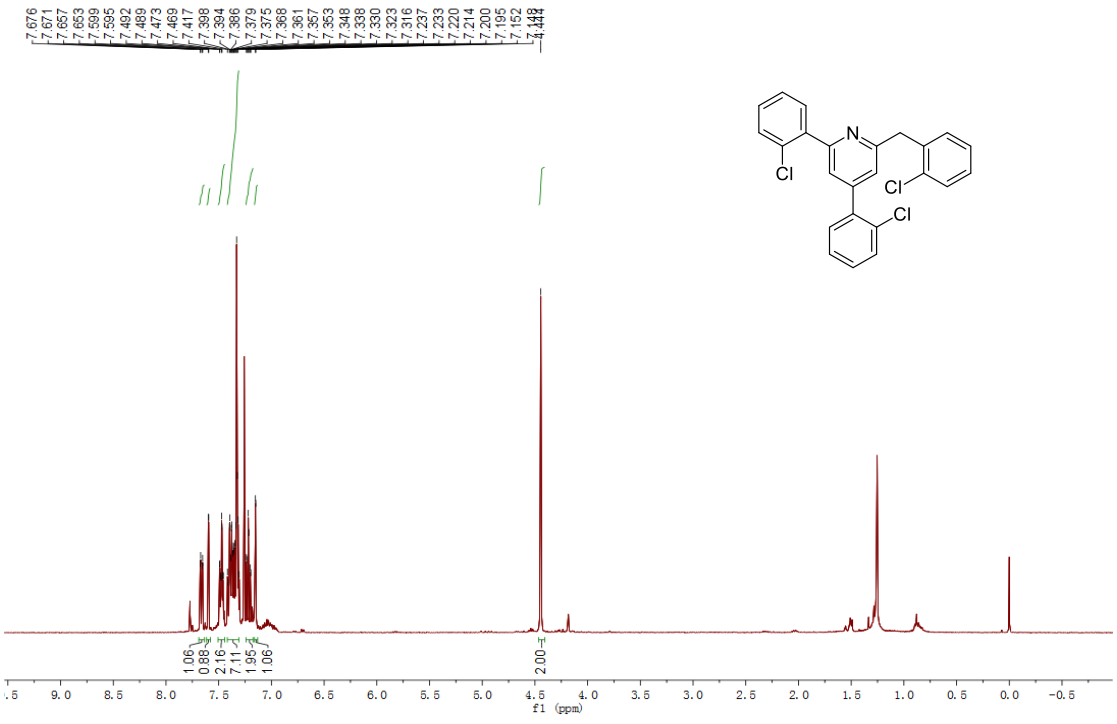

Figure 6.33 ^{1}H NMR spectrum of **5e**

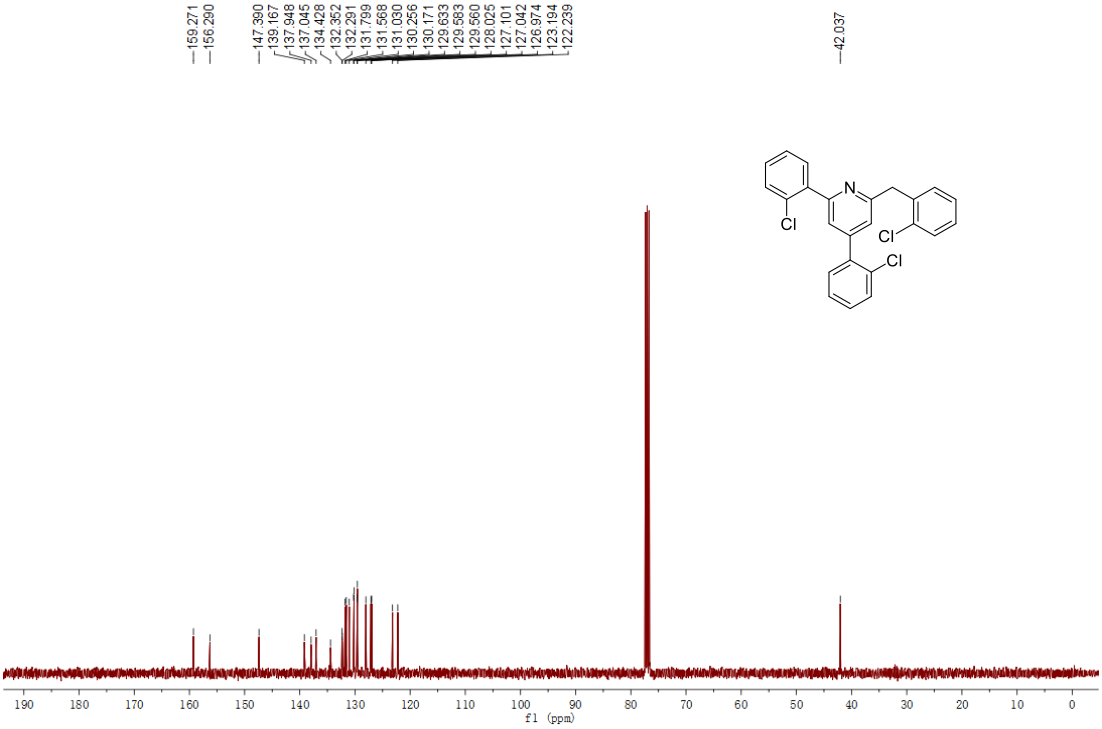

Figure 6.34 ^{13}C NMR spectrum of **5e**

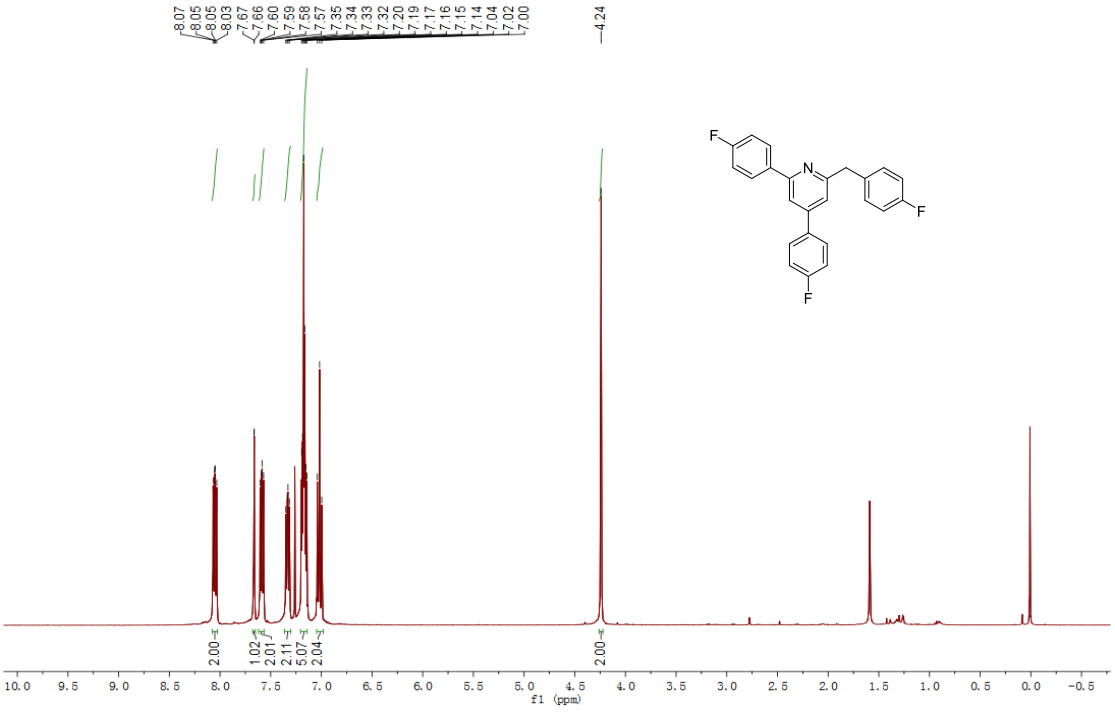

Figure 6.35 ^{1}H NMR spectrum of **5f**

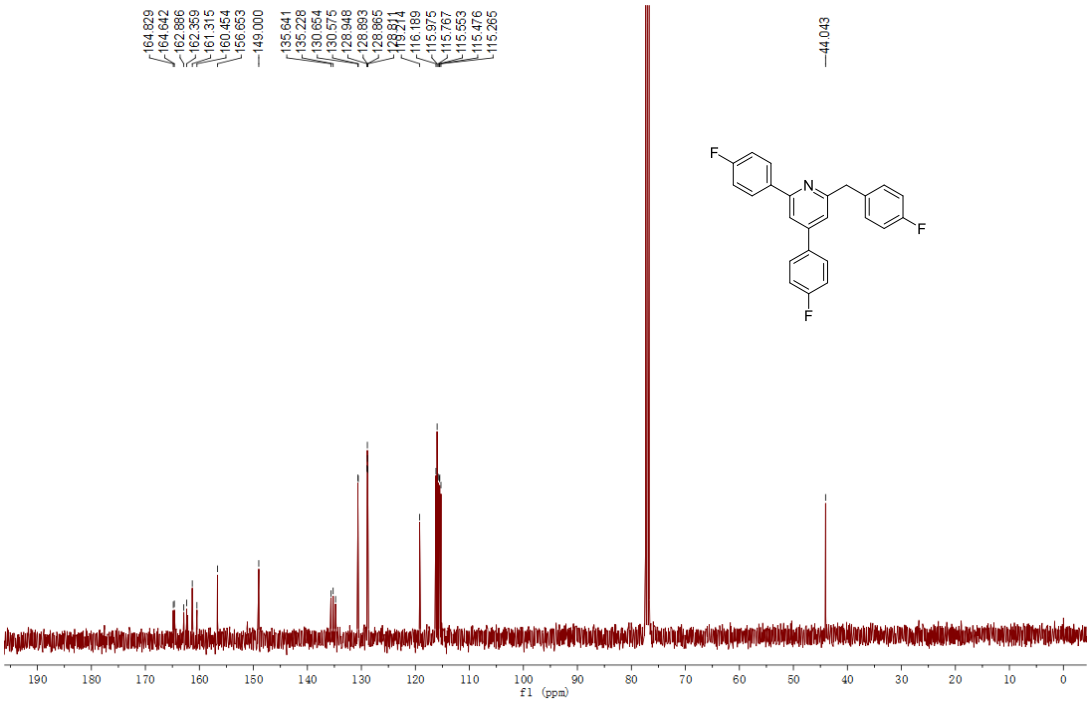

Figure 6.36 ^{13}C NMR spectrum of **5f**

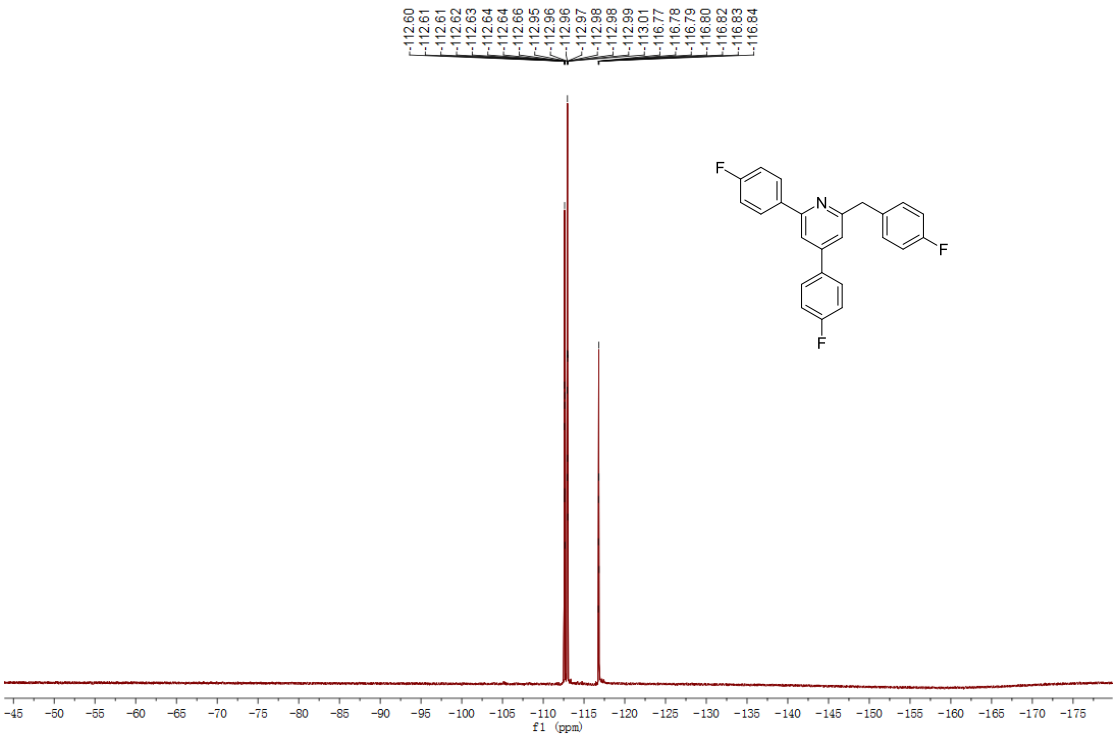

Figure 6.37 ^{19}F NMR spectrum of **5f**

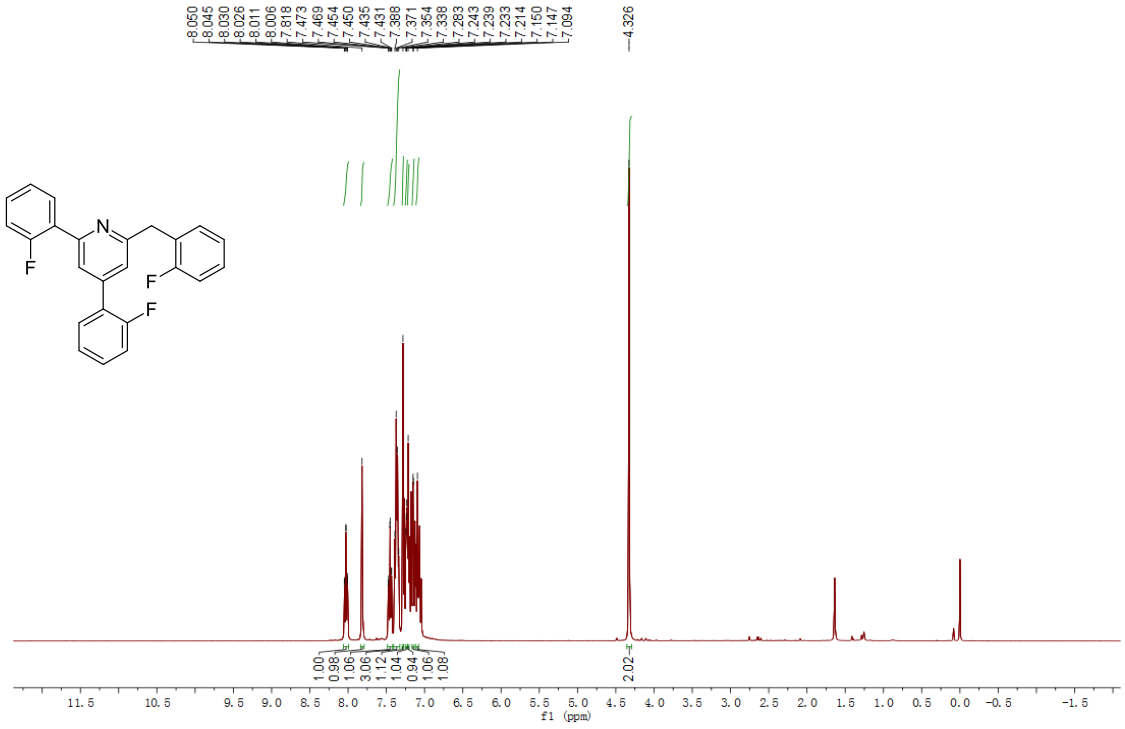

Figure 6.38 ^{1}H NMR spectrum of **5g**

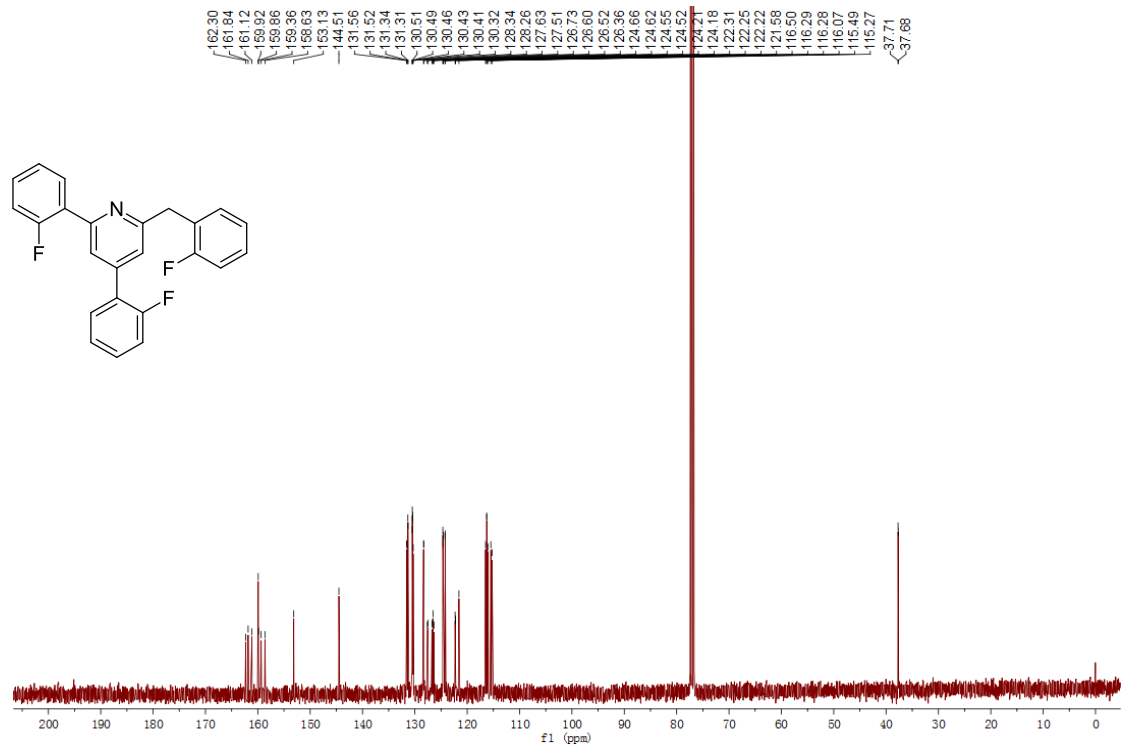

Figure 6.39 ^{13}C NMR spectrum of **5g**

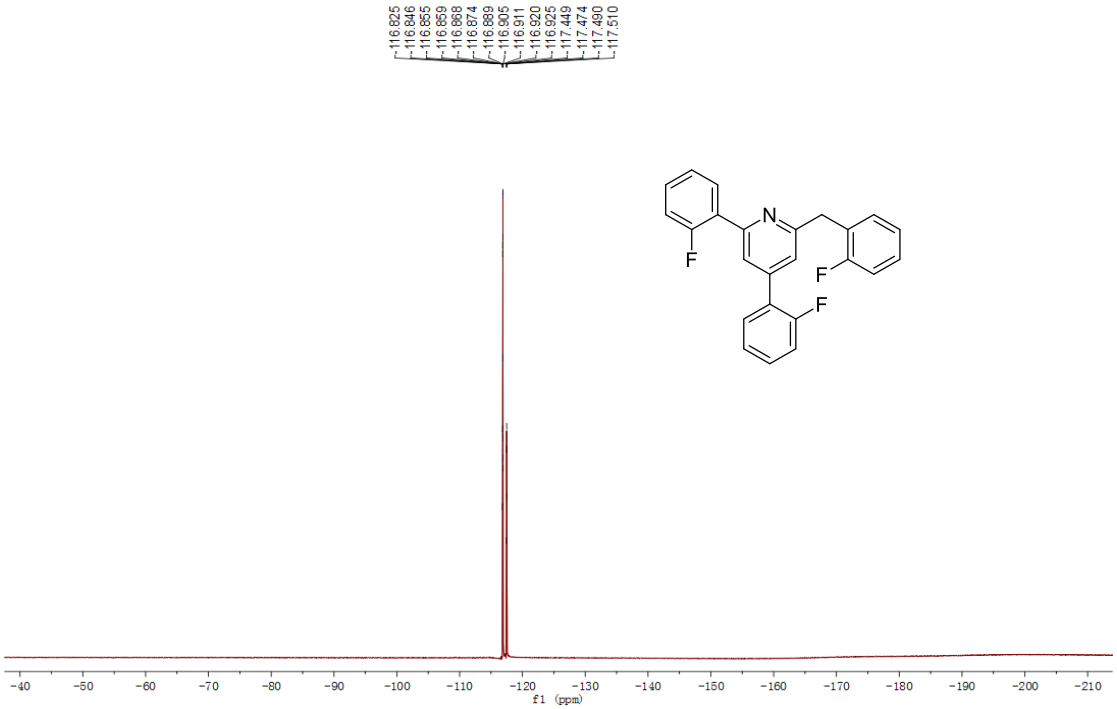

Figure 6.40 ^{19}F NMR spectrum of **5g**

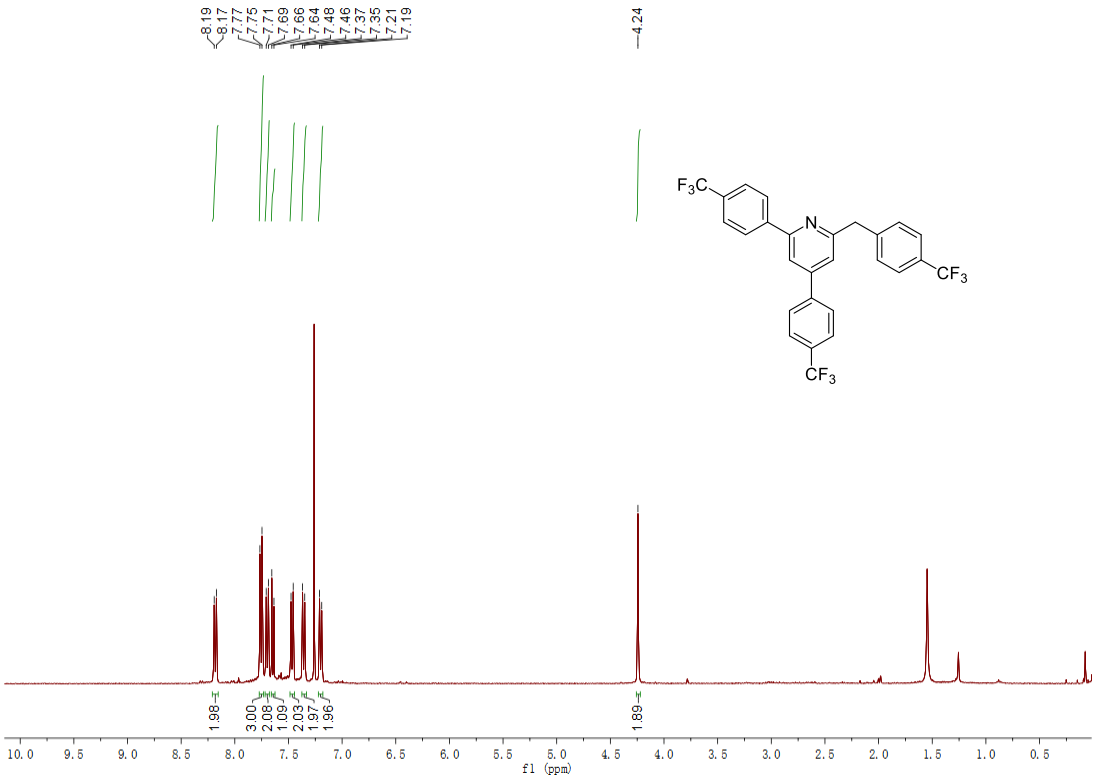

Figure 6.41 ^{1}H NMR spectrum of **5h**

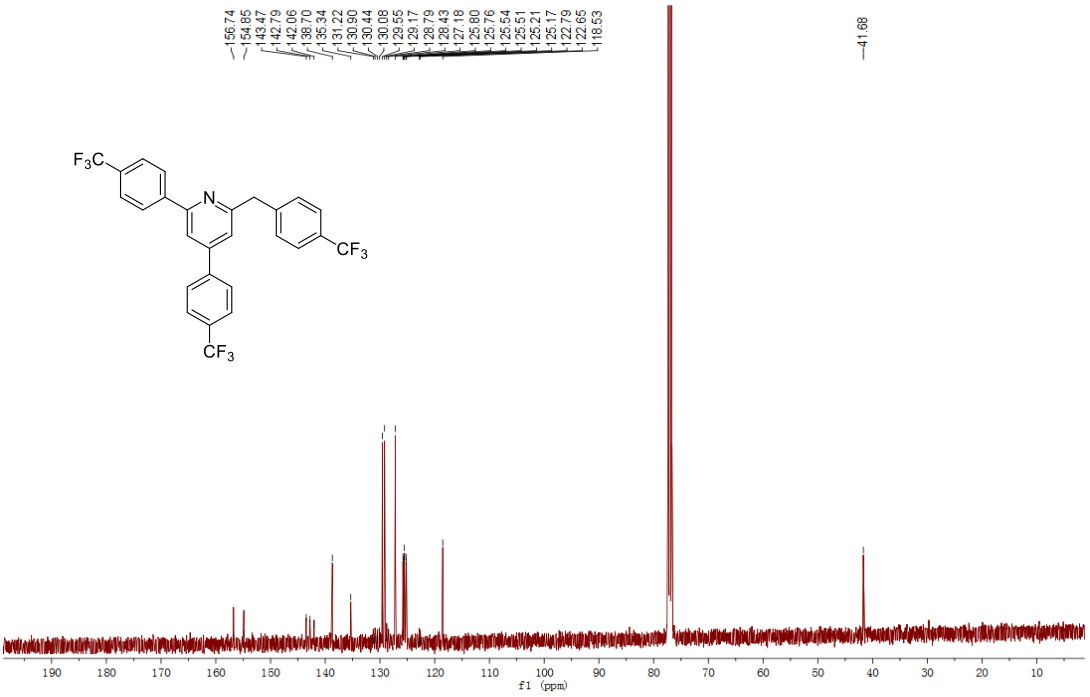

Figure 6.42 ^{13}C NMR spectrum of **5h**

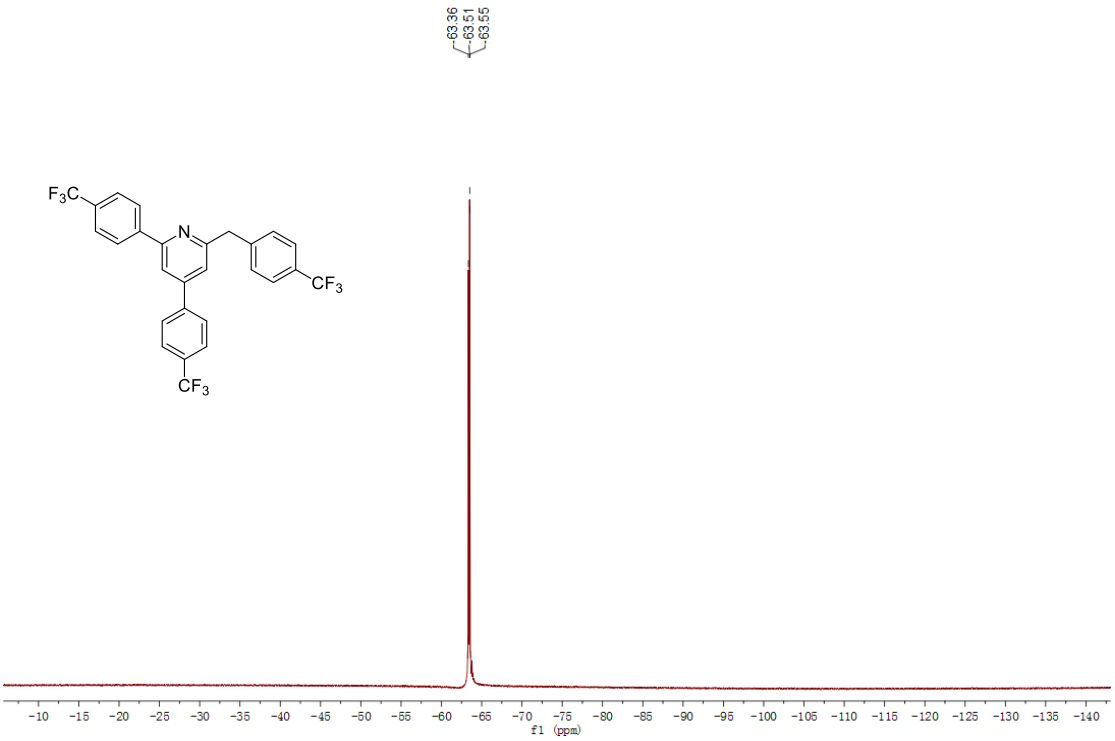

Figure 6.43 ^{19}F NMR spectrum of **5h**

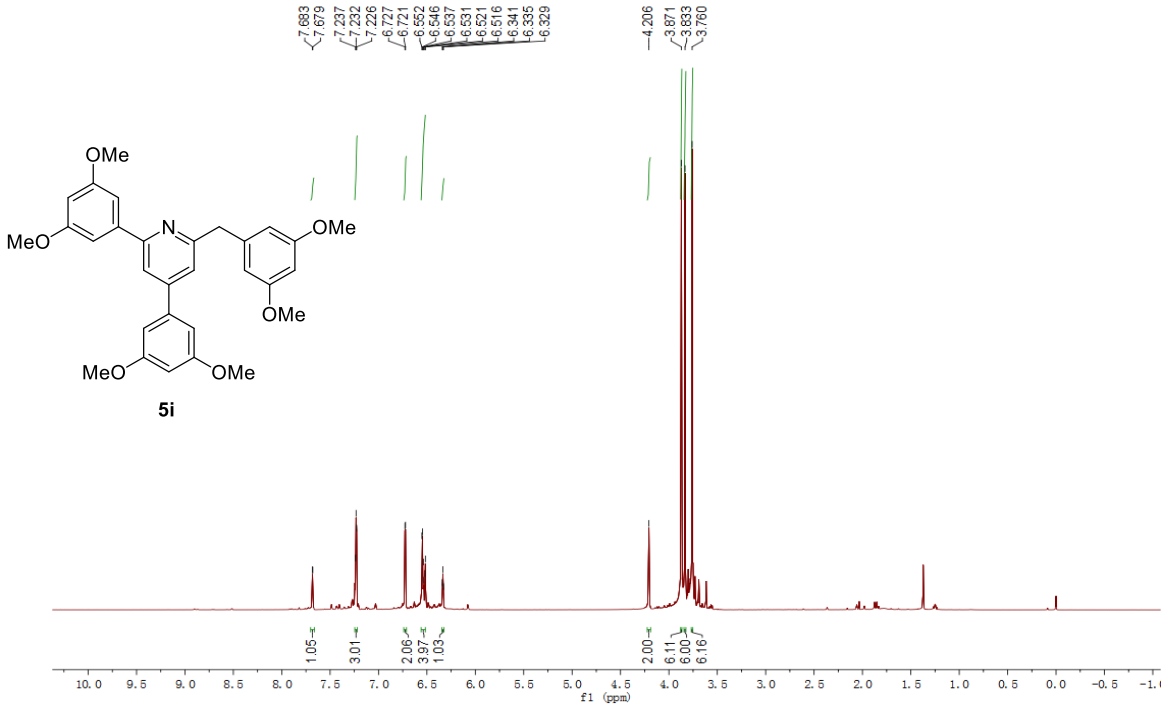

Figure 6.44 ^{1}H NMR spectrum of **5i**

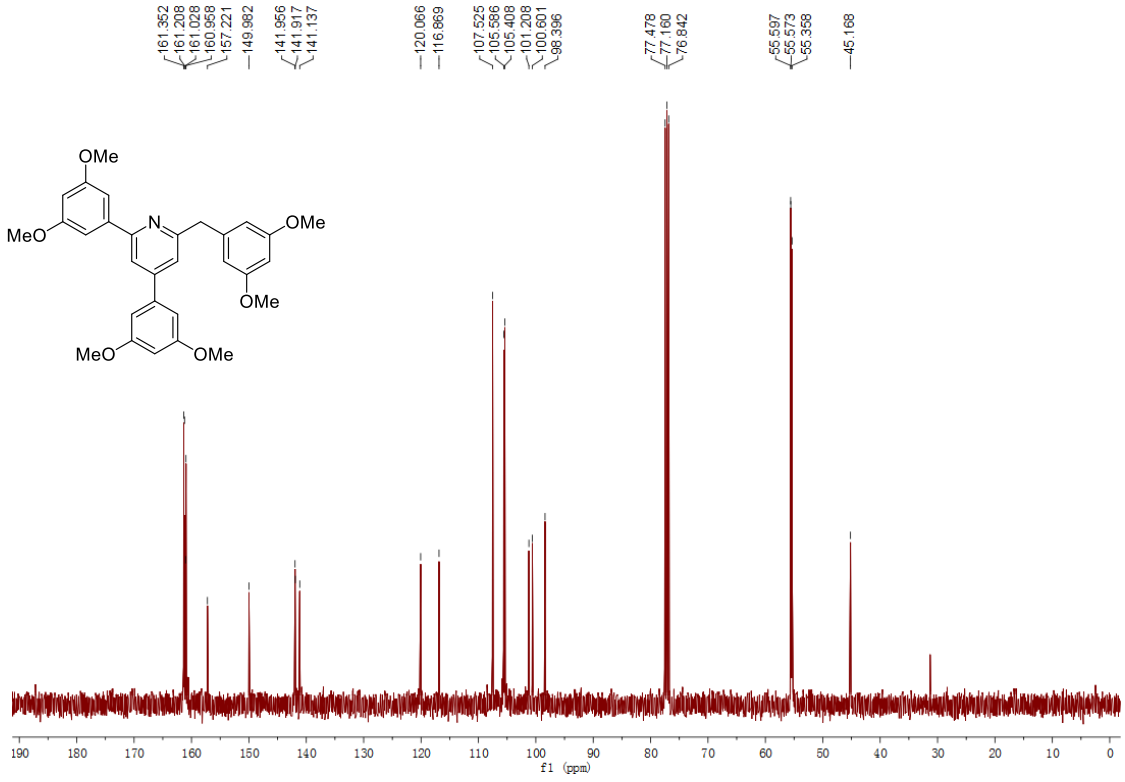

Figure 6.45 ^{13}C NMR spectrum of **5i**

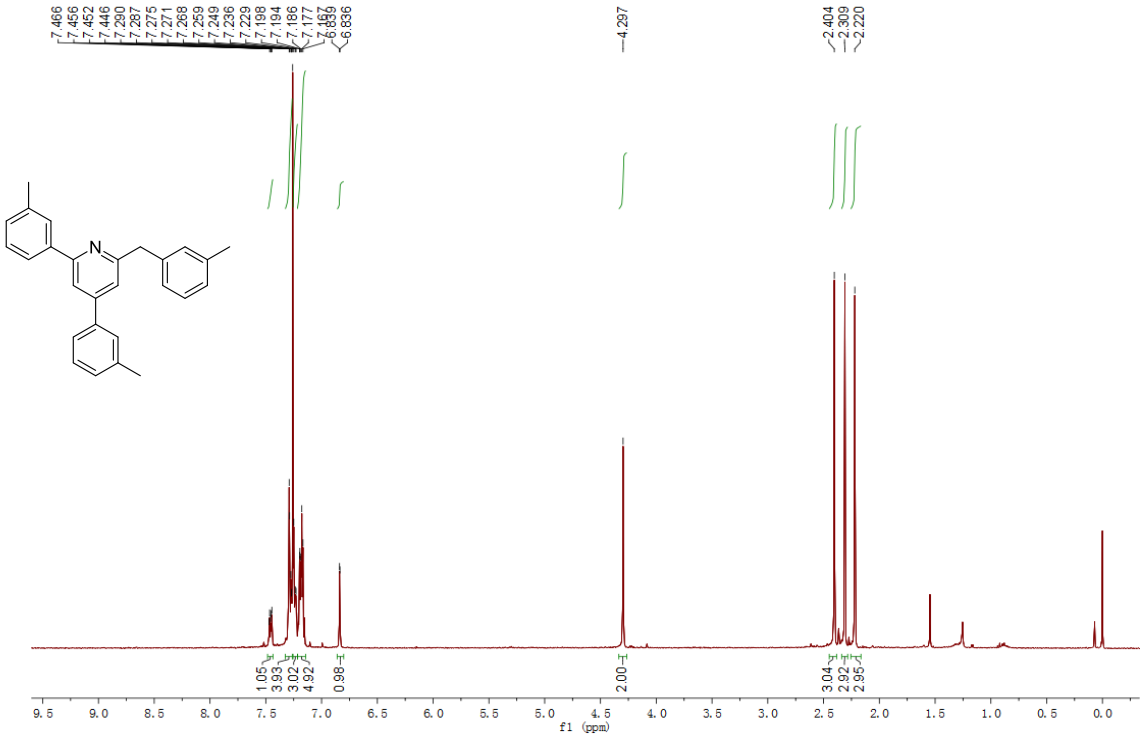

Figure 6.46 ^{1}H NMR spectrum of **5j**

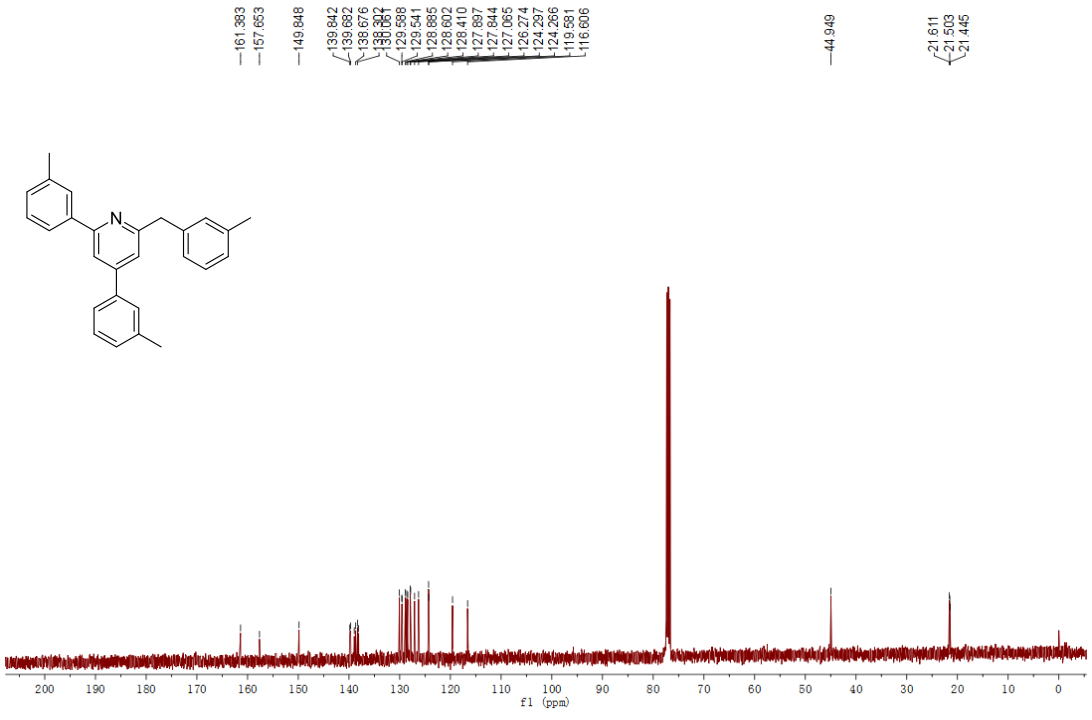

Figure 6.47 ^{13}C NMR spectrum of **5j**

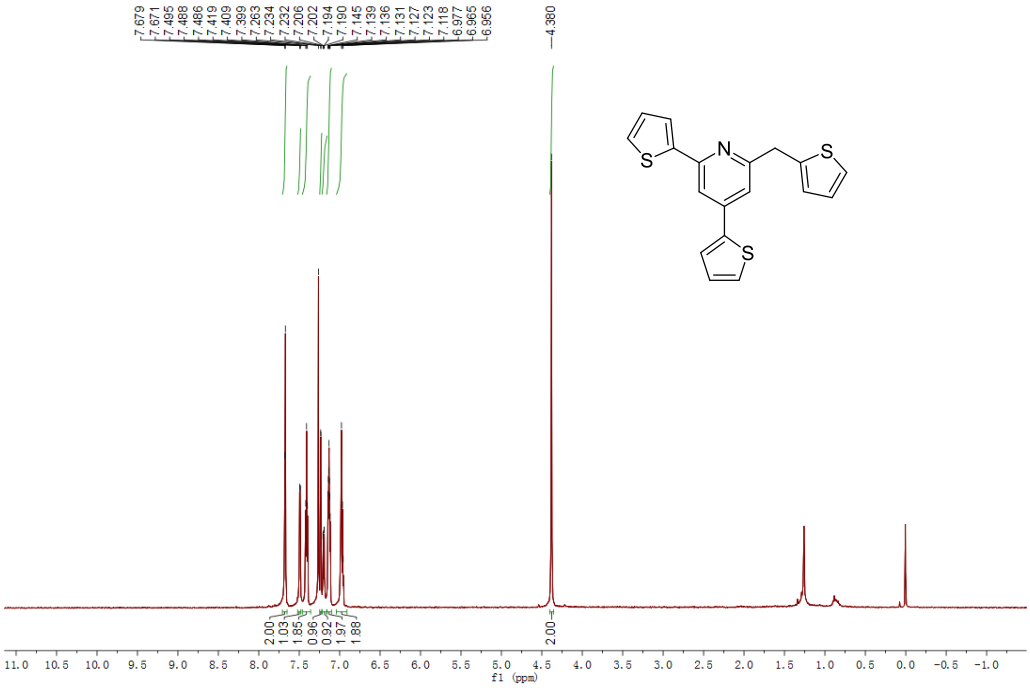

Figure 6.48 ^{1}H NMR spectrum of **5k**

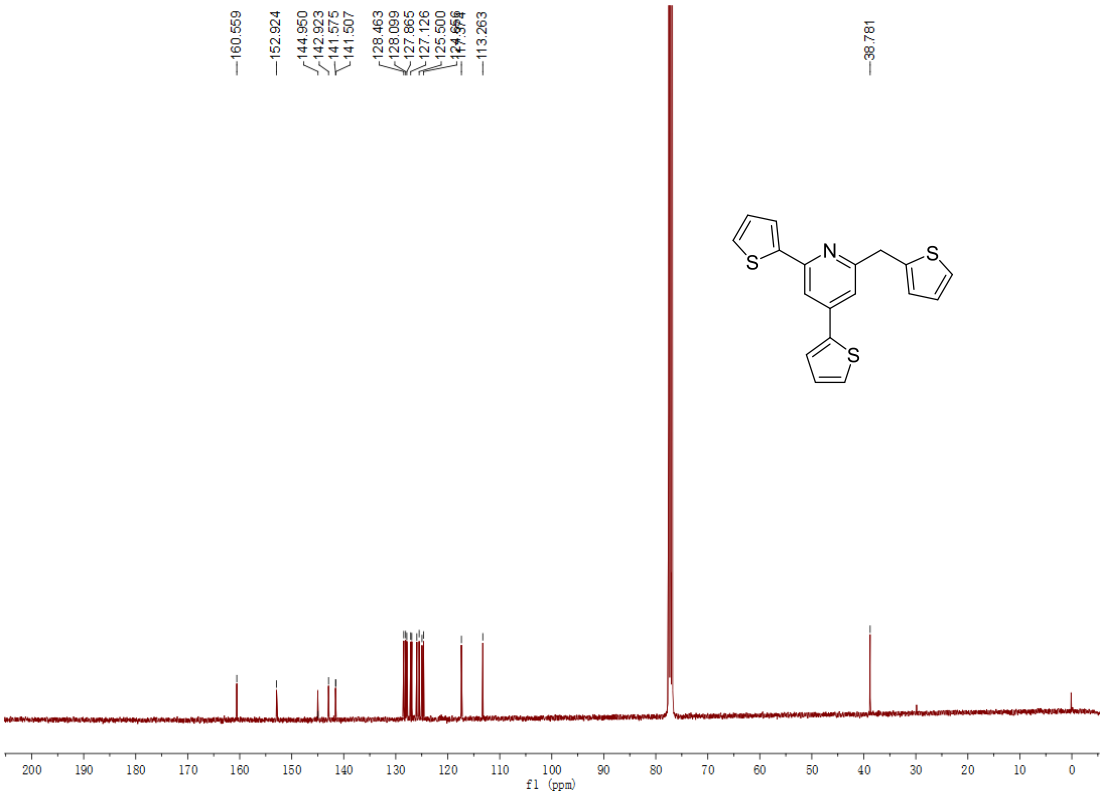

Figure 6.49 ^{13}C NMR spectrum of **5k**

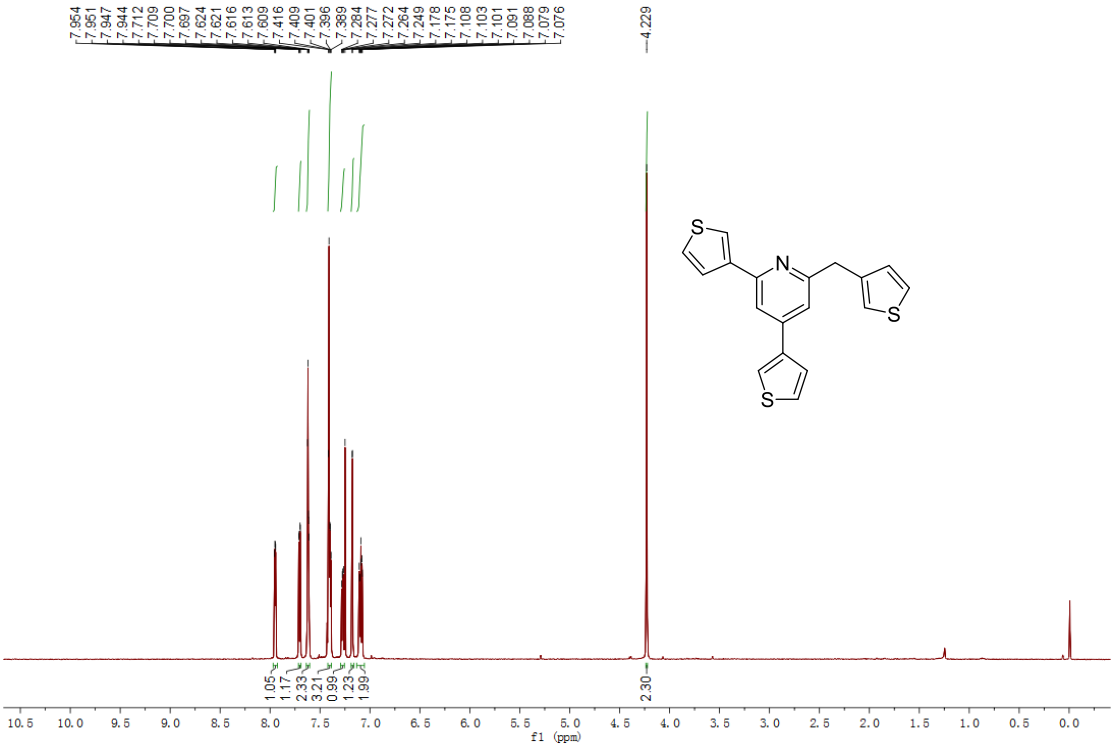

Figure 6.50 ^{1}H NMR spectrum of **5l**

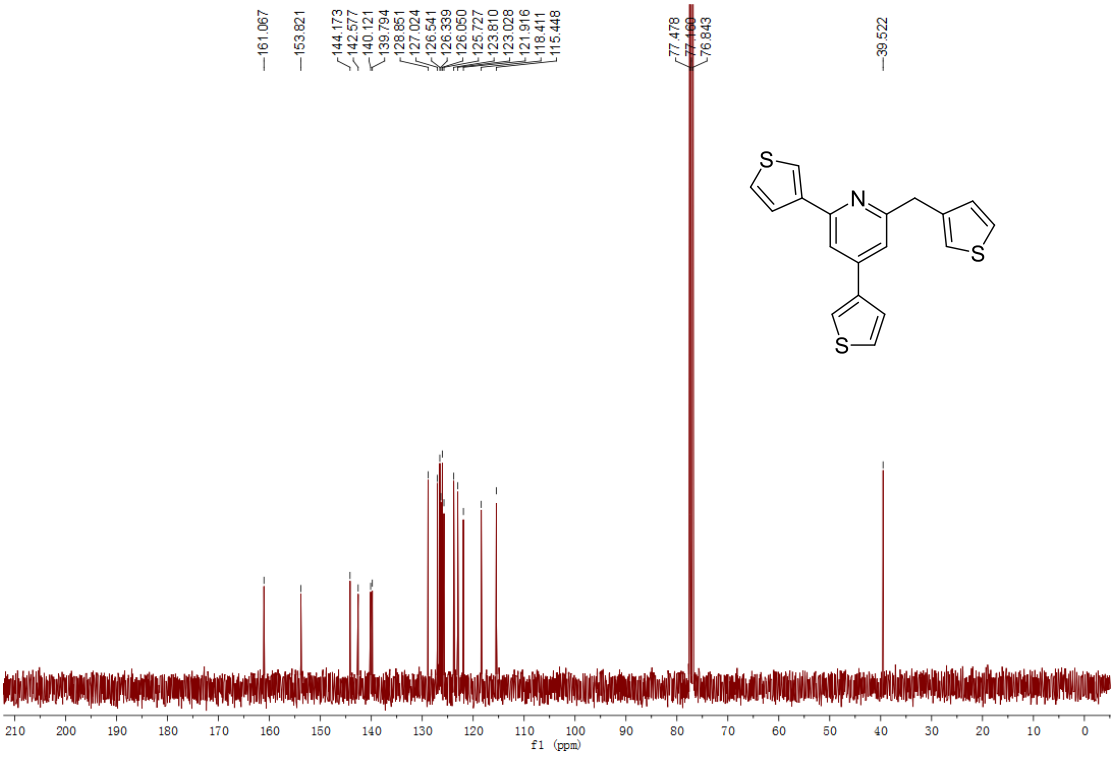

Figure 6.51 ^{13}C NMR spectrum of **5l**

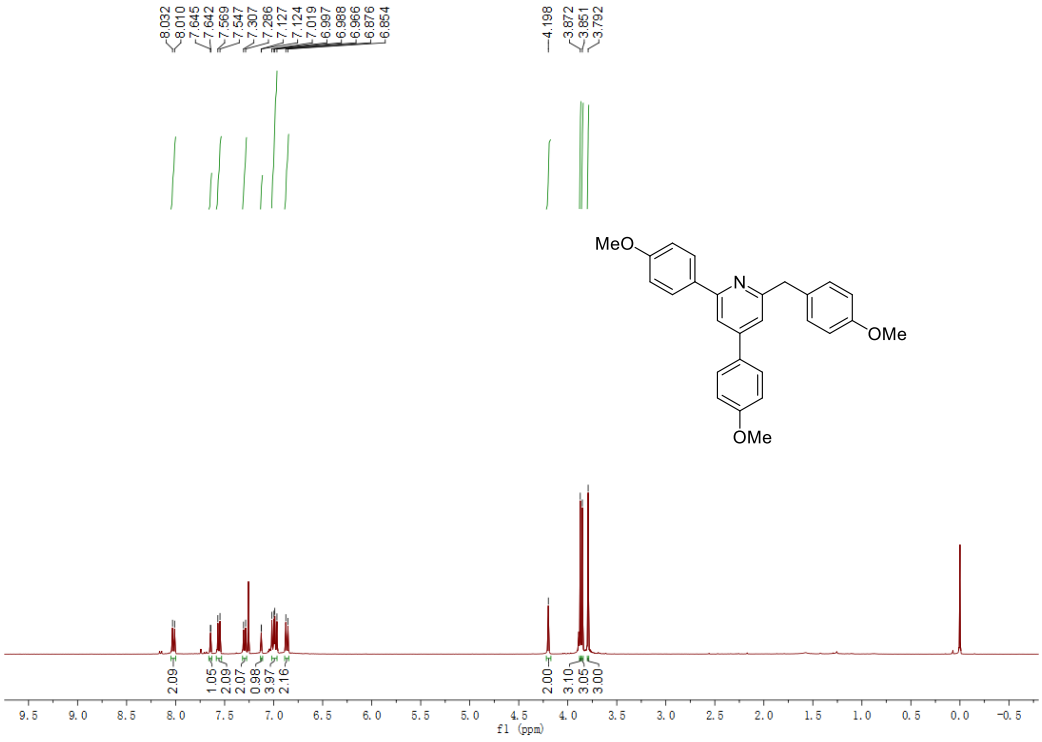

Figure 6.52 ^{1}H NMR spectrum of **5m**

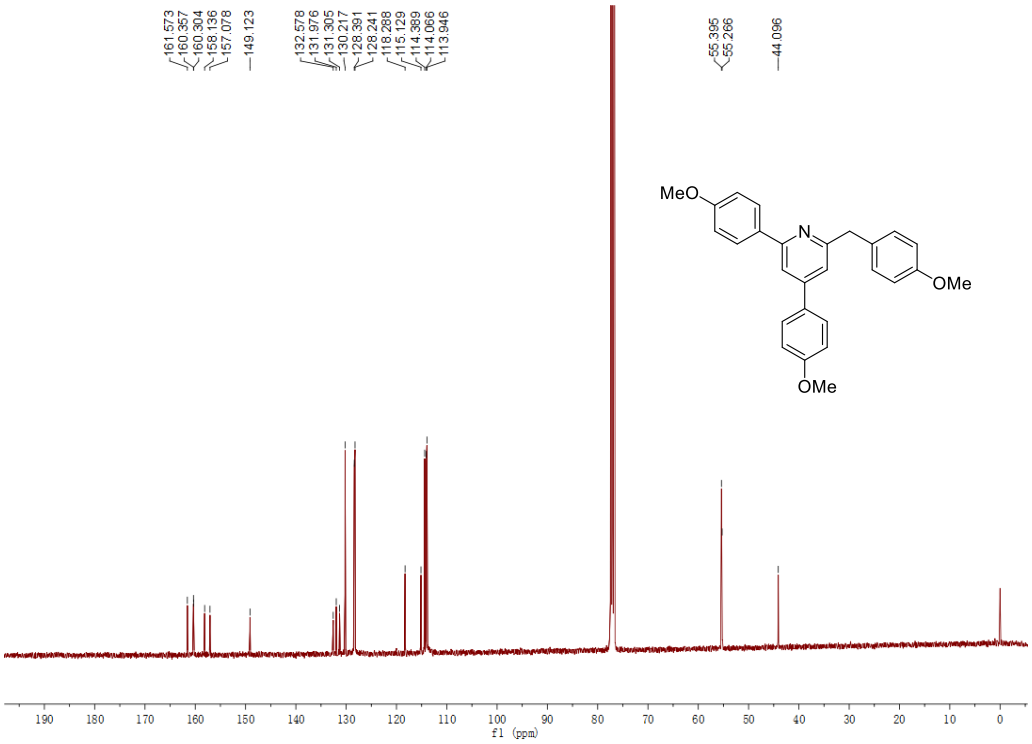

Figure 6.53 ^{13}C NMR spectrum of **5m**

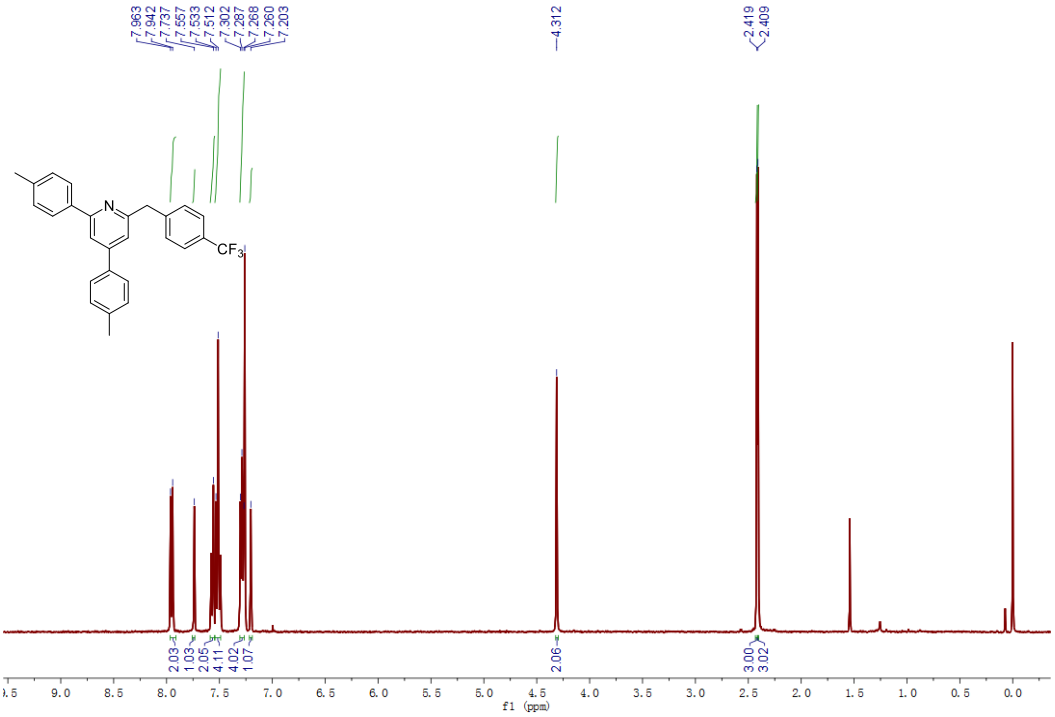

Figure 6.54 ^{1}H NMR spectrum of **16a**

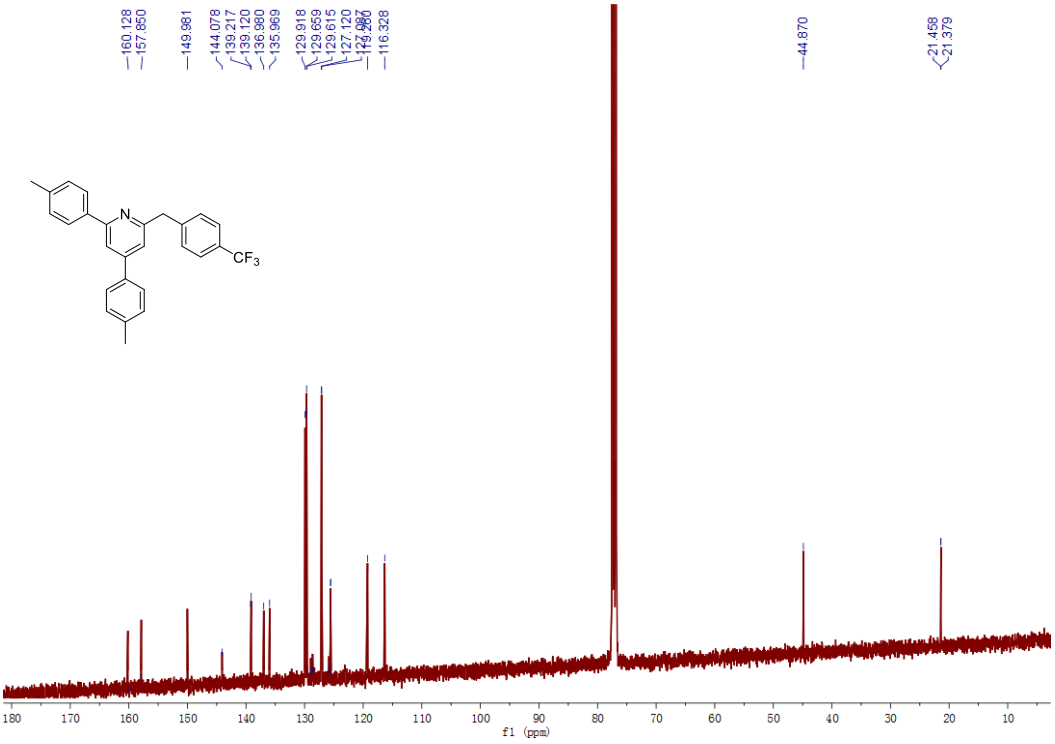

Figure 6.55 ^{13}C NMR spectrum of **16a**

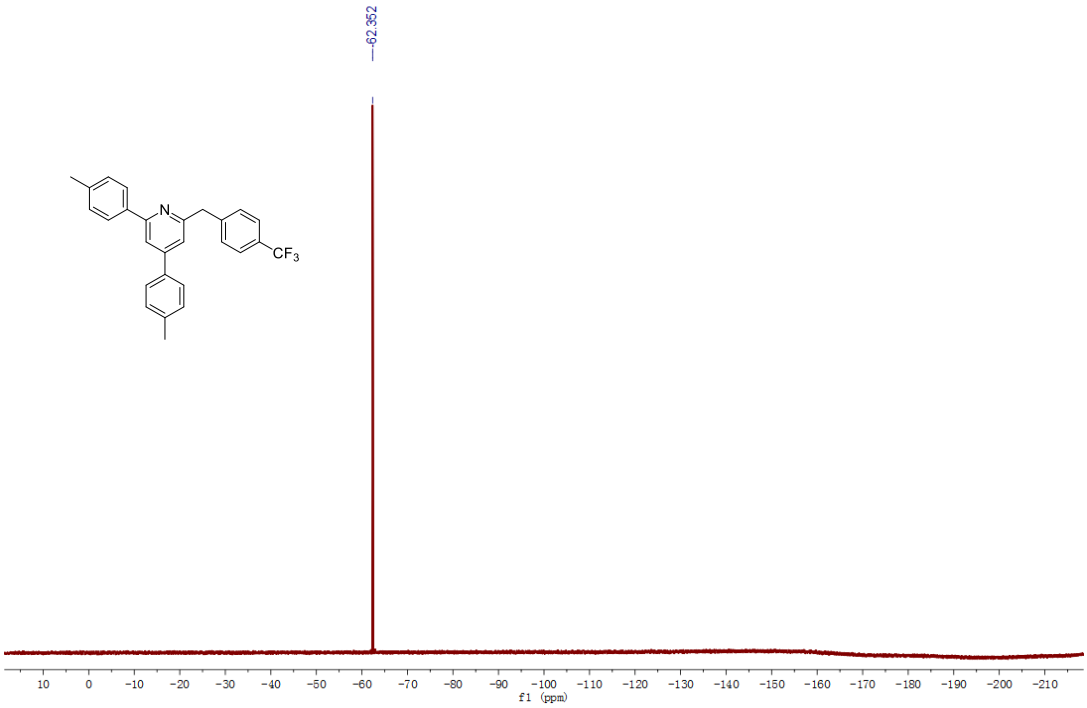

Figure 6.56 ^{19}F NMR spectrum of **16a**

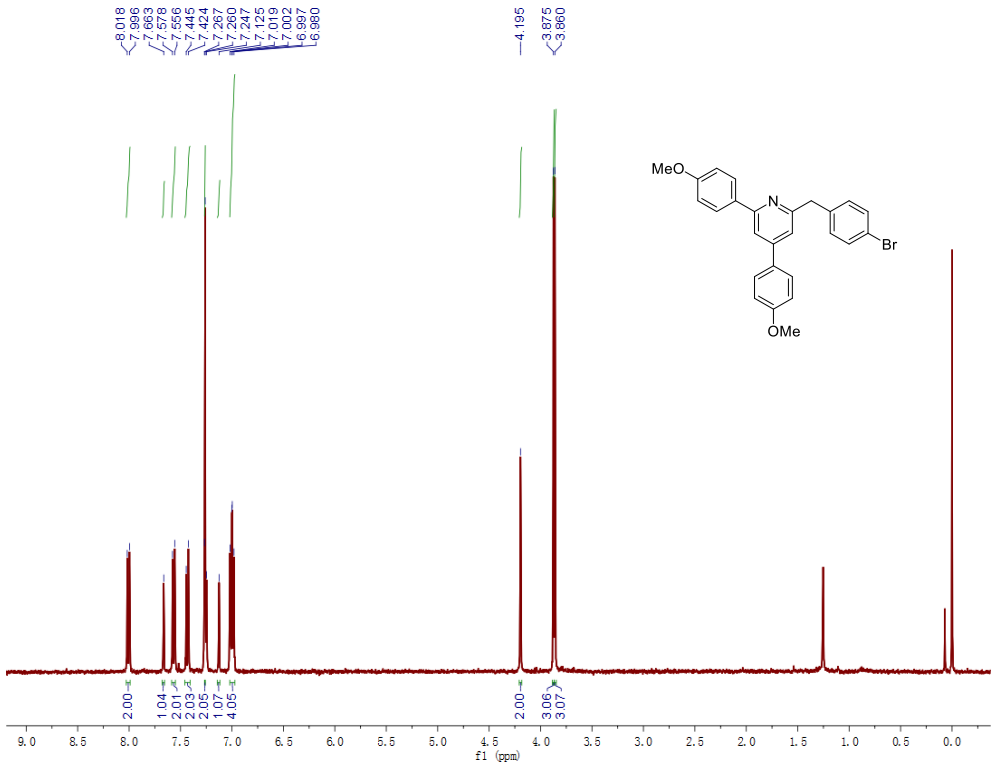

Figure 6.57 ^{1}H NMR spectrum of **16b**

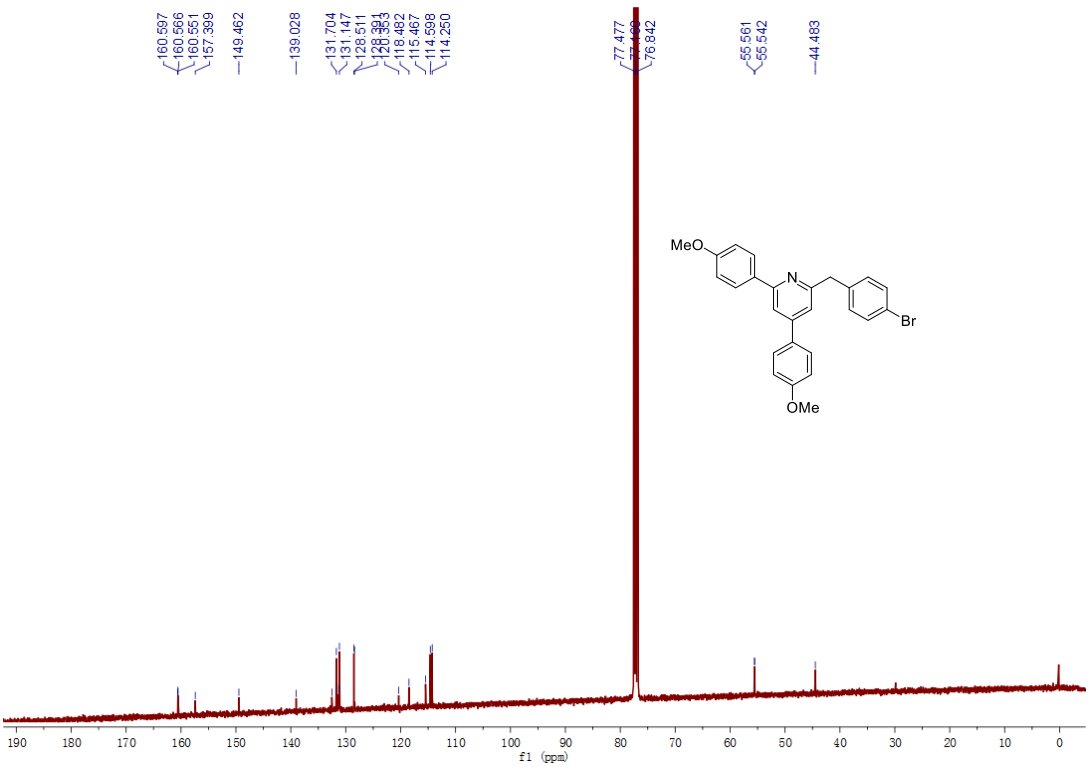

Figure 6.58 ^{13}C NMR spectrum of **16b**

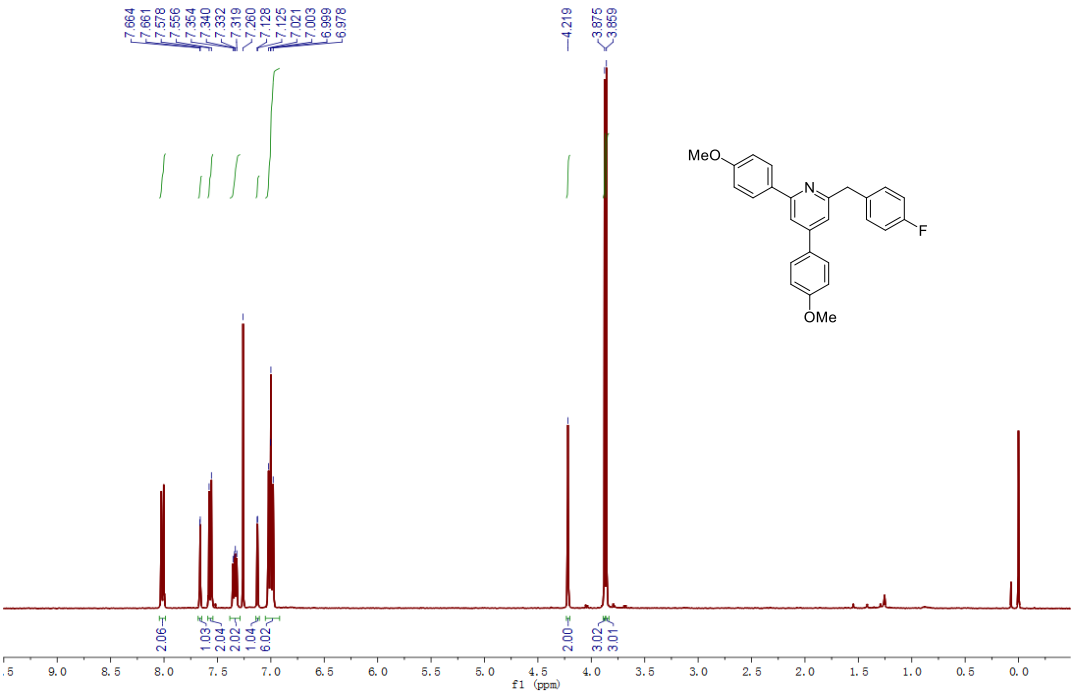

Figure 6.59 ^{1}H NMR spectrum of **16c**

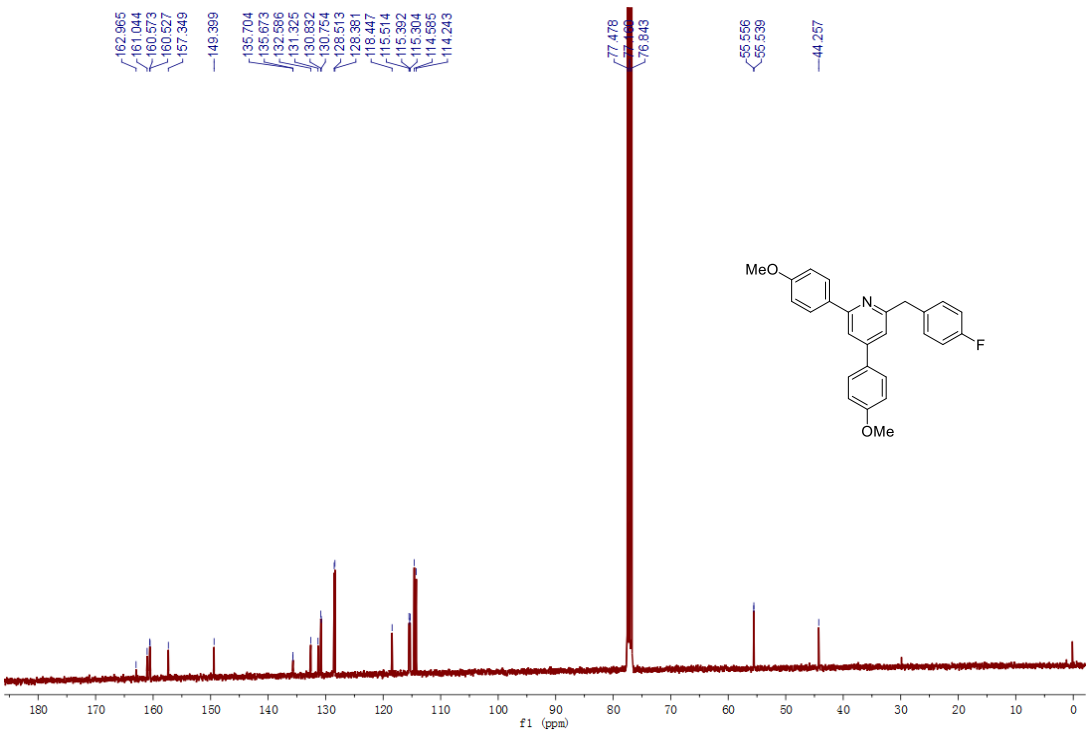

Figure 6.60 ^{13}C NMR spectrum of **16c**

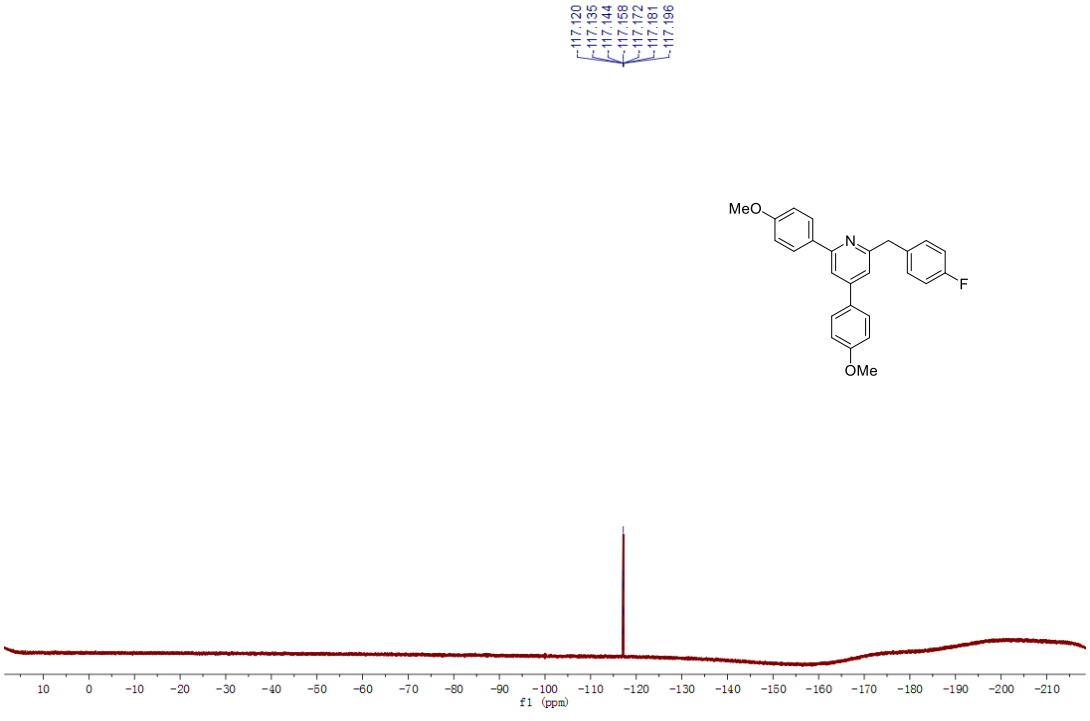

Figure 6.61 ^{19}F NMR spectrum of **16c**

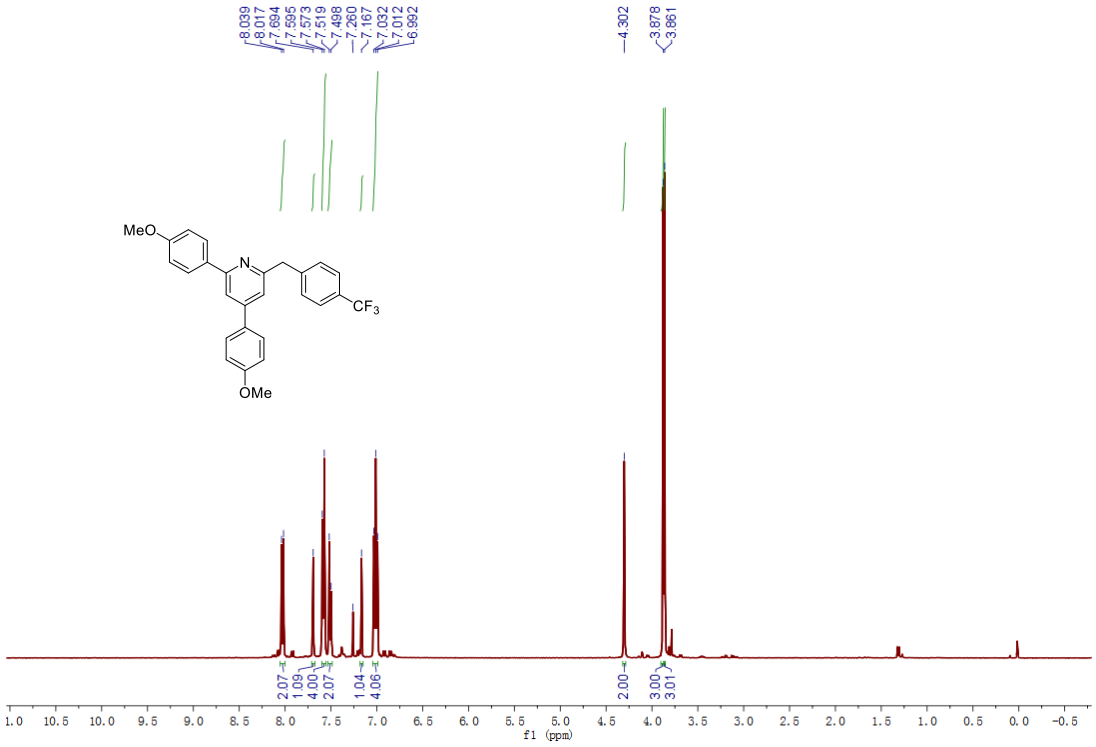

Figure 6.62 ^{1}H NMR spectrum of **16d**

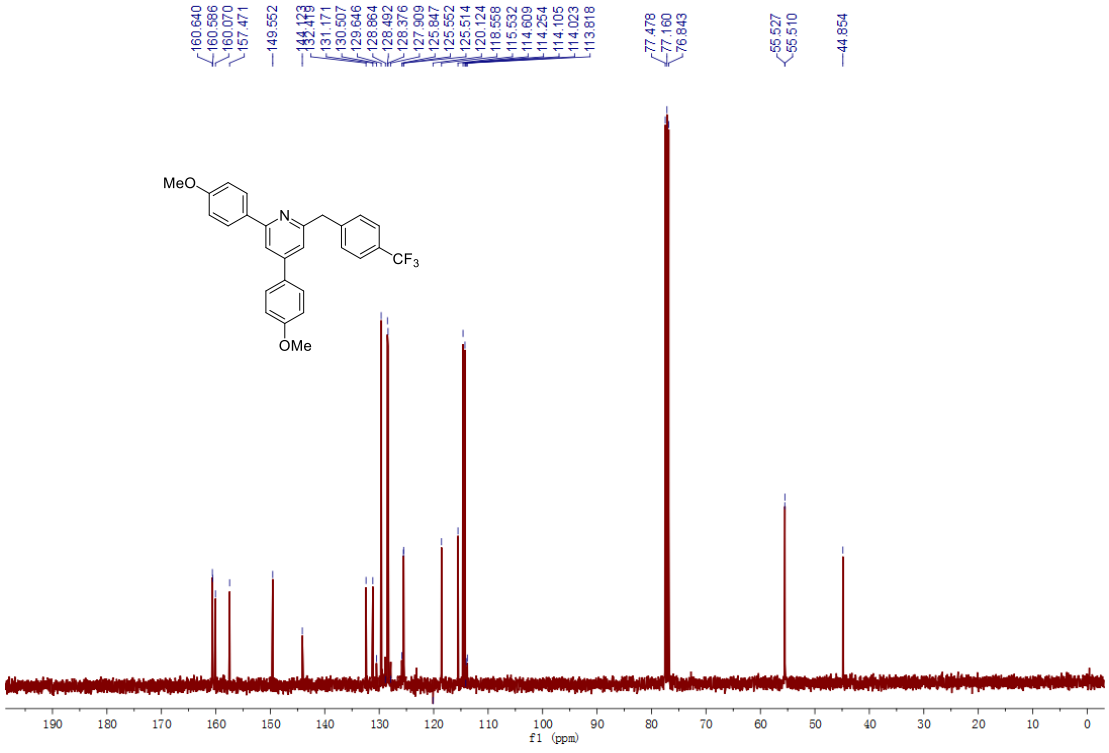

Figure 6.63 ^{13}C NMR spectrum of **16d**

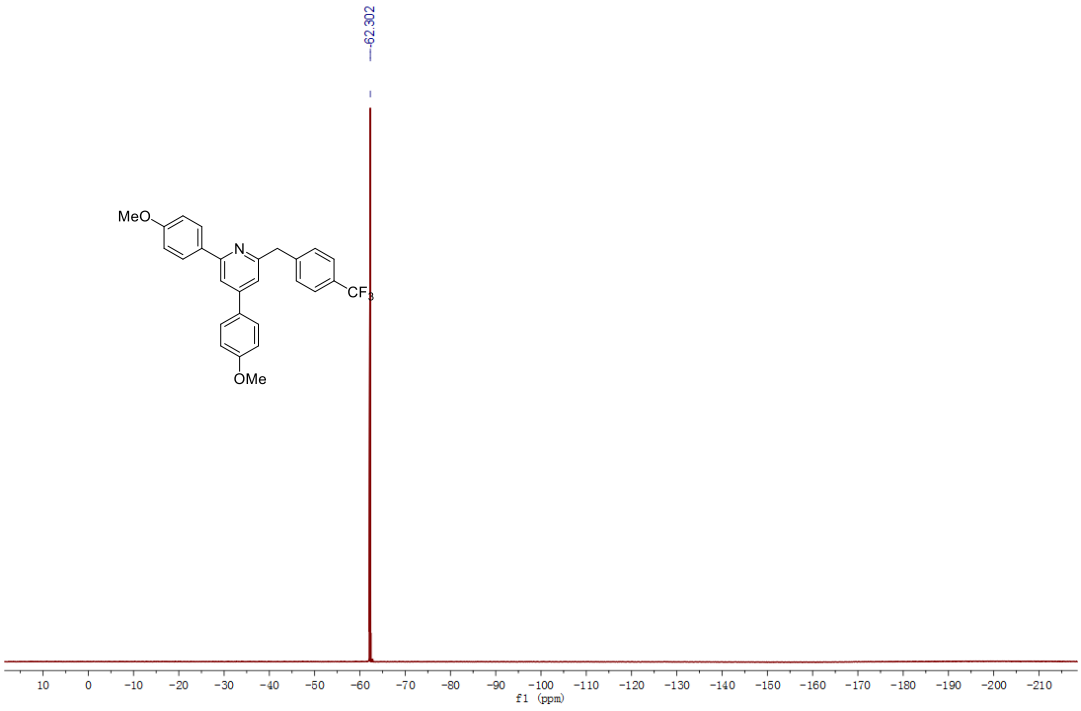

Figure 6.64 ^{19}F NMR spectrum of **16d**

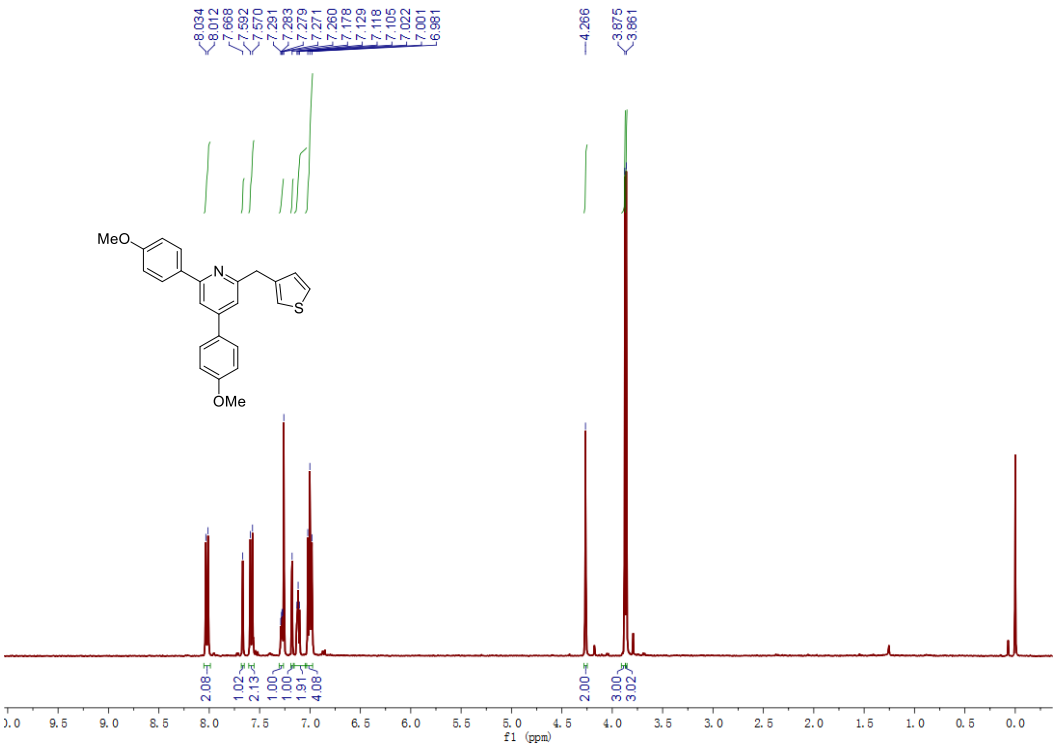

Figure 6.65 ^{1}H NMR spectrum of **16e**

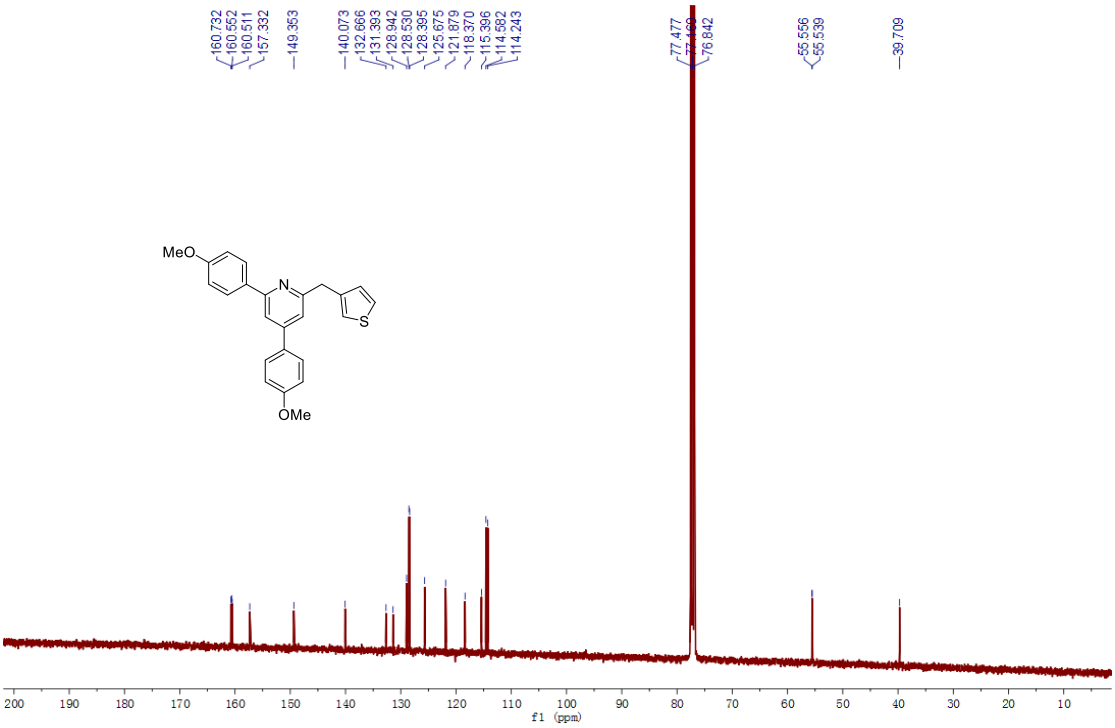

Figure 6.66 ^{13}C NMR spectrum of **16e**

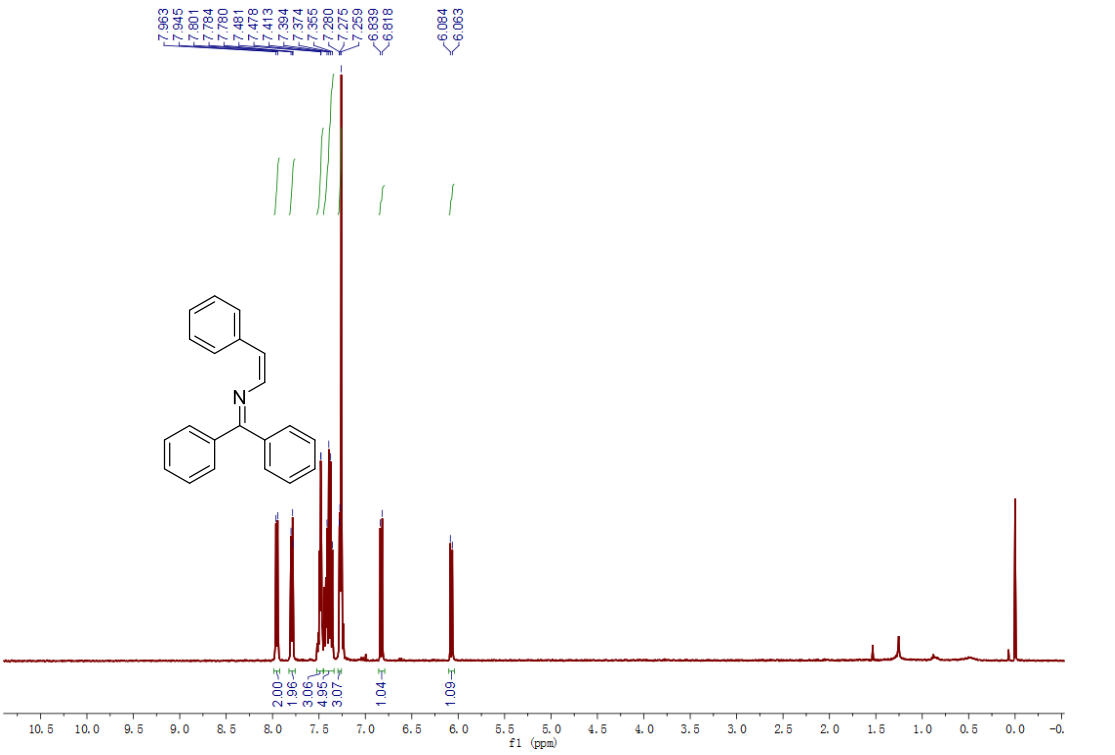

Figure 6.67 ^{1}H NMR spectrum of **18a**

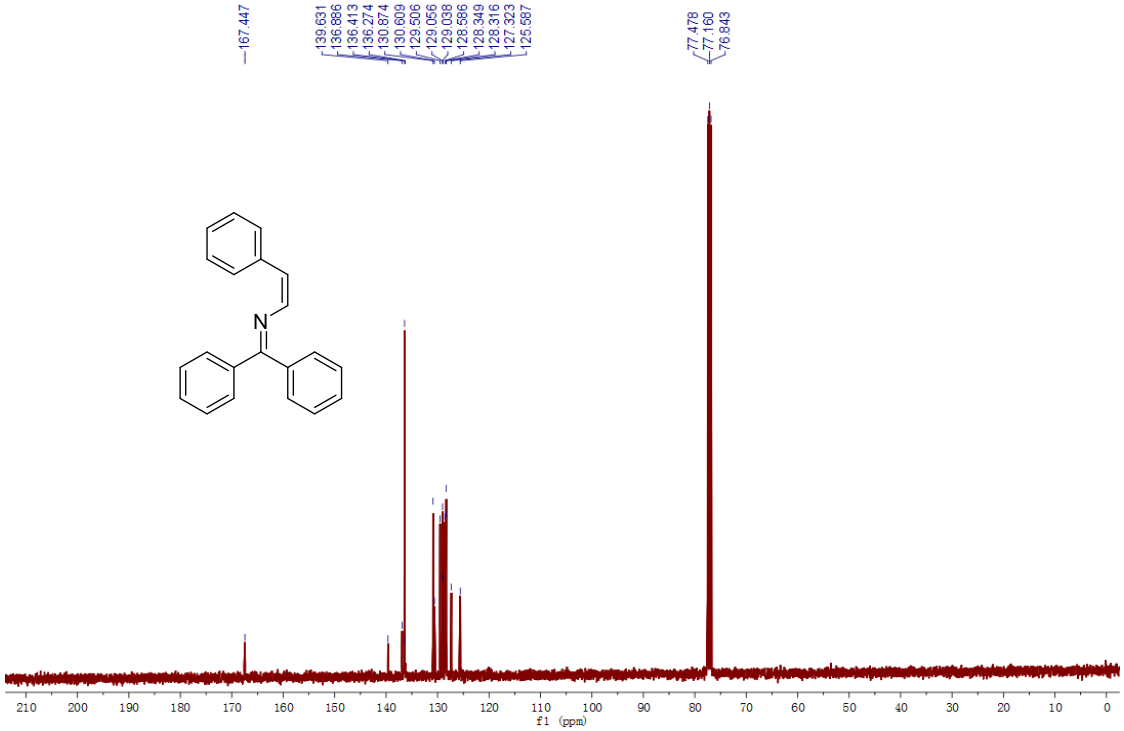

Figure 6.68 ^{13}C NMR spectrum of **18a**

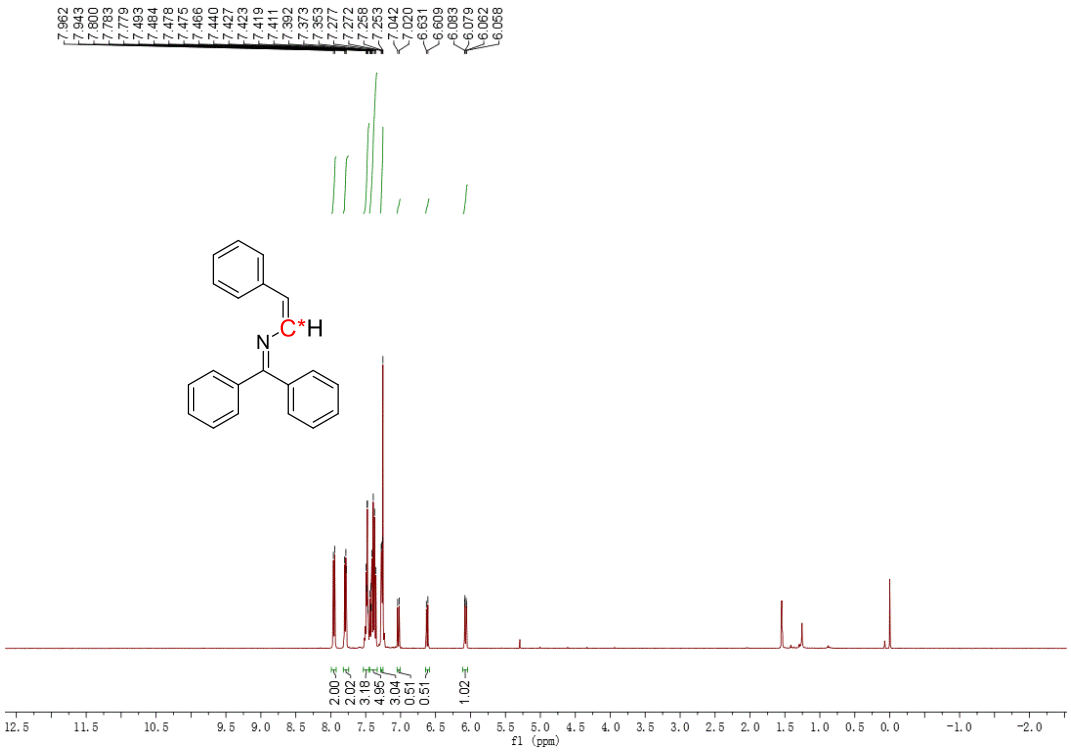

Figure 6.69 ^{1}H NMR spectrum of **18a***

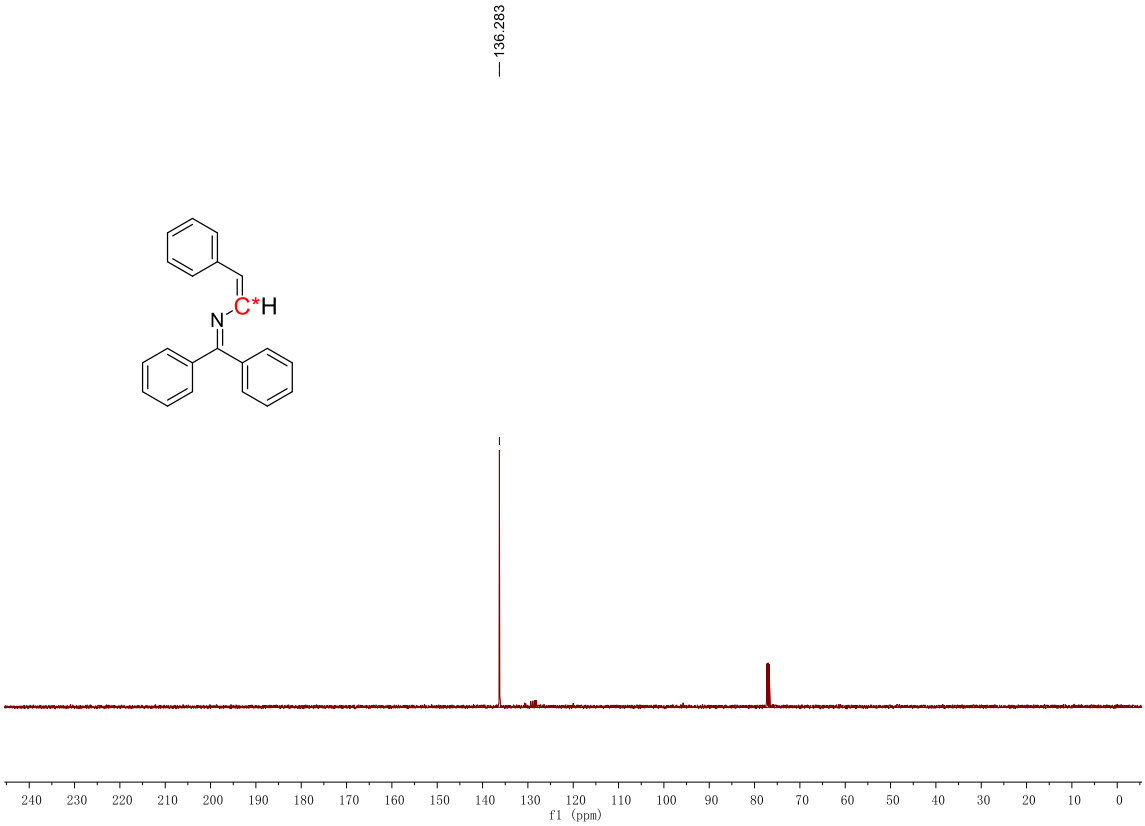

Figure 6.70 ^{13}C NMR spectrum of **18a***

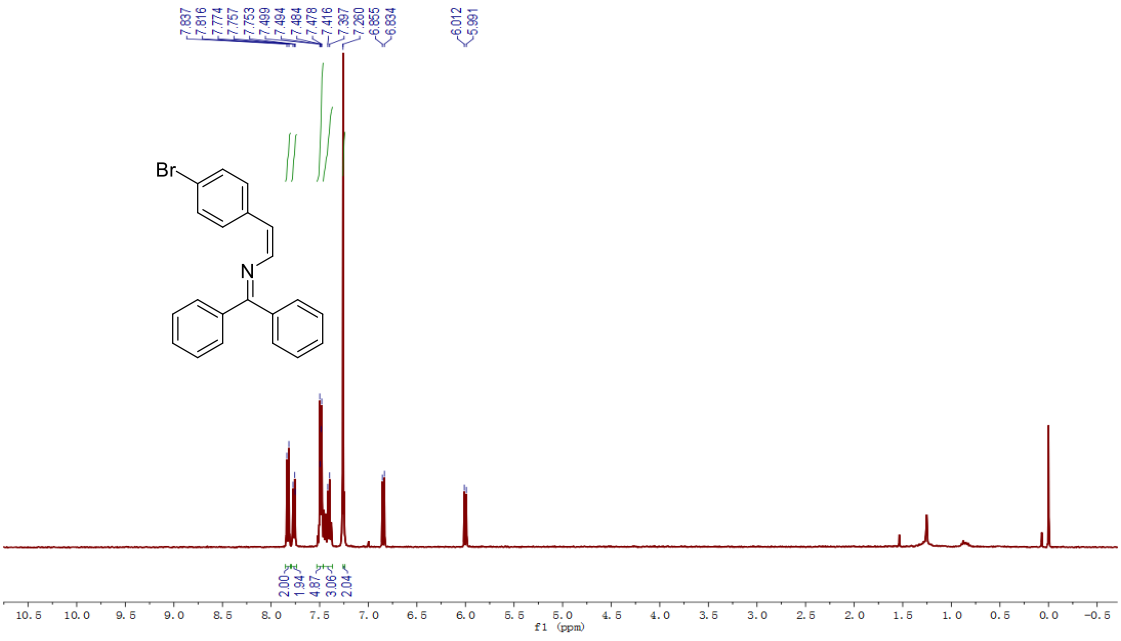

Figure 6.71 ^{1}H NMR spectrum of **18b**

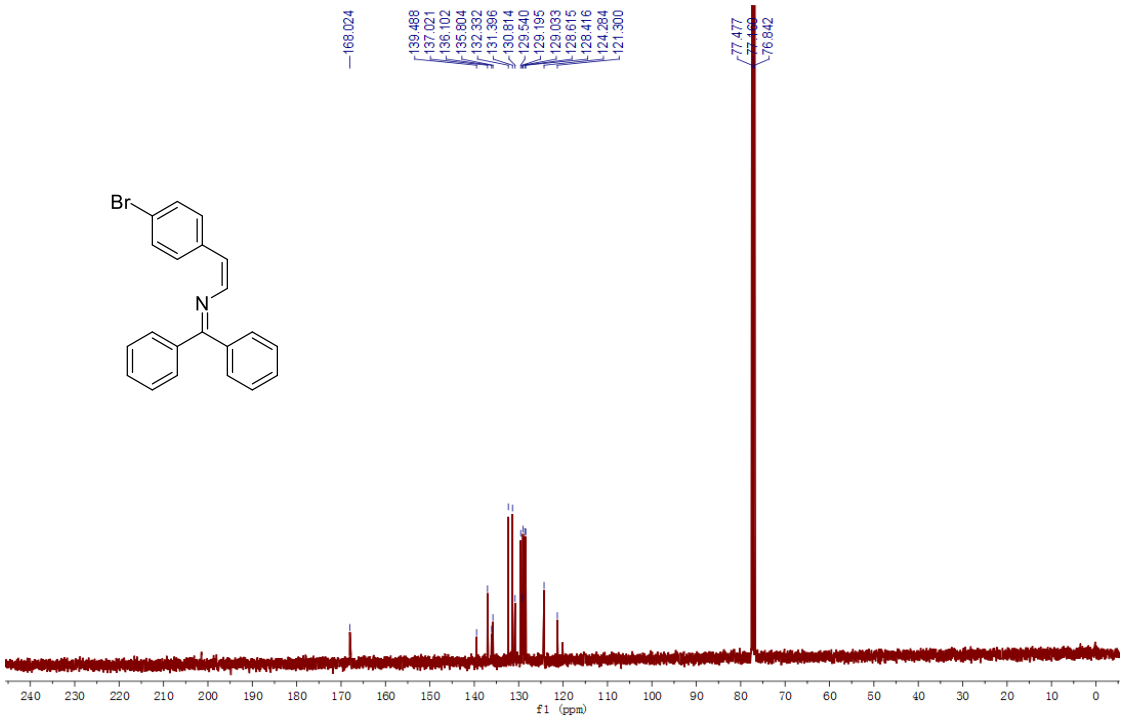

Figure 6.72 ^{13}C NMR spectrum of **18b**

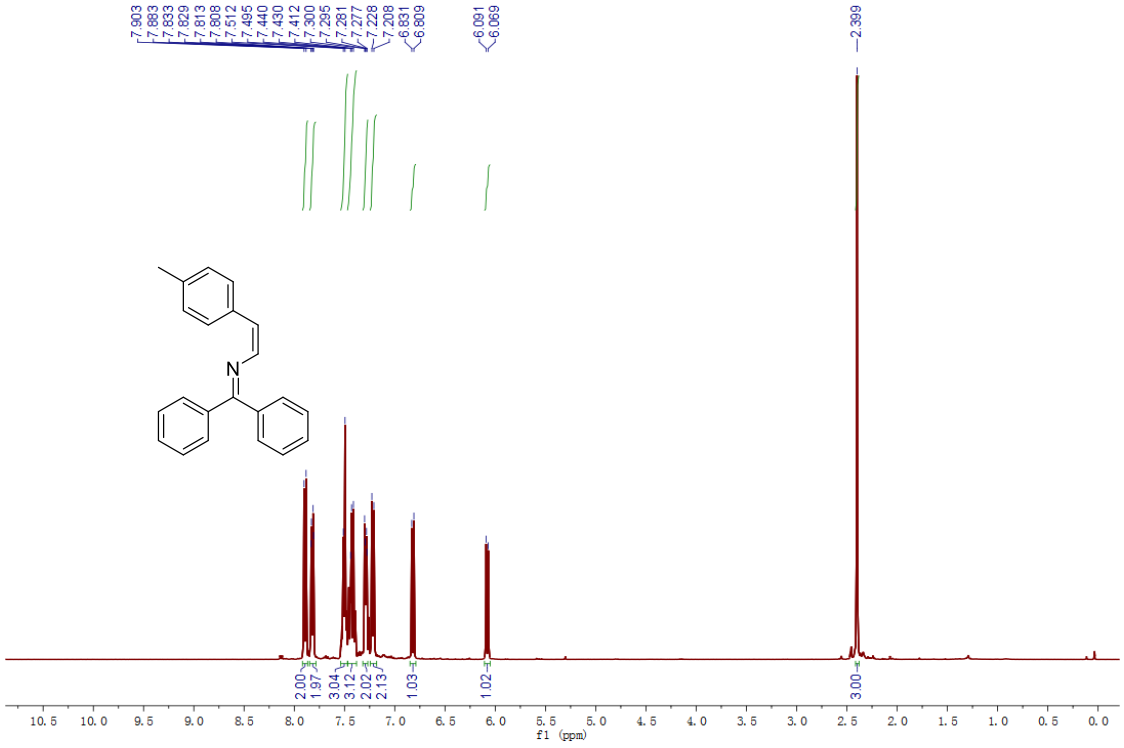

Figure 6.73 ^{1}H NMR spectrum of **18c**

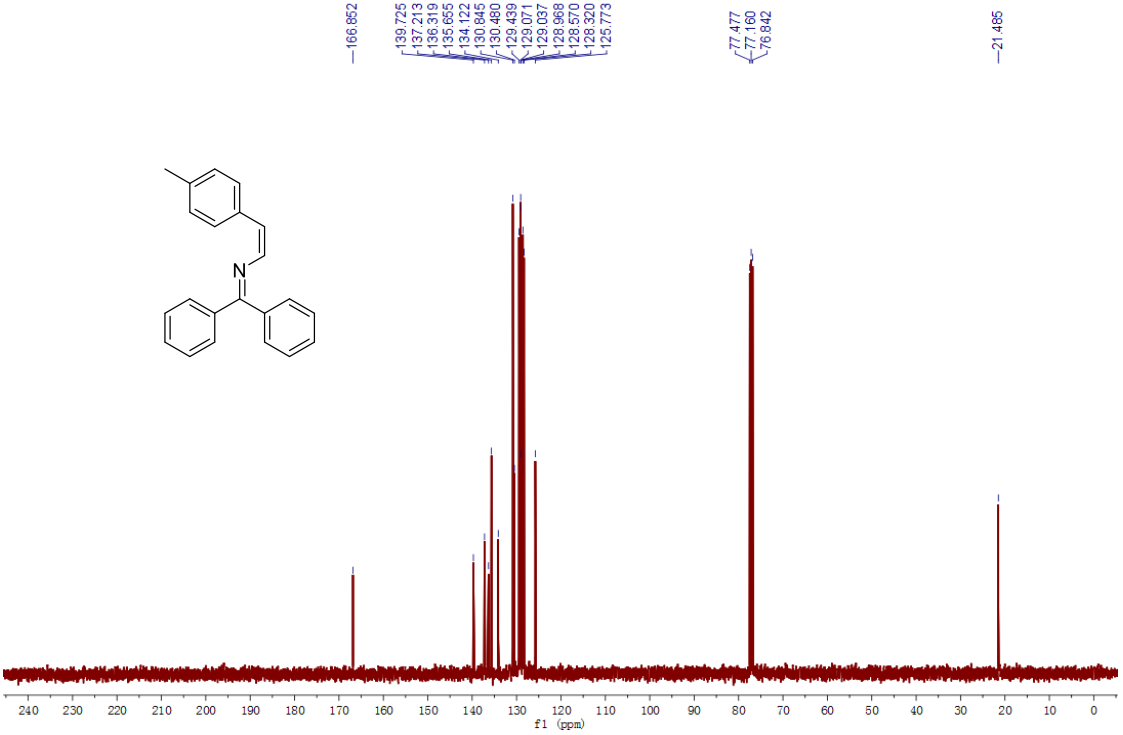

Figure 6.74 ^{13}C NMR spectrum of **18c**

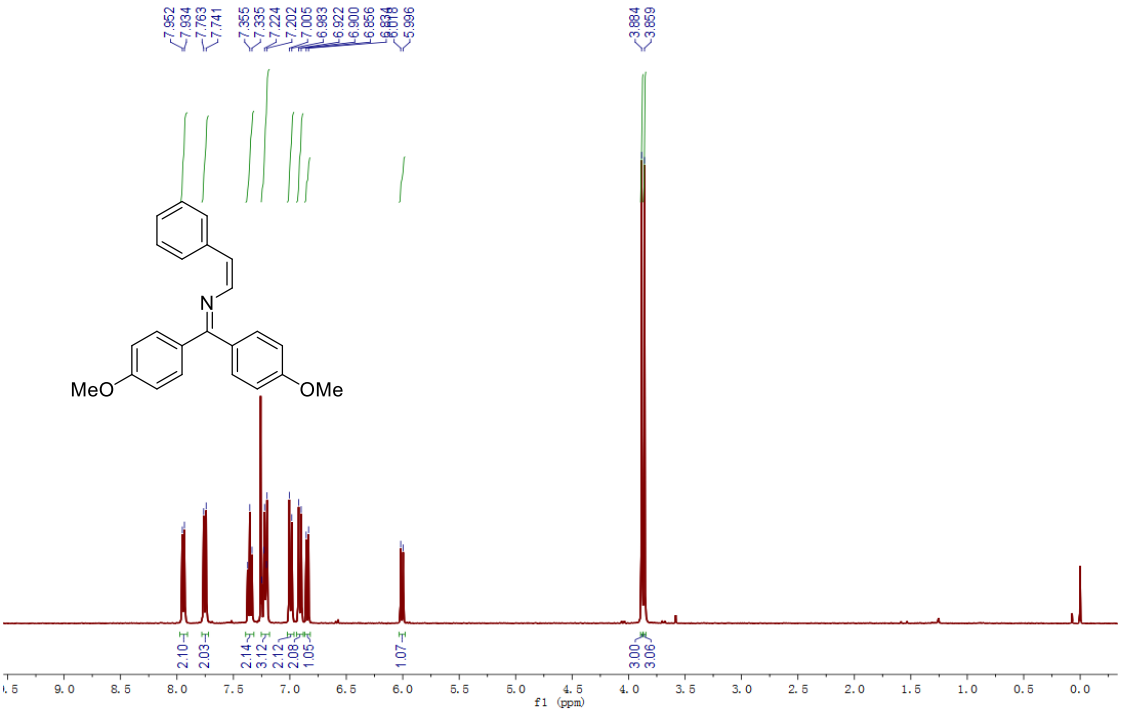

Figure 6.75 ^{1}H NMR spectrum of **18d**

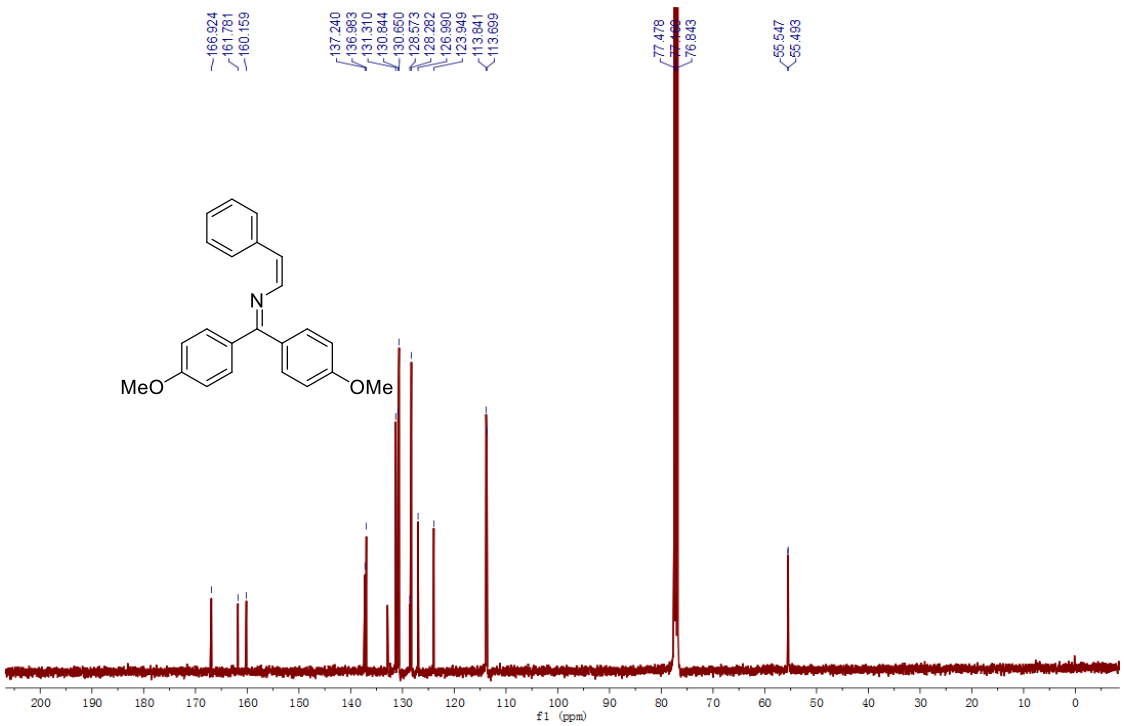

Figure 6.76 ^{13}C NMR spectrum of **18d**

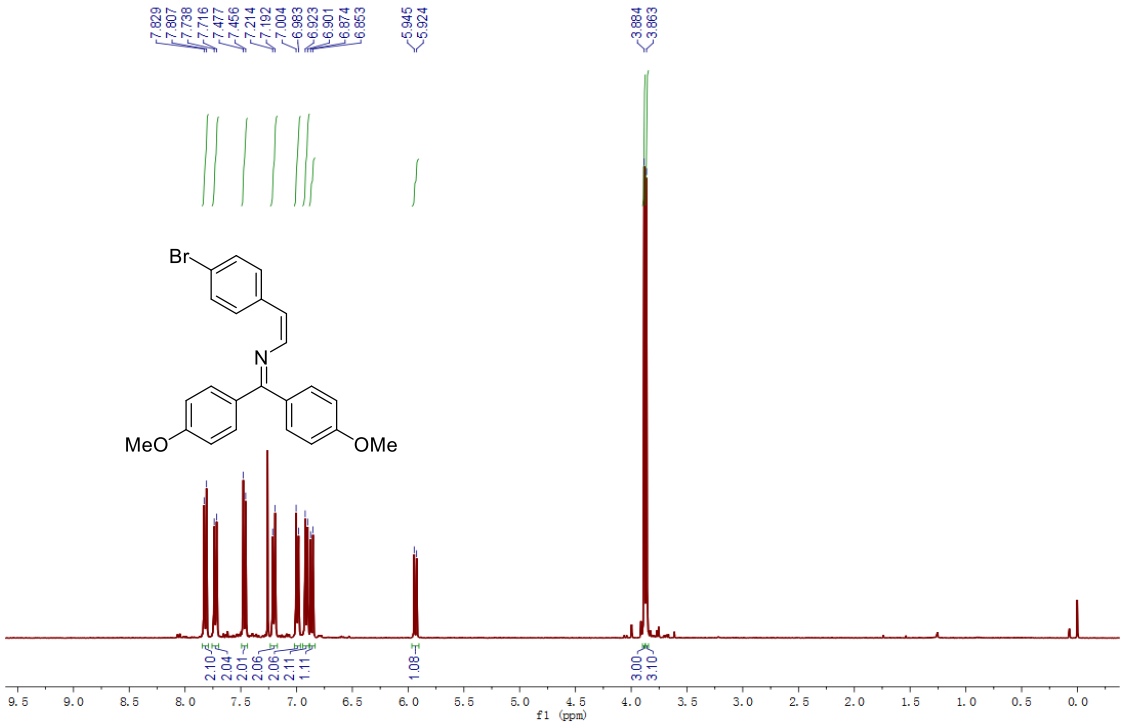

Figure 6.77 ^{1}H NMR spectrum of **18e**

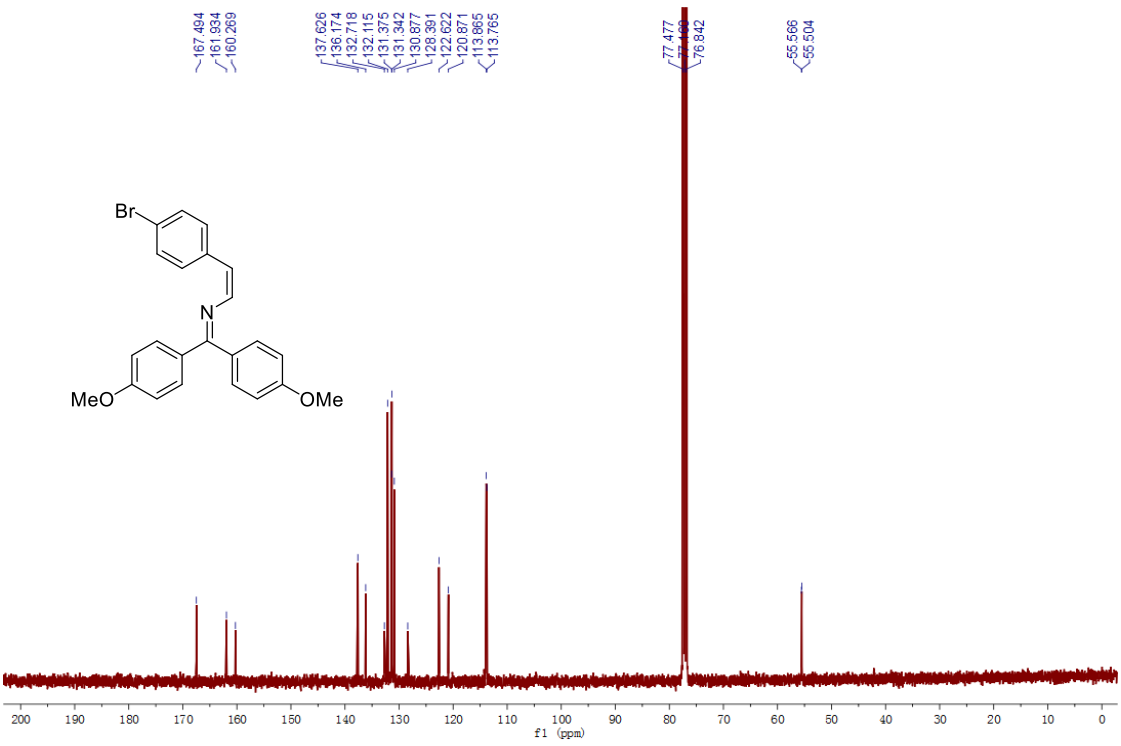

Figure 6.78 ^{13}C NMR spectrum of **18e**

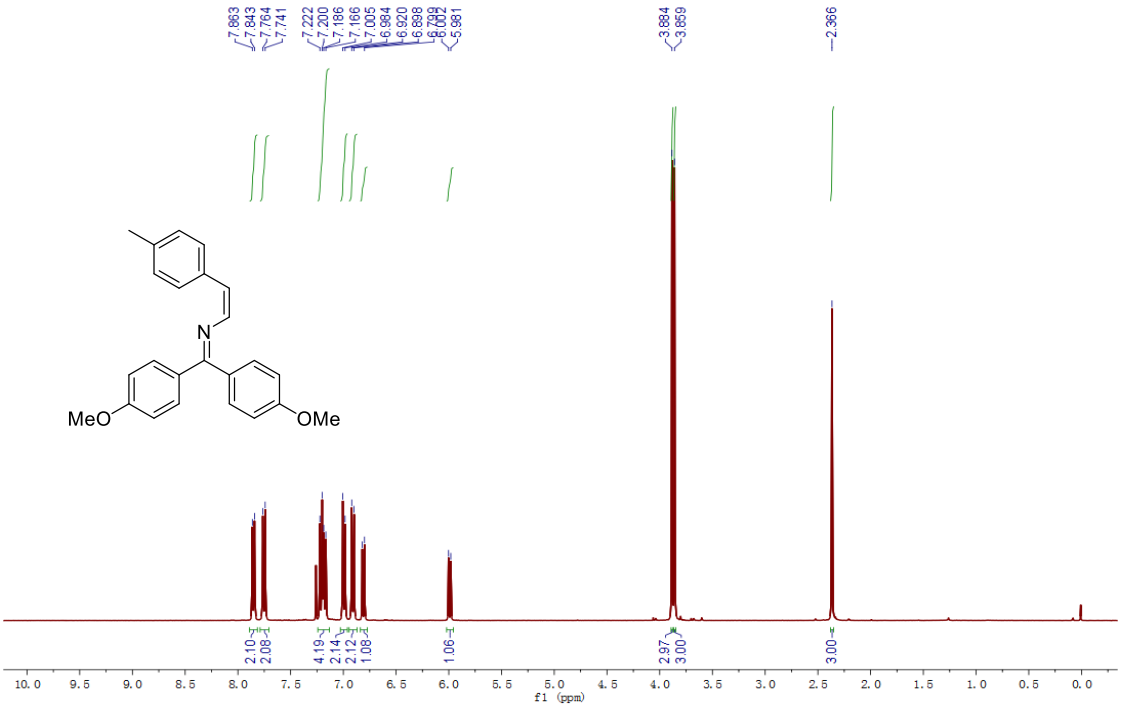

Figure 6.79 ^{1}H NMR spectrum of **18f**

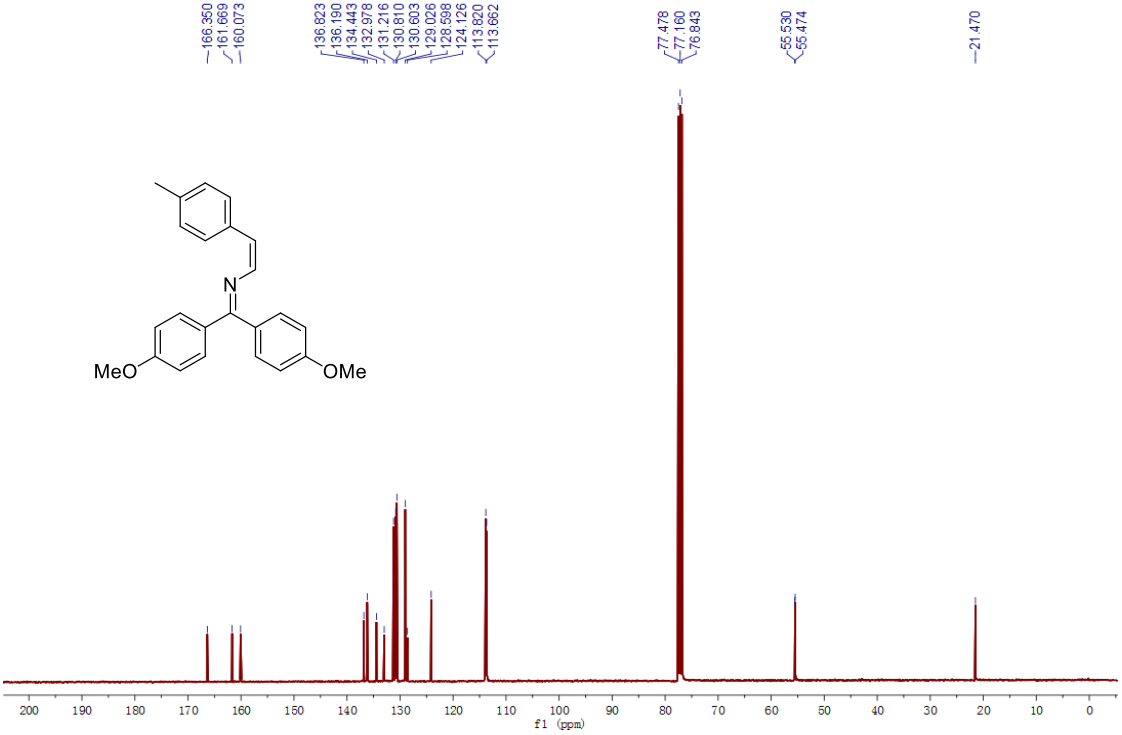

Figure 6.80 ^{13}C NMR spectrum of **18g**

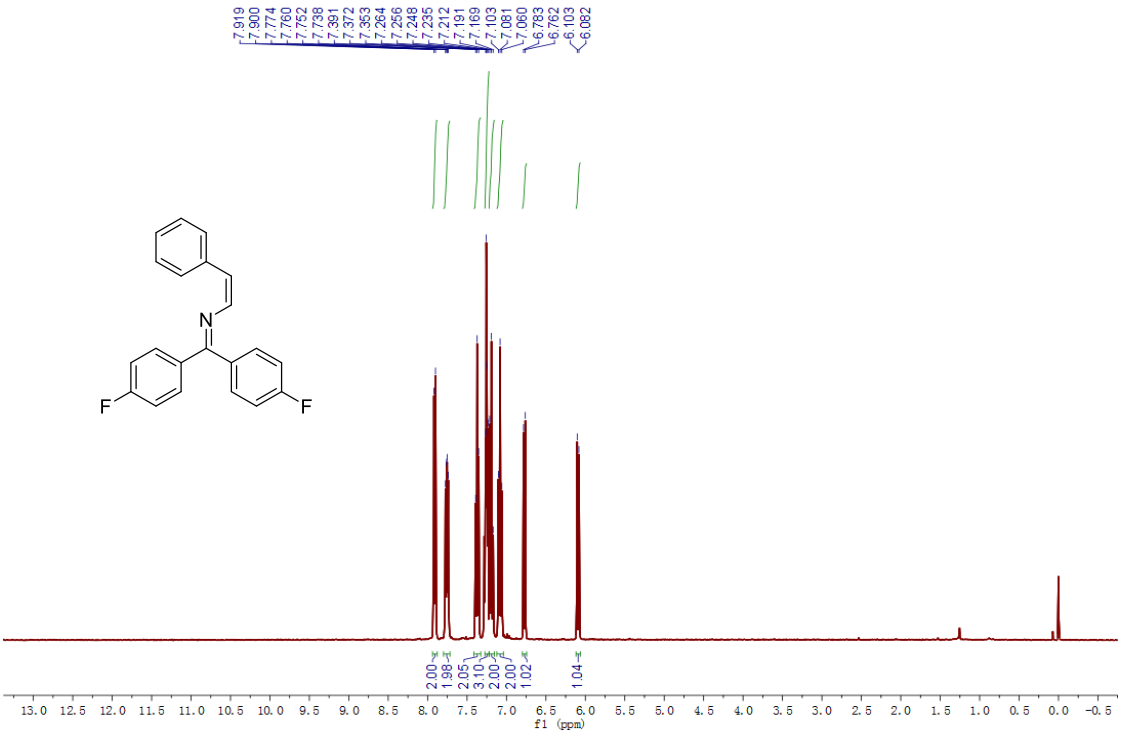

Figure 6.81 ^{1}H NMR spectrum of **18g**

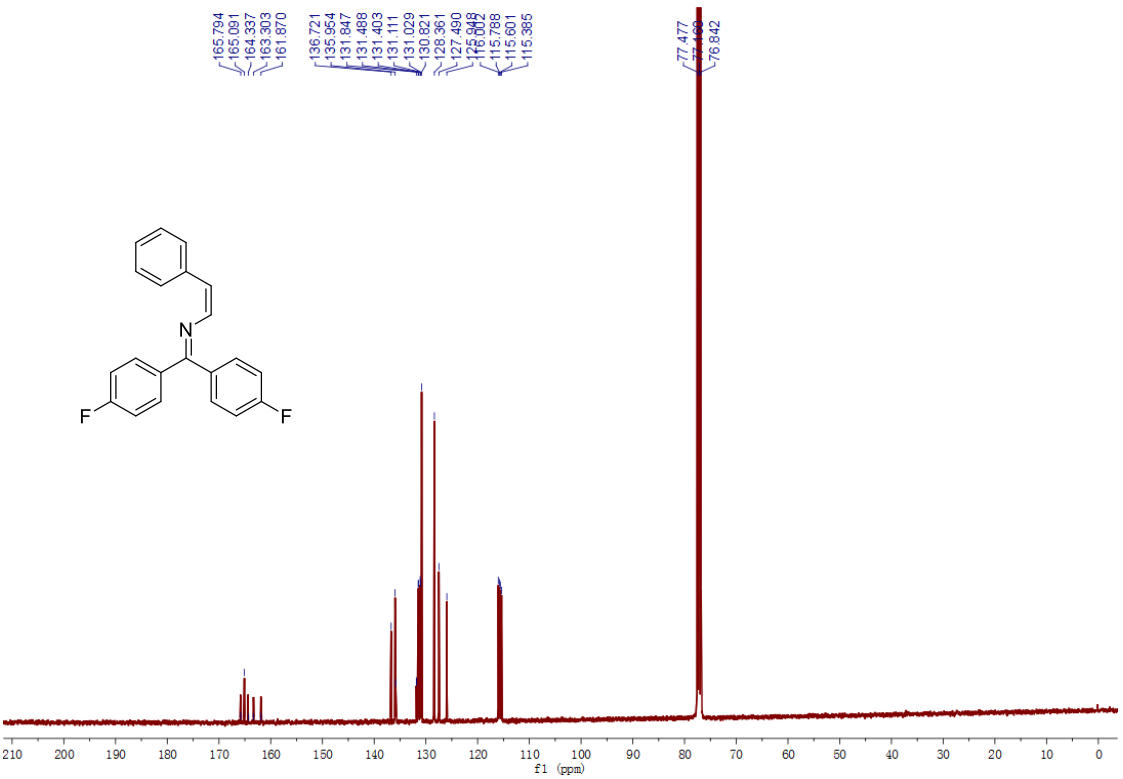

Figure 6.82 ^{13}C NMR spectrum of **18g**

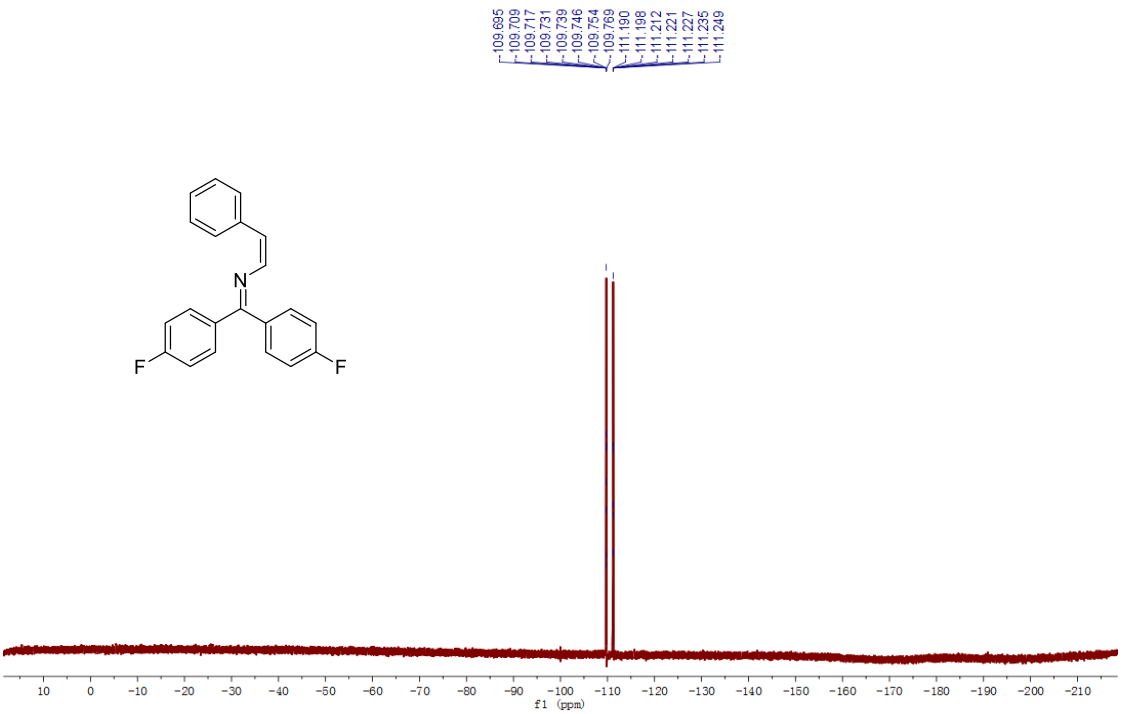

Figure 6.83 ^{19}F NMR spectrum of **18g**

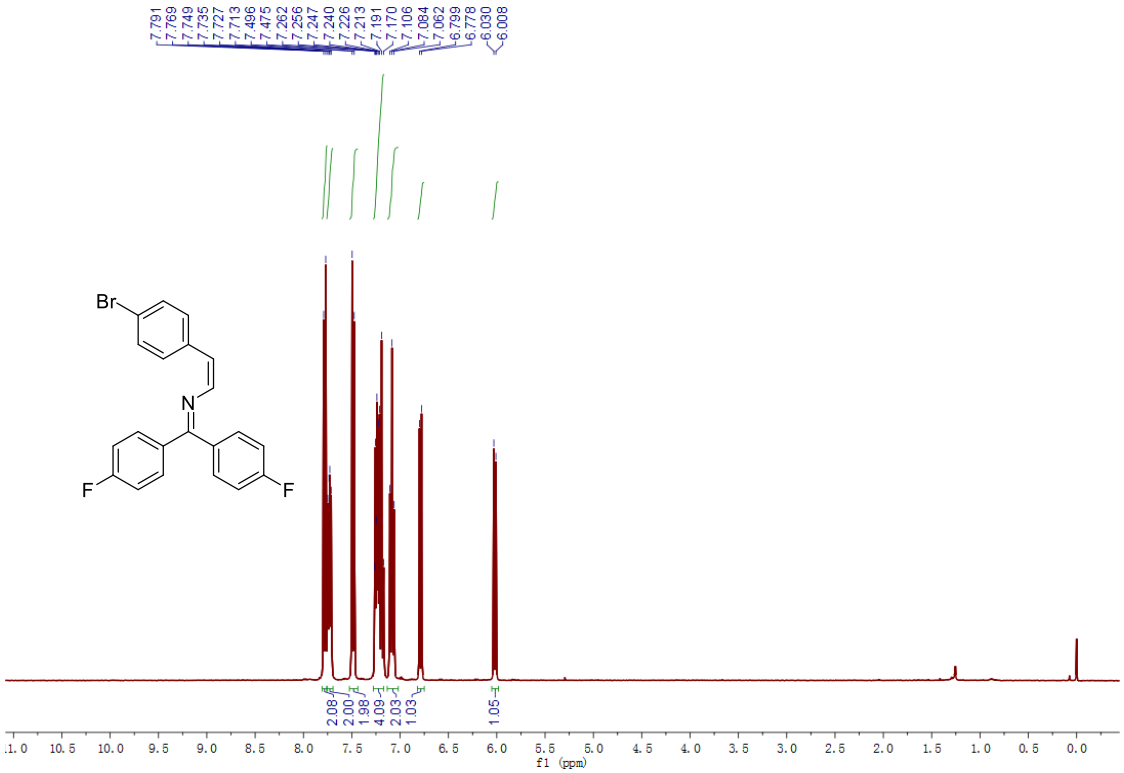

Figure 6.84 ^{1}H NMR spectrum of **18h**

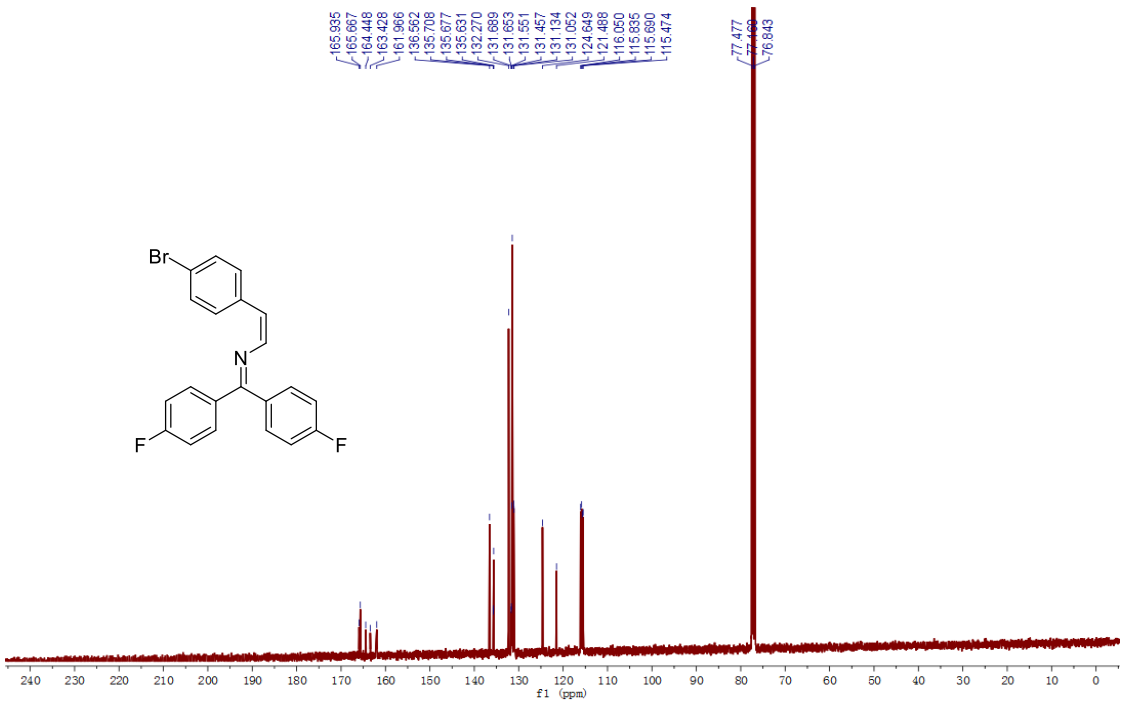

Figure 6.85 ^{13}C NMR spectrum of **18h**

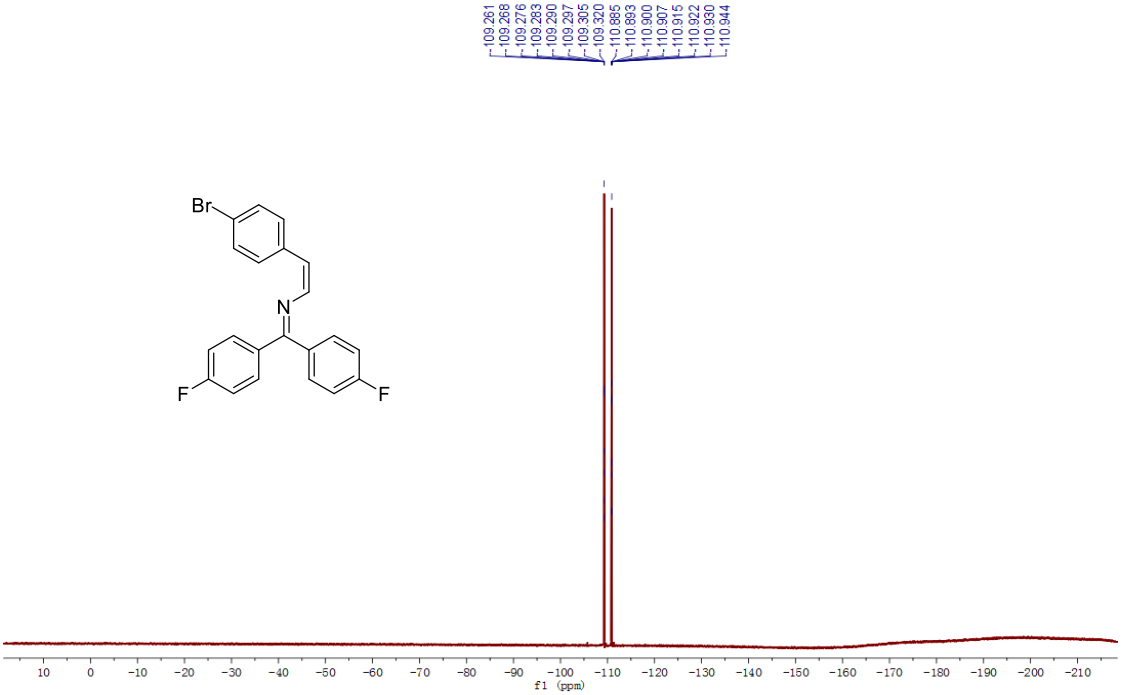

Figure 6.86 ^{19}F NMR spectrum of **18h**

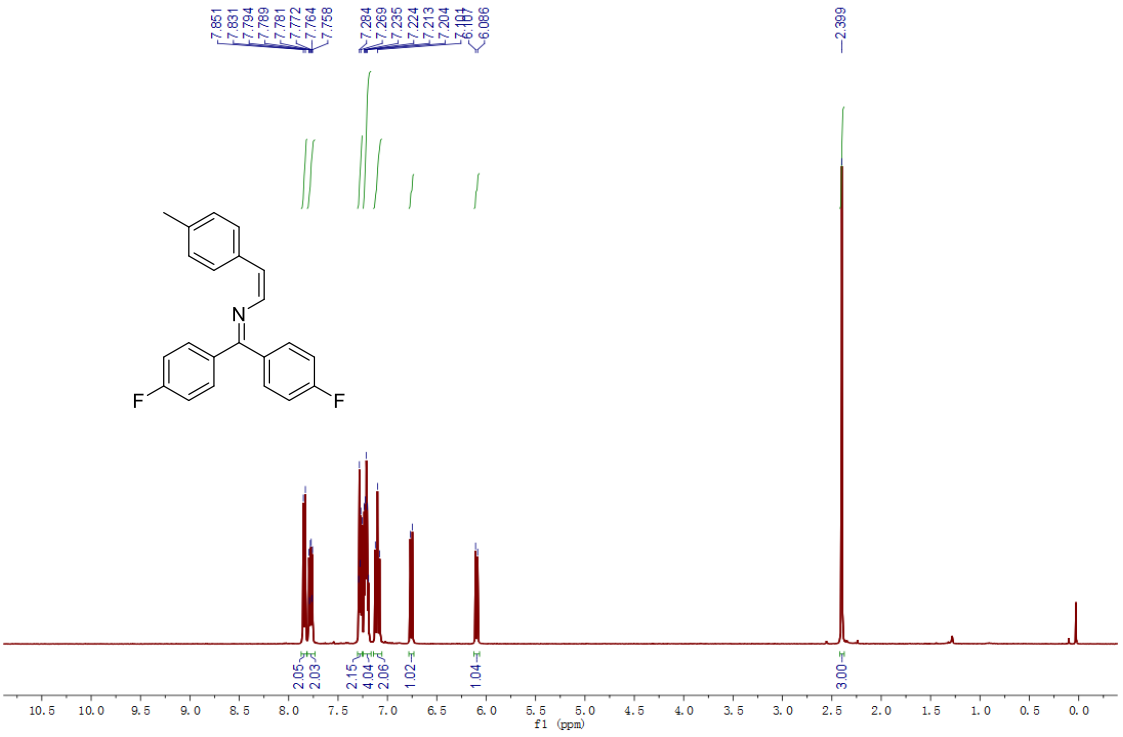

Figure 6.87 ^{1}H NMR spectrum of **18i**

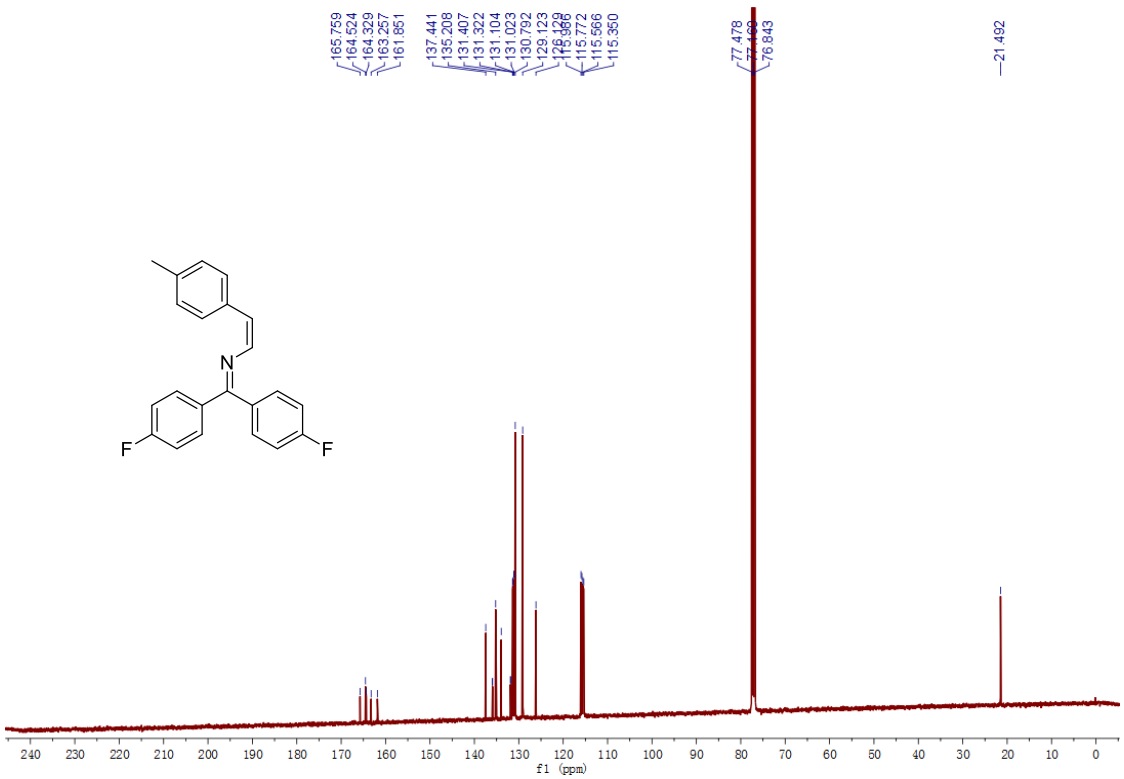

Figure 6.88 ^{13}C NMR spectrum of **18i**

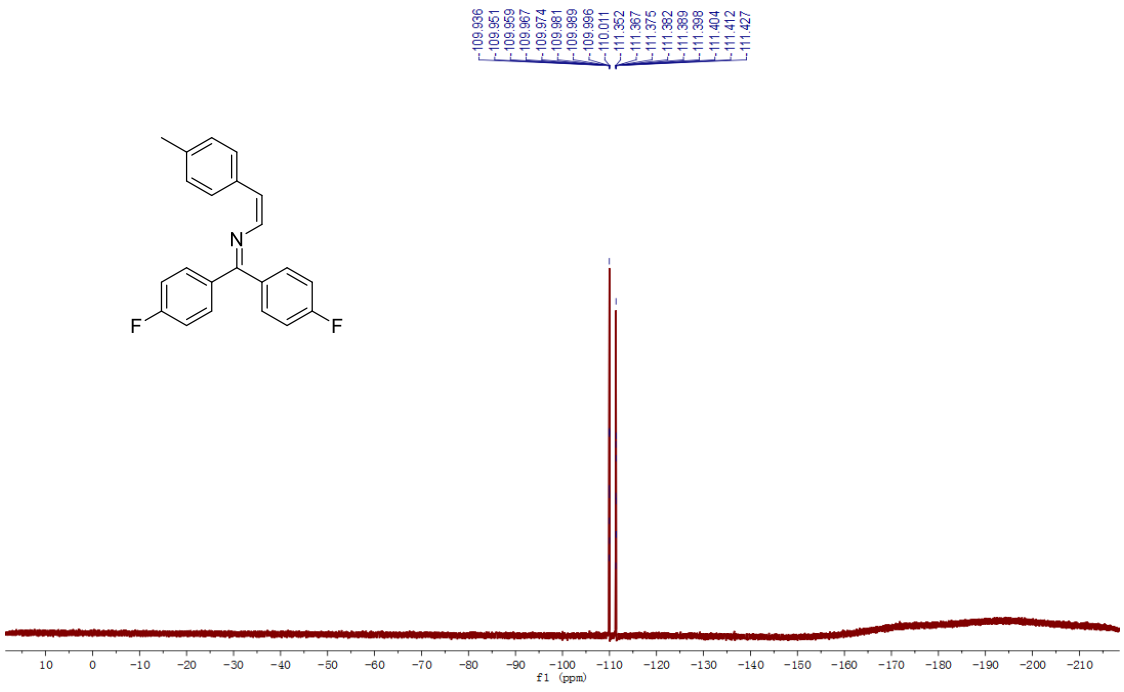

Figure 6.89 ^{19}F NMR spectrum of **18i**

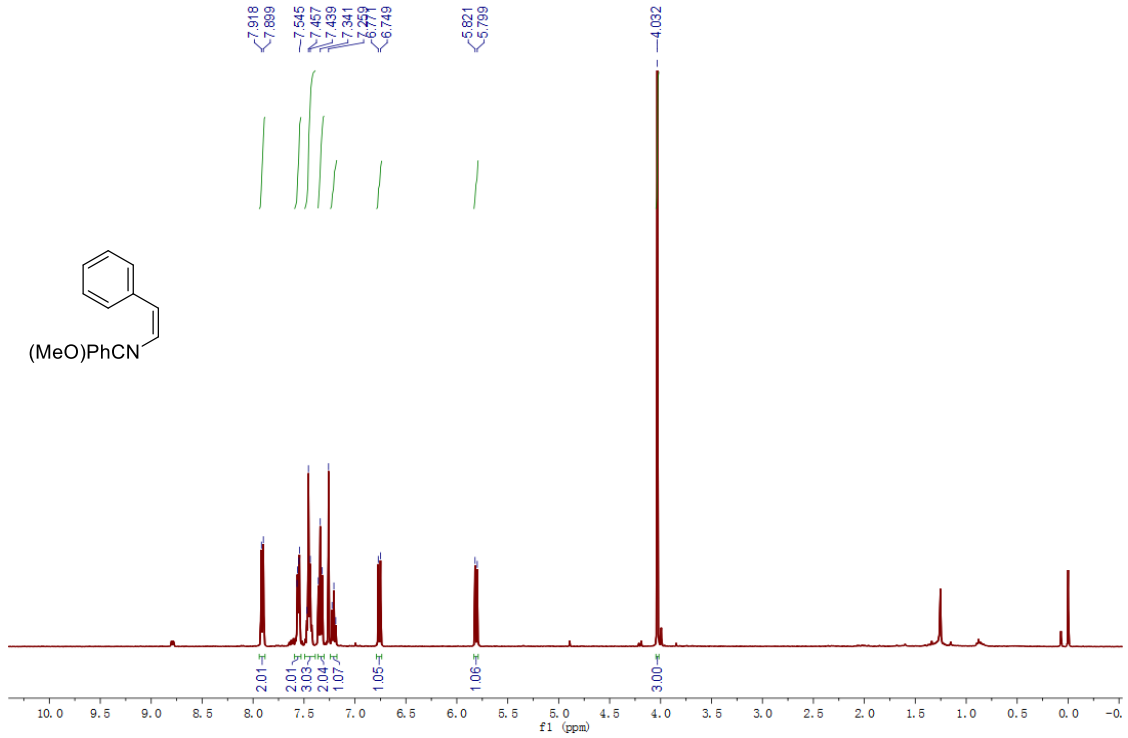

Figure 6.90 ^{1}H NMR spectrum of **18j**

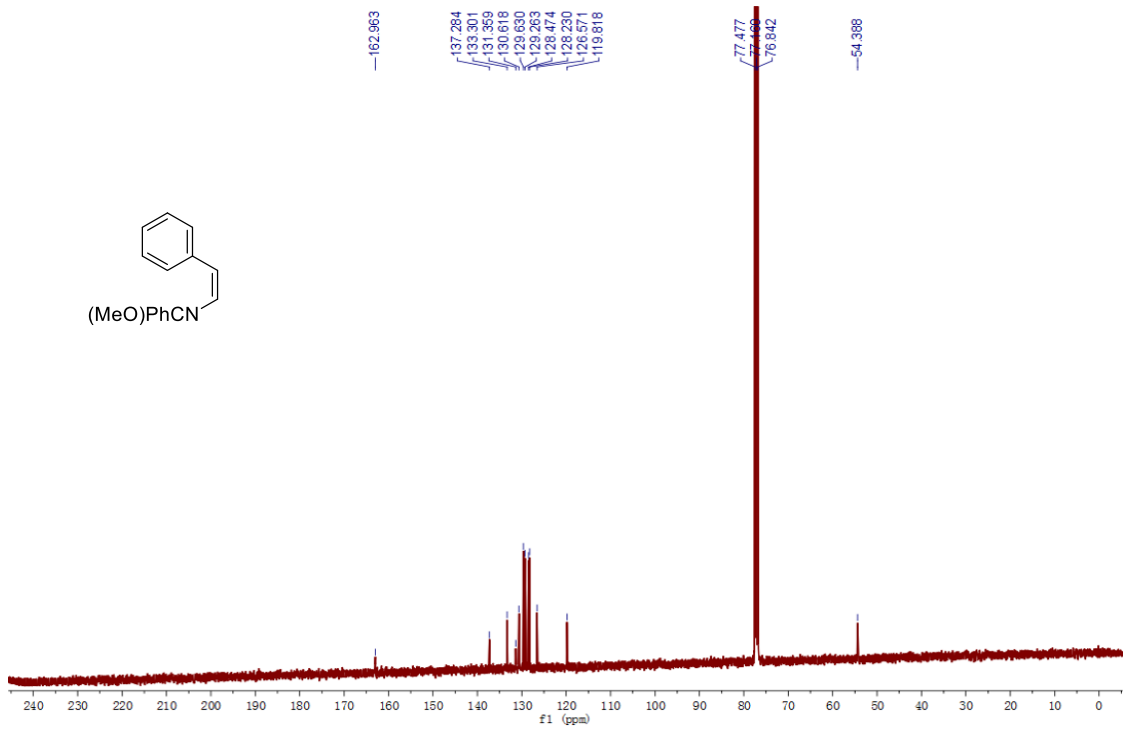

Figure 6.91 ^{13}C NMR spectrum of **18j**

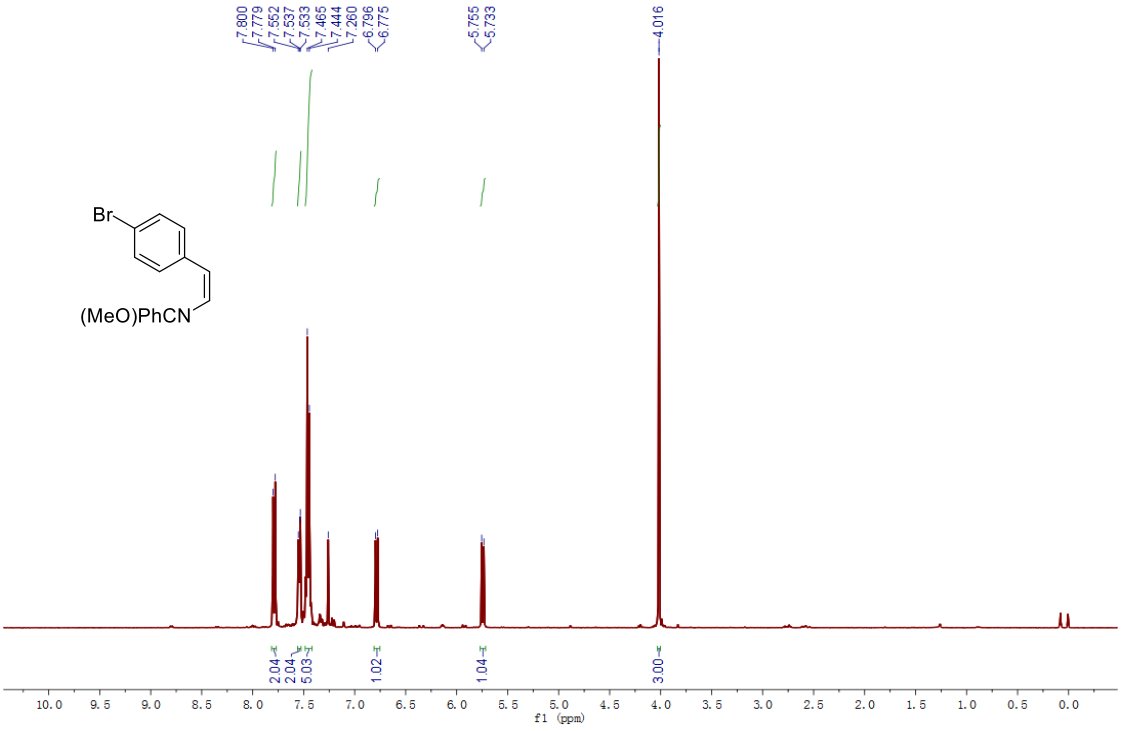

Figure 6.92 ^{1}H NMR spectrum of **18k**

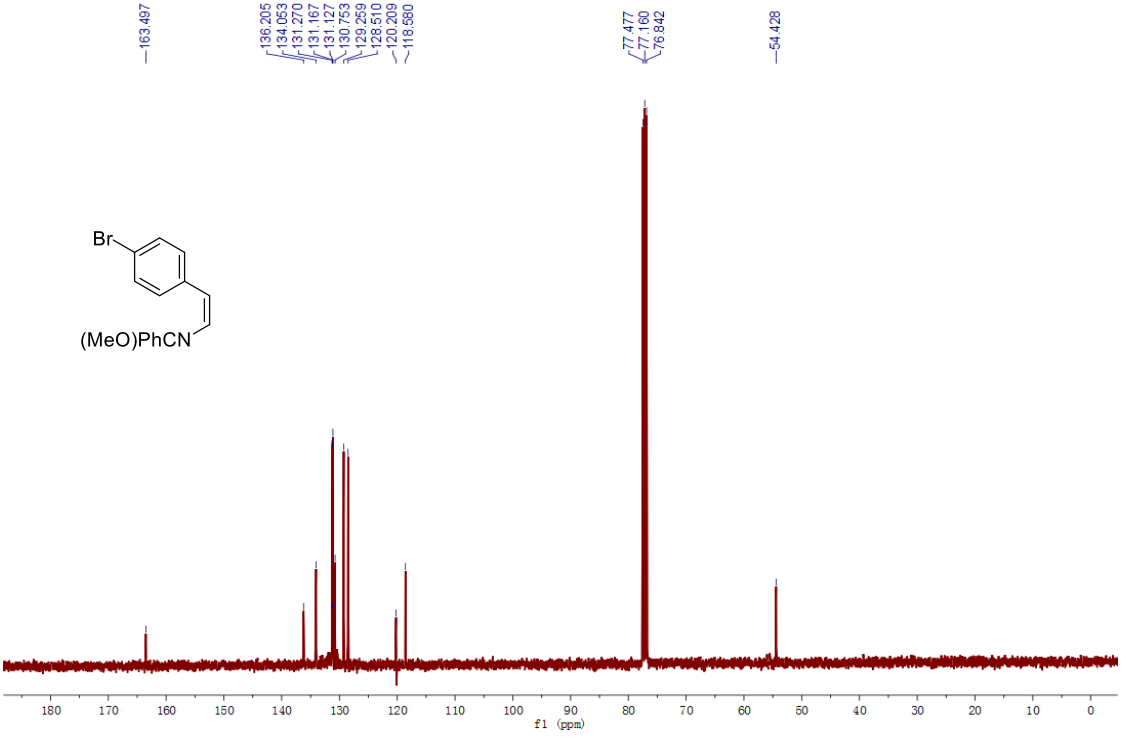

Figure 6.93 ^{13}C NMR spectrum of **18k**

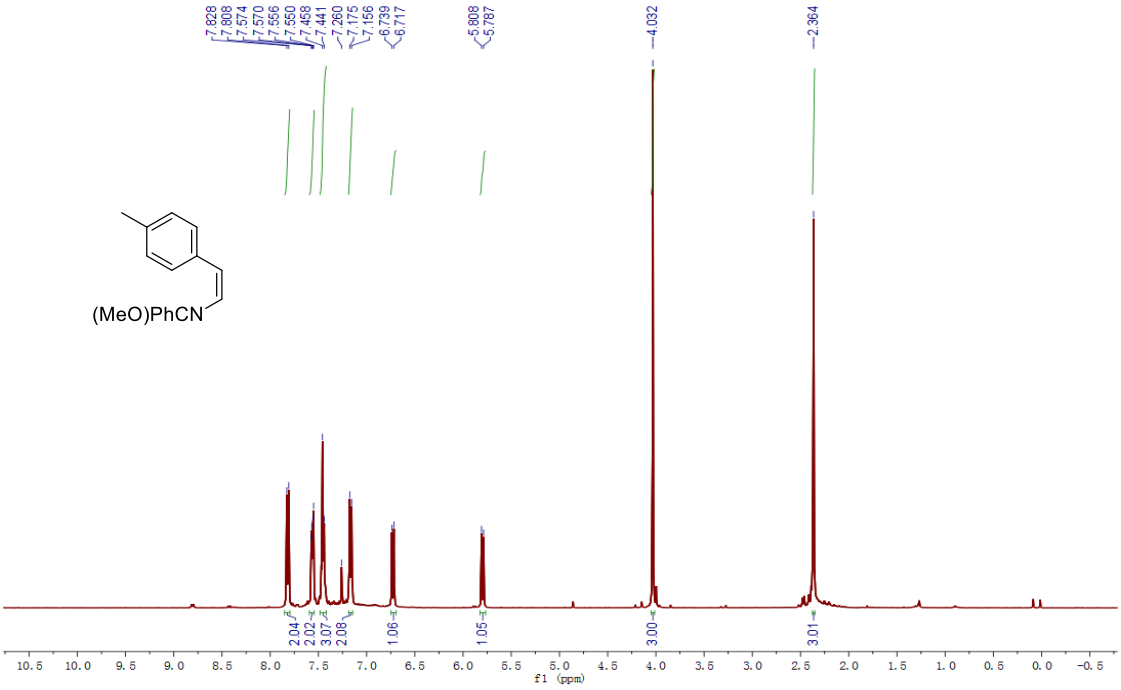

Figure 6.94 ^{1}H NMR spectrum of **18l**

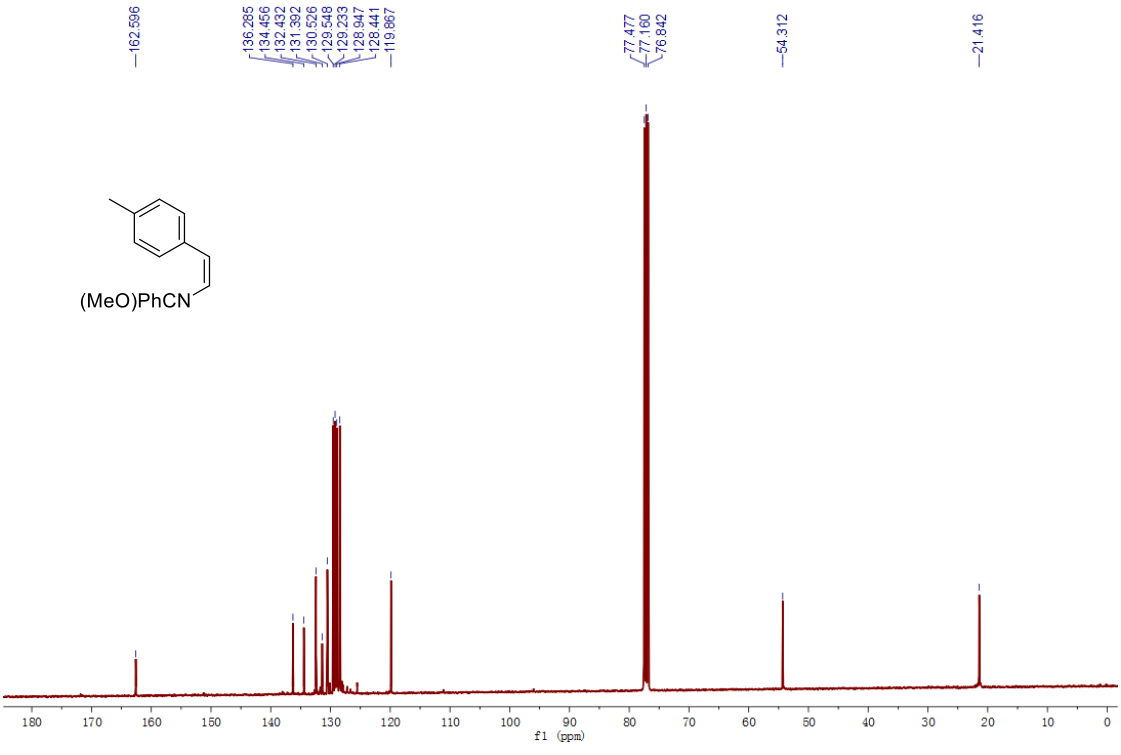

Figure 6.95 ^{13}C NMR spectrum of **18l**

6.5 Reference

1. Doherty, N. M.; Hoffmann, N. W., *Chem. Rev.* **1991,** *91*, 553-573.

2. Murphy, E. F.; Murugavel, R.; Roesky, H. W., *Chem. Rev.* **1997,** *97*, 3425-3468.

3. Grushin, V. V., *Chem.-Eur. J.* **2002,** *8*, 1006-1014.

4. de Frémont, P.; Marion, N.; Nolan, S. P., *Coord. Chem. Rev.* **2009,** *253*, 862-892.

5. Ferrando-Miguel, G.; Gérard, H.; Eisenstein, O.; Caulton, K. G., *Inorg. Chem.* **2002,** *41*, 6440-6449.

6. Jasim, N. A.; Perutz, R. N.; Whitwood, A. C.; Braun, T.; Izundu, J.; Neumann, B.; Rothfeld, S.; Stammler, H.-G., *Organometallics* **2004,** *23*, 6140-6149.

7. Jacobsen, H.; Correa, A.; Costabile, C.; Cavallo, L., *J. Organomet. Chem.* **2006,** *691*, 4350-4358.

8. Fischer, E. O.; Maasböl, A., *Angew. Chem. Int. Ed. Engl.* **1964,** *3*, 580-581.

9. Cardin, D. J.; Cetinkaya, B.; Lappert, M. F., *Chem. Rev.* **1972,** *72*, 545-574.

10. Igau, A.; Grutzmacher, H.; Baceiredo, A.; Bertrand, G., *J. Am. Chem. Soc.* **1988,** *110*, 6463-6466.

11. Bertrand, G.; Reed, R., *Coord. Chem. Rev.* **1994,** *137*, 323-355.

12. Igau, A.; Baceiredo, A.; Trinquier, G.; Bertrand, G., *Angew. Chem. Int. Ed. Engl.* **1989,** *28*, 621-622.

13. Igau, A.; Baceiredo, A.; Trinquier, G.; Bertrand, G., *Angew. Chem.* **1989,** *101*, 617-618.

14. Arduengo, A. J.; Harlow, R. L.; Kline, M., *J. Am. Chem. Soc.* **1991,** *113*, 361-363.

15. Arduengo, A. J.; Dias, H. V. R.; Harlow, R. L.; Kline, M., *J. Am. Chem. Soc.* **1992,** *114*, 5530-5534.

16. Canac, Y.; Soleilhavoup, M.; Conejero, S.; Bertrand, G., *J. Organomet. Chem.* **2004,** *689*, 3857-3865.

17. Vignolle, J.; Cattoën, X.; Bourissou, D., *Chem. Rev.* **2009,** *109*, 3333-3384.

18. Arduengo, A. J.; Krafczyk, R., *Chem. unserer Zeit* **1998,** *32*, 6-14.

19. Martin, D.; Soleilhavoup, M.; Bertrand, G., *Chem. Sci.* **2011,** *2*, 389-399.

20. Martin, C. D.; Soleilhavoup, M.; Bertrand, G., *Chem. Sci.* **2013,** *4*, 3020-3030.

21. Soleilhavoup, M.; Bertrand, G., *Acc. Chem. Res.* **2015,** *48*, 256-266.

22. Müller, T. E.; Hultzsch, K. C.; Yus, M.; Foubelo, F.; Tada, M., *Chem. Rev.* **2008,** *108*, 3795-3892.

23. Patil, N. T.; Singh, V., *J. Organomet. Chem.* **2011,** *696*, 419-432.

24. Hannedouche, J.; Schulz, E., *Chem. Eur. J.* **2013,** *19*, 4972-4985.

25. Dyker, G., *Angew. Chem. Int. Ed.* **1999,** *38*, 1698-1712.

26. Zhang, Y.-Q.; Zhu, D.-Y.; Li, B.-S.; Tu, Y.-Q.; Liu, J.-X.; Lu, Y.; Wang, S.-H., *J. Org. Chem.* **2012,** *77*, 4167-4170.

27. Kondo, T.; Okada, T.; Suzuki, T.; Mitsudo, T.-a., *J. Organomet. Chem.* **2001,** *622*, 149-154.

28. Tokunaga, M.; Eckert, M.; Wakatsuki, Y., *Angew. Chem. Int. Ed.* **1999,** *38*, 3222-3225.

29. Mizushima, E.; Chatani, N.; Kakiuchi, F., *J. Organomet. Chem.* **2006,** *691*, 5739-5745.

30. Yi, C. S.; Yun, S. Y., *J. Am. Chem. Soc.* **2005,** *127*, 17000-17006.

31. Field, L. D.; Messerle, B. A.; Vuong, K. Q.; Turner, P., *Dalton Trans.* **2009**, 3599-3614.

32. Burling, S.; Field, L. D.; Messerle, B. A.; Turner, P., *Organometallics* **2004,** *23*, 1714-1721.

33. Lai, R.-Y.; Surekha, K.; Hayashi, A.; Ozawa, F.; Liu, Y.-H.; Peng, S.-M.; Liu, S.-T., *Organometallics* **2007,** *26*, 1062-1068.

34. Motta, A.; Fragalà, I. L.; Marks, T. J., *Organometallics* **2006,** *25*, 5533-5539.

35. Beller, M.; Trauthwein, H.; Eichberger, M.; Breindl, C.; Müller, T. E., *Eur. J. Inorg. Chem.* **1999,** *1999*, 1121-1132.

36. Beller, M.; Trauthwein, H.; Eichberger, M.; Breindl, C.; Herwig, J.; Müller, T. E.; Thiel, O. R., *Chem. Eur. J.* **1999,** *5*, 1306-1319.

37. Burling, S.; Field, L. D.; Messerle, B. A., *Organometallics* **2000,** *19*, 87-90.

38. Müller, T. E.; Berger, M.; Grosche, M.; Herdtweck, E.; Schmidtchen, F. P., *Organometallics* **2001,** *20*, 4384-4393.

39. Müller, T. E.; Grosche, M.; Herdtweck, E.; Pleier, A.-K.; Walter, E.; Yan, Y.-K., *Organometallics* **2000,** *19*, 170-183.

40. Ackermann, L.; Sandmann, R.; Kondrashov, M. V., *Synlett* **2009,** *2009*, 1219-1222.

41. Lutete, L. M.; Kadota, I.; Yamamoto, Y., *J. Am. Chem. Soc.* **2004,** *126*, 1622-1623.

42. Patil, N. T.; Kavthe, R. D.; Raut, V. S.; Reddy, V. V. N., *J. Org. Chem.* **2009,** *74*, 6315-6318.

43. Tsipis, C. A.; Kefalidis, C. E., *Organometallics* **2006,** *25*, 1696-1706.

44. Pitzer, K. S., *J. Am. Chem. Soc.* **1948,** *70*, 2140-2145.

45. Wanzlick, H. W.; Schönherr, H. J., *Angew. Chem. Int. Ed. Engl.* **1968,** *7*, 141-142.

46. Leyva, A.; Corma, A., *Adv. Synth. Catal.* **2009,** *351*, 2876-2886.

47. Patil, N. T.; Mutyala, A. K.; Lakshmi, P. G. V. V.; Gajula, B.; Sridhar, B.; Pottireddygari, G. R.; Rao, T. P., *J. Org. Chem.* **2010,** *75*, 5963-5975.

48. Lavallo, V.; Frey, G. D.; Donnadieu, B.; Soleilhavoup, M.; Bertrand, G., *Angew. Chem. Int. Ed.* **2008,** *47*, 5224-5228.

49. Kinjo, R.; Donnadieu, B.; Bertrand, G., *Angew. Chem. Int. Ed.* **2011,** *50*, 5560-5563.

50. Biyikal, M.; Löhnwitz, K.; Meyer, N.; Dochnahl, M.; Roesky, P. W.; Blechert, S., *Eur. J. Inorg. Chem.* **2010,** *2010*, 1070-1081.

51. Okuma, K.; Seto, J.-i.; Sakaguchi, K.-i.; Ozaki, S.; Nagahora, N.; Shioji, K., *Tetrahedron Lett.* **2009,** *50*, 2943-2945.

52. Yamamoto, Y.; Gridnev, I. D.; Patil, N. T.; Jin, T., *Chem. Commun.* **2009**, 5075-5087.

53. Kirsch, S. F., *Synthesis* **2008,** *2008*, 3183-3204.

54. López, F.; Mascareñas, J. L., *Beilstein J. Org. Chem.* **2011,** *7*, 1075-1094.

55. Haggin, J., *Chem. Eng. News* **1993,** *71*, 23-27.

56. Klinkenberg, J. L.; Hartwig, J. F., *Angew. Chem. Int. Ed.* **2011,** *50*, 86-95.

57. Gunanathan, C.; Milstein, D., *Angew. Chem.* **2008,** *120*, 8789-8792.

58. Lang, F.; Zewge, D.; Houpis, I. N.; Volante, R. P., *Tetrahedron Lett.* **2001,** *42*, 3251-3254.

59. Xu, H.; Wolf, C., *Chem. Commun.* **2009**, 3035-3037.

60. Xia, N.; Taillefer, M., *Angew. Chem. Int. Ed.* **2009,** *48*, 337-339.

61. Wang, D.; Cai, Q.; Ding, K., *Adv. Synth. Catal.* **2009,** *351*, 1722-1726.

62. Kim, J.; Chang, S., *Chem. Commun.* **2008**, 3052-3054.

63. Kovács, G.; Lledós, A.; Ujaque, G., *Angew. Chem. Int. Ed.* **2011,** *50*, 11147-11151.

64. Tukov, A. A.; Normand, A. T.; Nechaev, M. S., *Dalton Trans.* **2009**, 7015-7028.

65. Dorta, R.; Stevens, E. D.; Scott, N. M.; Costabile, C.; Cavallo, L.; Hoff, C. D.; Nolan, S. P., *J. Am. Chem. Soc.* **2005,** *127*, 2485-2495.

66. Scott, N. M.; Nolan, S. P., *Eur. J. Inorg. Chem.* **2005,** *2005*, 1815-1828.

67. Chianese, A. R.; Li, X.; Janzen, M. C.; Faller, J. W.; Crabtree, R. H., *Organometallics* **2003,** *22*, 1663-1667.

68. Chianese, A. R.; Kovacevic, A.; Zeglis, B. M.; Faller, J. W.; Crabtree, R. H., *Organometallics* **2004,** *23*, 2461-2468.

69. Blanco Jaimes, M. C.; Böhling, C. R. N.; Serrano-Becerra, J. M.; Hashmi, A. S. K., *Angew. Chem. Int. Ed.* **2013,** *52*, 7963-7966.

70. Blanco Jaimes, M. C.; Rominger, F.; Pereira, M. M.; Carrilho, R. M. B.; Carabineiro, S. A. C.; Hashmi, A. S. K., *Chem. Commun.* **2014,** *50*, 4937-4940.

71. Hata, K.; Segawa, Y.; Itami, K., *Chem. Commun.* **2012,** *48*, 6642-6644.

72. Otsuka, M.; Takita, R.; Kanazawa, J.; Miyamoto, K.; Muranaka, A.; Uchiyama, M., *J. Am. Chem. Soc.* **2015,** *137*, 15082-15085.

73. Hansch, C.; Leo, A.; Taft, R. W., *Chem. Rev.* **1991,** *91*, 165-195.

74. Hartwig, J. F., *Chem. Soc. Rev.* **2011,** *40*, 1992-2002.

75. Wöß, E.; Monkowius, U.; Knör, G., *Chem. Eur. J.* **2013,** *19*, 1489-1495.

76. Michael, J. P., *Nat. Prod. Rep.* **2005,** *22*, 627-646.

77. Craig, D.; Henry, G. D., *Tetrahedron Lett.* **2005,** *46*, 2559-2562.

78. Roesch, K. R.; Larock, R. C., *J. Org. Chem.* **2002,** *67*, 86-94.

79. Suzuki, D.; Nobe, Y.; Watai, Y.; Tanaka, R.; Takayama, Y.; Sato, F.; Urabe, H., *J. Am. Chem. Soc.* **2005,** *127*, 7474-7479.

80. Jayakumar, S.; Ishar, M. P. S.; Mahajan, M. P., *Tetrahedron* **2002,** *58*, 379-471.

81. Weinreb, S. M.; Scola, P. M., *Chem. Rev.* **1989,** *89*, 1525-1534.

82. Campbell, M. J.; Toste, F. D., *Chem. Sci.* **2011,** *2*, 1369-1378.

83. Manan, R. S.; Kilaru, P.; Zhao, P., *J. Am. Chem. Soc.* **2015,** *137*, 6136-6139.

Conclusion

As mentioned *in Chapter 1*, the aim of the project is to investigate the synthesis and reactivities of novel Group 14 divalent species such as carbene and germylene. First, we have developed a cyclic (alkyl)(amino) germylene (**CAAGe**) in *Chapter 2*. **CAAGe** possesses the high-lying HOMO−1 and low-lying LUMO, which was supported by DFT calculations.

In *Chapter 3*, we have investigated the reactivity of CAAGe with S_8 and N_2O. The oxidation reaction of **CAAGe** by S_8 led to the formation of the sulfido-bridged dimers as a mixture of two diastereomers involving Ge_2S_2 four-membered ring framework. In contrast, when **CAAGe** was oxidized by N_2O, and only trans product containing the Ge_2O_2 four-membered ring skeleton was obtained. The reaction of **CAAGe** with TEMPO led to the formation of a 1:2 adduct.

In *Chapter 4*, a modified **CAAGe** with an adamantyl group on the N atom was developed. In the reaction of **CAAGe** with hydrosilanes in the presence of 20 mol% $B(C_6F_5)_3$, **CAAGe** was transformed into germylenes **10** and **11** via silyl group exchange. The corresponding kinetic studies have been performed to support the mechanism proposed.

In *Chapter 5*, the reactions of **CAAGe** with various gold(I), palladium(0) and palladium(II) complexes have been examined in *Chapter 5*. The Au−Cl bond insertion products [ClGe−Au−PPh_3] and [ClGe−Au−NHC] were formed in the reactions of **CAAGe** with triphenylphosphine gold(I) chloride and NHC gold(I) chloride respectively. The reactions of [ClGe−Au−NHC] with various silver reagents afforded the corresponding [Ge−Au−NHC]•X complex. Furthermore, the reaction of **CAAGe** with $Pd(PPh_3)_4$ resulted in the formation of germylene bis(triphenylphosphine) palladium(0), which was also formed by the reaction of **CAAGe** with $Pd(PPh_3)_2Cl_2$.

Lastly, a new gold(I) complex featuring a pyrid-*2*-ylidene ligand was synthesized and fully characterized. Gold(I) complex has been employed in hydroamination of alkynes with ammonia, which provided an efficient synthetic method for the construction of pyridine derivatives. Gold(I)

complex has also been utilized in the hydroimination of alkynes with imines, which indicated an apparent anti-Markovnikov regioselectivity to form 2-aza-1,3-dienes. A plausible mechanism involving both Markovnikov and Anti-Markovnikov addition was proposed and certified by the experimental studies.

List of Publications

1. **Liliang Wang**, Yi Shan Lim, Yongxin Li, Rakesh Ganguly, Rei Kinjo; Isolation of a Cyclic (Alkyl)(Amino)Germylene, *Molecules*, **2016,** *21*, 990.
2. **Liliang Wang**[#], Lingbing Kong[#], Yongxin Li, Rakesh Ganguly, Rei Kinjo; Anti-Markovnikov Hydroimination of Terminal Alkynes in Gold-Catalyzed Pyridine Construction using Ammonia, *Chem. Commun*. **2015,** *51*, 12419.

Appendix A Crystallographic details

X-ray data collection and structural refinement. Intensity data for all compounds were collected using a Bruker APEX II diffractometer. The structure was solved by direct phase determination (SHELX-2013) and refined for all data by full-matrix least-squares methods on F2[1]. All non-hydrogen atoms were subjected to anisotropic refinement. The hydrogen atoms were generated geometrically and allowed to ride in their respective parent atoms; they were assigned appropriate isotropic thermal parameters and included in the structure-factor calculations.

Chapter 2 **Supplementary table** | X-ray data for **3, 4** and **1**.

Compounds	**3**	**4**	**1**
Formula	$C_{21}H_{37}NSi_2$	$C_{21}H_{37}Cl_2GeNSi_2$	$C_{21}H_{37}GeNSi_2$
Fw	359.69	503.18	432.28
Crystsyst	monoclinic	monoclinic	orthorhombic
Space group	P 1 21/c 1	P 1 21/n 1	P n m a
Size (mm^3)	0.180 x 0.220 x 0.360	0.260 x 0.300 x 0.320	0.220 x 0.300 x 0.420
T/K	103(2)	103(2)	103(2)
a, Å	12.2230(12)	17.7322(15)	18.4853(11)
b, Å	12.3881(14)	7.2799(6)	10.4296(6)
c, Å	15.7504(16)	20.5722(17)	12.7509(8)
α, deg	90	90	90
β, deg	102.165(3)	104.674(3)	90
γ, deg	90	90	90
V, A^3	2331.4(4)	2569.0(4)	2458.3(3)
Z	4	4	4
d_{calcd} g·cm^{-3}	1.025	1.301	1.168
μ, mm^{-1}	0.155	1.501	1.348
Refl collected	31602	33105	18278
T_{max}/ T_{min}	0.9730/ 0.9460	0.6960/ 0.6450	0.7560/ 0.6010
N_{measd}	6254	8173	2656
[R int]	0.0749	0.0690	0.1358
R [I>2sigma(I)]	0.0448	0.0521	0.0629
R_w [I>2sigma(I)]	0.1044	0.1085	0.1149
GOF	1.033	1.154	1.030
Largest diff. peak/ hole[e. $Å^{-3}$]	0.362/ -0.236	1.283/-0.729	0.295/ -0.575

Chapter 3 **Supplementary table** ｜X-ray data for **2a, 2b, 3, 4** and **5**.

Compounds	**2a**	**2b**	**3**
Formula	$C_{42}H_{75}Ge_2N_2S_2Si_4$	$C_{42}H_{74}Ge_2N_2S_2Si_4$	$C_{21}H_{38}Cl_4GaGeNSi_2$
Fw	929.70	928.69	644.81
Crystsyst	monoclinic	triclinic	monoclinic
Space group	P 1 21/n 1	P -1	P 1 21/c 1
Size (mm^3)	0.220 x 0.300 x 0.420	0.200 x 0.240 x 0.420	0.020 x 0.080 x 0.140
T/K	103(2)	103(2)	103(2)
a, Å	10.2311(6)	10.489(4)	11.8503(2)
b, Å	26.3317(18)	11.566(4)	17.4160(3)
c, Å	18.5201(13)	12.544(5)	14.7239(3)
α, deg	90	105.736(8)	90
β, deg	91.640(2)	106.806(7)	107.3473(9)
γ, deg	90	111.124(7)	90
V, A^3	4987.3(6)	1233.0(8)	2900.57(9)
Z	4	1	4
d_{calcd} $g\cdot cm^{-3}$	1.238	1.251	1.477
μ, mm^{-1}	1.414	1.430	6.670
Refl collected	75028	4359	23363
T_{max}/ T_{min}	0.7460/ 0.5880	0.7630/ 0.5850	0.8780/ 0.4550
N_{measd}	15294	6915	5110
[R int]	0.1900	0.1031	0.0487
R [I>2sigma(I)]	0.0729	0.1238	0.0410
R_w [I>2sigma(I)]	0.1484	0.2585	0.1111
GOF	0.991	1.074	1.093
Largest diff. peak/ hole[e. $Å^{-3}$]	2.128/-1.539	1.336/ -0.450	0.835/ -0.894

Compounds	**4**	**5**
Formula	$C_{39}H_{73}GeN_3O_2Si_2$	$C_{21}H_{37}GeNOSi_2$
Fw	744.77	448.28
Crystsyst	triclinic	triclinic
Space group	P -1	P -1
Size (mm^3)	0.060 x 0.200 x 0.400	0.380 x 0.400 x 0.420
T/K	103(2)	103(2)
a, Å	12.027(3)	10.1766(6)
b, Å	17.639(4)	12.0888(7)
c, Å	19.606(4)	21.8730(14)
α, deg	98.477(2)	80.3144(18)
β, deg	92.2855(19)	80.8124(18)
γ, deg	90.304(2)	65.2397(18)
V, A^3	4110.3(15)	2396.7(3)
Z	4	4
d_{calcd} g·cm^{-3}	1.204	1.242
μ, mm^{-1}	0.839	1.388
Refl collected	19943	96838
T_{max}/ T_{min}	0.9510/ 0.7300	0.6210/ 0.5930
N_{measd}	19943	21165
[R int]	0.1425	0.1588
R [I>2sigma(I)]	0.0719	0.0606
R_w [I>2sigma(I)]	0.1366	0.1240
GOF	0.919	0.998
Largest diff. peak/ hole[e. $Å^{-3}$]	0.726/ -1.116	0.819/ -0.896

Chapter 4 **Supplementary table** | X-ray data for **7, 10, 12b** and **12d**.

Compounds	**7**	**10**	**12b**	**12d**
Formula	$C_{19}H_{35}GeNSi_2$	$C_{37}H_{39}GeNSi_2$	$C_{34}H_{51}GeNSe_2Si_2$	$C_{46}H_{51}GeNSe_2Si_2$
Fw	406.25	626.46	760.44	904.56
Crystsyst	monoclinic	triclinic	triclinic	monoclinic
Space group	P 1 21/m 1	P -1	P -1	P 1 21/n 1
Size (mm^3)	0.100 x 0.120 x 0.320	0.100 x 0.140 x 0.160	0.120 x 0.220 x 0.240	0.080 x 0.200 x 0.220
T/K	153(2) K	100(2)	100(2)	100(2)
a, Å	6.81090(10)	10.8487(4)	10.0277(5)	17.0042(16)
b, Å	39.6790(8)	11.8926(6)	11.6736(6)	13.6366(13)
c, Å	12.4192(2)	13.2375(6)	16.9271(9)	18.009(2)
α, deg	90	94.4802(19)	75.9599(16)	90
β, deg	104.2011(7)	111.5290(17)	86.3631(17)	103.789(4)
γ, deg	90	90.9025(16)	65.3770(15)	90
V, A^3	3253.72(10)	1582.06(12)	1745.89(16)	4055.6(7)
Z	6	2	2	4
d_{calcd} g·cm^{-3}	1.244	1.315	1.447	1.481
μ, mm^{-1}	2.957	1.071	3.054	2.643
Refl collected	16556	24268	74683	8859
T_{max}/ T_{min}	0.7560/ 0.4510	0.9000/ 0.8470	0.7110/ 0.5280	0.8160/ 0.5940
N_{measd}	5683	7910	9818	8859
[R int]	0.0454	0.0580	0.0994	0.0892
R [I>2sigma(I)]	0.0594	0.0477	0.0543	0.0669
R_w [I>2sigma(I)]	0.1831	0.1040	0.1141	0.1594
GOF	1.147	0.997	1.119	1.062
Largest diff. peak/ hole[e. $Å^{-3}$]	1.499/ -0.882	1.415/ -0.497	1.445/ -1.449	1.590/ -1.220

Chapter 5 **Supplementary table** | X-ray data for **3a, 3b, 4a, 4b, 5d** and **6**.

Compounds	**3a**	**3b**	**4a**
Formula	$C_{39}H_{52}AuClGeNPSi_2$	$C_{37}H_{50}AuClGeNPSi_2$	$C_{48}H_{73}AuClGeN_3Si_2$
Fw	926.97	900.93	1053.28
Crystsyst	monoclinic	monoclinic	monoclinic
Space group	C 1 2/c 1	P 1 21/c 1	P 1 21/c 1
Size (mm^3)	0.040 x 0.240 x	0.080 x 0.120 x	0.060 x 0.200 x
T/K	133(2) K	100(2)	103(2)
a, Å	17.7016(3)	12.8142(3)	18.0057(3)
b, Å	15.5137(3)	22.1010(5)	12.7387(2)
c, Å	29.9298(5)	14.3320(3)	22.8121(4)
α, deg	90	90	90
β, deg	100.4377(9)	113.2443(10)	107.8530(9)
γ, deg	90	90	90
V, A^3	8083.2(2)	3729.46(15)	4980.43(15)
Z	8	4	4
d_{calcd} g·cm^{-3}	1.523	1.605	1.405
μ, mm^{-1}	9.389	4.941	7.401
Refl collected	33896	52235	33537
T_{max}/ T_{min}	0.7050/ 0.1430	0.6930/ 0.3010	0.6650/ 0.2150
N_{measd}	6968	8153	8840
[R int]	0.0477	0.0782	0.0481
R	0.0306	0.0369	0.0391
R_w	0.0786	0.0663	0.1080
GOF	1.158	1.050	1.077
Largest diff. peak/ hole[e. $Å^{-3}$]	1.068/ -1.126	1.275/ -1.364	1.863/ -2.231

Compounds	**4b**	**5d**	**6**
Formula	$C_{47}H_{73}AuCl_3GeN_3Si_2$	$C_{64}H_{73}AlAuF_{36}GeN_3O_4Si_2$	$C_{57}H_{67}GeNP_2PdSi_2$
Fw	1112.17	1984.97	1063.22
Crystsyst	monoclinic	monoclinic	triclinic
Space group	P 1 21/n 1	P 1 21/c 1	P -1
Size (mm^3)	0.040 x 0.240 x 0.320	0.080 x 0.300 x 0.420	0.060 x 0.300 x 0.320
T/K	143(2)	103(2)	103(2)
a, Å	18.6200(2)	10.7385(5)	12.181(2)
b, Å	12.5818(2)	20.1534(9)	13.762(3)
c, Å	23.5793(3)	36.3744(16)	17.215(3)
α, deg	90	90	95.183(3)
β, deg	113.0519(7)	90.5836(18)	101.208(3)
γ, deg	90	90	105.736(2)
V, A^3	5082.91(12)	7871.6(6)	2693.2(9)
Z	4	4	2
d_{calcd} g·cm^{-3}	1.453	1.675	1.311
μ, mm^{-1}	8.227	2.416	1.032
Refl collected	49255	96044	13297
T_{max}/ T_{min}	0.7340/ 0.1780	0.8300/ 0.4300	0.9410/ 0.7340
N_{measd}	8949	20415	13297
[R int]	0.0662	0.0766	0
R [I>2sigma(I)]	0.0350	0.0618	0.0719
R_w [I>2sigma(I)]	0.0913	0.1464	0.1593
GOF	1.035	1.042	0.955
Largest diff. peak/ hole[e. $Å^{-3}$]	2.080/ -0.991	2.468/ -1.404	1.060/ -1.214

Chapter 6 **Supplementary table** ｜X-ray data for **1, 7b, 7g, 16d, 18h** and **18i**.

Compounds	**1**	**7b**	**7g**
Formula	C43H57AuCl3N	C24H16Br3N	C24H16F3N
Fw	891.21	558.11	376.38
Crystsyst	monoclinic	triclinic	triclinic
Space group	P 1 21/c 1	P -1	P 1
Size (mm^3)	0.040 x 0.160 x 0.220	0.080 x 0.240 x 0.280	0.010 x 0.040 x 0.120
T/K	103(2)	103(2)	103(2)
a, Å	20.7969(9)	9.8400(9)	11.219(5)
b, Å	9.1006(3)	13.6565(13	11.500(6)
c, Å	22.4423(10)	15.8730(16)	14.861(8)
α, deg	90	102.909(6)	72.70(3)
β, deg	104.9810(10)	93.588(6)	89.67(3)
γ, deg	90	95.664(6)	77.32(3)
V, A^3	4103.2(3)	2061.1(3)	1967.1(3)
Z	4	4	4
d_{calcd} g·cm^{-3}	1.443	1.799	1.399
μ, mm^{-1}	3.810	5.882	0.103
Refl collected	37965	40100	31706
T_{max}/ T_{min}	0.8600 / 0.5600	0.6500 / 0.2900	0.9990 / 0.9880
N_{measd}	10022	8099	14351
[R int]	0.0520	0.1300	0.1447
R [I>2sigma(I)]	0.0350	0.0613	0.0782
R_w [I>2sigma(I)]	0.1129	0.1927	0.2260
GOF	1.158	1.032	0.957
Largest diff. peak/ hole[e. $Å^{-3}$]	1.564 / -1.541	2.803 /-1.027	0.787 / -0.440

Compounds	**16d**	**18h**	**18i**
Formula	$C_{27}H_{22}F_3NO_2$	$C_{21}H_{14}BrF_2N$	$C_{22}H_{17}F_2N$
Fw	449.45	398.24	333.36
Crystsyst	monoclinic	monoclinic	triclinic
Space group	P 1 21/n 1	C 1 c 1	P -1
Size (mm^3)	0.040 x 0.220 x 0.320	0.200 x 0.220 x 0.280	0.140 x 0.180 x 0.260
T/K	103(2)	103(2)	296(2)
a, Å	17.8858(12)	11.1103(4)	8.7580(7)
b, Å	5.3984(4)	19.8612(7)	9.0189(7)
c, Å	24.0688(17)	8.6893(3)	12.1251(9)
α, deg	90	90	77.130(4)
β, deg	107.814(2)	119.1045(15)	80.995(4)
γ, deg	90	90	74.079(5)
V, A^3	2212.5(3)	675.31(10)	893.19(12)
Z	4	4	2
d_{calcd} g·cm^{-3}	1.349	1.579	1.240
μ, mm^{-1}	0.102	2.477	0.086
Refl collected	35846	11979	14211
T_{max}/ T_{min}	0.9960 /0.9680	0.6370/0.5440	0.9880/0.9780
N_{measd}	5465	4527	3508
[R int]	0.0944	0.0352	0.0556
R [I>2sigma(I)]	0.0630	0.0329	0.0482
R_w [I>2sigma(I)]	0.1793	0.0666	0.1626
GOF	1.040	1.011	1.049
Largest diff. peak/ hole[e. $Å^{-3}$]	0.426 /-0.277	0.374/-0.336	0.175/-0.214

Supplementary reference

1. Bruker AXS SHELXTL, Madison, WI; SHELX-97 Sheldrick, G. M. Acta Crystallogr. A. 2008, 64, 112; SHELX-2013, http://shelx.uni-ac. gwdg.de/SHELX/index.php.

Appendix B Theoretical calculation

Gaussian 09 was used for all density functional theory (DFT) calculations.[1] Geometry optimisation and frequency calculations were performed using the level of theory as stated in each chapter. Specific details for the DFT calculations for each chapter are stated as follow:

Chapter 2

Geometry optimization, frequency calculations, natural bond orbital (NBO) analysis of compound **1** were performed at the B3LYP/6-311G(d,p) level of theory. Geometry optimization and frequency calculations for **VIII', IX', XI' and 1'** were performed at the B3LYP/6-311G(d,p) level of theory.

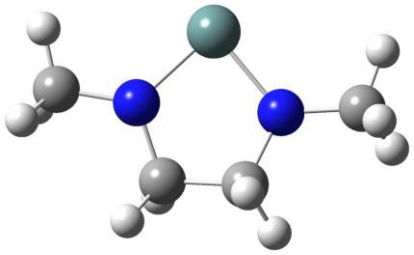

VIII'

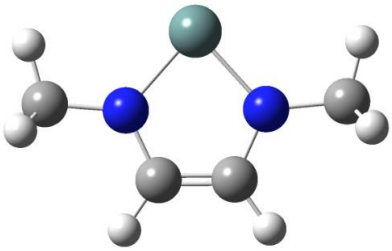

IX'

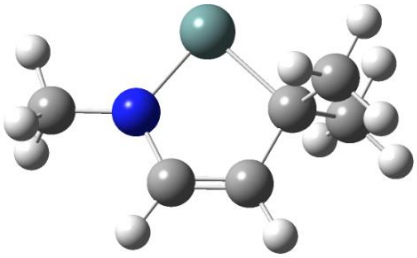

1'

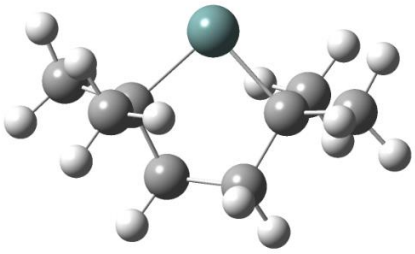

XI'

VIII'

C	0.74302498	-1.61271022	0.18178240
N	1.27078519	-0.28435381	-0.11946238
Ge	0.00000048	1.05725558	-0.00000009
N	-1.27078570	-0.28435276	0.11946059
C	-0.74302572	-1.61270976	-0.18178233
C	2.70556464	-0.12887246	-0.01946194
C	-2.70556527	-0.12887186	0.01946352

H	1.27987150	-2.39347663	-0.37575975
H	0.86702911	-1.83483303	1.25662167
H	-1.27987376	-2.39347566	0.37575903
H	-0.86702818	-1.83483292	-1.25662180
H	3.22979845	-0.75885342	-0.75335152
H	2.98843889	0.91086252	-0.21056523
H	3.08799469	-0.39982450	0.97864251
H	-2.98843790	0.91086652	0.21055087
H	-3.08799908	-0.39983931	-0.97863532
H	-3.22979727	-0.75884052	0.75336505

IX’

C	0.68102740	1.61109497	-0.00016495
N	1.25624747	0.36023206	-0.00016839
Ge	0.00000878	-1.04180876	-0.00008846
N	-1.25624751	0.36020679	-0.00007150
C	-0.68106474	1.61107484	-0.00013608
C	2.70532766	0.23370681	0.00035432
C	-2.70532733	0.23368961	0.00031830
H	1.29984116	2.50140102	-0.00021973
H	-1.29989169	2.50137188	-0.00015850
H	2.98404762	-0.82322362	-0.00057917
H	3.14823116	0.70115377	-0.88806874
H	3.14746703	0.69941176	0.89008155
H	-3.14811930	0.70110963	-0.88817825
H	-2.98406200	-0.82323772	-0.00057224
H	-3.14757252	0.69942433	0.88997542

1’

C	-0.80381010	1.61838581	-0.00010535
C	0.53673360	1.64579561	-0.00015341
C	1.24333285	0.31672105	-0.00004152
Ge	-0.23610794	-1.06506190	-0.00011557
N	-1.43092639	0.35870233	-0.00004714
C	-2.88478947	0.31609906	0.00004610
C	2.10344760	0.13757283	-1.26887990
C	2.10254083	0.13747129	1.26945438
H	-1.44243390	2.49936367	-0.00009278
H	1.08756214	2.58444311	-0.00023321
H	-3.22262137	-0.72280441	0.00016020
H	-3.30040230	0.81006375	0.88838380
H	-3.30050696	0.80990438	-0.88833225
H	2.57739752	-0.85079620	-1.29773738
H	1.50328234	0.24072528	-2.18041061

H	2.90383540	0.88916136	-1.31423948
H	2.57642179	-0.85092301	1.29862806
H	2.90293453	0.88901527	1.31541261
H	1.50173765	0.24063751	2.18056760

XI’

C	-0.69800882	1.63386532	0.31890426
C	0.69802275	1.63385319	-0.31897117
C	1.41225412	0.30289706	-0.02017543
Ge	0.00000674	-1.12791531	-0.00000954
C	-1.41224700	0.30289572	0.02016918
C	-2.62593162	0.06982692	0.91994103
C	-1.80965946	0.20153355	-1.47305365
C	2.62598909	0.06981866	-0.91987507
C	1.80956603	0.20156065	1.47307930
H	-1.29005961	2.49814313	-0.02077098
H	-0.59946038	1.74465552	1.40694352
H	1.29007419	2.49814427	0.02066813
H	0.59947466	1.74458792	-1.40701627
H	-3.09532402	-0.90040683	0.72169637
H	-2.33863738	0.07736782	1.97787721
H	-3.39454153	0.84458672	0.78113572
H	-2.41058004	-0.69377080	-1.66653019
H	-2.39614922	1.07675527	-1.78637966
H	-0.94508493	0.15055867	-2.15471931
H	3.09534806	-0.90042715	-0.72161350
H	2.33876198	0.07737966	-1.97782973
H	3.39460828	0.84455937	-0.78101201
H	2.41048553	-0.69373065	1.66661218
H	2.39601307	1.07679809	1.78644043
H	0.94494514	0.15058226	2.15469254

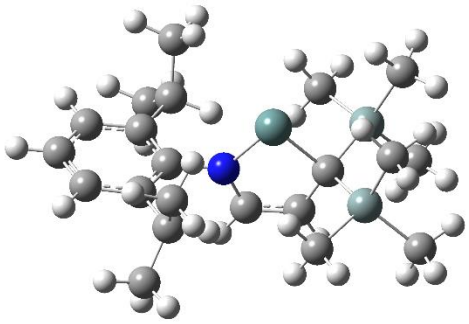

1

C	-2.28607731	0.00346427	0.19962120
C	-2.98328133	-1.22148539	0.10827528
C	-2.96603352	1.23958262	0.12632849
N	-0.85541345	-0.00640760	0.33178060
C	-4.35658094	1.22395475	-0.03289927
C	-2.21290262	2.56388012	0.17317321
C	-2.80317342	3.55232621	1.19313361
C	-2.13014195	3.19512977	-1.23114293
C	-5.05877948	0.02539167	-0.11805285
C	-4.37365140	-1.18393390	-0.05012634
C	-2.24978650	-2.55711213	0.13505467
C	-2.19140991	-3.17582164	-1.27579053
C	-2.84434678	-3.54543821	1.15272837
C	1.80288122	-0.00279849	0.32935939
C	1.08504393	-0.00374209	1.64076734
Si	2.76224173	-1.64935188	0.11986794
Si	2.77097272	1.63536056	0.08752416
Ge	0.39422639	-0.00428565	-1.07221312
C	3.46364194	1.80754428	-1.67107080
C	1.58432386	3.09032847	0.35002145
C	4.19814375	1.80789966	1.32527102
C	3.64554577	-1.74222783	-1.55614496
C	1.54129356	-3.10011879	0.18201470
C	4.01968109	-1.90848226	1.51415671
C	-0.26665204	-0.00710077	1.59473897
H	-1.19058149	2.34026896	0.48310470
H	-3.80984720	3.87994599	0.91218134
H	-2.17560301	4.44759793	1.25868898
H	-2.86380621	3.10699702	2.19114060
H	-3.12718355	3.41422864	-1.62897173
H	-1.63045852	2.52060918	-1.93457212
H	-1.56528908	4.13371902	-1.19989578
H	-4.89581884	2.16450309	-0.09630865
H	-6.13802439	0.03395348	-0.24175515

H	-4.92588313	-2.11592622	-0.12671061
H	-1.22091652	-2.35148325	0.43557517
H	-2.88517875	-3.10887402	2.15561465
H	-2.23177475	-4.45212413	1.20201820
H	-3.85997806	-3.85268189	0.88108410
H	-3.19561802	-3.38172321	-1.66253854
H	-1.63471333	-4.11956345	-1.26093398
H	-1.69501634	-2.49850621	-1.97884311
H	3.86605748	2.81847410	-1.80521080
H	2.68384935	1.65808992	-2.42616216
H	4.27160753	1.10297913	-1.88457264
H	1.02427174	2.99749645	1.28490862
H	0.86549194	3.16300043	-0.47294106
H	2.13992076	4.03401945	0.38743719
H	4.60115449	2.82669169	1.28651131
H	5.02134503	1.12150128	1.10359670
H	3.87526882	1.62024338	2.35455347
H	4.52490890	-1.09404505	-1.60985568
H	2.97147173	-1.46202089	-2.37328538
H	3.98361477	-2.76853100	-1.73952743
H	2.08725971	-4.04982984	0.21849067
H	0.89981399	-3.12391385	-0.70542030
H	0.90042382	-3.05499488	1.06745497
H	4.81531469	-1.15797077	1.50754668
H	4.48985249	-2.89324038	1.40917218
H	3.53997578	-1.87740750	2.49806782
H	-0.91968901	-0.00818133	2.46342179
H	1.60499705	-0.00287069	2.59530205

The NPA charges of **1**.

Atom	No	Natural Charge	Natural Population			
			Core	Valence	Rydberg	Total
C	1	0.14991	1.99884	3.83234	0.01892	5.85009
C	2	-0.01946	1.99898	4.00393	0.01655	6.01946
C	3	-0.01584	1.99901	4.00056	0.01627	6.01584
N	4	-0.80335	1.99948	5.78784	0.01603	7.80335
C	5	-0.21607	1.99916	4.20545	0.01146	6.21607
C	6	-0.23359	1.99922	4.22307	0.01130	6.23359
C	7	-0.63561	1.99944	4.62825	0.00793	6.63561
C	8	-0.62464	1.99941	4.61753	0.00770	6.62464
C	9	-0.18825	1.99927	4.17640	0.01258	6.18825
C	10	-0.21396	1.99916	4.20331	0.01150	6.21396
C	11	-0.23009	1.99922	4.21932	0.01155	6.23009
C	12	-0.63009	1.99941	4.62292	0.00776	6.63009
C	13	-0.63224	1.99944	4.62483	0.00798	6.63224
C	14	-1.51370	1.99933	5.50057	0.01380	7.51370
C	15	-0.25800	1.99925	4.23820	0.02054	6.25800
Si	16	1.83901	9.99797	2.12702	0.03600	12.16099
Si	17	1.84585	9.99807	2.12015	0.03593	12.15415
Ge	18	0.93639	27.99327	3.05612	0.01422	31.06361
C	19	-1.14738	1.99942	5.13543	0.01254	7.14738
C	20	-1.16093	1.99943	5.14916	0.01235	7.16093
C	21	-1.16818	1.99943	5.15684	0.01191	7.16818
C	22	-1.14159	1.99941	5.12969	0.01249	7.14159
C	23	-1.16134	1.99942	5.14957	0.01234	7.16134
C	24	-1.15168	1.99942	5.13983	0.01244	7.15168
C	25	0.00919	1.99914	3.97491	0.01677	5.99081
H	26	0.23321	0.00000	0.76349	0.00330	0.76679
H	27	0.21074	0.00000	0.78759	0.00167	0.78926
H	28	0.22157	0.00000	0.77697	0.00146	0.77843
H	29	0.22075	0.00000	0.77763	0.00162	0.77925
H	30	0.21428	0.00000	0.78402	0.00170	0.78572
H	31	0.22057	0.00000	0.77792	0.00150	0.77943
H	32	0.21505	0.00000	0.78335	0.00160	0.78495
H	33	0.20517	0.00000	0.79285	0.00199	0.79483
H	34	0.20558	0.00000	0.79270	0.00172	0.79442
H	35	0.20531	0.00000	0.79271	0.00197	0.79469
H	36	0.23152	0.00000	0.76499	0.00349	0.76848
H	37	0.21989	0.00000	0.77858	0.00153	0.78011
H	38	0.21982	0.00000	0.77870	0.00148	0.78018
H	39	0.20889	0.00000	0.78945	0.00166	0.79111
H	40	0.21400	0.00000	0.78417	0.00182	0.78600
H	41	0.21626	0.00000	0.78206	0.00168	0.78374
H	42	0.22230	0.00000	0.77614	0.00156	0.77770
H	43	0.23877	0.00000	0.75997	0.00126	0.76123
H	44	0.23929	0.00000	0.75926	0.00145	0.76071
H	45	0.23324	0.00000	0.76542	0.00134	0.76676

H	46	0.23933	0.00000	0.75899	0.00168	0.76067
H	47	0.23685	0.00000	0.76168	0.00147	0.76315
H	48	0.23994	0.00000	0.75880	0.00125	0.76006
H	49	0.24221	0.00000	0.75644	0.00135	0.75779
H	50	0.23394	0.00000	0.76469	0.00137	0.76606
H	51	0.23849	0.00000	0.76011	0.00140	0.76151
H	52	0.23227	0.00000	0.76640	0.00133	0.76773
H	53	0.23971	0.00000	0.75886	0.00143	0.76029
H	54	0.23843	0.00000	0.76036	0.00121	0.76157
H	55	0.23906	0.00000	0.75970	0.00124	0.76094
H	56	0.23564	0.00000	0.76290	0.00147	0.76436
H	57	0.24121	0.00000	0.75708	0.00172	0.75879
H	58	0.23211	0.00000	0.76642	0.00147	0.76789
H	59	0.23899	0.00000	0.75971	0.00130	0.76101
H	60	0.23624	0.00000	0.76237	0.00138	0.76376
H	61	0.20092	0.00000	0.79769	0.00139	0.79908
H	62	0.20415	0.00000	0.79360	0.00225	0.79585
* Total *		0.00000	91.97358	137.59707	0.42935	230.00000

Geometry optimization, frequency calculations of compound **7** were performed at the B3LYP/6-311G(d,p) level of theory.

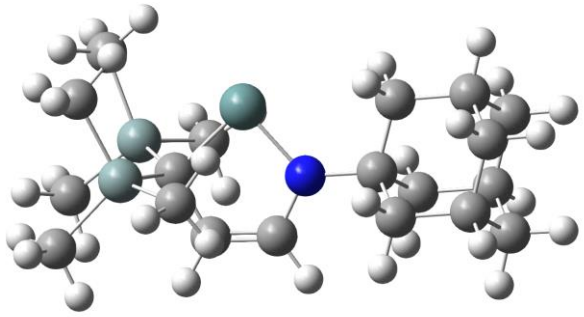

7

C	2.179022	-0.03999	0.206818
C	2.5644	-0.09975	-1.28579
C	4.096785	-0.07817	-1.45536
C	4.661339	1.222968	-0.85027
C	4.299008	1.287433	0.646625
C	2.764349	1.265191	0.803615
C	2.816534	-1.25977	0.920017
C	4.351647	-1.23203	0.763523
C	4.71496	-1.29169	-0.73288
C	4.906898	0.07093	1.376022
C	0.118692	-0.04223	1.590313
C	-1.23237	-0.02179	1.640327
C	-1.95124	-0.00927	0.331891
C	-3.60394	-1.80069	-1.67316
C	-4.38608	-1.76976	1.306958
C	-1.74581	-3.07488	0.421827
C	-3.62471	1.822614	-1.6116
C	-4.06082	2.05013	1.442878
C	-1.44226	3.036141	0.179477
Ge	-0.54477	-0.04121	-1.06956
N	0.711882	-0.05491	0.332665
Si	-2.93391	-1.6284	0.095037
Si	-2.78578	1.6929	0.085505
H	2.119814	0.751272	-1.81597
H	2.145318	-1.00818	-1.73636
H	4.336385	-0.1228	-2.52486
H	5.750971	1.257203	-0.97782

H	4.250056	2.094337	-1.37602
H	4.691864	2.213993	1.083815
H	2.305199	2.120082	0.292011
H	2.495463	1.34574	1.863835
H	2.395771	-2.17777	0.491463
H	2.553611	-1.25552	1.984358
H	4.780896	-2.09701	1.284486
H	5.805413	-1.29063	-0.85819
H	4.34314	-2.22515	-1.17479
H	6.000984	0.089518	1.290408
H	4.670577	0.115742	2.447276
H	0.749278	-0.04829	2.474546
H	-1.74996	-0.01561	2.596539
H	-4.03137	-2.80041	-1.81334
H	-2.81452	-1.66699	-2.42094
H	-4.39224	-1.07447	-1.89238
H	-4.83372	-2.76884	1.247584
H	-4.06784	-1.61227	2.342845
H	-5.17397	-1.04232	1.086121
H	-1.41943	-3.09289	1.465787
H	-2.22807	-4.0343	0.204098
H	-0.84756	-3.00056	-0.20149
H	-3.90342	2.862818	-1.816
H	-2.95152	1.493051	-2.41082
H	-4.53737	1.221937	-1.67506
H	-4.4718	3.05891	1.31926
H	-3.60939	1.998354	2.439205
H	-4.89755	1.344877	1.419531
H	-0.78874	2.877941	1.042692
H	-0.81344	3.047218	-0.71773
H	-1.8962	4.028689	0.278207

Geometry optimization, frequency calculations of compound **5d** were performed at the B3LYP/6-31G(d,p) level for Ge, Si, C, N, H and M05-2X/LANL2DZ level for Au.

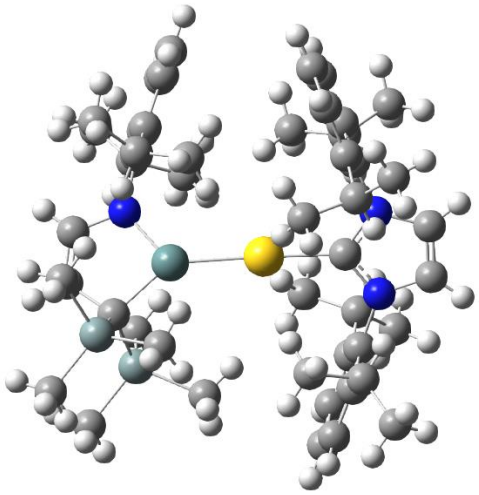

5d

Au	4.5309	6.334	23.1526
C	4.4324	8.3496	22.811
Ge	4.5563	3.9886	23.441
N	3.8707	3.0532	24.8275
C	3.5085	3.5893	26.1191
C	2.1668	3.7344	26.4828
C	4.5569	4.0569	26.9375
C	4.1959	4.7219	28.1123
C	6.0058	3.8654	26.5883
C	6.7413	3.0673	27.654
C	6.7227	5.1875	26.3155
H	6.038	3.3293	25.7445
H	6.4788	3.3878	28.5415
H	7.7089	3.1822	27.5376
H	6.5134	2.1181	27.5704
H	6.4155	5.8667	26.952
H	6.5323	5.4817	25.4026
H	7.6924	5.0605	26.421
C	2.8876	4.9053	28.4579
H	4.8773	5.0545	28.6834
C	1.8829	4.4035	27.6795
H	2.6724	5.387	29.2471
H	0.9803	4.5123	27.9523

C	1.0213	3.1963	25.6099
C	0.0421	2.3559	26.4355
C	0.251	4.333	24.9115
H	1.4172	2.6079	24.9043
H	-0.4527	2.9384	27.0466
H	0.5448	1.6889	26.9557
H	-0.5821	1.8985	25.8354
H	0.8772	4.857	24.3623
H	-0.1564	4.9134	25.5844
H	-0.4423	3.9521	24.3369
C	3.9249	1.6808	24.5689
C	4.404	1.316	23.3937
H	3.6317	1.0399	25.2062
C	4.9159	2.366	22.4706
H	4.4216	0.399	23.1402
Si	6.8309	2.0577	22.34
Si	3.7755	2.5413	20.8887
C	7.5486	1.5397	23.984
H	7.1182	0.7134	24.2823
H	7.3915	2.2471	24.646
H	8.5118	1.3906	23.8858
C	7.1616	0.653	21.1761
H	6.7992	-0.1753	21.5507
H	8.1316	0.5562	21.0488
H	6.7388	0.8364	20.3104
C	7.6999	3.6337	21.8926
H	7.6033	4.2786	22.6237
H	7.3044	4.0045	21.0779
H	8.6507	3.4523	21.7435
C	2.004	2.5232	21.4889
H	1.8633	3.2608	22.1181
H	1.8179	1.6707	21.9363
H	1.3975	2.628	20.7251
C	3.9877	1.1105	19.6703
H	3.6881	0.2761	20.0885
H	4.9394	1.0258	19.4302
H	3.4643	1.2838	18.8628
C	4.0392	4.1153	19.8812
H	3.5279	4.0629	19.0483
H	4.996	4.21	19.6703
H	3.7472	4.8912	20.4013
N	4.5198	9.325	23.7218
N	4.2372	8.9683	21.6318
C	4.2075	10.3407	21.8079
C	4.3822	10.5705	23.1093
H	4.0866	10.9937	21.1288
H	4.4079	11.4169	23.5367

C	4.7696	9.067	25.1334
C	6.1079	9.0489	25.5262
C	3.686	8.8655	25.9882
C	6.3626	8.8111	26.8757
C	7.2772	9.2	24.5915
C	8.1958	10.3185	25.0716
C	8.041	7.878	24.4605
H	6.9288	9.4499	23.6894
H	7.6666	11.1186	25.2607
H	8.8548	10.5221	24.3732
H	8.6633	10.0324	25.8827
H	8.3111	7.5676	25.348
H	8.8359	8.013	23.904
H	7.4611	7.2069	24.0422
C	5.3335	8.5692	27.7522
H	7.2614	8.8151	27.1921
C	4.0171	8.5974	27.3194
H	5.5272	8.3818	28.6615
H	3.3278	8.4282	27.945
C	2.2642	8.7163	25.4644
C	1.6493	7.3459	25.7372
C	1.3472	9.8691	25.879
H	2.3398	8.7808	24.4714
H	2.2771	6.6446	25.4571
H	0.8147	7.2552	25.2316
H	1.4667	7.2532	26.6938
H	1.7599	10.7236	25.6317
H	1.2031	9.8429	26.8466
H	0.4831	9.7804	25.4208
C	4.0581	8.1863	20.3468
C	2.7643	7.7832	20.0049
C	5.1895	7.9324	19.543
C	2.6398	7.0416	18.841
C	1.5549	8.0674	20.8742
C	1.0268	6.7715	21.4852
C	0.4504	8.7808	20.0922
H	1.8437	8.668	21.6198
H	0.7581	6.1569	20.7723
H	0.2468	6.9711	22.049
H	1.7246	6.3564	22.0308
H	0.0944	8.1803	19.4047
H	0.8145	9.585	19.6666
H	-0.2732	9.0348	20.7069
C	3.7283	6.7635	18.0371
H	1.7833	6.7151	18.59
C	4.9757	7.2008	18.3972
H	3.6119	6.2677	17.2369

H	5.7148	6.9952	17.8371
C	6.5815	8.3758	19.9394
C	7.3731	7.1706	20.4523
C	7.3461	9.0186	18.7719
H	6.5042	9.0469	20.6778
H	7.5815	8.3294	18.1172
H	8.1631	9.4419	19.1101
H	6.7813	9.6958	18.3463
H	6.9333	6.8018	21.2452
H	8.2834	7.4547	20.6887
H	7.4167	6.4854	19.7539

Supplementary reference

1. Gaussian 09, Revision B.01, M. J. Frisch, G. W. Trucks, H. B. Schlegel, G. E. Scuseria, M. A. Robb, J. R. Cheeseman, G. Scalmani, V. Barone, B. Mennucci, G. A. Petersson, H. Nakatsuji, M. Caricato, X. Li, H. P. Hratchian, A. F. Izmaylov, J. Bloino, G. Zheng, J. L. Sonnenberg, M. Hada, M. Ehara, K. Toyota, R. Fukuda, J. Hasegawa, M. Ishida, T. Nakajima, Y. Honda, O. Kitao, H. Nakai, T. Vreven, J. A. Montgomery, Jr., J. E. Peralta, F. Ogliaro, M. Bearpark, J. J. Heyd, E. Brothers, K. N. Kudin, V. N. Staroverov, T. Keith, R. Kobayashi, J. Normand, K. Raghavachari, A. Rendell, J. C. Burant, S. S. Iyengar, J. Tomasi, M. Cossi, N. Rega, J. M. Millam, M. Klene, J. E. Knox, J. B. Cross, V. Bakken, C. Adamo, J. Jaramillo, R. Gomperts, R. E. Stratmann, O. Yazyev, A. J. Austin, R. Cammi, C. Pomelli, J. W. Ochterski, R. L. Martin, K. Morokuma, V. G. Zakrzewski, G. A. Voth, P. Salvador, J. J. Dannenberg, S. Dapprich, A. D. Daniels, O. Farkas, J. B. Foresman, J. V. Ortiz, J. Cioslowski, D. J. Fox, Gaussian, Inc., Wallingford CT, **2010**.